Aus der Sektion für Translationale Neurodegeneration „Albrecht Kossel“ der Klinik für Neurologie der Universitätsmedizin Rostock
Sektionsleiter Prof. Dr. Dr. Andreas Hermann

Entwicklung individualisierter molekularer Therapien für lysosomale Speicherkrankheiten

Habilitationsschrift
zur
Erlangung des akademischen Grades
doctor rerum naturalium/ habilitatus rerum humanarum (Dr. rer. nat./ habil. rer. hum.)
der Universitätsmedizin Rostock

vorgelegt von: Dr. rer. nat. Jan Lukas,
geb. am 14. März 1980 in: Stade

Wohnhaft in Rostock

Rostock, im Januar 2024

https://doi.org/10.18453/rosdok_id00005126

Gutachter:

Prof. Dr. Dr. Andreas Hermann, Universitätsmedizin Rostock

Prof. Dr. Christine Kurschat, Universitätsmedizin Köln

Prof. Dr. Christoph Kampmann, Universitätsmedizin Mainz

Datum der Aufnahme des Verfahrens: 26.02.2024

Datum der Verteidigung: 27.01.2025

Die Habilitationsschrift wurde im Rahmen des Forschungsprojektes „PePPP“ angefertigt. Die Förderung des Projektes erfolgte aus Mitteln des Europäischen Sozialfonds (ESF) im Rahmen des Qualifikationsprogrammes „Förderung von Nachwuchswissenschaftlern in exzellenten Forschungsverbünden – Exzellenzforschungsprogramm des Landes Mecklenburg-Vorpommern“. (ESF/14-BM-A55-0046/16)

Inhalt

1 Einleitung

Für die Entwicklung von Therapien für seltene Mendelsche oder Stoffwechselkrankheiten stehen eine ganze Reihe verschiedener Konzepte zur Verfügung. Einige basieren auf der Nutzung von Nukleinsäuren, andere nutzen Proteine oder andere Stoffwechselprodukte oder steuern diese in der Zielzelle an. Auslöser der Krankheiten sind Genmutationen, die zu einem Mangel an Enzymen, Cofaktoren oder Transportern führen. Die lysosomalen Speicherkrankheiten (LSD von engl. l*ysosomal storage disorder*) sind eine heterogene Gruppe von weit über 50 Krankheiten, denen Defekte in Genen der lysosomalen Biogenese und Funktion zugrunde liegen. Die Anhäufung oder Fehlallokation von unabgebautem Stoffwechselmaterial führt schließlich zur beobachteten Pathophysiologie. Therapiekonzepte für die LSDs fußen auf der Verringerung der Substratakkumulation oder auf Ersatz oder Verstärkung des fehlenden oder unzureichend funktionierenden Enzyms. Bei Krankheiten wie Morbus Fabry (M. Fabry), Morbus Gaucher (M. Gaucher) und Morbus Pompe (M. Pompe, *Glycogen storage disease type II*) ist dem geschädigten Enzym durch das Vorliegen einer Punkt- oder Komplexmutation in vielen Fällen eine Proteinfehlfaltung inhärent. Neben der Enzymersatztherapie (ERT von engl. *enzyme replacement therapy*), die für alle drei Krankheiten zur Verfügung steht, liegt ein aktueller Schwerpunkt auf der Entwicklung von niedermolekularen Therapien, zu denen die so genannten pharmakologischen Chaperone (PCs) zählen, deren therapeutische Wirkung in der Verstärkung der reduzierten Aktivität des endogenen Enzyms liegt. Die angestrebten Vorteile der PC Therapie (PCT) im Vergleich zur ERT sind die orale Verfügbarkeit und eine verbesserte Bioverfügbarkeit, beispielsweise ins zentrale Nervensystem bei Erkrankungen mit neurologischer Symptomatik. Zu den vielen Herausforderungen für die Umsetzung dieses Ansatzes in die klinische Anwendung zählt, dass PCs in der Regel den natürlichen Substraten der Zielenzyme strukturähnlich sind und daher, speziell in hohen Konzentrationen, zu einer kompetitiven Hemmung führen können. Zudem sind PCs abhängig von der Genetik und daher nicht für die Anwendung bei jedem Patienten geeignet. Es bedarf der Entwicklung spezifischer pharmakogenetischer Testsysteme und robuster, prädiktiver Readouts für eine erfolgreiche medizinische Translation wirksamer PC Kandidaten.

1.1 Das lysosomale System

1.1.1 Aufbau und Funktion des Lysosoms

Das Lysosom ist ein vielschichtiger Reaktom-Komplex, dessen Funktionalität durch interne Interaktion der katabolischen Komponenten bestimmt wird und der durch Kommunikation mit externen regulatorischen Faktoren hochgradig mit der Zellumgebung vernetzt ist. In den 1950er und frühen 60er Jahren waren es Christian de Duve und seine Mitarbeiter, die erstmals saure Hydrolasen

enthaltende Kompartimente in der Zelle identifizierten und diese als Lysosomen bezeichneten (Uchiyama et al. 2008; Vikić-Topić und Carević 2009). Lysosomen kommen in allen pflanzlichen und tierischen Zellen außer ausgereiften Erythrozyten vor (Kurz et al. 2011). In den lysosomalen Kompartimenten werden Makromoleküle aus den Stoffklassen der Fette (Lipide), Zucker (Kohlenhydrate) und Eiweiße (Proteine) abgebaut, die der Zelle wieder als Bausteine zur Neusynthese zur Verfügung gestellt werden können (Lodish 2002; Jaishy und Abel 2016). Zu diesem Zweck wirken im Lysosom eine Vielzahl spezialisierter Enzyme aus der Klasse der Phosphatasen, Proteasen, DNAsen/RNAsen, Lipasen und Glykosidasen, welche, dem sauren intra-lysosomalen Milieu angepasst, eine erhöhte Stabilität und einen optimierten Aktivitätslevel bei tiefen pH Werten um 3-5 aufweisen (Abb. 1).

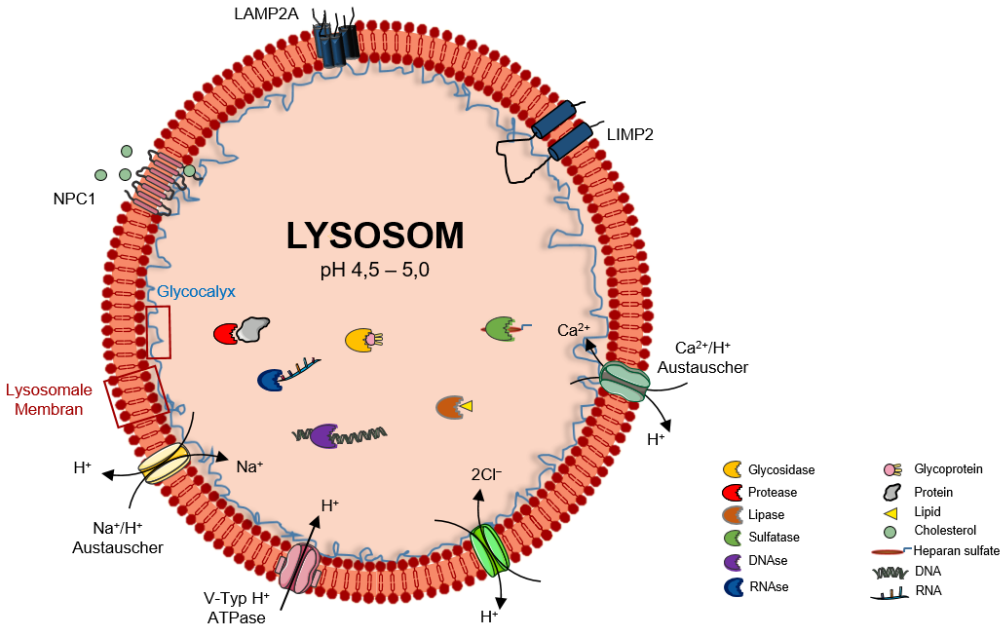

Abb. 1. Das Lysosom ist ein Organellensystem von enormer Bedeutung und mit vielfältigen Funktionen. Daher ist das System einzigartig in seiner Anpassung an spezifische Aufgaben in Bezug auf Redoxpotential und pH-Wert, gekennzeichnet durch Kanäle zur Regulierung des Ionengleichgewichts, die Ausstattung mit Proteinen und Enzymen mit charakteristischen Aktivitätsoptima und eine begrenzende Doppelmembran und innere Matrix, die die Bedürfnisse der Kommunikation und des Schutzes erfüllen und den Reaktionsraum von der äußeren zytosolischen Umgebung abgrenzen. Das lysosomale Lumen enthält eine Reihe von löslichen hydrolytischen Enzymen, die Proteine (Proteasen), Glykoproteine und Glykolipide (Glykosidasen), Lipide (Lipidasen), Phosphatester (z. B. DNAsen) und Heparansulfate (Sulfatasen) spalten. Die Abbildung wurde teilweise unter Verwendung von *Servier Medical Art* erstellt, bereitgestellt von Servier, lizenziert unter einer *Creative Commons Attribution 3.0 unported license*.

Aufgabe der Lysosomen sind das Recycling von Biomolekülen, sowie komplexe Vorgänge zur Überwindung des Zellverschleißes (Plasmamembranreparatur), der Sekretion, Instandhaltung des Cholesterolgleichgewichts, Steuerung des Energiehaushaltes der Zelle, Funktionen im Zusammenhang mit der Immunität sowie Beeinflussung von Signalwegen wie der Autophagie und dem programmierten Zelltod (Settembre et al. 2013; Turk und Turk 2009; Appelqvist et al. 2013). Der saure

lysosomale pH bedingt neben den genannten Anforderungen an die Beschaffenheit der residenten Proteine ebenfalls Besonderheit im Aufbau der begrenzenden selektiv-permeablen Membran, die aus einer Lipiddoppelschicht besteht und sich durch eine dicke Kohlenhydrat-haltige Glykokalyx auf der lumenalen Seite von anderen zellulären Organell-Membranen unterscheidet (Lodish 2002). Dieser Kohlenhydratanteil und eine Ausstattung mit spezifischen integralen Membranproteinen schaffen eine Barriere, die die Zelle vor dem Verdau durch die eigenen lysosomalen Hydrolasen schützt und die physiologische und biochemische Grundlage für die hochspezialisierte Funktionalisierung des Organells darstellt (Schulze et al. 2009).

1.1.2 Synthese, Reifung und Transport lysosomaler Proteine

Die endosomale Sortierung zum Lysosom erfolgt über zwei Hauptwege. Einmal die rezeptorvermittelte Internalisierung an der Plasmamembran, die im Gegensatz zum Biosyntheseweg steht. Im Letzteren werden neu synthetisierte Hydrolasen und andere lysosomale Proteine auf ihrem endozytischen Weg ins endosomale/lysosomale System sortiert. Abbildung 2 fasst die wesentlichen Schritte des Biosyntheseweges zusammen. Die Biosynthese lysosomaler Proteine beginnt mit der Transkription im Zellkern der Zelle (Abb. 2A). Lange Zeit wurde angenommen, dass lysosomale Gene konstitutiv exprimiert werden und zu den so genannten »*housekeeping*« Genen zu zählen sind. Die Entdeckung des als CLEAR (*Coordinated Lysosomal Expression and Regulation*) bezeichneten regulatorischen Netzwerkes (Sardiello et al. 2009) um den Master Regulator Trancription factor EB (TFEB) wies eine koordinierte Transkriptionsregulation lysosomaler Gene nach und lieferte mechanistische Details aktiver lysosomaler Funktionssteuerung als Anpassung auf zelluläre Bedürfnisse bei wechselnden Umweltreizen (Ballabio und Bonifacino 2020).

Lysosomale Proteine sind mit einer N-terminalen Signalsequenz versehen, die während der Synthese der Polypeptidkette über Signalpeptidasen abgespalten wird. Das Ribosom, welches das Protein synthetisiert, ist direkt mit der Membran des endoplasmatischen Retikulums (ER) verbunden. Mit Ribosomen besetzte Regionen des ER werden als raues endoplasmatisches Retikulum (rER) bezeichnet. Die naszente Polypeptidkette wird am rER in einem co-translationalen Prozess durch die ER Membran transloziert und im Lumen freigesetzt (Alberts 2002). Die Translokation wird über *signal recognition protein* (SRP-) Komplex und das SEC61-Porenprotein vermittelt, die das ER Translocon bilden (Mandon et al. 2013) (Abb. 2B). Lysosomale Proteine sind Glykoproteine, die an Asparaginresten innerhalb einer Asn-X-(Ser/Thr)-Sequenz glykosyliert werden. Bei der N-Glykosylierung kommt es zum Anhängen von Glykosylgruppen an Aminogruppen (»N«-Gruppen) des Proteins. Diese Art der posttranslationalen Modifikation hat direkte Auswirkungen auf Eigenschaften und Bioaktivität des Proteins. Entfällt die initiale N-Glykosylierung im ER, so konnte für lysosomale Hydrolasen eine Beeinträchtigung der strukturellen Integrität, des subzellulären Transports und der katalytischen

Funktion festgestellt werden (Gieselmann et al. 1992; Ioannou et al. 1998). Die Glykosylierung wird durch Oligosaccharyltransferasen getrieben, welche ein aus Glucose$_3$-Mannose$_9$-*N*-Acetylglucosamin$_2$ ($Glc_3Man_9GlcNAc_2$) vorgefertigtes Kernglykan-Gerüst an die Aminogruppe des Asparagins transferieren (Moremen und Molinari 2006). Eine entscheidende Rolle spielt die Glykanprozessierung im ER für die Proteinfaltung und den anterograden Transport zum Golgi Apparat. Unmittelbar nach der Übertragung von $Glc_3Man_9GlcNAc_2$ werden Glucosidase I und II aktiv, die die terminalen Glucosereste abspalten. Das $Glc_1Man_9GlcNAc_2$ Glykangerüst wird von den Lektinen Calnexin (CANX) und Calreticulin (CRT) erkannt und das Protein durchläuft den Calnexinzyklus, die wichtigste Qualitätskontrolle der Proteostase des ER. Nach Entfernen des letzten Glucoserestes durch Glucosidase II werden Proteine, die den Faltungsprozess nicht abgeschlossen haben, vom Faltungssensor UDP-glucose:glycoprotein glucosyltransferase (UGT1) erkannt und erneut glykosyliert. Diese Zurückbehaltung unreifer Proteine im ER ist der erste Schritt der Qualitätssicherung. Proteine, die auch bei wiederholtem Durchlaufen des Calnexinzyklus von UGT1 als unreif erkannt werden, werden dem BiP Chaperon System, der zweiten Qualitätssicherungsphase, überantwortet oder über die ER-assoziierte Degradation (ERAD) endgültig entsorgt. Der Signalgeber für den finalen Abbau ist »Mannosetrimming« über ER-residente α-Mannosidasen. Korrekt gefaltete Glykoproteine verlassen den Calnexinzyklus und werden in anterograde Transportvesikel verpackt (Moremen und Molinari 2006). Die lysosomalen Proteine treten dann auf der cis-Seite in den Golgi Apparat ein, dessen Golgi-Stapel sie von cis nach trans durchqueren. Es wird angenommen, dass sowohl das cis-Golgi-Netzwerk (CGN) als auch das trans-Golgi-Netzwerk (TGN) für die Proteinsortierung wichtig sind. Dabei werden die Proteine auf ihrem Weg weiteren Modifikationen ihrer N-gebundenen Oligosaccharide unterzogen (Abb. 2C). Bei der Art der Glykosylierung werden komplexe Oligosaccharide und Oligosaccharide mit hohem Mannosegehalt unterschieden. Hoch-Mannose Oligosaccharide werden im Golgi Apparat nicht mit neuen Zuckern angereichert. Sie entsprechen im Wesentlichen der ER Vorstufe bestehend aus zwei N-Acetylglucosaminen und einer hohen Anzahl an Mannoseresten. Im Gegensatz dazu werden komplexe Oligosaccharide durch eine Kombination aus Entfernen der ursprünglichen im ER konjugierten N-gebundenen Oligosaccharide und dem Anreichern durch weitere Zucker wie Galactose- und Sialinsäureresten sowie Fucose erzeugt. Die Prozessierung zu komplexen oder mannosereichen Oligosacchariden im Golgi-Apparat wird weitgehend durch das Protein und die Position der N-glykosylierten Aminosäure auf dem Proteinmolekül bestimmt (Alberts 2002). Phosphomonoester- und Phosphodiesterbindungen an endständigen Mannoseresten werden im CGN durch die aufeinanderfolgende Wirkung von zwei Enzymen, einer Phosphotransferase und einer Diesterase, hergestellt.

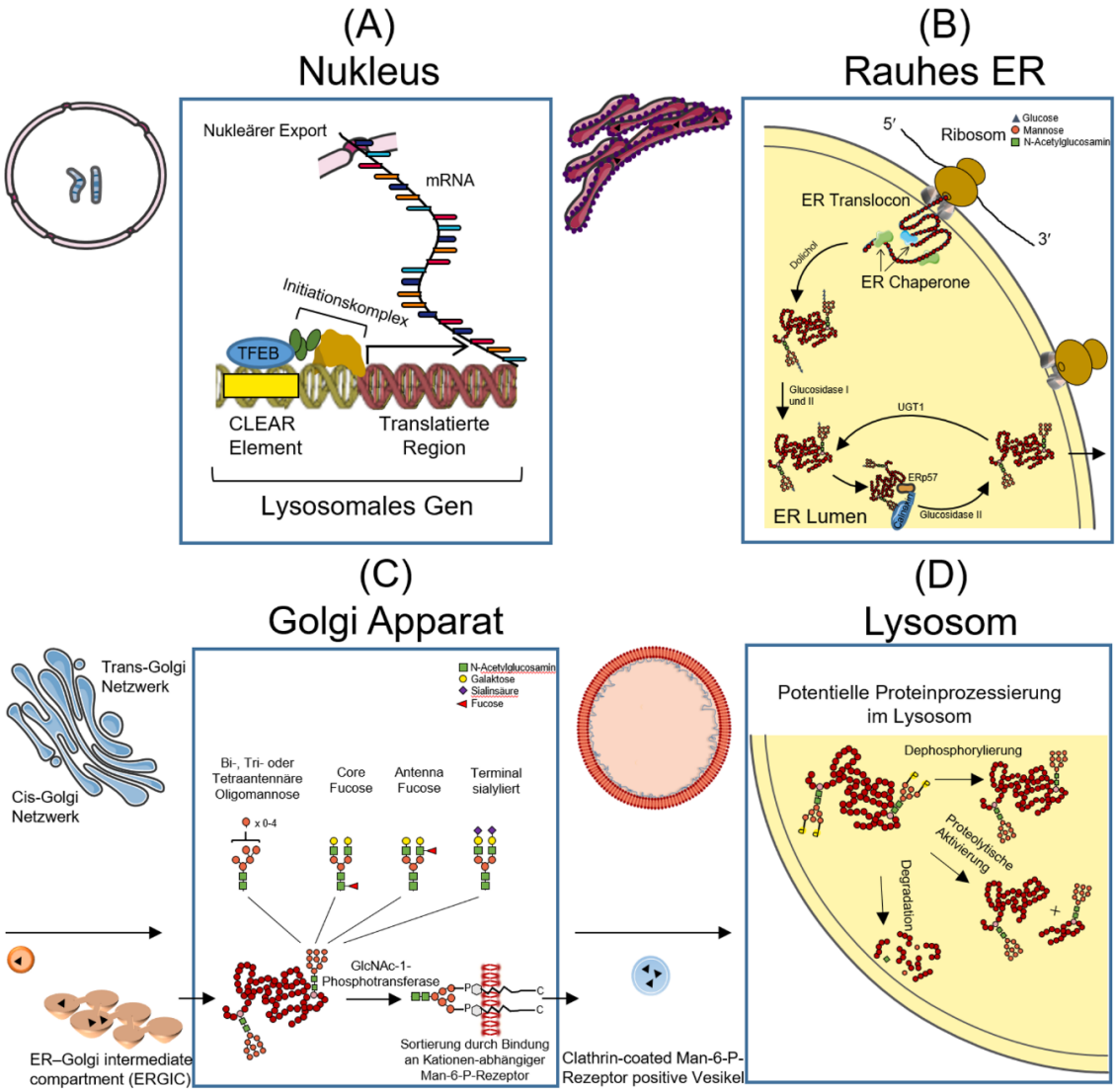

Abb. 2. Endozytischer Transport lysosomaler Proteine ins Lysosom. Die Abbildung stellt die wesentlichen Prozesse und Meilensteine lysosomaler Proteine von ihrer Synthese bis ins Zielorganell dar. (A) Im Zellkern erfolgt die Transkription lysosomaler Gene in Abhängigkeit von CLEAR Sequenzelementen in der Promotorregion, die vom Master Regulator Trancription factor EB (TFEB) gebunden werden, woraufhin die Transkription angeschaltet wird. (B) Nach dem nukleären Export der reifen mRNA wird diese von ER-assoziierten Ribosomen am rauhen ER (rER) gebunden. Die naszente Polypeptidkette transloziert co-translational über das SEC61-Porenprotein (ER Translocon) in das Innere des ER und die Faltung des Proteins wird über ER Chaperone ermöglicht, die eine vorzeitige Proteinaggregation verhindern und intramolekulare Bindungen knüpfen. Im ER Lumen erfolgt der Transfer eines vorgefertigten Kernglykan-Gerüsts auf Asparaginreste durch Oligosaccharyltransferasen. Als ein entscheidender Teil der Qualitätskontrolle im ER erfolgt die Qualitätsprüfung von Glykoproteinen über den Calnexinzyklus als Voraussetzung für die Sortierung in Transportvesikel in Richtung Golgi-Apparat. (C) Im CGN wird das Zuckergerüst weiter prozessiert und terminale Mannosereste werden durch die N-Acetylglucosamin-1-Phosphotransferase phosphoryliert, um die lysosomale Sortierung über Mannose-6-Phosphat Rezeptoren (Man-6-P-Rezeptoren) zu gewährleisten. (D) Im Lysosom kommt es zu einer Abspaltung der Phosphatreste und in einigen Fällen zu einer proteolytischen Spaltung, die über die Freisetzung der katalytischen Domäne Enzym-aktivierend wirkt. Auf Grund der harschen Umgebungsbedingungen ist die Halbwertzeit lysosomaler Proteine begrenzt. Die ultimative Degradation beendet den Lebenszyklus des Proteins im Lysosom. Der Transport zwischen ER und Golgi-Apparat sowie Golgi-Apparat und Lysosom (endosomal/lysosomalem System) erfolgt Vesikel-basiert, so dass lysosomale Proteine niemals im direkten Kontakt mit dem Zytosol stehen. Die Abbildung wurde teilweise unter Verwendung von *Servier Medical Art* erstellt, bereitgestellt von Servier, lizenziert unter einer *Creative Commons Attribution 3.0 unported license*.

Die bei den meisten lysosomalen Proteinen zu findende Mannose-6-Phosphat (Man-6-P) Markierung dient der Identifizierung der Proteine durch spezifische Kationen-abhängige Man-6-P-Rezeptoren, die eine Sortierung des Proteins in Vesikel mit dem Bestimmungsort Lysosom ermöglichen (Braulke und Bonifacino 2009). Dieser Prozess ist bei der I-Zellkrankheit (Mukolipidose Typ II), bei der eine Untereinheit der N-Acetylglucosamin-1-Phosphotransferase mutiert ist, gestört und löst eine Fehlsortierung multipler lysosomaler Enzyme aus. Auch wenn das mutierte Enzym nicht selbst im Lysosom wirkt, so gilt die I-Zellkrankheit als LSD (Brooks et al. 2007). Es existieren auch Man-6-P unabhängige Transportmechanismen lysosomaler Proteine, zum Beispiel über das Adapterproteinkomplex-1/Clathrin System oder Bindung an weitere Proteinrezeptoren (VAMP7, LIMP-2, Sortilin) (Pols et al. 2013; Reczek et al. 2007; Zeng et al. 2009).

Mit dem Eintritt ins Lysosom ist das optimale saure Milieu für die residenten Proteine gegeben, um an den katabolischen Prozessen teilnehmen zu können. Allerdings ist der Reifungsprozess der Enzyme auch mit dem Eintritt ins Lysosom noch nicht abgeschlossen (Abb. 2D). Reife, lysosomale Enzyme sind auf Grund eines intralysosomalen Abbaus der Phosphatreste wenig phosphoryliert (Matsuura et al. 1998). Zusätzlich benötigen einige lysosomale Enzyme wie die heparan sulfate acetyl-CoA: α-glucosaminide N-acetyltransferase, verantwortlich für Mucopolysaccharidose IIIC (Sanfilippo Syndrom), eine Umwandlung in eine aktive und gleichzeitig stabilere Form durch proteolytische Spaltung über saure Proteasen, die Cathepsine (Braulke und Bonifacino 2009).

1.2 Allgemeine Aspekte lysosomaler Speicherkrankheiten

1.2.1 Geschichte und klinische Einordnung der lysosomalen Speicherkrankheiten

Lysosomale Speicherkrankheiten (LSDs) umfassen eine Gruppe verwandter Erkrankungen, bei denen auf Grund spezifischer Gendefekte eine ungesteuerte Speicherung von Makromolekülen in Lysosomen hervorgerufen wird. Die erste klinisch durch den Ophthalmologen Warren Tay beschriebene LSD war GM_2-Gangliosidose (Tay-Sachs Syndrom) im Jahre 1881 (Walker 2007). Wenig später folgten Morbus Gaucher (M. Gaucher) (1882) und Morbus Fabry (M. Fabry) (1898). M. Fabry wurde im selben Jahr unabhängig voneinander von dem deutschen Dermatologen Johannes Fabry und dem britischen Chirurg William Anderson beschrieben. Trotz der Bekanntheit der meisten LSDs seit dem endenden 19. und beginnenden 20. Jahrhundert konnten die zugrundeliegenden physiologischen Defekte erst durch die Identifizierung und Charakterisierung des Lysosoms und die Entdeckungen der Krankheits-assoziierten lysosomalen Gene in den 1960er Jahren schrittweise aufgedeckt werden. Die zu M. Pompe führende saure α-Glucosidase (GAA) Defizienz war die erste Entdeckung eines Krankheits-assoziierten lysosomalen Gens im Jahre 1963. Das für M. Gaucher verantwortliche *GBA1* Gen wurde Mitte der 60er Jahre (Brady et al. 1966), die für M. Fabry verantwortliche Enzymdefizienz

erstmals im Jahr 1967 beschrieben (Brady et al. 1967), das zugehörige Gen der α-Galactosidase A (AGAL) einige Zeit später im Jahr 1970 (Kint 1970).

Die meisten LSDs zeichnen sich durch einen progredienten Verlauf aus, was häufig zu einer schweren Krankheitsmanifestation und frühzeitigem Tod führt. Mit wenigen Ausnahmen folgen die LSDs einem autosomal rezessiven Erbgang, molekular damit einem *loss-of-function* Prinzip. Es existieren sowohl pädiatrisch-neurologische als auch rein viszerale Verlaufsformen mit sehr heterogenen Verläufen. Auf Grund der fehlenden Spezifität des Großteils der Symptome sollten LSDs bei der Differentialdiagnose vieler systemischer Erkrankungen berücksichtigt werden. Es wird postuliert, dass eine hohe Rate nicht oder falsch diagnostizierter Fälle zu einer weltweiten Unterschätzung der Häufigkeit von LSDs führt. Einzeln betrachtet gehören die LSDs zu den seltenen Krankheiten, wobei die gemeldeten Inzidenzen von 1 zu 45 000 Lebendgeburten bei Morbus Niemann-Pick Typ C (NP-C) bis zu 1 zu 4,2 Millionen bei Mucolipidose Typ I variieren (Gieselmann 2006). Die Zahlen können auch von der ethnischen Zugehörigkeit der untersuchten Bevölkerungsgruppe abhängen. Beispielsweise ist der M. Gaucher bei Menschen mit aschkenasisch-jüdischer Abstammung mit 1:450 beziffert (Zimran et al. 1991). Auch Tay-Sachs Syndrom tritt in dieser ethnischen Gruppe etwa 100-fach häufiger auf als in anderen Ethnien. Bei NP-C wird eine erhöhte Prävalenz in der kanadischen Provinz Nova Scotia beschrieben (Vanier 2010). M. Fabry hingegen zeigt eine panethnisch homogene Verteilung (Germain 2010).

1.2.2 Molekulare Grundlagen lysosomaler Speicherkrankheiten

Die über 50 LSD-assoziierten Gene sind gemeinsam Bestandteil des CLEAR Netzwerks. Die Ausbildung der Pathologie basiert auf dem Totalausfall oder nicht ausreichender Funktionalität eines Gens mit der Folge eines zellulären Stoffwechseldefizits (Wenger et al. 2003). Man unterscheidet die LSDs anhand des akkumulierten Speichermaterials oder des defekten Gens in Sphingolipidosen, Mucopolysaccharidosen, Glykoproteinosen, Glykogenspeicherkrankheiten, Lipidosen, lysosomalen Transportdefekten und anderen Krankheiten beruhend auf Defekten lysosomaler Proteine (Vellodi 2005). Durch eine Schaden-induzierende Genmutation beispielsweise eines der katabolischen Hydrolasegene des Netzwerks kann der zelluläre Stoffwechsel derart aus dem Gleichgewicht geraten, dass eine schwerwiegende klinische Symptomatik resultiert. Im Allgemeinen werden in betroffenen Patienten und in Tier- und Zellmodellen neben der verschlechterten lysosomalen Funktion und Biogenese weitere Fehlfunktionen wie oxidativer Stress, ER Stress, gestörte Autophagie, veränderte Kalzium-Homöostase, abnormaler Transport verschiedener Zellkomponenten, Entzündungsprozesse, Autoimmunreaktionen, Energieungleichgewicht, peroxisomale Dysfunktion, mitochondriale Dysfunktion, Dysfunktion des Golgi-Apparats usw. festgestellt.

Eine der zentralen pathophysiologischen Fragen bei allen LSDs ist, wie das Speichermaterial den Stoffwechsel einer Zelle beeinflusst und in der Folge zu Organpathologie und klinischen Symptomen führt (Gieselmann 2006). Dabei haben die chemische Natur der Speicherverbindung, das Ausmaß und die Kinetik der Speicherung sowie die Art und das Spektrum der betroffenen Speicherzellen meist einen offensichtlichen Einfluss auf die Pathophysiologie. So bietet der Glykogengehalt der Muskeln eine Erklärung dafür, warum bei der Pompe-Krankheit die Myopathie die dominierende Rolle in der Pathophysiologie einnimmt (Gieselmann 2006). Beim M. Gaucher wird angenommen, dass die Pathophysiologie durch Glucozerebrosid-angereicherte Makrophagen angetrieben wird (Scharenberg et al. 2020), was die Einordnung von M. Gaucher als in erster Linie hämatologische Krankheit erklären kann.

1.2.3 Die Primärmutation als Haupteinflussfaktor auf die Pathophysiologie

Die Sequenzen der für die LSDs verantwortlichen Gene wurden aufgeklärt, die Funktionen der meisten Gene ebenso und es wurden viele Mutationen, die zu Funktionsverlust (z.B. Enzymmangel) bei den verschiedenen Erkrankungen führten, aufgedeckt. Durch die Fortschritte in der DNA Sequenzierungstechnologie der vergangenen beiden Jahrzehnte wurden für die meisten LSDs eine Vielzahl an Mutationen entdeckt, in der Regel zwischen einigen Hundert bis zu über Tausend Mutationen. Diese große Anzahl erklärt sich daraus, dass die Mutationen normalerweise auf eine einzige Familie oder eine sehr kleine Population beschränkt sind; man spricht von so genannten »privaten Mutatonen«. Auch wenn regelmäßig neue Mutationen beschrieben werden, sind die LSDs daher auf genetisch-deskriptiver Ebene gut verstanden. Punktmutationen werden solche Mutationen genannt, die auf eine einzelne Genregion und eines oder wenige Nukleotide beschränkt sind. Nonsense-Mutationen und Deletionen/Insertionen in exonischen, Protein-kodierenden, Genbereichen sowie von größeren Intra- oder Interlokus Umstrukturierungen bewirken eine vorzeitige Beendigung der Translation und/oder eine Leserasterverschiebung und damit eine veränderte Aminosäurekette (Abb. 3). Die molekulare Folge all dieser Veränderungen ist offensichtlich ein vollständiger Funktionsverlust des Genprodukts. Störungen des mRNA Splicing sind schwerer zu bewerten. Die Beeinflussung eines Splicing Consensus durch eine Mutation ist oft nicht absolut, weshalb der Krankheitsschweregrad mit dem sich einstellenden Gleichgewicht zwischen falsch und richtig gespleißter mRNA zusammenhängen mag. Die in Asien häufige *GLA* Variante c.640-801G>A (IVS4 +919G>A) mit einer Häufigkeit von 1 in 823 X-Chromosomen (Chien et al. 2012) führt zur Aktivierung eines Pseudoexons und einer erhöhten Expression eines um 57 Nukleotide verlängerten mRNA Moleküls (Palhais et al. 2016). Diese Mutation wird ausschließlich in Patienten mit atypisch-abgeschwächten, meist kardialen, M. Fabry Verläufen gefunden (Filoni et al. 2008).

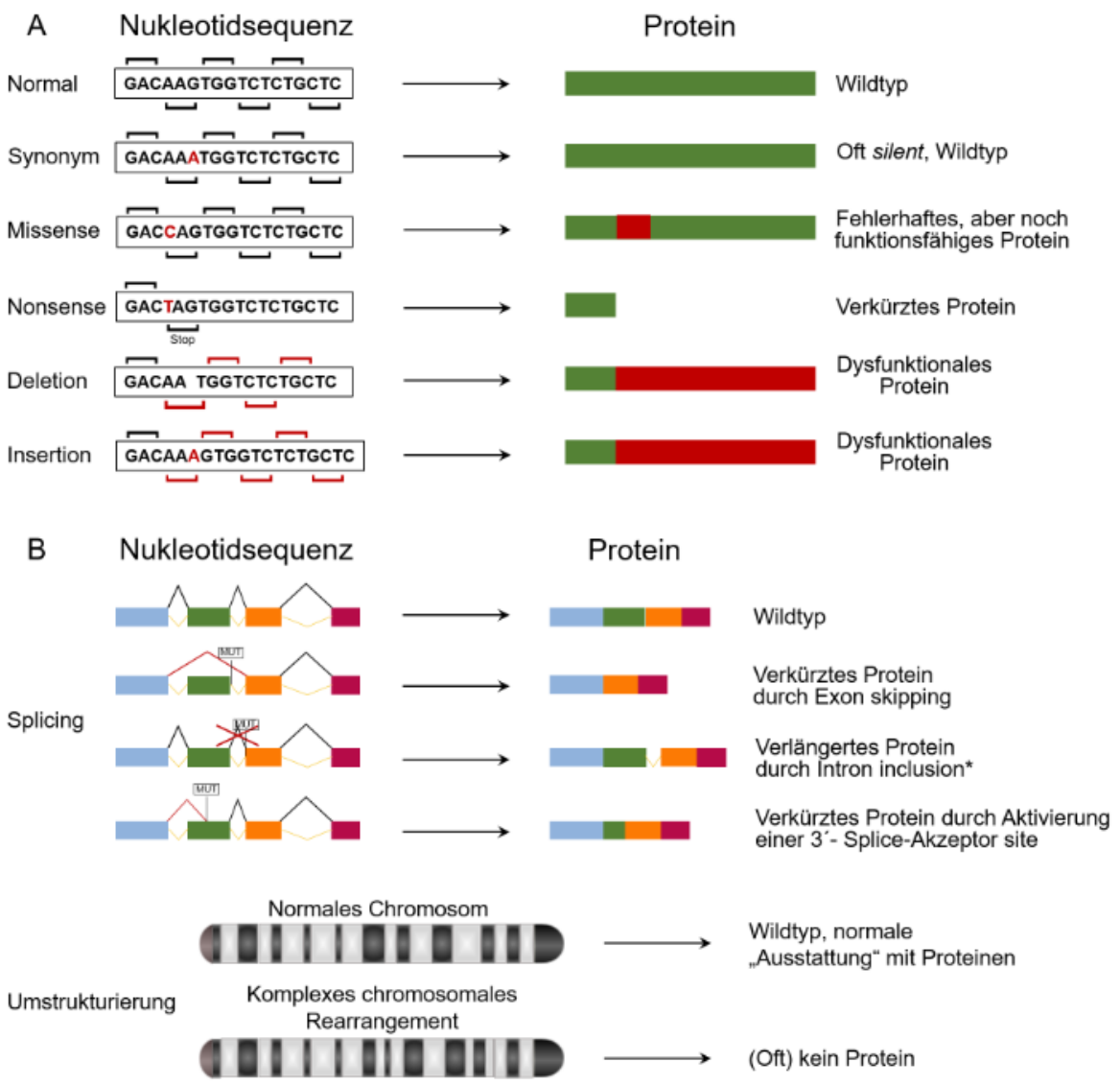

Abb. 3. Typen von Mutationen in genetischen Krankheiten. **A**. Arten und Auswirkungen exonischer Punktmutationen. Rote Buchstaben markieren die punktuelle Veränderung. Die schwarzen Klammern bezeichnen den normalen Leserahmen, rote Klammern weisen auf einen veränderten Leserahmen hin. **B**. RNA Splicing Mutationen und große chromosomale Umstrukturierung und ihre Auswirkungen. *Gezeigt sind drei Beispiele für die Konsequenzen aus Mutationen, die das RNA Splicing beeinflussen. Das gezeigte Protein ist ein theoretisches Produkt, dessen tatsächliche Synthese meist unbekannt ist und weiteren Faktoren unterliegt. **In der Human Genome Mutation Database (HGMD) werden Mutationen als »große Rearrangements« bezeichnet, wenn mehr als 20 Nukleotide betroffen sind. Komplexe chromosomale Umstrukturierungen können zu Krankheitsbildern führen, die atypisch für monogenetische Krankheiten sind. Die Abbildung wurde teilweise unter Verwendung von *Servier Medical Art* erstellt, bereitgestellt von Servier, lizenziert unter einer *Creative Commons Attribution 3.0 unported license*.

Besonders bei der prozentual bei den LSDs häufigsten Klasse der Mutationen, den Missense oder nichtsynonymen Missense Mutationen, ist die Auswirkung auf einen eventuell entstehenden Enzymmangel kaum offensichtlich. Zuverlässige Vorhersagemethoden sind für diese Mutationen daher von diagnostischem und prognostischem Interesse. Wenn Aminosäurereste betroffen sind, die an der Architektur des aktiven Zentrums direkt beteiligt sind, ist ein schädliches Resultat für das Enzym

sehr wahrscheinlich (Saito et al. 2010). Derartige Mutationen bilden allerdings nur einen verhältnismäßig kleinen Teil aller Mutationen. Beispielsweise betreffen beim M. Fabry laut Human Genome Mutation Database (HGMD) nur 8,9% aller bekannten Mutationen (HGMD professional, abgefragt im 4. Quartal 2015) das aktive Zentrum, die Aminosäurereste Trp47, Asp92, Asp93, Tyr134, Cys142, Lys168, Asp170, Glu203, Leu206, Tyr207, Arg227, Asp231, Asp266, und Met267. Weitere 5,4 % entfallen auf den Austausch von Cysteinresten, die für die Faltung wichtige Disulfidbrücken bilden. Auf Grund der Tatsache, dass sich für die Mehrzahl an Missense Mutationen bei den LSDs eine Schadensvorhersage komplex darstellt, können durch den Einsatz von Computer-gestützten Prädiktionsprogrammen wie PolyPhen-2 (Adzhubei et al. 2010), SIFT (Ng und Henikoff 2003) und Mutation Taster (Schwarz et al. 2010) biochemische Auswirkungen auf das Enzym anhand der Art der Aminosäuresubstitution, Konservierung der Aminosäure und struktureller Folgen (Proteinfaltungsverhalten) ermittelt werden. Die Computer-unterstützte Vorhersage ist jedoch mit Problemen verbunden und lässt nur begrenzt Rückschlüsse für eine klinische Interpretation zu, was das folgende Beispiel veranschaulicht. Die zwei M. Fabry auslösenden *GLA* Mutationen c.335G>A (p.Arg112His) und c.725T>A (p.Ile242Asn) waren beide sind in der Vorhersage mit dem höchsten Pathogenitäts-Score von 1.000 (Bereich 0-1) bei PolyPhen-2 assoziiert. Jedoch wurde p.Arg112His ausschließlich in Patienten mit milderen Krankheitsverläufen gefunden, während die p.Ile242Asn Variante in Patienten mit der klassisch-schweren Verlaufsform gefunden wurde. Eine im zellulären Expressionssystem durchgeführte molekularbiologische Untersuchung wies für die klinisch mildere p.Arg112His Variante sogar eine leicht geringere Enzymaktivität auf (Lukas et al. 2013). Allerdings zeigten beide Enzymvarianten eine Aktivität von unter 5% der normalen Aktivität, was die Polyphen-2 Vorhersage einer biochemisch stark beschädigten Enzymvariante mit einer um >95% reduzierten Aktivität stützte. Es ist der Redundanz des lysosomalen Systems zuzuschreiben, dass eine geringe Enzymaktivität wie die der AGAL Variante p.Arg112His zu milden M. Fabry Verlaufsformen führen kann. Dennoch wirft das Beispiel der beiden beschriebenen Mutationen die Frage auf, inwieweit der Verlauf der Fabry-Krankheit mit der Enzymaktivität der zugrundeliegenden AGAL Mutante korreliert oder ob es Aktivitätsgrenzen oder -bereiche gibt, anhand derer der klinische Verlauf prognostiziert werden kann. Dieselbe Frage stellt sich für eine eventuelle Untergrenze der Enzymaktivität oberhalb der ein asymptomatischer Verlauf erwartet werden kann. Kann daher eine holistische Untersuchung von *GLA*-Genvarianten neue Erkenntnisse zu diesem Sachverhalt beisteuern? Verschiedene Verfahren wurden - meist im Rahmen einer einzigen Studie - zur Untersuchung von Restenzymaktivität, Enzymmaturierung und intrazellulären Transport angewendet (Ishii et al. 2007; Ron und Horowitz 2005; Schmitz et al. 2005; Yang et al. 2015; Lukas et al. 2013). Eine systematische Charakterisierung der Genvarianten war zum Beginn unserer Studien jedoch noch nicht publiziert.

1.3 Therapieformen lysosomaler Speicherkrankheiten

1.3.1 Enzymersatztherapie (ERT)

Bei den drei in dieser Abhandlung thematisierten Krankheiten, M. Fabry (MIM #301500), M. Gaucher (MIM #230800, #230900, #231000) und M. Pompe (MIM #232200), handelt es sich im molekularen Sinn um Enzym-basierte Krankheiten. M. Fabry und M. Gaucher sind Glykosphingolipidosen und M. Pompe ist eine Glykogenspeicherkrankheit oder Glykogenose nach den jeweils betroffenen Stoffwechselpfaden. Es existiert mit der Enzymersatztherapie (ERT) eine gemeinsame häufigste Therapieform. Wie alle anderen Therapieformen ist die ERT kein Heilmittel für LSDs und sie erfordert lebenslange Infusionen des therapeutischen Enzyms. Eine Übersichtsdarstellung aller bekannten kausativen als auch begleitenden symptomatischen Behandlungsformen von LSDs ist in Abbildung 4 gezeigt. Kausative Therapieformen sind in ihrer Wirkung unterschiedlich effektiv und hängen von allgemeinen Parametern wie dem Krankheitsfortschritt bei Therapiebeginn als auch krankheitsspezifisch von der Art des geschädigten Gewebes und der Pharmakokinetik und –dynamik des Medikaments ab.

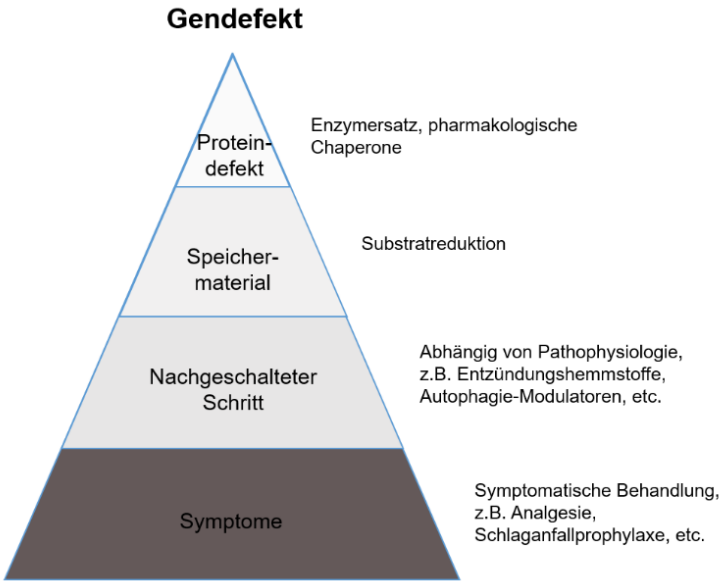

Abb. 4. Therapieformen für LSDs. Behandlungsmöglichkeiten für LSDs reichen von kausativ bis symptomatisch. Add-on Therapien durch Ansteuerung sekundär beeinträchtigter biologischer Prozesse sind ebenfalls verbreitet.

Bei M. Fabry sind weltweit zwei rekombinante Enzymformulierungen für die ERT zugelassen. Agalsidase beta (Fabrazyme™; Genzyme Corporation, Cambridge, MA, USA) wurde in den Jahren 2001 und 2003 durch die Europäische Arzneimittelagentur (EMA von engl. European Medicines Agency) bzw. die Food and Drug Administration (FDA) in Europa und den USA zugelassen. Fabrazyme wird in gentechnisch veränderten CHO-Zellen (von engl. *Chinese hamster ovary*) hergestellt, die die *GLA*-Gen-DNA erhalten haben, die sie zur Produktion des Enzyms befähigt (Lee et al. 2003). Im Gegensatz dazu wird Agalsidase alfa (Replagal™; Takeda Pharmaceutical Company Limited, Tokio, Japan; ehemals Shire Human Genetic Therapies AB, Danderyd, Schweden) nicht rekombinant hergestellt, sondern aus

kultivierten menschlichen Fibroblasten gewonnen, deren *GLA* Expression durch Aktivierung angeworfen wird (Sakuraba et al. 2006). Replagal ist für die Verwendung in einer Dosis von 0,2 mg/kg und Fabrazyme für die Verwendung in einer Dosis von 1,0 mg/kg alle zwei Wochen zugelassen. Wirksamkeit und Sicherheit beider ERTs wurden in verschiedenen Studien verglichen, und es wurden keine signifikanten Vorteile einer der beiden Formulierungen festgestellt (Vedder et al. 2007; Pisani et al. 2013). Ein weiteres Produkt erwartet in Pegunigalsidase alfa, das in BY2-Tabakzellkultur exprimiert wird, auf die Zulassung durch die EMA. Die ERT für den M. Pompe erfolgt mit alglucosidase alfa (Lumizyme®, Sanofi Genzyme, Cambridge, MA, USA) und ist seit 2006 die zunächst einzige zugelassene Behandlung des M. Pompe. Die GAA-Dosen sind deutlich höher als die Dosen, die für eine ERT bei anderen lysosomalen Speicherkrankheiten erforderlich sind, da die Schwelle für die Korrektur des GAA-Mangels in den Skelettmuskeln von M. Pompe Patienten sehr hoch ist (Sun et al. 2015). Seit 2021 ist das zweite-Generation ERT Präparat avalglucosidase alfa (Nexviazyme™, ebenfalls Sanofi Genzyme) erhältlich, welches einen erhöhten Grad terminaler Phosphoglykogenierung zur spezifischen Versorgung des Skelettmuskels durch das Enzym aufweist, um eine verbesserte Aufnahme durch Mannose-6-Phosphat-Rezeptoren zu ermöglichen (Pena et al. 2019). Gleich drei unterschiedliche ERT Präparate stehen zur Behandlung von M. Gaucher zur Verfügung (Imiglucerase, Genzyme Corporation, Cambridge, MA, USA; Velaglucerase alfa, Takeda Pharmaceutical Company Limited; Taliglucerase alfa, Protalix, Carmiel, Israel). Im Jahr 2009 musste Genzyme eine virale Kontamination seiner Bioreaktoren bekannt geben, die zu einer weltweiten Verknappung von Imiglucerase führte und eine sofortige Zulassung der rekombinanten Enzyme Taliglucerase alfa und Velaglucerase alfa zur Deckung des Patientenbedarfs zur Folge hatte (Hofstetter et al. 2015). Die ERT bei M. Gaucher wird in der Regel gut vertragen, überwindet die katabolische Blockade, indem sie ausreichend exogenes Enzym bereitstellt, das gespeicherte Substrat abbaut und die Beteiligung peripherer Organe sowie Leber- und Milzschäden rückgängig macht (Gregory M Pastores und Derralynn A Hughes 2018). Leider ist die ERT nicht zur Behandlung von akut neuronopathischem M. Gaucher Typ II (MIM #230900) und nur bedingt zur Behandlung von subakutem neuronopathischem M. Gaucher Typ III (MIM #231000) geeignet, da es zwar fast alle systemischen Manifestationen bei diesen Patienten aufhebt, aber die Blut-Hirn-Schranke nicht überqueren kann (Altarescu et al. 2001; Zimran und Elstein 2014). Den zahlreichen Belegen für die Wirksamkeit und Sicherheit und der langen klinischen Erfahrung mit der ERT stehen die begrenzte Gewebepenetration (z.B. keine Überwindung der Blut-Hirn-Schranke), die unvollständige Rückbildung der Pathologie, unerwünschte Reaktionen bei der Infusion, weitere die Wirksamkeit verringernde Effekte wie die Bildung neutralisierender Antikörper und die hohen jährlichen Therapiekosten gegenüber (Azevedo et al. 2020). Die lebenslange, intravenöse Verabreichung des Enzyms wird von den Patienten überdies als unangenehme Bürde empfunden, weshalb oral verfügbare Therapieformen angestrebt werden.

1.3.2 Substratreduktionstherapie (SRT)

Ebenfalls eine lebenslange Behandlung erfordert der unter dem Namen Substratreduktionstherapie (SRT von engl. *substrate reduction therapy*) bekannte Therapieansatz. Die Grundidee hinter der SRT besteht darin, die Bildung von Metaboliten zu begrenzen, die auf Grund des zugrunde liegenden enzymatischen Defekts nicht abgebaut werden können (van der Veen et al. 2020). Bei Patienten mit ausreichender Restenzymaktivität kann eine SRT die Produktion des Substrats auf ein Niveau reduzieren, das mit der verbleibenden Enzymaktivität vereinbar ist. Bei Patienten mit minimaler oder ohne Restenzymaktivität reicht die SRT als alleinige Therapie möglicherweise nicht aus, könnte aber als Ergänzung zur ERT dennoch von Nutzen sein. Im Gegensatz zur ERT basiert die SRT auf einem niedermolekularen Prinzip. Es handelt sich um eine Klasse von Stoffen mit einer Molekülmasse von unter 800 g/mol, die in der Regel oral verabreicht werden kann und eine im Vergleich zur ERT erhöhte Bioverfügbarkeit zum Beispiel durch die Überwindung der Blut-Hirn-Schranke ermöglicht. Allerdings bestätigte sich die Hoffnung auf Behandelbarkeit von neuronopathischem M. Gaucher mittels des Iminozuckers N-Butyldeoxynojirimycin (NB-DNJ, Miglustat, Zavesca®, Actelion Pharmaceutical Ltd, Schweiz) nicht, weshalb es aktuell nicht zur Behandlung von neuronopathischem M. Gaucher zugelassen ist. Das seit 2002 (Europa) bzw. 2003 (USA) zugelassene Miglustat hemmt den ersten Schritt der Glykosphingolipid-Synthese durch Hemmung der Glucosylceramid-Synthase (GCS). Auf Grund schwerer Nebenwirkungen stellt es nur dann eine Therapiealternative dar, wenn Patienten Anzeichen einer Unverträglichkeit gegenüber einer ERT zeigen (Substrathemmung durch Miglustat 2022). Eliglustat (Cerdelga™, Sanofi Genzyme) ist hingegen ein Ceramid-ähnliches GCS-hemmendes Pharmacophor, welches im Jahr 2014 seine erste Zulassung für die M. Gaucher-Therapie in den USA erhielt (Poole 2014). Auch bei der Anwendung von Eliglustat gibt es allerdings Einschränkungen wie bestimmte Stoffwechselstörungen und Leberschäden (Committee for Medicinal Products for Human Use 2015) und auch dieses Medikament ist nicht für die Verwendung bei neuronopathischen Formen von M. Gaucher indiziert. Außerdem sind die Auswirkungen einer dauerhaften Abschaltung des Glykosphingolipid-Synthesewegs auf die Homöostase und Zellgesundheit kaum untersucht. Der Stoffwechselweg ist von derart basaler Bedeutung, dass er auch in der M. Fabry Forschung ins Zentrum der Aufmerksamkeit geraten ist (Abe et al. 2001). Allerdings führten schwere Nebenwirkungen (unerwünschte neurologische Ereignisse, Gewichtsverlust und Atrophie lymphoider Organe) letztlich zu einer zu großen Skepsis gegenüber Miglustat als Therapieoption für M. Fabry, so dass weitere klinische Studien eingestellt wurden. Neue Kandidatenverbindungen wie das Ceramid-ähnliche Venglustat und das Galactose-Derivat Lucerastat wurden seitdem identifiziert (van der Veen et al. 2020) und befinden sich aktuell in klinischen PhaseI/II Studien (z.B. NCT05206773, NCT03425539). Es ist nur ein einziger Ansatz bekannt, um eine Substratreduktion bei M. Pompe durchzuführen. Dieser basiert auf der Reduktion der Muskelglykogensynthase 1 (Gys1) mit Hilfe von Nukleinsäuresonden,

was zu einem genetischen Knockdown und damit zu einer verminderten Bildung von lysosomalem Glykogen führen soll (Douillard-Guilloux et al. 2008; Clayton et al. 2014).

1.3.3 Pharmakologische Chaperon Therapie (PCT)

Sowohl die ERT als auch die SRT sind prinzipiell in ihrer Wirkweise unabhängig vom Genotyp, da sie nicht das veränderte Enzym selbst zum therapeutischen Ziel haben. Anders verhält es sich mit den so genannten pharmakologischen Chaperonen (PCs), welche als ebenfalls niedermolekulare Alternative spezifisch die Funktion des körpereigenen mutierten Enzyms (zumindest teilweise) wiederherstellen. Mit dem Iminozucker-Analogon des terminalen Galactoserestes des neutralen Glykosphingolipid-Substrates, Migalastat (Galafold™, Amicus, NJ), das experimentell unter dem Namen 1-Deoxygalactonojirimycin (DGJ) im Jahr 1999 entdeckt wurde (Fan et al. 1999), erhielt im Jahr 2016 das erste PC für eine LSD die internationale Zulassung (Markham 2016). Das Wirkprinzip dieses Wirkstoffs ist die Stabilisierung jener ansprechbaren Formen des Zielproteins über direkte Bindung, im Fall von DGJ an das aktive Zentrum mutierter AGAL-Formen des M. Fabry, so dass deren Zurückhaltung und Abbau im ER verhindert und der Transport zu den Lysosomen ermöglicht wird (Abb. 5). DGJ wurde als PC der ersten Generation bezeichnet (Liguori et al. 2020), da seine Entdeckung als Stabilisator der AGAL aus der begründeten Vermutung entstand, dass DGJ als ein Glykomimetikum mit einem Sechsatomring dem natürlichen Substrat Galactose so ähnelt, dass es in das aktive Zentrum des Enzyms eintreten kann (Citro et al. 2016). Es ist wichtig, sich bewusst zu machen, dass die meisten bisher getesteten PCs Inhibitoren ihrer Zielenzyme sind. Ein PC ist nur für Patienten mit ansprechbaren *GLA*-Mutationen eine therapeutische Option, so dass die Eignung jedes Patienten von der Genetik abhängt und aktuell nur ein in vitro-Test zur Verfügung steht, um die in vivo-Responsivität zu bestimmen oder vorherzusagen (Benjamin et al. 2017). Frühere Studien schätzen das Potential der auf DGJ ansprechbaren Mutationen auf 35-50% (Hughes et al. 2017) bis zu 60% (Wu et al. 2011) aller *GLA*-Mutationen. Trotz der Seltenheit der Krankheit weist M. Fabry eine stetig wachsende Zahl von Mutationen auf. Durch die Häufigkeit privater Mutationen hat die Gesamtzahl der bekannten Mutationen mittlerweile die 2000er-Marke überschritten (View GALAFOLD® Amenability Table 2022).

Für die Anwendung von PCT bei M. Gaucher ist der *GBA1* Genotyp ebenso entscheidend wie der *GLA* Genotyp bei M. Fabry. Obwohl PCT in den vergangenen Jahren bemerkenswerte Fortschritte gemacht hat, wies von den initial für M. Fabry, M. Gaucher (Isofagomin, Plicera™, IFG, AT2101) und M. Pompe (1-Deoxynojirimycin, duvoglustat, DNJ, AT2220) in klinischen Studien getesteten PCs (Parenti et al. 2015) nur das M. Fabry PC DGJ eine ausreichende Wirksamkeit und Sicherheit für eine internationale Zulassung nach. Auf Grund der häufigen Allele wird in vitro Expressionsuntersuchungen zur Ansprechbarkeit von *GBA1* Mutationen auf eine Behandlung mit kleinen Molekülen offenbar weniger Relevanz beigemessen als beim M. Fabry, denn es existiert keine systematisch durchgeführte

Studie. Aus Expressionsstudien zu den häufigen Allelen p.Asn370Ser und der mit neuronopathischem M. Gaucher Typ-assoziierten p.Leu444Pro ist abzuleiten, dass eine große Anzahl an Patienten auf molekulare Therapien wie PCs, Proteasomhemmstoffe, Proteostaseregulatoren und andere Mutations-abhängig wirkende Stoffe (Chen et al. 2018) geeignet sein könnten. Zudem stehen mit dem bei Atemwegserkrankungen eingesetzten Sekretolytikum Ambroxol (ABX) (Maegawa et al. 2009), Isofagomin Nachfolge-Verbindungen (z.B. AT3375) (Sun et al. 2012) und auch PCs anderer Substanzklassen (Scherer et al. 2021) neue Kandidatenverbindungen zur Verfügung, so dass zukünftig mit derartigen Studien, die die Ansprechbarkeit weiterer *GBA1* Missense Mutationen thematisieren und somit die Pharmakogenetik in den Mittelpunkt stellen, zu rechnen sein wird.

Wie erwähnt gab es bereits Bestrebungen auch beim M. Pompe eine PCT zu realisieren. Die erste Erwähnung effektiver PC-Kandidaten in M. Pompe Zellen geht auf zwei fast zeitgleich erschienene Arbeiten der beiden Pioniere der PC-Forschung, Giancarlo Parenti und Arnold Reuser, aus dem Jahr 2007 zurück (Parenti et al. 2007; Okumiya et al. 2007). Auch hier handelte es sich wieder um Substratanaloga, die beiden bereits weiter oben erwähnten Iminozucker DNJ und NB-DNJ, die über spezifische Bindung an das aktive Zentrum des Enzyms die Aktivität der mutierten GAA in der Zellkultur erhöhten. Es folgten weitere Studien, in denen das Wirkungsspektrum der PCs auf eine breitere Basis von *GAA*-Mutationen und die Eignung als Kombinationsbehandlung mit rekombinanter GAA zur ERT-Verstärkung untersucht wurden (Flanagan et al. 2009; Porto et al. 2009; Khanna et al. 2012). Mit N-

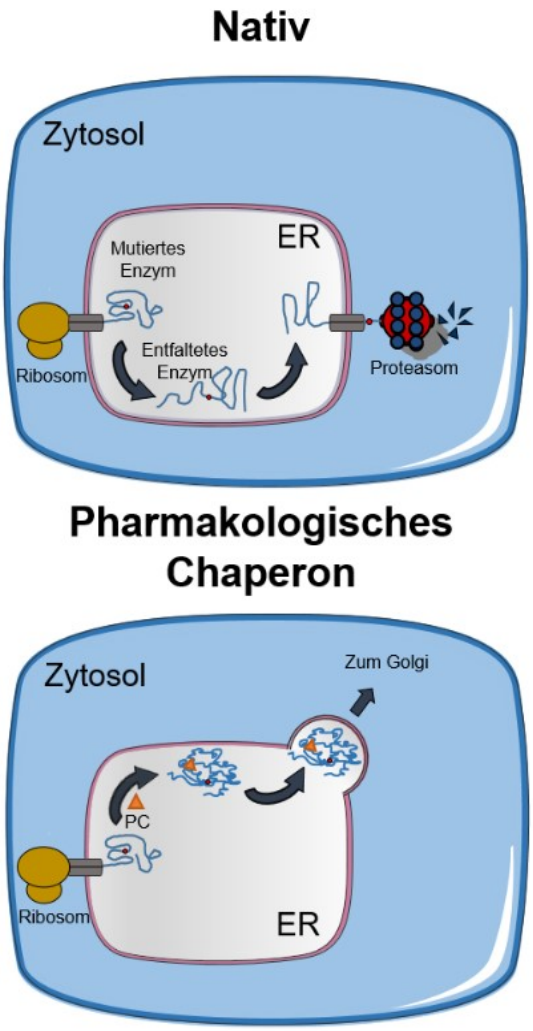

Abb. 5. Wirkweise eines Pharmakologischen Chaperons (PCs). Abhängig von der Art der Mutation unterliegt das mutierte Proteine vielfach einer Fehlfaltung im ER. Nicht zur Faltung fähiges Protein wird über Membrankanalproteine ins Zytosol geschleust, wo sie proteasomal abgebaut werden (oben). PCs binden co-translational an das sich faltende Protein und führen zu einer Korrektur der Faltung, wodurch der Weitertransport des Proteins über abgeschnürte Vesikel über den Golgi-Apparat und in die Lysosomen gelingt (unten). Die Abbildung wurde teilweise unter Verwendung von *Servier Medical Art* erstellt, bereitgestellt von Servier, lizenziert unter einer *Creative Commons Attribution 3.0 unported license*.

Acetylcystein, welches überschüssigen Schleim in den Atemwegen reduziert und zur Behandlung von chronischen Atemwegserkrankungen, als Gegenmittel bei Überdosierung von Paracetamol und bei anderen Erkrankungen im Zusammenhang mit Cystein/GSH-Mangel eingesetzt wird, befindet sich ein Kandidat für ein allosterisches PC in der Testung (Porto et al. 2012). Allosterische PCs könnten eine verbesserte Anwendersicherheit und ein verbreitertes Wirkspektrum als ein isosterisches PC zur Folge haben.

Es existieren mit der hämatopoetischen Stammzelltransplantation, Gen- und Zelltherapieansätzen weitere Therapiemöglichkeiten, welche in manchen Fällen bereits erfolgreiche Anwendung gefunden haben. Da diese aber für die vorgestellten Studien nicht relevant waren, sollen sie an dieser Stelle der Vollständigkeit halber lediglich Erwähnung finden. Auf Grund der vorhandenen Therapien gilt allgemein, dass eine frühzeitige Diagnose die Prognose für die Patienten verbessert. Derzeit hat sich jedoch keine der technischen Plattformen, die bereits für den klinischen Einsatz zugelassen sind, für eine generelle Anwendung bei den LSDs geeignet erwiesen. Im Gegenteil, die Wirksamkeit aller zugelassenen Medikamente ist in der klinischen Praxis bei einer beträchtlichen Anzahl von Patienten erheblich eingeschränkt. Das breite klinische Spektrum und die unterschiedlichen Krankheitsverläufe weisen auf unterschiedliche Patientenbedürfnisse und somit unterschiedliche Anforderungen an die Medikamente hin und machen die Entwicklung neuer, individualisierter Therapieformen einen lohnenswerten Ansatz.

1.4 Die lysosomalen Speicherkrankheiten M. Fabrym M. Gaucher und M. Pompe

Im folgenden Abschnitt werden M. Fabry, M. Gaucher und M. Pompe in Form kurzer Steckbriefe vorgestellt und auf wesentliche unerfüllte Anforderungen zum Zeitpunkt des Beginns der durchgeführten Studien fokussiert.

1.4.1 Steckbrief: M. Fabry

M. Fabry (MIM #301500) ist eine X-chromosomale Erkrankung mit einer Prävalenz von etwa 1:40.000. Für die Krankheit ist eine Mutation im langen Arm des X-Chromosoms (Xq22.1) verantwortlich (Kornreich et al. 1989). Das hier lokalisierte *GLA*-Gen kodiert für ein Glykosidhydrolase-Familie 27 Enzym, α-Galactosidase A (AGAL, EC-Nummer 3.2.1.22). Das Gen umspannt bei 7 Exons einen genomischen Bereich von 12 kb (Kornreich et al. 1990). Mutationen gehen einher mit der Unfähigkeit, neutrale Glykosphingolipide, hauptsächlich Globotriaosylceramid (Gb3), abzubauen. Ablagerungen von nicht abgebautem Gb3 treten in praktisch allen Zellen auf, insbesondere in vaskulärem Endothel und glatten Muskelzellen, glomerulären und tubulären Epithelzellen der Nieren,

Myokardzellen und Neuronen der Spinalganglien und des autonomen Nervensystems, was zu einer multisystemischen Beteiligung führt. M. Fabry ist gekennzeichnet durch Rheuma-ähnliche Schmerzen mit akuten und episodischen Schmerzkrisen, gastrointestinalen Beschwerden, Verdickung der Interventrikelscheidewand, Bluthochdruck, Proteinurie, Hitze- oder Kälteunverträglichkeit, Augenanomalien und *angiokeratomas corporis diffusum* (Hauser et al. 2004). Hauptursachen für den vorzeitigen Tod bei M. Fabry umfassen Nierenerkrankung im Endstadium, Herzrhythmusstörungen und Schlaganfall. Während die klassisch-schwerwiegende Form in der Regel in der Kindheit auftritt, manifestiert sich die atypisch-milde Form von M. Fabry im Allgemeinen in der dritten oder vierten Lebensdekade. Unbehandelt führt der klassisch-schwerwiegende Verlauf bei männlichen Patienten mit M. Fabry im Durchschnitt zu einer um etwa zwanzig Jahre reduzierten Lebenserwartung (Miller et al. 2020). Eine hohe Inzidenz veränderter *GLA* Allele von 1:3.100 (Spada et al. 2006) in Italien, 1:1.250 (Hwu et al. 2009) in Taiwan und 1:13.341 (Wittmann et al. 2012) in Ungarn suggeriert eine größere Häufigkeit der Krankheit als in älteren Studien. Dies kann auf eine Unterdiagnose von M. Fabry hinweisen, die auf milde und daher übersehene Symptome im Verlauf der Krankheit zurückzuführen ist. Es fügt sich ins Schema, dass lange Zeit angenommen wurde, dass heterozygote weibliche *GLA* Mutations-Trägerinnen nicht an M. Fabry leiden können (MacDermot et al. 2001). Auf Grund der zufälligen Inaktivierung des gesunden elterlichen X-Chromosoms kann M. Fabry jedoch auch heterozygote Frauen betreffen, die sogar ähnlich schwere oder, typischer, mildere Symptome aufweisen als männliche Patienten mit der gleichen Mutation (Hauser et al. 2004).

Mutationen, die zu einem kompletten Verlust der Enzymaktivität führen, werden bei Patienten mit klassisch-schwerwiegendem Verlauf diagnostiziert, bei atypisch-milden Verläufen werden mutierte Enzyme mit Restaktivität entdeckt. Diese Mutationen haben hauptsächlich einen ER-Abbau-Phänotyp und sind ansonsten unverändert kinetisch aktiv (Ishii et al. 2007). Eine weitreichende Ergänzung dieses Klassifizierungssystems konnte in molekularen Studien zur Auswirkung der Mutationen verfeinert werden (Lukas et al. 2013). Es zeigte sich überdies wie konsistent in vitro Enzymmessungen im Überexpressionssystem mit dem kürzlich entwickelten klinischen Biomarker Globotriaosylsphingosin (Lyso-Gb3) übereinstimmen, was Lyso-Gb3 nicht nur als diagnostischen, sondern auch als prognostischen und therapiebegleitenden Follow-Up Biomarker interessant macht. Es zeigten sich überdies gute Hinweise auf eine Genotyp-Phänotyp-Korrelation. Mutationen mit mehr als 20% Restaktivität waren mit milden Krankheitsverläufen assoziiert und führten in der Regel nicht zu einer Biomarker-Erhöhung. Es blieb die Frage offen, ob Lyso-Gb3 nicht empfindlich genug war oder ob es sich um gutartige Genvarianten gehandelt haben könnte. In anderen Worten, ob neben den schwerwiegenden und milden Mutationen im *GLA*-Gen auch eine beträchtliche Anzahl insignifikanter Polymorphismen vorliegen, eine Betrachtungsweise, die bisher nicht viel Aufmerksamkeit erhalten hatte.

1.4.2 Steckbrief: M. Gaucher

M. Gaucher (MIM #230800, #230900, #231000) ist eine autosomal rezessive Erkrankung, welche durch homozygote oder gemischt heterozygote Mutationen im für die Glucocerebrosidase (β-Glu, EC-Nummer 3.2.1.45) kodierenden *GBA1* Gen verursacht wird. *GBA1* Mutationen führen zu einer extensiven Anhäufung von GlcCer, speziell in Zellen des angeborenen und adaptiven Immunsystems, was zu chronischen Entzündungen führt (Pandey et al. 2017). M. Gaucher wird phänotypisch in drei Hauptuntertypen eingeteilt: Nicht-neuronopathischer Typ I, akuter neuronopathischer Typ II und subakuter neuronopathischer Typ III. Typischerweise tritt M. Gaucher (Typ I) in Erscheinung mit Hepatosplenomegalie, Panzytopenie (insbesondere Thrombozytopenie), Anämie, Epistaxis, Skelettanomalien, Knochenschmerzen und Manifestationen einer Organinfiltration durch charakteristische »Gaucher-Zellen«, große, vakuolisierte Makrophagen, die aus dem retikuloendothelialen System stammen (Goldblatt 1988; Park et al. 2001). Die Typen II und III haben eine Beteiligung des zentralen Nervensystems und neurologische Manifestationen. Typ I ist die häufigste Form von M. Gaucher, speziell in der aschkenasisch-jüdischen Bevölkerung ist Typ I die am häufigsten anzutreffende Form (Jmoudiak und Futerman 2005), was auf Homozygotie oder gemischt-Heterozygotie mit der Mutation c.1226A>G (p.Asn370Ser) zurückzuführen ist. Das Auftreten dieser Mutation ist ausschließlich mit dem klinischen Typ I verbunden (Koprivica et al. 2000) und macht etwa 75% aller M. Gaucher Allele in der aschkenasisch-jüdischen Bevölkerung aus, während der Anteil dieses Allels in nicht-jüdischen Patienten mit einem Drittel der Allele deutlich seltener ist (Zimran et al. 1991). Das breite klinische Spektrum reicht von betroffenen Säuglingen bis zu asymptomatischen Erwachsenen. Insgesamt liegt die jährliche Inzidenz von M. Gaucher in der Allgemeinbevölkerung bei etwa 1:60.000 bis 1:100.000, kann aber bei den Aschkenasiern bis zu 1 in 450 Geburten betragen (Zimran et al. 1991). Anders als beim Typ I gibt es keine ethnische Prävalenz bei M. Gaucher Typ II und Typ III. Bisher wurden etwa 600 Mutationen im *GBA1* Gen identifiziert, von denen die meisten Missense Mutationen sind. Wie oben angedeutet sind anders als bei M. Fabry wenige Allele für eine Vielzahl der klinischen Fälle verantwortlich. Die vier häufigsten mutierten Allele p.Asn370Ser, c.84-85insG, IVS2+1G>A und p.Leu444Pro machen sogar 93 % aller Allele in der aschkenasisch-jüdischen Bevölkerung aus (Koprivica et al. 2000). Das p.Leu444Pro Allel steht bei Fehlen einer leichten Mutation wie p.Asn370Ser mit neuronopathischen Formen der Erkrankung in Verbindung. Eine andere, ebenfalls häufig auftretende Mutation, c.1342G>C (p.Asp409His), wurde mit einem spezifischen Typ III-Phänotyp in Verbindung gebracht, der eine schwere kardiale Beteiligung und okulomotorische Apraxie aufweist (Montfort et al. 2004). Ähnlich wie bei M. Fabry sind Mutationen mit höherer Aktivität mit milderen Krankheitsverläufen verbunden, aber im Allgemeinen sind die Mutationen zu selten, um eine exakte Genotyp-Phänotyp-Korrelation herzustellen, und das Vorhandensein von gemischt-heterozygoten Patienten erschwert die Situation zusätzlich.

Das *GBA1* Gen befindet sich auf dem Chromosom 1q21 und besteht aus 11 Exons und 10 Introns, die eine Sequenz von 7,6 kb umfassen (Zampieri et al. 2017). Eine Besonderheit des *GBA1* Gens ist das Vorhandensein eines hochgradig homologen Pseudogens, das sich etwa 16 kb downstream des funktionellen *GBA1* Gens befindet und dessen exonische Region 96% Sequenzhomologie aufweist. Diese Konstellation ist der Grund für Gen/Pseudogen Rearrangements, welche das Spektrum der *GBA1* Genmutationen zu den Punktmutations-Ereignissen wie Missense/Nonsense, Splicingveränderungen, Basendeletionen/-insertionen ergänzen (Balwani et al. 2011). Hinzu kommt, dass die molekulargenetische Diagnose von M. Gaucher durch das Pseudogen erschwert wird. Dennoch ist die Sequenzierung des *GBA1*-Gens Teil der Standarddiagnostik der Gaucher-Krankheit. Des Weiteren beruht die M. Gaucher Diagnostik auf dem Nachweis eines Mangels an β-Glu basierend auf der Messung einer verminderten Enzymaktivität in peripheren Blutleukozyten und der massiv erhöhten Plasmaspiegel von Biomarker-Material wie Glucosylsphingosin (Gregory M Pastores und Derralynn A Hughes 2018).

1.4.3 Steckbrief: M. Pompe

M. Pompe (MIM #232200) folgt wie M. Gaucher einem autosomal rezessiven Erbschema. Die Krankheit wird durch homozygote oder gemischt heterozygote Mutationen im Gen der sauren α-Glucosidase (GAA, EC 3.2.1.20), auch als saure Maltase bekannt, auf Chromosom 17q25, ausgelöst. GAA wird als 110 kDa-Glykoprotein synthetisiert, das über den Mannose-6-Phosphat-Rezeptor zum Lysosom transportiert wird und im späten endosomalen/lysosomalen Kompartiment nach einer Reihe von proteolytischen und N-Glykan-prozessierenden Schritten die reife, aktive Form annimmt (Roig-Zamboni et al. 2017).

M. Pompe Patienten weisen eine Gewebe-Glykogen Akkumulation in der Skelettmuskulatur, den viszeralen Organen und dem zentralen Nervensystem auf, was zu einer Pathologie der Skelettmuskulatur und bei schweren Formen schließlich zu Ateminsuffizienz und Tod führt (Fuller et al. 2013). Die klinische Einteilung erfolgt ähnlich wie bei M. Fabry in eine klassisch-schwere Form, IOPD (von engl. *infantile-onset Pompe disease*) und eine später einsetzende, meist milder verlaufende Form, LOPD (von engl. *late-onset Pompe disease*). Bei der klassischen Form M. Pompe herrschen Muskelschwäche und Herzbeteiligung vor. Die betroffenen Kinder sind niedergeschlagen, stark hypoton, das Herz sowie die Zunge sind in der Regel stark vergrößert. Schlafstörungen/Apnoe, Wachstumsstörungen, Skelettmuskel-Beteiligung, Magenreflux, chronische Mittelohrentzündung und Hörverlust treten bei der schweren IOPD Form häufiger auf als bei LOPD (Kishnani et al. 2019). M. Pompe wird mit einer Häufigkeit von 1:40.000 angegeben, wobei LOPD die häufigere Form ist (Ausems et al. 1999). Der Verlust der Enzymaktivität ist bei den frühen Formen der Krankheit ausgeprägter als bei den späten Formen (Reuser et al. 1987), aber eine eindeutige Genotyp-Phänotyp-Korrelation ist in

einzelnen Studien meist nicht herstellbar (Laforêt et al. 2000). Dennoch gibt es eine Reihe von häufigen Genotypen, bei denen eine Genotyp-Phänotyp-Korrelation etabliert ist. Eines oder zwei der drei Allele IVS1-13T-G, 525delT und EX18DEL werden in 63% der niederländischen M. Pompe Patienten gefunden (Kroos et al. 1995). Nonsense-Deletionen wie 525delT (p.Glu176fs*45) sind am häufigsten mit IOPD und das intronische IVS1-13T-G-Allel ist mit LOPD verbunden. Obwohl die häufigsten Allele bei M. Pompe keine Missense Mutationen sind, ist die Mehrheit (~ 60%) der insgesamt etwa 700 Mutationen der Missense Kategorie zuzuordnen. Im Zellkulturmaßstab exprimierte GAA wird auch beim M. Pompe für in vitro Enzymmessungen als diagnostisches Hilfsmittel eingesetzt, um den katalytischen Defekt und den Schweregrad der Mutation zu bestätigen (Kroos et al. 1998; Kroos et al. 2012; Ngiwsara et al. 2019).

2 Zielstellung der experimentellen Studien

Eine Verbesserung der Situation für die Patienten in Bezug auf Diagnostik und Prognostik erfordert ein umfangreiches molekulares Verständnis der Pathophysiologie sowie der Mechanismen potentieller Kandidaten-Verbindungen für eine molekulare Therapie. Die vorliegende kumulative Schrift verwendet pharmakodynamische in vitro Modellstudien, die sich, unter besonderer Berücksichtigung der Pharmakogenetik, quantitativ-statistischer und mechanistischer molekularbiologischer Methodik der Arzneimittelentwicklung und -bewertung widmen. Dabei wird das Potential niedermolekularer Therapien untersucht, insbesondere der pharmakologischen Chaperone, welche spezifisch die Funktion eines mutierten Enzyms wiederherstellen, dessen inhärenter Defekt die Destabilisierung der Faltstruktur ist.

Die vorliegende kumulative Arbeit gliedert sich in die folgenden übergeordneten Zielstellungen und experimentellen Einzelstudien:

Ziel 1: Quantitative Untersuchungen zur molekularen Klassifizierung von *GLA* Mutationen bei M. Fabry

Studie 1: Molekulare Charakterisierung und Phänotypisierung neuer *GLA* Mutationen bei M. Fabry mit Schwerpunkt auf Genvarianten von unklarer Bedeutung. Hum Mutat. 2016 Jan;37(1):43-51. doi: 10.1002/humu.22910.

Studie 2: Meta-Analyse aller Studien, die sich mit der Messung der Enzymaktivität und DGJ-Ansprechbarkeitsuntersuchungen im zellulären In-vitro-Maßstab befassen, um die Gültigkeit der vorgenommenen Klassifizierungen in Abhängigkeit vom verwendeten zellulären System

und die Diskrepanzen zwischen den Laboren zu bewerten. Int J Mol Sci. 2016 Dec 1;17(12):2010. DOI: 10.3390/ijms17122010.

Studie 3: Ein hochgradig standardisiertes Protokoll für die in vitro-Messung der lysosomalen Enzymaktivität als Plattform für die Erprobung der Reaktionsfähigkeit auf pharmakologische Chaperone. .J Vis Exp. 2017 Dec 20;(130). doi: 10.3791/56550.

Studie 4: Untersuchung zur Verifizierbarkeit der klinisch validierten Methode zur Identifizierung von Fabry Patienten zur Eignung für die PCT. Int J Mol Sci. 2020 Jan 31;21(3):956. doi: 10.3390/ijms21030956.

Ziel 2: Mechanistische Untersuchungen und Entwicklung neuer niedermolekularer Wirkstoffe bei M. Fabry, M. Gaucher und M. Pompe

Studie 5: Korrektur des Phänotyps der Fehlfaltung und Proteinaggregation von α-Galactosidase A im Fliegenmodell *Drosophila melanogaster* durch das pharmakologische Chaperon 1-Desoxygalactonojirimycin. Int J Mol Sci. 2020 Oct 7;21(19):7397. doi: 10.3390/ijms21197397.

Studie 6: Ambroxol hat in cellulo eine signifikant-positive Wirkung auf die häufige M. Gaucher Variante p.Asn370Ser von β-Glu, hat aber in vitro, verglichen mit dem für das aktive Zentrum spezifischen ersten Generation PC Isofagomin, eine geringe Fähigkeit, als PC zu wirken. Int J Mol Sci. 2022 Mar 24;23(7):3536. doi: 10.3390/ijms23073536.

Studie 7: 2,6-Dithiopurin ist ein allosterisch bindendes pharmakologisches Chaperon der zweiten Generation, stabilisiert lysosomale AGAL in vitro und rettet eine Mutation, die nicht auf eine Behandlung mit dem zugelassenen pharmakologischen Chaperonen anspricht. PLoS One. 2016 Oct 27;11(10):e0165463. doi: 10.1371/journal.pone.0165463. eCollection 2016.

Studie 8: Das Expektorans Ambroxol und der Peroxisom-Proliferator-aktivierter Rezeptor (PPAR)-γ-Agonist Rosiglitazon eignen sich als Enzym-*Enhancer* (EE) und können die reduzierte Enzymaktivität bestimmter AGAL Mutationen in Kombination mit dem pharmakologischen Chaperon 1-Deoxygalactonojirimycin fast zur Vollständigkeit wiederherstellen. Mol Ther. 2015 Mar;23(3):456-64. doi: 10.1038/mt.2014.22.

Studie 9: Enzym-*Enhancer* (EE) der lysosomalen AGAL aus der Klasse der Proteostaseregulatoren modulieren die zelluläre Proteasom-Aktivität und Genexpression und steigern in Kombinationsbehandlung die Effektivität des pharmakologischen Chaperons in vitro. Biochem J. 2020 Jan 31;477(2):359-380. doi:10.1042/BCJ20190513.

3 Kumulative Darstellung der Studienergebnisse und Diskussion

3.1 Proteinbiochemische Charakterisierung und Phänotypisierung von M. Fabry-assoziierten Mutationen des *GLA*-Gens

3.1.1 In vitro Enzymmessung als Instrument zur Vorhersage des Krankheitsverlaufs bei M. Fabry (Studie 1)

Die klare molekulare Abgrenzbarkeit zwischen atypisch-oligosymptomatischen und klassisch-schweren Krankheitsverläufen beim M. Fabry weist auf eine starke Genotyp-Phänotyp-Korrelation hin. In vitro Enzymmessungen im heterologen Expressionssystem eignen sich als ergänzendes Instrument zur Biomarker-Bestimmung als Grundlage für ein verbessertes Gesundheitsmanagement im Hinblick auf Prognose und Therapieentscheidungen. In der Studie »*Functional characterisation of alpha-galactosidase a mutations as a basis for a new classification system in Fabry disease*« (Lukas et al. 2013) wurde ein neues Klassifikationsmodell für M. Fabry Mutationen vorgeschlagen, das auf der Messung der Enzymaktivität in vitro basiert. Um das Modell zu bestätigen und ein ganzheitliches Profil der pathologischen Folgen einer Vielzahl von M. Fabry Mutationen zu erstellen, wurden paraklinische Daten des kürzlich entwickelten M. Fabry-Biomarkers Lyso-Gb3 (Aerts et al. 2008; Togawa et al. 2010) und weitere klinische Details in die Analyse einbezogen. Allein die In vitro Enzymaktivität im isogenen Zellkultursystem zeigte mit 83,3 % eine sehr gute Vorhersagequalität des erwarteten klinischen Phänotyps einer vorliegenden Mutation. Bei der Betrachtung des klinischen Biomarkers fällt auf, dass die Vorhersagequalität vom Geschlecht des Patienten abhängt, wobei die klinischen Parameter von weiblichen Patienten den Phänotyp weniger zuverlässig wiedergeben. Dies lässt sich durch die zufällige mosaikartige Inaktivierung der elterlichen X-Chromosomen erklären, die dazu führt, dass auch weibliche Patienten mit klassischen Mutationen häufig atypisch-milde Verläufe aufweisen. Dennoch ist die Bestimmung von Lyso-Gb3 auch bei weiblichen Patienten sinnvoll, da bei Vorliegen einer *GLA*-Mutation, die mit dem klassisch-schweren Phänotyp verbunden ist, in der Regel eine Erhöhung beobachtet wird.

Ziel der vorliegenden Studie war zum einen die Einbeziehung weiterer neuer Mutationen, die im Rahmen der M. Fabry Diagnostik gefunden wurden, und zum anderen die Verfeinerung der klinischen Phänotypisierung von Mutationen anhand von Parametern wie Biomarker und Symptomspektrum. Ein besonderes Augenmerk galt in dieser Studie den »milden Mutationen«, da die Durchführung von Screenings bei Neugeborenen und verschiedenen Risikopopulationen (Patienten mit Niereninsuffizienz, Schlaganfall und Kardiomyopathie) viele neue *GLA* Mutationen zutage förderte (Spada et al. 2006; Andrade et al. 2008; Brouns et al. 2010; Hwu et al. 2009; Wittmann et al. 2012; Fan et al. 2021). Die signifikante Prävalenz von *GLA*-Mutationen in symptomatischen Populationen könnte

auf eine unterschätzte Anzahl von mit atypisch-oligosymptomatischen Krankheitsverläufen assoziierten *GLA*-Mutationen schließen lassen und somit auf eine hohe Dunkelziffer fehldiagnostizierter M. Fabry Patienten in diesen Kohorten. Die Befunde erweiterten somit das Spektrum solcher »milden Mutationen« und ebenfalls die Datenlage zu denjenigen genetischen Varianten unbekannter Signifikanz (GVUS von engl. *genetic variant of unknown significance*), deren pathogenes Potential kontrovers betrachtet wird wie beispielsweise die Fälle von p.Ala143Thr und p.Asp313Tyr zeigen (Hauth et al. 2018; Lenders et al. 2016; Palaiodimou et al. 2022). Diese Varianten sind durch minimal erhöhte oder normale Lyso-Gb3-Biomarkerwerte charakterisiert und zeigen meist in vitro Enzymaktivität >20% des Wildtyp-Niveaus. Zu den bekannten Mutationen wurden die bis dahin unpublizierten Mutationen p.Leu3Pro, p.Leu3Val, p.Asp33Gly, p.Gly35Glu, p.Glu71Gly, p.Gly80Asp, p.Ala121Thr, p.Ile154Thr, p.Val164Leu, p.Leu180Phe, p.Arg196Ser, p.Ile198Thr, p.Lys213Arg, p.Asn228Ser, p.Ile242Val p.Ile253Thr, p.Val254Ala, p.Ile289Val, p.Ala309Val, p.Asp313Asn, Asp315Asn, p.Val316Ala, p.Pro323Arg p.Gln333Arg, p.Ala352Arg, p.Gly375Ala, p.Arg392Ser und p.Trp399Ser hinzugefügt, welche mit 61% (28/46) aller neu beschriebenen Mutationen den Hauptanteil der Mutationen in der Studie ausmachten. Bei Patienten mit diesen Genotypen zeigten sich gleichwohl mit M. Fabry vereinbare Symptome. Die Mutationen, die in der untersuchten Kohorte oligosymptomatischer M. Fabry Patienten gefunden wurden, wiesen eine hohe mittlere Enzymaktivität von >50% auf. Überdies waren die wenigen asymptomatischen Patienten dieser Kohorte, die durch Familientests identifiziert wurden, signifikant jünger (24,0 (m) und 24,4 (w) Jahre) als die symptomatischen Patienten (51,6 (m) und 44,7 (w) Jahre), was auf einen sehr späten Ausbruch dieses M. Fabry-Subtyps hinweist. Es muss jedoch berücksichtigt werden, dass chronische kardiovaskuläre Erkrankungen und Symptome wie Nierenversagen, Schlaganfall und periphere Nervenschäden bei älteren Menschen häufiger vorkommen und andere Pathologien in die Differentialdiagnose einbezogen werden müssen. Die Studie liefert Hinweise auf die Pathologie zahlreicher *GLA* Mutationen, erfährt aber eine Einschränkung durch die einerseits allgemein geringe Patientenzahl und andererseits die nicht genau bestimmbare Häufigkeit der untersuchten Mutationen in der gesunden Bevölkerung, so dass die Signifikanz dieser Mutationen weiterhin als unklar zu bezeichnen ist.

Zum Zeitpunkt der Studie wurde eine neue Webanwendung angeboten, die entwickelt wurde, um »Kliniker bei der Auswahl geeigneter Patienten für eine pharmakologische Chaperontherapie zu unterstützen«[1] (Cammisa et al. 2013), basierend auf experimentellen Daten und einem Vorhersagealgorithmus für Mutationen, die noch nicht experimentell auf ihre Ansprechbarkeit

[1] Übersetzt aus dem Englischen nach Cammisa et al. 2013. Fabry_CEP: a tool to identify Fabry mutations responsive to pharmacological chaperones. *Orphanet journal of rare diseases* 8, S. 111.

getestet wurden. Der für die Mutationen in der vorliegenden Studie erhaltene Vorhersagewert von 0,81 (0 - 1) war vergleichbar mit dem in der früheren Studie veröffentlichen Wert (Cammisa et al. 2013) und hebt die Wichtigkeit der experimentellen Prüfung der biochemischen Ansprechbarkeit einer Mutation hervor.

3.1.2 Interassay-Variabilität in der Enzymmessung von *GLA* Mutationen (Studie 2)

Neben genetischen Modifikatoren und anderen extragenetischen (epigenetische, umweltbedingte) Faktoren stellen die Missense Mutationen auf Grund der Variabilität der verbleibenden Enzymaktivität einen Erklärungsansatz für das breite phänotypische Spektrum bei M. Fabry dar. *GLA*-Gen Missense Mutationen bedürfen daher einer besonderen Herangehensweise bei der Diagnosestellung. Überdies existiert seit 2016 eine zusätzliche Therapieoption mit dem PC DGJ für geeignete Patienten (Markham 2016), wodurch ein weiterer Aspekt der Untersuchungen in den Fokus rückt, die Pharmakogenetik. Der Vorteil der PCT gegenüber der ERT ist die orale Verfügbarkeit. Allerdings muss die Eignung der Patienten für jede individuelle Mutation festgestellt werden, während die ERT unabhängig von der Genetik prinzipiell für alle Patienten geeignet ist (Liguori et al. 2020). Die vorliegende Studie beschreibt die Reproduzierbarkeit von in vitro und ex vivo Enzymaktivität in Bezug auf den Phänotyp und die Zuverlässigkeit der Aussage über die Ansprechbarkeit auf das PC vor dem Hintergrund der wachsenden Bedeutung neuer therapeutischer Alternativen. Die Ergebnisse von insgesamt 13 Studien wurden miteinander verglichen, in denen im Wesentlichen dieselbe Methodik zur Bestimmung der AGAL in vitro Enzymaktivität in Anwesenheit und Abwesenheit von DGJ angewandt wurde. Die Zellen, die in diesen Studien verwendet wurden, stammten entweder von Patienten (ex vivo Enzymaktivität) oder waren in den meisten Fällen Standard-Zellmodelle wie HEK293- oder COS-Zellen, die transient mit Expressionsvektoren transfiziert wurden (in vitro). Die Basalaktivität (ohne PC) und der Anstieg von Enzymlevel sowie Enzymaktivität wurden gemessen und durch den Gesamtproteingehalt in den Zellextrakten normalisiert. Die in den Überexpressionsmodellen gewonnenen Daten zeigten eine starke Korrelation und hingen nicht von der Art der Empfängerzellen ab, die für die Transfektion verwendet wurden, während die erhaltenen absoluten Daten aus Patientenzellen (Lymphoblasten und Fibroblasten), die dieselbe Mutation trugen, weniger reproduzierbar waren. Im Vergleich der Werte zwischen den Patientenzellen und den Überexpressionssystemen fiel auf, dass die gemessenen absoluten Werte der AGAL Aktivität ohne PC, trotz vorhandener Korrelation (r = 0.7), in den Patientenzellen insgesamt deutlich niedriger waren als in den Überexpressionsmodellen. Für die Mutation p.Leu180Phe wurde ein Durchschnittswert von 32,4% WT Aktivität in HEK293 Zellen ermittelt. In Leukozyten zweier unabhängiger Individuen hingegen nur 6,0% (± 2,0). Ähnlich gravierend stellten sich die berechneten Abweichungen für die Mutationen p.Asn215Ser und p.Ile253Thr dar. Dies kann summa summarum das Risiko einer

Unterschätzung der Pathogenität der Mutationen durch den in vitro Assay bedeuten. Dieser bedeutsamen Einschränkung der in vitro Enzymmessungen durch die Interassay Variabilität steht die über alle untersuchten Arbeitsgruppen robust darstellbare Ansprechbarkeit der Mutationen für das PC gegenüber.

Im zweiten Teil des Artikels wurden solche Mutationen genauer betrachtet, die als GVUS einzustufen sind. Die zuvor eingeführte Größe der PSSM (von engl. *position specific substitution matrix*) kann dann eine bei der Schadenvorhersage für die entsprechende Mutation oder zur Vorhersage von deren Ansprechbarkeit auf das neue PC DGJ eine Rolle spielen, wenn in vitro Daten nicht vorliegen (Andreotti et al. 2011; Andreotti et al. 2010). Wir rekapitulierten, dass Mutationen am aktiven Zentrum erwartungsgemäß keine Restaktivität hatten und entsprechend nicht auf DGJ reagierten, während Mutationen an nicht konservierten Stellen in der Regel ansprachen. In Zahlen bedeutete das, dass Mutationen mit einem Score >-1 meist responsiv waren und Mutationen mit einem Score <-2 nicht responsiv waren. Für alle in ExAC (fasst Exom-Sequenzierungsdaten aus einer Vielzahl großer Sequenzierungsprojekte zusammen) beschriebenen Mutationen (N=304) ergaben sich PSSM zwischen 0 bis -7. Für die Varianten mit nachgewiesen hoher Enzymaktivität und unklarem klinischem Outcome p.Arg118Cys (in vitro Aktivität: 24,5%; PSSM: -2), p.Ala143Thr (in vitro Aktivität: 39,7%; PSSM: -1), p.Glu66Gln (in vitro Aktivität: 47,6%; PSSM: -2) und p.Asp313Tyr (in vitro Aktivität: 75,5%; PSSM: -1), ergab sich ein konsistentes Bild. Tatsächlich erwiesen sich p.Arg118Cys und p.Glu66Gln mit absoluter Aktivitätserhöhung von +3,3% (des WT-Wertes) bzw. +6,1% (des WT-Wertes) und einer relativen 1,13-fachen Erhöhung zum unbehandelten Wert experimentell als schwach responsiv. In der Literatur werden diese Mutationen teilweise als M. Fabry-assoziiert, aber in einer steigenden Anzahl von Berichten als genetische Modifikatoren oder Risikofaktoren für bestimmte Pathologien wie Schlaganfall, Nieren- und Herz-Kreislauf-Erkrankungen betrachtet (Nakamura et al. 2014; Schiffmann et al. 2016). Interessanterweise wurde die Pathogenität der Variante p.Asn215Ser niemals angezweifelt. Wie gezeigt können auch diese hochaktiven Varianten einen Nutzen durch die Behandlung mit DGJ erfahren, allerdings ist die Aktivitätssteigerung verglichen mit der ohnehin hohen Restaktivität gering, wodurch sich die Frage der Notwendigkeit und der Effektivität einer Behandlung anschließt.

3.1.3 Visualisiertes Plattenleser-Protokoll zur in vitro Enzymmessung lysosomaler AGAL und GAA (Studie 3)

Die Inzidenz von M. Fabry wird mit 1:40.000 bis 1:117.000 angegeben (Śnit et al. 2022). Gleichwohl deuten Neugeborenen-Screenings und Screenings von Risikopatientengruppen auf wesentlich höhere Raten hin (Spada et al. 2006; Hwu et al. 2009; Wittmann et al. 2012; Brouns et al. 2010). Darunter sind jedoch viele Fälle von Mutationsvarianten, bei denen die Krankheit nicht wie bei

den klassischen Mutationen in vollem Umfang ausbricht. Eine ähnliche Situation finden wir bei M. Pompe vor. Mit fast identischen Zahlen, z.B. einer Häufigkeit von etwa 1 zu 40.000 Geburten in den Niederlanden gehört M. Pompe mit klassischem Auftreten ebenfalls zu den seltenen Krankheiten (Kanters et al. 2011). In Risikokohorten mit neuromuskulären Erkrankungen ist die Allelfrequenz der GAA-Mutation mit 2,4 % jedoch keineswegs selten (Lukacs et al. 2016), was auf eine Untererfassung der Pompe-Krankheit hindeuten kann.

Neben der Entwicklung effektiver Therapiestrategien konnte in den vergangenen Jahren auch eine Beschleunigung der Diagnose für die Erkrankten erzielt werden, so dass die Verzögerung zwischen dem Auftreten der ersten Symptome und der Diagnose bei vielen LSDs beträchtlich reduziert werden konnte. Eine rasche Diagnose verbessert die Prognose für den Patienten vor allem dann, wenn wirksame therapeutische Maßnahmen ergriffen werden können, wie es bei M. Fabry und M. Pompe durch den Einsatz von ERT der Fall ist. Durch die Einführung individualisierter Therapieansätze wie der PCT bei M. Fabry kommt der Pharmakogenetik eine hohe Bedeutung zu. Während alle M. Fabry Patienten unabhängig vom Genotyp von einer ERT profitieren können, sind nur Patienten mit bestimmten ansprechenden Mutationen für eine Therapie mit dem PC geeignet. Wie bei M. Fabry sind auch bei M. Pompe Hunderte von mutierten Allelen des beteiligten sauren Hydrolase-Gens an der Krankheitsentstehung involviert. Typischerweise behindern kostspielige komplexe klinische Studien mit geringen Patientenzahlen die Zulassungsverfahren, so dass die Anreize neue Therapien auf den Markt zu bringen geschmälert sind. Im Fall von Galafold™ wurden große Anstrengungen unternommen, um ansprechende Mutationen mittels eines eigens dafür GLP-validierten in vitro Test-Screenings Hunderter Genotypen vorherzusagen (Benjamin et al. 2017). Wie auch die Daten der 2016 veröffentlichten Meta-Analyse (Studie 2) zeigen, wurden bisher verschiedene Zellsysteme basierend auf Fibroblasten-/Leukozytenkulturen von Patienten und transient transfizierten COS- oder HEK-Zellen verwendet und Arbeitsgruppen-spezifische Protokolle zur Charakterisierung und Klassifizierung von AGAL-Enzymmutationen kamen zum Einsatz. Zeitgleich zur Veröffentlichung der Daten der präklinischen Untersuchungen von Benjamin und Kollegen im Jahr 2017 haben wir unsere »*in-house*« durchgeführte molekulare Enzymanalytik zur Charakterisierung von AGAL und GAA Mutationen ebenfalls standardisiert und ein visualisiertes Protokoll publiziert. Gleichwohl für die Therapie des M. Pompe aktuell keine PCT zugelassen ist, so gibt es mit DNJ und NB-DNJ zwei Verbindungen, die als PC wirken (Okumiya et al. 2007; Parenti et al. 2007). Diese können eine potentielle Ansprechbarkeit einer GAA Mutation vorhersagen und als Leitstrukturen für zukünftige Wirkstoffentwicklung bedeutsam sein. Daher wurde die Bestimmung der GAA Enzymaktivität unter den beschriebenen Standardbedingungen mit ins Protokoll aufgenommen.

Der Artikel besteht aus einer Einleitung, einem in vier Schritte gegliederten Protokoll (1. Herstellung von mutierten pcDNA3.1/GLA- und pcDNA3.1/GAA-Konstrukten; 2. Kultivierung von

HEK293-H-Zellen; 3. pcDNA3.1/GLA und pcDNA3.1/GAA Plasmid-Transfektion und Behandlung von HEK293-H; 4. Zellernte und Messung der Aktivität von α-Galactosidase A oder saurer α-Glucosidase), einem Teil, der repräsentative Daten vorstellt und einer kurzen Diskussion, sowie aus einem Videoformat, das ausgewählte Schritte dokumentiert. Das veröffentlichte Protokoll stellt zunächst die vereinfachten molekulargenetischen Vorarbeiten zur Herstellung der Mutationen in den vorgestellten Vektoren pcDNA3.1/GLA und pcDNA3.1/GAA (Lukas et al. 2013) vor. Der Zellkultur-Anteil des Protokolls ist von zentraler Bedeutung. Hier sind die Einhaltung genauer Kulturbedingungen und Zeitvorgaben wie dargestellt unbedingt zu beachten, u.a. Zelldichte bei Aussaat der Zellen, der Zeitpunkt von Transfektion und Ernte sowie Dauer der Behandlung mit dem PC (Tabelle 1). Typischerweise pendeln die Angaben in den Behandlungsprotokollen zwischen 48 Stunden und 5 Tagen Behandlungsdauer, was ergebnisrelevante Interassay Unterschiede hervorrufen kann.

Tabelle 1. Standardisierte Versuchsbedingungen der AGAL Aktivitätsmessung.

Parameter	**Standardisierte Bedingung**
Zelllinie	HEK293-H
Plasmid-Vektor-System	pcDNA3.1/v5-His TOPO
Zellkulturformat/ Zelldichte bei der Aussaat	24-Well/ 1.5 x 10^5 Zellen
Medium	DMEM, 4,5 g/l Glucose (+GlutaMAX), 10 % FBS und 1% P/S*
Transfektion	24 Std nach Aussaat mit Lipofectamin 2000
Inkubationszeit (post-Transfektion)	66 Std (60 Std. mit Behandlung)
DGJ Konzentration	20 µM
Mediumwchsel	Ja; 42 Std post-Transfektion
Zelllyse	Gefrieren und Tauen in 200 µl bidestilliertem Wasser
Enzymmessung	
- Substrat/Puffer	1,34 mM 4-Methylumbelliferyl-α-D-galactopyranosid in 0,06 M Phosphat-Citrat-Puffer, pH 4,7
- Reaktionsformat	96-Well
- Reaktionsvolumen	30 µl
- Probenkonzentration	50 ng Gesamtprotein/ µl
Unabhängige Versuchswiederholungen	n = 5 (Duplikate)

*P/S = Penicillin/ Streptomycin

Das Rational zur Anfertigung eines standardisierten Protokolls bestand vorwiegend in der Festlegung bestimmter Zellkultur-Bedingungen (z.B. Kulturbedingungen der HEK293-H Zellen, Transfektion und Ernte) und der Straffung zeitaufwendiger Schritte wie dem Herstellungsprozess der mutanten Plasmid-Vektoren. Die bedeutendste Anpassung des Protokolls im Vergleich zu den zuvor veröffentlichten Studien der Jahre 2013 und 2016 (Lukas et al. 2013) lag in der Erhöhung der unabhängigen experimentellen Wiederholungen, wodurch die Robustheit und Signifikanz der Ergebnisse verbessert wurde.

3.1.4 Untersuchung der Reproduzierbarkeit der Ergebnisse der GLP-validierten Methode zur Identifizierung PCT-geeigneten Fabry Patienten (Studie 4)

Die Studie 1 widmete sich der Objektivierung der Schadensbestimmung lysosomaler AGAL anhand einer holistischen molekularen und klinischen Charakterisierung. Die Daten ließen den Schluss zu, dass in vitro Enzymmessung einen prädiktiven Wert für eine klinische Phänotypisierung hat. In den Studien 2 und 3 lag der Schwerpunkt auf Grund der Fortschritte bei der Entwicklung der PCT zunehmend auf dem Wert des Systems im Hinblick auf die Vorhersage, wann eine Mutation als ansprechend betrachtet werden kann. Studie 4 knüpft an dieser Stelle an. Gerade bei der Feststellung der Eignung einer Mutation für eine PC-Behandlung muss bei einer Fehleinschätzung mit gravierenden medizinischen Konsequenzen zum Nachteil des Patienten gerechnet werden.

Wie erwähnt erschien in kurzem zeitlichen Abstand der Studien 1, 2 und 3 ein kongruenter Bericht über die Entwicklung eines GLP-validierten pharmakogenetischen Enzymtests zur Bestimmung der Ansprechbarkeit von AGAL Mutanten auf eine DGJ-Behandlung (Benjamin et al. 2017). In der selben Studie wurde auch der prädiktive Wert des Assays anhand pharmakodynamischer DGJ-Daten der klinischen Studien der Phase II und III überprüft. In einer folgenden Studie wurde die Zuverlässigkeit der Vorhersage des GLP-validierten Assays getestet, indem 59 der 2017 von Benjamin und Kollegen veröffentlichten *GLA*-Genmutationen in einem Messsystem, das den GLP-Assay replizierte, erneut gemessen wurden (Oommen et al. 2019). Verglichen wurden nicht nur die Reproduzierbarkeit der erhaltenen Rohmessergebnisse, sondern auch die endgültige Abschätzung der Ansprechbarkeit auf der Grundlage der Definition für eine ansprechbare Mutation. Als Schwellenwert für eine ansprechbare Mutation gilt offiziell eine absolute Zunahme der Enzymaktivität um ≥3% WT und eine relative Zunahme der Enzymaktivität um das 1,2-fache nach Inkubation mit 10 µM DGJ (Committee for Medicinal Products for Human Use).

Absolute Steigerung der Aktivität (% WT):

$$\left[\frac{Mut + DGJ}{WT - DGJ} \times 100\right] - \left[\frac{Mut - DGJ}{WT - DGJ} \times 100\right] \geq 3$$

∧

Relative Steigerung gegenüber dem Ausgangswert (*fold change*):

$$\left[\frac{Mut + DGJ}{WT - DGJ} \times 100\right] \div \left[\frac{Mut - DGJ}{WT - DGJ} \times 100\right] \geq 1{,}2$$

Trotz der identischen Versuchsanordnung stellten die Autoren des Artikels eine »offensichtliche Diskrepanz zwischen den Laboratorien bei der Messung der AGAL-Aktivität«[2] fest, was mit den zuvor beobachteten Unterschieden bei den Schätzungen der Ansprechbarkeit übereinstimme. In der Tat wurde in früheren Studien ermittelt, dass die Anzahl der ansprechbaren *GLA* Missense Mutationen zwischen etwa 40 und 60 % schwankte (Lukas et al. 2013; Wu et al. 2011). Unterschiedliche Bewertungen einzelner Mutationen kamen ebenfalls vor, wobei zu beachten ist, dass neben unterschiedlichen Messprotokollen auch unsere eigene Definition für eine ansprechbare Mutation von den Fremdstudien abwich:

Absolute Steigerung der Aktivität (% WT):

$$\left[\frac{Mut + DGJ}{WT - DGJ} \times 100\right] - \left[\frac{Mut - DGJ}{WT - DGJ} \times 100\right] \geq 5$$

V

Relative Steigerung gegenüber dem Ausgangswert (*fold change*):

$$\left[\frac{Mut + DGJ}{WT - DGJ} \times 100\right] \div \left[\frac{Mut - DGJ}{WT - DGJ} \times 100\right] \geq 1{,}5$$

Voraussetzung zur Erfüllung der Ansprechbarkeitskriterien ist eine Zunahme der Enzymaktivität auf mindestens 5% WT Aktivität.

Die Studie von Oommen und Kollegen (2019) veranlasste uns zu einem Vergleich der im GLP-Assay erhaltenen Daten (Benjamin et al. 2017) mit den eigenen AGAL Enzymaktivitätsdaten aus unserem sehr ähnlichen, intern entwickelten Test (Lukas et al. 2013). Wir verglichen 160 Mutationen, zu denen Datensätze beider Arbeitsgruppen vorlagen. Wir stellten fest, dass im Allgemeinen eine gute Übereinstimmung sowohl bei den biochemischen Daten als auch bei der Bewertung der Ansprechbarkeit gegeben war. Dennoch ergab ein Vergleich der Daten, dass 12,9 % aller Varianten unterschiedlich klassifiziert wurden, als die internen experimentellen Daten mit denen des GLP-validierten Assays und seinen dualen Ansprechbarkeitskriterien verglichen wurden. Es gab keine Neigung zu responsiven oder nicht responsiven Mutationen, die im anderen System jeweils unterschiedlich bewertet wurden, was auf einen systemischen Unterschied hindeuten würde. Wir stellten die Frage, ob die abweichende Einordnung hauptsächlich an unterschiedlichen biochemischen Enzymaktivitätswerten oder der unterschiedlichen Definition für eine ansprechbare Mutation liegen würde. Die beste Übereinstimmung mit der offiziellen Ansprechbarkeitsklassifizierung auf der

[2] Übersetzt aus dem Englischen nach Oommen et al. 2019. Inter-assay variability influences migalastat amenability assessments among Fabry disease variants. *Molecular genetics and metabolism* 127 (1), S. 74 – 85.

Grundlage der GLP-validierten Benjamin-Studie wurde erzielt, wenn die Enzymdaten der GLP-Studie und die Ansprechbarkeitskriterien aus unseren Studien verwendet wurden (Abweichung 6,2 %), während die größte Abweichung bei der Verwendung eigener Enzymdaten und der Ansprechbarkeitskriterien der GLP-Studie zu beobachten war (Abweichung 18 %). Dies deutete darauf hin, dass hauptsächlich die Interassay-Variabilität bei den Enzymdaten und nicht die unterschiedlichen Ansprechbarkeitskriterien für die Nichtübereinstimmung verantwortlich waren. Anhand unserer Datensätze wurde auch deutlich, dass eine niedrige Ausgangsaktivität und eine grenzwertige biochemische Ansprechbarkeit Risikofaktoren für eine Fehlklassifizierung von *GLA*-Genvariante waren. Die Messung der Ansprechbarkeit auf DGJ in zellbasierten In vitro Assays ist jedoch eine Methode, zu der es derzeit keine Alternative gibt, um die Eignung von Patienten zu bestimmen.

3.2 Studien zu mechanistischen Aspekten neuer therapeutischer Ansätze bei LSDs

3.2.1 Expression menschlicher *GLA* Mutationen in Drosophila führt zu Enzymfehlfaltung, Tod dopaminerger Zellen und einer kürzeren Lebensdauer (Studie 5)

Pathophysiologische Studien bei M. Fabry und M. Gaucher sind im Wesentlichen auf Nagetiermodelle beschränkt (Mark E Haskins et al. 2006; Farfel-Becker et al. 2011). Das für M. Fabry verfügbare murine Knockout-Modell weist ein vollständiges Fehlen der AGAL Aktivität auf und repräsentiert weder die genetischen noch die krankheitsspezifischen Aspekte von M. Fabry in angemessener Weise (Ohshima et al. 1997). Die unter beachtlichem Aufwand entwickelten Modelle für den M. Gaucher lassen den Ansatz erkennen, Genotyp-vermittelten Besonderheiten in humanisierten Tiermodellen Rechnung zu tragen. Doch in Bezug auf die Phänotypisierung stellten sich die Mausmodelle mit den häufigen Mutationen p.Asn370Ser und p.Leu444Pro als Enttäuschung heraus. Das p.Asn370Ser Modell, welches den milden, non-neuronopathischen M. Gaucher Typ I abbilden sollte, verstarben in den ersten 24 Stunden nach der Geburt an einem schweren ichthyotischen Zustand der Haut (Xu et al. 2003). Mäuse, die die Typ III/Typ II-Mutation p.Leu444Pro trugen, wiesen je nach Labor, in dem die Maus hergestellt wurden, sehr unterschiedliche Phänotypen auf, die von sehr mild bis hin zu unmittelbar tödlich reichten, so dass der Wert der Modelle begrenzt war (Liu et al. 1998; Mizukami et al. 2002). Für den M. Fabry existiert ebenfalls ein humanisiertes Mausmodell mit der gut charakterisierten *GLA*-Genmutation p.Arg301Gln, aber diese Maus zeigt keinen Phänotyp außer einer verminderten AGAL Aktivität und einer moderaten Gb3-Akkumulation. Sie wurde bislang ausschließlich für prä-klinische Wirksamkeits- und Dosierungstests für das PC DGJ eingesetzt (Khanna et al. 2010). Auf Grund des erheblichen Aufwands in der Haltung, Zucht und

Durchführung von Experimenten eignen sich diese Modelle nur bedingt zur Untersuchung pharmakologischer Beeinflussung zellulärer Pathways mit dem Ziel molekularer Therapieentwicklung.

Im Jahr 2013 wurde ein *Drosophila melanogaster*-Modell für M. Gaucher etabliert (Maor et al. 2013). Die ektopische Expression der Mutanten p.Asn370Ser und p.Leu444Pro in dopaminergen/serotonergen Zellen der Fliegen führte zu erhöhter Aktivität der UPR (von engl. *unfolded protein response*), Bewegungsstörungen, die an die Parkinson-Krankheit erinnerten und zum Tod in frühen Entwicklungsstadien. Die Fliegen wiesen gleichwohl keinerlei GlcCer Akkumulation auf und stellten ein reines Proteinfehlfaltungsmodell dar anhand dessen die Fehlfaltung mutierter β-Glu, UPR Aktivierung und Enzymretention im ER in einen kausalen Zusammenhang mit der Stabilisierung, Aggregation und Akkumulation von zellulärem α-Synuclein gebracht werden konnten (Maor et al. 2016; Maor et al. 2019).

Studie 5 überträgt den für die Gaucher-Krankheit beschriebenen Ansatz der Expression einer potenziell fehlgefalteten Genmutation in Zellen des zentralen Nervensystems von *D. melanogaster* auf die Fabry-Krankheit. Zu diesem Zweck wurden transgene Fliegen erzeugt, die die mutierten AGAL-Varianten p.Ala156Val und p.Ala285Asp exprimierten. Beide Varianten sind mit dem klassischen Krankheitsverlauf bei M. Fabry assoziiert, wobei die erste Variante eine signifikante Restaktivität von etwa 5 % in HEK293-H-Zellen aufweist und auf das PC DGJ anspricht; p.Ala285Asp hat keine Restaktivität und spricht nicht auf eine PC-Behandlung an (Lukas et al. 2013). Bei ubiquitärer Expression der AGAL-Varianten wurde in Fliegenzellen eine ER-Stressreaktion und eine Aktivierung der UPR in Form von erhöhtem Hsc-70-3, gespleißtem Xbp1 und ATF4 beobachtet. Darüber hinaus wurden für die AGAL Enzymvarianten selbst eine Verringerung des zellulären Levels und eine vorwiegende ER-Lokalisation als Indikator unreifen, inaktiven Enzyms beobachtet. Eine Normalisierung des Zustandes wurde für p.Ala156Val exprimierende Fliegen über die Gabe von DGJ erreicht. Zwar konnte auch der Enzymlevel von p.Ala285Asp durch die Gabe von 20 µM DGJ signifikant erhöht werden, die übrigen Parameter normalisierten sich hingegen nicht, was darauf schließen lässt, dass die durch die Proteinfehlfaltung der p.Ala285Asp-Mutante ausgelösten Folgen durch das PC nicht behoben werden konnten. Die Zelltyp-spezifische Expression von *GLA* durch einen in dopaminergen Zellen aktiven Promotor erzeugte eine Unfähigkeit zu klettern (»Negative Geotaxis«-Versuch) in Mutation-exprimierenden Fliegen, die mit einem vermehrten Absterben dopaminerger Zellen und einer verkürzten Lebensspanne einherging. Im Gegensatz dazu war die Lebensspanne von WT AGAL-exprimierenden Fliegen nicht beeinträchtigt. Die DGJ-Behandlung von p.Ala156Val-exprimierenden Fliegen führte zu einer Erholung auf nahezu Kontrollniveau, d. h. Fliegen, die kein Transgen exprimierten. Die Ergebnisse bei p.Ala285Asp-exprimierenden Fliegen zeigten keine signifikante Verbesserung. Zusammengenommen zeigte sich, dass die ektopische Expression fehlgefalteter AGAL in neuronalen Zellen der Fliege motorische Verhaltensstörungen hervorrufen konnte, die nicht auf

einen Mangel an Enzymaktivität zurückzuführen waren. Der Phänotyp war durch das PC teilweise reversibel, wenn eine durch DGJ korrigierbare Fehlfaltungsmutante exprimiert wurde.

3.2.2 Ambroxol als ein intrazellulärer *Enhancer* mutierter β-Glu (Studie 6)

In der Erstpublikation des AGAL *Enhancers* 1-Deoxygalactonijirimycin wird die Verbindung als *'chemical chaperon*' bezeichnet (Fan et al. 1999). Dies ist eine der ersten Studien überhaupt, die kompetitive Inhibitoren als neue molekulare therapeutische Strategie für die Behandlung genetischer Stoffwechselkrankheiten vorschlägt. In der Folge wurden strukturell vergleichbare Zuckermimetika aus der Klasse der Iminozucker verwendet, um geeignete Inhibitoren für β-Glu (M. Gaucher) und GAA (M. Pompe) zu identifizieren, die sich auch als Chaperone eignen (Sawkar et al. 2002; Steet et al. 2006; Okumiya et al. 2007; Parenti et al. 2007). Bald darauf wurden PCs für weitere Hydrolase-Enzym-basierte LSDs entdeckt (Maegawa et al. 2007; Lee et al. 2010; Hoshina et al. 2018). Der Wirkmechanismus beruhte stets auf der Bindung an das aktive Zentrum des Enzyms. Doch nicht alle der Wirkstoffkandidaten waren offensichtliche Mimetika des natürlichen Enzymsubstrats. Das Vorgehen der Wissenschaftler zeigte ein breites Spektrum, das vom »*educated guess*«-Ansatz (ähnlich der DGJ-Studie) über ein automatisiertes Hemmstoffscreening potenzieller Kandidaten, bei dem die Substanzbibliotheken oft aus für andere Krankheiten zugelassenen Wirkstoffen bestanden (Maegawa et al. 2007), bis hin zu Studien reichte, die ein durch Bioinformatik gestütztes Vorscreening, das so genannte molekulare Docking (MD) oder in silico-MD (Subramaniyan et al. 2018), verwendeten. Screening (Zheng et al. 2007), *Repurposing*/*Repositioning* (Hay Mele et al. 2015) und rationales Arzneimitteldesign (Zhu et al. 2005; Atrian et al. 2008) waren seither die Ansätze, die zur Entdeckung einer Vielzahl an Leitstrukturen und deren Weiterentwicklung zur Behandlung von *GBA1* Proteinfehlfaltungsmutationen bei M. Gaucher führten. Ambroxol wurde als β-Glu-*Enhancer* im Rahmen einer Studie entdeckt, in der erstmals nicht nach Hemmstoffen gesucht wurde, sondern nach Verbindungen, die in der Lage waren, die thermische Denaturierung des Enzyms abzuschwächen, also Enzymstabilisatoren (Maegawa et al. 2009). Die Ausgangsbedingung sah eine 10 mM Behandlungskonzentration der zu untersuchenden Verbindung vor. In weiteren Untersuchungen zur Bindungskinetik wurden ebenfalls hohe Konzentrationen von mindestens 2 mM eingesetzt, was höchstwahrscheinlich eine klinisch unerreichbare Konzentration darstellt (Kim et al. 2020). Gleichwohl konnte ABX die β-Glu Aktivität verschiedener Mutationen in Patientenzellen und im Fliegenmodell im mittleren zweistelligen micromolaren Bereich erhöhen, darunter auch die Aktivität der beiden häufigen Mutationen p.Asn370Ser und p.Leu444Pro (Bendikov-Bar et al. 2011; Castilla et al. 2012; McNeill et al. 2014; Ivanova et al. 2018; Maor et al. 2016). Auch die klinische Anwendung bei Patienten mit M. Gaucher Typ I verlief erfolgversprechend (Zimran et al. 2013). Die Ansprechbarkeit von p.Leu444Pro nährte überdies die Hoffnung auf eine erste effektive Behandlungsform für den

subakuten neuronopathischen M. Gaucher Typ III. Durch diese aussichtsreichen Daten verdient ABX unsere Aufmerksamkeit als Medikamentenkandidat für die Behandlung von M. Gaucher. ABX wurde zuletzt meist als pharmakologisches Chaperon bezeichnet (Enshaei et al. 2019; Kopytova et al. 2021), was allerdings einen spezifischen Wirkmechanismus unterstellt, der auf einer Stabilisierung des Enzyms beruht. Gleichwohl konnte dieser Wirkmechanismus in den zahlreichen in cellulo Studien für ABX bislang nicht nachgewiesen werden. Die hohen Konzentrationen, die in zellfreien Experimenten verwendet wurden, um eine β-Glu Reaktion auszulösen, könnten auf einen anderen Mechanismus der enzymstimulierenden Wirkung von ABX hinweisen, der auf komplexeren intrazellulären Prozessen beruht. In der vorliegenden Studie 6 wurde ein klassisches PC in Form des hochkompetenten Iminozucker-Inhibitors IFG mit ABX verglichen. Untersucht wurden verschiedene bekannte Parameter wie Hemmungseffizienz, Effektivität auf die intrazelluläre β-Glu-Aktivität in patienteneigenen Zellen und erstmals Enzym-stabilisierende Wirkung in einem quantifizierbaren Modell (TSA von engl. *thermal shift assay*). In Übereinstimmung mit vorherigen Studien konnte bei pH 4,7 nur minimale Hemmwirkung von ABX festgestellt werden, während IFG eine vollständige Hemmwirkung entfaltete (IC_{50} = 0,32 µM). Es wurde berichtet, dass die inhibitorische Wirkung von ABX pH-abhängig war und eine vollständige Hemmung von β-Glu bei einem pH 6,7, wie er im ER der Zelle herrscht, erreicht werden konnte. Dies könne von Vorteil sein, da die Interaktion zwischen Enzym und Ligand im ER am Ort der Enzymsynthese erwünscht und am Ort der katabolen Funktion im Lysosom unerwünscht ist. Wir sahen allerdings von einer enzymatischen Bestimmung unter neutralen pH-Bedingungen ab, da das Enzym hier kaum aktiv ist (Aerts et al. 2003). Da beide Verbindungen in zwei heterozygoten Zelllinien (p.Asn370Ser/ 84GG) eine nahezu identische Steigerung der β-Glu-Enzymaktivität bewirkten, stellten wir stattdessen ein hitzeinduziertes Schmelzprofil des rekombinanten β-Glu-Enzyms mittels TSA her. Hierin zeigte sich, dass das mit 2 mM IFG behandelte Enzym bei pH 5,5 eine um 22°C verzögerte Denaturierung von 42°C auf 64°C aufwies. Unter gleichen Bedingungen konnte ABX nur eine insignifikante thermische Stabilisierung von 2,3°C erzielen. In Übereinstimmung hiermit zeigte sich ABX-behandelte β-Glu im Zellkulturmodell instabiler und eine größere unreife β-Glu Fraktion als in IFG-behandelten Zellen wurde evident. Wir argumentierten, dass frühere Studien gezeigt hatten, dass ABX nicht nur als PC, sondern auch auf zellbiologischer Ebene als Transkriptionsregulator wirkt, indem es *GBA1* durch Erhöhung des lysosomalen Hauptregulators Transkriptionsfaktor EB, und CHOP, einem weiteren ER-Stress-relevanten Transkriptionsfaktor, der an der *GBA1*-Regulierung beteiligt ist, erhöht. Durch Nutzung spezifischer ABX-Strukturanaloga lieferte Studie 6 weiterhin Informationen zur Struktur-Funktionsbeziehung von ABX. Die Daten zeigten, dass sowohl die 4-Hydroxylgruppe als auch das Fehlen der Aminomethylgruppe (im Unterschied zum Strukturanalog Bromhexin) als Charakteristika entscheidende Strukturmerkmale für die Effektivität von ABX als β-Glu-*Enhancer*

darstellen, was für die künftige rationale Entwicklung von Arzneimitteln für M. Gaucher auf der Basis von ABX als Leitstruktur Einschränkungen in der Derivatisierbarkeit mit sich bringt.

3.2.3 Entwicklung nicht-inhibitorischer PCs der »zweiten Generation« für M. Fabry (Studie 7)

Der Einsatz von in silico-MD ist ein leistungsfähiges Instrument zur Abschätzung der Bindungsfähigkeit potenzieller Interaktionspartner für bei LSDs mutierte Hydrolasen. Diese Technologie wurde bereits erfolgreich bei diversen Krankheiten wie M. Gaucher, M. Pompe und NP-C angewandt (Subramaniyan et al. 2018; Borie-Guichot et al. 2021; Völkner et al. 2022). Computergestützte MD Experimente im eigenen Labor verwendeten die N-terminale Domäne, die die Cholesterol-Bindungsstelle am NPC1 Protein beinhaltet (Kwon et al. 2009). Die N-terminale Domäne besteht aus ∼240 Aminosäuren und entspricht der ersten luminalen Domäne des 13 Transmembrandomänen umfassenden NPC1-Proteins. Hier bot sich der natürliche Ligand als Leitstruktur für eine kompetitive Proteinbindung an der Cholesterolbindungstasche an. Das strukturbasierte Wirkstoffdesign wurde zum einen mit Hilfe oxygenierter Derivate (z.B. 25-Hydroxycholesterol und 27- Hydroxycholesterol) (Porter et al. 2010; Ohgane et al. 2014) und zum anderen mit Hilfe großer Substanzbibliotheken (Wishart et al. 2006) durch in silico-MD durchgeführt. So konnten sowohl steroidale als auch nicht-steroidale (nicht substratmimetische) PC-Kandidaten identifiziert werden. Neben der freien Bindungsenergie war ein wesentlicher Parameter zur Bestimmung der Bindungsqualität der pKb-Wert der Verbindung, da die pH-abhängige Bindungsstärke durch den Unterschied zwischen dem Syntheseort und dem Wirkungsort des lysosomalen Proteins eine Rolle spielt. Auf diese Weise kann eine erleichterte Reversibilität der Bindung sichergestellt und eine verbesserte PC Wirkung erzeugt werden. Am Beispiel von NP-C lässt sich auch die Bedeutung von PCs aufzeigen, die nicht kompetitiv an das aktive Zentrum des Proteins andocken. Ohgane und Kollegen fanden Hinweise auf eine zweite Cholesterol-Bindungsstelle, deren Besetzung ebenfalls zu einer Stabilisierung des mutierten Proteins führen könnte (Ohgane et al. 2013). Die Dynamik der Cholesterolbindung sowie die Spezifität der zweiten Bindungsstelle ist nur unzureichend verstanden (Dubey et al. 2020), birgt aber die Hoffnung auf stabilisierende Ligandenbindung ohne gleichzeitige Hemmung des Cholesteroltransports.

In einer früheren Studie wurde an der AGAL ebenfalls eine zweite, allosterische Zucker-Bindungsstelle distal des aktiven Zentrums mit erhöhter Affinität zu β-D-Galactose aufgedeckt. Da die hemmende Wirkung dem therapeutischen Ziel der PCT im Wege steht und eine immer noch signifikante Anzahl von Mutationen durch den isosterischen Iminozucker DGJ nicht adressiert werden konnte, wurde im Rahmen der Studie 7 ein in silico-MD-Screening mit über 10.000 kommerziell erhältlichen Verbindungen aus der ZINC-Datenbank (Irwin und Shoichet 2005) an der allosterischen

Zucker-Bindungsstelle durchgeführt. Die Bindungsstelle bot eine veränderte Ligandenspezifität über die mutmaßliche Bindung an Asp255 und Lys374 und damit die potentielle Umgehung von Kreuzinhibition mit der primären Zucker-Bindungsstelle sowie die Möglichkeit, zusätzliche Mutationen anzuvisieren, die von DGJ nicht angesprochen werden konnten. Von den zugelassenen Medikamenten tat sich im virtuellen Screening keine Verbindung hervor, die sich für das *drug repositioning* anbot, aber ein Treffer stellte das 2,6-Dithiopurin (DTP) dar, welches zwar kein zugelassenes Medikament, aber in Zellkulturexperimenten gut verträglich war. DTP hemmte rekombinante AGAL (Fabrazyme, Genzyme Corporation) bei einer Konzentration von 6 mM in einem enzymatischen Test mit dem synthetischen Substrat 4-Nitrophenyl-α-D-Galactopyranosid nicht. Demgegenüber stand eine nahezu vollständige Hemmung durch DGJ bei gleichem Versuchsaufbau und bei einer Konzentration von 1 µM. Im TSA zeigte DTP allein und in Synergie mit DGJ eine stabilisierende Wirkung auf Fabrazyme. Im Überexpressionssystem in COS-7 Zellen wurde die Ansprechbarkeit verschiedener *GLA* Mutationen auf DTP untersucht. Zwar erwies sich das Wirkspektrum von DTP als begrenzt, beispielsweise waren Mutationen in unmittelbarer Nähe der allosterischen Bindungsstelle, p.Ala37Thr, p.Pro40Ser, p.Met42Thr und p.Met42Val, nicht ansprechbar, gleichwohl zeigte sich die DGJ-irresponsive p.Ala230Thr ansprechbar. Die durchgeführten Untersuchungen wiesen auf ein erweitertes Potential für niedermolekulare PCT hin und lieferten Aussagen zur Vorhersagbarkeit der Ansprechbarkeit von *GLA* Mutationen bei Adressierung der allosterischen Bindungsstelle.

3.2.4 Prüfung potenzieller enzymverstärkender Verbindungen für AGAL und GAA (Studie 8)

Verschiedene Punkte sprechen für eine gemeinsame Betrachtung Hydrolase-assoziierter LSDs in Bezug auf ein therapeutisches *Targeting*. Das Vorhandensein eines lysosomalen Netzwerks (CLEAR) zentral regulierter Gene (Sardiello et al. 2009) und die weitgehende Identität proteinbiosynthetischer Prozessierungsabläufe lysosomaler Hydrolasen in der Zelle (siehe Abschnitt 1.1.2) öffnet die Möglichkeit eines pharmakologischen Eingriffes mittels funktionaler ERAD-Inhibitoren, Transkriptionsregulatoren und anderer Proteostaseregulatoren. Die lysosomalen Enzyme AGAL und GAA weisen überdies viele weitere Gemeinsamkeiten auf. Sie bilden den Glykosylhydrolase-Clan »GH-D«, eine Superfamilie von Alpha-Galactosidasen und anderen zuckerspaltenden Hydrolasen, die neben einem gemeinsamen katalytischen Mechanismus eine gemeinsame strukturelle Topologie bestehend aus einer α/β_8-*barrel fold* in der Domäne, die das aktive Zentrum enthält, aufweisen.

Das größte Manko der konventionellen ERT ist die begrenzte Effektivität bei bestimmten Gewebsmanifestationen. So z.B. ist die Blut-Hirn-Schranke eine unüberwindbare Barriere für diese Therapie und Patienten mit zerebrovaskulären Komplikationen und neuropathischen Schmerzen (M. Fabry) können nur unzureichend profitieren (Azevedo et al. 2020). Ebenso verhält es sich mit

Symptomen der Herz- und Atemmuskulatur (M. Pompe) (Sun et al. 2015). Eine weitere Gefahr besteht in einer möglichen Immunreaktion gegen die applizierten Enzyme, die das Risiko einer Effektivitätsminderung beherbergen (El Dib und Pastores 2010; Wilcox et al. 2012; Azevedo et al. 2020). Patienten mit NULL Mutationen und besonders schädlichen Missense Mutationen, die mit schweren Krankheitsverläufen assoziiert sind, sind demnach besonders gefährdet, während der ERT neutralisierende Antikörper zu entwickeln (Wang et al. 2008).

Die in Studie 8 untersuchten niedermolekularen Verbindungen ABX und Rosiglitazon (RSG) wurden in früheren Studien als genregulatorisch (McNeill et al. 2014) bzw. ERAD-hemmend (Motomura et al. 2004) beschrieben. RSG hat durch seinen Einfluss auf PPARy und NFkB eine massive Wirksamkeit auf zellphysiologische Wege, deren Beeinträchtigung in LSD Modellen bekannt ist und deren pharmakologische Ansteuerung potenziell bedeutsam sein kann, z.B. als direkt schmerzlinderndes Mittel gegen die M. Fabry Neuropathie (Formaggio et al. 2022). Weitere systematisch untersuchte niedermolekulare Wirkstoffe, die den Prozess von Synthese und Transport lysosomaler Enzyme unterstützen können wurden in ER Stress-Auslösern (z.B. Tunicamycin), Inaktivatoren des proteasomalen Abbaus (z.B. MG-132) und anderen PPAR-modulierenden Wirkstoffe (z.B. Bezafibrat) analysiert. Die Verbindungen wurden zunächst im in vitro Überexpressionsmodell an neun ausgewählten M. Fabry Mutationen untersucht. Die Mutationen wurden dergestalt selektiert, dass sie in HEK293-H-Zellen (i) eine Restaktivität (≥1 % des Wildtyps) und (ii) Ansprechbarkeit auf DGJ (≥1,5-facher Anstieg, insgesamt ≥5 % des Wildtyps) aufwiesen, um deren Responsivitätspotential zu gewährleisten. Zum Zeitpunkt der vorliegenden Studie wurde ABX erst kürzlich als PC für M. Gaucher identifiziert. Bei Einzelverabreichung einer Konzentration von 40 µM zeigte es nur auf wenige AGAL-Formen eine signifikante Wirkung, darunter der Wildtyp, p.Ala156Val und p.Arg301Gln. Die Konzentrations-Wirkungs-Beziehung ergab eine EC_{50} von 17,4 µM für das Wildtyp-Enzym unter Verwendung eines sigmoidalen Kurvenanpassungsmodells. In Zellkultur als Kombinationsbehandlung mit DGJ eingesetzt, zeigte ABX eine signifikante zusätzliche Steigerung auf die Enzymaktivität aller neun getesteten AGAL Mutationen. In gleicher Weise verstärkte ABX synergistisch die Wirkung des ebenfalls als PC bekannten natürlichen Substrats Galactose (Frustaci et al. 2001) auf die untersuchten Mutationen. Die thermische Denaturierung unter steigenden DGJ- und ABX-Konzentrationen und die anschließende Enzymmessung wurden analog zu den Arbeiten von Maegawa und Kollegen (Maegawa et al. 2009) durchgeführt. Dabei zeigte sich kein nachweisbarer Effekt auf die Stabilität von rekombinantem AGAL (Agalsidase alfa) durch ABX. Dennoch zeigte sich ein zusätzlicher stabilisierender Effekt zur DGJ-vermittelten Stabilisierung bei zusätzlicher Gabe von 2,5 mM ABX. Zudem fungierte ABX nicht als Inhibitor von Agalsidase alfa. In Zellkultur erhöhte ABX die durch die beiden PCs DNJ und NB-DNJ erhöhte GAA Aktivität dreier ansprechbarer M. Pompe-assoziierter Mutationen in additiver Weise.

ABX konnte nach unseren Untersuchungen als potentiell LSD-übergreifender PC-*Enhancer* etabliert werden.

Die weiteren Substanzen wurden *bona fide* an der AGAL Mutante p.Arg301Gln getestet. Der PPARγ Agonist RSG zeigte eine synergistische Wirkung mit DGJ in ähnlicher Weise wie ABX. Allerdings schien die Wirkung der Einzelbehandlung mit RSG ausgeprägter zu sein, so dass RSG bei zusätzlichen grenzwertig DGJ-ansprechbaren Mutationen, p.Arg118Cys und p.Thr385Ala, erfolgreich getestet wurde. Eine eventuell unterschiedliche Mutationsspezifität verschiedener Proteostaseregulatoren könnte das Therapiespektrum niedermolekularer Substanzen erweitern, bedarf aber weiterführender mechanistischer Studien, um die Vorhersagbarkeit zu verbessern. Das RSG-Struktur- und Funktionsanalog Pioglitazon als auch das eine höhere Spezifität für PPARα aufweisende Bezafibrat wiesen ebenfalls aktivitätssteigernde Wirkung auf die AGAL Mutante p.Arg301Gln auf. Die proteasomalen Inhibitoren MG-132 und Lactacystin zeigten eine enzymstabilisierende Wirkung, aber keine Erhöhung der Aktivität, so dass davon auszugehen war, dass der Enzymabbau in gewissem Maße verhindert wurde, der Weitertransport und die Prozessierung von AGAL im HEK293-H-System jedoch nicht stattfanden oder nicht abgebildet werden konnten. Zum Vergleich, Ishii und Kollegen wiesen ebenfalls einen verringerten Abbau von AGAL-Mutanten in überexprimierenden COS-7 Zellen nach, maßen in ihrer Studie jedoch nicht die Enzymaktivität (Ishii et al. 2007). Daher stehen unsere Daten nicht im Widerspruch zu dieser Studie. Im Gegensatz dazu wurden positive Auswirkungen von proteasomalen Inhibitoren auf die β-Glu-Mutante anhand von Enzymaktivitätsmessungen gezeigt, die aber an patienteneigenen Zellen vorgenommen wurden (Mu et al. 2008). Das große Potential der Substanzklasse der proteasomalen Inhibitoren als Wirkstoffe bei LSDs ist ebenfalls an der Durchführung klinischer Studien zu NP-C und M. Pompe ablesbar (Sitarska et al. 2021), (NCT02525172[3]), so dass zu diesem Zeitpunkt offen bleiben muss, ob Proteasom-Inhibitoren eine wirksame Behandlungsoption für M. Fabry sein könnten. Die anderen Substanzen, die auf verschiedene Weise in die ER-Physiologie eingreifen und ER-Stress erzeugen, Kifunensin, Thapsigargin und Tunicamycin, hatten im Expressionssystem ebenfalls keine Wirkung auf p.Arg301Gln.

Sowohl ABX als auch RSG haben eine ganze Reihe von unterschiedlichen Auswirkungen auf die Zellphysiologie. Ein klarer Mechanismus kann für beide Wirkstoffe ohne weitere Untersuchungen noch nicht definiert werden. ABX ist ein nicht hemmender PC-*Enhancer*, der sowohl Auswirkungen auf den Kalziumhaushalt der Zelle als auch erweiterte genregulatorische Effekte ausübt. RSG zeigte in einer früheren Studie Ubiquitin-hemmende Wirkungen (Marfella et al. 2006). Wir konnten keinen Hinweis auf Hemmung des Proteasoms in der applizierten Konzentration feststellen. Um die Rolle des

[3] In dieser klinischen Studie wird Bortezomib als immunmodulatorisches Medikament zur Reduzierung von IgG Antikörpern auf die ERT eingesetzt.

Ubiquitin-Proteasom-Systems beim beobachteten RSG-Effekt zu untersuchen, behandelten wir die Zellen mit dem E1-Enzym-Hemmstoff Pyr-41, was weder einen Effekt auf die Aktivität noch auf den Abbau des AGAL Enzyms hatte, so dass die Ergebnisse dieser Studie die Modulation PPAR-regulierter Stoffwechselwege als wahrscheinlicheren Wirkmechanismus erscheinen lassen.

3.2.5 Identifizierung und mechanistische Untersuchungen an niedermolekularen Enzym-*Enhancern* (Studie 9)

Wenn es sich um Wirkstoffverbindungen handelt, die die Funktion einzelner Proteine oder ganzer molekularer Prozesse ausnutzen, um eine verstärkende Wirkung des mutierten lysosomalen Enzyms zu erreichen, sind Überexpressionsmodelle für die Translation in die Anwendung fehleranfälliger als endogene Modelle. Beispielsweise sind HEK293-H-Zellen auf Grund ihres stark abweichenden Karyotyps für Studien, welche genregulatorische Wirkstoffe nutzen, ungeeignet (Stepanenko und Dmitrenko 2015). Weitere Eingriffe in die Zellphysiologie wie die Veränderung durch Plasmidvektor-vermittelten Gentransfer erzeugen weitere Artefakte und schränken die Signifikanz mechanistischer Studien ein. PCs nehmen eine Ausnahmestellung bei den niedermolekularen Wirkstoffen ein und können daher in der Regel auch in Überexpressionsmodellen eingesetzt werden (Flanagan et al. 2009; Wu et al. 2011). Eine mögliche Erklärung ist, dass die Klasse der PCs direkt mit dem mutierten lysosomalen Enzym interagiert, dessen für die Ansprechbarkeit relevante strukturelle Charakteristika weitgehend unabhängig von Zelltyp und Expressionslevel zu sein scheinen. Gleichwohl ist die Liste an PC Molekülen noch kurz, deren Wirksamkeit sowohl im Überexpressionssystem als auch im endogenen Modell empirisch belegt wurde. In wirkmechanistischen Studien an M. Gaucher kommen so gut wie ausschließlich Patientenzellen zum Einsatz. Der Umweg über Expressionsmodelle ist unnötig, da die Verfügbarkeit geeigneter endogener Zellmodelle auf Grund der Häufigkeit bestimmter Missense Mutationen (c.1226A>G (p.Asn370Ser); c.1448T>C (p.Leu444Pro)) gegeben ist. Diese Mutationen stehen im Zentrum des Behandlungsinteresses. Derzeit gibt es keine Berichte zur Ansprechbarkeit auf niedermolekulare Medikamente, die den Hunderten von *GBA1* Missense Mutationen Rechnung tragen wie bei den breit angelegten Studien bei M. Fabry. Im Gegensatz zu den häufigen Mutationen bei M. Gaucher sind die häufigen Mutationen bei M. Fabry deutlich weniger verbreitet. Das Auftreten von Mutationen ist in der Regel auf eine oder wenige Familien beschränkt, was die Wahl einer Modellmutation für Medikamententests erschwert und die Verfügbarkeit geeigneter endogener Zellmodelle begrenzt. Dank intensiver Forschung an DGJ ist jedoch die Ansprechbarkeit der Mehrzahl aller bekannten *GLA* Missense Mutationen bekannt. Die Punktmutation c.902G>A (p.Arg301Gln) hat sich wiederholt als Beispiel für eine Proteinfehlfaltungsmutante (mit restlicher katalytischer Funktionalität) erwiesen, die sich demnach für die Untersuchung neuer niedermolekularer Wirkstoffkandidaten eignet (Ishii et al. 2007; Khanna et al. 2010; Lukas et al. 2013).

Für die vorliegende Studie erhielten wir mit freundlicher Genehmigung von Amicus Therapeutics (Cranbury, NJ, USA) eine hemizygote Fibroblastenlinie eines männlichen Patienten mit der c.902G>A Variante. Darüber hinaus konnte eine Fibroblastenlinie über das Coriell Institute for Medical Research (Camden, NJ, USA) bezogen werden, die hemizygot für eine C>G-Transversion im selben Codon in Exon 6 (c.901C>G) war, was zur Substitution von Arginin durch Glycin (p.Arg301Gly) führt.

Auf Grund der unbekannten Kohärenz der zuvor erhaltenen Daten im Überexpressionssystem haben wir nicht nur bereits positiv getestete Verbindungen (ABX, RSG) in den Fibroblasten getestet, sondern erneut ein Screening mit 23 Proteostase-regulierenden Verbindungen (PR) mit einer Vielzahl von Funktionen (Ionenkanalmodulatoren, UPR Stimulatoren, ERAD-Inhibitoren, Energiestoffwechselmodulatoren) durchgeführt. Die proteasomalen Regulatoren (PRs) wurden auf ihr Potenzial zur Steigerung der zellulären AGAL-Enzymaktivität untersucht. Als wichtigste Eigenschaften wirksamer PRs bei M. Fabry erwiesen sich die Fähigkeiten, die *GLA*-Genexpression zu induzieren und das Proteasom zu hemmen (insbesondere die Chymotrypsin-ähnliche Aktivität). Darüber hinaus wurde ein charakteristisches Transkriptionsmuster beobachtet, das aus 29 Genen bestand. Hierbei fiel auf, dass die regulierten Gene direkt mit Proteostase-assoziierten Prozessen, »Proteasomaler Abbau«, »Parkin-Ubiquitin-Proteasom-System« und der »NRF2-Abbauweg« (nach Wikipathways (Kutmon et al. 2016)) in Verbindung standen. Wir vermuteten daher, dass diese Transkriptionseffekte auf wichtige Mechanismen hinweisen und hilfreich für künftige Wirksamkeitsvorhersagen potentieller PRs sein können. Wichtige Genexpressionssignaturen sind aus Datenbanken wie iLINCS extrahierbar (Pilarczyk et al. 2022) und können künftige Arzneimittelentdeckungsprojekte unterstützen. Darüber hinaus mag es Kausalitäten geben, die eines Tages therapeutische *Targets* werden definieren können.

Die wesentlichen wirksamen Verbindungen entstammten hier der Klasse der proteasomalen Inhibitoren wie Bortezomib/MG-132/Lactacystin, gleichwohl sich der Inhibitor Celastrol, der sowohl zu einer erhöhten *GLA*-Genexpression als auch zu einer verringerten proteasomalen Aktivität führte, als unwirksam herausstellte. Gründe hierfür könnten eine unzureichende Erhöhung der Genexpression bzw. eine unzureichende Hemmung der Proteasom-Aktivität oder andere ungünstige, noch unbekannte Einflussfaktoren sein, die einer Verstärkung von AGAL entgegenwirkten.

Weitere Erkenntnisse waren insbesondere der synergistische Effekt der PRs im Rahmen einer Kombinationsbehandlung mit dem klinisch zugelassenen DGJ. Dies könnte ein Indikator für eine klinisch relevante Steigerung der Wirksamkeit der PCT und eine Ausweitung des Wirkungsspektrums auf Mutationen sein, die bisher als unzureichend ansprechbar galten. Darüber hinaus wurde gezeigt, dass Verbindungen, die sich auf die Mutation c.902G>A positiv auswirkten, die AGAL-Aktivität von c.901C>G (p.Arg301Gly) in ähnlicher Weise positiv beeinflussten.

4 Zusammenfassung

Die vergleichsweise intensiv erforschten lysosomalen Speicherkrankheiten M. Fabry, M. Gaucher und M. Pompe zeigen eindrucksvoll die Fortschritte auf dem Gebiet der Diagnostik und Therapie. In den letzten zwanzig Jahren wurden in diesem Bereich technologische Errungenschaften wie die genetische Sequenzierung mit der Next Generation Sequencing-Technologie sowie die Entdeckung und Entwicklung von Biomarkern mit Hilfe fortschrittlicher spektrometrischer Methoden zu Diagnosezwecken implementiert.

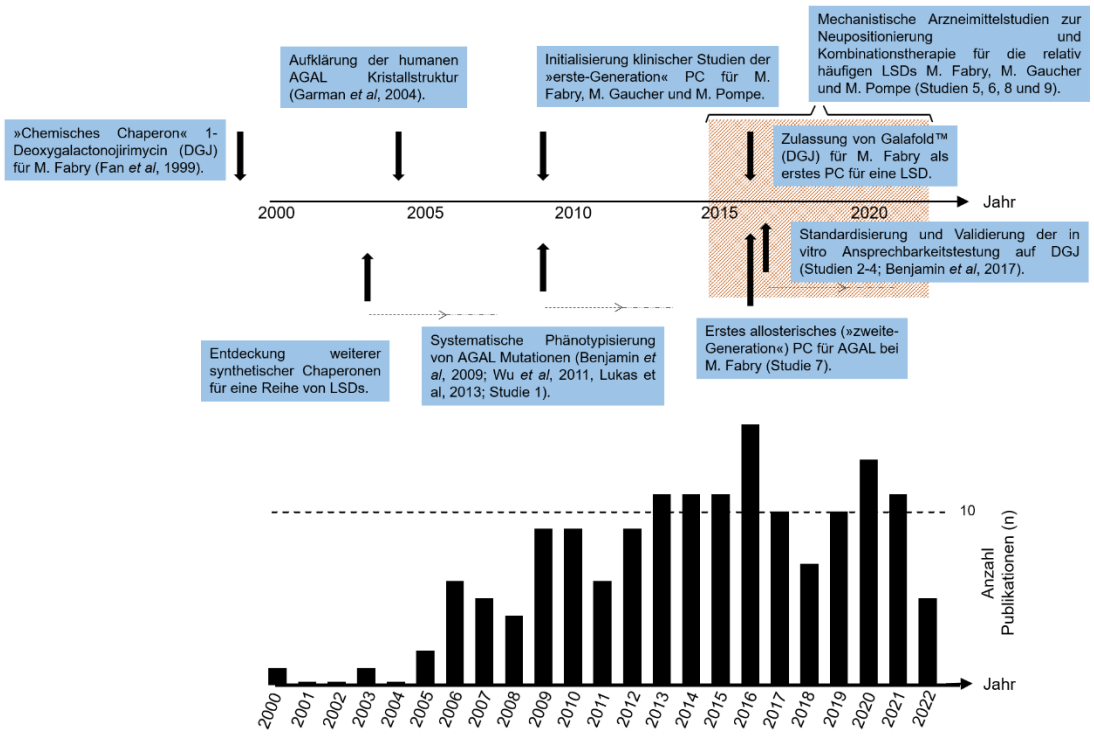

Abb. 6. Pharmakologische Chaperone bei M. Fabry. Oben: Das Diagramm zeigt einige wegweisende Entwicklungen in der Forschung und Medizin von niedermolekularen PCs in LSDs (hier mit Fokus auf M. Fabry) in den Jahren 1999 bis 2022. Die neun eigenen Studien sind im Diagramm ebenso benannt und in den Kontext der Forschung eingebettet wie die einflussreichsten externen Studien. Der rot schraffierte Bereich kennzeichnet den Zeitraum von 2015 bis 2022, in dem die hier zusammengefassten Studien durchgeführt wurden. Unten: Entwicklung der Literatur zu LSDs und pharmakologischen Chaperonen in Zahlen. Gezeigt ist die Anzahl an Studienveröffentlichungen in Abhängigkeit des Veröffentlichungsjahres. Es wurden die Suchanfragen [„lysosomal storage*“ AND „pharmacological chaperone“] als auch [„lysosomal storage*“ AND „chemical chaperone“] verwendet, um einerseits der Tatsache Rechnung zu tragen, dass die gebräuchlichen Begriffe *lysosomal storage disease* als auch *lysosomal storage disorder* in der Suchanfrage berücksichtigt werden und andererseits, dass der Terminus *pharmacological chaperone* in der LSD Literatur erst im Jahr 2006 erstmalig auftaucht.

Die Entdeckung und Weiterentwicklung neuer und alternativer Therapieformen waren sicherlich eine Triebkraft für diesen Fortschritt, da dadurch das Interesse von pharmazeutischer Seite geweckt war, die Identifizierung von Patienten im Rahmen großer Screening-Programme wirtschaftlich zu unterstützen. Dies wirkte sich wiederum sowohl für die Anbieter der pharmazeutischen Produkte

als auch für die Patienten vorteilhaft aus, denn eine frühzeitig erkannte und behandelte Symptomatik führt zu einer deutlichen Verbesserung und damit der Prognose der Erkrankung. Da die meisten Therapeutika unabhängig der Patientengenetik funktionieren, hinkten mechanistische Untersuchung an individuellen Mutationen zum zeitlichen Beginn der hier vorgestellten Studien der Entwicklung hinterher. Relativ neu war die Erkenntnis, dass einige Genmutationen mit einer Fehlfaltung des Proteins oder Enzyms einhergingen, was einen Rückbehalt des Enzyms im ER und schließlich einem vorzeitigen Abbau im Proteasom zur Folge hatte. Gleichwohl rückte die Genetik der Patienten erst eine ganze Weile nach der Entdeckung des ersten pharmakologischen Chaperons für M. Fabry, dem Iminozucker 1-Deoxygalactonojirimycin, im Jahr 1999 in den Fokus. Ein wichtiger Meilenstein in dieser Entwicklung war die Entschlüsselung der Kristallstruktur des menschlichen AGAL Enzyms, die eine computergestützte Vorhersagbarkeit des durch Missense Mutationen verursachten biochemischen Defekts verbesserte (Abb. 6, oberer Teil). Nach und nach zeigte sich in der pathomechanistischen Betrachtung, dass eine Vielzahl der zahlreichen Missense Mutationen bei M. Fabry (und anderen LSDs) von Proteinfehlfaltung betroffen waren. Therapietheoretisch wurde somit die Aufmerksamkeit von der Funktionalität der Enzyme im Lysosom einerseits und vom lysosomalen Speichermaterial andererseits hin zur Bildung und Reifung des Enzyms im ER verschoben. Mit dem neuen Thema der Wirkstoffe, die die Faltung der mutierten Enzyme im ER positiv beeinflussen könnten, wurden in den 2000er Jahren PC-Kandidaten für weitere LSDs entdeckt (Abb. 6, oberer Teil). Diese ähnelten dem natürlichen Substrat und traten mit der Bindungsstelle im aktiven Zentrum in Wechselwirkung, so dass sie in ihrer Eigenschaft als Hemmstoffe auch als »erste Generation« PCs bezeichnet wurden. In den Jahren 2009 und 2011 wurde in zwei Publikationen erstmals ein systematischer Ansatz zur Bewertung der Ansprechbarkeit von 80 *GLA* Missense Mutationen auf das PC verfolgt, der erstmals das pharmazeutische Potenzial im Hinblick auf die Wirksamkeit aufzeigte und eine Vorstellung von der Anzahl der ansprechbaren Patienten gab. Die hier vorgestellten neun Studien der Jahre 2015 - 2022 fallen zeitlich in eine Phase, in der bereits die ersten klinischen Studien für M. Fabry, M. Gaucher und M. Pompe dieser ersten Generation PCs abgeschlossen waren. Die zunächst steigende und dann auf einem gleichen Niveau bleibende Zahl von Primärartikeln in PubMed (Abb. 6, unterer Teil) kann als Indikator für die zunehmend vielversprechende Forschung an neuen PC-Kandidaten dienen, deren Entdeckung mit DGJ bei M. Fabry begann und sich bald auf andere LSDs erstreckte.

Unsere Untersuchungen legten das Augenmerk auf die Analyse weiterer Mutationen unter Erweiterung um klinische, biochemische und bioinformatische Analysetechniken, der Standardisierung der AGAL (und GAA) Enzymaktivitätsmessung und trugen zur systematischen Phänotypisierung der Mutationen in Hinblick auf deren Pathogenitätspotential und somit zum heutigen umfassenden molekularen Verständnis über diese Mutationen bei (Lukas et al. 2013; Studien 1-4). Ein Wandel im Grundverständnis der Bewertung von Mutationen im *GLA*-Gen lässt sich an folgendem Beispiel

aufzeigen: In älteren Studien werden niedrigere Prävalenzen für das Auftreten von M. Fabry von 1:40.000 bis 1:117.000 angegeben (Śnit et al. 2022). Neuere Studien der späten 2000er Jahre ließen auf eine wesentlich höhere Häufigkeit von M. Fabry-assoziierten *GLA*-Mutationen schließen (Spada et al. 2006; Hwu et al. 2009; Wittmann et al. 2012). Diese Befunde führten zu der Annahme, dass nur etwa 10-20 % der M. Fabry-Fälle mit dem klassisch-schweren Krankheitsverlauf assoziiert sind, während die weitaus höhere Zahl auf zuvor häufig übersehene mildere Krankheitsvarianten zurückzuführen ist. Die Thematik wurde durch unsere Studien erneut aufgegriffen und das bisherige Bild geschärft. Durch die vielen *GLA*-Genvarianten mit hoher Enzymaktivität und unklarer klinischer Kennzeichen ist zu erwarten, dass es sich bei einer großen Zahl dieser *GLA*-Varianten um gutartige Varianten handelt, bei deren Vorkommen es nur in seltenen Fällen zum Ausbruch einer M. Fabry-Symptomatik kommt (Duro et al. 2018). Mit anderen Worten: Die hohen Zahlen an *GLA*-Gen Varianten beschreiben zunächst Allelhäufigkeiten, die nicht zwingend mit M. Fabry in Einklang stehen, so dass die Prävalenz der atypisch-milden M. Fabry-Krankheit spekulativ bleibt, aber sehr wahrscheinlich niedriger liegt als in den 2000er Studien gezeichneten Szenarien. Denkbar ist auch ein abweichender Pathomechanismus fußend auf fehlerhafter Proteinfaltung, die zu toxischem *gain of function* führen könnte, was sich aus unserem Fliegenmodell-Ansatz ableiten lässt (Studie 5) und auch in neueren Studien dokumentiert wird (Riillo et al. 2023).

Überdies gelang es den Ansprechbarkeitslevel zahlreicher *GLA*-Mutationen für das PC DGJ zu bestimmen und die Datenlage für behandelnde Ärzte zu verbessern, indem der klinisch zugelassene pharmakogenetische Enzymassays (GLP-HEK) einer unabhängigen Validierung unterzogen wurde. Die Robustheit der Performance des PCs zeigte sich auch in anderen Krankheitsmodellen wie der Fruchtfliege *D. melanogaster* (Studie 5). Zusammenfassend zeigen unsere Studien ein großes Potenzial für die therapeutische Anwendung von DGJ bei M. Fabry, da etwa die Hälfte aller untersuchten Missense Mutationen einen biochemischen Gewinn durch die Behandlung mit diesem niedermolekularen Substratmimetikum zeigte. Die Identifizierung nicht-inhibitorischer PC Kandidaten der zweiten Generation für M. Fabry waren Gegenstand einer weiteren Studie, die offenbarte, dass der nukleophile Radikalfänger 2,6-Dithiopurin ein verändertes Wirkspektrum als PC für mutierte AGAL besitzt (Studie 7). Es besteht daher Hoffnung, dass in Zukunft Patienten mit solchen Mutationen individuell behandelt werden können, die bisher nicht auf das zugelassene PC angesprochen haben.

Ambroxol ist ein Kandidat für ein pharmakologisches Chaperon bei M. Gaucher und könnte dank seiner nur schwachen Hemmwirkung auf die β-Glu und seine allgemein sehr gute Verträglichkeit die Problemfelder bisheriger PCT Kandidaten bei M. Gaucher beseitigen. Mechanistische Untersuchungen konnten die enzymfördernde Wirkung auf β-Glu bestätigen (Studie 6). In Verbindung mit den zwischenzeitlich veröffentlichten Studien von Zimran *et al*. (2013) und Narita *et al*. (2016) legen die Daten nahe, dass ABX als adjuvante Medikation zur derzeitigen ERT-Standardbehandlung

oder als Verstärker eines PC Wirkstoffs wie IFG eine Option zur Steigerung der Effektivität bekannter M. Gaucher Therapeutika darstellen kann. Ein derartiger kombinatorischer Ansatz verschiedener Wirkstoffkandidaten zur Steigerung von GAA und AGAL war Gegenstand der Studien 8 und 9, in denen verschiedene proteostaseregulierende Wirkstoffkandidaten (PRs) zum Einsatz kamen. Sowohl bei der singulären als auch bei der kombinatorischen Anwendung zeigten diverse Verbindungen wie ABX und Bortezomib wirksame Verstärkungseffekte auf die mutierten Enzymformen. Ein spezifisches Funktionsprofil einer solchen wirksamen Verbindung zur Steigerung der AGAL Enzymaktivität beruhte u.a. auf der Hemmung der proteasomalen Aktivität und der Steigerung der mRNA-Expression des mutierten *GLA*-Gens in Patientenzellen. Darüber hinaus wiesen die Verbindungen globale Auswirkungen auf die zelluläre mRNA Transkription aus, so dass charakteristische Transkriptionssignaturen entstanden, die bei der zukünftigen Suche nach Wirkstoffkandidaten helfen können.

Die präsentierten neun Studien liefern Anhaltspunkte für eine effiziente Identifizierung künftiger Arzneimittel. Da die derzeitigen Behandlungsmethoden, z. B. die Einzelwirkstofftherapie durch Enzymersatz, Substratreduzierung oder pharmakologische Chaperone, für eine große Zahl schwer erkrankter Patienten (und damit verbundener Genetik) auf Grund unzureichender Wirksamkeit ungeeignet sind, nähren unsere Studien an niedermolekularen Wirkstoffkandidaten die Hoffnung, dass diese therapeutischen Konzepte in Zukunft wirksamer und angemessener sein werden.

5 Zukunftsperspektive

Die derzeitigen experimentellen Ansätze zur Behandlung von LSDs zielen auf eine Vielzahl von zellulären Prozessen und Pfaden ab. Zu den möglichen Zielen pharmakologischer Interventionen gehören Transkription und Translation, das Autophagie-/Lysosom-System (Rega et al. 2016), die ER-Proteostase, der Proteintransport (Yam et al. 2007), oxidative und entzündliche Prozesse (Tarallo et al. 2021; Zhang et al. 2022) sowie der Kalziumhaushalt (Wang et al. 2011; Zhong et al. 2016) und die Änderung der Membraneigenschaften (Kakhlon et al. 2020). Die Stoff- und Funktionsklassen der Medikamente sind noch vielfältiger. Neben der bekannten ERT, die über die Aufnahme von Man-6-P-Rezeptoren in der äußeren Zellmembran (und anderen Aufnahmemechanismen, z.B. über Fusionsprotein-ERT mit anti-Human-Transferrin-Rezeptor-Antikörper) funktionieren, Hemmstoffen der Substratbildung und pharmakologischen Chaperonen gibt es eine ganze Reihe an Verbindungen, die therapeutisch diskutiert werden. Unter ihnen sind Hemmstoffe von Histon-Deacetylase, Hemmstoffe der ERAD, UPR Stimulatoren, Energie- und Lipidstoffwechsel Modulatoren, TFEB und mTOR (*mechanistic Target of Rapamycin*) Regulatoren, miRNAs und translationale *read-through*-induzierende Wirkstoffe (auch als *nonsense suppressors* bekannt). Mechanistisch greifen viele dieser

Stoffe als Regulatoren der Transkription in den zellulären Stoffwechsel ein und beeinflussen mehrere Pathways gleichzeitig. Doch selbst unter normalen Bedingungen sind viele der oben genannten Pathways nur unzureichend erforscht, und die Komplexität von Arzneimittelwirkungen und –wechselwirkungen mit anderen Pathways unterbewertet. Eine Vielzahl an Arzneistoffen sind wahre »*black boxes*«. Bei nur etwa der Hälfte der von der FDA zugelassenen Medikamente ist der Wirkmechanismus laut offizieller Kennzeichnung vollständig geklärt, da die Kenntnis des genauen Wirkmechanismus keine regulatorische Voraussetzung für die Zulassung eines Medikaments ist (Davis 2020). Die konsequente Weiterentwicklung zentraler, autoritativer Dokumentationssysteme wie der »*Guide to PHARMACOLOGY*« (Pawson et al. 2014), welcher alle zellulären Folgen einer Behandlung mit jedem der derzeit zugelassenen und experimentellen Arzneimittel nachvollziehbar zugänglich machen, muss in Zukunft ein Forschungsimperativ sein. Die Grundlagenforschung an seltenen Mendelschen Krankheiten ist daher so wertvoll, weil die beobachtete Pathophysiologie auf einer monogenen Störung beruht. Die Entwicklung von Modellsystemen zur Wirkstofftestung für seltene monogene LSDs kann somit den Zweck erfüllen, ein besseres Verständnis über die physiologischen und pathophysiologischen Abläufe und neue Zusammenhänge zu erlangen, woraus sich wiederum das Verständnis von Medikamentenwirkung verbessern und weitere Therapieansätze ableiten lassen. Am besten geeignet für translationale Studien an Erbkrankheiten sind Patienten-abgeleitete endogene Mutationszellmodelle, da sich diagnostische, prognostische und vor allem therapeutische Verfahren hierin effizient entwickeln lassen. Ein besonderes Augenmerk sollte daher der Einrichtung und Pflege von Zellarchiven zur Verbesserung der Forschungsinfrastruktur gewidmet werden, um die aktuell defizitäre Verfügbarkeit wichtiger Materialien für Forschungsarbeiten zur Herstellung genetischer Zellmodelle zu gewährleisten. Anfänge wurden durch die Errichtung des Telethon Network of Genetic Biobanks oder das vor 50 Jahren ins Leben gerufene und durch das Coriell Institute for Medical Research (Camden, NJ, USA) betriebene Human Genetic Cell Repository des National Institute of General Medical Sciences gemacht. Der Ansatz setzt die Bereitschaft von Patienten und Patientenorganisationen voraus, sich an den Forschungsbemühungen zu beteiligen. Es ist festzuhalten, dass die Beteiligung von Patientenorganisationen als ein positives Kriterium für die Förderwürdigkeit eines Forschungsprojektes durch öffentliche und nicht-öffentliche Projektträger immer größere Bedeutung erlangt.

Natürlich existieren auch Limitationen für den Einsatz von Patientenzellen in der Wirkstofferprobung. LSDs stehen meist in Verbindung mit Hunderten unterschiedlicher Mutationen, die verschiedene pathogene Mechanismen in Gang setzen - eine besondere Bedeutung fällt den so genannten Missense Mutationen zu – und deren funktionsschädigende Effekte sowie Einfluss auf die Pharmakogenetik, die Wirksamkeit eines Medikaments, schwer vorhersehbar machen. Ein individualisierter Ansatz wie der der pharmakologischen Chaperone bedarf eines Systems, welches die

Testung von Wirkstoffkandidaten an einem breiten Spektrum von Mutationen ermöglicht, um die Wirkstoffe in angemessenen Modellen zu testen, so dass jene, die nur für eine kleinere Gruppe von Patienten geeignet sind, in der Klinik nicht an falsch konzipierten Studien scheitern. Der seit 2016 klinisch validierte und von den Gesundheitsbehörden zugelassene pharmakogenetische »GLP HEK« Assay für die Beurteilung, ob ein M. Fabry Patient für die DGJ-Behandlung geeignet ist oder nicht, ist ein Beispiel für die erfolgreiche Implementierung eines Expressionsmodells in die klinische Praxis (Benjamin et al. 2017). Gleichwohl konnte in unseren Studien nachgewiesen werden, dass der beobachtete pharmakologische Effekt des DGJ im endogenen System vergleichsweise etwas niedrigere Effekte aufwies als im Expressionsmodell. Es ist daher Vorsicht geboten, die in Überexpressionsmodellen wie dem »GLP HEK« erzielten Effekte nicht zu überschätzen. Darüber hinaus zeigten wir, dass das Expressionssystem nicht für jede Wirkklasse von Verbindungen geeignet war einen Behandlungseffekt nachzuweisen.

Ein weiterer wichtiger Aspekt, der sich in den letzten Jahren der Forschung herauskristallisiert hat und den unsere Studien kontinuierlich verfolgen, ist die Kombinationstherapie. Klinische Wirkstoffstudien sind bei seltenen Erkrankungen besonders durch geringe Teilnehmerzahl, geografische Streuung der Patienten und geringe Anzahl von interessierten oder angemessen ausgebildeten Forschern und Ärzten und nicht zuletzt Vor-Zulassungskosten in Höhe von über 800 Millionen Dollar (Augustine et al. 2013). Die Entwicklung eines neuen Medikaments ist nicht nur kostspielig; seltene, tödliche und schnell fortschreitende pädiatrische Erkrankungen erlauben nicht den Luxus von über einen langen Zeitraum angelegten Studien. Bei einem individuellen Ansatz wie den PCs kommt die Pharmakogenetik als einzubeziehendes Kriterium für eine Therapie im Vergleich zu prinzipiell uneingeschränkt einsetzbaren Behandlungsformen wie der ERT als begrenzender Faktor hinzu. Die tendenziell aufwendigeren Testverfahren unter Einbezug der Pharmakogenetik (z.B. "GLP HEK"-Test) zur Erhöhung der Verschreibungssicherheit und Wirksamkeit sind oben bereits angeführt. Abhilfe können hier *Repurposing*/*Repositioning* Ansätze schaffen, um Kosten- und Zeitfaktor signifikant zu senken, da bekannte, verträgliche und teils für andere Erkrankungen zugelassene Wirkstoffe zugängig gemacht werden. Allerdings wirkt sich hierin bei einem Medikament wie ABX die begrenzte Marktexklusivität mindernd auf die Aussicht auf Profite aus (Pearson et al. 2022). Dementsprechend sind aufwendige Entdeckungsprozesse, ein begrenztes Wirkungsspektrum und eine unzureichende klinische Wirksamkeit gewichtige Argumente für eine eher abwartende Haltung der Industrie, so dass bestimmte Wirkstoffe in Schubladen landen, anstatt in aufwendigen Zulassungsverfahren eine Chance zu erhalten. Nur 15 % der neuen Wirkstoffe in der klinischen Prüfung sind Monotherapien mit niedermolekularen Verbindungen, und nur 3 % sind PC (Verma et al. 2021).

Kombinationstherapien können eine passende Lösung für die fehlende Wirksamkeit und die geringe Zahl zugänglicher Patienten für niedermolekulare Therapieansätze sein. Zur Behandlung der

Mukoviszidose wurde kürzlich der dreifach-Wirkkomplex Trikafta® (Vertex Pharmaceuticals Inc., Boston, MA, USA) zugelassen, dessen Komponenten aus Elexacaftor, Ivacaftor und Tezacaftor bestehen. Bei allen drei Einzelwirkstoffen handelt es sich um mutationsspezifische Korrektoren des CFTR (Cystic Fibrosis Transmembrane Conductance Regulator) Chloridkanals. Daher ist das Präparat nur für Patienten zugelassen, die mindestens eine F508del-Mutation im *CFTR*-Gen aufweisen, was auf geschätzt 90 % der Mukoviszidose-Patienten zutrifft. An den Beispielen die ERT durch Zugabe des PCT-Medikaments DNJ (M. Pompe) bzw. des EET Medikaments ABX (M. Gaucher Typ III) effektiver zu machen, zeigt die Bemühung diesen Ansatz bei den LSD Krankheiten einzusetzen (Khanna et al. 2012; Narita et al. 2016; Charkhand et al. 2019).

Was die Kosten der PCT/ERT-Kombinationstherapie betrifft, so lohnt sich ein Blick auf die Situation bei M. Fabry. Die Kosten für die ERT belaufen sich auf etwa 300.000 US$. Die Kosten der PCT mit dem Iminozucker DGJ liegen in der gleichen Größenordnung (Pharmacoeconomic Review Report: Migalastat (Galafold): (Amicus Therapeutics): Indication: Fabry Disease [Internet] 2018). Geht man davon aus, dass eine Therapie mit DNJ bei M. Pompe in einer ähnlichen Größenordnung liegen würde und unterstellt, dass keine Dosisanpassung der einzelnen Wirkstoffkomponenten vorgenommen wird, würden die Kosten für eine *Next-Generation* ERT somit potenziell astronomische Höhen erreichen. Die ergänzte Medikamentenkomponente ABX bei M. Gaucher könnte dagegen eine kostengünstigere Alternative sein. Ausgehend vom Grundpreis des Hustensaftes Mucosolvan® mit dem Wirkstoff Ambroxolhydrochlorid wären die jährlichen Kosten von zusätzlich 5.000 € für die Supplementierung vergleichsweise gering. Die Frage, ob ABX als Ergänzung zur ERT für eine breite Anwendung bei M. Gaucher Typ III wirksam genug ist, bedarf weiterer Klärung im Rahmen klinischer Studien, hat allerdings neben dem medizinischen auch einen politischen Aspekt.

6 Literaturverzeichnis

Abe, A.; Wild, S. R.; Lee, W. L.; Shayman, J. A. (2001): Agents for the treatment of glycosphingolipid storage disorders. In: *Current drug metabolism* 2 (3), S. 331–338. DOI: 10.2174/1389200013338414.

Adzhubei, Ivan A.; Schmidt, Steffen; Peshkin, Leonid; Ramensky, Vasily E.; Gerasimova, Anna; Bork, Peer et al. (2010): A method and server for predicting damaging missense mutations. In: *Nature methods* 7 (4), S. 248–249. DOI: 10.1038/nmeth0410-248.

Aerts, Johannes M.; Groener, Johanna E.; Kuiper, Sijmen; Donker-Koopman, Wilma E.; Strijland, Anneke; Ottenhoff, Roelof et al. (2008): Elevated globotriaosylsphingosine is a hallmark of Fabry disease. In: *Proceedings of the National Academy of Sciences of the United States of America* 105 (8), S. 2812–2817. DOI: 10.1073/pnas.0712309105.

Aerts, Johannes M.; Hollak, Carla; Boot, Rolf; Groener, Ans (2003): Biochemistry of glycosphingolipid storage disorders: implications for therapeutic intervention. In: *Philosophical transactions of the Royal Society of London. Series B, Biological sciences* 358 (1433), S. 905–914. DOI: 10.1098/rstb.2003.1273.

Alberts, Bruce (2002): Molecular biology of the cell. 4. ed. New York, NY: Garland Science.

Altarescu, G.; Hill, S.; Wiggs, E.; Jeffries, N.; Kreps, C.; Parker, C. C. et al. (2001): The efficacy of enzyme replacement therapy in patients with chronic neuronopathic Gaucher's disease. In: *The Journal of pediatrics* 138 (4), S. 539–547. DOI: 10.1067/mpd.2001.112171.

Andrade, Jason; Waters, Paula J.; Singh, R. Suneet; Levin, Adeera; Toh, Bee-Chin; Vallance, Hilary D.; Sirrs, Sandra (2008): Screening for Fabry disease in patients with chronic kidney disease: limitations of plasma alpha-galactosidase assay as a screening test. In: *Clinical journal of the American Society of Nephrology : CJASN* 3 (1), S. 139–145. DOI: 10.2215/CJN.02490607.

Andreotti, Giuseppina; Citro, Valentina; Crescenzo, Agostina de; Orlando, Pierangelo; Cammisa, Marco; Correra, Antonella; Cubellis, Maria Vittoria (2011): Therapy of Fabry disease with pharmacological chaperones: from in silico predictions to in vitro tests. In: *Orphanet journal of rare diseases* 6, S. 66. DOI: 10.1186/1750-1172-6-66.

Andreotti, Giuseppina; Guarracino, Mario R.; Cammisa, Marco; Correra, Antonella; Cubellis, Maria Vittoria (2010): Prediction of the responsiveness to pharmacological chaperones: lysosomal human alpha-galactosidase, a case of study. In: *Orphanet journal of rare diseases* 5, S. 36. DOI: 10.1186/1750-1172-5-36.

Appelqvist, Hanna; Wäster, Petra; Kågedal, Katarina; Öllinger, Karin (2013): The lysosome. From waste bag to potential therapeutic target. In: *Journal of molecular cell biology* 5 (4), S. 214–226. DOI: 10.1093/jmcb/mjt022.

Atrian, Sílvia; López-Viñas, Eduardo; Gómez-Puertas, Paulino; Chabás, Amparo; Vilageliu, Lluïsa; Grinberg, Daniel (2008): An evolutionary and structure-based docking model for glucocerebrosidase-saposin C and glucocerebrosidase-substrate interactions - relevance for Gaucher disease. In: *Proteins* 70 (3), S. 882–891. DOI: 10.1002/prot.21554.

Augustine, Erika F.; Adams, Heather R.; Mink, Jonathan W. (2013): Clinical trials in rare disease: challenges and opportunities. In: *Journal of child neurology* 28 (9), S. 1142–1150. DOI: 10.1177/0883073813495959.

Ausems, M. G.; Verbiest, J.; Hermans, M. P.; Kroos, M. A.; Beemer, F. A.; Wokke, J. H. et al. (1999): Frequency of glycogen storage disease type II in The Netherlands: implications for diagnosis and genetic counselling. In: *European journal of human genetics : EJHG* 7 (6), S. 713–716. DOI: 10.1038/sj.ejhg.5200367.

Azevedo, Olga; Gago, Miguel Fernandes; Miltenberger-Miltenyi, Gabriel; Sousa, Nuno; Cunha, Damião (2020): Fabry Disease Therapy: State-of-the-Art and Current Challenges. In: *International journal of molecular sciences* 22 (1). DOI: 10.3390/ijms22010206.

Ballabio, Andrea; Bonifacino, Juan S. (2020): Lysosomes as dynamic regulators of cell and organismal homeostasis. In: *Nature reviews. Molecular cell biology* 21 (2), S. 101–118. DOI: 10.1038/s41580-019-0185-4.

Balwani, Manisha; Grace, Marie E.; Desnick, Robert J. (2011): Gaucher disease: when molecular testing and clinical presentation disagree -the novel c.1226AG(p.N370S)--RecNcil allele. In: *Journal of inherited metabolic disease* 34 (3), S. 789–793. DOI: 10.1007/s10545-011-9307-7.

Bendikov-Bar, Inna; Ron, Idit; Filocamo, Mirella; Horowitz, Mia (2011): Characterization of the ERAD process of the L444P mutant glucocerebrosidase variant. In: *Blood cells, molecules & diseases* 46 (1), S. 4–10. DOI: 10.1016/j.bcmd.2010.10.012.

Benjamin, Elfrida R.; Della Valle, Maria Cecilia; Wu, Xiaoyang; Katz, Evan; Pruthi, Farhana; Bond, Sarah et al. (2017): The validation of pharmacogenetics for the identification of Fabry patients to be treated with migalastat. In: *Genetics in medicine : official journal of the American College of Medical Genetics* 19 (4), S. 430–438. DOI: 10.1038/gim.2016.122.

Borie-Guichot, Marc; Tran, My Lan; Génisson, Yves; Ballereau, Stéphanie; Dehoux, Cécile (2021): Pharmacological Chaperone Therapy for Pompe Disease. In: *Molecules (Basel, Switzerland)* 26 (23). DOI: 10.3390/molecules26237223.

Brady, R. O.; Gal, A. E.; Bradley, R. M.; Martensson, E.; Warshaw, A. L.; Laster, L. (1967): Enzymatic defect in Fabry's disease. Ceramidetrihexosidase deficiency. In: *The New England journal of medicine* 276 (21), S. 1163–1167. DOI: 10.1056/NEJM196705252762101.

Brady, R. O.; Kanfer, J. N.; Bradley, R. M.; Shapiro, D. (1966): Demonstration of a deficiency of glucocerebroside-cleaving enzyme in Gaucher's disease. In: *The Journal of clinical investigation* 45 (7), S. 1112–1115. DOI: 10.1172/JCI105417.

Braulke, Thomas; Bonifacino, Juan S. (2009): Sorting of lysosomal proteins. In: *Biochimica et biophysica acta* 1793 (4), S. 605–614. DOI: 10.1016/j.bbamcr.2008.10.016.

Brooks, Doug; Turner, Chris; Muller, Viv; Hopwood, John J.; Meikle, Peter (2007): I-Cell Disease: Springer US (Lysosomal Storage Disorders).

Brouns, Raf; Thijs, Vincent; Eyskens, François; van den Broeck, Marleen; Belachew, Shibeshih; van Broeckhoven, Christine et al. (2010): Belgian Fabry study. Prevalence of Fabry disease in a cohort of 1000 young patients with cerebrovascular disease. In: *Stroke* 41 (5), S. 863–868. DOI: 10.1161/STROKEAHA.110.579409.

Cammisa, Marco; Correra, Antonella; Andreotti, Giuseppina; Cubellis, Maria Vittoria (2013): Fabry_CEP: a tool to identify Fabry mutations responsive to pharmacological chaperones. In: *Orphanet journal of rare diseases* 8, S. 111. DOI: 10.1186/1750-1172-8-111.

Castilla, Javier; Rísquez, Rocío; Cruz, Deysi; Higaki, Katsumi; Nanba, Eiji; Ohno, Kousaku et al. (2012): Conformationally-locked N-glycosides with selective β-glucosidase inhibitory activity: identification of a new non-iminosugar-type pharmacological chaperone for Gaucher disease. In: *Journal of medicinal chemistry* 55 (15), S. 6857–6865. DOI: 10.1021/jm3006178.

Charkhand, Behshad; Scantlebury, Morris H.; Narita, Aya; Zimran, Ari; Al-Hertani, Walla (2019): Effect of Ambroxol chaperone therapy on Glucosylsphingosine (Lyso-Gb1) levels in two Canadian patients with type 3 Gaucher disease. In: *Molecular genetics and metabolism reports* 20, S. 100476. DOI: 10.1016/j.ymgmr.2019.100476.

Chen, Yuehong; Sud, Neetu; Hettinghouse, Aubryanna; Liu, Chuan-ju (2018): Molecular regulations and therapeutic targets of Gaucher Disease. In: *Cytokine & growth factor reviews* 41, S. 65–74. DOI: 10.1016/j.cytogfr.2018.04.003.

Chien, Yin-Hsiu; Lee, Ni-Chung; Chiang, Shu-Chuan; Desnick, Robert J.; Hwu, Wuh-Liang (2012): Fabry disease. Incidence of the common later-onset α -galactosidase A IVS4+919G → A mutation in Taiwanese newborns--superiority of DNA-based to enzyme-based newborn screening for common mutations. In: *Molecular medicine (Cambridge, Mass.)* 18, S. 780–784. DOI: 10.2119/molmed.2012.00002.

Citro, Valentina; Cammisa, Marco; Liguori, Ludovica; Cimmaruta, Chiara; Lukas, Jan; Cubellis, Maria Vittoria; Andreotti, Giuseppina (2016): The Large Phenotypic Spectrum of Fabry Disease Requires Graduated Diagnosis and Personalized Therapy: A Meta-Analysis Can Help to Differentiate Missense Mutations. In: *International journal of molecular sciences* 17 (12). DOI: 10.3390/ijms17122010.

Clayton, Nicholas P.; Nelson, Carol A.; Weeden, Timothy; Taylor, Kristin M.; Moreland, Rodney J.; Scheule, Ronald K. et al. (2014): Antisense Oligonucleotide-mediated Suppression of Muscle Glycogen Synthase 1 Synthesis as an Approach for Substrate Reduction Therapy of Pompe Disease. In: *Molecular therapy. Nucleic acids* 3, e206. DOI: 10.1038/mtna.2014.57.

Committee for Medicinal Products for Human Use: Galafold, INN-migalastat hydrochloride. Online verfügbar unter https://www.ema.europa.eu/en/documents/assessment-report/galafold-epar-public-assessment-report_en.pdf, zuletzt geprüft am 11.11.2022.

Committee for Medicinal Products for Human Use (2015): Summary of Product Characteristics. In: Ian P. Stolerman und Lawrence H. Price (Hg.): Encyclopedia of Psychopharmacology. Berlin, Heidelberg: Springer Berlin Heidelberg, S. 1687.

Davis, Ronald L. (2020): Mechanism of Action and Target Identification: A Matter of Timing in Drug Discovery. In: *iScience* 23 (9), S. 101487. DOI: 10.1016/j.isci.2020.101487.

Douillard-Guilloux, Gaelle; Raben, Nina; Takikita, Shoichi; Batista, Lionel; Caillaud, Catherine; Richard, Emmanuel (2008): Modulation of glycogen synthesis by RNA interference: towards a new therapeutic approach for glycogenosis type II. In: *Human molecular genetics* 17 (24), S. 3876–3886. DOI: 10.1093/hmg/ddn290.

Dubey, Vikas; Bozorg, Behruz; Wüstner, Daniel; Khandelia, Himanshu (2020): Cholesterol binding to the sterol-sensing region of Niemann Pick C1 protein confines dynamics of its N-terminal domain. In: *PLoS computational biology* 16 (10), e1007554. DOI: 10.1371/journal.pcbi.1007554.

Duro, Giovanni; Zizzo, Carmela; Cammarata, Giuseppe; Burlina, Alessandro; Burlina, Alberto; Polo, Giulia et al. (2018): Mutations in the GLA Gene and LysoGb3: Is It Really Anderson-Fabry Disease? In: *International journal of molecular sciences* 19 (12). DOI: 10.3390/ijms19123726.

El Dib, Regina P.; Pastores, Gregory M. (2010): Enzyme replacement therapy for Anderson-Fabry disease. In: *The Cochrane database of systematic reviews* (5), CD006663. DOI: 10.1002/14651858.CD006663.pub2.

Enshaei, Hamidreza; Molina, Brenda G.; Del Valle, Luis J.; Estrany, Francesc; Arnan, Carme; Puiggalí, Jordi et al. (2019): Scaffolds for Sustained Release of Ambroxol Hydrochloride, a Pharmacological Chaperone That Increases the Activity of Misfolded β-Glucocerebrosidase. In: *Macromolecular bioscience* 19 (8), e1900130. DOI: 10.1002/mabi.201900130.

Fan, J. Q.; Ishii, S.; Asano, N.; Suzuki, Y. (1999): Accelerated transport and maturation of lysosomal alpha-galactosidase A in Fabry lymphoblasts by an enzyme inhibitor. In: *Nature medicine* 5 (1), S. 112–115. DOI: 10.1038/4801.

Fan, Yiting; Chan, Tsz-Ngai; Chow, Josie T. Y.; Kam, Kevin K. H.; Chi, Wai-Kin; Chan, Joseph Y. S. et al. (2021): High Prevalence of Late-Onset Fabry Cardiomyopathy in a Cohort of 499 Non-Selective Patients with Left Ventricular Hypertrophy: The Asian Fabry Cardiomyopathy High-Risk Screening Study (ASIAN-FAME). In: *Journal of clinical medicine* 10 (10). DOI: 10.3390/jcm10102160.

Farfel-Becker, Tamar; Vitner, Einat B.; Futerman, Anthony H. (2011): Animal models for Gaucher disease research. In: *Disease models & mechanisms* 4 (6), S. 746–752. DOI: 10.1242/dmm.008185.

Filoni, Camilla; Caciotti, Anna; Carraresi, Laura; Donati, Maria Alice; Mignani, Renzo; Parini, Rossella et al. (2008): Unbalanced GLA mRNAs ratio quantified by real-time PCR in Fabry patients' fibroblasts results in Fabry disease. In: *European journal of human genetics : EJHG* 16 (11), S. 1311–1317. DOI: 10.1038/ejhg.2008.109.

Flanagan, John J.; Rossi, Barbara; Tang, Katherine; Wu, Xiaoyang; Mascioli, Kirsten; Donaudy, Francesca et al. (2009): The pharmacological chaperone 1-deoxynojirimycin increases the activity and lysosomal trafficking of multiple mutant forms of acid alpha-glucosidase. In: *Human mutation* 30 (12), S. 1683–1692. DOI: 10.1002/humu.21121.

Formaggio, Francesco; Rimondini, Roberto; Delprete, Cecilia; Scalia, Leonardo; Merlo Pich, Emilio; Liguori, Rocco et al. (2022): L-Acetylcarnitine causes analgesia in mice modeling Fabry disease by up-regulating type-2 metabotropic glutamate receptors. In: *Molecular pain* 18, 17448069221087033. DOI: 10.1177/17448069221087033.

Frustaci, A.; Chimenti, C.; Ricci, R.; Natale, L.; Russo, M. A.; Pieroni, M. et al. (2001): Improvement in cardiac function in the cardiac variant of Fabry's disease with galactose-infusion therapy. In: *The New England journal of medicine* 345 (1), S. 25–32. DOI: 10.1056/NEJM200107053450104.

Fuller, David D.; ElMallah, Mai K.; Smith, Barbara K.; Corti, Manuela; Lawson, Lee Ann; Falk, Darin J.; Byrne, Barry J. (2013): The respiratory neuromuscular system in Pompe disease. In: *Respiratory physiology & neurobiology* 189 (2), S. 241–249. DOI: 10.1016/j.resp.2013.06.007.

Germain, Dominique P. (2010): Fabry disease. In: *Orphanet journal of rare diseases* 5, S. 30. DOI: 10.1186/1750-1172-5-30.

Gieselmann, V.; Schmidt, B.; Figura, K. von (1992): In vitro mutagenesis of potential N-glycosylation sites of arylsulfatase A. Effects on glycosylation, phosphorylation, and intracellular sorting. In: *The Journal of biological chemistry* 267 (19), S. 13262–13266. DOI: 10.1016/S0021-9258(18)42204-1.

Gieselmann, Volkmar (2006): Fabry Disease: Perspectives from 5 Years of FOS. Cellular pathophysiology of lysosomal storage diseases. Hg. v. Atul Mehta, Michael Beck und Gere Sunder-Plassmann. Oxford.

Goldblatt, J. (1988): Type I Gaucher disease. In: *Journal of medical genetics* 25 (6), S. 415–418. DOI: 10.1136/jmg.25.6.415.

Gregory M Pastores; Derralynn A Hughes (2018): Gaucher Disease. In: Gregory M. Pastores und Derralynn A. Hughes (Hg.): GeneReviews® [Internet]: University of Washington, Seattle. Online verfügbar unter https://www.ncbi.nlm.nih.gov/books/NBK1269/.

Hauser, A. C.; Lorenz, M.; Sunder-Plassmann, G. (2004): The expanding clinical spectrum of Anderson-Fabry disease: a challenge to diagnosis in the novel era of enzyme replacement therapy. In: *Journal of internal medicine* 255 (6), S. 629–636. DOI: 10.1111/j.1365-2796.2004.01300.x.

Hauth, Lothar; Kerstens, Jeroen; Yperzeele, Laetitia; Eyskens, François; Parizel, Paul M.; Willekens, Barbara (2018): Galactosidase Alpha p.A143T Variant Fabry Disease May Result in a Phenotype With Multifocal Microvascular Cerebral Involvement at a Young Age. In: *Frontiers in neurology* 9, S. 336. DOI: 10.3389/fneur.2018.00336.

Hay Mele, Bruno; Citro, Valentina; Andreotti, Giuseppina; Cubellis, Maria Vittoria (2015): Drug repositioning can accelerate discovery of pharmacological chaperones. In: *Orphanet journal of rare diseases* 10, S. 55. DOI: 10.1186/s13023-015-0273-2.

Hofstetter, K.; Raspe, H.; Stumpf, S.; Framke, S. (2015): M. Gaucher und Imiglucerase 2009/2010: Was leitet eine plötzlich erzwungene Priorisierung? In: *Gesundheitswesen (Bundesverband der Arzte des Offentlichen Gesundheitsdienstes (Germany))* 77 (2), S. 86–92. DOI: 10.1055/s-0034-1370997.

Hoshina, Hiroo; Shimada, Yohta; Higuchi, Takashi; Kobayashi, Hiroshi; Ida, Hiroyuki; Ohashi, Toya (2018): Chaperone effect of sulfated disaccharide from heparin on mutant iduronate-2-sulfatase in mucopolysaccharidosis type II. In: *Molecular genetics and metabolism* 123 (2), S. 118–122. DOI: 10.1016/j.ymgme.2017.12.428.

Hughes, Derralynn A.; Nicholls, Kathleen; Shankar, Suma P.; Sunder-Plassmann, Gere; Koeller, David; Nedd, Khan et al. (2017): Oral pharmacological chaperone migalastat compared with enzyme replacement therapy in Fabry disease: 18-month results from the randomised phase III ATTRACT study. In: *Journal of medical genetics* 54 (4), S. 288–296. DOI: 10.1136/jmedgenet-2016-104178.

Hwu, Wuh-Liang; Chien, Yin-Hsiu; Lee, Ni-Chung; Chiang, Shu-Chuan; Dobrovolny, Robert; Huang, Ai-Chu et al. (2009): Newborn screening for Fabry disease in Taiwan reveals a high incidence of the later-onset GLA mutation c.936+919GA (IVS4+919GA). In: *Human mutation* 30 (10), S. 1397–1405. DOI: 10.1002/humu.21074.

Ioannou, Y. A.; Zeidner, K. M.; Grace, M. E.; Desnick, R. J. (1998): Human alpha-galactosidase A. Glycosylation site 3 is essential for enzyme solubility. In: *The Biochemical journal* 332 (Pt 3), S. 789–797. DOI: 10.1042/bj3320789.

Irwin, John J.; Shoichet, Brian K. (2005): ZINC--a free database of commercially available compounds for virtual screening. In: *Journal of chemical information and modeling* 45 (1), S. 177–182. DOI: 10.1021/ci049714+.

Ishii, Satoshi; Chang, Hui-Hwa; Kawasaki, Kunito; Yasuda, Kayo; Wu, Hui-Li; Garman, Scott C.; Fan, Jian-Qiang (2007): Mutant alpha-galactosidase A enzymes identified in Fabry disease patients with residual enzyme activity. Biochemical characterization and restoration of normal intracellular processing by 1-deoxygalactonojirimycin. In: *The Biochemical journal* 406 (2), S. 285–295. DOI: 10.1042/BJ20070479.

Ivanova, Margarita M.; Changsila, Erk; Turgut, Alper; Goker-Alpan, Ozlem (2018): Individualized screening for chaperone activity in Gaucher disease using multiple patient derived primary cell lines. In: *American Journal of Translational Research* 10 (11), S. 3750–3761.

Jaishy, Bharat; Abel, E. Dale (2016): Lipids, lysosomes, and autophagy. In: *Journal of lipid research* 57 (9), S. 1619–1635. DOI: 10.1194/jlr.R067520.

Jmoudiak, Marina; Futerman, Anthony H. (2005): Gaucher disease: pathological mechanisms and modern management. In: *British journal of haematology* 129 (2), S. 178–188. DOI: 10.1111/j.1365-2141.2004.05351.x.

Kakhlon, Or; Escriba, Pablo V.; Akman, Hasan O.; Weil, Miguel (2020): Editorial: Using Small Molecules to Treat Macromolecule Storage Disorders. In: *Frontiers in cell and developmental biology* 8, S. 623613. DOI: 10.3389/fcell.2020.623613.

Kanters, Tim A.; Hagemans, Marloes L. C.; van der Beek, Nadine A. M. E.; Rutten, Frans F. H.; van der Ploeg, Ans T.; Hakkaart, Leona (2011): Burden of illness of Pompe disease in patients only receiving supportive care. In: *Journal of inherited metabolic disease* 34 (5), S. 1045–1052. DOI: 10.1007/s10545-011-9320-x.

Khanna, Richie; Flanagan, John J.; Feng, Jessie; Soska, Rebecca; Frascella, Michelle; Pellegrino, Lee J. et al. (2012): The pharmacological chaperone AT2220 increases recombinant human acid α-glucosidase uptake and glycogen reduction in a mouse model of Pompe disease. In: *PloS one* 7 (7), e40776. DOI: 10.1371/journal.pone.0040776.

Khanna, Richie; Soska, Rebecca; Lun, Yi; Feng, Jessie; Frascella, Michelle; Young, Brandy et al. (2010): The pharmacological chaperone 1-deoxygalactonojirimycin reduces tissue globotriaosylceramide levels in a mouse model of Fabry disease. In: *Molecular therapy : the journal of the American Society of Gene Therapy* 18 (1), S. 23–33. DOI: 10.1038/mt.2009.220.

Kim, Yoon-Myung; Yum, Mi-Sun; Heo, Sun Hee; Kim, Taeho; Jin, Hee Kyung; Bae, Jae-Sung et al. (2020): Pharmacologic properties of high-dose ambroxol in four patients with Gaucher disease and myoclonic epilepsy. In: *Journal of medical genetics* 57 (2), S. 124–131. DOI: 10.1136/jmedgenet-2019-106132.

Kint, J. A. (1970): Fabry's disease. Alpha-galactosidase deficiency. In: *Science (New York, N.Y.)* 167 (3922), S. 1268–1269. DOI: 10.1126/science.167.3922.1268.

Kishnani, Priya S.; Gibson, James B.; Gambello, Michael J.; Hillman, Richard; Stockton, David W.; Kronn, David et al. (2019): Clinical characteristics and genotypes in the ADVANCE baseline data set, a comprehensive cohort of US children and adolescents with Pompe disease. In: *Genetics in medicine : official journal of the American College of Medical Genetics* 21 (11), S. 2543–2551. DOI: 10.1038/s41436-019-0527-9.

Koprivica, V.; Stone, D. L.; Park, J. K.; Callahan, M.; Frisch, A.; Cohen, I. J. et al. (2000): Analysis and classification of 304 mutant alleles in patients with type 1 and type 3 Gaucher disease. In: *American journal of human genetics* 66 (6), S. 1777–1786. DOI: 10.1086/302925.

Kopytova, A. E.; Rychkov, G. N.; Nikolaev, M. A.; Baydakova, G. V.; Cheblokov, A. A.; Senkevich, K. A. et al. (2021): Ambroxol increases glucocerebrosidase (GCase) activity and restores GCase translocation in primary patient-derived macrophages in Gaucher disease and Parkinsonism. In: *Parkinsonism & related disorders* 84, S. 112–121. DOI: 10.1016/j.parkreldis.2021.02.003.

Kornreich, R.; Bishop, D. F.; Desnick, R. J. (1989): The gene encoding alpha-galactosidase A and gene rearrangements causing Fabry disease. In: *Transactions of the Association of American Physicians* 102, S. 30–43.

Kornreich, R.; Bishop, D. F.; Desnick, R. J. (1990): Alpha-galactosidase A gene rearrangements causing Fabry disease. Identification of short direct repeats at breakpoints in an Alu-rich gene. In: *The Journal of biological chemistry* 265 (16), S. 9319–9326. DOI: 10.1016/S0021-9258(19)38851-9.

Kroos, M. A.; van der Kraan, M.; van Diggelen, O. P.; Kleijer, W. J.; Reuser, A. J.; van den Boogaard, M. J. et al. (1995): Glycogen storage disease type II: frequency of three common mutant alleles and their associated clinical phenotypes studied in 121 patients. In: *Journal of medical genetics* 32 (10), S. 836–837. DOI: 10.1136/jmg.32.10.836-a.

Kroos, M. A.; van Leenen, D.; Verbiest, J.; Reuser, A. J.; Hermans, M. M. (1998): Glycogen storage disease type II: identification of a dinucleotide deletion and a common missense mutation in the lysosomal alpha-glucosidase gene. In: *Clinical genetics* 53 (5), S. 379–382. DOI: 10.1111/j.1399-0004.1998.tb02749.x.

Kroos, Marian; Hoogeveen-Westerveld, Marianne; Michelakakis, Helen; Pomponio, Robert; van der Ploeg, Ans; Halley, Dicky; Reuser, Arnold (2012): Update of the pompe disease mutation database with 60 novel GAA sequence variants and additional studies on the functional effect of 34 previously reported variants. In: *Human mutation* 33 (8), S. 1161–1165. DOI: 10.1002/humu.22108.

Kurz, Tino; Eaton, John W.; Brunk, Ulf T. (2011): The role of lysosomes in iron metabolism and recycling. In: *The international journal of biochemistry & cell biology* 43 (12), S. 1686–1697. DOI: 10.1016/j.biocel.2011.08.016.

Kutmon, Martina; Riutta, Anders; Nunes, Nuno; Hanspers, Kristina; Willighagen, Egon L.; Bohler, Anwesha et al. (2016): WikiPathways: capturing the full diversity of pathway knowledge. In: *Nucleic acids research* 44 (D1), D488-94. DOI: 10.1093/nar/gkv1024.

Kwon, Hyock Joo; Abi-Mosleh, Lina; Wang, Michael L.; Deisenhofer, Johann; Goldstein, Joseph L.; Brown, Michael S.; Infante, Rodney E. (2009): Structure of N-terminal domain of NPC1 reveals distinct subdomains for binding and transfer of cholesterol. In: *Cell* 137 (7), S. 1213–1224. DOI: 10.1016/j.cell.2009.03.049.

Laforêt, P.; Nicolino, M.; Eymard, P. B.; Puech, J. P.; Caillaud, C.; Poenaru, L.; Fardeau, M. (2000): Juvenile and adult-onset acid maltase deficiency in France: genotype-phenotype correlation. In: *Neurology* 55 (8), S. 1122–1128. DOI: 10.1212/wnl.55.8.1122.

Lee, Karen; Jin, Xiaoying; Zhang, Kate; Copertino, Lorraine; Andrews, Laura; Baker-Malcolm, Jennifer et al. (2003): A biochemical and pharmacological comparison of enzyme replacement therapies for the glycolipid storage disorder Fabry disease. In: *Glycobiology* 13 (4), S. 305–313. DOI: 10.1093/glycob/cwg034.

Lee, Wing C.; Kang, Dongcheul; Causevic, Ena; Herdt, Aimee R.; Eckman, Elizabeth A.; Eckman, Christopher B. (2010): Molecular characterization of mutations that cause globoid cell leukodystrophy and pharmacological rescue using small molecule chemical chaperones. In: *The Journal of neuroscience : the official journal of the Society for Neuroscience* 30 (16), S. 5489–5497. DOI: 10.1523/JNEUROSCI.6383-09.2010.

Lenders, Malte; Weidemann, Frank; Kurschat, Christine; Canaan-Kühl, Sima; Duning, Thomas; Stypmann, Jörg et al. (2016): Alpha-Galactosidase A p.A143T, a non-Fabry disease-causing variant. In: *Orphanet journal of rare diseases* 11 (1), S. 54. DOI: 10.1186/s13023-016-0441-z.

Liguori, Ludovica; Monticelli, Maria; Allocca, Mariateresa; Hay Mele, Bruno; Lukas, Jan; Cubellis, Maria Vittoria; Andreotti, Giuseppina (2020): Pharmacological Chaperones: A Therapeutic Approach for Diseases Caused by Destabilizing Missense Mutations. In: *International journal of molecular sciences* 21 (2). DOI: 10.3390/ijms21020489.

Liu, Y.; Suzuki, K.; Reed, J. D.; Grinberg, A.; Westphal, H.; Hoffmann, A. et al. (1998): Mice with type 2 and 3 Gaucher disease point mutations generated by a single insertion mutagenesis procedure. In: *Proceedings of the National Academy of Sciences of the United States of America* 95 (5), S. 2503–2508. DOI: 10.1073/pnas.95.5.2503.

Lodish, Harvey (2002): Molecular cell biology. 4. ed., [Nachdr.]. New York, NY: Freeman (Media connected).

Lukacs, Zoltan; Nieves Cobos, Paulina; Wenninger, Stephan; Willis, Tracey A.; Guglieri, Michela; Roberts, Marc et al. (2016): Prevalence of Pompe disease in 3,076 patients with hyperCKemia and limb-girdle muscular weakness. In: *Neurology* 87 (3), S. 295–298. DOI: 10.1212/WNL.0000000000002758.

Lukas, Jan; Giese, Anne-Katrin; Markoff, Arseni; Grittner, Ulrike; Kolodny, Ed; Mascher, Hermann et al. (2013): Functional characterisation of alpha-galactosidase a mutations as a basis for a new classification system in fabry disease. In: *PLoS genetics* 9 (8), e1003632. DOI: 10.1371/journal.pgen.1003632.

MacDermot, K. D.; Holmes, A.; Miners, A. H. (2001): Anderson-Fabry disease. Clinical manifestations and impact of disease in a cohort of 60 obligate carrier females. In: *Journal of medical genetics* 38 (11), S. 769–775. DOI: 10.1136/jmg.38.11.769.

Maegawa, Gustavo H. B.; Tropak, Michael; Buttner, Justin; Stockley, Tracy; Kok, Fernando; Clarke, Joe T. R.; Mahuran, Don J. (2007): Pyrimethamine as a potential pharmacological chaperone for late-onset forms of GM2 gangliosidosis. In: *The Journal of biological chemistry* 282 (12), S. 9150–9161. DOI: 10.1074/jbc.M609304200.

Maegawa, Gustavo H. B.; Tropak, Michael B.; Buttner, Justin D.; Rigat, Brigitte A.; Fuller, Maria; Pandit, Deepangi et al. (2009): Identification and characterization of ambroxol as an enzyme enhancement agent for Gaucher disease. In: *The Journal of biological chemistry* 284 (35), S. 23502–23516. DOI: 10.1074/jbc.M109.012393.

Mandon, Elisabet C.; Trueman, Steven F.; Gilmore, Reid (2013): Protein translocation across the rough endoplasmic reticulum. In: *Cold Spring Harbor perspectives in biology* 5 (2). DOI: 10.1101/cshperspect.a013342.

Maor, Gali; Cabasso, Or; Krivoruk, Olga; Rodriguez, Joe; Steller, Hermann; Segal, Daniel; Horowitz, Mia (2016): The contribution of mutant GBA to the development of Parkinson disease in Drosophila. In: *Human molecular genetics* 25 (13), S. 2712–2727. DOI: 10.1093/hmg/ddw129.

Maor, Gali; Rapaport, Debora; Horowitz, Mia (2019): The effect of mutant GBA1 on accumulation and aggregation of α-synuclein. In: *Human molecular genetics* 28 (11), S. 1768–1781. DOI: 10.1093/hmg/ddz005.

Maor, Gali; Rencus-Lazar, Sigal; Filocamo, Mirella; Steller, Hermann; Segal, Daniel; Horowitz, Mia (2013): Unfolded protein response in Gaucher disease: from human to Drosophila. In: *Orphanet journal of rare diseases* 8, S. 140. DOI: 10.1186/1750-1172-8-140.

Marfella, Raffaele; D'Amico, Michele; Esposito, Katherine; Baldi, Alfonso; Di Filippo, Clara; Siniscalchi, Mario et al. (2006): The ubiquitin-proteasome system and inflammatory activity in diabetic

atherosclerotic plaques: effects of rosiglitazone treatment. In: *Diabetes* 55 (3), S. 622–632. DOI: 10.2337/diabetes.55.03.06.db05-0832.

Mark E Haskins; Urs Giger; Donald F Patterson (2006): Animal models of lysosomal storage diseases: their development and clinical relevance. In: Mark E. Haskins, Urs Giger und Donald F. Patterson (Hg.): Fabry Disease: Perspectives from 5 Years of FOS: Oxford PharmaGenesis. Online verfügbar unter https://www.ncbi.nlm.nih.gov/books/NBK11578/.

Markham, Anthony (2016): Migalastat: First Global Approval. In: *Drugs* 76 (11), S. 1147–1152. DOI: 10.1007/s40265-016-0607-y.

Matsuura, F.; Ohta, M.; Ioannou, Y. A.; Desnick, R. J. (1998): Human alpha-galactosidase A. Characterization of the N-linked oligosaccharides on the intracellular and secreted glycoforms overexpressed by Chinese hamster ovary cells. In: *Glycobiology* 8 (4), S. 329–339. DOI: 10.1093/glycob/8.4.329.

McNeill, Alisdair; Magalhaes, Joana; Shen, Chengguo; Chau, Kai-Yin; Hughes, Derralyn; Mehta, Atul et al. (2014): Ambroxol improves lysosomal biochemistry in glucocerebrosidase mutation-linked Parkinson disease cells. In: *Brain : a journal of neurology* 137 (Pt 5), S. 1481–1495. DOI: 10.1093/brain/awu020.

Miller, James J.; Kanack, Adam J.; Dahms, Nancy M. (2020): Progress in the understanding and treatment of Fabry disease. In: *Biochimica et biophysica acta. General subjects* 1864 (1), S. 129437. DOI: 10.1016/j.bbagen.2019.129437.

Mizukami, Hiroki; Mi, Yide; Wada, Ryuichi; Kono, Mari; Yamashita, Tadashi; Liu, Yujing et al. (2002): Systemic inflammation in glucocerebrosidase-deficient mice with minimal glucosylceramide storage. In: *The Journal of clinical investigation* 109 (9), S. 1215–1221. DOI: 10.1172/JCI14530.

Montfort, Magda; Chabás, Amparo; Vilageliu, Lluïsa; Grinberg, Daniel (2004): Functional analysis of 13 GBA mutant alleles identified in Gaucher disease patients: Pathogenic changes and "modifier" polymorphisms. In: *Human mutation* 23 (6), S. 567–575. DOI: 10.1002/humu.20043.

Moremen, Kelley W.; Molinari, Maurizio (2006): N-linked glycan recognition and processing. The molecular basis of endoplasmic reticulum quality control. In: *Current opinion in structural biology* 16 (5), S. 592–599. DOI: 10.1016/j.sbi.2006.08.005.

Motomura, Wataru; Takahashi, Nobuhiko; Nagamine, Miho; Sawamukai, Mitsuko; Tanno, Satoshi; Kohgo, Yutaka; Okumura, Toshikatsu (2004): Growth arrest by troglitazone is mediated by p27Kip1 accumulation, which results from dual inhibition of proteasome activity and Skp2 expression in human hepatocellular carcinoma cells. In: *International journal of cancer* 108 (1), S. 41–46. DOI: 10.1002/ijc.11561.

Mu, Ting-Wei; Ong, Derrick Sek Tong; Wang, Ya-Juan; Balch, William E.; Yates, John R.; Segatori, Laura; Kelly, Jeffery W. (2008): Chemical and biological approaches synergize to ameliorate protein-folding diseases. In: *Cell* 134 (5), S. 769–781. DOI: 10.1016/j.cell.2008.06.037.

Nakamura, K.; Sekijima, Y.; Hattori, K.; Nagamatsu, K.; Shimizu, Y.; Yazaki, M. et al. (2014): p.E66Q mutation in the GLA gene is associated with a high risk of cerebral small-vessel occlusion in elderly Japanese males. In: *European journal of neurology* 21 (1), S. 49–56. DOI: 10.1111/ene.12214.

Narita, Aya; Shirai, Kentarou; Itamura, Shinji; Matsuda, Atsue; Ishihara, Akiko; Matsushita, Kumi et al. (2016): Ambroxol chaperone therapy for neuronopathic Gaucher disease: A pilot study. In: *Annals of clinical and translational neurology* 3 (3), S. 200–215. DOI: 10.1002/acn3.292.

Ng, Pauline C.; Henikoff, Steven (2003): SIFT. Predicting amino acid changes that affect protein function. In: *Nucleic acids research* 31 (13), S. 3812–3814. DOI: 10.1093/nar/gkg509.

Ngiwsara, Lukana; Wattanasirichaigoon, Duangrurdee; Tim-Aroon, Thipwimol; Rojnueangnit, Kitiwan; Noojaroen, Saisuda; Khongkraparn, Arthaporn et al. (2019): Clinical course, mutations and its functional characteristics of infantile-onset Pompe disease in Thailand. In: *BMC medical genetics* 20 (1), S. 156. DOI: 10.1186/s12881-019-0878-8.

Ohgane, Kenji; Karaki, Fumika; Dodo, Kosuke; Hashimoto, Yuichi (2013): Discovery of oxysterol-derived pharmacological chaperones for NPC1: implication for the existence of second sterol-binding site. In: *Chemistry & biology* 20 (3), S. 391–402. DOI: 10.1016/j.chembiol.2013.02.009.

Ohgane, Kenji; Karaki, Fumika; Noguchi-Yachide, Tomomi; Dodo, Kosuke; Hashimoto, Yuichi (2014): Structure-activity relationships of oxysterol-derived pharmacological chaperones for Niemann-Pick type C1 protein. In: *Bioorganic & medicinal chemistry letters* 24 (15), S. 3480–3485. DOI: 10.1016/j.bmcl.2014.05.064.

Ohshima, T.; Murray, G. J.; Swaim, W. D.; Longenecker, G.; Quirk, J. M.; Cardarelli, C. O. et al. (1997): alpha-Galactosidase A deficient mice: a model of Fabry disease. In: *Proceedings of the National Academy of Sciences of the United States of America* 94 (6), S. 2540–2544. DOI: 10.1073/pnas.94.6.2540.

Okumiya, Toshika; Kroos, Marian A.; van Vliet, Laura; Takeuchi, Hiroaki; van der Ploeg, Ans T.; Reuser, Arnold J. J. (2007): Chemical chaperones improve transport and enhance stability of mutant alpha-glucosidases in glycogen storage disease type II. In: *Molecular genetics and metabolism* 90 (1), S. 49–57. DOI: 10.1016/j.ymgme.2006.09.010.

Oommen, Susan; Zhou, Yanfeng; Meiyappan, Muthuraman; Gurevich, Andrey; Qiu, Yongchang (2019): Inter-assay variability influences migalastat amenability assessments among Fabry disease variants. In: *Molecular genetics and metabolism* 127 (1), S. 74–85. DOI: 10.1016/j.ymgme.2019.04.005.

Palaiodimou, Lina; Stefanou, Maria-Ioanna; Bakola, Eleni; Papadopoulou, Marianna; Kokotis, Panagiotis; Vrettou, Agathi-Rosa et al. (2022): D313Y Variant in Fabry Disease: A Systematic Review and Meta-analysis. In: *Neurology* 99 (19), e2188-e2200. DOI: 10.1212/WNL.0000000000201102.

Palhais, Bruno; Dembic, Maja; Sabaratnam, Rugivan; Nielsen, Kira S.; Doktor, Thomas Koed; Bruun, Gitte Hoffmann; Andresen, Brage Storstein (2016): The prevalent deep intronic c. 639+919 GA GLA mutation causes pseudoexon activation and Fabry disease by abolishing the binding of hnRNPA1 and hnRNP A2/B1 to a splicing silencer. In: *Molecular genetics and metabolism* 119 (3), S. 258–269. DOI: 10.1016/j.ymgme.2016.08.007.

Pandey, Manoj K.; Burrow, Thomas A.; Rani, Reena; Martin, Lisa J.; Witte, David; Setchell, Kenneth D. et al. (2017): Complement drives glucosylceramide accumulation and tissue inflammation in Gaucher disease. In: *Nature* 543 (7643), S. 108–112. DOI: 10.1038/nature21368.

Parenti, Giancarlo; Andria, Generoso; Valenzano, Kenneth J. (2015): Pharmacological Chaperone Therapy. Preclinical Development, Clinical Translation, and Prospects for the Treatment of Lysosomal Storage Disorders. In: *Molecular therapy : the journal of the American Society of Gene Therapy* 23 (7), S. 1138–1148. DOI: 10.1038/mt.2015.62.

Parenti, Giancarlo; Zuppaldi, Alfredo; Gabriela Pittis, M.; Rosaria Tuzzi, M.; Annunziata, Ida; Meroni, Germana et al. (2007): Pharmacological Enhancement of Mutated α-Glucosidase Activity in Fibroblasts from Patients with Pompe Disease. In: *Molecular Therapy* 15 (3), S. 508–514. DOI: 10.1038/sj.mt.6300074.

Park, J. K.; Koprivica, V.; Andrews, D. Q.; Madike, V.; Tayebi, N.; Stone, D. L.; Sidransky, E. (2001): Glucocerebrosidase mutations among African-American patients with type 1 Gaucher disease. In: *American journal of medical genetics* 99 (2), S. 147–151. DOI: 10.1002/1096-8628(2001)9999:9999<::aid-ajmg1144>3.0.co;2-1.

Pawson, Adam J.; Sharman, Joanna L.; Benson, Helen E.; Faccenda, Elena; Alexander, Stephen P. H.; Buneman, O. Peter et al. (2014): The IUPHAR/BPS Guide to PHARMACOLOGY: an expert-driven knowledgebase of drug targets and their ligands. In: *Nucleic acids research* 42 (Database issue), D1098-106. DOI: 10.1093/nar/gkt1143.

Pearson, Caroline; Schapiro, Lindsey; Pearson, Steven D. (2022): The next generation of rare disease drug policy: ensuring both innovation and affordability. In: *Journal of comparative effectiveness research* 11 (14), S. 999–1010. DOI: 10.2217/cer-2022-0120.

Pena, Loren D. M.; Barohn, Richard J.; Byrne, Barry J.; Desnuelle, Claude; Goker-Alpan, Ozlem; Ladha, Shafeeq et al. (2019): Safety, tolerability, pharmacokinetics, pharmacodynamics, and exploratory efficacy of the novel enzyme replacement therapy avalglucosidase alfa (neoGAA) in treatment-naïve and alglucosidase alfa-treated patients with late-onset Pompe disease: A phase 1, open-label, multicenter, multinational, ascending dose study. In: *Neuromuscular disorders : NMD* 29 (3), S. 167–186. DOI: 10.1016/j.nmd.2018.12.004.

Pharmacoeconomic Review Report: Migalastat (Galafold): (Amicus Therapeutics): Indication: Fabry Disease [Internet] (2018): Canadian Agency for Drugs and Technologies in Health.

Pilarczyk, Marcin; Fazel-Najafabadi, Mehdi; Kouril, Michal; Shamsaei, Behrouz; Vasiliauskas, Juozas; Niu, Wen et al. (2022): Connecting omics signatures and revealing biological mechanisms with iLINCS. In: *Nature communications* 13 (1), S. 4678. DOI: 10.1038/s41467-022-32205-3.

Pisani, A.; Spinelli, L.; Visciano, B.; Capuano, I.; Sabbatini, M.; Riccio, E. et al. (2013): Effects of switching from agalsidase Beta to agalsidase alfa in 10 patients with anderson-fabry disease. In: *JIMD reports* 9, S. 41–48. DOI: 10.1007/8904_2012_177.

Pols, Maaike S.; van Meel, Eline; Oorschot, Viola; Brink, Corlinda ten; Fukuda, Minoru; Swetha, M. G. et al. (2013): hVps41 and VAMP7 function in direct TGN to late endosome transport of lysosomal membrane proteins. In: *Nature communications* 4, S. 1361. DOI: 10.1038/ncomms2360.

Poole, Raewyn M. (2014): Eliglustat: first global approval. In: *Drugs* 74 (15), S. 1829–1836. DOI: 10.1007/s40265-014-0296-3.

Porter, Forbes D.; Scherrer, David E.; Lanier, Michael H.; Langmade, S. Joshua; Molugu, Vasumathi; Gale, Sarah E. et al. (2010): Cholesterol oxidation products are sensitive and specific blood-based biomarkers for Niemann-Pick C1 disease. In: *Science translational medicine* 2 (56), 56ra81. DOI: 10.1126/scitranslmed.3001417.

Porto, Caterina; Cardone, Monica; Fontana, Federica; Rossi, Barbara; Tuzzi, Maria Rosaria; Tarallo, Antonietta et al. (2009): The pharmacological chaperone N-butyldeoxynojirimycin enhances enzyme replacement therapy in Pompe disease fibroblasts. In: *Molecular therapy : the journal of the American Society of Gene Therapy* 17 (6), S. 964–971. DOI: 10.1038/mt.2009.53.

Porto, Caterina; Ferrara, Maria C.; Meli, Massimiliano; Acampora, Emma; Avolio, Valeria; Rosa, Margherita et al. (2012): Pharmacological enhancement of α-glucosidase by the allosteric chaperone N-acetylcysteine. In: *Molecular therapy : the journal of the American Society of Gene Therapy* 20 (12), S. 2201–2211. DOI: 10.1038/mt.2012.152.

Reczek, David; Schwake, Michael; Schröder, Jenny; Hughes, Heather; Blanz, Judith; Jin, Xiaoying et al. (2007): LIMP-2 is a receptor for lysosomal mannose-6-phosphate-independent targeting of beta-glucocerebrosidase. In: *Cell* 131 (4), S. 770–783. DOI: 10.1016/j.cell.2007.10.018.

Rega, Laura R.; Polishchuk, Elena; Montefusco, Sandro; Napolitano, Gennaro; Tozzi, Giulia; Zhang, Jinzhong et al. (2016): Activation of the transcription factor EB rescues lysosomal abnormalities in cystinotic kidney cells. In: *Kidney international* 89 (4), S. 862–873. DOI: 10.1016/j.kint.2015.12.045.

Reuser, A. J.; Kroos, M.; Willemsen, R.; Swallow, D.; Tager, J. M.; Galjaard, H. (1987): Clinical diversity in glycogenosis type II. Biosynthesis and in situ localization of acid alpha-glucosidase in mutant fibroblasts. In: *The Journal of clinical investigation* 79 (6), S. 1689–1699. DOI: 10.1172/JCI113008.

Riillo, Concetta; Bonapace, Giuseppe; Moricca, Maria Teresa; Sestito, Simona; Salatino, Alessandro; Concolino, Daniela (2023): c.376A>G, (p.S126G) Alpha Galactosidase A Mutation Induces ER Stress, Unfolded Protein Response and Reduced Enzyme Transport to Lysosome: Possible Relevance in the Pathogenesis of Late Onset Forms of Fabry Disease.

Roig-Zamboni, Véronique; Cobucci-Ponzano, Beatrice; Iacono, Roberta; Ferrara, Maria Carmina; Germany, Stanley; Bourne, Yves et al. (2017): Structure of human lysosomal acid α-glucosidase-a guide for the treatment of Pompe disease. In: *Nature communications* 8 (1), S. 1111. DOI: 10.1038/s41467-017-01263-3.

Ron, Idit; Horowitz, Mia (2005): ER retention and degradation as the molecular basis underlying Gaucher disease heterogeneity. In: *Human molecular genetics* 14 (16), S. 2387–2398. DOI: 10.1093/hmg/ddi240.

Saito, Seiji; Ohno, Kazuki; Sese, Jun; Sugawara, Kanako; Sakuraba, Hitoshi (2010): Prediction of the clinical phenotype of Fabry disease based on protein sequential and structural information. In: *Journal of human genetics* 55 (3), S. 175–178. DOI: 10.1038/jhg.2010.5.

Sakuraba, Hitoshi; Murata-Ohsawa, Mai; Kawashima, Ikuo; Tajima, Youichi; Kotani, Masaharu; Ohshima, Toshio et al. (2006): Comparison of the effects of agalsidase alfa and agalsidase beta on cultured human Fabry fibroblasts and Fabry mice. In: *Journal of human genetics* 51 (3), S. 180–188. DOI: 10.1007/s10038-005-0342-9.

Sardiello, Marco; Palmieri, Michela; Di Ronza, Alberto; Medina, Diego Luis; Valenza, Marta; Gennarino, Vincenzo Alessandro et al. (2009): A gene network regulating lysosomal biogenesis and function. In: *Science (New York, N.Y.)* 325 (5939), S. 473–477. DOI: 10.1126/science.1174447.

Sawkar, Anu R.; Cheng, Wei-Chieh; Beutler, Ernest; Wong, Chi-Huey; Balch, William E.; Kelly, Jeffery W. (2002): Chemical chaperones increase the cellular activity of N370S beta -glucosidase: a therapeutic strategy for Gaucher disease. In: *Proceedings of the National Academy of Sciences of the United States of America* 99 (24), S. 15428–15433. DOI: 10.1073/pnas.192582899.

Scharenberg, Samantha G.; Poletto, Edina; Lucot, Katherine L.; Colella, Pasqualina; Sheikali, Adam; Montine, Thomas J. et al. (2020): Engineering monocyte/macrophage-specific glucocerebrosidase expression in human hematopoietic stem cells using genome editing. In: *Nature communications* 11 (1), S. 3327. DOI: 10.1038/s41467-020-17148-x.

Scherer, Manuel; Santana, Andrés G.; Robinson, Kyle; Zhou, Steven; Overkleeft, Hermen S.; Clarke, Lorne; Withers, Stephen G. (2021): Lipid-mimicking phosphorus-based glycosidase inactivators as pharmacological chaperones for the treatment of Gaucher's disease. In: *Chemical science* 12 (41), S. 13909–13913. DOI: 10.1039/d1sc03831a.

Schiffmann, Raphael; Fuller, Maria; Clarke, Lorne A.; Aerts, Johannes M. F. G. (2016): Is it Fabry disease? In: *Genetics in medicine : official journal of the American College of Medical Genetics* 18 (12), S. 1181–1185. DOI: 10.1038/gim.2016.55.

Schmitz, Martina; Alfalah, Marwan; Aerts, Johannes M. F. G.; Naim, Hassan Y.; Zimmer, Klaus-Peter (2005): Impaired trafficking of mutants of lysosomal glucocerebrosidase in Gaucher's disease. In: *The international journal of biochemistry & cell biology* 37 (11), S. 2310–2320. DOI: 10.1016/j.biocel.2005.05.008.

Schulze, Heike; Kolter, Thomas; Sandhoff, Konrad (2009): Principles of lysosomal membrane degradation. Cellular topology and biochemistry of lysosomal lipid degradation. In: *Biochimica et biophysica acta* 1793 (4), S. 674–683. DOI: 10.1016/j.bbamcr.2008.09.020.

Schwarz, Jana Marie; Rödelsperger, Christian; Schuelke, Markus; Seelow, Dominik (2010): MutationTaster evaluates disease-causing potential of sequence alterations. In: *Nature methods* 7 (8), S. 575–576. DOI: 10.1038/nmeth0810-575.

Settembre, Carmine; Fraldi, Alessandro; Medina, Diego L.; Ballabio, Andrea (2013): Signals from the lysosome. A control centre for cellular clearance and energy metabolism. In: *Nature reviews. Molecular cell biology* 14 (5), S. 283–296. DOI: 10.1038/nrm3565.

Sitarska, Dominika; Tylki-Szymańska, Anna; Ługowska, Agnieszka (2021): Treatment trials in Niemann-Pick type C disease. In: *Metabolic brain disease* 36 (8), S. 2215–2221. DOI: 10.1007/s11011-021-00842-0.

Śnit, Mirosław; Przyłudzka, Marcela; Grzeszczak, Władysław (2022): Fabry disease - a genetically conditioned extremely rare disease with a very unusual course. In: *Intractable & rare diseases research* 11 (1), S. 34–36. DOI: 10.5582/irdr.2021.01132.

Spada, Marco; Pagliardini, Severo; Yasuda, Makiko; Tukel, Turgut; Thiagarajan, Geetha; Sakuraba, Hitoshi et al. (2006): High incidence of later-onset fabry disease revealed by newborn screening. In: *American journal of human genetics* 79 (1), S. 31–40. DOI: 10.1086/504601.

Steet, Richard A.; Chung, Stephen; Wustman, Brandon; Powe, Allan; Do, Hung; Kornfeld, Stuart A. (2006): The iminosugar isofagomine increases the activity of N370S mutant acid beta-glucosidase in Gaucher fibroblasts by several mechanisms. In: *Proceedings of the National Academy of Sciences of the United States of America* 103 (37), S. 13813–13818. DOI: 10.1073/pnas.0605928103.

Stepanenko, A. A.; Dmitrenko, V. V. (2015): HEK293 in cell biology and cancer research: phenotype, karyotype, tumorigenicity, and stress-induced genome-phenotype evolution. In: *Gene* 569 (2), S. 182–190. DOI: 10.1016/j.gene.2015.05.065.

Subramaniyan, Vijayakumar; Mathiyalagan, Sathiya; Praveenkumar, Arulmozhi; Srinivasan, Prabhu; Palani, Manogar; Ravichandran, Vinothkannan; Nallasamy, Parameswari (2018): Molecular docking and ADME properties of bioactive molecules against human acid-beta-glucosidase enzyme, cause of Gaucher's disease. In: *In silico pharmacology* 6 (1), S. 3. DOI: 10.1007/s40203-018-0039-3.

Substrathemmung durch Miglustat (2022). Online verfügbar unter https://www.arzneimitteltherapie.de/heftarchiv/2004/05/substrathemmung-durch-miglustat-neue-behandlungsstrategie-der-gaucher-krankheit.html, zuletzt aktualisiert am 24.06.2022, zuletzt geprüft am 24.06.2022.

Sun, Baodong; Brooks, Elizabeth D.; Koeberl, Dwight D. (2015): Preclinical Development of New Therapy for Glycogen Storage Diseases. In: *Current gene therapy* 15 (4), S. 338–347. DOI: 10.2174/1566523215666150630132253.

Sun, Ying; Liou, Benjamin; Xu, You-Hai; Quinn, Brian; Zhang, Wujuan; Hamler, Rick et al. (2012): Ex vivo and in vivo effects of isofagomine on acid β-glucosidase variants and substrate levels in Gaucher disease. In: *The Journal of biological chemistry* 287 (6), S. 4275–4287. DOI: 10.1074/jbc.M111.280016.

Tarallo, Antonietta; Damiano, Carla; Strollo, Sandra; Minopoli, Nadia; Indrieri, Alessia; Polishchuk, Elena et al. (2021): Correction of oxidative stress enhances enzyme replacement therapy in Pompe disease. In: *EMBO molecular medicine* 13 (11), e14434. DOI: 10.15252/emmm.202114434.

Togawa, Tadayasu; Kodama, Takashi; Suzuki, Toshihiro; Sugawara, Kanako; Tsukimura, Takahiro; Ohashi, Toya et al. (2010): Plasma globotriaosylsphingosine as a biomarker of Fabry disease. In: *Molecular genetics and metabolism* 100 (3), S. 257–261. DOI: 10.1016/j.ymgme.2010.03.020.

Turk, Boris; Turk, Vito (2009): Lysosomes as "suicide bags" in cell death. Myth or reality? In: *The Journal of biological chemistry* 284 (33), S. 21783–21787. DOI: 10.1074/jbc.R109.023820.

Uchiyama, Yasuo; Shibata, Masahiro; Koike, Masato; Yoshimura, Kentaro; Sasaki, Mitsuho (2008): Autophagy-physiology and pathophysiology. In: *Histochemistry and cell biology* 129 (4), S. 407–420. DOI: 10.1007/s00418-008-0406-y.

van der Veen, Sanne J.; Hollak, Carla E. M.; van Kuilenburg, André B. P.; Langeveld, Mirjam (2020): Developments in the treatment of Fabry disease. In: *Journal of inherited metabolic disease* 43 (5), S. 908–921. DOI: 10.1002/jimd.12228.

Vanier, Marie T. (2010): Niemann-Pick disease type C. In: *Orphanet journal of rare diseases* 5, S. 16. DOI: 10.1186/1750-1172-5-16.

Vedder, Anouk C.; Linthorst, Gabor E.; Houge, Gunnar; Groener, Johannna E. M.; Ormel, Els E.; Bouma, Berto J. et al. (2007): Treatment of Fabry disease: outcome of a comparative trial with agalsidase alfa or beta at a dose of 0.2 mg/kg. In: *PloS one* 2 (7), e598. DOI: 10.1371/journal.pone.0000598.

Vellodi, Ashok (2005): Lysosomal storage disorders. In: *British journal of haematology* 128 (4), S. 413–431. DOI: 10.1111/j.1365-2141.2004.05293.x.

Verma, Shalja; Pantoom, Supansa; Petters, Janine; Pandey, Anand Kumar; Hermann, Andreas; Lukas, Jan (2021): A molecular genetics view on Mucopolysaccharidosis Type II. In: *Mutation research. Reviews in mutation research* 788, S. 108392. DOI: 10.1016/j.mrrev.2021.108392.

View GALAFOLD® Amenability Table (2022). Online verfügbar unter https://www.galafoldamenabilitytable.com/reference, zuletzt aktualisiert am 28.06.2022, zuletzt geprüft am 28.06.2022.

Vikić-Topić, Drazen; Carević, Olga (2009): Lizosomi i apoptoza. In: *Acta medica Croatica : casopis Hravatske akademije medicinskih znanosti* 63 Suppl 2, S. 21–25.

Völkner, Christin; Pantoom, Supansa; Liedtke, Maik; Lukas, Jan; Hermann, Andreas; Frech, Moritz J. (2022): Assessment of FDA-Approved Drugs as a Therapeutic Approach for Niemann-Pick Disease Type C1 Using Patient-Specific iPSC-Based Model Systems. In: *Cells* 11 (3). DOI: 10.3390/cells11030319.

Walker, Julie (2007): Tay-Sachs disease. 1st ed. New York: Rosen Pub. Group (Genetic diseases and disorders).

Wang, Fan; Agnello, Giulia; Sotolongo, Natasha; Segatori, Laura (2011): Ca2+ homeostasis modulation enhances the amenability of L444P glucosylcerebrosidase to proteostasis regulation in patient-derived fibroblasts. In: *ACS chemical biology* 6 (2), S. 158–168. DOI: 10.1021/cb100321m.

Wang, Jinhai; Lozier, Jay; Johnson, Gibbes; Kirshner, Susan; Verthelyi, Daniela; Pariser, Anne et al. (2008): Neutralizing antibodies to therapeutic enzymes: considerations for testing, prevention and treatment. In: *Nature biotechnology* 26 (8), S. 901–908. DOI: 10.1038/nbt.1484.

Wenger, David A.; Coppola, Stephanie; Liu, Shu-Ling (2003): Insights into the diagnosis and treatment of lysosomal storage diseases. In: *Archives of neurology* 60 (3), S. 322–328. DOI: 10.1001/archneur.60.3.322.

Wilcox, William R.; Linthorst, Gabor E.; Germain, Dominique P.; Feldt-Rasmussen, Ulla; Waldek, Stephen; Richards, Susan M. et al. (2012): Anti-α-galactosidase A antibody response to agalsidase beta treatment: data from the Fabry Registry. In: *Molecular genetics and metabolism* 105 (3), S. 443–449. DOI: 10.1016/j.ymgme.2011.12.006.

Wishart, David S.; Knox, Craig; Guo, An Chi; Shrivastava, Savita; Hassanali, Murtaza; Stothard, Paul et al. (2006): DrugBank: a comprehensive resource for in silico drug discovery and exploration. In: *Nucleic acids research* 34 (Database issue), D668-72. DOI: 10.1093/nar/gkj067.

Wittmann, Judit; Karg, Eszter; Turi, Sàndor; Legnini, Elisa; Wittmann, Gyula; Giese, Anne-Katrin et al. (2012): Newborn screening for lysosomal storage disorders in hungary. In: *JIMD reports* 6, S. 117–125. DOI: 10.1007/8904_2012_130.

Wu, Xiaoyang; Katz, Evan; Della Valle, Maria Cecilia; Mascioli, Kirsten; Flanagan, John J.; Castelli, Jeffrey P. et al. (2011): A pharmacogenetic approach to identify mutant forms of α-galactosidase A that respond to a pharmacological chaperone for Fabry disease. In: *Human mutation* 32 (8), S. 965–977. DOI: 10.1002/humu.21530.

Xu, You-Hai; Quinn, Brian; Witte, David; Grabowski, Gregory A. (2003): Viable Mouse Models of Acid β-Glucosidase Deficiency. In: *The American Journal of Pathology* 163 (5), S. 2093–2101. DOI: 10.1016/s0002-9440(10)63566-3.

Yam, Gary Hin-Fai; Roth, Jürgen; Zuber, Christian (2007): 4-Phenylbutyrate rescues trafficking incompetent mutant alpha-galactosidase A without restoring its functionality. In: *Biochemical and biophysical research communications* 360 (2), S. 375–380. DOI: 10.1016/j.bbrc.2007.06.048.

Yang, Chunzhang; Wang, Herui; Zhu, Dongwang; Hong, Christopher S.; Dmitriev, Pauline; Zhang, Chao et al. (2015): Mutant glucocerebrosidase in Gaucher disease recruits Hsp27 to the Hsp90 chaperone complex for proteasomal degradation. In: *Proceedings of the National Academy of Sciences of the United States of America* 112 (4), S. 1137–1142. DOI: 10.1073/pnas.1424288112.

Zampieri, Stefania; Cattarossi, Silvia; Bembi, Bruno; Dardis, Andrea (2017): GBA Analysis in Next-Generation Era: Pitfalls, Challenges, and Possible Solutions. In: *The Journal of molecular diagnostics : JMD* 19 (5), S. 733–741. DOI: 10.1016/j.jmoldx.2017.05.005.

Zeng, Jibin; Racicott, Jesse; Morales, Carlos R. (2009): The inactivation of the sortilin gene leads to a partial disruption of prosaposin trafficking to the lysosomes. In: *Experimental cell research* 315 (18), S. 3112–3124. DOI: 10.1016/j.yexcr.2009.08.016.

Zhang, Xiao-Wen; Feng, Na; Liu, Yan-Chen; Guo, Qiang; Wang, Jing-Kang; Bai, Yi-Zhen et al. (2022): Neuroinflammation inhibition by small-molecule targeting USP7 noncatalytic domain for neurodegenerative disease therapy. In: *Science advances* 8 (32), eabo0789. DOI: 10.1126/sciadv.abo0789.

Zheng, Wei; Padia, Janak; Urban, Daniel J.; Jadhav, Ajit; Goker-Alpan, Ozlem; Simeonov, Anton et al. (2007): Three classes of glucocerebrosidase inhibitors identified by quantitative high-throughput screening are chaperone leads for Gaucher disease. In: *Proceedings of the National Academy of Sciences of the United States of America* 104 (32), S. 13192–13197. DOI: 10.1073/pnas.0705637104.

Zhong, Xi Zoë; Sun, Xue; Cao, Qi; Dong, Gaofeng; Schiffmann, Raphael; Dong, Xian-Ping (2016): BK channel agonist represents a potential therapeutic approach for lysosomal storage diseases. In: *Scientific reports* 6, S. 33684. DOI: 10.1038/srep33684.

Zhu, Xiaoxiang; Sheth, Kamlesh A.; Li, Shihong; Chang, Hui-Hwa; Fan, Jian-Qiang (2005): Rational design and synthesis of highly potent beta-glucocerebrosidase inhibitors. In: *Angewandte Chemie (International ed. in English)* 44 (45), S. 7450–7453. DOI: 10.1002/anie.200502662.

Zimran, A.; Gelbart, T.; Westwood, B.; Grabowski, G. A.; Beutler, E. (1991): High frequency of the Gaucher disease mutation at nucleotide 1226 among Ashkenazi Jews. In: *American journal of human genetics* 49 (4), S. 855–859.

Zimran, Ari; Altarescu, Gheona; Elstein, Deborah (2013): Pilot study using ambroxol as a pharmacological chaperone in type 1 Gaucher disease. In: *Blood cells, molecules & diseases* 50 (2), S. 134–137. DOI: 10.1016/j.bcmd.2012.09.006.

Zimran, Ari; Elstein, Deborah (2014): Management of Gaucher disease: enzyme replacement therapy. In: *Pediatric endocrinology reviews : PER* 12 Suppl 1, S. 82–87. DOI: Review.

7 Anhang

7.1 Abkürzungsverzeichnis

Abb.	Abbildung
ABX	Ambroxol
AGAL	α-Galactosidase A
Ala	Aminosäure Alanin
Arg	Aminosäure Arginin
Asn	Aminosäure Asparagin
Asp	Aminosäure Asparaginsäure
β-Glu	Glucocerebrosidase
c.	Angabe einer kodierenden DNA-Referenzsequenz nach Human Genome Variation Society
CGN	cis-Golgi-Netzwerk
CHO-Zellen	aus Ovarien der chinesischen Hamsterart Cricetulus griseus isolierte Zelllinie
CLEAR	*Coordinated Lysosomal Expression and Regulation*
COS-Zellen	aus dem Nierenbindegewebe der afrikanischen grünen Meerkatze Chlorocebus aethiops isolierte Zelllinie
Cys	Aminosäure Cystein
DGJ	1-Deoxygalactonojirimycin
DNJ	1-Deoxynojirimycin
DNA	Desoxyribonukleinsäure
DTP	2,6-Dithiopurin
EC_{50}	halbe maximale effektive Konzentration
EMA	European Medicines Agency, europäische Arzneimittelbehörde
ER	Endoplasmatisches Retikulum
ERAD	ER-assoziierte Degradation
ERT	Enzymersatztherapie
FDA	Food and Drug Administration, US-amerikanische Arzneimittelbehörde
GAA	saure α-Glucosidase
Gb3	Globotriaosylceramid
GCS	Glucosylceramid-Synthase
Glc	Glucose
GlcNAc	N-Acetylglucosamin
Gln	Aminosäure Glutamin
Glu	Aminosäure Glutaminsäure
Gly	Aminosäure Glycin
GM_2	Monosialinsäure-Gangliosid Typ 2
GVUS	genetische Variante unbekannter Signifikanz
HEK/HEK293	humane embryonale Nierenzelllinie
HGMD	Human Genome Mutation Database
His	Aminosäure Histidin
IC_{50}	halbe maximale Hemmstoffkonzentration
IFG	Isofagomin
Ile	Aminosäure Isoleucin
IOPD	infantile-onset Pompe disease
Leu	Aminosäure Leucin
LOPD	late-onset Pompe disease
LSD	lysosomale Speicherkrankheit
Lyso-Gb3	Globotriaosylsphingosin
M.	Morbus

Man	Mannose
Man-6-P	Mannose-6-Phosphat
MD	molekulares Docking
MIM	Mendelian Inheritance in Man, Kompendium humaner Gene und Phänotypen
mRNA	Boten Ribonukleinsäure
N	Aminogruppe
NB-DNJ	N-Butyldeoxynojirimycin
NP-C	Morbus Niemann-Pick Typ C
NPC1	Niemann-Pick C1 Protein
p.	Angabe für eine Protein-Referenzsequenz nach Human Genome Variation Society
PC	pharmakologisches Chaperon
PCT	pharmakologisches Chaperon Therapie
PR	proteasomaler Regulator
Pro	Prolin
PSSM	position specific substitution matrix
rER	raues endoplasmatisches Retikulum
RSG	Rosiglitazon
Ser	Aminosäure Serin
SRT	Substratreduktionstherapie
TFEB	Trankriptionsfaktor EB
TGN	trans-Golgi-Netzwerk
Thr	Aminosäure Threonin
Trp	Aminosäure Tryptophan
TSA	thermal shift assay
Tyr	Aminosäure Tyrosin
UPR	unfolded protein response
Val	Aminosäure Valin
WT	Wildtyp
X	beliebige Aminosäure
Xq	langer Arm des X-Chromosoms

7.2 Kopien der inkludierten Studien

RESEARCH ARTICLE

Human Mutation

OFFICIAL JOURNAL HGVS HUMAN GENOME VARIATION SOCIETY www.hgvs.org

Functional and Clinical Consequences of Novel α-Galactosidase A Mutations in Fabry Disease

Jan Lukas,[1]* Simone Scalia,[2] Sabrina Eichler,[3] Anne-Marie Pockrandt,[1] Nicole Dehn,[1] Claudia Cozma,[3] Anne-Katrin Giese,[1] and Arndt Rolfs[1,3]

[1] *Albrecht-Kossel-Institute for Neuroregeneration, Medical University Rostock, Rostock, Germany;* [2] *Institute of Biomedicine and Molecular Immunology "A. Monroy" (IBIM), National Research Council (CNR), Palermo, Italy;* [3] *Centogene AG, Rostock, Germany*

Communicated by David S. Rosenblatt

Received 14 July 2015; accepted revised manuscript 10 September 2015.
Published online 29 September 2015 in Wiley Online Library (www.wiley.com/humanmutation). DOI: 10.1002/humu.22910

ABSTRACT: Fabry disease (FD) is a rare metabolic disorder of glycosphingolipid storage caused by mutations in the *GLA* gene encoding lysosomal hydrolase α-galactosidase A (α-gal A). Recently, the diagnostic procedure for FD has advanced in several ways, through the development of a specific biomarker (lyso-Gb3) and the implementation of newborn screenings, which acted as a catalyst to augment general awareness of the disease. Heterologous over-expression of α-gal A variants and subsequent in vitro measurement of enzyme activity provided molecular data to elucidate the relationship between mutation, enzyme damage, lyso-Gb3 biomarker levels, and clinical phenotype. This knowledge is the foundation for improved counseling with regard to prognosis and therapeutic decisions. Herein, we resume the approach of in vitro characterization, with a further 73 mainly novel *GLA* gene mutations. Patient lyso-Gb3 data were available for most of the mutations. All mutations were tested for responsiveness to pharmacological chaperone treatment and phenotypic data for 61 hemizygous male and 116 heterozygous female patients carrying a mutation associated with ≥20% residual activity, formerly classified as "mild" variant, were collected in order to evaluate the pathogenicity. We conclude that a mild *GLA* variant is typically characterized by high residual enzyme activity and normal biomarker levels. We found evidence that these variants can still be classified as a distinctive, but milder, sub-type of FD.
Hum Mutat 37:43–51, 2016. © 2015 Wiley Periodicals, Inc.

KEY WORDS: Fabry disease; GLA; variants of unknown significance; GVUS; pharmacological chaperone therapy

Introduction

Fabry disease (FD; MIM# 301500) is a lysosomal storage disorder caused by mutations in the X-chromosomal *GLA* gene (Xq22), encoding α-galactosidase A (α-gal A; MIM# 300644). The estimated number of *GLA* gene variations is approaching four-figure number (Supp. Table S1; HGMD® Professional 2015.1 [http://www.hgmd.cf.ac.uk/]; and Fabry-database [http://fabry-database.org], accessed on 01-15-2015). Pathological changes in *GLA*—both the gene and its encoded protein—result in storage of complex sphingolipids in the lysosome, mainly Globotriaosylceramide (Gb3), which in turn causes FD, a cellular and microvascular dysfunction with multiple organ involvement.

In the classical form of FD, symptoms are typically first experienced in early childhood, consisting of acroparesthesia, abdominal pain and fever. During adolescence, the affected subjects exhibit angiokeratomas, decreased ability to perspire, proteinuria and progressive renal insufficiency and cornea verticillata. Progressing with age, the patients manifest cardiomyopathy and arrhythmia and cerebrovascular complications [Germain, 2010]. Formerly, the estimated prevalence of FD has been reported as one out of 40,000 to one out of 117,000 in males [Meikle et al., 1999, Desnick et al., 2001]. However, newborn screening initiatives suggest that the rate of *GLA* gene alterations exceeds this number by an order of magnitude. Indicated incidences range from about 1:1,500 in the Taiwanese [Hwu et al., 2009] to 1:13,341 in the Hungarian population [Wittmann et al., 2012] considering exonic changes only. Evidently, the elevated incidence of *GLA* mutations is due to the fact that many patients who present with a mild, late-onset symptomatology or with single organ involvement—as observed in cardiac, renal, and cerebrovascular variants of FD [Nakao et al., 1995; Nance et al., 2006; Rolfs et al., 2005; Brouns et al., 2010]—are screened for variations in the *GLA* gene to determine the etiology. This has led to the discovery of many novel mutations within the last two decades (Supp. Table S1). Moreover, adaptation of clinical management led to the inclusion of female heterozygous mutation carriers affected by FD [Guffon, 2003]. A study in Italy, however, reported an unchanged incidence of classic FD [Spada et al., 2006].

If a previously undescribed novel *GLA* variant is detected in a patient who lacks typical clinical features of FD, prognosis is often difficult, especially in females. Information gleaned from familial testing may be limited because members can remain symptom-free until the fifth or sixth decade or even throughout their entire life. Incorrect interpretation of the clinical significance of a *GLA* variant can cause inappropriate disease counseling. In order to improve the interpretation of uncertain *GLA* gene variants, we developed a cell-culture based system to investigate the downstream enzyme damage [Lukas et al., 2013]. A high proportion of mutations (60%–70%) lead to complete abolishment of, or very low, enzyme activity. In such cases, the prognosis is clear and respective patients are predicted to develop classic FD with all its phenotypic consequences. Enzyme replacement therapy (ERT) can be initiated immediately thus reaping the benefits of earlier treatment which is the most efficacious.

Additional Supporting Information may be found in the online version of this article.

*Correspondence to: Jan Lukas, Albrecht-Kossel-Institute for Neuroregeneration, Department of Medical Genetics, Medical University of Rostock, Gehlsheimer Str. 20, 18147 Rostock, Germany. E-mail: jan.lukas@med.uni-rostock.de

However, the number of *GLA* mutations known to result in α-gal A retaining a remarkable residual activity of about 20% or more of the normal level has increased dramatically. These so-called "mild" mutations generally occur in mono-, bi-, or oligo-symptomatic patients and are partially referred to as gene variants of unclear significance (GVUS) [van der Tol et al., 2014]. As all symptoms are not exclusive to FD (e.g., stroke, cardiomyopathy), but rather represent a differential diagnosis for a series of other disorders, the pathogenic nature of some mutations requires further investigation.

The present article describes 73 mutations, which underwent in vitro analysis. The aim of the study was to analyze *GLA* mutations in-depth on the basis of a holistic approach involving in vitro enzyme activity measurement of the mutant α-gal A enzyme in cell culture (over-expression) as well as determination of the biomarker globotriaosylsphingosine (lyso-Gb3) from either plasma or dried blood spots (DBS). Lyso-Gb3 is a deacylated metabolite of Gb3 with a higher sensitivity than Gb3 and a good correlation to the FD phenotype [Tsukimura et al., 2014, Smid et al., 2015(II)]. Furthermore, we introduce outline data for 61 male and 116 female patients with atypical FD (including age of diagnosis and symptomatic spectrum) in concurrence with one of 26 GVUS described in this study, in an attempt to elucidate the pathogenesis of these specific cases.

As mentioned, FD is currently treated with ERT. A paradigm shift in the approach to therapy was inspired by the fact that many of the mutations cause the protein to misfold, with the consequence of early ER-associated proteasomal degradation [Fan et al., 2007]. We therefore advocate that a great fraction of mutations can potentially be treated by an alternative therapeutic approach involving genotype-dependent pharmacological chaperone therapy (PCT). Consequently, every α-gal A mutant was tested for responsiveness to the pharmacological chaperone (PC) deoxygalactonojirimycin (DGJ; AT1001, Migalastat) in our cell culture system in order to establish whether PCT is a potentially suitable treatment option for patients with these genotypes. This experimental step provides preclinical evidence as to whether a mutation is a potential target for PCT with DGJ [Wu et al., 2011] which is currently investigated in a phase 3 clinical trial (ClinicalTrials.gov Identifier: NCT01458119).

Materials and Methods

Patients and Blood Samples

Blood samples were obtained from patients undergoing biochemical analysis or genetic testing for FD by Centogene AG (Rostock, Germany). All patients agreed for testing of their blood samples. The project was in concordance with the regulations of the local Ethical Committee of the University Rostock.

Cell Culture

HEK-293H cells were maintained in DMEM (Dulbecco's Modified Eagle Medium; Invitrogen, Karlsruhe, Germany) supplemented with 10% FBS (fetal bovine serum; PAA Laboratories, Pasching, Austria) and 1% penicillin/streptomycin (Invitrogen). All cells were incubated in a water-jacket incubator (Binder, Tuttlingen, Germany) under standard cultivation conditions (37°C, 5% CO_2).

Site-Directed Mutagenesis of α-Gal A

Expression vectors harboring *GLA* mutations were generated by site-directed PCR mutagenesis using the Q5 Site-Directed Mutagenesis Kit (New England Biolabs, Ipswich, MA). The expression vector harboring the wild-type cDNA of *GLA* has been introduced before [Lukas et al., 2013]. Nucleotide exchanges or deletions were individually introduced by PCR amplification using sense and antisense primers designed according to the exponential amplification principle. Each mutant plasmid was sequenced at Source Bioscience (Berlin, Germany) to ensure sequence integrity. Throughout the manuscript, we refer to the *GLA* reference sequence: GenBank NM_000169.2. In accordance with HGVS recommendations (v 2.0), nucleotide numbering uses +1 as the A of the ATG translation initiation codon in the reference sequence, with the initiation codon as codon 1. Variants were submitted to the ClinVar (NCBI) public database (http://www.ncbi.nlm.nih.gov/clinvar/).

Transient Expression and Enzymatic Measurement of Mutant α-Gal A in HEK-293H Cells

The method for transient expression of mutant α-gal A in HEK-293H cells and subsequent determination of enzymatic activity has been carried out as described previously [Lukas et al., 2013]. In brief, we seeded HEK-293H cells on the day before transfection using 24-well culture plates (Sarstedt, Nümbrecht, Germany) and antibiotic-free high glucose DMEM supplemented with 10% FBS. On the day of transfection, the cells reached 70%–80% confluency. Lipofectamin 2000 (Invitrogen, Carlsbad, CA) and the *GLA* cDNA containing plasmid vector was added according to the instruction manual. After 4 hr incubation, the antibiotic-free medium was removed and 500 μl fresh DMEM supplemented with 10% FBS and 1% penicillin/streptomycin was added. In this step, DGJ (BIOZOL Diagnostica, Eching, Germany) was added to the culture medium from an aqueous stock solution (10 mM) where intended. The cells were incubated for another 60 hr before being harvested. After this period, the cells were homogenized in 200 μl deionized water and subjected to five freeze/thaw cycles using liquid nitrogen. The homogenate was centrifuged at 10,000*g* for 5 min in order to obtain the supernatant for the enzyme activity assay. The artificial substrate 4-MU-α-D-galactopyranoside (2 mM; Sigma–Aldrich, Munich, Germany) in 0.06 M phosphate citrate buffer (pH 4.7) was added to 50 ng of total protein. Protein measurement was carried out using BCA assay reagent (Thermo Fisher, Braunschweig, Germany). Enzyme reactions were terminated by the addition of 0.2 ml of 1.0 M glycine buffer (pH 10.5). The released 4-MU was determined by fluorescence measurement in a microplate fluorescence reader (Tecan, Männedorf, Switzerland). The measured enzyme activity was calculated as nmol 4-MU/mg protein and normalized to one hundred percent wild-type activity.

Lyso-Gb3 Level Determination from Plasma and DBS

For detailed methods, see the Supporting Information.

Statistical Tests

All statistical tests were carried out using GraphPad Prism5 software. To study the correlation of lyso-Gb3 with in vitro enzyme activity and age non-parametric rank correlation test to calculate spearman's *rho* was used.

Results

In Vitro Enzyme Activity Measurement of α-Gal A Mutants

Seventy-three mutations were tested for residual enzyme activity, and responsiveness to the PC DGJ (see Table 1). The majority of mutations have not previously been reported (45 out of 73) or have not been tested in a comparable overexpression system (63 out of 73). The remainder of the mutations (c.58G>C (p.A20P), c.118C>T (p.P40S), c.272T>C (p.I91T), c.281G>C (p.C94S), c.605G>A (p.C202Y), c.776C>G (p.P259R), c.826A>G (p.S276G), c.958A>T (p.N320Y), c.982G>C (p.G328R), c.1072G>A (p.E358K), RNA not analyzed) showed similar behavior to that observed by other groups, with regard to residual activity and responsiveness towards DGJ (Supp. Table S2). Altogether, 34 out of 73 of the mutant enzymes responded to DGJ treatment with a resulting elevation in activity according to the criteria established by our previous work [Lukas et al., 2013, also summarized in Table 1].

The data set was opposed to the DGJ-responsiveness prediction algorithm "Fabry-cep" (available at http://www.icb.cnr.it/project/fabry_cep/). "Fabry-cep" rated 19 out of 70 as "unclear". Mutations affecting the N-terminal signal peptide ($N = 5$) and nonsense mutations ($N = 3$) were excluded from the analysis. Comparison with the experimental data revealed 19 true negatives (in vitro non-responders), 13 true positives (in vitro responders), but also 11 false negatives and three false positives. Supp. Table S3 summarizes the results for all 46 predicted mutations indicating a positive predictive value (0.81) comparable to the former report [Cammisa et al., 2013].

Biomarker Globotriaosylsphingosine

Globotriaosylsphingosine (lyso-Gb3) is an effective biomarker for the classification of FD severity [Smid et al., 2015(II)]. In the present study, we measured this marker in plasma or DBS (for details see Supp. Methods S1). Records from 207 (132w/75m) patients with a *GLA* variant were collected (Table 1). There is a strong negative correlation between residual enzyme activity and height of the biomarker in the male portion of the cohort (Spearman's *rho*: −0.73, $P < 0.0001$, compare Fig. 1) and a moderate correlation for the females (Spearman's *rho*: −0.44, $P < 0.0001$). Most male individuals, even these with mutations with high residual in vitro enzyme activity (≥20%), showed increased biomarker values. Only few mutations caused inconspicuous biomarker levels in males, that is, lower than the estimated pathological cut-off of 0.9 ng/ml (c.7C>G (p.L3V), c.8T>C (p.L3P), c.683A>G (p.N228S), c.926C>T (p.A309V), c.968C>G (p.P323R), c.989A>G (p.Q330R), c.1055C>G (p.A352G), RNA not analyzed; in vitro enzyme activity range: 48.0%–117.7%). Lyso-Gb3 levels were only slightly elevated by mean (<5 ng/ml) in male patients with mutations c.179C>T (p.P60L), c.239G>A (p.G80D), c.337T>A (p.F113I), c.593T>C (p.I198T), c.641C>T (p.P214L), c.724A>G (p.I242V), c.1196G>C (p.W399S), RNA not analyzed (in vitro enzyme activity range: 15.6%–70.6%), whereas single individuals even had normal lyso-Gb3.

Mutations resulting in less than 1% residual enzyme activity were mostly associated with classic FD [Lukas et al., 2013]. Among these, all male patients had pathologically elevated biomarker levels. For the females, there appear to be factors other than *GLA* mutation type that determine biomarker elevation. Analyzing two extensive families with a classic FD-related mutation, p.C94Y [Eng et al., 1997] and p.E358K [Germain et al., 2002], respectively, we set out to test whether biomarker level is correlated with age (Fig. 2). Both mutant enzymes did not display any residual activity in the over-expression system. In the family with the p.E358K genotype, two out of four individuals between 3 and 22 years of age show normal lyso-Gb3, and other two patients show only a mild elevation. Individuals aged 25–63 years show modest to strong biomarker elevation. However, the relationship between elevated biomarker and age is not significant as determined by Mann–Whitney *U* test (data not shown). The same holds true for the 21 female patients with the c.281G>A (p.C94Y, RNA not analyzed) genotype. Even though it can be assumed that lyso-Gb3 increases progressively with age in a single patient, the variation between family members with the same genotype implies that factors other than age determine the biomarker level. This finding highlights the clinical heterogeneity of the disease even in patients with the same genotype.

"Mild" Mutations can Provoke FD Symptoms

Patients carrying mild mutations (≥20% residual in vitro activity) usually present with later-onset disease and a symptom spectrum different from the classically affected patients. In order to investigate disease severity in patients with mild mutations, we collected the clinical records from 61 male and 116 female patients. The clinical spectrum for this sub-fraction of mutations encompasses the whole spectrum of typical FD symptoms (Fig. 3A). However, the frequency of mono- or bi-symptomatic cases is high, 59.0% in males and 43.1% in females, respectively and in a small proportion of patients (seven out of 61 males and 15 out of 116 females) no apparent FD symptoms were detected; these patients were recruited as family members of affected patients. The median age of the asymptomatic (24.0/m and 24.4/f yrs) versus affected (51.6/m and 44.7/f yrs) individuals differed significantly ($P = 0.0276$/m and $P = 0.001$/f), using Mann–Whitney *U* test. This may argue for a potential very late onset pathogenicity of the mutations. In addition, 18 out of 61(m) and 51 out of 116(f) had a more severe clinical record with three or more symptoms. Interestingly, there is apparently no sex-dependent difference in disease severity, unlike patients with classic mutations [Vedder et al., 2007].

Discussion

In order to accurately interpret the various *GLA* gene mutations potentially causing FD, systematic biochemical in vitro characterization with a clear and comprehensive read-out is imperative for good clinical counseling. Cell culture-based over-expression and in vitro enzyme activity measurement was carried out for 73, partially novel, α-gal A variants.

In accordance with our preceding study we found good correlation between in vitro activity of the mutants and the patient's biomarker level (Fig. 1) which illustrates that this method delivers solid and clinically relevant data regardless of the sub-fraction of mutations under investigation. Even though, not surprisingly, the correlation is better in male patients, females tend to display genotype-dependent biomarker elevation related to the biochemical damage of the α-gal A enzyme. Despite the fact that the wide spectrum of clinical manifestations in FD is presumably influenced by the effects of a great number of modifier genes [Altarescu et al., 2005] and epigenetic factors [Barba-Romero et al., 2010], this study provides further evidence that reduced enzyme activity is actually the main determinant for biomarker elevation and, hence, phenotypic severity.

HUMAN MUTATION, Vol. 37, No. 1, 43–51, 2016

Table 1. Summary of Tested *GLA* Variants

N	Amino acid	cDNA	In vitro enzyme activity [% WT] in mean ± SEM (N)		Responder[a]	Responder prediction (Fabry_cep)[b]	Blood lyso-Gb3 [mean (N)][c]		PolyPhen-2[d]
			−DGJ	+DGJ			Male	Female	
1	**p.L3V**	**c.7C>G**	81.5 ± 9.2 (5)	88.0 ± 12.4 (5)	Yes	–	0.5 (1)	0.5 (1)	Benign
2	**p.L3P**	**c.8T>C**	117.7 ± 13.7 (4)	129.4 ± 12.6 (4)	Yes	–	0.5 (1)	0.5 (1)	Benign
3	p.A20P	c.58G>C	2.5 ± 0.4 (11)	4.9 ± 0.8 (12)	No	–	8.5 (1)	0.7 (1)	Benign
4	**p.A20D**	**c.59C>A**	2.8 ± 0.1 (3)	4.5 ± 0.2 (3)	No	–		3.7 (1)	Possibly damaging
5	**p.L21P**	**c.62T>C**	0.6 ± 0.1 (3)	1.7 ± 0.3 (3)	No	–	70.9 (1)		Probably damaging
6	**p.D33G**	**c.98A>G**	37.4 ± 5.1 (3)	62.0 ± 4.8 (3)	Yes	Unclear	17.6 (1)	1.0 (2)	Possibly damaging
7	**p.G35E**	**c.104G>A**	38.0 ± 7.8 (4)	70.8 ± 14.6 (4)	Yes	No	45.3 (1)	0.7 (1)	Probably damaging
8	**p.L36W**	**c.107T>G**	2.3 ± 0.6 (5)	22.3 ± 1.5 (5)	Yes	No	31.7 (1)	0.5 (1)	Probably damaging
9	p.P40S	c.118C>T	0 (4)	1.4 ± 0.5 (3)	No	No	11.8 (2)	1.6 (2)	Probably damaging
10	p.M42T	c.125T>C	2.9 ± 0.3 (4)	21.4 ± 5.0 (4)	Yes	No		0.5 (1)	Probably damaging
11	p.L45P	c.134T>C	0 (4)	0 (4)	No	Unclear	42.7 (2)	9.8 (1)	Probably damaging
12	p.E48D	c.144G>C	0 (4)	0 (4)	No	Unclear	82.2 (2)	11.4 (1)	Probably damaging
13	p.C56Y	c.167G>A	0 (4)	3.3 ± 1.1 (3)	No	No	28.4 (1)	2.5 (3)	Probably damaging
14	p.P60L	c.179C>T	15.6 ± 0.2 (3)	33.1 ± 1.0 (3)	Yes	No	1.4 (3)	2.2 (4)	Probably damaging
15	**p.I64F**	**c.190A>T**	0 (3)	0 (3)	No	Unclear	41.4 (1)	1.2 (2)	Probably damaging
16	**p.E71G**	**c.212A>G**	87.0 ± 4.8 (4)	104.6 ± 7.4 (4)	Yes	Unclear		0.5 (1)	Benign
17	**p.G80D**	**c.239G>A**	29.3 ± 5.7 (4)	30.4 ± 5.4 (4)	No	No	1.6 (3)	1.4 (5)	Probably damaging
18	**p.Y86H**	**c.256T>C**	0 (3)	0.7 ± 0.1 (3)	No	Unclear	23.7 (1)	0.8 (4)	Probably damaging
19	**p.I91N**	**c.272T>A**	0 (3)	0 (3)	No	No	104.0 (1)		Probably damaging
20	p.I91T	c.272T>C	0.7 ± 0.3 (7)	7.0 ± 1.0 (7)	Yes	No	12.9 (1)	0.6 (2)	Probably damaging
21	p.C94Y	c.281G>A	0 (6)	0 (6)	No	No	55.8 (7)	18.2 (20)	Probably damaging
22	p.C94S	c.281G>C	0 (6)	0 (6)	No	No	32.9 (2)	5.7 (1)	Probably damaging
23	**p.F113I**	**c.337T>A**	15.6 ± 1.9 (7)	34.0 ± 5.5 (3)	Yes	No	1.3 (1)	0.5 (3)	Probably damaging
24	**p.A121T**	**c.361G>A**	50.0 ± 8.4 (7)	55.5 ± 6.2 (7)	Yes	Unclear		0.5 (2)	Probably damaging
25	**p.I154T**	**c.461T>C**	98.0 ± 16.4 (8)	108.0 ± 18.6 (8)	Yes	Yes		0.5 (1)	Benign
26	p.W162*	c.485G>A	0 (5)	0 (5)	No	–			–
27	**p. V164L**	**c.490G>T**	43.1 ± 1.0 (5)	47.8 ± 1.1 (5)	No	Unclear			Possibly damaging
28	p.V164G	c.491T>G	1.4 ± 0.1 (6)	2.8 ± 0.5 (6)	No	No			Probably damaging
29	p.L167Q	c.500T>A	0 (6)	0.7 ± 0.3 (6)	No	No		10.7 (1)	Probably damaging
30	**p.L180F**	**c.540G>T**	32.4 ± 9.3 (8)	80.7 ± 15.6 (8)	Yes	Yes	12.2 (2)	1.0 (4)	Possibly damaging
31	p.M187V	c.599A>G	22.8 ± 5.0 (7)	67.0 ± 7.8 (7)	Yes	Unclear			Probably damaging
32	**p.M187I**	**c.561G>A**	3.1 ± 0.6 (5)	31.2 ± 4.5 (5)	Yes	Unclear			Probably damaging
33	**p.R196S**	**c.588A>C**	42.1 ± 2.5 (4)	67.8 ± 6.6 (4)	Yes	No		0.5 (1)	Probably damaging
34	**p.I198T**	**c.593T>C**	38.7 ± 3.1 (3)	50.4 ± 3.2 (3)	Yes	No	4.7 (1)		Probably damaging
35	p.C202Y	c.605G>A	0 (5)	1.4 ± 0.5 (5)	No	No	31.8 (1)	5.5 (1)	Probably damaging
36	**p.W204R**	**c.610T>C**	0 (3)	0 (3)	No	No	101 (1)		Probably damaging
37	**p.K213R**	**c.638A>G**[e]	68.1 ± 8.5 (4)	65.3 ± 11.4 (4)	No	Yes	30.4 (1)	0.9 (1)	Benign
38	**p.P214L**	**c.641C>T**	19.4 ± 1.4 (3)	64.1 ± 9.8 (3)	Yes	Unclear	4.6 (1)	1.0 (7)	Probably damaging
39	**p.I219M**	**c.657C>G**	15.2 ± 2.2 (5)	56.5 ± 9.4 (5)	Yes	Yes			Probably damaging
40	p.R220*	c.658C>T	0 (5)	0 (5)	No	–	62.8 (3)	7.1 (2)	–
41	**p.R227P**	**c.680G>C**	0 (7)	0 (7)	No	No		4.9 (1)	Probably damaging
42	**p.N228S**	**c.683A>G**	59.5 ± 9.8 (5)	70.6 ± 13.1 (5)	Yes	Yes	0.5 (1)		Probably damaging
43	**p.I242V**	**c.724A>G**	70.6 ± 15.7 (9)	89.4 ± 21.2 (9)	Yes	Yes	2.0 (2)		Benign

(*Continued*)

Table 1. Continued

N	Amino acid	cDNA	In vitro enzyme activity [% WT] in mean ± SEM (N) –DGJ	In vitro enzyme activity [% WT] in mean ± SEM (N) +DGJ	Responder[a]	Responder prediction (Fabry_cep)[b]	Blood lyso-Gb3 [mean (N)][c] Male	Blood lyso-Gb3 [mean (N)][c] Female	PolyPhen-2[d]
44	p.L243F	c.729G>C	11.4 ± 2.0 (10)	70.8 ± 10.5 (10)	Yes	Yes		0.7 (2)	Probably damaging
45	p.S247P	c.739T>C	0 (6)	5.8 ± 1.5 (6)	Yes	Yes	81.9 (1)		Probably damaging
46	p.N249K	c.747C>A	23.7 ± 1.7 (4)	54.6 ± 3.4 (4)	Yes	Yes			Benign
47	**p.I253T**	**c.758T>C**	73.0 ± 4.8 (3)	115.8 ± 6.9 (3)	Yes	Unclear	8.45 (2)	1.4 (3)	Probably damaging
48	**p.V254A**	**c.761T>C**	26.4 ± 2.4 (3)	39.3 ± 3.2 (3)	Yes	Yes		2.5 (1)	Probably damaging
49	p.P259R	c.776C>G	20.5 ± 2.6 (12)	40.0 ± 4.5 (12)	Yes	No	44.8 (1)		Probably damaging
50	**p.W262R**	**c.784T>C**	0 (3)	0 (3)	No	No		12.3 (1)	Probably damaging
51	**p.V269G**	**c.806T>G**	0 (5)	0 (5)	No	Unclear	15.1 (3)	27.8 (2)	Probably damaging
52	p.S276G	c.826A>G	0 (5)	5.6 ± 1.4 (5)	Yes	Unclear	11.8 (2)	0.9 (4)	Probably damaging
53	**p.I289V**	**c.865A>G**	79.9 ± 6.4 (4)	95.0 ± 4.3(3)	Yes	Yes		0.5 (4)	Probably damaging
54	**p.A309V**	**c.926C>T**	48.0 ± 0.5 (5)	46.6 ± 1.6 (5)	No	Yes	0.5 (1)		Possibly damaging
55	**p.D313N**	**c.937G>A**	90.1 ± 23.0 (4)	95.2 ± 18.7 (3)	Yes	Yes			Benign
56	**p.D315N**	**c.943G>A**	65.3 ± 7.4 (7)	72.4 ± 12.4 (7)	Yes	Yes			Possibly damaging
57	**p.V316A**	**c.947T>C**	49.1 ± 5.5 (3)	58.3 ± 7.7 (3)	Yes	No		0.5 (1)	Probably damaging
58	**p.I317S**	**c.950T>G**	0 (4)	2.7 ± 0.7 (4)	No	No		0.8 (4)	Probably damaging
59	p.N320Y	c.958A>T	0 (6)	0 (6)	No	No		7.0 (2)	Probably damaging
60	**p.P323R**	**c.968C>G**	62.7 ± 4.4 (4)	63.7 ± 3.1 (4)	No	No	0.8 (1)	1.1 (2)	Benign
61	**p.Q327R**	**c.980A>G**	0 (5)	3.9 ± 0.1 (5)	No	Unclear		11.1 (1)	Probably damaging
62	**p.Q327L**	**c.980A>T**	0.6 ± 0.1 (5)	20.0 ± 3.0 (5)	Yes	No	24.0 (1)	5.5 (1)	Probably damaging
63	p.G328R	c.982G>C	0 (8)	0 (4)	No	No		6.8 (5)	Probably damaging
64	**p.Q330R**	**c.989A>G**	54.9 ± 5.4 (5)	62.8 ± 11.9 (5)	Yes	Yes	0.6 (1)		Benign
65	p.R342P	c.1025G>C	0 (7)	0 (7)	No	No	38.6 (4)	2.8 (6)	Probably damaging
66	**p.A352G**	**c.1055C>G**	53.7 ± 4.2 (4)	56.4 ± 2.9 (4)	No	Unclear	0.5 (1)	0.5 (1)	Probably damaging
67	**p.R356P**	**c.1067G>C**	2.1 ± 0.6 (6)	6.7 ± 2.3 (6)	No	No		0.5 (2)	Benign
68	p.E358K	c.1072G>A	0 (3)	0 (3)	No	Yes	45.8 (8)	27.1 (10)	Probably damaging
69	p.G360S	c.1078G>A	0 (3)	0.4 ± 0.2 (3)	No	Unclear			Probably damaging
70	**p.G375A**	**c.1124G>C**	44.1 ± 10.1 (5)	48.8 ± 12.6 (5)	No	Unclear		2.5 (2)	Benign
71	**p.R392S**	**c.1176G>T**	44.3 ± 1.6 (4)	46.2 ± 1.7 (4)	No	Unclear		4.3 (1)	Benign
72	**p.W399S**	**c.1196G>C**	53.0 ± 4.3 (3)	51.5 ± 5.1 (3)	No	No	1.2 (2)		Possibly damaging
73	p.R404del	*c.1212-14 del AAG*	0 (3)	0 (3)	No	–			–

Bold mutations are novel.
[a]According to responder criteria introduced in Lukas et al. (2013); increased enzyme activity of 1.5-fold or >5% compared with the untreated value.
[b]Fabry_cep estimates the likelihood of a mutants' responsiveness to DGJ. We examined a PSSM score of ≥–1 as presumed responder and ≤–3 as presumed non-responder. A score of –2 was regarded unclear according to the basic principles of the algorithm introduced in Andreotti et al. (2011).
[c]lyso-Gb3 values below 0.9 can be considered normal.
[d]PolyPhen-2 (Polymorphism Phenotyping v2.2.2) URL: http://genetics.bwh.harvard.edu/pph2/ (requested during May 2014) (Adzhubei et al., 2010).
[e]Likely splice site mutation

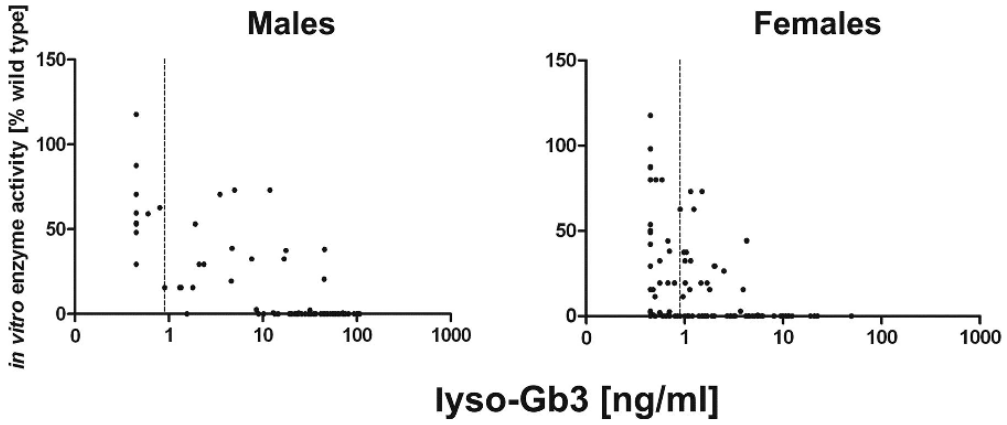

Figure 1. In vitro enzyme activity correlates with lyso-Gb3 level in males and females. The in vitro enzyme activity values of over-expressed α-gal A mutants measured in HEK-293H cell homogenates were plotted against the mean lyso-Gb3 of the patients with the corresponding mutation, that is, each dot represents one genotype (not one patient) (for details see Table 1). The dotted line indicates the pathological cut-off for lyso-Gb3. Individuals with lyso-Gb3 values below the limit of quantitation were calculated to display 50% of pathological cutoff value (0.45 ng/ml).

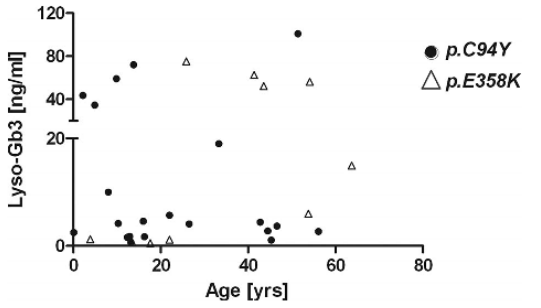

Figure 2. Lyso-Gb3 in female patients with classical FD mutations. The diagram shows lyso-Gb3 values as a function of age in female patients with p.C94Y (black circles) and p.E358K (open triangles). There is no age-dependence of biomarker level in female patients from both families.

However, even though we detected correlation between the enzyme damage (as can be interpolated from the enzyme activity assay) and patient lyso-Gb3 as reflected by Spearman's coefficients of −0.73(m) and −0.44(f), there are still a few specific cases of equivocal compliance between the two parameters. For example, the three mutants p.D33G, p.G35E, and p.G80D had a similar activity (29.3%–38.0% of normal) and were consequently labelled as "mild." Although two male patients with either p.D33G or p.G35E showed strong lyso-Gb3 elevation, the three hemizygous individuals carrying p.G80D only had normal to slightly elevated biomarker values (Table 1). One reasonable explanation is that the patients with unexpectedly high biomarker values had a greater chromosomal rearrangement not detectable by standard sequencing. There is also a certain chance that the assay conditions might not totally reflect the biochemical damage of these specific enzymes because excess amounts of an artificial fluorogenic α-gal A substrate have been used for the assay which may cause disparate kinetics than the natural substrate. However, it is interesting to note that the conversion from glycine to arginine at codon position 35 also leads to a significant residual enzyme activity, but three male patients had strongly elevated lyso-Gb3 of 63.0, 70.4, and 73.2 ng/ml (norm: <0.9 ng/ml) [Lukas et al., 2013]. Therefore, it can be argued that there is some unforeseen damage occurring to mutations at that particular site that cannot be resolved in the cell culture over-expression assay. For this reason, we carefully investigated the mutations that are situated in the vicinity of splice sites. We identified c.638A>G (→ p.K213R) as a potential splice site mutation (Alamut Visual version 2.7; Interactive Biosoftware, Rouen, France) which explains the high lyso-Gb3 despite of the high residual activity after over-expression. However, this analysis did not reveal splice site changes for c.540G>T (p.L180F) and c.641C>T (p.P214L).

In heterozygous female carriers, in addition to the enzyme activity the X-inactivation process plays a crucial role in determining the biomarker level by turning off either the normal or mutated allele. In terms of the *GLA* gene, balanced ratios of mutant:normal alleles reflecting random X-inactivation have been found, as well as evidence for skewed X-inactivation leading to ratios of 70:30 and higher which seems to firmly affect the phenotype [Echevarria et al., 2015]. Overall, lyso-Gb3-levels are highly variable across the whole spectrum of Fabry-related mutations and even intra-familial variation remains high. It can be speculated that biomarker levels are more deeply rooted in ontogenesis, rather than tied to a simple age-related progression. Further investigation is required to clarify how, and to what extent, lyso-Gb3 exposure time and level affect disease burden. Conceivably, long-term investigations on ERT (and substrate reduction therapy) effectiveness will facilitate the establishment and validation of biomarker-based therapeutic goals of FD.

Some genotypes are associated with normal lyso-Gb3, even in male patients. Moreover, these genotypes are characterized by absent classical FD symptoms with onset in the 5th to 7th decade of life. This holds true for many mutations with a residual activity ≥20% of normal. As an example, there is a controversial discussion about *GLA* mutation p.D313Y. Based on an earlier in vitro study, this mutation was labeled as a pseudodeficient variant [Yasuda et al., 2003], but is still deemed relevant in most recent literature [Bono et al., 2011] and screening programs [Baptista et al., 2010; Brouns et al., 2010] with evidence that this mutation leads to a particular CNS involvement [Brouns et al., 2010; Lenders et al., 2013]. However, the mutation is

A Distribution of symptoms in males and females with "mild" FD mutations

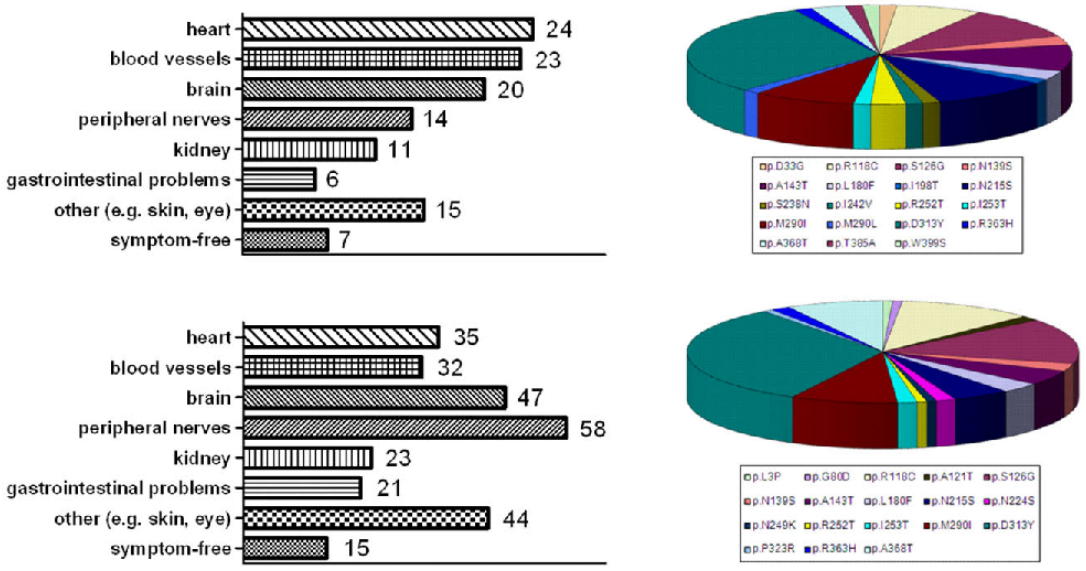

B

	no. of individuals	median age at onset (IQR)	median lyso-Gb3 (IQR) [norm: <0.9]	Symptoms no/mono/bi/multiple	median *in vitro* enzyme activity (IQR)
male	61	51.6 yrs (22.0)	0.47 ng/ml (1.4)	7/22/14/18	51.3 (45.9)
female	116	44.7 yrs (21.4)	0.65 ng/ml (1.1)	15/27/23/51	51.3 (44.9)

Figure 3. Spectrum of symptoms in patients with mild mutations. The patient cohort harbors a total of 153 male and 246 female patients with mild mutations (in vitro enzyme activity > 20% of wild type). **A**: The figure illustrates the symptom spectrum for 61 male (upper) and 116 female (lower) individuals. The fractions of genotypes represented for each group is shown in the pie charts. **B**: Statistics of the patients represented above. Age at disease onset was equated with age at diagnosis and only symptomatic patients were included.

associated with normal plasma lyso-Gb3 in patients [Niemann et al., 2013]. Other recent reports questioned the pathology of mutations formerly regarded as pathogenic, for example, p.P60L, c.352C>T (p.R118C) and c.888G>A (p.M296I), RNA not analyzed [Mitobe et al., 2012; Smid et al., 2015(I); Ferreira et al., 2015].

A glance at the symptom spectrum of individuals harboring mutations with high residual enzyme activity in the over-expression system revealed evidence that the mutation was causative for the observed phenotype. (1) The number of patients with exonic *GLA* alterations in patients with FD symptoms is too high to be coincidental; (2) in the investigated cohort, median age at symptom onset in males and females was significantly higher than median age of the asymptomatic mild mutation carriers ($P = 0.0276$/m and $P = 0.001$/f); (3) in specific genotypes, for example, p.P60L, some individuals had slightly elevated biomarker, some did not, indicating that certain mutations may play the role of a genetic risk factor for common disease, that is, stroke or renal insufficiency, under certain genetic or extra-genetic conditions. However, genetic testing was typically carried out when the patient had a physical symptom. A large cohort of symptom-free and, reasonably, older individuals need to be screened for the presence or absence of mild *GLA* mutations in order to support the finding that these can nevertheless cause FD. Patients with early symptom onset (e.g., <40 years) are particularly good candidates for whole genome/exome analysis, in comparison with symptom-free mutation carriers.

To put it into perspective, some genotypes are probable targets for an alternative therapeutic approach with PCT. The question as to whether a given mutation can be addressed with a small molecule like DGJ has been approached by an in silico prediction algorithm "Fabry-cep" [Cammisa et al., 2013]. We examined PPV, sensitivity (true negatives) and specificity (true positives) for a total of 46 mutations (compare Supp. Table S3). While principally valuable (as indicated by a PPV of 0.81), "Fabry-cep" produced a high number of false-negative predictions leading to a low sensitivity of 0.54. However, "Fabry-cep" identified non-responders accurately leading to a specificity of 0.86 suggesting that this tool is capable of offering a deliberated prediction of possible responders in the absence of experimental data. Interestingly, our experimental analysis revealed that the fraction of responding mutants proved to be higher amongst mutations with residual activity in vitro. Mild mutations

with biochemical behaviour comparable to the wild type should also benefit from PCT. Even though the increase in enzyme activity is merely mild to moderate, the enzyme is stabilized and less vulnerable to heat denaturation and resistant to protease attack [Guce et al., 2011]. Therefore, an orally administered drug might be a preferable option, rendering the more torturous life-long intravenous therapy obsolete.

Of note, we have confirmed a positive genetic diagnosis by detection of a *GLA* mutation in about 1,205 patients with suspected FD, since 2010. The obtained numbers of 771 out of 434 (females/males) approach the expected Mendelian ratio of 2:1 for X-linked diseases, which indicates that female carriers are rarely asymptomatic throughout their entire lives.

Conclusions

We have characterized 73 GLA mutations (45 of which were novel) in a cell culture over-expression system. Most of the corresponding mutant enzymes display absent or strongly reduced enzyme activity. Hence the number of GLA mutations resulting in a residual activity ≥20% of normal level is increased (42.5%) relative to our previous study (26.9%, Lukas et al., 2013). Biomarker lyso-Gb3 is normal in most male and female patients with these mutations, so for this reason cannot serve as a surrogate for genetic diagnosis in these cases. There is, however, strong clinical evidence that mild mutations may lead to a mono- or oligo-symptomatic form of FD later in life. Based on in vitro testing, we predict a high proportion of responders to small molecule treatment (PCT based on the PC DGJ) among mildly affected patients.

Acknowledgments

We are very thankful to all participating patients. A special thanks goes to Jenny Creed Geraghty for excellent advice and proofreading of the manuscript.

Disclosure statement: The authors declare no conflict of interest.

References

Adzhubei IA, Schmidt S, Peshkin L, Ramensky VE, Gerasimova A, Bork P, Kondrashov AS, Sunyaev SR. 2010. A method and server for predicting damaging missense mutations. Nat Methods 7:248–249.

Altarescu G, Moore DF, Schiffmann R. 2005. Effect of genetic modifiers on cerebral lesions in Fabry disease. Neurology 64:2148–2150.

Andreotti G, Citro V, De Crescenzo A, Orlando P, Cammisa M, Correra A, Cubellis MV. 2011. Therapy of Fabry disease with pharmacological chaperones: from in silico predictions to in vitro tests. Orphanet J Rare Dis 6:66.

Baptista MV, Ferreira S, Pinho-E-Melo T, Carvalho M, Cruz VT, Carmona C, Silva FA, Tuna A, Rodrigues M, Ferreira C, Pinto AA, Leitão A, et al. 2010. Mutations of the GLA gene in young patients with stroke: the PORTYSTROKE study–screening genetic conditions in Portuguese young stroke patients. Stroke 41:431–436.

Barba-Romero MA, Deegan P, Giugliani R, Hughes D. 2010. Does geographical location influence the phenotype of Fabry disease in women in Europe? Clin Genet 77:131–140.

Bono C1, Nuzzo D, Albeggiani G, Zizzo C, Francofonte D, Iemolo F, Sanzaro E, Duro G. 2011. Genetic screening of Fabry patients with EcoTILLING and HRM technology. BMC Res Notes 4:323.

Brouns R, Thijs V, Eyskens F, Van den Broeck M, Belachew S, Van Broeckhoven C, Redondo P, Hemelsoet D, Fumal A, Jeangette S, Verslegers W, Baker R, et al. 2010. Belgian Fabry study: prevalence of fabry disease in a cohort of 1000 young patients with cerebrovascular disease. Stroke 41:863–868.

Cammisa M, Correra A, Andreotti G, Cubellis MV. 2013. Fabry_CEP: a tool to identify Fabry mutations responsive to pharmacological chaperones Orphanet. J Rare Dis 8:111.

Desnick RJ, Joannou YA, Eng CM. 2001. α-Galactosidase A deficiency: Fabry disease. *In The metabolic and molecular bases of inherited disease*. New York: McGraw Hill. 3733–3774.

Echevarria L, Benistan K, Toussaint A, Dubourg O, Hagege AA, Eladari D, Jabbour F, Beldjord C, de Mazancourt P, Germain DP. 2015. X chromosome inactivation in female patients with Fabry disease. Clin Genet. 2015 May 14. doi: 10.1111/cge.12613. [Epub ahead of print]

Eng CM, Ashley GA, Burgert TS, Enriquez AL, D'Souza M, Desnick RJ. 1997. Fabry disease: thirty-five mutations in the alpha-galactosidase A gene in patients with classic and variant phenotypes. Mol Med 3:174–182.

Fan JQ, Ishii S. 2007. Active-site-specific chaperone therapy for Fabry disease: Yin and Yang of enzyme inhibitors. FEBS J 274:4962–4971.

Ferreira S, Ortiz A, Germain DP, Viana-Baptista M, Caldeira-Gomes A, Camprecios M, Fenollar-Cortés M, Gallegos-Villalobos Á, Garcia D, García-Robles JA, Egido J, Gutiérrez-Rivas E, et al. 2015. The alpha-galactosidase A p.Arg118Cys variant does not cause a Fabry disease phenotype: data from individual patients and family studies. Mol Genet Metab 114:248–258.

Germain DP, Shabbeer J, Cotigny S, Desnick RJ. 2002. Fabry disease: twenty novel alpha-galactosidase A mutations and genotype-phenotype correlations in classic and variant phenotypes. Mol Med 8:306–312.

Germain DP. 2010. Fabry Disease. Orphanet J Rare Dis 5:30.

Guffon N. 2003. Clinical presentation in female patients with Fabry disease. J Med Genet 40:e38.

Guce AI, Clark NE, Rogich JJ, Garman SC. 2011. The molecular basis of pharmacological chaperoning in human α-galactosidase. Chem Biol 18:1521–1526.

Hwu WL, Chien YH, Lee NC, Chiang SC, Dobrovolny R, Huang AC, Yeh HY, Chao MC, Lin SJ, Kitagawa T, Desnick RJ, Hsu LW. 2009. Newborn screening for Fabry disease in Taiwan reveals a high incidence of the later-onset GLA mutation c.936+919G>A (IVS4+919G>A). Hum Mutat 30:1397–1405.

Lenders M, Duning T, Schelleckes M, Schmitz B, Stander S, Rolfs A, Brand SM, Brand E. 2013. Multifocal white matter lesions associated with the D313Y mutation of the α-galactosidase A gene. PLoS One 8:e55565.

Lukas J, Giese AK, Markoff A, Grittner U, Kolodny E, Mascher H, Lackner KJ, Meyer W, Wree P, Saviouk V, Rolfs A. 2013. Functional characterisation of alpha-galactosidase a mutations as a basis for a new classification system in fabry disease. PLoS Genet 9:e1003632.

Meikle PJ, Hopwood JJ, Clague AE, Carey WF. 1999. Prevalence of lysosomal storage disorders. JAMA 281:249–254.

Mitobe S, Togawa T, Tsukimura T, Kodama T, Tanaka T, Doi K, Noiri E, Akai Y, Saito Y, Yoshino M, Takenaka T, Saito S, et al. 2012. Mutant α-galactosidase A with M296I does not cause elevation of the plasma globotriaosylsphingosine level. Mol Genet Metab 107:623–626.

Nance CS, Klein CJ, Banikazemi M, Dikman SH, Phelps RG, McArthur JC, Rodriguez M, Desnick RJ. 2006. Later-onset Fabry disease: an adult variant presenting with the cramp-fasciculation syndrome. Arch Neurol 63:453–457.

Nakao S, Takenaka T, Maeda M, Kodama C, Tanaka A, Tahara M, Yoshida A, Kuriyama M, Hayashibe H, Sakuraba H, Tanaka H. 1995. An atypical variant of Fabry's disease in men with left ventricular hypertrophy. N Engl J Med 333: 288–293.

Niemann M, Rolfs A, Giese A, Mascher H, Breunig F, Ertl G, Wanner C, Weidemann F. 2013. Lyso-Gb3 indicates that the alpha-galactosidase A mutation D313Y is not clinically relevant for Fabry disease. JIMD Rep 7:99–102.

Rolfs A, Böttcher T, Zschiesche M Morris P, Winchester B, Bauer P, Walter U, Mix E, Löhr M, Harzer K, Strauss U, Pahnke J, et al. 2005. Prevalence of Fabry disease in patients with cryptogenic stroke: a prospective study. Lancet 366:1794–1796.

Smid BE, Hollak CE, Poorthuis BJ, van den Bergh Weerman MA, Florquin S, Kok WE, Lekanne Deprez RH, Timmermans J, Linthorst GE. 2015. Diagnostic dilemmas in Fabry disease: a case series study on GLA mutations of unknown clinical significance. Clin Genet 88:161–166.

Smid BE, van der Tol L, Biegstraaten M, Linthorst GE, Hollak CE, Poorthuis BJ. 2015. Plasma globotriaosylsphingosine in relation to phenotypes of Fabry disease. J Med Genet 52:262–268.

Spada M, Pagliardini S, Yasuda M, Tukel T, Thiagarajan G, Sakuraba H, Ponzone A, Desnick RJ. 2006. High incidence of later-onset fabry disease revealed by newborn screening. Am J Hum Genet 79:31–40.

Tsukimura T, Nakano S, Togawa T, Tanaka T, Saito S, Ohno K, Shibasaki F, Sakuraba H. 2014. Plasma mutant α-galactosidase A protein and globotriaosylsphingosine level in Fabry disease. Mol Genet Metab Rep 1:288–298.

van der Tol L, Smid BE, Poorthuis BJ, Biegstraaten M, Deprez RH, Linthorst GE, Hollak CE. 2014. A systematic review on screening for Fabry disease: prevalence of individuals with genetic variants of unknown significance. J Med Genet 51:1–9.

Vedder AC, Linthorst GE, van Breemen MJ, Groener JE, Bemelman FJ, Strijland A, Mannens MM, Aerts JM, Hollak CE. 2007. The Dutch Fabry cohort: diversity of clinical manifestations and Gb3 levels. J Inherit Metab Dis 30:68–78.

Wittmann J, Karg E, Turi S, Legnini E, Wittmann G, Giese AK, Lukas J, Gölnitz U, Klingenhäger M, Bodamer O, Mühl A, Rolfs A. 2012. Newborn screening for lysosomal storage disorders in hungary. JIMD Rep 6:117–125.

Wu X, Katz E, Della Valle MC, Mascioli K, Flanagan JJ, Castelli JP, Schiffmann R, Boudes P, Lockhart DJ, Valenzano KJ, Benjamin ER. 2011. A pharmacogenetic approach to identify mutant forms of α-galactosidase A that respond to a pharmacological chaperone for Fabry disease. Hum Mutat 32:965–977.

Yasuda M, Shabbeer J, Benson SD, Maire I, Burnett RM, Desnick RJ. 2003. Fabry disease: characterization of alpha-galactosidase A double mutations and the D313Y plasma enzyme pseudodeficiency allele. Hum Mutat 22:486–492.

International Journal of
Molecular Sciences

MDPI

Article

The Large Phenotypic Spectrum of Fabry Disease Requires Graduated Diagnosis and Personalized Therapy: A Meta-Analysis Can Help to Differentiate Missense Mutations

Valentina Citro [1], Marco Cammisa [2], Ludovica Liguori [3], Chiara Cimmaruta [1,3], Jan Lukas [4,*], Maria Vittoria Cubellis [1,*] and Giuseppina Andreotti [3]

1 Dipartimento di Biologia, Università Federico II, 80126 Napoli, Italy; vale.ctr@gmail.com (V.C.); chiaracimmaruta@yahoo.it (C.C.)
2 Istituto di Genetica e Biofisica 'A. Buzzati-Traverso', CNR, 80131 Napoli, Italy; cammisamarco.py@gmail.com
3 Istituto di Chimica Biomolecolare, CNR, 80078 Pozzuoli, Italy; lud.liguori@gmail.com (L.L.); gandreotti@icb.cnr.it (G.A.)
4 Albrecht-Kossel-Institute for Neuroregeneration, University Rostock Medical Center, 18147 Rostock, Germany
* Correspondence: jan.lukas@med.uni-rostock.de (J.L.); cubellis@unina.it (M.V.C.); Tel.: +49-381-494-4713 (J.L.); +39-081-679-118 (M.V.C.); Fax: +49-381-494-4899 (J.L.); +39-081-679-233 (M.V.C.)

Academic Editor: Ritva Tikkanen
Received: 9 October 2016; Accepted: 24 November 2016; Published: 1 December 2016

Abstract: Fabry disease is caused by mutations in the *GLA* gene and is characterized by a large genotypic and phenotypic spectrum. Missense mutations pose a special problem for graduating diagnosis and choosing a cost-effective therapy. Some mutants retain enzymatic activity, but are less stable than the wild type protein. These mutants can be stabilized by small molecules which are defined as pharmacological chaperones. The first chaperone to reach clinical trial is 1-deoxygalactonojirimycin, but others have been tested in vitro. Residual activity of *GLA* mutants has been measured in the presence or absence of pharmacological chaperones by several authors. Data obtained from transfected cells correlate with those obtained in cells derived from patients, regardless of whether 1-deoxygalactonojirimycin was present or not. The extent to which missense mutations respond to 1-deoxygalactonojirimycin is variable and a reference table of the results obtained by independent groups that is provided with this paper can facilitate the choice of eligible patients. A review of other pharmacological chaperones is provided as well. Frequent mutations can have residual activity as low as one-fourth of normal enzyme in vitro. The reference table with residual activity of the mutants facilitates the identification of non-pathological variants.

Keywords: Fabry disease/drug therapy; α-galactosidase; pharmacological chaperones; 1-deoxynojirimycin

1. Introduction

Fabry disease (FD, OMIM #301500) is a rare pathology, but accounts for 8.8% of the patients affected by inherited disorders of metabolism [1] and is the second most common lysosomal storage disorder [2]. FD is caused by those mutations in the *GLA* gene that result in a deficiency of the protein product, lysosomal α-galactosidase (AGAL Uniprot: AGAL_HUMAN P06280; EC: 3.2.1.22), and the accumulation of its substrates. The real incidence of FD is difficult to establish. It was estimated at 1 in 100,000 [3].

Screening of various at-risk populations, patients with renal failure [4,5], stroke [6], and cardiomyopathy [7,8], have shown a significant prevalence of FD in symptomatic population. *GLA* gene variations have been found in newborn screening with a frequency as high as 1 in 1200 or 1 in 3100 [9,10]. Some of the found variations remain unclear with respect to clinical significance.

Although *GLA* is located on X chromosome (Xq22.1), heterozygous females can be symptomatic. This is due to random inactivation and lack of cross-correction that occurs in other lysosomal storage disorders such as mucopolysaccharidosis type II [11]. Random X-chromosome inactivation in heterozygous females leads to a mosaic of cells, half of which express wild-type AGAL. Under these circumstances, female patients have mild or no signs of the disease. In some cases, however, a skewed inactivation, which occurs for unknown reasons, leads to the preferential expression either of the chromosome carrying the wild type or the mutant *GLA*. Under these circumstances, female patients can be as severely affected as much as the male patients carrying the same mutation [12].

AGAL is a homodimeric glycoprotein with 429 amino acids per chain and shares structural similarities with the other lysosomal glycosidases. It catalyzes the removal of α-galactosyl residues from glycosphingolipids, in particular globotriaosylceramide, Gb3 or GL-3 (also known as ceramide trihexoside). Its products are lactosylceramide and galactose. Gb3 mainly occurs in the endothelial, kidney, heart, and nervous cells and there is evidence suggesting its involvement in the renal pathology [13,14], but the underlying mechanism remains largely unknown [15]. Gb3 and its isoforms based on ceramide modification are detectable in blood and urinary samples [16,17] from the patients for the use as diagnostic and prognostic biomarkers following and supporting genetic testing. Meanwhile, a deacylated metabolite of Gb3, globotriaosylsphingosine (lyso-Gb3) has emerged as a superior biomarker demonstrating higher sensitivity than Gb3 and a good correlation to the FD phenotype [18].

FD is characterized by a large phenotypic spectrum, with mildly and severely affected patients, and shares many symptoms with common diseases. In severe cases, often referred to as classic FD, the first specific signs appearing in childhood or adolescence are angiokeratoma, cornea verticillata, neuropathic pain, acroparesthesias and hypohidrosis. These are followed by progressive proteinuric renal insufficiency, rhythm and conductance disorders with progressive hypertrophic cardiomyopathy and cerebrovascular stroke [19–21]. In mild cases, often referred to as atypical FD, only some symptoms are present, usually the cardiac ones. The Mainz Severity Score Index (MSSI) [22,23] was developed to measure the severity of FD and to monitor the clinical course of the disease in response to therapy. The MSSI includes four components or sub-scores that assess the general, neurological, cardiovascular and renal signs and symptoms. Although the MSSI score is able to differentiate FD from other severe debilitating diseases, a minor, still significant overlap, in particular for cardiac sub-scores, between healthy and FD affected persons was observed. MSSI was originally developed for classic FD. Other tools, such as Fabry Disease Severity Scoring System (DS3) [24] and Fabry STabilization indEX (FASTEX) [25], were subsequently developed to cover a broader range of cases.

The broad heterogeneous symptom spectrum might be due in part to genetic modifiers and other extra-genetic (epigenetic, environmental) factors that are currently discussed [26,27].

Enzyme replacement therapy (ERT) has been approved for the last 15 years. There exist two formulations of the recombinant AGAL, agalsidase α or β, that are commercialized by Shire, Lexington, MA, USA and Genzyme, a Sanofi company, Cambridge, MA, USA respectively [28]. ERT may decrease cardiac mass [29–32] and reduce the accumulation of the substrate Gb3 in the kidney [33–35], but the effects on nervous system and renal function have not been definitively assessed [36–39]. Early start of ERT has been suggested because irreversible organ damage, cardiac fibrosis or severe renal dysfunction, would render the therapy ineffective [34,36,40]. Recommendations for initiation and cessation of enzyme replacement therapy in patients with Fabry disease have recently been provided by the European Fabry Working Group consensus document [28]. The effect of ERT on patients with mild mutations, which retain some residual AGAL activity, has not been considered separately [41]. This is unfortunate because ERT is not the only possible therapy for

FD. A new approach with pharmacological chaperones (PC) has been proposed and a small molecular weight molecule is on the verge of being approved with the commercial name of Galafold™. This drug is an iminosugar, which closely resembles the natural product of AGAL galactose, and has been known by different names, 1-deoxygalactonojirimycin (DGJ), migalastat, AMIGAL, AT1001. DGJ inhibits reversibly AGAL at nanomolar concentrations, but stabilizes the wild type enzyme in vitro against thermal [42] and chemical induced denaturation [43] too. DGJ can be used in synergy with ERT either co-administrating both drugs intravenously or one orally (DGJ) and the other intravenously (recombinant enzyme). DGJ prolongs the half-life of AGAL in vivo, both in mouse models and in humans and leads to an improved clearance of Gb3 [44–46].

DGJ can be used for a stand-alone oral therapy of FD for specific missense genotypes. The efficacy of DGJ was tested in vitro, ex vivo, in cells derived from patients, and in vivo. Oral administration of DGJ reduces Gb3 in kidney, heart and skin of Fabry transgenic mice carrying the responsive human mutation R301Q [47]. When administered with an oral dose of 150 mg, it was well tolerated, increased AGAL activity [48] and decreased plasma lyso-Gb3 [47] in the majority of the patients with responsive *GLA* mutations. Interestingly, the best results are obtained when an intermittent regimen is used. The results of a clinical trial phase 3 study carried out on males and females affected by FD has been recently published. Patients received 150 mg of Galafold™ or placebo every other day. The study began with six months of double-blind administration and proceeded with 6 + 12 months of open-label administration. Although the authors conclude their abstract stating quite cautiously that "the percentage of patients who had a response at 6 months did not differ significantly between the migalastat (DGJ) group and the placebo group", promising results are shown. A reduction of the number of Gb3 inclusions per kidney interstitial capillary as well as a reduction of plasma lyso-Gb3 were observed [49].

More than 700 variants have been reported in HGMD for the *GLA* gene so far and, differently from other lysosomal disorders such as Gaucher, there are not prevalent mutations, on the contrary most are usually found only in a single family. The number of missense mutations, 467 described so far, is a surprisingly high value for a medium size protein, such as AGAL. In order to appreciate this finding it should be considered that more than 70,000 missense mutations affecting proteins associated to human diseases have been reported, with seven variants per protein on average. The large number of missense mutations poses several problems for making a diagnosis and initiating the most appropriate therapy. Recently, it was proposed to use residual activity measured in vitro to classify mutations. We wish to contribute to the evaluation of such a proposal with the first meta-analysis of the residual activity of *GLA* missense mutations measured by several independent research groups employing different protocols, either ex vivo, in cells derived from patients, or in vitro, in transiently transfected cells. Results covering 317 of missense mutants, mostly cases reported in HGMD and associated to FD, were collected. Data were obtained in the absence or in the presence of DGJ. For this reason, our analysis provides an independent perspective on the amenability to pharmacological chaperones. In addition to this we reviewed other small molecules that were reported to have a stabilizing effect on some *GLA* missense mutations in vitro and might be developed to act in synergy or as an alternative to DGJ.

2. Results

Meta-Analysis of Data Reporting Residual Activity and Responsiveness to DGJ of GLA Missense Mutations

Several independent groups have tested the effect of DGJ on AGAL mutants, administering the drug to cells derived from patients, or most frequently, to HEK293 or COS cell transiently transfected with expression plasmids. The enhancement of enzyme levels and that of the total enzyme activity is monitored in the cells extracts and is regarded as a proof of the stabilization of the mutant in the cell by DGJ. Residual activity is normalized by the total amount of protein in the cell and should not be confused with specific activity, which is normalized by the amount of AGAL. Residual activity

is influenced by the stability of the mutant in the cell and by its specific activity. In general, a fixed concentration of DGJ was used, usually 20 μM, in some cases, however, IC_{50} was determined and the optimal concentration was used. The results gathered from literature are reported in Supplementary File S1 and the methods employed in each study are summarized in Table 1.

Table 1. Experimental conditions under which DGJ responsiveness has been assessed.

Reference	Cell Type	Concentration and Incubation Time
Ishii_2000 [50]	Transfection COS1	20 μM DGJ 1 day
Spada_2006 [10]	Transfection COS7	20 μM DGJ 72 h
Shin_2007 [51]	T-cells and fibroblasts	20 μM DGJ 3 or 4 days
Ishii_2007 [52]	Lymphoblasts and fibroblasts	20 μM DGJ 5 days
Shin_2008 [53]	T-cells	20 μM DGJ 3 days
Park_2009 [54]	Transfection COS7	20 μM DGJ 2 days
Benjamin_2009 [55]	Lymphoblasts and fibroblasts	Depending on EC50 5 days
Filoni_2010 [56]	Transfection COS1 and lymphocytes	20 μM DGJ 72 h
Wu_2011 [57]	Transfection HEK293	Depending on EC50 4 to 5 days
Andreotti_2011 [58]	Transfection COS7	20 μM DGJ 48 h
Lukas_2013 [2]	Transfection HEK293H	20 μM DGJ 60 h
Giugliani_2013 [59]	Transfection HEK293	10 μM DGJ
Lukas_2016 [60]	Transfection HEK293	20 μM DGJ 60 h

The last criteria for responsiveness were adopted for the clinical trial phase 3 published in 2016 [49] and require a relative increase in AGAL activity ≥1.2-fold above baseline and an absolute increase in AGAL ≥ 3% of wild type after incubation with 10 μM DGJ. The concentration of 10 μM is the Cmax concentration in plasma when patients are treated with 150 mg of DGJ, as was the case in clinical trials [47,49]. Ten micromolar, however, is not the highest concentration that can be safely reached in plasma [59,61] and the data obtained before 2016 with 20 μM DGJ, can still be useful to choose eligible patients.

In vitro results are robust and do not depend on the type of recipient cells used for transfection (Figure 1).

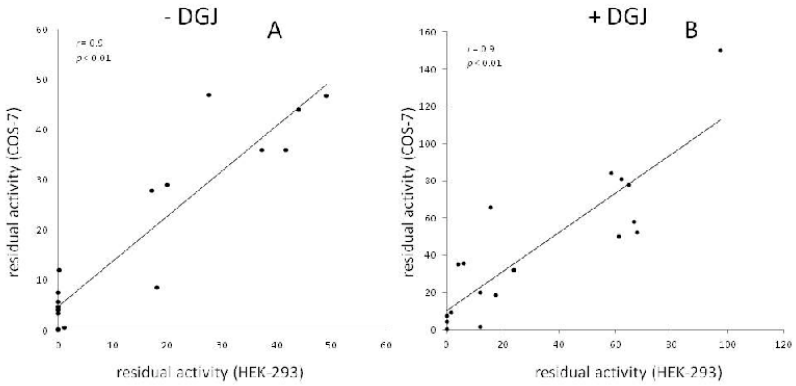

Figure 1. The residual activity of mutants transiently transfected and expressed in COS7 and in HEK293 is shown. In the case that multiple reports are available for a given mutant and a given recipient cell type, the average value was plotted. Results in the absence of DGJ (**A**) or in the presence of DGJ (**B**) are reported.

On the other hand, residual activity measured ex vivo varies among individuals and type of cells. A few examples of the levels measured in white blood cells are provided with the average,

standard deviation and number of individuals: E66Q 42.3 ± 12.5 (n = 9) [62]; A143T 35.9 ± 7.2 (n = 4), R112H 7.2 ± 7.0 (n = 5), R301Q 7.3 ± 2.7 (n = 6), R356W 1.2 ± 1.9 (n = 4) (Supplementary File S1).

Figure 2 shows the average residual activity measured in lymphoblasts or in fibroblasts harboring the same mutation. A moderate yet statistically significant correlation of the data is observed only in the presence of DGJ.

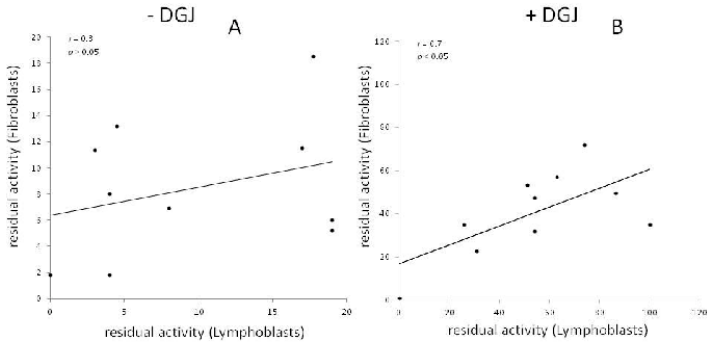

Figure 2. The residual activity of mutants measured in fibroblasts and lymphoblasts derived from patients is shown. In case that multiple reports are available for a given mutant and a given cell type, the average value was plotted. Results in the absence of DGJ (**A**) or in the presence of DGJ (**B**) are reported.

Figure 3 compares the residual activity measured ex vivo in cells derived from patients, (mostly lymphocytes or, in a few cases, fibroblasts), with that measured, in vitro, in transfected cells (HEK293, COS7 or COS1). For each mutant, the averages among results obtained by different authors without (Figure 3A) or with DGJ (Figure 3B) was determined. It can be observed that the residual activity measured in cells derived from patients tends to be lower than that measured in transfected cells, in particular in the absence of DGJ. A few examples are provided indicating in vitro result in HEK293H cells, ex vivo results in leucocytes with average, standard deviation and number of individuals: L180F: 32.4%, 6.0 ± 2.0 (n = 2); N215S: 39.5%, 27.1 ± 16.3 (n = 10); and I253T: 73.0%, 22.6 ± 6.9 (n = 3).

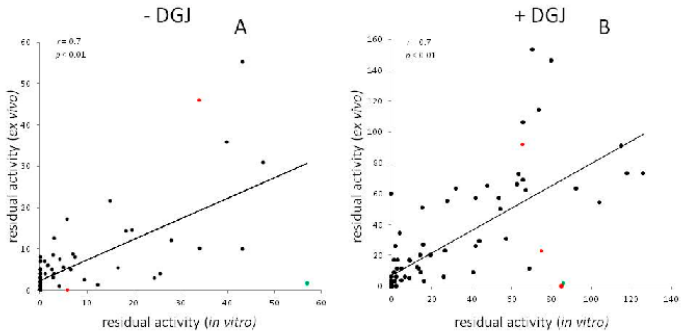

Figure 3. The residual activity of mutants transiently transfected and expressed in vitro and derived from patient cells is shown. In case that multiple reports are available for a given mutant, the average value was plotted. Results in the absence of DGJ (**A**) or in the presence of DGJ (**B**) are reported. Mutations affecting a site of splicing and corresponding to G183, are represented by red symbols, G128E is represented by a green symbol.

However, the residual activities in vitro and ex vivo correlate (Figure 3A $r = 0.7$, $p < 0.01$; Figure 3B $r = 0.7$, $p < 0.01$). Thus, it can be concluded that tests in vitro can generally recapitulate the residual activity ex vivo and responsiveness to DGJ.

When this manuscript had been completed, we became aware of a recent publication that reports residual activity of AGAL mutants expressed in HEK293 cells and tested with DGJ 10 μM [63]. These data correlate with those reported in Supplementary File S1 (−DGJ $r = 0.8$, $p < 0.000001$; +DGJ $r = 0.7$, $p < 0.000001$).

Test in vitro have a limitation because they cannot account for the effect of exonic mutation on splicing. In fact, mutants are encoded by plasmids that do not contain introns. It is interesting to analyze the case of the mutations affecting a site of splicing and corresponding to G183 represented by red symbols in Figure 3. Substitution of GLY by SER results in a mutant that does not retain activity in cells derived from patients and does not recover activity with DGJ. The same mutant recovers activity with DGJ in vitro. We can hypothesize that the drug has a stabilizing effect on the protein, but cannot correct the effect on splicing. On the other hand, G183A and G183D are responsive to the drug both in vitro and ex vivo suggesting that these mutations mainly affect the protein, but not the splicing. K213M might be another example where splicing could play a role to explain the in vitro and ex vivo differences. Mutations not occurring at splicing sites can have effect on the maturation of RNA too. We suspect that this might be the case for G128E, green symbol in Figure 3, because very low residual activity was measured by several authors in cells derived from patients, either in the presence or in the absence of DGJ, whereas the mutation retains residual activity and is responsive to DGJ in vitro. Although a putative consensus for an exonic splicing enhancer including the triplet 128 was found, further experiments are needed to confirm the influence of the mutation on RNA processing.

We report the score obtained by a position specific substitution matrix (PSSM) that measures whether the mutation was tolerated during the evolution of homologous proteins in Supplementary File S2. Mutations affecting the active site, as expected, have no residual activity and do not respond to DGJ, mutations occurring at non-conserved sites tend to be responsive.

Predictions were obtained with Web based Polyphen2 using HumDiv or HumVar as the training set and are reported in Supplementary File S2. Both sets use disease mutations in UniprotKB as positive controls, but differ for the negative control set. HumDiv uses differences between human proteins and their closely related mammalian homologs, whereas HumVar uses common human SNPs (MAF > 1%) without annotated involvement in disease. HumVar-trained model is suitable to distinguish mild mutations, the HumDiv-trained model, considers also mild mutations as deleterious one. Although, on average, the residual activity of mutations that are predicted as probably damaging with both training sets is very different from the residual activity of mutations predicted as benign, exceptions can be observed in particular with HumVar-trained model (Table 2).

Other in silico approaches based on the structural features of AGAL, some from our group [64], have been attempted [65,66], to predict the severity of FD genotypes. We believe that data obtained in vitro should always be preferred whenever available.

In Supplementary File S2, all missense variants of *GLA* described in ExAC [67] are reported. ExAC summarizes exome sequencing data from a wide variety of large-scale sequencing projects. Variants reported in this database, in particular those observed with higher frequency, are likely to be non-pathogenic. The mean residual activity measured in vitro for a subset of ExAC variants, i.e., those observed in more than one male is reported in Table 2. The number of hemizygous individuals reported in ExAC, the PSSM score, Polyphen2 prediction and the reference found in HGMD are reported in the same table.

Table 2. Putative non-pathological AGAL mutants: features and residual activity in vitro.

Mutation	No. Hemiz	−DGJ	+DGJ	PSSM	Humdiv	Humvar	Reference
L3P	4	117.7	129.4	−3	Probably damaging	Probably damaging	[60]
E66Q	3	47.6	53.66	−2	Probably damaging	Probably damaging	[68]
R118C	8	24.5	27.8	−2	Probably damaging	Possibly damaging	[10]
N139S	7	147.8	176.4	−1	Benign	Benign	[69]
S126G	18	51.3	67.4	−2	Benign	Benign	[70]
A143T	19	39.7	63.7	−1	Probably damaging	Possibly damaging	[71]
I289V	3	79.9	95	0	Probably damaging	Possibly damaging	
D313Y	129	75.5	100.3	−1	Probably damaging	Possibly damaging	[71]
R363H	3	28	65.7	−1	Benign	Benign	[72]
A368T	3	103.7	93.3	0	Benign	Benign	[2]
T385A	36	45	48.9	−2	Possibly damaging	Benign	[2]
W399S	5	53	51.5	−4	Possibly damaging	Benign	[60]

R118C is the variant with the lowest residual activity, only 24.5% of wild type when tested in transiently transfected cells. It is relatively frequent in the European population, but it is predicted as deleterious both by Polyphen_Humvar and Polyphen_Humdiv. Oliveira and colleagues reviewed the clinical, biochemical and histopathology data obtained from 22 individual carriers and reached the conclusion that it "does not segregate with FD manifestations at least in a highly-penetrant Mendelian fashion", but might be a risk factor for stroke [73]. In accordance with this, low levels of lyso-Gb3, a biomarker of FD, were measured in the carriers [2]. R118C is considered amenable to DGJ according to galafold amenability table [63]. R118C was tested with DGJ and with Rosiglitazone by Lukas et al. [74]. Although in terms of activity fold increase, the effect of mono-therapy with either drug was small, the combinatorial effect was significantly higher.

A143T has an average residual activity of approximately 39.7% of wild type. Brand and coworkers [75] analyzed 15 females and 10 males carrying this mutation. They observed that female and male A143T carriers showed less organ involvement in comparison to FD patients with other missense mutations and those suffering from stroke/TIA showed no further FD-typical organ manifestations. They came to the conclusion that "A143T seems not to be causal for FD, but rather a genetic variant of unknown significance or a genetic modifier". A143T is considered amenable for the therapy with DGJ according to the galafold amenability table.

E66Q has specific activity, *V*max, and affinity for the artificial substrate 4-methylumbelliferyl-α-galactopyranoside, *K*m, similar to those of wild type, but residual activity in transfected cells is approximately one half of the wild type, possibly because the stability at neutral pH is reduced [52]. The mutation is relatively frequent in East Asian population. Sakuraba and coworkers measured the activity in 20 Japanese or Korean male carriers with renal and cardiovascular disorders and found 13% to 26% of the normal mean values for plasma and 24% to 65% of the normal mean values for white blood cells, but the lyso-Gb3 levels were as low as those of healthy controls and no inclusion bodies were found [62]. Hu and co-workers found that the mutation segregated with renal disease in a very large Chinese family, but they did not measure the accumulation of the substrate or of lyso-Gb3 in the same patients [76]. The involvement in cardiovascular disease has also been suspected, but no accumulation of Gb3 was found in the heart of a patient carrying E66Q [77]. The association between E66Q and the risk cerebral small-vessel occlusion is debated [78,79]. In conclusion, pathogenicity of E66Q is still vexata quaestio. E66Q is considered non amenable for DGJ according to galafold amenability table, but an increase in activity upon drug administration was measured by other authors [52,55,57,80].

D313Y was first associated to classic phenotype [71]. Subsequent data clinically and biochemically indicated that D313Y should be considered a variant [81]. Cardiac, nephrological, neurological, laboratory and quality of life data were collected from carriers of D313Y with a 4-year follow up and the results indicated that the mutation is non pathological. Very low levels of lyso-Gb3 were found [2]. The opinion that D313Y is a non-pathological variant is supported by the fact that its frequency of

0.4% in the non-Finnish European population is much higher than the prevalence of FD in the same population. D313Y is considered amenable for DGJ.

For other mutations such as S126G and N139S, the clinical picture did not include specific signs of FD [69,70]. Both mutations are considered amenable for DGJ.

This survey would suggest that a residual activity higher than 25% can indicate a non-pathological variant. Nonetheless, when considering administration of a therapy, if any, clinicians should be aware of the fact that the severity of the disease depends not only on the damage caused to the protein itself by the mutation, but also by other factors, which regrettably have not yet been clarified. It should be considered that the phenotype can differ even among the members of the same family [82] and that the residual activity in plasma or in white blood cells can vary largely in people carrying the same mutation [62].

N215S is a mutation affecting glycosylation of the AGAL enzyme [83]. It presents with a proportionally high residual activity >25% of normal. It is considered a distinct sub-type of FD due to its elevated prevalence compared to non-N215S FD cases and late-onset occurrence [60,84]. Interestingly, this variant has never been scrutinized to cause a pathogenic phenotype. By contrast, it is believed to cause a specific cardiac phenotype. Other cardiac-prone mutations might exist, e.g., the so-called IVS4 + 919G > A splice mutation highly prevalent in the Taiwanese population. A clinical trial investigating the long term clinical course of N215S patients is currently ongoing (clinicaltrials.gov, NCT01429597). In this case, the diagnostic and prognostic value of biomarker lyso-Gb3 can be appreciated. While apparently all (genetically) found patients were identified it was demonstrated that Gb3 was normal in a great fraction of patients. Meehan et al. [85] showed that N215S was present in a patient with renal manifestation and is, thus, suggestive to cause mainly cardiac and renal symptoms. N215S is amenable for DGJ.

3. Future Perspectives for Therapy

DGJ is a promising drug, but it might not be the ideal drug yet. DGJ inhibits AGAL at nanomolar concentration and stabilizes it at micromolar concentrations. Therefore a continuous exposure to the drug can promote AGAL levels, but not AGAL intracellular activity. Reduction of Gb3 concentration was not observed in fibroblasts derived from patients carrying the mutations R301Q or L300P and incubated with DGJ for 10 days, but was observed if the incubation of seven days with the drug was followed by a three day wash-out [55].

The discovery of DGJ was the result of an educated guess, and not of a methodical screening [86]. In fact, DGJ is a glycomimetic with a six-atom ring and very closely resembles the galactose, which is the natural product and inhibitor, and also the first chaperone described for AGAL [87]. A more systematic search was started with the aim of finding other drugs that might have a better ratio between the stabilizing and the inhibitory effect. Most of the molecules considered so far are glycomimetics as DGJ itself. DGJ is an amine and is positively charged at neutral pH. In order to facilitate its diffusion through membranes, alkylation was proposed [88]. Contrary to what was observed for analogous iminosugars active on other lysosomal glycosidases, alkyl-DGJ derivatives had a lower affinity for AGAL and apparently a lower chaperoning potential probably because one important hydrogen-bond, the one established between the heterocyclic NH proton and D170 of AGAL, is lost.

On the contrary, aryl DGJ-derivatives (1-deoxygalactonojirimycin-arylthioureas) that form a hydrogen bond between the aryl-N'H thiourea proton and D231 of AGAL, act as reversible inhibitors and chaperones. When tested at 30 μM concentration on Q279E or R301Q mutants, the best candidate, namely *N'-p*-methoxyphenyl-DGJ-Aryl thiourea, had a seven fold higher chaperoning activity than DGJ at its optimal concentration [89].

Iminosugars characterized by a smaller, five-atom ring system, have been described [90,91]. 2,5-dideoxy-2,5-imino-D-altritol (DIA) inhibited AGAL and stabilized it against thermal denaturation and acted as a chaperone when tested on Fabry R301Q lymphoblasts although at a concentration 20 times higher than the optimal one for DGJ. The effect on Gb3 accumulation was not tested.

One derivative of DIA possessing an aminomethyl group showed a chaperoning effect higher than DGJ when administered to N215S patient lymphocyte cell line at high concentration (100 μM) [92].

DGJ binds and inhibits AGAL both at neutral pH, which is required, and at acidic pH, which is not required [42]. It would be useful to find molecules that bind and stabilize AGAL mutants when they are in the neutral environment of the endoplasmic reticulum, but dissociate when the protein reaches the lysosome. This point was specifically addressed incorporating an orthoester segment into DGJ [93].

Glycomimetics require a precise dosing, whereas non carbohydrate mimetics might offer a larger therapeutic window and an improved therapeutic index. In order to look for chemically diverse drugs, a library of 230,000 diverse compounds was screened but no inhibitors or activators of a-Gal A with an IC_{50} below 50 μM were identified. Unfortunately the screening procedure relied only on an enzymatic assay carried out at pH 5.9, but not at neutral pH or on assays based on AGAL stabilization [94].

So far reversible inhibitors of AGAL that act as PC have been described. The association between the two effects, inhibition and stabilization, is avoidable because active sites are not the only targets for chaperones. Allosteric ligands might act as pharmacological chaperones, and might be more effective than reversible inhibitors, since they would perform their stabilizing action without competing with the natural substrate. Looking for allosteric PC is difficult because they do not resemble chemically known substrates. Large libraries of structurally diverse compounds should be tested and preliminary screening in silico might be functional. Allosteric ligands do not bind the active site, but one of the many pockets occurring on the surface of a protein. Therefore it is difficult to restrict the area where binding is allowed as required by structure based virtual screening. A recent screening, carried out on 10,000 molecules, showed that it is possible to find molecules that, at least in silico, preferentially bind an allosteric site than the active site. The two sites are located at the opposite sides of the catalytic domain of AGAL [95].

The PC that have been described previously are specific ligands of AGAL. They are effective on missense mutations that cause destabilization of the enzyme and, ultimately, its early degradation. Other small molecules that do not physically interact with AGAL, but have effect on proteostasis, can be considered for the treatment of these cases as well. Proteostasis regulators can be used in synergy with specific PC potentiating their action or allowing lower dosages.

The before mentioned Rosiglitazone, a Peroxisome proliferator-activated receptor gamma (PPARγ) agonist rearranges global cellular ubiquitination by inhibiting the ubiquitin-proteasome system (UPS). It displayed the highest beneficial effect on mutations with a significant residual activity (e.g., R118C and T385A) and was even more effective in combination with a PC [60]. Mechanistic studies are required to explain why other ubiquitination inhibitors such as Pyr-41 failed to increase AGAL activity. This finding might be ascribed to intense adverse effects of cellular ubiquitination inhibition caused by Pyr-41 and associated toxicological aspects.

Ambroxol, a mucolytic agent used in the treatment of respiratory diseases, was identified as an enhancer of AGAL activity. The compound has formerly been demonstrated to act as a PC on mutant Glucocerebrosidase in Gaucher disease. Even though its mechanism of action is not known it was demonstrated to increase cellular AGAL level and activity of most (DGJ−) amenable mutations (E59K, A73V, A143T, A156V, I232T, R301G, R301Q, R356W and R363H) indicating an impact on AGAL proteostasis. Ambroxol was, however, not effective as a monotherapy, but only in the combination with a PC, galactose or DGJ [60].

The synergistic effect of *N′-p*-methoxyphenyl-DGJ-Aryl thiourea with two proteostasis regulators, 4-phenylbutyric acid and celastrol has been assessed. The latter compound was not effective, but 4-phenylbutyric acid at 0.1 mM concentration was able to enhance the chaperoning activity of the aryl-thiourea (20 μM) on the fibroblasts harbouring Q279E [89].

The effects of lactacystin 2 μM (a proteasome inhibitor) and kifunensine 0.2 mM (an inhibitor of ER α-mannosidase I) on the processing on some mutants assessing the amount of protein was tested

by Fan and coworkers [52] They found that some mutants responded to both drugs (F113L, N215S, and M296I), one responded only to lactacystin (E66Q), others only to kifunesine (M72V, I91T, A97V, R112H, L166V, and Q279E), and others had low or no response to either (A20P, A156V, M296V, R356W, G373D, G373S, E59K, and P146S). All mutants that are responsive to kifunensine or lactacystin are also responsive to DGJ, while A156V, M269V, R356W, and E59K are responsive only to DGJ. These results suggest that a different cocktail of drugs might be ideal for specific AGAL mutations.

4. Methods

Residual activities in Supplementary File S1 were obtained from the literature. In those cases where the authors did not report the normalized percentage values, the activity of the mutant in the presence of DGJ was divided by the activity of wild type AGAL multiplied by 100 (+DGJ/wild $\times$ 100). The reference wild type activity, measured in the absence of DGJ was obtained for each mutation from the appropriate paper. IC_{50} values are reported when available.

Pearson correlation coefficients and two tailed *p*-values were calculated as described by Lowry [96].

PSSM values were calculated as described [97,98]. Active site residues were identified with DrosteP [99]. Predictions were obtained with Web based Polyphen2 using HumDiv or HumVar as the training set under default conditions [100].

Supplementary Materials: Supplementary materials can be found at www.mdpi.com/1422-0067/17/12/2010/s1.

Acknowledgments: Funding was provided by Telethon-Italy (Grant no. GGP12108). The funders had no role in study design, data collection and analysis, decision to publish, or preparation of the manuscript. We thank Gaetano Viscido and Mario D'Andrea for technical assistance. This work is dedicated to our friend and colleague Maria Malanga.

Author Contributions: Valentina Citro, Maria Vittoria Cubellis and Giuseppina Andreotti conceived and designed the study and wrote the manuscript. Marco Cammisa analyzed the data and prepared the figures. Chiara Cimmaruta and Ludovica Liguori gathered the data. Jan Lukas contributed to the discussion. All authors read and approved the final manuscript.

Conflicts of Interest: The authors declare no conflict of interest.

References

1. Sirrs, S.; Hollak, C.; Merkel, M.; Sechi, A.; Glamuzina, E.; Janssen, M.C.; Lachmann, R.; Langendonk, J.; Scarpelli, M.; Ben Omran, T.; et al. The frequencies of different inborn errors of metabolism in adult metabolic centres: Report from the ssiem adult metabolic physicians group. *JIMD Rep.* **2016**, *27*, 85–91. [PubMed]
2. Lukas, J.; Giese, A.K.; Markoff, A.; Grittner, U.; Kolodny, E.; Mascher, H.; Lackner, K.J.; Meyer, W.; Wree, P.; Saviouk, V.; et al. Functional characterisation of α-galactosidase a mutations as a basis for a new classification system in Fabry disease. *PLoS Genet.* **2013**, *9*, e1003632. [CrossRef] [PubMed]
3. Germain, D.P. Fabry disease. *Orphanet. J. Rare Dis.* **2010**, *5*, 30. [CrossRef] [PubMed]
4. Wallin, E.F.; Clatworthy, M.R.; Pritchard, N.R. Fabry disease: Results of the first UK hemodialysis screening study. *Clin. Nephrol.* **2011**, *75*, 506–510. [CrossRef] [PubMed]
5. Doi, K.; Noiri, E.; Ishizu, T.; Negishi, K.; Suzuki, Y.; Hamasaki, Y.; Honda, K.; Fujita, T.; Tsukimura, T.; Togawa, T.; et al. High-throughput screening identified disease-causing mutants and functional variants of α-galactosidase a gene in japanese male hemodialysis patients. *J. Hum. Genet.* **2012**, *57*, 575–579. [CrossRef] [PubMed]
6. Rolfs, A.; Fazekas, F.; Grittner, U.; Dichgans, M.; Martus, P.; Holzhausen, M.; Bottcher, T.; Heuschmann, P.U.; Tatlisumak, T.; Tanislav, C.; et al. Acute cerebrovascular disease in the young: The stroke in young Fabry patients study. *Stroke* **2013**, *44*, 340–349. [CrossRef] [PubMed]
7. Sachdev, B.; Takenaka, T.; Teraguchi, H.; Tei, C.; Lee, P.; McKenna, W.J.; Elliott, P.M. Prevalence of anderson-Fabry disease in male patients with late onset hypertrophic cardiomyopathy. *Circulation* **2002**, *105*, 1407–1411. [CrossRef] [PubMed]

8. Monserrat, L.; Gimeno-Blanes, J.R.; Marin, F.; Hermida-Prieto, M.; Garcia-Honrubia, A.; Perez, I.; Fernandez, X.; de Nicolas, R.; de la Morena, G.; Paya, E.; et al. Prevalence of Fabry disease in a cohort of 508 unrelated patients with hypertrophic cardiomyopathy. *J. Am. Coll. Cardiol.* **2007**, *50*, 2399–2403. [CrossRef] [PubMed]
9. Hwu, W.L.; Chien, Y.H.; Lee, N.C.; Chiang, S.C.; Dobrovolny, R.; Huang, A.C.; Yeh, H.Y.; Chao, M.C.; Lin, S.J.; Kitagawa, T.; et al. Newborn screening for Fabry disease in taiwan reveals a high incidence of the later-onset GLA mutation C.936 + 919G > A (IVS4 + 919G > A). *Hum. Mutat.* **2009**, *30*, 1397–1405. [CrossRef] [PubMed]
10. Spada, M.; Pagliardini, S.; Yasuda, M.; Tukel, T.; Thiagarajan, G.; Sakuraba, H.; Ponzone, A.; Desnick, R.J. High incidence of later-onset Fabry disease revealed by newborn screening. *Am. J. Hum. Genet.* **2006**, *79*, 31–40. [CrossRef] [PubMed]
11. Fuller, M.; Mellett, N.; Hein, L.K.; Brooks, D.A.; Meikle, P.J. Absence of α-galactosidase cross-correction in Fabry heterozygote cultured skin fibroblasts. *Mol. Genet. Metab.* **2015**, *114*, 268–273. [CrossRef] [PubMed]
12. Echevarria, L.; Benistan, K.; Toussaint, A.; Dubourg, O.; Hagege, A.A.; Eladari, D.; Jabbour, F.; Beldjord, C.; de Mazancourt, P.; Germain, D.P. X-chromosome inactivation in female patients with Fabry disease. *Clin. Genet.* **2016**, *89*, 44–54. [CrossRef] [PubMed]
13. Hoffmann, B. Fabry disease: Recent advances in pathology, diagnosis, treatment and monitoring. *Orphanet. J. Rare Dis.* **2009**, *4*, 21. [CrossRef] [PubMed]
14. Taguchi, A.; Maruyama, H.; Nameta, M.; Yamamoto, T.; Matsuda, J.; Kulkarni, A.B.; Yoshioka, H.; Ishii, S. A symptomatic Fabry disease mouse model generated by inducing globotriaosylceramide synthesis. *Biochem. J.* **2013**, *456*, 373–383. [CrossRef] [PubMed]
15. Shin, Y.J.; Jeon, Y.J.; Jung, N.; Park, J.W.; Park, H.Y.; Jung, S.C. Substrate-specific gene expression profiles in different kidney cell types are associated with Fabry disease. *Mol. Med. Rep.* **2015**, *12*, 5049–5057. [CrossRef] [PubMed]
16. Mills, K.; Johnson, A.; Winchester, B. Synthesis of novel internal standards for the quantitative determination of plasma ceramide trihexoside in Fabry disease by tandem mass spectrometry. *FEBS Lett.* **2002**, *515*, 171–176. [CrossRef]
17. Auray-Blais, C.; Cyr, D.; Ntwari, A.; West, M.L.; Cox-Brinkman, J.; Bichet, D.G.; Germain, D.P.; Laframboise, R.; Melancon, S.B.; Stockley, T.; et al. Urinary globotriaosylceramide excretion correlates with the genotype in children and adults with Fabry disease. *Mol. Genet. Metab.* **2008**, *93*, 331–340. [CrossRef] [PubMed]
18. Smid, B.E.; van der Tol, L.; Biegstraaten, M.; Linthorst, G.E.; Hollak, C.E.; Poorthuis, B.J. Plasma globotriaosylsphingosine in relation to phenotypes of Fabry disease. *J. Med. Genet.* **2015**, *52*, 262–268. [CrossRef] [PubMed]
19. Linhart, A.; Elliott, P.M. The heart in anderson-Fabry disease and other lysosomal storage disorders. *Heart* **2007**, *93*, 528–535. [CrossRef] [PubMed]
20. Schiffmann, R.; Moore, D.F. Neurological manifestations of Fabry disease. In *Fabry Disease: Perspectives from 5 Years of FOS*; Mehta, A., Beck, M., Sunder-Plassmann, G., Eds.; Oxford PharmaGenesis: Oxford, UK, 2006.
21. Sunder-Plassmann, G. Renal manifestations of Fabry disease. In *Fabry Disease: Perspectives from 5 Years of FOS*; Mehta, A., Beck, M., Sunder-Plassmann, G., Eds.; Oxford PharmaGenesis: Oxford, UK, 2006.
22. Whybra, C.; Bahner, F.; Baron, K. Measurement of disease severity and progression in Fabry disease. In *Fabry Disease: Perspectives from 5 Years of FOS*; Mehta, A., Beck, M., Sunder-Plassmann, G., Eds.; Oxford PharmaGenesis: Oxford, UK, 2006.
23. Whybra, C.; Kampmann, C.; Krummenauer, F.; Ries, M.; Mengel, E.; Miebach, E.; Baehner, F.; Kim, K.; Bajbouj, M.; Schwarting, A.; et al. The mainz severity score index: A new instrument for quantifying the anderson-Fabry disease phenotype, and the response of patients to enzyme replacement therapy. *Clin. Genet.* **2004**, *65*, 299–307. [CrossRef] [PubMed]
24. Giannini, E.H.; Mehta, A.B.; Hilz, M.J.; Beck, M.; Bichet, D.G.; Brady, R.O.; West, M.; Germain, D.P.; Wanner, C.; Waldek, S.; et al. A validated disease severity scoring system for Fabry disease. *Mol. Genet. Metab.* **2010**, *99*, 283–290. [CrossRef] [PubMed]
25. Mignani, R.; Pieruzzi, F.; Berri, F.; Burlina, A.; Chinea, B.; Gallieni, M.; Pieroni, M.; Salviati, A.; Spada, M. Fabry stabilization index (fastex): An innovative tool for the assessment of clinical stabilization in Fabry disease. *Clin. Kidney J.* **2016**, *9*, 739–747. [CrossRef] [PubMed]

26. Teitcher, M.; Weinerman, S.; Whybra, C.; Beck, M.; Sharon, N.; Elstein, D.; Altarescu, G. Genetic polymorphisms of vitamin D receptor (VDR) in Fabry disease. *Genetica* **2008**, *134*, 377–383. [CrossRef] [PubMed]
27. Altarescu, G.; Moore, D.F.; Schiffmann, R. Effect of genetic modifiers on cerebral lesions in Fabry disease. *Neurology* **2005**, *64*, 2148–2150. [CrossRef] [PubMed]
28. Biegstraaten, M.; Arngrimsson, R.; Barbey, F.; Boks, L.; Cecchi, F.; Deegan, P.B.; Feldt-Rasmussen, U.; Geberhiwot, T.; Germain, D.P.; Hendriksz, C.; et al. Recommendations for initiation and cessation of enzyme replacement therapy in patients with Fabry disease: The european Fabry working group consensus document. *Orphanet. J. Rare Dis.* **2015**, *10*, 36. [CrossRef] [PubMed]
29. Banikazemi, M.; Bultas, J.; Waldek, S.; Wilcox, W.R.; Whitley, C.B.; McDonald, M.; Finkel, R.; Packman, S.; Bichet, D.G.; Warnock, D.G.; et al. Agalsidase-β therapy for advanced Fabry disease: A randomized trial. *Ann. Intern. Med.* **2007**, *146*, 77–86. [CrossRef] [PubMed]
30. Bierer, G.; Balfe, D.; Wilcox, W.R.; Mosenifar, Z. Improvement in serial cardiopulmonary exercise testing following enzyme replacement therapy in Fabry disease. *J. Inherit. Metab. Dis.* **2006**, *29*, 572–579. [CrossRef] [PubMed]
31. Hughes, D.A.; Elliott, P.M.; Shah, J.; Zuckerman, J.; Coghlan, G.; Brookes, J.; Mehta, A.B. Effects of enzyme replacement therapy on the cardiomyopathy of anderson-Fabry disease: A randomised, double-blind, placebo-controlled clinical trial of agalsidase alfa. *Heart* **2008**, *94*, 153–158. [CrossRef] [PubMed]
32. Rombach, S.M.; Smid, B.E.; Linthorst, G.E.; Dijkgraaf, M.G.; Hollak, C.E. Natural course of Fabry disease and the effectiveness of enzyme replacement therapy: A systematic review and meta-analysis: Effectiveness of ert in different disease stages. *J. Inherit. Metab. Dis.* **2014**, *37*, 341–352. [CrossRef] [PubMed]
33. Thurberg, B.L.; Rennke, H.; Colvin, R.B.; Dikman, S.; Gordon, R.E.; Collins, A.B.; Desnick, R.J.; O'Callaghan, M. Globotriaosylceramide accumulation in the Fabry kidney is cleared from multiple cell types after enzyme replacement therapy. *Kidney Int.* **2002**, *62*, 1933–1946. [CrossRef] [PubMed]
34. Germain, D.P.; Waldek, S.; Banikazemi, M.; Bushinsky, D.A.; Charrow, J.; Desnick, R.J.; Lee, P.; Loew, T.; Vedder, A.C.; Abichandani, R.; et al. Sustained, long-term renal stabilization after 54 months of agalsidase β therapy in patients with Fabry disease. *J. Am. Soc. Nephrol.* **2007**, *18*, 1547–1557. [CrossRef] [PubMed]
35. Tondel, C.; Bostad, L.; Larsen, K.K.; Hirth, A.; Vikse, B.E.; Houge, G.; Svarstad, E. Agalsidase benefits renal histology in young patients with Fabry disease. *J. Am. Soc. Nephrol.* **2013**, *24*, 137–148. [CrossRef] [PubMed]
36. Rombach, S.M.; Smid, B.E.; Bouwman, M.G.; Linthorst, G.E.; Dijkgraaf, M.G.; Hollak, C.E. Long term enzyme replacement therapy for Fabry disease: Effectiveness on kidney, heart and brain. *Orphanet. J. Rare Dis.* **2013**, *8*, 47. [CrossRef] [PubMed]
37. Buechner, S.; Moretti, M.; Burlina, A.P.; Cei, G.; Manara, R.; Ricci, R.; Mignani, R.; Parini, R.; di Vito, R.; Giordano, G.P.; et al. Central nervous system involvement in anderson-Fabry disease: A clinical and MRI retrospective study. *J. Neurol. Neurosurg. Psychiatry* **2008**, *79*, 1249–1254. [CrossRef] [PubMed]
38. Jardim, L.; Vedolin, L.; Schwartz, I.V.; Burin, M.G.; Cecchin, C.; Kalakun, L.; Matte, U.; Aesse, F.; Pitta-Pinheiro, C.; Marconato, J.; et al. Cns involvement in Fabry disease: Clinical and imaging studies before and after 12 months of enzyme replacement therapy. *J. Inherit. Metab. Dis.* **2004**, *27*, 229–240. [CrossRef] [PubMed]
39. Jardim, L.B.; Aesse, F.; Vedolin, L.M.; Pitta-Pinheiro, C.; Marconato, J.; Burin, M.G.; Cecchin, C.; Netto, C.B.; Matte, U.S.; Pereira, F.; et al. White matter lesions in Fabry disease before and after enzyme replacement therapy: A 2-year follow-up. *Arq. Neuropsiquiatr.* **2006**, *64*, 711–717. [CrossRef] [PubMed]
40. Weidemann, F.; Niemann, M.; Stork, S.; Breunig, F.; Beer, M.; Sommer, C.; Herrmann, S.; Ertl, G.; Wanner, C. Long-term outcome of enzyme-replacement therapy in advanced Fabry disease: Evidence for disease progression towards serious complications. *J. Intern. Med.* **2013**, *274*, 331–341. [CrossRef] [PubMed]
41. Hollak, C.E.; Weinreb, N.J. The attenuated/late onset lysosomal storage disorders: Therapeutic goals and indications for enzyme replacement treatment in gaucher and Fabry disease. *Best Pract. Res. Clin. Endocrinol. Metab.* **2015**, *29*, 205–218. [CrossRef] [PubMed]
42. Andreotti, G.; Monticelli, M.; Cubellis, M.V. Looking for protein stabilizing drugs with thermal shift assay. *Drug Test. Anal.* **2015**, *7*, 831–834. [CrossRef] [PubMed]
43. Andreotti, G.; Citro, V.; Correra, A.; Cubellis, M.V. A thermodynamic assay to test pharmacological chaperones for Fabry disease. *Biochim. Biophys. Acta* **2014**, *1840*, 1214–1224. [CrossRef] [PubMed]

44. Benjamin, E.R.; Khanna, R.; Schilling, A.; Flanagan, J.J.; Pellegrino, L.J.; Brignol, N.; Lun, Y.; Guillen, D.; Ranes, B.E.; Frascella, M.; et al. Co-administration with the pharmacological chaperone AT1001 increases recombinant human α-galactosidase a tissue uptake and improves substrate reduction in Fabry mice. *Mol. Ther.* **2012**, *20*, 717–726. [CrossRef] [PubMed]
45. Warnock, D.G.; Bichet, D.G.; Holida, M.; Goker-Alpan, O.; Nicholls, K.; Thomas, M.; Eyskens, F.; Shankar, S.; Adera, M.; Sitaraman, S.; et al. Oral migalastat HCL leads to greater systemic exposure and tissue levels of active α-galactosidase a in Fabry patients when co-administered with infused agalsidase. *PLoS ONE* **2015**, *10*, e0134341. [CrossRef] [PubMed]
46. Xu, S.; Lun, Y.; Brignol, N.; Hamler, R.; Schilling, A.; Frascella, M.; Sullivan, S.; Boyd, R.E.; Chang, K.; Soska, R.; et al. Coformulation of a novel human α-galactosidase a with the pharmacological chaperone AT1001 leads to improved substrate reduction in Fabry mice. *Mol. Ther.* **2015**, *23*, 1169–1181. [CrossRef] [PubMed]
47. Young-Gqamana, B.; Brignol, N.; Chang, H.H.; Khanna, R.; Soska, R.; Fuller, M.; Sitaraman, S.A.; Germain, D.P.; Giugliani, R.; Hughes, D.A.; et al. Migalastat hcl reduces globotriaosylsphingosine (lyso-Gb3) in Fabry transgenic mice and in the plasma of Fabry patients. *PLoS ONE* **2013**, *8*, e57631. [CrossRef] [PubMed]
48. Germain, D.P.; Fan, J.Q. Pharmacological chaperone therapy by active-site-specific chaperones in Fabry disease: In vitro and preclinical studies. *Int. J. Clin. Pharmacol. Ther.* **2009**, *47*, S111–S117. [PubMed]
49. Germain, D.P.; Hughes, D.A.; Nicholls, K.; Bichet, D.G.; Giugliani, R.; Wilcox, W.R.; Feliciani, C.; Shankar, S.P.; Ezgu, F.; Amartino, H.; et al. Treatment of fabry's disease with the pharmacologic chaperone migalastat. *N. Engl. J. Med.* **2016**, *375*, 545–555. [CrossRef] [PubMed]
50. Ishii, S.; Suzuki, Y.; Fan, J.Q. Role of ser-65 in the activity of α-galactosidase a: Characterization of a point mutation (S65T) detected in a patient with Fabry disease. *Arch. Biochem. Biophys.* **2000**, *377*, 228–233. [CrossRef] [PubMed]
51. Shin, S.H.; Murray, G.J.; Kluepfel-Stahl, S.; Cooney, A.M.; Quirk, J.M.; Schiffmann, R.; Brady, R.O.; Kaneski, C.R. Screening for pharmacological chaperones in Fabry disease. *Biochem. Biophys. Res. Commun.* **2007**, *359*, 168–173. [CrossRef] [PubMed]
52. Ishii, S.; Chang, H.H.; Kawasaki, K.; Yasuda, K.; Wu, H.L.; Garman, S.C.; Fan, J.Q. Mutant α-galactosidase a enzymes identified in Fabry disease patients with residual enzyme activity: Biochemical characterization and restoration of normal intracellular processing by 1-deoxygalactonojirimycin. *Biochem. J.* **2007**, *406*, 285–295. [CrossRef] [PubMed]
53. Shin, S.H.; Kluepfel-Stahl, S.; Cooney, A.M.; Kaneski, C.R.; Quirk, J.M.; Schiffmann, R.; Brady, R.O.; Murray, G.J. Prediction of response of mutated α-galactosidase a to a pharmacological chaperone. *Pharmacogenet. Genom.* **2008**, *18*, 773–780. [CrossRef] [PubMed]
54. Park, J.Y.; Kim, G.H.; Kim, S.S.; Ko, J.M.; Lee, J.J.; Yoo, H.W. Effects of a chemical chaperone on genetic mutations in α-galactosidase a in Korean patients with Fabry disease. *Exp. Mol. Med.* **2009**, *41*, 1–7. [CrossRef] [PubMed]
55. Benjamin, E.R.; Flanagan, J.J.; Schilling, A.; Chang, H.H.; Agarwal, L.; Katz, E.; Wu, X.; Pine, C.; Wustman, B.; Desnick, R.J.; et al. The pharmacological chaperone 1-deoxygalactonojirimycin increases α-galactosidase a levels in Fabry patient cell lines. *J. Inherit. Metab. Dis.* **2009**, *32*, 424–440. [CrossRef] [PubMed]
56. Filoni, C.; Caciotti, A.; Carraresi, L.; Cavicchi, C.; Parini, R.; Antuzzi, D.; Zampetti, A.; Feriozzi, S.; Poisetti, P.; Garman, S.C.; et al. Functional studies of new *GLA* gene mutations leading to conformational Fabry disease. *Biochim. Biophys. Acta* **2010**, *1802*, 247–252. [CrossRef] [PubMed]
57. Wu, X.; Katz, E.; Della Valle, M.C.; Mascioli, K.; Flanagan, J.J.; Castelli, J.P.; Schiffmann, R.; Boudes, P.; Lockhart, D.J.; Valenzano, K.J.; et al. A pharmacogenetic approach to identify mutant forms of α-galactosidase a that respond to a pharmacological chaperone for Fabry disease. *Hum. Mutat.* **2011**, *32*, 965–977. [CrossRef] [PubMed]
58. Andreotti, G.; Citro, V.; de Crescenzo, A.; Orlando, P.; Cammisa, M.; Correra, A.; Cubellis, M.V. Therapy of Fabry disease with pharmacological chaperones: From in silico predictions to in vitro tests. *Orphanet. J. Rare Dis.* **2011**, *6*, 66. [CrossRef] [PubMed]

59. Giugliani, R.; Waldek, S.; Germain, D.P.; Nicholls, K.; Bichet, D.G.; Simosky, J.K.; Bragat, A.C.; Castelli, J.P.; Benjamin, E.R.; Boudes, P.F. A phase 2 study of migalastat hydrochloride in females with Fabry disease: Selection of population, safety and pharmacodynamic effects. *Mol. Genet. Metab.* **2013**, *109*, 86–92. [CrossRef] [PubMed]
60. Lukas, J.; Scalia, S.; Eichler, S.; Pockrandt, A.M.; Dehn, N.; Cozma, C.; Giese, A.K.; Rolfs, A. Functional and clinical consequences of novel α-galactosidase a mutations in Fabry disease. *Hum. Mutat.* **2016**, *37*, 43–51. [CrossRef] [PubMed]
61. Johnson, F.K.; Mudd, P.N., Jr.; Bragat, A.; Adera, M.; Boudes, P. Pharmacokinetics and safety of migalastat HCL and effects on agalsidase activity in healthy volunteers. *Clin. Pharmacol. Drug Dev.* **2013**, *2*, 120–132. [CrossRef] [PubMed]
62. Togawa, T.; Tsukimura, T.; Kodama, T.; Tanaka, T.; Kawashima, I.; Saito, S.; Ohno, K.; Fukushige, T.; Kanekura, T.; Satomura, A.; et al. Fabry disease: Biochemical, pathological and structural studies of the α-galactosidase a with E66Q amino acid substitution. *Mol. Genet. Metab.* **2012**, *105*, 615–620. [CrossRef] [PubMed]
63. Benjamin, E.R.; Della Valle, M.C.; Wu, X.; Katz, E.; Pruthi, F.; Bond, S.; Bronfin, B.; Williams, H.; Yu, J.; Bichet, D.G.; et al. The validation of pharmacogenetics for the identification of Fabry patients to be treated with migalastat. *Genet. Med.* **2016**. [CrossRef] [PubMed]
64. Cubellis, M.V.; Baaden, M.; Andreotti, G. Taming molecular flexibility to tackle rare diseases. *Biochimie* **2015**, *113*, 54–58. [CrossRef] [PubMed]
65. Saito, S.; Ohno, K.; Sese, J.; Sugawara, K.; Sakuraba, H. Prediction of the clinical phenotype of Fabry disease based on protein sequential and structural information. *J. Hum. Genet.* **2010**, *55*, 175–178. [CrossRef] [PubMed]
66. Riera, C.; Lois, S.; Dominguez, C.; Fernandez-Cadenas, I.; Montaner, J.; Rodriguez-Sureda, V.; de la Cruz, X. Molecular damage in Fabry disease: Characterization and prediction of α-galactosidase a pathological mutations. *Proteins* **2015**, *83*, 91–104. [CrossRef] [PubMed]
67. Lek, M.; Karczewski, K.J.; Minikel, E.V.; Samocha, K.E.; Banks, E.; Fennell, T.; O'Donnell-Luria, A.H.; Ware, J.S.; Hill, A.J.; Cummings, B.B.; et al. Analysis of protein-coding genetic variation in 60,706 humans. *Nature* **2016**, *536*, 285–291. [CrossRef] [PubMed]
68. Ishii, S.; Sakuraba, H.; Suzuki, Y. Point mutations in the upstream region of the α-galactosidase a gene exon 6 in an atypical variant of Fabry disease. *Hum. Genet.* **1992**, *89*, 29–32. [CrossRef] [PubMed]
69. Havndrup, O.; Christiansen, M.; Stoevring, B.; Jensen, M.; Hoffman-Bang, J.; Andersen, P.S.; Hasholt, L.; Norremolle, A.; Feldt-Rasmussen, U.; Kober, L.; et al. Fabry disease mimicking hypertrophic cardiomyopathy: Genetic screening needed for establishing the diagnosis in women. *Eur. J. Heart Fail.* **2010**, *12*, 535–540. [CrossRef] [PubMed]
70. Branton, M.H.; Schiffmann, R.; Sabnis, S.G.; Murray, G.J.; Quirk, J.M.; Altarescu, G.; Goldfarb, L.; Brady, R.O.; Balow, J.E.; Austin Iii, H.A.; et al. Natural history of Fabry renal disease: Influence of α-galactosidase a activity and genetic mutations on clinical course. *Medicine (Baltimore)* **2002**, *81*, 122–138. [CrossRef] [PubMed]
71. Eng, C.M.; Resnick-Silverman, L.A.; Niehaus, D.J.; Astrin, K.H.; Desnick, R.J. Nature and frequency of mutations in the α-galactosidase a gene that cause Fabry disease. *Am. J. Hum. Genet.* **1993**, *53*, 1186–1197. [PubMed]
72. Shabbeer, J.; Yasuda, M.; Luca, E.; Desnick, R.J. Fabry disease: 45 novel mutations in the α-galactosidase a gene causing the classical phenotype. *Mol. Genet. Metab.* **2002**, *76*, 23–30. [CrossRef]
73. Ferreira, S.; Ortiz, A.; Germain, D.P.; Viana-Baptista, M.; Caldeira-Gomes, A.; Camprecios, M.; Fenollar-Cortes, M.; Gallegos-Villalobos, A.; Garcia, D.; Garcia-Robles, J.A.; et al. The α-galactosidase a p.Arg118cys variant does not cause a Fabry disease phenotype: Data from individual patients and family studies. *Mol. Genet. Metab.* **2015**, *114*, 248–258. [CrossRef] [PubMed]
74. Lukas, J.; Pockrandt, A.M.; Seemann, S.; Sharif, M.; Runge, F.; Pohlers, S.; Zheng, C.; Glaser, A.; Beller, M.; Rolfs, A.; et al. Enzyme enhancers for the treatment of Fabry and pompe disease. *Mol. Ther.* **2015**, *23*, 456–464. [CrossRef] [PubMed]
75. Lenders, M.; Weidemann, F.; Kurschat, C.; Canaan-Kuhl, S.; Duning, T.; Stypmann, J.; Schmitz, B.; Reiermann, S.; Kramer, J.; Blaschke, D.; et al. α-Galactosidase A p.A143T, a non-Fabry disease-causing variant. *Orphanet. J. Rare Dis.* **2016**, *11*, 54. [CrossRef] [PubMed]

76. Peng, H.; Xu, X.; Zhang, L.; Zhang, X.; Zheng, Y.; Luo, S.; Guo, H.; Xia, K.; Li, J.; Yao, H.; et al. GLA variation p.E66Q identified as the genetic etiology of Fabry disease using exome sequencing. *Gene* **2016**, *575*, 363–367. [CrossRef] [PubMed]
77. Oikawa, M.; Sakamoto, N.; Kobayashi, A.; Suzuki, S.; Yoshihisa, A.; Yamaki, T.; Nakazato, K.; Suzuki, H.; Saitoh, S.; Kiko, Y.; et al. Familial hypertrophic obstructive cardiomyopathy with the GLA E66Q mutation and zebra body. *BMC Cardiovasc. Disord.* **2016**, *16*, 83. [CrossRef] [PubMed]
78. Nakamura, K.; Sekijima, Y.; Hattori, K.; Nagamatsu, K.; Shimizu, Y.; Yazaki, M.; Sakurai, A.; Endo, F.; Fukushima, Y.; Ikeda, S.I. P.E66Q mutation in the *GLA* gene is associated with a high risk of cerebral small-vessel occlusion in elderly Japanese males. *Eur. J. Neurol.* **2014**, *21*, 49–56. [CrossRef] [PubMed]
79. Satomura, A.; Yanai, M.; Fujita, T.; Nakayama, T. Comment on 'p.E66q mutation in the *GLA* gene is associated with a high risk of cerebral small-vessel occlusion in elderly japanese males'. *Eur. J. Neurol.* **2014**, *21*, e62. [CrossRef] [PubMed]
80. Shimotori, M.; Maruyama, H.; Nakamura, G.; Suyama, T.; Sakamoto, F.; Itoh, M.; Miyabayashi, S.; Ohnishi, T.; Sakai, N.; Wataya-Kaneda, M.; et al. Novel mutations of the *GLA* gene in Japanese patients with Fabry disease and their functional characterization by active site specific chaperone. *Hum. Mutat.* **2008**, *29*, 331. [CrossRef] [PubMed]
81. Niemann, M.; Rolfs, A.; Giese, A.; Mascher, H.; Breunig, F.; Ertl, G.; Wanner, C.; Weidemann, F. Lyso-Gb3 indicates that the α-galactosidase a mutation D313Y is not clinically relevant for Fabry disease. *JIMD Rep.* **2013**, *7*, 99–102. [PubMed]
82. Rigoldi, M.; Concolino, D.; Morrone, A.; Pieruzzi, F.; Ravaglia, R.; Furlan, F.; Santus, F.; Strisciuglio, P.; Torti, G.; Parini, R. Intrafamilial phenotypic variability in four families with anderson-Fabry disease. *Clin. Genet.* **2014**, *86*, 258–263. [CrossRef] [PubMed]
83. Ioannou, Y.A.; Zeidner, K.M.; Grace, M.E.; Desnick, R.J. Human α-galactosidase A: Glycosylation site 3 is essential for enzyme solubility. *Biochem. J.* **1998**, *332*, 789–797. [CrossRef] [PubMed]
84. Thomas, A.; Baker, R.; Mehta, A.; Hughes, D. The N215S mutation results in a distinct subtype of Fabry disease. *Mol. Genet. Metab.* **2015**, *114*, S113. [CrossRef]
85. Meehan, S.M.; Junsanto, T.; Rydel, J.J.; Desnick, R.J. Fabry disease: Renal involvement limited to podocyte pathology and proteinuria in a septuagenarian cardiac variant. Pathologic and therapeutic implications. *Am. J. Kidney Dis.* **2004**, *43*, 164–171. [CrossRef] [PubMed]
86. Fan, J.Q.; Ishii, S.; Asano, N.; Suzuki, Y. Accelerated transport and maturation of lysosomal α-galactosidase A in Fabry lymphoblasts by an enzyme inhibitor. *Nat. Med.* **1999**, *5*, 112–115. [CrossRef] [PubMed]
87. Okumiya, T.; Ishii, S.; Takenaka, T.; Kase, R.; Kamei, S.; Sakuraba, H.; Suzuki, Y. Galactose stabilizes various missense mutants of α-galactosidase in Fabry disease. *Biochem. Biophys. Res. Commun.* **1995**, *214*, 1219–1224. [CrossRef] [PubMed]
88. Asano, N.; Ishii, S.; Kizu, H.; Ikeda, K.; Yasuda, K.; Kato, A.; Martin, O.R.; Fan, J.Q. In vitro inhibition and intracellular enhancement of lysosomal α-galactosidase A activity in Fabry lymphoblasts by 1-deoxygalactonojirimycin and its derivatives. *Eur. J. Biochem.* **2000**, *267*, 4179–4186. [CrossRef] [PubMed]
89. Yu, Y.; Mena-Barragan, T.; Higaki, K.; Johnson, J.L.; Drury, J.E.; Lieberman, R.L.; Nakasone, N.; Ninomiya, H.; Tsukimura, T.; Sakuraba, H.; et al. Molecular basis of 1-deoxygalactonojirimycin arylthiourea binding to human α-galactosidase A: Pharmacological chaperoning efficacy on Fabry disease mutants. *ACS Chem. Biol.* **2014**, *9*, 1460–1469. [CrossRef] [PubMed]
90. Kato, A.; Yamashita, Y.; Nakagawa, S.; Koike, Y.; Adachi, I.; Hollinshead, J.; Nash, R.J.; Ikeda, K.; Asano, N. 2,5-dideoxy-2,5-imino-d-altritol as a new class of pharmacological chaperone for Fabry disease. *Bioorg. Med. Chem.* **2010**, *18*, 3790–3794. [CrossRef] [PubMed]
91. Ayers, B.J.; Ngo, N.; Jenkinson, S.F.; Martinez, R.F.; Shimada, Y.; Adachi, I.; Weymouth-Wilson, A.C.; Kato, A.; Fleet, G.W. Glycosidase inhibition by all 10 stereoisomeric 2,5-dideoxy-2,5-iminohexitols prepared from the enantiomers of glucuronolactone. *J. Org. Chem.* **2012**, *77*, 7777–7792. [CrossRef] [PubMed]
92. Cheng, W.C.; Wang, J.H.; Li, H.Y.; Lu, S.J.; Hu, J.M.; Yun, W.Y.; Chiu, C.H.; Yang, W.B.; Chien, Y.H.; Hwu, W.L. Bioevaluation of sixteen admdp stereoisomers toward α-galactosidase A: Development of a new pharmacological chaperone for the treatment of Fabry disease and potential enhancement of enzyme replacement therapy efficiency. *Eur. J. Med. Chem.* **2016**, *123*, 14–20. [CrossRef] [PubMed]

93. Mena-Barragan, T.; Narita, A.; Matias, D.; Tiscornia, G.; Nanba, E.; Ohno, K.; Suzuki, Y.; Higaki, K.; Garcia Fernandez, J.M.; Ortiz Mellet, C. pH-responsive pharmacological chaperones for rescuing mutant glycosidases. *Angew. Chem. Int. Ed. Engl.* **2015**, *54*, 11696–11700. [CrossRef] [PubMed]
94. Motabar, O.; Liu, K.; Southall, N.; Marugan, J.J.; Goldin, E.; Sidransky, E.; Zheng, W. High throughput screening for inhibitors of α-galactosidase. *Curr. Chem. Genom.* **2010**, *4*, 67–73. [CrossRef] [PubMed]
95. Citro, V.; Peña-García, J.; den-Haan, H.; Pérez-Sánchez, H.; del Prete, R.; Liguori, L.; Cimmaruta, C.; Lukas, J.; Cubellis, M.V.; Andreotti, G. Identification of an allosteric binding site on human lysosomal α-galactosidase opens the way to new pharmacological chaperones for Fabry disease. *PLoS ONE* **2016**, *11*, e0165463. [CrossRef] [PubMed]
96. Linear Correlation and Regression. Available online: http://vassarstats.net/corr_big.html (accessed on 30 November 2016).
97. Andreotti, G.; Guarracino, M.R.; Cammisa, M.; Correra, A.; Cubellis, M.V. Prediction of the responsiveness to pharmacological chaperones: Lysosomal human α-galactosidase, a case of study. *Orphanet. J. Rare Dis.* **2010**, *5*, 36. [CrossRef] [PubMed]
98. Cammisa, M.; Correra, A.; Andreotti, G.; Cubellis, M.V. Fabry_cep: A tool to identify Fabry mutations responsive to pharmacological chaperones. *Orphanet. J. Rare Dis.* **2013**, *8*, 111. [CrossRef] [PubMed]
99. Cammisa, M.; Correra, A.; Andreotti, G.; Cubellis, M.V. Identification and analysis of conserved pockets on protein surfaces. *BMC Bioinform.* **2013**, *14*, S9. [CrossRef] [PubMed]
100. Adzhubei, I.A.; Schmidt, S.; Peshkin, L.; Ramensky, V.E.; Gerasimova, A.; Bork, P.; Kondrashov, A.S.; Sunyaev, S.R. A method and server for predicting damaging missense mutations. *Nat. Methods* **2010**, *7*, 248–249. [CrossRef] [PubMed]

jove Journal of Visualized Experiments www.jove.com

Video Article

In Vitro Enzyme Measurement to Test Pharmacological Chaperone Responsiveness in Fabry and Pompe Disease

Jan Lukas[1], Anne-Marie Knospe[1], Susanne Seemann[1], Valentina Citro[2], Maria V Cubellis[2], Arndt Rolfs[1,3]

[1]Albrecht-Kossel-Institute, University Rostock Medical Center

[2]Department of Biology, University Federico II

[3]Centogene AG

Correspondence to: Jan Lukas at jan.lukas@med.uni-rostock.de

URL: https://www.jove.com/video/56550
DOI: doi:10.3791/56550

Keywords: Lysosomal storage disorder, phenotype, glycosidase, small molecule drugs, preclinical test, personalised therapy

Date Published: 11/14/2017

Citation: Lukas, J., Knospe, A.M., Seemann, S., Citro, V., Cubellis, M.V., Rolfs, A. *In Vitro* Enzyme Measurement to Test Pharmacological Chaperone Responsiveness in Fabry and Pompe Disease. *J. Vis. Exp.* (), e56550, doi:10.3791/56550 (2017).

Abstract

The use of personalized medicine to treat rare monogenic diseases like lysosomal storage disorders (LSDs) is challenged by complex clinical trial designs, high costs, and low patient numbers. Hundreds of mutant alleles are implicated in most of the LSDs. The diseases are typically classified into 2 to 3 different clinical types according to severity. Moreover, molecular characterization of the genotype can help predict clinical outcomes and inform patient care. Therefore, we developed a simple cell culture assay based on HEK293H cells heterologously over-expressing the mutations identified in Fabry and Pompe disease. A similar assay has recently been introduced as a preclinical test to identify amenable mutations for Pharmacological Chaperone Therapy (PCT) in Fabry disease. This manuscript describes an amended cell culture assay which enables rapid phenotypic assessment of allelic variants in Fabry and Pompe disease to identify eligible patients for PCT and may aid in the development of novel pharmacochaperones.

Video Link

The video component of this article can be found at https://www.jove.com/video/56550/

Introduction

There are over a dozen lysosomal storage disorders (LSDs) related to glycosidase dysfunction as a result of primary gene mutations. In Fabry (OMIM #301500) and Pompe (OMIM #232300) disease, more than 500 and 200 missense mutations[1,2,3] have been reported, respectively, which corresponds to about 60% of the total mutation count. Numerous new gene variants are still being identified, many of which have unknown significance. Extensive biochemical studies revealed that certain genotypes do not lead to a complete loss-of-function of the *GLA* gene (OMIM *300644) in Fabry disease, but cause the corresponding enzyme to fail to reach a thermodynamically favored folding state[4]. This results in ER retention and premature degradation of the otherwise functional enzyme. Similar conclusions have been drawn in other LSDs including Pompe disease[5]. Moreover, molecular characterization of enzyme variants can facilitate clinical interpretation of the mutations at the time of diagnosis[6], suggesting that LSD progression is an individual process based on the nature of the mutation. Therefore, the conventional classification into typically 2 to 3 different clinical types should be reassessed in order to streamline clinical counselling and therapeutic decisions.

Enzyme Replacement Therapy (ERT) is available for both diseases. ERT, however, has limited efficacy in affected tissues/organs such as the brain and skeletal muscle. Furthermore, ERT can elicit an immunogenic response that jeopardizes its therapeutic benefits. Pharmacological Chaperones (PCs) are an attractive treatment alternative for patients with so-called responsive mutations. PCs serve as a molecular scaffold for correct protein folding and stabilization which in turn prevents endoplasmic reticulum (ER) retention and ER-associated degradation of the enzyme. Moreover, PCs can be administered orally and are potentially able to cross the blood brain barrier. Therefore, PCT might be a more viable option for treating patients with certain genotypes. For an extensive review on PC application in LSDs, refer to the excellent review by Parenti[7].

The discovery of hundreds of disease causing mutant alleles challenges pre-clinical drug testing and necessitates a simple, fast, and highly standardized assessment of amenable patients for a personalized medicine approach. In order to assess the detrimental effects of LSD gene mutations and to test candidate mutations to predict amenable patients for PCT, a highly standardized over-expression system in HEK293H cells that allows for fast and reliable enzyme activity measurement was developed. Similar over-expression systems have been previously described for Fabry and Pompe disease using either COS-7[8,9,10,11], HeLa cells[12], or HEK293[13,14,15,16] cells for the glycosidase gene.

A very similar method has even been patented as a "Method to predict response to Pharmacological Chaperone treatment of diseases"[17] indicating the relevance of a cell culture system capable of being integrated into clinical practice.

jove Journal of Visualized Experiments www.jove.com

Protocol

1. Preparation of Mutant pcDNA3.1/GLA and pcDNA3.1/GAA Constructs

NOTE: The cloning strategies for the *GLA* and *GAA* coding sequences (cds) have been reported earlier[15,18].

1. **Site-directed Mutagenesis Using Site-Directed Mutagenesis**
    1. Use the reference sequences NM_000169.2 and NM_000152.4 as templates for the mutagenesis of *GLA* and *GAA* genes, respectively. Have a set of high purity salt free primers (25-37-mers) synthesized by a commercial provider, with sense and antisense primers carrying one of the respective sequence modifications central to their length to individually introduce the mutation. Use the free primer design tool to support the primer design[19].
    2. For the reaction mixture, use the standard conditions for the reaction solution and PCR conditions provided by the manufacturer.
        1. Mix 5 µL of 10x reaction buffer, 10 ng of double-stranded template plasmid DNA (pcDNA3.1/GLA or pcDNA3.1/GAA), 125 ng of each primer, 1 µL of the provided dNTP mixture, 3 µL of DMSO reagent in an appropriate volume of deionized water (final reaction volume: 50 µL). Finally, add 2.5 U of DNA polymerase and mix by pipetting up and down. As a negative control, carry along a no-primer sample.
    3. Start the PCR using the following program: step 1: 95 °C for 1 min, step 2: 95 °C for 50 s, step 3: 60 °C for 50 s, step 4: 68 °C for 8 min, repeat step 2-4 18 times, and step 5: 68 °C for 10 min.
        1. Following PCR, add 1 µL of the *Dpn*I restriction enzyme (10 U/µL) and further incubate the reaction vial at 37 °C for 1 h.

2. **Transformation and Screening for the Desired Clone**
    1. Transform an aliquot of ultracompetent cells in accordance with the manufacturer's recommendations. Use SOC medium (tryptone 2% (w/v), yeast extract 0.5% (w/v), NaCl 10 mM, KCl 2.5 mM, sterilize at 121 °C, and then add sterile-filtered solutions of $MgCl_2$ and glucose up to final concentrations of 10 and 20 mM, respectively) instead of the manufacturer's medium. After the procedure, plate 250 µL of the sample mutagenesis on an LB plate containing 100 µg/mL ampicillin and incubate at 37 °C for 18 h.
    2. Assure that the number of transformants is >10 and the reaction yields at least three times as many colonies as the no-primer control reaction, *e.g.*, using a luminous plate to facilitate colony counting. Then pick 3 colonies and prepare 3 mL overnight cultures in LB Broth medium.
    3. The next day, carry out plasmid preparation with a standard kit and analyze whole sequence using T7 (5'-TAA TAC GAC TCA CTA TAG GG-3') and BGHr (5'-TAG AAG GCA CAG TCG AGG-3') primers via standard Sanger sequencing.
    4. Use a suitable molecular biology tool to analyze the sequence. When the desired mutation is detected and no further sequence abnormality compared to NM_000169.2 (α-galactosidase A) or NM_000152.4 (acid α-glucosidase) is seen, select the clone for transfection-grade plasmid purification.
    5. Determine the purity of the DNA by measuring the absorbance in a spectrophotometer.
    NOTE: Allow only preparations that yield a plasmid purity with a 260/280 absorbance ratio of >1.8 for cell culture experiments.

2. Cultivation of HEK293H Cells

1. Maintain HEK293H cells in high glucose (4.5 g/L) Dulbecco´s Modified Eagle Medium (DMEM) supplemented with 10% fetal bovine serum (FBS) and 1% penicillin/streptomycin. Keep the cells in a water-jacket incubator at 37 °C under a 5% CO_2 atmosphere.
2. Cultivate the cells to a density of 80 - 90%.
3. Aspirate the medium and wash once using phosphate buffered saline (PBS) without Ca^{2+} and Mg^{2+}.
4. Passage by adding 0.05% Trypsin-EDTA and incubate for 5 min at 37 °C and 5% CO_2.
5. Split the cells 1:15 in fresh medium and seed into a new T75 flask to maintain the permanent culture. Do not use cells with more than 25 passages.

3. pcDNA3.1/GLA and pcDNA3.1/GAA Plasmid Transfection and Treatment of HEK293H

1. 24 h prior to the transfection, wash the HEK293H cells in a T75 cell culture flask once with PBS with Ca^{2+}, Mg^{2+}. Harvest the cells with 0.05% Trypsin-EDTA as stated above and seed 1.5 x 10^5 cells in the cavities of a 24 well culture plate using 500 µL DMEM medium supplemented with 10% FBS without antibiotics.
2. Carry out a transfection protocol according to the manufacturer's manual. Typically, use a mixture of 1 µg of plasmid DNA and 2.5 µL of transfection reagent in 100 µL of serum-free DMEM. Incubate for 20 min at room temperature and add to the cells in a drop-wise manner thereafter.
3. Remove the medium containing the transfection reagent after a period of 4 h at 37 °C/5% CO_2 and add 500 µL of fresh DMEM with 10% FBS/ 1% penicillin/streptomycin.
    NOTE: During this step, 1-Deoxygalactonojirimycin Hydrochloride (DGJ) or 1-Deoxynojirimycin Hydrochloride (DNJ) might be added to the culture medium where intended (use an aqueous stock solution of 10 mM in order to obtain a final concentration of 20 µM DGJ and DNJ). Fresh DGJ or DNJ was added 42 h after plasmid transfection.

4. Cell Harvest and α-galactosidase A or Acid α-glucosidase Activity Measurement

1. **Cell harvest**

1. On the day of the harvest, remove the cells from the incubator and aspirate the medium. Carefully wash the cells 2 times with PBS with Ca^{2+} and Mg^{2+}.
   NOTE: This step is critical because DGJ and DNJ are potent inhibitors of α-galactosidase and α-glucosidase, respectively, and any leftover would invalidate the test.
2. Add 200 µL of deionized water directly on top of the cells. Rinse the cells from the plate and transfer them to a 1.5 mL reaction tube.

2. **Homogenization by freezing and thawing**
   1. Put the samples in an appropriate foam rack and vortex for 5 s to make the lysis more efficient. Put the samples alternating in liquid nitrogen for 10 s and in a room temperature water bath until the thawing was complete (5 min).
   2. Repeat this procedure 5 times and then spin the samples for 5 min at 10,000 x g. Retain the supernatant and pipette in a new reaction tube.

3. **Protein concentration determination using bicinchoninic acid (BCA) assay**
   1. Prepare a fresh tube for each sample containing 40 µL of deionized H_2O and add 10 µL of sample. Mix solution by vortexing briefly and transfer 10 µL into a cavity of a 96 well plate (each sample in triplicate). Dilute a 2 mg/mL bovine serum albumin (BSA) stock solution in deionized H_2O as follows to obtain a standard curve: 50 µL H_2O/50 µL BSA; 60 µL H_2O/40 µL BSA; 70 µL H_2O/30 µL BSA; 80 µL H_2O/20 µL BSA; 90 µL H_2O/10 µL BSA; 100 µL H_2O.
   2. Start the reaction by adding 200 µL of BCA reagent (Reagent A and reagent B mixed at a 50:1 ratio) and incubate for 1 h in the dark at 37 °C under slight agitation on an orbital shaker (300 rpm). Measure the absorbance at 560 nm in a plate reader.
      NOTE: The samples typically contain between 1 and 1.5 µg protein per µL.

4. **Enzyme activity measurement with artificial 4-Methylumbelliferyl substrates (4-MUG)**
   1. Dilute the calculated amount of each sample and pipet into fresh 1.5 mL reaction tubes to obtain 0.05 (for α-galactosidase A) or 0.5 (for acid α-glucosidase) µg protein/µL solutions. Vortex the samples for 5 s again and pipet 10 µL of this dilution into a 96 well plate (each sample in duplicate).
   2. Start the reaction by adding 20 µL of the respective substrate solution:
      For α-galactosidase A: 2 mM 4-Methylumbelliferyl-α-D-galactopyranoside (4-MU-gal) in 0.06 M phosphate citrate buffer, pH 4.7.
      For acid α-glucosidase: 2 mM 4-methylumbelliferyl α-D-glucopyranoside (4-MU-glu) in 0.025 M sodium acetate, pH 4.0.
   3. Incubate the enzyme reactions for 1 h in the dark at 37 °C under slight agitation on an orbital shaker (300 rpm). Terminate the reaction by the addition of 200 µL of 1.0 M, pH 10.5 adjusted glycine-NaOH buffer.
   4. Prepare a standard curve of 4-methylumbelliferone (4-MU) from a 0.01 mg/mL stock as follows:
      100 µL H_2O/ no 4-MU; 80 µL H_2O/ 20 µL 4-MU; 60 µL H_2O/ 40 µL 4-MU; 40 µL H_2O/ 60 µL 4-MU; 20 µL H_2O/ 80 µL 4-MU; no H_2O/ 100 µL 4-MU, pipet 10 µL of each dilution into the 96 well plate (in duplicates) and add 200 µL of the 1.0 M glycine-NaOH buffer to each well in order to adjust the volume and pH.
   5. Measure the enzyme activity in a fluorescence reader equipped with the appropriate filter set and analyze the data using the appropriate software for the fluorescence reader device.
      NOTE: Both 4-MUG substrates are reduced to 4-MU during exposure to α-galactosidase A or acid α-glucosidase. Released 4-MU is a fluorochrome, which can be measured at 360 and 465 nm as the excitation and emission wavelengths, respectively, using a microplate fluorescence reader.

Representative Results

The mutagenesis procedure: To assess the efficiency of *GLA* gene mutagenesis, the mutations were classified into one of the following categories. This approach to generate mutations revealed that about 66.5% of the *GLA* mutations were obtained in the first attempt. A further 25% could be obtained after a slightly modified second PCR.

Category 1: The mutagenesis PCR was effective at first attempt.

Category 2: First mutagenesis PCR failed (no colonies on the plate, no inserted mutation); repetition using the same primer set by increasing the annealing temperature up to 68 °C was effective.

Category 3: More effort had to be undertaken to yield the desired clone (*e.g.*, typically one or more new sets of primers were designed).

α-galactosidase A and acid α-glucosidase enzyme activity measurement: Enzyme activity of the different mutant enzymes was recorded after previous incubation of the transiently transfected cells in the presence or absence of a PC. **Table 1** refers to the results for 3 α-galactosidase A and 3 acid α-glucosidase mutations. Data are displayed as (1) absolute values for the substrate turnover (nmol 4-MU* mg $protein^{-1}$* h^{-1}) and as (2) relative values normalized to the wild type enzyme. Both expressions are useful, since total substrate turnover illustrates the efficiency of the reaction and the sensitivity of the system, while the normalized values can give important hints for the likelihood of the malignancy of the mutation on the one hand and the efficiency of the applied PC treatment on the other hand. For the experimental phase, the work flow depicted in **Figure 1** was set up, which scheduled a 60 h incubation period with the compound (due to technical reasons, *e.g.* fast HEK293H cell growth under the introduced conditions). Even though it has been stated that 10 µM was the approximate maximum achievable plasma concentration for DGJ[14], the current protocol uses 20 µM as a reasonable concentration for the purpose of a screening for PC responsiveness as supported by numerous earlier works[4,20,21,22,23]. Moreover, it has been postulated that higher plasma levels can be reached[24].

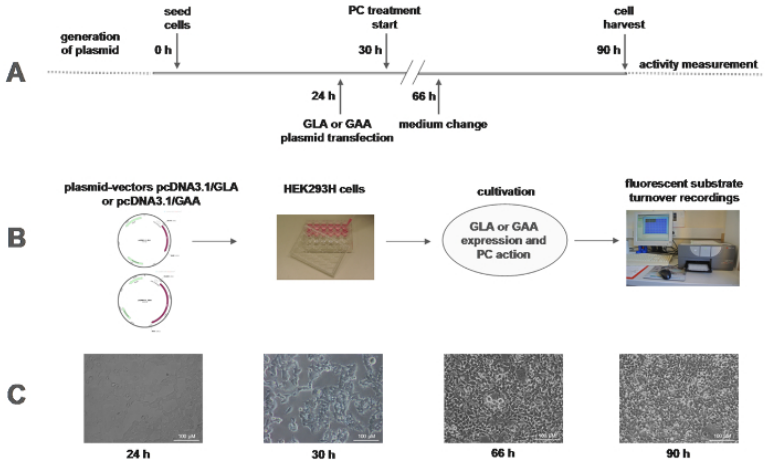

Figure 1: Work flow of the *in vitro* enzyme activity measurement. (A) The timeline of the experiment shows a 90 h cell culture effort with relatively little hands-on-time required at the indicated time points. **(B)** Representative plasmid vectors pcDNA3.1 containing the wild type cds of *GLA* and *GAA* are shown. *GLA* and *GAA* wild type plasmids and plasmids including the respective inserted mutation of interest were used to transiently transfect HEK293H cells plated in 24 well format. After a period to allow the cells to synthesize the respective gene products and allow for enzyme processing, lysosomal transport, and PC action, the cells were lysed and measured in a fluorescence plate reader and analyzed using the respective software. C: Cell morphology and growth status of the HEK293H cells are shown throughout the time course of the experiment. Scale bars = 100 µm Please click here to view a larger version of this figure.

	in vitro enzyme activity				
GLA	**native**		**20 µM DGJ**		
mutation (AA)	nmol 4-MUG-gal /mg/ h (mean)	% mean (±SD, N)	nmol 4-MUG-gal /mg/ h (mean)	% mean (±SD, N)	significance
p.A143T	2384.7	29.2 (±2.6, 5)	4223.0	52.0 (±4.4, 5)	***
p.A156V	379.2	4.3 (±.8, 5)	1437.5	16.3 (±1.3, 5)	****
p.R301Q	777.4	8.8 (±1.1, 5)	3002.6	44.2 (±3.6, 5)	****
GAA	**native**		**20 µM DNJ**		
mutation (AA)	nmol 4-MUG-glu /mg/ h (mean)	% mean (±SD, N)	nmol 4-MUG-glu /mg/ h (mean)	% mean (±SD, N)	significance
p.Y455F	41.1	5.4 (±.4, 5)	246.6	31.4 (±2.8, 5)	***
p.P545L	65.7	6.6 (±.4, 5)	166.5	16.7 (±1.5, 5)	**
p.L552P	0.0	0.0 (±.2, 5)	104.3	10.4 (±1.4, 5)	***

Table 1: Enzyme activity of α-galactosidase A and acid α-glucosidase. The table shows representative results for 3 α-galactosidase A and 3 acid α-glucosidase mutants with and without the PCs DGJ or DNJ. Absolute enzyme activity data was corrected for endogenous enzyme activity of the HEK293H cells. To evaluate endogenous enzyme activity, the cells were transfected with a pcDNA3.1 empty vector. The values were 97.5 nmol 4-MU* mg protein^{-1}* h^{-1} for α-galactosidase A and 41.6 nmol 4-MU* mg protein^{-1}* h^{-1} for acid α-glucosidase, respectively; enzyme activity values were normalized to wild type enzyme from corresponding experiments, which explains the deviations of relative values between the different mutants. After 5 independent cell culture experiments (N=5), each carried out in technical duplicates, the standard deviation was not allowed to be >15% of the mean. Ratio T-Tests were used to calculate the difference between untreated and PC-treated enzyme.
*p<0.05, **p<0.01, ***p<0.005, ****p<0.001

Discussion

The protocol described herein delivers robust results for enzyme damage assessment in hereditary lysosomal diseases of metabolism. This manuscript is an amendment to the protocol published earlier[15]. The most crucial modifications involve stringency (*i.e.*, in the process of mutant vector construct preparation), standardization of the cell culture protocol (*i.e.*, HEK293H cell maintenance and transfection conditions), and the high number of experimental repetitions (at least 5), which highly contributed to the reproducibility of the results. Altogether, both target genes have been easily accessible for mutagenesis and a multiplicity of mutations can be assembled in parallel. A relatively high signal/noise ratio was achieved considering that endogenous enzyme activity within the HEK293H cells was a negligible 1/50 (α-galactosidase A) and 1/20 (acid α-glucosidase) of the over-expressed wild type gene. Thus, there is an excellent resolution between wild type and mutant enzyme. It should be

noted that a different amount of total protein was applied for the activity assay of both enzymes (0.5 and 5 µg, respectively), because acid α-glucosidase activity was an order of magnitude lower than that of α-galactosidase A.

As stated above, assay parameters are often controversial, since many laboratories have developed their own assays to investigate lysosomal glycosidases. The systems can differ in cell type, plasmid-vector design, cultivation conditions, and period of drug exposure just to name a few of the numerous parameters. A recently published meta-analysis for Fabry disease demonstrated that enzyme activity recordings (with and without PC) of transfected cell models (*e.g.*, HEK293, COS-7) was largely in accordance with the results obtained from patient-derived cells (mostly lymphocytes or fibroblasts) with regard to the question, whether a mutation is responsive to the PC[24]. Earlier reports directly comparing patient-derived cells and transfection models demonstrated that over-expression systems reflect the situation in patient cells without compromising the conclusion[13,14]. It can therefore be concluded that, regardless of the particular protocol, the results obtained by different authors was not changed by the different cellular systems, even though responder definitions can be divergent. The current definition for a responding mutation is 20% relative enzyme activity increase and 5% absolute enzyme activity increase compared to the wild type enzyme after incubation with 20 µM DGJ for 60 h. A comprehensive database, FabryCEP, permits the comparison of results obtained by different experimental approaches for hundreds of α-galactosidase mutants[25].

Whether these criteria are sufficient to predict clinical benefits of DGJ and DNJ remains unclear, since the level of activity necessary to prevent symptomatic disease is controversial. A former study suggested that 10 to 15% of residual activity might be sufficient for the system to work properly[26]. However, in a recently published report from a phase 2 clinical study for DGJ, a 1% activity increase was deemed potentially beneficial for the patient, when the baseline activity was less than 1% of normal[27]. Recent clinical results suggest that patients predicted to respond to PCs by the responder definition of ≥20% relative increase and ≥3% absolute increase of wild type α-galactosidase A activity in HEK293H cells after incubation with 10 µM DGJ actually derived clinical benefit with disease stabilization or even improvement by renal and cardiac parameters[28]. Whereas DGJ has already been approved by the FDA and the European Commission as a monotherapy for Fabry disease, the course of PCs such as DNJ and the derivative N-Butyl-DNJ in Pompe disease appears to be different. A monotherapeutical approach with DNJ has been terminated during a Phase II clinical trial due to severe adverse events in some of the patients[29]. However, PC treatment in combination with approved ERT showed significantly improved results with regards to disease substrate (glycogen) reduction compared to the ERT monotherapy[30].

We suggest that the presented approach can be extended to other LSDs and other PCs such as Gaucher, Krabbe, Tay-Sachs/Sandhoff, and GM1 gangliosidosis, but this might not work in specific cases, where for example the signal/noise ratio of the system is insufficient. Care should be taken to select a suitable cell disruption method to prepare a cell lysate for enzyme activity determination, because the addition of detergents into the lysis buffer might be indicative of membrane-bound enzymes such as glucocerebrosidase in Gaucher disease while similar amounts of detergent may harm other enzymes. For α-galactosidase A, a sonication-based cell disruption method should be avoided.

Disclosures

The authors declare that they have no competing financial interests.

Acknowledgements

The authors would like to acknowledge Mandy Loebert and Tina Czajka for excellent technical support. We thank Flora Luo (Harvard Medical School, Boston, MA, USA) for language editing help.

References

1. Cardiff University. *http://www.hgmd.cf.ac.uk/ac/index.php.* (2017).
2. Meiji Pharmaceutical University. *http://fabry-database.org/.* (2017).
3. Erasmus Medical Center. *Mutations In Human Acid Alpha-Glucosidase.* http://cluster15.erasmusmc.nl/klgn/pompe/mutations.html?lang=en (2017).
4. Ishii, S., *et al.* Mutant alpha-galactosidase A enzymes identified in Fabry disease patients with residual enzyme activity: biochemical characterization and restoration of normal intracellular processing by 1-deoxygalactonojirimycin. *Biochem J.* **406**, 285-95 (2007).
5. Tajima, Y., *et al.* Structural and biochemical studies on Pompe disease and a "pseudodeficiency of acid alpha-glucosidase". *J Hum Genet.* **52**, 898-906 (2007).
6. Lukas, J., *et al.* Functional and Clinical Consequences of Novel α-Galactosidase A Mutations in Fabry Disease. *Hum Mutat.* **37**, 43-51 (2016).
7. Parenti, G. Treating lysosomal storage diseases with pharmacological chaperones: from concept to clinics. *EMBO Mol Med.* **1**, 268-279 (2009).
8. Yasuda, M., *et al.* Fabry disease: characterization of alpha-galactosidase A double mutations and the D313Y plasma enzyme pseudodeficiency allele. *Hum Mutat.* **22**, 486-92 (2003).
9. Shimotori, M., Maruyama, H., Nakamura, G., Suyama, T., Sakamoto, F., Itoh, M., Miyabayashi, S., Ohnishi, T., *et al.* Novel mutations of the GLA gene in Japanese patients with Fabry disease and their functional characterization by active site specific chaperone. *Hum Mutat.* 29, 331 (2008).
10. Andreotti, G., *et al.* Therapy of Fabry disease with pharmacological chaperones: from in silico predictions to in vitro tests. *Orphanet J Rare Dis.* **6**, 66 (2011).
11. Khanna, R., *et al.* The pharmacological chaperone AT2220 increases the specific activity and lysosomal delivery of mutant acid alpha-glucosidase, and promotes glycogen reduction in a transgenic mouse model of Pompe disease. *PLoS One.* **9**, e102092 (2014).
12. Siekierska, A., *et al.* α-Galactosidase aggregation is a determinant of pharmacological chaperone efficacy on Fabry disease mutants. *J Biol Chem.* **287**, 28386-97 (2012).

13. Parenti, G., *et al.* Pharmacological enhancement of mutated alpha-glucosidase activity in fibroblasts from patients with Pompe disease. *Mol Ther.* **15**, 508-14 (2007).
14. Wu, X., *et al.* A pharmacogenetic approach to identify mutant forms of α-galactosidase A that respond to a pharmacological chaperone for Fabry disease. *Hum Mutat.* **32**, 965-77 (2011).
15. Lukas, J., *et al.* Functional characterisation of alpha-galactosidase a mutations as a basis for a new classification system in fabry disease. *PLoS Genet.* **9**, e1003632 (2013).
16. Andreotti, G., Citro, V., Correra, A., Cubellis, M.V. A thermodynamic assay to test pharmacological chaperones for Fabry disease. *Biochim Biophys Acta.* **1840**, 1214-1224 (2014).
17. *https://www.google.ch/patents/US9095584.* (2017).
18. Lukas, J., *et al.* Enzyme enhancers for the treatment of Fabry and Pompe disease. *Mol Ther.* **23**, 456-64 (2015).
19. *http://www.genomics.agilent.com/primerDesignProgram.jsp.* (2017).
20. Yam, G.H., Bosshard, N., Zuber, C., Steinmann, B., Roth, J. Pharmacological chaperone corrects lysosomal storage in Fabry disease caused by trafficking-incompetent variants. *Am J Physiol Cell Physiol.* **290**, C1076-82 (2006).
21. Shin, S.H., *et al.* Screening for pharmacological chaperones in Fabry disease. *Biochem Biophys Res Commun.* **359**, 168-73 (2007).
22. Shin, S.H., *et al.* Prediction of response of mutated alpha-galactosidase A to a pharmacological chaperone. *Pharmacogenet Genomics.* **18**, 773-80 (2008).
23. Filoni, C., *et al.* Functional studies of new GLA gene mutations leading to conformational Fabry disease. *Biochim Biophys Acta.* **1802**, 247-52 (2010).
24. Citro, V., *et al.* The Large Phenotypic Spectrum of Fabry Disease Requires Graduated Diagnosis and Personalized Therapy: A Meta-Analysis Can Help to Differentiate Missense Mutations. *Int J Mol Sci.* **17** (2016).
25. Cammisa M., Correra, A., Andreotti, G., Cubellis, M.V. Fabry_CEP: a tool to identify Fabry mutations responsive to pharmacological chaperones. *Orphanet J Rare Dis.* **8**, 111 (2013).
26. Leinekugel, P., Michel, S., Conzelmann, E., Sandhoff, K. Quantitative correlation between the residual activity of beta-hexosaminidase A and arylsulfatase A and the severity of the resulting lysosomal storage disease. *Hum Genet.* **88**, 513-23 (1992).
27. Germain, D.P., *et al.* Safety and pharmacodynamic effects of a pharmacological chaperone on α-galactosidase A activity and globotriaosylceramide clearance in Fabry disease: report from two phase 2 clinical studies. *Orphanet J Rare Dis.* **7**, 91 (2012).
28. Hughes, D.A., *et al.* Oral pharmacological chaperone migalastat compared with enzyme replacement therapy in Fabry disease: 18-month results from the randomised phase III ATTRACT study. *J Med Genet.* **54**, 288-296 (2017).
29. Parenti, G., Andria, G., Valenzano, K.J. Pharmacological Chaperone Therapy: Preclinical Development, Clinical Translation, and Prospects for the Treatment of Lysosomal Storage Disorders. *Mol Ther.* **23**, 1138-48 (2015).
30. Parenti, G., *et al.* A Chaperone Enhances Blood α-Glucosidase Activity in Pompe Disease Patients Treated With Enzyme Replacement Therapy. *Mol Ther.* **22**, 2004-12 (2014).

International Journal of *Molecular Sciences*

MDPI

Article

Assessment of Gene Variant Amenability for Pharmacological Chaperone Therapy with 1-Deoxygalactonojirimycin in Fabry Disease

Jan Lukas [1,2,*], Chiara Cimmaruta [1], Ludovica Liguori [3,4], Supansa Pantoom [1], Katharina Iwanov [1], Janine Petters [1], Christina Hund [1], Maik Bunschkowski [5], Andreas Hermann [1,2,6], Maria Vittoria Cubellis [4,7] and Arndt Rolfs [5,8]

1 Translational Neurodegeneration Section "Albrecht-Kossel", Department of Neurology, University Medical Center Rostock, 18147 Rostock, Germany; chiara.cimmaruta@med.uni-rostock.de (C.C.); Supansa.Pantoom@med.uni-rostock.de (S.P.); katharina.iwanov@med.uni-rostock.de (K.I.); janine.petters@med.uni-rostock.de (J.P.); christina.hund@med.uni-rostock.de (C.H.); andreas.hermann@med.uni-rostock.de (A.H.)
2 Center for Transdisciplinary Neurosciences Rostock (CTNR), University Medical Center Rostock, University of Rostock, 18147 Rostock, Germany
3 Dipartimento di Scienze e Tecnologie Ambientali, Biologiche e Farmaceutiche, Università degli Studi della Campania "Luigi Vanvitelli", 81100 Caserta, Italy; lud.liguori@gmail.com
4 Institute of Biomolecular Chemistry, CNR, 80078 Pozzuoli, Italy; cubellis@unina.it
5 Centogene AG, 18055 Rostock, Germany; Maik.Bunschkowski@centogene.com (M.B.); Arndt.Rolfs@centogene.com (A.R.)
6 German Center for Neurodegenerative Diseases (DZNE) Rostock/Greifswald, 18147 Rostock, Germany
7 Department of Biology, University Federico II, 80126 Naples, Italy
8 University Medical Center Rostock, University of Rostock, 18057 Rostock, Germany
* Correspondence: jan.lukas@med.uni-rostock.de; Tel.: +49-0381-494-4894

Received: 21 December 2019; Accepted: 29 January 2020; Published: 31 January 2020

Abstract: Fabry disease is one of the most common lysosomal storage disorders caused by mutations in the gene encoding lysosomal α-galactosidase A (α-Gal A) and resultant accumulation of glycosphingolipids. The sugar mimetic 1-deoxygalactonojirimycin (DGJ), an orally available pharmacological chaperone, was clinically approved as an alternative to intravenous enzyme replacement therapy. The decision as to whether a patient should be treated with DGJ depends on the genetic variant within the α-galactosidase A encoding gene (*GLA*). A good laboratory practice (GLP)-validated cell culture-based assay to investigate the biochemical responsiveness of the variants is currently the only source available to obtain pivotal information about susceptibility to treatment. Herein, variants were defined amenable when an absolute increase in enzyme activity of ≥3% of wild type enzyme activity and a relative increase in enzyme activity of ≥1.2-fold was achieved following DGJ treatment. Efficacy testing was carried out for over 1000 identified *GLA* variants in cell culture. Recent data suggest that about one-third of the variants comply with the amenability criteria. A recent study highlighted the impact of inter-assay variability on DGJ amenability, thereby reducing the power of the assay to predict eligible patients. This prompted us to compare our own α-galactosidase A enzyme activity data in a very similar in-house developed assay with those from the GLP assay. In an essentially retrospective approach, we reviewed 148 *GLA* gene variants from our former studies for which enzyme data from the GLP study were available and added novel data for 30 variants. We also present data for 18 *GLA* gene variants for which no data from the GLP assay are currently available. We found that both differences in experimental biochemical data and the criteria for the classification of amenability cause inter-assay discrepancy. We conclude that low baseline activity, borderline biochemical responsiveness, and inter-assay discrepancy are alarm signals for misclassifying a variant that must not be ignored. Furthermore, there is no solid basis for setting a minimum response threshold on which a clinical indication with DGJ can be justified.

Keywords: Lysosomal storage disorders; pharmacological chaperones; method comparison study; personalized medicine

1. Introduction

Fabry disease (FD; MIM# 301500) is a rare X–linked lysosomal storage disorder caused by mutations in the *GLA* gene encoding for the lysosomal enzyme α-galactosidase A (α-Gal A, E.C. 3.2.1.22). Pathological changes in the gene and its encoded protein result in a complete cellular absence or insufficiency of α-Gal A enzyme activity. The consequence is a cellular and microvascular dysfunction with multiple organ involvement [1]. The resulting storage of complex sphingolipids in the lysosomes, mainly globotriaosylceramide (Gb3) and its metabolite globotriaosylsphingosine (lyso-Gb3) serve as biomarkers in the diagnosis of FD [2] and are believed to play a major role in disease pathophysiology [3].

Clinical FD manifestation involves acroparesthesia, abdominal pain and fever, angiokeratomas, cornea verticillata, decreased ability to perspire, proteinuria, and progressive renal insufficiency. Considerable morbidity in patients with FD is due to kidney failure, cardiac disease, and stroke in the third to fifth decade of life [4–6]. However, a broad heterogeneous symptom spectrum can be observed, which is largely associated with the genotype [7].

To date, more than 1000 mostly private *GLA* gene variants were found related to FD [8]. A majority of approximately 60% of the variants are missense mutations associated with single amino-acid substitutions [9]. Enzyme replacement therapy (ERT) can principally be administered to all FD patients regardless of the underlying *GLA* gene constitution. However, the benefit of ERT is disadvantaged by a number of limitations such as insufficient penetration of relevant tissues [10] and an immune response that can lead to the formation of neutralizing immunoglobulin G (IgG) antibodies [11]. Therefore, the orally available pharmacological chaperone 1-deoxygalactonojirimycin (DGJ or migalastat, trade name Galafold® [12]) was recently developed as an alternative to ERT, but is suitable only for patients carrying biochemically responding gene variants. Typically, variants with residual enzyme activity are likely to respond to chaperone treatment at a higher level [13]. Nevertheless, even gene variants that severely affect enzyme activity can be classified as so-called "amenable". In addition to the missense variants, these may include nonsense variants near the carboxyl terminus, in-frame small deletions and insertions, and variants with more than one nucleotide exchange on the same allele [14]. A large number of studies concerned the assessment of variant α-Gal A enzyme activity in different cell culture systems. It was found that inter-assay discrepancies in residual activity and DGJ responsivity of the variants persist [15]. During the clinical phase 3 study, a standardized good laboratory practice (GLP)-validated human embryonic kidney cell-based in vitro assay was established to identify DGJ amenability of *GLA* gene variants [14], and it is currently the only approved method for this assessment. A very recent study stressed a significant inter-assay variability between the GLP-validated assay and an in-house assay adapted to it [16]. Due to the impact of this study for physicians, patients, and the relatives of patients, we felt that this study called on our own recent experience with further mutation data in order to contribute to the important topic of amenability of *GLA* gene variants. Thus, we comparatively analyzed the results from our in-house *GLA* gene variant amenability assessment with the GLP study data for reproducibility of enzymatic data and DGJ amenability classification of 178 *GLA* variants.

2. Results

Before the 178 datasets of the GLP-validated assay were compared with our in-house assay, the following 10 *GLA* gene variants from previous articles [7,13] were reexamined according to the in-house protocol to evaluate the robustness and reproducibility of the assay: M42V, N139S, G183V, N215S, S247P, L268S, L310F, S345P, R356Q, and G360C. Differences in the reexamination are shown in

Table A1 (Appendix A). Herein, one variant, L310F, changed category from non-amenable to amenable in accordance with the GLP-validated study and another former study [17]. Furthermore, a strong linear correlation of baseline activity and activity after DGJ treatment was obtained (Pearson $r = 0.9484$, $p < 0.0001$; $r = 0.8864$, $p = 0.0006$). However, there was no correlation with the DGJ-induced activity change (Pearson $r = 0.01734$, not significant), which can probably be explained by the small case size and the significantly different results for the three variants N139S, L310F (category switch), and R356Q.

2.1. Global Description of the Investigated Gene Variants in the In-House Assay

Among the 178 gene variants implemented in the present study, 88 were classified amenable and 90 were classified non-amenable by our in-house assay using our amenability criteria (Table 1). Amenability classification requires an absolute increase in α-Gal A ≥ 5% of wild type (WT) or a relative increase in α-Gal A activity ≥ 1.5-fold above baseline plus a minimum of 5% activity (%WT) after incubation with 20 μM DGJ. Of the 88 amenable variants, all showed the required increase in absolute enzyme activity of 5%. Only 58 of these showed the 1.5-fold relative increase compared to baseline activity. For 15 of the 30 remaining variants, no fold change could be calculated due to lack of baseline activity. Among the 90 non-amenable gene variants, six (A20D, A20P, L21P, V164G, G261V, and G271C) had a fold increase >1.5, but did not comply with the 5% threshold for minimal enzyme activity (see Table A2, Appendix A). Notably, 86.7% of the non-amenable variants had baseline enzyme activity <1%, another 5.6% showed enzyme activity >50%, and only 7.8% an intermediate enzyme activity between 1% and 50%. The amenable variants showed a different profile. Only 14.8% had baseline enzyme activity <1%, 68.2% had intermediate enzyme activity, and 17.0% had enzyme activity >50% baseline activity. The high percentage of variants with high baseline enzyme activity >50% is especially important as these patients should be carefully evaluated in an initial clinical examination as to whether chaperone therapy is appropriate, e.g., if sufficient evidence is available that the mutation is causal for the symptomatology. This is particularly delicate if certain outcome measures are not available to assess the success of the therapy. A different distribution was also observed for the clinical phenotype of the non-amenable as compared to the amenable variants. In total, 73.3% (66/90) of the non-amenable variants were associated with the classical phenotype, whereas the percentage of classical variants within the amenable group was only 51.1% (45/88) (see Table A2, Appendix A).

Table 1. Comparison of the good laboratory practice (GLP)-validated assay and the in-house assay.

Parameter	Good laboratory practice (GLP) Assay	In-House Assay
Cell culture	GripTite™ HEK293 MSR	HEK293H
Assay format	96 well	24 well
Transfection reagent	Fugene HD	Lipofectamine 2000
Incubation time	120 h	60 h
1-Deoxygalactonojirimycin (DGJ) concentration	10 μM	20 μM
Cell lysis condition	Lysis buffer containing 0.5% Triton X-100	Freeze and thaw in High Pure Water
Plasmid vector system	pcDNA6/v5-His A	pcDNA3.1/v5-His TOPO
Number of measurements	$n = 5$, quadruplicate	$n \geq 3$, duplicate
Criteria for amenability	≥3% absolute increase of wild type (%WT) AND 1.2-fold increase relative to baseline α-galactosidase A (α-Gal A) activity	≥5% absolute increase (%WT) OR 1.5-fold increase relative to baseline α-Gal A activity plus a minimum of 5% activity (%WT)

2.2. Inter-Assay Comparison of In Vitro Enzyme Activity between In-House and GLP Assay Data

Despite some differences in design parameters between the in-house measurements and the GLP-validated study, especially concerning cultivation time and concentration of the pharmacological chaperone DGJ, both assays were designed to test the in vitro responsiveness of mutations and predict the responsiveness of patients. Table 1 shows the differences between the two assays under investigation here. We compared α-Gal A activity of all 178 *GLA* gene variants, presented as a percentage of WT (%WT) activity, without and with the addition of DGJ (see Figure A1, Appendix A) and separated the variants initially according to whether amenability was testified (see Figure A1A and Table A2, upper section, Appendix A) or not (see Figure A1B and Table A2, lower section, Appendix A) using the data obtained in our in-house assay. It is important to note that amenability classification was strictly applied according to the protocol of the respective study as summarized together with all crucial differences between the two compared assays (Table 1); therefore, the in-house data were assessed with the corresponding amenability criteria, whereas the data from the GLP-validated assay were evaluated with the dual criteria previously described [14]. Following this evaluation there was agreement between our in-house assessment and the GLP-validated study for 155 (87.1%) of the gene variants with a balanced number of amenable (11) and non-amenable (12) variants (see Table A2, Appendix A). The baseline activity appears to have a significant effect on the classification of amenability as shown above. We used the Pearson *r* linearity coefficient to test associations between the in-house and the GLP-validated assay, which revealed a good correlation for the baseline enzyme activity (Pearson correlation coefficient $r = 0.8729$, $p < 0.0001$, Figure 1A). Moreover, a similar correlation was observed between the two datasets comparing the α-Gal A activity with DGJ ($r = 0.9448$, $p < 0.0001$, Figure 1B). We also examined the DGJ-induced α-Gal A activity change over baseline as %WT and found a Pearson *r* of 0.7992 (Figure 1C). For a better comparison of the data with the previous study from Oommen and colleagues [16], we also indicated the R^2 from linear regression analysis which indicated higher agreement of the data despite using different assays. We obtained R^2 of 0.7620, 0.7692, and 0.6388 for baseline activity, activity after DGJ treatment, and DGJ-induced activity change, respectively, compared to 0.514, 0.4019, and 0.382 for the same parameters [16]. Still, the Bland–Altman analysis was in line with the previous study demonstrating a weak inter-assay correlation with 95% limits of agreement of −194.3% to 178.7% determined for the baseline activity without DGJ (Figure 2A) and −150.7% to 175.6% with DGJ (Figure 2B). The α-Gal A activity change in %WT showed 95% limits of agreement from Bland–Altman analysis of −242.5% to 228.3% between the in-house assay and the GLP-validated assay (Figure 2C). With the exclusion of the extreme result for variant A368T (red dot in Figure 2C), the 95% limits of agreement were −197.7% to 195.3%. This analysis indicated significant disagreement in the measurement of enzyme activity depending on the examining laboratory.

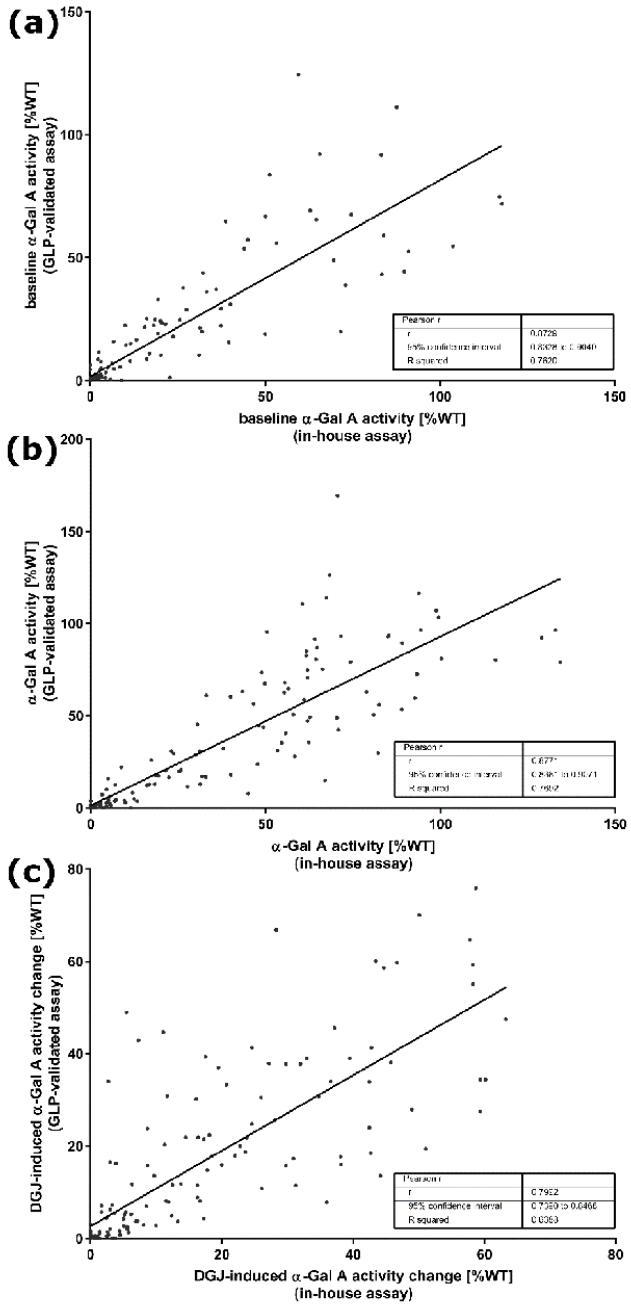

Figure 1. Linear correlation analysis of α-galactosidase A (α-Gal A) activity presented as absolute increase (%WT) of *GLA* variants (**a**) without and (**b**) with DGJ between the in-house assay and the GLP-validated assay. (**c**) Linear correlation analysis of DGJ-induced α-Gal A activity change over baseline (%WT) of the *GLA* variants.

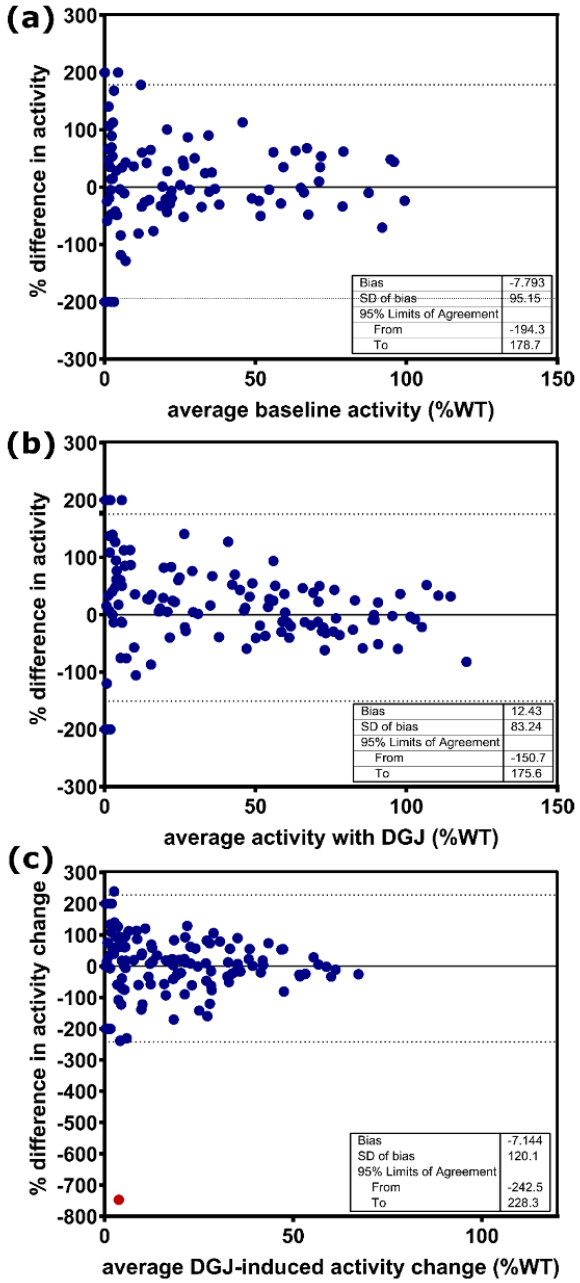

Figure 2. Bland–Altman analysis of α-Gal A activity for *GLA* variants expressed as percentage difference in activity (%WT) between the in-house assay and the GLP-validated assay. (**a**) Baseline α-Gal A activity without the addition of DGJ. (**b**) α-Gal A activity with DGJ. (**c**) DGJ-induced α-Gal A activity change. The dotted line indicates the 95% limit of agreement. SD: standard deviation.

2.3. Comparison of Amenability Classification

The relatively weak inter-assay correlation observed in the Bland–Altman plots was reinforced by the fact that the classification of amenable versus non-amenable variants was inconsistent for 12.9% (23/178) of the variants. We considered what the main risk might be for a variant classified differently. Therefore, we compared the 23 differently categorized gene variants with the remaining consistently classified variants. As observed in the former study by Oommen and colleagues [16], a high percentage of 34.8% (8/23) of the differently classified variants had high enzyme activity >50%, including D175E, K213M, R252T, V316I, A368T, F396Y, and L415F, with an essentially normal enzyme activity (min/max = 50.1%/117.9%; mean activity = 85.1%). These variants may be benign with an uncertain clinical significance. Moreover, F396Y was terminated from the Human Gene Mutation Database (HGMD) because it is not a genomic mutation [13]. Interestingly, when analyzing the isolated 23 differently classified *GLA* gene variants using Bland–Altmann analysis, the 95% limit of agreement did not differ much from the value obtained for all 178 variants: −164.8% to 155.3% (without DGJ) and −162.7% to 182.9% (with DGJ) (see Figure A2A,B, Appendix A). However, not surprisingly, for the DGJ-induced α-Gal A activity change, the Bland–Altman analysis revealed a large difference between the assays with a 95% limits of agreement from −441.1% to 338.3% (see Figure A2C, Appendix A). It is important to note that the difference in the DGJ-induced activity change of 82.6% (19/23) of the variants was higher than the applied threshold of ≥3% absolute increase from the amenability criteria of the GLP study.

2.4. Reconsideration of Amenability

There were 89/178 *GLA* variants classified as non-amenable according to the GLP-validated assay [14] (see Table A2, Appendix A). In total, 84/89 variants lacked the required DGJ-induced 3% increase in absolute enzyme activity, whereas 75/84 had no baseline activity and, hence, no fold over baseline value was calculated. Lastly, 6/84 showed at least the required fold over baseline activity. We tested whether a better agreement between the two datasets from the in-house assay and the GLP-validated assay could be achieved by exchanging the amenability criteria. To this end, we applied the amenability definition from the GLP-validated assay on our in-house dataset. Surprisingly, 9.6% (n = 17) of the variants switched categories. All switches from amenable to non-amenable (n = 11) were explained by an insufficient (<1.2) fold over baseline activity. Only gene variants of the category 50% activity and higher were involved (min/max = 50.0%/117.7%; mean activity = 79.3%). The cases in which the switch from non-amenable to amenable occurred (n = 6) could be attributed to the lower threshold of 3% absolute activity. However, the application of the different amenability definition did not lead to an improved agreement between the assays. In this analysis, 18.0% (32/178) of the variants had a discordant amenability classification with the earlier study [14], which argues for an experimental discrepancy rather than one of definition. However, when we exerted our amenability definition on the GLP-validated assay dataset, 11 variants switched category. Here, a preferred switch from amenable to non-amenable (n = 7) was also observed compared to the reversed direction (n = 4). A summary of this analysis is shown in Table 2.

Table 2. Impact of the different amenability definitions on *GLA* variant classification.

Reference *GLA* Variant Amenability Classification from the GLP Study [14] Was Compared to Amenability Classification Obtained Using	Number (%) of *GLA* Variants Classified Differently from the GLP Study; n = 178
In-house assay and amenability criteria from in-house study [13]	23 (12.9)
In-house assay and amenability criteria from the GLP-validated study [14]	32 (18.0)
GLP-validated study and amenability criteria from [13]	11 (6.2)

The variants that failed at the fold over baseline threshold usually exhibited >50% enzyme activity and were, therefore, variants of uncertain significance, which could be associated with benign outcomes. The most frequent finding among the non-amenable variants was a non-calculable fold over baseline due to a lack of baseline activity, which, however, is not an exclusion criterion for amenability as long as the 3% threshold absolute enzyme activity is reached. Therefore, we considered the absolute %WT increase in enzyme activity to be the more relevant of the two parameters of the amenability criteria and abandoned the dual criteria in favor of a more stringent threshold for the absolute increase. We further figured that this strategy may lead to better compliance of the amenability classification. We defined common thresholds of 3%, 5%, 7%, 8%, and 10%, and then compared the data of the in-house assay and the GLP-validated assay. Interestingly, the best achievable agreement was found at a threshold of 7%. Here, only 9.0% (16/178) of gene variants were classified differently (Table 3), but the number of amenable variants was reduced to 76 or 80, depending on whether the in-house or GLP assay dataset was used. In order to achieve agreement between both datasets, the number of amenable variants was even reduced to 71. A lower set threshold or even higher threshold values also led to a slightly improved agreement compared to the use of different amenability criteria.

Table 3. Effects of different thresholds for absolute enzyme activity increase (%WT) as the only criterion for defining amenability of *GLA* variants when comparing data from the in-house assay and the GLP-validated assay.

Absolute Increase in α-Gal A Activity (%WT) to Define DGJ Amenability	Number (%) of *GLA* Variants Classified Differently between the GLP-Validated Assay and the In-House Assay; *n* = 178
3%	19 (10.7)
5%	22 (12.4)
7%	16 (9.0)
8%	17 (9.6)
10%	20 (11.2)

2.5. First Evaluation of DGJ amenability for 18 GLA Gene Variants

New *GLA* variants are being identified continuously, for which no treatment recommendation with DGJ can be published so promptly. We tested 18 novel *GLA* variants from the CentoMD® 5.4 database [18] (CentoMD® 5.4 database, queried 02/2018) for their DGJ amenability (Table 4). In total, 33.3% (6/18) of the variants had residual activity >50%, which suggests that they may have been found during differential diagnosis in patients with mild disease progression of unknown etiology [7]. Of the 18 variants, 14 were biochemically responsive to 20 µM DGJ. Eight of the 14 amenable variants met both amenability criteria, i.e., the absolute enzyme activity increase of at least 5% of WT and the 1.5-fold over baseline (D165E, F169L, G171V, M208K, P214A, Y222D, V269L, and G271A). Five of the 14 variants were classified as amenable exclusively due to the sufficient absolute increase in activity (V22A, D25V, S188A, R193S, and M208I), and for one variant the fold over baseline could not be determined due to lack of activity (G183C).

Table 4. Enzyme activity and DGJ amenability classification of 18 novel *GLA* gene variants.

Amino Acid	cDNA	In Vitro Enzyme Activity (%WT) in Mean ± SEM		Absolute Increase (%WT)	Fold over Baseline	Amenable According to Present Study
		Without DGJ	With DGJ			
p.L16R	c.47T > G	0.0	0.0	0.0	n/c	No
p.V22A	c.65T > C	33.2	43.3	10.2	1.3	Yes
p.D25V	c.74A > T	110.0	128.0	18.0	1.2	Yes
p.D165E	c.495T > G	7.8	19.2	11.4	2.5	Yes
p.F169L	c.505T > C	47.7	76.8	29.1	1.6	Yes
p.G171V	c.512G > T	3.6	17.0	13.4	4.8	Yes
p.G183C	c.547G > T	0.0	9.7	9.7	n/c	Yes
p.S188A	c.562T > G	91.5	116.1	24.6	1.3	Yes
p.R193S	c.579G > C	48.7	62.5	13.8	1.3	Yes
p.M208K	c.623T > A	2.7	49.6	46.9	18.5	Yes
p.M208I	c.624G > A	45.6	62.5	16.9	1.4	Yes
p.P214A	c.640C > G	63.9	130.6	66.7	2.0	Yes
p.Q221H	c.663G > C	63.2	67.1	3.9	1.1	No
p.Y222D	c.664T > G	5.2	45.9	40.7	8.9	Yes
p.F248S	c.743T > C	108.2	90.4	−17.9	0.8	No
p.D255E	c.765T > A	79.8	77.2	−2.6	1.0	No
p.V269L	c.805G > C	2.8	48.8	46.0	17.6	Yes
p.G271A	c.812G > C	12.2	60.1	47.8	4.9	Yes

Green: Result complies with in-house amenability criterion. Red: Result does not comply with in-house amenability criterion.

3. Discussion

Pharmacological chaperone therapy with the novel chaperone DGJ in Fabry disease depends on the biochemical responsiveness of the *GLA* gene variant. It was demonstrated that residual baseline activity of a gene variant has a positive effect on the likelihood of being responsive [13]; however, due to the wide range of baseline α-Gal A levels among non-amenable and amenable variants, amenability is difficult to predict and demands empirical testing. An amenability prediction method was also developed [19,20], but did not completely represent the experimental investigations [7]. We introduced a method to measure α-Gal A activity to assess the damage of *GLA* gene variants in FD [7,9,13]. A very similar method was engineered using a GLP-validated assay to predict the clinical outcome of the chaperone therapy [14]. To date, the latter assay is the only source available to obtain pivotal information on patients' receptivity to treatment. In the present study, we compared the outcomes of the GLP-validated assay and our in-house assay. Despite experimental differences, both assays pursue the purpose of predicting patient treatment response. Amenability classification was already carried out for more than 1000 *GLA* gene variants and compiled in the current summary of product characteristics [8]. In the present study, complementary data for a subset of 178 gene variants were compared for enzymatic data and amenability classification.

Correlation analysis suggested a strong correlation of in vitro enzyme activity data between the in-house assay results and the GLP study (Figure 1). Moreover, linear regression analysis showed improved R^2 for baseline activity, activity after DGJ treatment, and DGJ-induced activity change as compared to the study by Oommen and colleagues [16], even though the latter study adopted the conditions of the GLP study in detail. However, this may partially be attributed to the larger number of variants investigated, because Bland–Altman analysis revealed rather strong deviation between the activity values for the individual variants in line with the former study [16]. More critically, a level of differently classified variants of 12.9% between the present study and the GLP study regarding DGJ amenability was found. However, since a higher DGJ concentration was used in combination with a shortened incubation period of 60 h in our in-house assay as compared to the GLP-validated study, one could speculate that this difference has a significant systematic impact on the reproducibility of the results. Nevertheless, it was impressively shown that even data from different cell systems (COS-7 vs. HEK293 cells) correlate very well as long as they were obtained from

in vitro overexpression systems [15]. It was also reported that there was a discrepancy of 10.5% in the amenability classification [16] between a pre-GLP HEK assay developed in clinical phase II [21] and the GLP-validated study [14]. A less pronounced correlation was determined when comparing enzyme activity between overexpression systems and cells derived from patients. This finding is reflected in various clinical trial studies. The study introducing the preliminary HEK assay showed that one of eight *GLA* variants (12.5%) previously classified as amenable (F295C) failed biochemical response in DGJ-treated patients that were tested for in vivo α-Gal A activity in peripheral blood mononuclear cells (PBMCs) [21]. In another cohort, two of 16 (12.5%) variants (G144V, G325R) failed to achieve biochemical response. However, both patients showed clinical response in terms of biomarker reduction [14]; version the other hand, one patient of another cohort harboring the variant S276G showed unexpected responsiveness in the PBMC assay, but showed no reduction of biomarker. Notably, S276G is one of the variants switching category from amenable to non-amenable between References [21] and [14]. This variant is classified amenable in our in-house assay in contrast with the GLP study. All 14 patients (representing nine different *GLA* variants) in another cohort showed clinical responses in accordance with the classification of the GLP assay [14].

We hypothesized that, although the definitions of amenability appear similar, their impact on the indication of whether treatment with DGJ should be initiated may be significant. Based on the observation that many variants failed to meet the dual criteria of amenability, we considered the influence of different definitions of amenability on the observed discrepancy of 12.9% of differently classified variants. The application of the different amenability criteria to the datasets led to further inconsistencies (Table 2). Thus, we endeavored to make use of a uniform simplified amenability classification in order to achieve a better reproducibility between the assays. Since the fold over baseline criterion is invalid for many variants due to a lack of baseline activity, we based this analysis on absolute activity increase (%WT). It was assumed that the deviating classification particularly affected those gene variants that showed DGJ-induced α-Gal A in the range of the thresholds defined. Therefore, thresholds between 3% and 10% activity gain were set as a single amenability criterion. This strategy led to the conclusion that a more stringent threshold of 7% absolute activity increase led to the best compliance of the analyzed datasets with only 9.0% of the variants being differently classified (Table 3). On this basis, it could be discussed whether amenable variants that lead to a lower increase in activity should be labeled as mild or moderate responders.

To date, there is no established correlation between the biochemical enzyme activity increase induced by DGJ and the clinical benefit. Although a minimal increase in enzyme activity to 1%–6% of WT activity was suggested to be sufficient to achieve clinical benefits [22], it is highly questionable whether such an increase, observed in the in vitro cell-based assay, allows conclusions to be drawn about a beneficial outcome in vivo. It should also be considered that DGJ is an active site-specific inhibitor of α-Gal A, which may lead to total inhibition of the enzyme and worsening of the patient's condition in gene variants with very low baseline activity. In a former study, patients with amenable *GLA* gene variants were switched from ERT to chaperone. The general result suggested that the DGJ influence on renal function and other disease-specific markers was stabilizing or even improving over the duration of the study in contrast to patients with non-amenable variants where lyso-Gb3 increased during the treatment period with DGJ [23]. In a recent study in patients with the variant N215S associated with the atypical cardiac phenotype of FD, which, to our understanding, is a strongly responsive *GLA* gene variant, an overall good outcome was shown, including increased α-Gal A activity in leucocytes and reduced plasma lyso-Gb3 [24]. However, the same study revealed that patients harboring the variant L294S, which is associated with classical FD, no baseline activity, and a moderate biochemical responsiveness of in vitro enzyme activity, did not show a beneficial outcome. This *GLA* gene variant was classified as amenable in both the GLP-validated and the in-house assay. However, the biochemical responsiveness in the GLP assay was so low that it would have been considered non-amenable according to our criteria. A recent study revealed that a patient carrying the presumed amenable variant S276N had to be switched back to ERT due to biomarker escalation [25].

It certainly remains a matter of debate whether amenability testing can still be improved by, for example, the use of *GLA* knockout cell models as recently introduced [24]. However, the cases of the variants L294S, S276G, S276N, and F295C seem to suggest that only clinical data will be able to unveil whether patients with variants of mild to moderate responsiveness will experience an equivalent benefit from the treatment as patients with strongly responding variants. Nevertheless, G325R seems to be strongly responsive in the GLP-validated assay and shows an inconsistent picture in the paraclinical data, which may be a hint that not only borderline amenable variants may show unpredictable clinical findings.

4. Materials and Methods

4.1. Material

All materials were purchased as described in the preliminary studies [7,9,13]. In brief, HEK293H cells, culture medium, all supplements, pcDNA3.1/v5-His TOPOplasmid vector, and the transfection reagent were purchased from Thermo Fisher Scientific (Carlsbad, CA, USA). Additionally, 1-deoxygalactonojirimycin hydrochloride and the synthetic fluorogenic substrate 4-methylumbelliferyl-α-D-galactopyranoside (4-MUG) for α-Gal A activity measurement were purchased from Sigma Aldrich (Steinheim, Germany).

4.2. Study Design and Selection of Mutations

In the present study, α-Gal A enzyme activity data from our in-house human embryonic kidney cell-based assay were compared to the good laboratory practice (GLP)-validated assay for 178 *GLA* gene variants. The differences of the assays are displayed in Table 1. The results of the α-Gal A activity measurement for 148 variants were taken from previous studies; 114 variants were measured in References [9,13], and 34 variants were measured in Reference [7]. The previously published variants M42V, N139S, G183V, N215S, L268S, L310F, S345P, R356Q, G360C [13], and S247P [7] were reassessed for the current study. Further variants A15P, W162C, D170H, G183A, M187R, E203K, P205T, Y207C, P214S, Y216C, W226R, A230T, I239T, Q250P, N263S, P265S, G271C, G271D, G274S, and M284V were selected from the CentoMD database [18] (CentoMD® 5.4 database, queried 02/2018). Nonsense variants and variants where no enzyme activity was published from the GLP-validated reference assay were excluded from the study.

4.3. Generation of Novel GLA Mutations

The plasmid vectors containing the mutant *GLA* complementary DNA (cDNA) were produced inpcDNA3.1/v5-His TOPO using site-directed mutagenesis PCR and were analyzed according to our previous protocols [7,13].

4.4. In-House α-Gal A Activity Assay

The α-Gal A activity was measured as described previously [7,13]. In brief, HEK293H cells were harvested in High Pure Water (TKA Wasseraufbereitungssysteme GmbH, Niedererlberg, Germany) and lysed using the freeze and thaw method. The protein content of each sample was determined using the bicinchoninic acid (BCA) Assay Kit (Thermo Fisher, Braunschweig, Germany). Enzyme activity was measured in a sample containing 0.5 µg of total protein using the fluorogenic substrate 4-MUG. The lysates of each well were measured in duplicates in a plate reader (Tecan AG, Männedorf, Switzerland) at 360 and 465 nm, as the excitation and emission wavelength, respectively.

4.5. Enzyme Activity Calculation

In each experiment, the measured variant enzyme activity was corrected for endogenous enzyme activity by subtracting the average activity obtained from two wells containing pcDNA3.1/v5-His TOPOvector-only transfected cells. Enzyme activity was normalized to WT-*GLA* vector-transfected

HEK293H cells (%WT) from corresponding experiments. Absolute increase in α-Gal A activity was calculated by subtracting untreated (baseline) activity from the activity after addition of 20 μM DGJ as %WT. Relative enzyme activity was determined as fold increase above baseline. Endogenous α-Gal A enzyme activity in pcDNA3.1/v5-His TOPOvector control-transfected HEK293H cells was 137.3 ± 12.0 nmol 4-MU·mg protein^{-1}·h^{-1} without and 173.1 ± 11.8 nmol 4-MU·mg protein^{-1}·h^{-1} (mean ± SD) with the addition of 20 μM DGJ. Wild type enzyme activity was 7333.1 ± 734.0 nmol 4-MU·mg protein^{-1}·h^{-1} and 7985.7 ± 768.4 nmol 4-MU·mg protein^{-1}·h^{-1} with and without DGJ, respectively.

4.6. Statistical Evaluation

Correlation and Bland–Altman analyses were calculated using GraphPad Prism, version 5.01.

5. Conclusions

The pharmacological chaperone DGJ is the model of an experimental drug. It provides highly reproducible data in different in vitro systems for assessing the amenability of different *GLA* gene variants. Treatment with the DGJ relies on biochemical responsiveness of the gene variant underlying the disease. Therefore, the genetic profile of the patients will be an essential feature for future assessment of the evaluation of treatment success with DGJ. The measurement of the responsiveness to DGJ in in vitro cell-based assays is currently a method that has no alternative for determining amenability. In comparisons of inter-assay reproducibility, a certain variability of the results of enzyme activity and the amenability classification can virtually not be prevented. An accurate appraisal should be taken into account for a treatment decision with DGJ especially in cases of low baseline activity, borderline biochemical responsiveness, and inter-assay discrepancy as risk factors to misinterpret the potential of a *GLA* gene variant to be amenable to DGJ treatment. We also recommend a very close monitoring of the patient's well-being and biomarkers, especially lyso-Gb3 to monitor treatment response in patients.

Author Contributions: All authors read and agreed to the published version of the manuscript. Conceptualization, J.L., C.C., M.V.C., and A.R.; methodology, L.L. and S.P.; validation, J.L., C.C., K.I., and A.H.; formal analysis, J.L., C.C., L.L., and M.B.; investigation, J.P. and C.H.; resources, A.H. and A.R.; data curation, K.I., J.P., M.B., and A.R.; writing—original draft preparation, J.L. and C.C.; writing—review and editing, C.C., L.L., K.I., J.P., C.H., A.H., and M.V.C.; visualization, C.C., S.P., J.P., and C.H.; supervision, A.H. and M.V.C.; project administration, A.R.; funding acquisition, J.L. and A.R.

Funding: This work was supported by the European Union (grant number ESF/14-BM-A55-0046/16).

Acknowledgments: We would like to thank Katja Bovensiepen for technical support and data administration and Gene Frickey for constructive criticism of the manuscript. A.H. is supported by the Hermann und Lilly Schilling-Stiftung für medizinische Forschung im Stifterverband.

Conflicts of Interest: The authors A.R. and J.L. received financial support from Shire Pharmaceuticals in the past. M.B. is an employee at Centogene. A.R. is CEO at Centogene. The authors declare no conflict of interest.

Abbreviations

α-Gal A	α-galactosidase A
DGJ	1-deoxygalactonojirimycin
ERT	enzyme replacement therapy
FD	Fabry disease
GLP	good laboratory practice
HEK	human embryonic kidney cell
PBMC	peripheral blood mononuclear cells

Appendix A

Figure A1. Comparison of α-Gal A activity of *GLA* gene variants without and with the addition of DGJ between the in-house assay and GLP-validated assay [14]. (**a**) *GLA* gene variants that were classified as amenable according to in-house data. (**b**) *GLA* gene variants that were classified as non-amenable according to in-house data. *GLA* variants were ordered with respect to their positions on the amino-acid sequence. Variants with no associated bar had no quantifiable α-Gal A activity without or with the addition of DGJ.

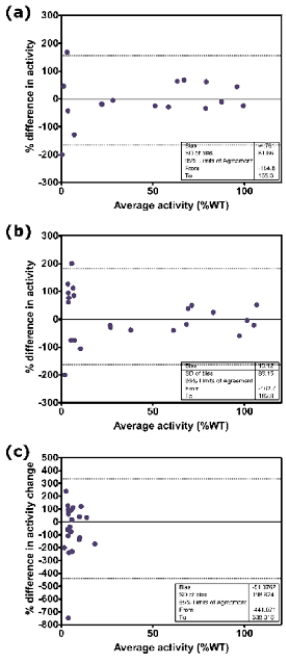

Figure A2. Bland–Altman analysis of α-Gal A activity for the 23 differently classified *GLA* gene variants expressed as % difference in activity (%WT) between the in-house assay and the GLP validated assay. (**a**) Baseline α-Gal A activity without the addition of DGJ. (**b**) α-Gal A activity with DGJ and (**c**) DGJ-induced α-Gal A activity change. The dotted line indicates the 95% limit of agreement. SD: standard deviation.

Table A1. Reexamination of selected *GLA* variants.

Amino Acid	cDNA	Mean In Vitro Enzyme Activity as %WT (Initial Study Result [7,13])		Absolute Increase as %WT	Fold over Baseline	Amenable According to Present Study	Category Switch Compared to Initial Study
		No DGJ	20 μM DGJ				
p.M42V	c.124A > G	0.0 (0)	7.2 (11.9)	7.2	n/c	Yes	No
p.N139S	c.416A > G	64.6 (147.8)	74.3 (176.4)	9.7	1.1	Yes	No
p.G183V	c.548G > T	0.0 (0)	6.9 (6.7)	6.9	n/c	Yes	No
p.N215S	c.644A > G	36.7 (39.5)	61.5 (63.9)	24.9	1.7	Yes	No
p.S247P	c.739T > C	0.0 (0)	6.8 (5.8)	6.4	n/c	Yes	No
p.L268S	c803T > C	0.0 (0)	7.4 (10.8)	7.0	n/c	Yes	No
p.L310F	c.928C > T	1.6 (0)	27.7 (4.1)	17.7	13.4	Yes	Yes
p.S345P	c.1033T > C	0.0 (0)	9.7 (13.3)	9.5	n/c	Yes	No
p.R356Q	c.1067G > A	33.3 (89.1)	66.3 (99.4)	33.0	2.0	Yes	No
p.G360C	c.1078G > T	16.2 (11.9)	32.9 (26.5)	15.4	2.2	Yes	No

Green: Result complies with in-house amenability criterion. Red: Result does not comply with in-house amenability criterion.

Table A2. *GLA* variant enzyme activity and amenability table. Upper: amenable variants; lower: non-amenable variants.

Amenable Variants											
Amino Acid	cDNA	Clinical Phenotype	Mean In Vitro Enzyme Activity as %WT (In-House)		Absolute Increase as %WT	Fold over Baseline	Mean In Vitro Enzyme Activity as %WT (GLP-Validated Assay [13])		Absolute Increase as %WT	Fold over Baseline	Amenable (In-House)	Amenable (GLP-Validated [14])
			Without DGJ	With DGJ			Without DGJ	With DGJ				
p.L3P	c.8T > C	Uncertain	117.7	129	11.3	1.1	71.9	92.2	20.3	1.3	Yes	Yes
p.D33G	c.98A > G	n/a	37.4	62	24.6	1.7	29.3	70.6	41.3	2.4	Yes	Yes
p.L36W	c.107T > G	n/a	2.3	22.3	20	9.7	0.7	16.6	15.9	23.7	Yes	Yes
p.A37T	c.109G > A	Atypical	69.6	132.9	63.3	1.9	48.9	96.4	47.5	2	Yes	Yes
p.M42V	c.124A > G	Classic	0	7.2	7.2	n/c	0.5	4.3	3.8	8.6	Yes	Yes
p.M42T	c.125T > C	Classic	2.9	21.4	18.5	7.4	2.5	20.3	17.8	8.1	Yes	Yes
p.H46P	c.137A > C	Atypical	40.1	98.8	58.7	2.5	31	106.9	75.9	3.4	Yes	Yes

Table A2. *Cont.*

Amenable Variants												
Amino Acid	**cDNA**	**Clinical Phenotype**	**Mean In Vitro Enzyme Activity as %WT (In-House)**		**Absolute Increase as %WT**	**Fold over Baseline**	**Mean In Vitro Enzyme Activity as %WT (GLP-Validated Assay [13])**		**Absolute Increase as %WT**	**Fold over Baseline**	**Amenable (In-House)**	**Amenable (GLP-Validated [14])**
			Without DGJ	With DGJ			Without DGJ	With DGJ				
p.R49C	**c.145C > T**	**Classic**	**0**	**5.1**	**5.1**	**n/c**	**0**	**2.7**	**2.7**	**n/c**	**Yes**	**No**
p.M51K	c.152T > A	Classic	0	8.7	8.7	n/c	6.3	22.1	15.8	3.5	Yes	Yes
p.M51I	c.153G > A	Atypical	37.4	62	24.6	1.7	22.3	47.1	24.8	2.1	Yes	Yes
p.E59K	c.175G > A	Classic	2.2	18.5	16.3	8.4	8.6	17.5	8.9	2	Yes	Yes
p.P60L	c.179C > T	Uncertain	15.6	33.1	17.5	2.1	21.7	61	39.3	2.8	Yes	Yes
p.E66K	c.196G > A	Classic	6.8	18.3	11.5	2.7	4.8	12.9	8.1	2.7	Yes	Yes
p.A73V	c.218C > T	Atypical	44	64.7	20.7	1.5	53.6	86.9	33.3	1.6	Yes	Yes
p.D83N	c.247G > A	n/a	62.9	71.6	8.7	1.1	69.2	93	23.8	1.3	Yes	Yes
p.I91T	c.272T > C	Atypical	0.7	7	6.3	10	0.9	12.6	11.7	14	Yes	Yes
p.S102L	c.305C > T	n/a	71.6	78.9	7.3	1.1	19.9	62.8	42.9	3.2	Yes	Yes
p.R112H	c.335G > A	Atypical	1.6	19.4	17.8	12.1	2.6	17.4	14.8	6.7	Yes	Yes
p.L120V	**c.358C > G**	**Atypical**	**50.1**	**62**	**11.9**	**1.2**	**66.8**	**74.7**	**7.9**	**1.1**	**Yes**	**No**
p.A121T	c.361G > A	Classic	50	55.5	5.5	1.1	18.9	67.9	49	3.6	Yes	Yes
p.S126G	c.376A > G	Uncertain	51.3	67.4	16.1	1.3	83.7	113.9	30.2	1.4	Yes	Yes
p.A135V	c.404C > T	Classic	0	6.9	6.9	n/c	0	3.7	3.7	n/c	Yes	Yes
p.D136E	c.408T > A	Classic	0	31.3	31.3	n/c	1.4	12.9	11.5	9.2	Yes	Yes
p.N139S	c.416A > G	Uncertain	64.6	74.3	9.7	1.2	65.5	79.1	13.6	1.2	Yes	Yes
p.A143T	c.427G > A	Atypical	31.3	49.4	18.1	1.6	21.4	43.8	22.4	2	Yes	Yes
p.A156V	c.467C > T	Classic	4.3	16.8	12.5	3.9	1.2	12.8	11.6	10.7	Yes	Yes
p.W162G	c.484T > G	Classic	0	5.2	5.2	n/c	0.8	5.9	5.1	7.4	Yes	Yes
p.W162C	**c.486G > C**	**Classic**	**5.8**	**11.4**	**5.6**	**2**	**0.5**	**0**	**−0.5**	**0**	**Yes**	**No**
p.D165H	c.493G > C	Classic	3.4	11.9	8.5	3.5	1.3	8.3	7	6.4	Yes	Yes
p.G183A	c.548G > C	n/a	10	46.6	36.6	4.6	22.4	56.4	34	2.5	Yes	Yes
p.G183V	**c.548G > T**	**Classic**	**0**	**6.9**	**6.9**	**n/c**	**0**	**2.5**	**2.5**	**n/c**	**Yes**	**No**
p.M187V	c.559A > G	Classic	22.8	67	44.2	2.9	1.3	14.9	13.6	11.5	Yes	Yes
p.M187I	c.561G > A	n/a	3.1	31.2	28.1	10.1	5.1	30.7	25.6	6	Yes	Yes
p.I198T	c.593T > C	n/a	38.7	50.4	11.7	1.3	64.7	95.5	30.8	1.5	Yes	Yes
p.P205T	c.613C > A	Classic	10.2	70.4	60.2	6.9	14.4	48.8	34.4	3.4	Yes	Yes
p.P214S	c.640C > T	n/a	18.1	61.6	43.5	3.4	22.4	82.5	60.1	3.7	Yes	Yes
p.P214L	c.641C > T	n/a	19.4	64.1	44.7	3.3	33	91.6	58.6	2.8	Yes	Yes
p.N215S	c.644A > G	Atypical	36.7	61.5	24.9	1.7	15.6	35.6	20	2.3	Yes	Yes
p.Y216C	c.647A > G	Classic	2.3	25.9	23.6	11.2	2	20.7	18.7	10.4	Yes	Yes
p.I219T	c.656T > C	Atypical	53.3	85.3	32	1.6	55.8	93.6	37.8	1.7	Yes	Yes
p.N224S	c.671A > G	Classic	31.1	82.2	51.1	2.6	10.3	29.7	19.4	2.9	Yes	Yes

Table A2. *Cont.*

Amenable Variants												
Amino Acid	**cDNA**	**Clinical Phenotype**	**Mean In Vitro Enzyme Activity as %WT (In-House)**		**Absolute Increase as %WT**	**Fold over Baseline**	**Mean In Vitro Enzyme Activity as %WT (GLP-Validated Assay [13])**		**Absolute Increase as %WT**	**Fold over Baseline**	**Amenable (In-House)**	**Amenable (GLP-Validated [14])**
			Without DGJ	With DGJ			Without DGJ	With DGJ				
p.H225D	c.673C > G	n/a	32.2	60.5	28.3	1.9	43.8	110.6	66.8	2.5	Yes	Yes
p.N228S	c.683A > G	n/a	59.5	70.6	11.1	1.2	124.5	169.2	44.7	1.4	Yes	Yes
p.I232T	c.695T > C	Atypical	11.5	61.6	50.1	5.4	15	85	70	5.7	Yes	Yes
p.S238N	c.713G > A	Atypical	36	94.3	58.3	2.6	37.1	96.4	59.3	2.6	Yes	Yes
p.I239T	c.716T > C	Classic	26.6	85	58.3	3.2	37.7	92.8	55.1	2.5	Yes	Yes
p.I242N	c725T > A	Classic	3.1	49.8	46.7	16.1	7.6	67.4	59.8	8.9	Yes	Yes
p.L243F	c.729G > C	Classic	11.4	70.8	59.4	6.2	7.9	42.3	34.4	5.4	Yes	Yes
p.S247P	**c.739T > C**	**Classic**	**0**	**6.8**	**6.8**	**n/c**	**0**	**1.3**	**1.3**	**n/c**	**Yes**	**No**
p.N249K	c.747C > A	Classic	23.7	54.6	30.9	2.3	17.9	35.2	17.3	2	Yes	Yes
p.Q250P	c.749A > C	Classic	18.5	61	42.5	3.3	24.8	58.7	33.9	2.4	Yes	Yes
p.R252T	**c.755G > C**	**Uncertain**	**117**	**134.3**	**17.3**	**1.1**	**74.8**	**79.1**	**4.3**	**1.1**	**Yes**	**No**
p.I253T	c.758T > C	Classic	73	115.8	42.8	1.6	38.9	80.2	41.3	2.1	Yes	Yes
p.I253S	c.758T > G	n/a	4.4	53.4	49	12.1	3.3	31.2	27.9	9.5	Yes	Yes
p.P259R	c.776C > G	Classic	20.5	40	19.5	2	23.3	60.3	37	2.6	Yes	Yes
p.N263S	c.788A > G	Classic	6.7	64.4	57.8	9.7	15.8	80.5	64.7	5.1	Yes	Yes
p.D264Y	c.790G > T	Classic	0	5.4	5.4	n/c	0.5	6.2	5.7	12.4	Yes	Yes
p.P265S	**c.793C > T**	**n/a**	**1.6**	**9.7**	**8.1**	**5.9**	**1**	**3.9**	**2.9**	**3.9**	**Yes**	**No**
p.L268S	**c.803T > C**	**Classic**	**0**	**7.4**	**7.4**	**n/c**	**0**	**2.8**	**2.8**	**n/c**	**Yes**	**No**
p.V269M	c.805G > A	Classic	0	17.3	17.3	n/c	4.4	25.9	21.5	5.9	Yes	Yes
p.V269A	c.806T > C	Classic	9	45	36	5	0	7.8	7.8	n/c	Yes	Yes
p.G271D	c.812G > A	n/a	3.1	37.9	34.8	12.3	1.5	32.2	30.7	21.5	Yes	Yes
p.S276G	**c.826A > G**	**Classic**	**0**	**5.6**	**5.6**	**n/c**	**0**	**2**	**2**	**n/c**	**Yes**	**No**
p.T282I	c.845C > T	n/a	5	47.7	42.7	9.5	5.2	23.7	18.5	4.6	Yes	Yes
p.M284V	c.850A > G	n/a	16.2	43.4	27.2	2.7	25.2	63.1	37.9	2.5	Yes	Yes
p.A291T	c.871G > A	Classic	13.2	55.7	42.5	4.2	16.5	40.5	24	2.5	Yes	Yes
p.L294S	c.881T > C	Classic	0	12.4	12.4	n/c	0	4.9	4.9	n/c	Yes	Yes
p.R301G	c.901C > G	Classic	19.3	56.5	37.2	2.9	19.1	64.7	45.6	3.4	Yes	Yes
p.R301Q	c.902G > A	Atypical	8.5	48	39.5	5.6	5.5	44.5	39	8.1	Yes	Yes
p.R301P	c.902G > C	Classic	0	5	5	n/c	0	4.2	4.2	n/c	Yes	Yes
p.L310F	c.928C > T	Classic	1.6	27.7	26.1	17.3	0.8	11.6	10.8	14.5	Yes	Yes
p.L311V	c.931C > G	n/a	1.9	40.1	38.2	21.1	2	18	16	9	Yes	Yes
p.D313Y	c.937G > T	Uncertain	83.9	100.3	16.4	1.2	59	80.9	21.9	1.4	Yes	Yes
p.I319T	c.956T > C	Classic	20.2	58.3	38.1	2.9	10.3	28	17.7	2.7	Yes	Yes

Table A2. *Cont.*

Amenable Variants												
Amino Acid	**cDNA**	**Clinical Phenotype**	**Mean In Vitro Enzyme Activity as %WT (In-House)**		**Absolute Increase as %WT**	**Fold over Baseline**	**Mean In Vitro Enzyme Activity as %WT (GLP-Validated Assay [13])**		**Absolute Increase as %WT**	**Fold over Baseline**	**Amenable (In-House)**	**Amenable (GLP-Validated [14])**
			Without DGJ	With DGJ			Without DGJ	With DGJ				
p.N320I	c.959A > T	Classic	2	31.8	29.8	15.9	1.4	17.1	15.7	12.2	Yes	Yes
p.Q321H	c.963G > C	n/a	3.3	25.3	22	7.7	1.9	19.8	17.9	10.4	Yes	Yes
p.G325S	c.973G > A	Classic	25.6	55.4	29.8	2.2	24.7	62.5	37.8	2.5	Yes	Yes
p.Q327E	c.979C > G	n/a	21.5	80.9	59.4	3.8	22.9	50.4	27.5	2.2	Yes	Yes
p.G328A	c.983G > C	Classic	6.2	30	23.8	4.8	6.9	28.7	21.8	4.2	Yes	Yes
p.S345P	c.1033T > C	Classic	0	9.7	9.7	n/c	0	3.7	3.7	n/c	Yes	Yes
p.R356W	c.1066C > T	Classic	16.9	62.7	45.8	3.7	11	49.1	38.1	4.5	Yes	Yes
p.R356Q	c.1067G > A	Atypical	33.3	66.3	33	2	36.1	75.1	39	2.1	Yes	Yes
p.G360C	c.1078G > T	Classic	16.2	32.9	16.7	2	8.7	16.8	8.1	1.9	Yes	Yes
p.R363H	c.1088G > A	Classic	31.9	57.9	26	1.8	20	50.5	30.5	2.5	Yes	Yes
p.F396Y	**c.1187T > A**	**n/a**	**87.6**	**93.8**	**6.2**	**1.1**	**111.2**	**116.4**	**5.2**	**1**	**Yes**	**No**
p.T410I	c.1229C > T	n/a	2.3	16.1	13.8	7	0.4	12.2	11.8	30.5	Yes	Yes
p.L415F	**c.1243C > T**	**n/a**	**83.2**	**99.5**	**16.3**	**1.2**	**91.8**	**103.3**	**11.5**	**1.1**	**Yes**	**No**
p.E418G	c.1253A > G	n/a	74.6	89.1	14.5	1.2	67.5	89.4	21.9	1.3	Yes	Yes
Non-Amenable Variants												
Amino Acid	**cDNA**	**Clinical Phenotype**	**Mean In Vitro Enzyme Activity as %WT (In-House)**		**Absolute Increase as %WT**	**Fold over Baseline**	**Mean In Vitro Enzyme Activity as %WT (GLP-Validated Assay [13])**		**Absolute Increase as %WT**	**Fold over Baseline**	**Amenable (In-House)**	**Amenable (GLP-Validated [14])**
			without DGJ	with DGJ			without DGJ	with DGJ				
p.A15P	c.43G > C	n/a	0	0.3	0.3	n/c	0.9	1.2	0.3	1.3	No	No
p.A20P	**c.58G > C**	**Atypical**	**2.5**	**4.9**	**2.4**	**2**	**11.5**	**15.9**	**4.4**	**1.4**	**No**	**Yes**
p.A20D	**c.59C > A**	**n/a**	**2.8**	**4.5**	**1.7**	**1.6**	**4.3**	**10**	**5.7**	**2.3**	**No**	**Yes**
p.L21P	c.62T > C	Classic	0.6	1.7	1.1	2.8	1.1	1.6	0.5	1.5	No	No
p.P40S	c.118C > T	Classic	0	1.4	1.4	n/c	0	1	1	n/c	No	No
p.G43S	c.127G > A	n/a	0	0	0	n/c	0	0	0	n/c	No	No
p.L45P	c.134T > C	Classic	0	0	0	n/c	0	0	0	n/c	No	No
p.R49G	c.145C > G	Classic	0	0	0	n/c	0	0	0	n/c	No	No
p.C52W	c.156C > G	n/a	0	0	0	n/c	0	0	0	n/c	No	No
p.C56Y	c.167G > A	Classic	0	3.3	3.3	n/c	0	7.3	7.3	n/c	No	Yes
p.C63Y	c.188G > A	Classic	0	0	0	n/c	0	0	0	n/c	No	No
p.L68F	c.202C > T	Classic	0	4.5	4.5	n/c	0	0.8	0.8	n/c	No	No
p.Y86H	c.256T > C	Classic	0	0.7	0.7	n/c	0	0	0	n/c	No	No
p.Y86D	c.256T > G	Classic	0	0	0	n/c	0	0	0	n/c	No	No

Table A2. *Cont.*

Non-Amenable Variants												
Amino Acid	**cDNA**	**Clinical Phenotype**	**Mean In Vitro Enzyme Activity as %WT (In-House)**		**Absolute Increase as %WT**	**Fold over Baseline**	**Mean In Vitro Enzyme Activity as %WT (GLP-Validated Assay [13])**		**Absolute Increase as %WT**	**Fold over Baseline**	**Amenable (In-House)**	**Amenable (GLP-Validated [14])**
			without DGJ	with DGJ			without DGJ	with DGJ				
p.D93Y	c.277G > T	Atypical	0	0	0	n/c	0	0	0	n/c	No	No
p.D93E	c.279C > G	Classic	0	0	0	n/c	0	0	0	n/c	No	No
p.C94Y	c.281G > A	Classic	0	0	0	n/c	0	0	0	n/c	No	No
p.C94S	c.281G > C	Classic	0	0	0	n/c	0	0	0	n/c	No	No
p.W95L	c.284G > T	Classic	0	0	0	n/c	0	0	0	n/c	No	No
p.R100T	c.299G > C	Classic	0	0	0	n/c	0	0	0	n/c	No	No
p.R112C	c.334C > T	Classic	0	0	0	n/c	0	0	0	n/c	No	No
p.R118C	**c.352C > T**	**Atypical**	**20**	**23.7**	**3.7**	**1.2**	**24**	**29.5**	**5.5**	**1.2**	**No**	**Yes**
p.H125P	c.374A > C	n/a	0	0	0	n/c	0	0	0	n/c	No	No
p.L129P	c.386T > C	Classic	0	0	0	n/c	0	0	0	n/c	No	No
p.L131P	c.392T > C	Classic	0	0	0	n/c	0	0	0	n/c	No	No
p.G132R	c.394G > A	Classic	0	0	0	n/c	0	0	0	n/c	No	No
p.G132E	c.395G > A	n/a	0	0	0	n/c	0	0	0	n/c	No	No
p.G138R	c.412G > A	Classic	0	0	0	n/c	0	0	0	n/c	No	No
p.T141I	c.422C > T	Classic	0	0	0	n/c	0	0	0	n/c	No	No
p.C142R	c.424T > C	Classic	0	0	0	n/c	0.4	0	−0.4	0	No	No
p.A143P	c.427G > A	Classic	0	0	0	n/c	0	0	0	n/c	No	No
p.G147R	c.439G > A	n/a	0	0	0	n/c	0	0	0	n/c	No	No
p.A156D	c.467C > A	Classic	0	0	0	n/c	0	0	0	n/c	No	No
p.V164G	c.491T > G	Classic	1.4	2.8	1.4	2	1.7	3.2	1.5	1.9	No	No
p.D165Y	c.493G > T	Classic	0	0	0	n/c	0	1.3	1.3	n/c	No	No
p.D165V	c.494A > T	Classic	0	0	0	n/c	0	0	0	n/c	No	No
p.L167Q	c.500T > A	Classic	0	0.7	0.7	n/c	0	0.6	0.6	n/c	No	No
p.D170N	c.508G > A	Classic	0	0	0	n/c	0	0	0	n/c	No	No
p.D170H	c.508G > C	Classic	0	0	0	n/c	0	0	0	n/c	No	No
p.C172G	c.514T > G	Classic	0	4.4	4.4	n/c	1.1	2.7	1.6	2.5	No	No
p.C172Y	c.515G > A	Classic	0	0	0	n/c	0	0	0	n/c	No	No
p.D175E	**c.525C > G**	**n/a**	**89.8**	**89**	**−0.8**	**1**	**44.3**	**53.4**	**9.1**	**1.2**	**No**	**Yes**
p.M187R	c.560T > G	Classic	0	0	0	n/c	0	0	0	n/c	No	No
p.L191P	c.572T > C	Classic	0	0	0	n/c	0	0	0	n/c	No	No
p.C202Y	c.605G > A	Classic	0	1.4	1.4	n/c	0	0	0	n/c	No	No
p.E203K	c.607G > A	n/a	0	0	0	n/c	0	0	0	n/c	No	No
p.Y207C	c.620A > G	Classic	0	1.1	1.1	n/c	0	0	0	n/c	No	No
p.K213M	**c.638A > T**	**Classic**	**83.4**	**82.5**	**−0.9**	**1**	**43.2**	**55.9**	**12.7**	**1.3**	**No**	**Yes**

Table A2. *Cont.*

Non-Amenable Variants												
Amino Acid	**cDNA**	**Clinical Phenotype**	**Mean In Vitro Enzyme Activity as %WT (In-House)**		**Absolute Increase as %WT**	**Fold over Baseline**	**Mean In Vitro Enzyme Activity as %WT (GLP-Validated Assay [13])**		**Absolute Increase as %WT**	**Fold over Baseline**	**Amenable (In-House)**	**Amenable (GLP-Validated [14])**
			without DGJ	with DGJ			without DGJ	with DGJ				
p.H225R	c.674A > G	Classic	0	3	3	n/c	0	2	2	n/c	No	No
p.W226R	c.676T > A	Classic	0	0	0	n/c	0	0	0	n/c	No	No
p.R227Q	c.680G > A	Classic	0	0	0	n/c	0	0	0	n/c	No	No
p.R227P	c.680G > C	Classic	0	0	0	n/c	0	0	0	n/c	No	No
p.A230T	c.688G > A	Classic	0	0	0	n/c	0	0	0	n/c	No	No
p.D231N	c.691G > A	Classic	0	0	0	n/c	0.5	0	−0.5	0	No	No
p.G261V	c.782G > T	Classic	0.2	3.5	3.3	17.5	0	0	0	n/c	No	No
p.W262C	c.786G > C	Classic	0	0	0	n/c	0	0	0	n/c	No	No
p.D264A	c.791A > C	n/a	0	0	0	n/c	0	0	0	n/c	No	No
p.D264V	c.791A > T	Classic	0	0	0	n/c	0	0	0	n/c	No	No
p.M267T	**c.800T > C**	**Classic**	**27.5**	**30.5**	**3**	**1.1**	**28.8**	**45.3**	**16.5**	**1.6**	**No**	**Yes**
p.G271C	c.811G > T	Classic	0.2	2.7	2.5	14.8	0	0.5	0.5	n/c	No	No
p.N272S	c.815A > G	Classic	0	0	0	n/c	0	0	0	n/c	No	No
p.G274S	c.820G > A	n/a	0	0	0	n/c	0	0	0	n/c	No	No
p.L275F	c.823C > T	Classic	0	0	0	n/c	0	0	0	n/c	No	No
p.Q283P	c.848A > C	Classic	0	0	0	n/c	0	0	0	n/c	No	No
p.A285D	c.854C > A	Classic	0	0	0	n/c	0	0	0	n/c	No	No
p.S297C	c.890C > G	Classic	0	3.8	3.8	n/c	0	0	0	n/c	No	No
p.V316I	**c.946G > A**	**n/a**	**65.6**	**68.3**	**2.7**	**1**	**92.1**	**126.1**	**34**	**1.4**	**No**	**Yes**
p.V316G	**c.947T > G**	**Classic**	**0**	**0**	**0**	**n/c**	**0.7**	**3.8**	**3.1**	**5.4**	**No**	**Yes**
p.I317S	c.950T > G	n/a	0	2.7	2.7	n/c	0	0.8	0.8	n/c	No	No
p.N320Y	c.958A > T	Classic	0	0	0	n/c	0	0.6	0.6	n/c	No	No
p.Q327K	c.979C > A	Classic	0	0	0	n/c	0	0	0	n/c	No	No
p.E341K	c.1021G > A	Classic	0	0	0	n/c	0	0	0	n/c	No	No
p.E341D	c.1023A > C	Classic	0	0	0	n/c	0	1.6	1.6	n/c	No	No
p.R342Q	c.1025G > A	Classic	0	0	0	n/c	0	0.9	0.9	n/c	No	No
p.R342P	c.1025G > C	n/a	0	0	0	n/c	0	0	0	n/c	No	No
p.R342L	c.1025G > T	Classic	0	0	0	n/c	0	0	0	n/c	No	No
p.L344P	c.1031T > C	Classic	0	0	0	n/c	0	0	0	n/c	No	No
p.E358K	c.1072G > A	Classic	0	0	0	n/c	0	0	0	n/c	No	No
p.A368T	**c.1102G > A**	**Atypical**	**103.7**	**93.3**	**−10.4**	**0.9**	**54.6**	**72.6**	**18**	**1.3**	**No**	**Yes**
p.L372P	c.1115T > C	n/a	0	2.6	2.6	n/c	1.2	2.6	1.4	2.2	No	No
p.L372R	c.1115T > G	Classic	0	0	0	n/c	0	0	0	n/c	No	No

Table A2. *Cont.*

Non-Amenable Variants												
Amino Acid	**cDNA**	**Clinical Phenotype**	**Mean In Vitro Enzyme Activity as %WT (In-House)**		**Absolute Increase as %WT**	**Fold over Baseline**	**Mean In Vitro Enzyme Activity as %WT (GLP-Validated Assay [13])**		**Absolute Increase as %WT**	**Fold over Baseline**	**Amenable (In-House)**	**Amenable (GLP-Validated [14])**
			without DGJ	with DGJ			without DGJ	with DGJ				
p.G373D	c.1118G > A	Classic	0	0	0	n/c	0	0	0	n/c	No	No
p.C378R	c.1132T > C	n/a	0	0	0	n/c	0	0	0	n/c	No	No
p.I384N	c.1151T > A	Classic	0	0	0	n/c	0	0.8	0.8	n/c	No	No
p.T385A	**c.1153A > G**	**n/a**	**45**	**48.9**	**3.9**	**1.1**	**57.3**	**73.5**	**16.2**	**1.3**	**No**	**Yes**
p.Q386P	c.1157A > C	Classic	0	0	0	n/c	0	0	0	n/c	No	No
p.P389L	c.1166C > T	n/a	0	0	0	n/c	0	0.6	0.6	n/c	No	No
p.G395A	**c.1184G > C**	**n/a**	**20.1**	**23.1**	**3**	**1.1**	**24.4**	**30.7**	**6.3**	**1.3**	**No**	**Yes**
p.S405R	c.1213A > C	n/a	91	92.7	1.7	1	52.5	59.6	7.1	1.1	No	No
p.L415P	c.1244T > C	Classic	0	0	0	n/c	0	0	0	n/c	No	No

Bold = different conclusions of both assays toward DGJ amenability; n/a = not analyzed; n/c = not calculated.

References

1. Germain, D.P. Fabry Disease. *Orphanet J. Rare Dis.* **2010**, *5*, 30. [CrossRef] [PubMed]
2. Aerts, J.M.; Groener, J.E.; Kuiper, S.; Donker-Koopman, W.E.; Strijland, A.; Ottenhoff, R.; Van Roomen, C.; Mirzaian, M.; Wijburg, F.A.; Linthorst, G.E.; et al. Elevated Globotriaosylsphingosine Is a Hallmark of Fabry Disease. *Proc. Natl. Acad. Sci. USA* **2008**, *105*, 2812–2817. [CrossRef] [PubMed]
3. Olivera-González, S.; Josa-Laorden, C.; Torralba-Cabeza, M.A. The Pathophysiology of Fabry Disease. *Revista Clínica Española (Engl. Ed.)* **2018**, *218*, 22–28.
4. Alroy, J.; Sabnis, S.; Kopp, J.B. Renal Pathology in Fabry Disease. *JASN* **2002**, *13*, S134–S138. [CrossRef]
5. Linhart, A.; Kampmann, C.; Zamorano, J.L.; Sunder-Plassmann, G.; Beck, M.; Mehta, A.; Elliott, P.M. Cardiac Manifestations of Anderson-Fabry Disease: Results from the International Fabry Outcome Survey. *Eur. Heart J.* **2007**, *28*, 1228–1235. [CrossRef] [PubMed]
6. Sims, K.; Politei, J.; Banikazemi, M.; Lee, P. Stroke in Fabry Disease Frequently Occurs Before Diagnosis and in the Absence of other Clinical Events: Natural History Data from The Fabry Registry. *Stroke* **2009**, *40*, 788–794. [CrossRef]
7. Lukas, J.; Scalia, S.; Eichler, S.; Pockrandt, A.-M.; Dehn, N.; Cozma, C.; Giese, A.-K.; Rolfs, A. Functional and Clinical Consequences of Novel A-Galactosidase A Mutations in Fabry Disease. *Hum. Mutat.* **2016**, *37*, 43–51. [CrossRef]
8. Chmp. Galafold, Inn-Migalastat Hydrochloride. Available online: https://www.ema.europa.eu/en/documents/assessment-report/galafold-epar-public-assessment-report_en.pdf (accessed on 1 October 2019).
9. Lukas, J.; Knospe, A.-M.; Seemann, S.; Citro, V.; Cubellis, M.V.; Rolfs, A. In Vitro Enzyme Measurement to Test Pharmacological Chaperone Responsiveness in Fabry And Pompe Disease. *J. Vis. Exp.: Jove* **2017**. [CrossRef]
10. Parenti, G. Treating Lysosomal Storage Diseases with Pharmacological Chaperones: From Concept to Clinics. *EMBO Mol. Med.* **2009**, *1*, 268–279. [CrossRef]
11. Van Der Veen, S.J.; Van Kuilenburg, A.B.P.; Hollak, C.E.M.; Kaijen, P.H.P.; Voorberg, J.; Langeveld, M. Antibodies Against Recombinant Alpha-Galactosidase A in Fabry Disease: Subclass Analysis and Impact on Response to Treatment. *Mol. Genet. Metab.* **2019**, *126*, 162–168. [CrossRef]
12. Markham, A. Migalastat: First Global Approval. *Drugs* **2016**, *76*, 1147–1152. [CrossRef]
13. Lukas, J.; Giese, A.-K.; Markoff, A.; Grittner, U.; Kolodny, E.; Mascher, H.; Lackner, K.J.; Meyer, W.; Wree, P.; Saviouk, V.; et al. Functional Characterisation Of Alpha-Galactosidase A Mutations as A Basis for A New Classification System in Fabry Disease. *PLoS Genet.* **2013**, *9*, E1003632. [CrossRef]
14. Benjamin, E.R.; Della Valle, M.C.; Wu, X.; Katz, E.; Pruthi, F.; Bond, S.; Bronfin, B.; Williams, H.; Yu, J.; Bichet, D.G.; et al. The Validation of Pharmacogenetics for the Identification of Fabry Patients to be Treated with Migalastat. *Genet. Med.: Off. J. Am. Coll. Med Genet.* **2017**, *19*, 430–438. [CrossRef] [PubMed]
15. Citro, V.; Cammisa, M.; Liguori, L.; Cimmaruta, C.; Lukas, J.; Cubellis, M.V.; Andreotti, G. The Large Phenotypic Spectrum of Fabry Disease Requires Graduated Diagnosis and Personalized Therapy: A Meta-Analysis Can Help to Differentiate Missense Mutations. *Int. J. Mol. Sci.* **2016**, *17*, 2010. [CrossRef] [PubMed]
16. Oommen, S.; Zhou, Y.; Meiyappan, M.; Gurevich, A.; Qiu, Y. Inter-Assay Variability Influences Migalastat Amenability Assessments Among Fabry Disease Variants. *Mol. Genet. Metab.* **2019**, *127*, 74–85. [CrossRef] [PubMed]
17. Andreotti, G.; Citro, V.; De Crescenzo, A.; Orlando, P.; Cammisa, M.; Correra, A.; Cubellis, M.V. Therapy of Fabry Disease with Pharmacological Chaperones: From in Silico Predictions To In Vitro Tests. *Orphanet J. Rare Dis.* **2011**, *6*, 66. [CrossRef]
18. Trujillano, D.; Oprea, G.-E.; Schmitz, Y.; Bertoli-Avella, A.M.; Abou Jamra, R.; Rolfs, A. A Comprehensive Global Genotype-Phenotype Database for Rare Diseases. *Mol. Genet. Genom. Med.* **2017**, *5*, 66–75. [CrossRef]
19. Andreotti, G.; Guarracino, M.R.; Cammisa, M.; Correra, A.; Cubellis, M.V. Prediction of the Responsiveness to Pharmacological Chaperones: Lysosomal Human Alpha-Galactosidase, A Case of Study. *Orphanet J. Rare Dis.* **2010**, *5*, 36. [CrossRef]
20. Cammisa, M.; Correra, A.; Andreotti, G.; Cubellis, M.V. Fabry_Cep: A Tool to Identify Fabry Mutations Responsive to Pharmacological Chaperones. *Orphanet J. Rare Dis.* **2013**, *8*, 111. [CrossRef]

21. Wu, X.; Katz, E.; Della Valle, M.C.; Mascioli, K.; Flanagan, J.J.; Castelli, J.P.; Schiffmann, R.; Boudes, P.; Lockhart, D.J.; Valenzano, K.J.; et al. A Pharmacogenetic Approach to Identify Mutant Forms of A-Galactosidase A that Respond to A Pharmacological Chaperone for Fabry Disease. *Hum. Mutat.* **2011**, *32*, 965–977. [CrossRef]
22. Benjamin, E. Methods of treating fabry disease in patients having the g9331a mutation in the gla gene. WO2017165164A1, 28 September 2017.
23. Hughes, D.A.; Nicholls, K.; Shankar, S.P.; Sunder-Plassmann, G.; Koeller, D.; Nedd, K.; Vockley, G.; Hamazaki, T.; Lachmann, R.; Ohashi, T.; et al. Oral Pharmacological Chaperone Migalastat Compared with Enzyme Replacement Therapy in Fabry Disease: 18-Month Results From The Randomised Phase Iii Attract Study. *J. Med. Genet.* **2017**, *54*, 288–296. [CrossRef] [PubMed]
24. Lenders, M.; Stappers, F.; Niemietz, C.; Schmitz, B.; Boutin, M.; Ballmaier, P.J.; Zibert, A.; Schmidt, H.; Brand, S.-M.; Auray-Blais, C.; et al. Mutation-Specific Fabry Disease Patient-Derived Cell Model to Evaluate the Amenability to Chaperone Therapy. *J. Med. Genet.* **2019**, *56*, 548–556. [CrossRef] [PubMed]
25. Nowak, A.; Huynh-Do, U.; Krayenbuehl, P.-A.; Beuschlein, F.; Schiffmann, R.; Barbey, F. Fabry Disease Genotype, Phenotype, And Migalastat Amenability: Insights from A National Cohort. *J. Inherit. Metab. Dis.* **2019**. [CrossRef] [PubMed]

International Journal of
Molecular Sciences

MDPI

Article

Misfolding of Lysosomal α-Galactosidase a in a Fly Model and Its Alleviation by the Pharmacological Chaperone Migalastat

Hila Braunstein [1], Maria Papazian [1], Gali Maor [1], Jan Lukas [2,3], Arndt Rolfs [4] and Mia Horowitz [1,*]

[1] The Shmunis School of Biomedicine and Cancer Research, Life Sciences, Tel Aviv University, Ramat Aviv 69978, Israel; brown_hila@walla.co.il (H.B.); mari.papazian@gmail.com (M.P.); galifit@gmail.com (G.M.)
[2] Department of Neurology, Translational Neurodegeneration Section "Albrecht-Kossel", University Medical Center Rostock, Rostock 18051, Germany; jan.lukas@med.uni-rostock.de
[3] Center for Transdisciplinary Neurosciences Rostock (CTNR), University Medical Center Rostock, University of Rostock, 18051 Rostock, Germany
[4] Centogene AG, 18055 Rostock, Germany; arndt.rolfs@med.uni-rostock.de
* Correspondence: horwitzm@tauex.tau.ac.il; Tel.: +011-972-3-640-9285

Received: 15 July 2020; Accepted: 5 October 2020; Published: 7 October 2020

Abstract: Fabry disease, an X-linked recessive lysosomal disease, results from mutations in the *GLA* gene encoding lysosomal α-galactosidase A (α-Gal A). Due to these mutations, there is accumulation of globotriaosylceramide (GL-3) in plasma and in a wide range of cells throughout the body. Like other lysosomal enzymes, α-Gal A is synthesized on endoplasmic reticulum (ER) bound polyribosomes, and upon entry into the ER it undergoes glycosylation and folding. It was previously suggested that α-Gal A variants are recognized as misfolded in the ER and undergo ER-associated degradation (ERAD). In the present study, we used *Drosophila melanogaster* to model misfolding of α-Gal A mutants. We did so by creating transgenic flies expressing mutant α-Gal A variants and assessing development of ER stress, activation of the ER stress response and their relief with a known α-Gal A chaperone, migalastat. Our results showed that the A156V and the A285D α-Gal A mutants underwent ER retention, which led to activation of unfolded protein response (UPR) and ERAD. UPR could be alleviated by migalastat. When expressed in the fly's dopaminergic cells, misfolding of α-Gal A and UPR activation led to death of these cells and to a shorter life span, which could be improved, in a mutation-dependent manner, by migalastat.

Keywords: Fabry disease 1; misfolding 2; UPR 3; ERAD 4; migalastat 5

1. Introduction

In misfolding diseases such as lysosomal storage diseases (LSDs) there is chronic retention of misfolded proteins in the endoplasmic reticulum (ER), which leads to their ER-associated degradation (ERAD) and causes ER stress and activation of the ER stress response in cells, known as the unfolded protein response (UPR) [1,2].

Our lab showed in the past that in Gaucher disease (GD), resulting from accumulation of glucosylceramides due to mutations in the *GBA1* gene, encoding acid-β-glucocerebrosidase (GCase), the mutant variants are retained in the ER and activate the UPR [3–8]. Using *Drosophila melanogaster* as an animal model, Maor et al. showed that expression of mutant human GCase in the dopaminergic cells of the fly activated UPR, which led to death of these cells, to motoric disabilities and to shorter

life span. The phenotype could be rescued by treatment with the known pharmacological chaperone ambroxol [3,8].

In the present study we used *Drosophila melanogaster* as an in-vivo model to analyze misfolding of α-Gal A, linked with Fabry disease, and its associated UPR, and to test whether we can improve UPR-associated pathology by applying a pharmacological chaperone.

Fabry disease is the second most common lysosomal disorder, inherited as an X-linked recessive disease. It results from mutations in the *GLA* gene, encoding alpha galactosidase A (α-Gal A, EC 3.2.1.22, NM_000169.2), leading to accumulation of globotriaosylceramide (GL-3) and its acylated form lyso-GL3 (lyso-Gb3) [9–13] in various types of cells, including vascular endothelial cells, podocytes, cardiomyocytes, arterial smooth muscle cells and kidney cells, peripheral and central nervous systems, skin and eyes [10–13]. Death occurs mainly because of renal failure along with premature myocardial infarction and strokes [11,14,15].

Fabry disease is broadly divided into "classic" and "late onset" phenotypes. Patients with the classic phenotype of Fabry disease are usually males with significantly low or undetectable (<3% of mean normal) α-Gal A activity, who present multiple organ manifestations. Patients with the late-onset phenotype have varied ages of onset and clinical manifestations, with typical cardiac and renal symptoms [16,17]. Fabry disease females are heterozygous and present varying degrees of symptoms, ranging from asymptomatic to severe [18–20]. This phenotypic is due, most probably, to X-inactivation. There are more than 1000 mutations in the *GLA* gene known to be associated with Fabry disease [17,21]. It was estimated that 35–50% of patients with Fabry disease have mutations that are amenable to migalastat therapy [17,22]. The amenability of *GLA* mutations to migalastat therapy is determined by an in-vitro assay, in which human embryonic kidney (HEK) 293 cells are transfected with individual *GLA*-containing DNA plasmids, with and without migalastat. Migalastat-amenable mutations are defined as those that present absolute increases of ≥3% over wild-type α-Gal A activity in the presence of 10 μM migalastat [17,22].

Enzyme replacement therapy (ERT) based on intravenous administration of recombinant human enzyme has been available for Fabry disease since 2001 (Raplagal, Shire Human Genetic Therapies AB; Fabrazyme, Sanofi Genzyme) [23–26]. One main shortcoming of ERT is limited tissue penetrance. Central nervous system manifestations such as cerebrovascular complications and neuropathic pain in Fabry disease cannot be addressed due to the blood–brain barrier, which is not penetrated by ERT. Another shortcoming is the risk of an immune response with potentially neutralizing antibodies generated against the therapeutic enzymes [16,24,27]. Treatment with a pharmacological chaperone is another option for Fabry disease patients. Pharmacological chaperones are small molecules with the ability to cross the blood–brain barrier, which bind misfolded proteins in the ER to allow their correct folding and trafficking via the secretory pathway to the lysosomes. In the case of a lysosomal enzyme, the pharmacological chaperone dissociates in the lysosome from the enzyme, which binds to its substrate and catalyzes its hydrolysis according to its residual activity [9,28,29]. One approved chaperone for the treatment of Fabry disease patients is migalastat (AT1001, DGJ-1-deoxygalactonojirimycin, commercial name Galafold) [17]. Migalastat is an analogue of α-Gal A substrate that binds to the active site of the enzyme [30,31]. Treatment with migalastat was shown to increase enzyme activity in cell culture and in mice expressing amenable mutations [32–37].

In the present study, we established transgenic flies harboring mutant (A156V, A285D) α-Gal A variants to model their misfolding and to address the effect of a known pharmacological chaperone on this misfolding. Mutant or WT *GLA* mutant or WT *GLA* cDNAs, coupled to a yeast upstream activating sequence (UAS), which is inactive in the fly, were introduced into normal flies Expression of the transgenes was controlled by the UAS/GAL4 system. In this system, the GAL4 gene is placed under the control of a native gene promoter. When expressed, GAL4 binds and activates the UAS, which is coupled to the gene of interest. Thus, expression of a target gene (a *GLA* variant in the present study) is achieved by the presence of active GAL4 [38].

Our results strongly indicated that the mutant variants, but not the WT α-Gal A variant, were retained in the ER and underwent ERAD. Their retention in the ER activated the UPR machinery. When expression of the mutant α-Gal A variants was driven in the dopaminergic cells of the fly, misfolding and UPR activation led to death of these cells and to premature death of the flies, which could be improved, in a mutation dependent manner, by migalastat.

2. Results

2.1. Alpha-Gal a Is ER Retained and Undergoes ERAD

Three fly lines harboring different variants of the *GLA* gene were generated: a WT human α-Gal A, a mutated human A156V α-Gal A variant and a mutated human A285D variant. The two latter are considered classical mutations, the A156V variant has 4.3% in vitro residual activity while the A285D mutant has no detectable activity [21]. All were introduced as cDNAs, coupled to a yeast upstream activating sequence (UAS), which is inactive in the fly, and binds the transcription factor GAL4. Thus, UAS-linked transgenes can be expressed in specific cell types under the control of a *Drosophila* promoter linked to the GAL4 sequence [39].

Western blot analysis of lysates prepared from flies expressing the different α-Gal A variants under the ubiquitous daughterless-GAL4 (DaGAL4) driver [40] depicted lower levels of α-Gal A in flies expressing the mutant forms of α-Gal A (A156V and A285D) in comparison to flies expressing the WT variant (Figure 1A,B). Moreover, the level of the more severe A285D mutant protein was lower than that of the A156V variant (Figure 1A). The appearance of a major band in the WT sample, with a minor upper band, two bands in the A156V lysate and only the upper one in the A285D mutant, suggested that they represent different glycosylation states and cellular localization. Thus, we assumed that the upper band was ER retained protein, while the lower band represented the mature lysosomal α-Gal A form. To confirm our assumption, we treated the lysates with endoglycosidase-H (endo-H). Endo-H is a specific endo-glycosidase that cleaves a high mannose (more than four residues) *N*-glycan complex and not a mature counterpart [41,42]. Since high mannose structures (with 8–9 mannose residues in the N-glycan trees) are mostly found on glycoproteins present in the ER, this fraction of glycoproteins is endo-H sensitive. However, once glycoproteins arrive to the cis-Golgi network, five mannose residues are removed from their *N*-glycans, rendering them with only four to three mannoses on the *N*-glycan tree [43,44]. The oligosaccharide chain with four to three mannoses is not recognized by endoH. Hence, this fraction of glycoproteins, which is mostly lysosomal, is endo-H resistant. All three α-Gal A proteins showed sensitivity to endo-H cleavage, indicating that in all three variants, there was an ER retained endo-H sensitive protein. The endo-H sensitive fraction was increased with mutation severity. While ~17% of the WT protein was endo-H sensitive, ~46% and ~96% were endo-H sensitive in the A156V and the A285D mutants, respectively (Figure 1C,D). The results indicated that most of the A285D protein was ER retained, while a significant fraction of the A156V mutant variant was able to exit the ER. A small fraction of WT α-Gal A resided in the ER. Thus, the results of the endo-H resistance experiment confirmed that the upper α-Gal A band (seen in Figure 1A) represented the ER retained, most probably the unfolded form of the enzyme, while the lower protein was a mature lysosomal α-Gal A.

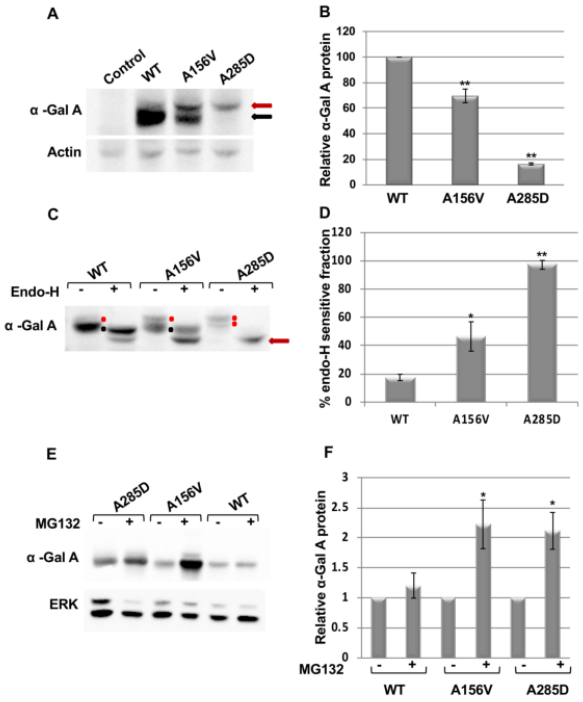

Figure 1. Alpha-Gal A expression in *Drosophila melanogaster*. (**A**) Lysates prepared from 15 day old flies were subjected to sodium dodecyl sulphate polyacrylamise gel electrophoresis (SDS–PAGE) and interaction with anti-Myc antibody, to identify α-Gal A and anti actin antibodies, as a loading control. The red arrow indicates the higher molecular weight, endoplasmic reticulum (ER) retained fraction of the protein; the black arrow indicates the lower molecular weight lysosomal fraction of the protein. (**B**) Quantification of results as seen in A of three independent experiments (mean ± standard error of mean (SEM)). To quantify the results, α-Gal A intensity in each lane was divided by that of actin in the same lane, and the number obtained for wild type (WT) was considered to be 100. Statistical analysis included one-way ANOVA followed by one-sample t-test. (**C**) Lysates prepared as in A were treated with endo-H and analyzed by Western blotting. The red dot indicates the higher molecular weight, ER retained fraction of the protein before endo-H treatment; the red arrow indicates the ER retained fraction of the protein after endo-H treatment; and the black dot marks the lower molecular weight, endo-H resistant lysosomal fraction of the protein. (**D**) Quantification of results as shown in (**C**). The amount of endo-H sensitive α-Gal A fraction in each treated lane was divided by the total amount of protein in the same lane. The results are the mean ± SEM of five independent experiments. Statistical analysis included one-way ANOVA followed by post-hoc Dunnett test. (**E**) Twenty-four hours after transfection of HEK293T cells with pcDNA4-MycHis-α-Gal A plasmids (human WT, A156V, A285D), they were treated with 25 μM MG132 for 20 h, and their lysates were subjected to Western blotting and interaction with anti-Myc antibody, to identify α-Gal A and anti ERK antibodies, as a loading control. (**F**) Quantification of results as shown in (**E**). To quantify the results, α-Gal A intensity in each lane was divided by that of ERK in the same lane, and the number obtained for every variant without treatment was considered to be 1. The results are the mean ± SEM of three independent experiments. Statistical analysis included one-sample t-test. Significance: * $p < 0.05$; ** $p < 0.01$. The expression of the α-Gal A mutant variants was under the daughterless GAL4 driver (DaGAL4).

To test whether mutant α-Gal A variants undergo ERAD due to their misfolding, and due to sensitivity of flies to treatment with proteasome inhibitors like bortezomib or MG132, we performed

the experiment in tissue culture. HEK293T cells, transfected with plasmids expressing the three different α-Gal A variants, were treated with MG132 after which their lysates were subjected to Western blot analysis. MG132 is a synthetic, membrane permeable, peptidyl aldehyde that effectively blocks the proteolytic activity of the S28 proteasome [45–47]. Therefore, treatment with MG132 leads to an increase in the amount of proteins that are otherwise degraded by ERAD. The results (Figure 1E,F) showed that the amount of mutant A156V and of the A285D α-Gal A proteins increased by MG132 treatment. There were 2.2- and 2.1-fold increases in the amount of A156V and A285D variants, respectively (Figure 1E,F), while the increase in the amount of the WT α-Gal A variant was non-significant. The results strongly indicate that mutant α-Gal A variants underwent ERAD (Supplementary Figure S1).

In order to examine the effect of chaperone treatment on the expression of the α-Gal A variants in transgenic flies, α-Gal A-expressing flies were treated with different concentrations of migalastat for 22 days post-eclosion. Western blots of the proteins indicated that there was an increase in stability of WT α-Gal A in flies treated with 50 μM migalastat (Figure 2A,B). There was a 2.5- and a 3-fold increase in the total amount of the A156V α-Gal A following 10 μM and 50 μM chaperone treatment, respectively, and elevation in the lysosomal fraction of the mutant protein, indicating that migalastat is able to bind the protein and to assist in its folding and trafficking from the ER to the lysosomes (Figure 2C,D). Moreover, even in the A285D-expressing flies, there was a 2.5-fold increase in the total amount of α-Gal A, as well as appearance of a small lysosomal fraction, following 20 μM migalastat treatment (Figure 2E,F).

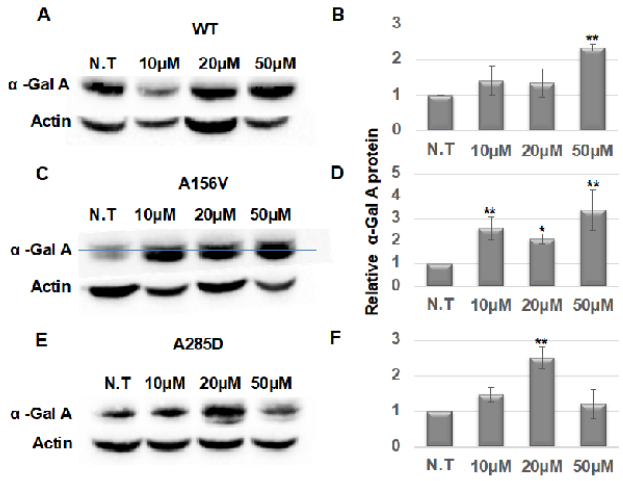

Figure 2. Alpha-Gal A expression following migalastat treatment. (**A**,**C**,**E**) Lysates prepared from 22 day old flies, carrying the different α-Gal A variants, as indicated in the graph, treated with different migalastat concentrations, were subjected to SDS–PAGE and interaction with anti-Myc antibody, to identify α-Gal A and anti actin antibodies, as a loading control. Blue lines separate the higher molecular weight ER retained fraction of the protein from the lower molecular weight lysosomal fraction (when applicable). (**B**,**D**,**F**) Quantification of results as shown in (**A**,**C**,**E**), respectively. To quantify the results, α-Gal A intensity in each lane was divided by that of actin in the same lane, and the number obtained for N.T. in each experiment was considered to be 1. The results are the mean ± SEM of three independent experiments. The expression of the α-Gal A mutant variants was under the daughterless GAL4 driver (DaGAL4). Statistical analysis included two-way ANOVA (to determine significant differences between genotypes' reactions to concentrations) followed by one-way ANOVA with post-hoc Dunnett t-tests. Significance: * $p < 0.05$; ** $p < 0.01$. N.T: Non-Treated.

2.2. UPR Activation in Transgenic α-Gal a Expressing Flies

Our results strongly indicated that when expressed in flies, mutant α-Gal A variants were misfolded, were retained in the ER and underwent ERAD.

ER retention of misfolded proteins leads to ER stress and to activation of UPR. To examine UPR activation in flies expressing different mutant α-Gal A variants, RNA was extracted from 22 day old flies and was subjected to qRT-PCR. Changes in the levels of known UPR-induced fly genes were monitored [8]. The results showed activation of the tested UPR markers: Hsc-70-3 (the fly BiP homolog), spliced Xbp1 and ATF4 (Figure 3A). In order to test the effect of migalastat on UPR, flies, collected at the day of eclosion, were treated with different concentrations of the chaperone for 22 days, after which RNA was extracted and subjected to real-time quantitative polymerase chain reaction (qRT-PCR) analysis. The results (Figure 3B–E) strongly indicated that only the A156V α-Gal A mutation was responsive to the chaperone treatment. There was a decrease in the level of the tested UPR parameters: Hsc-70-3, spliced Xbp1 and ATF4 in flies expressing the A156V α-Gal A mutant after 22 days of migalastat treatment (Figure 3D). The highest concentration used, 50 μM, was proven to be the most effective. There was no significant change in UPR parameters in flies expressing the A285D α-Gal A variant (Figure 3E). There was a decrease in the level of spliced Xbp1 in flies expressing the WT α-Gal A only at 50 μM (Figure 3C) with no accompanied change in other genes. We, therefore, believe it does not reflect a real decrease in UPR. Interestingly, though there was a small increase in the lysosomal fraction of the A285D mutant (Figure 2E,F), it was not significant enough to cause a decrease in UPR.

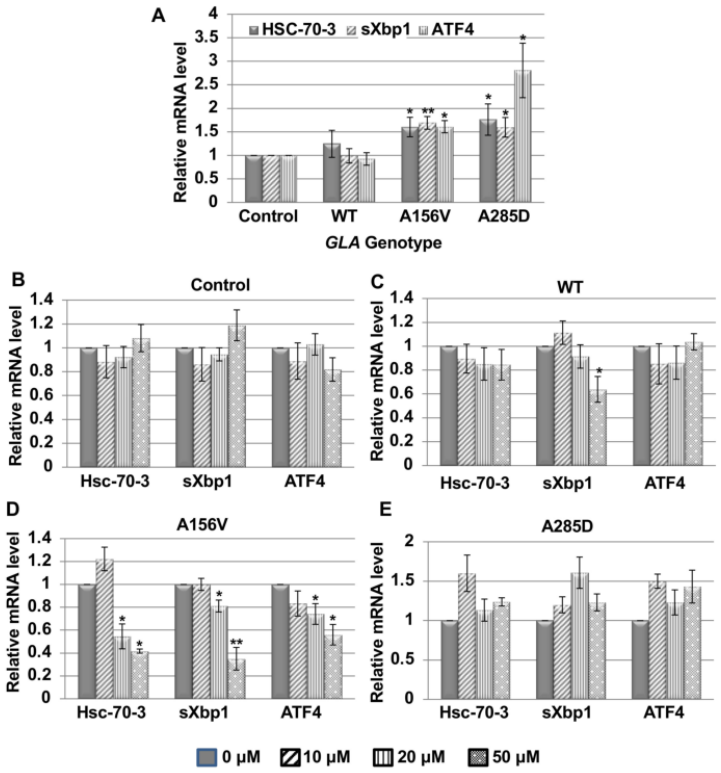

Figure 3. Unfolded protein response (UPR) activation in *GLA* transgenic flies and its alleviation following migalastat treatment. RNA was isolated from untreated (**A**) or from migalastat treated flies

(**B**–**E**), expressing the different α-Gal A variants, as indicated in the graph. The extracted RNA was subjected to real-time quantitative polymerase chain reaction (qRT-PCR) with primers specific for Hsc-70-3, spliced Xbp1 (sXbp1) and ATF4 mRNAs (as specified in Table 2), representing the three UPR arms. The expression of the α-Gal A mutant variants was under the daughterless GAL4 driver (DaGAL4). The results are the mean ± SEM of five independent experiments. Each bar represents the results of five different experiments. Statistical analysis included two-way ANOVA (to show the significance of the reaction of the different genotypes to different migalastat concentrations), followed by one-sample t-test. Significance: * $p < 0.05$; ** $p < 0.01$.

2.3. Climbing Ability of Transgenic α-Gal a Expressing Flies

Negative geotaxis (climbing) of the flies, commonly used for assaying motor deficits as a result of misexpression of neuron-specific proteins [48], was employed to assess the neural dysfunction caused to the flies by expression of mutant α-Gal A in their dopaminergic cells. We monitored the climbing ability of the flies at ages of 15- and 22-days post-eclosion. The results presented significant locomotion dysfunction in flies expressing both A156V and A285D α-Gal A mutants compared to flies expressing the WT *GLA* variant or control flies (Figure 4A,B).

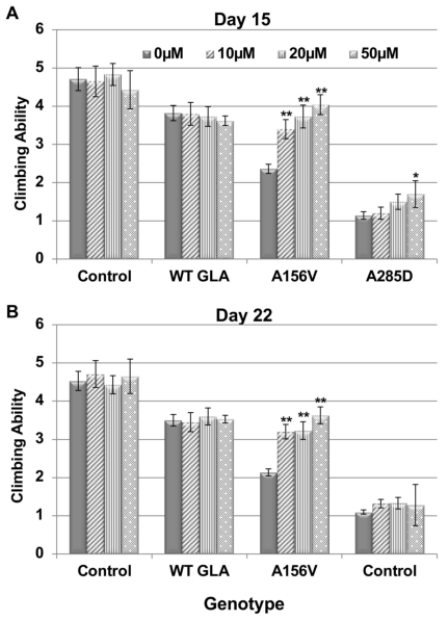

Figure 4. Climbing ability of *GLA* transgenic flies. (**A**,**B**) Transgenic flies treated with different concentrations of migalastat were analyzed for climbing ability at days 15 (**A**) or 22 (**B**) post-eclosion. The results are the mean ± SEM of three independent experiments. The expression of the α-Gal A mutant variants was under the dopa decarboxylase GAL4 driver (DdcGAL4). Statistical analysis included three-way ANOVA (to show the significance of the reaction of the different genotypes to different migalastat concentrations and test if there is a difference between the different days evaluated), followed by one-way ANOVA with post-hoc Dunnett test. Significance: * $p < 0.05$; ** $p < 0.01$.

Climbing ability of flies, treated with different concentrations of migalastat, was evaluated as well. The results (Figure 4A,B) showed a significant improvement in climbing ability of the A156V mutant α-Gal A-expressing flies following chaperone treatment in all the tested concentrations. There was a slight change in the climbing ability of flies expressing the A285D mutation at day 15 post-eclosion; however, it did not reach statistical significance and was not recapitulated at day 22 post-eclosion.

2.4. Death of Dopaminergic Cells in Brains of GLA Flies

Thus far we have shown that mutant α-Gal A variants underwent ERAD, and that their ER retention led to UPR activation. This UPR activation, which affects the motor skills of the flies, could be significantly alleviated in flies expressing the A156V α-Gal A mutant variant by migalastat treatment.

To further explore UPR activation in the flies, we followed the death of their dopaminergic cells. To do that, we quantified the amount of tyrosine hydroxylase (TH), as a marker of dopaminergic cells, in heads of aging flies. Fluorescence intensity of TH was analyzed in the posterior region of the brain, where ~70 dopaminergic cells occupy very distinct areas [49]. The results showed significantly decreased fluorescence intensity in brains of 22 day old mutant flies. We did not observe a significant difference in flies expressing WT α-Gal A following chaperone treatment at 10–20 μM concentrations, with a 40% increase in the presence of 50 μM migalastat. This increase is in line with the increased amount of WT α-Gal A in the presence of 50 μM migalastat (Figure 2A,B). Fluorescence intensity was significantly increased in brains of the A156V α-Gal A-expressing flies. In contrast, the increase in fluorescence intensity was mild and only statistically significant at the 50 μM concentration in flies expressing the A285D mutant α-Gal A (Figure 5A,B).

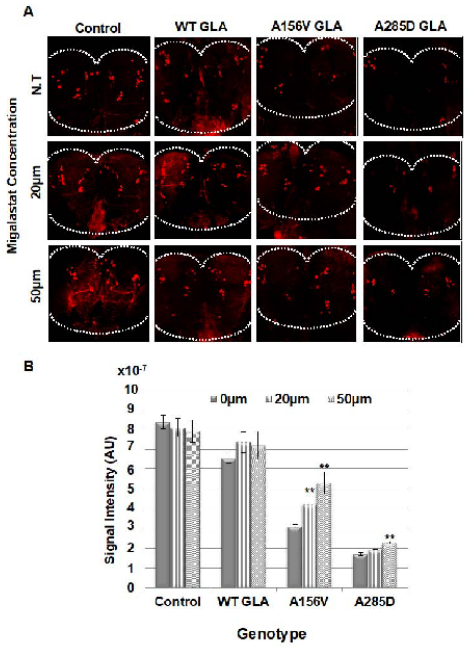

Figure 5. Immunostaining of dopaminergic cells in *GLA* transgenic flies. (**A**) Representative confocal images of adult brains of transgenic flies, expressing the human WT or mutant *GLA* variants, untreated or migalastat treated, stained with anti-TH antibodies at day 22 post-eclosion. (**B**) Quantification of TH signal intensity obtained from six tested brains as shown in (**A**). The expression of the α-Gal A mutant variants was under the dopa decarboxylase GAL4 driver (DdcGAL4). Statistical analysis included two-way ANOVA (to determine significant differences between genotypes' reaction to concentrations) followed by one-way ANOVA with post-hoc Dunnett t-tests. Significance: ** $p < 0.01$. N.T: Non-Treated.

To verify our results, we analyzed TH levels in head lysates of non-treated (Figure 6 A,B) and treated (Figure 6C–H) flies by Western blotting. The results strongly indicated that while 22 days treatment with migalastat had no effect in flies expressing the WT α-Gal A variant (Figure 6C,D), it had a significant effect on the amount of TH produced in the brains of A156V α-Gal A-expressing flies,

which is a measure of surviving dopaminergic cells (Figure 6E,F). There was also a significant (though lower than that seen in the A156V α-Gal A-expressing flies) increase in the amount of TH in flies expressing the A285D mutant α-Gal A variant (Figure 6G,H).

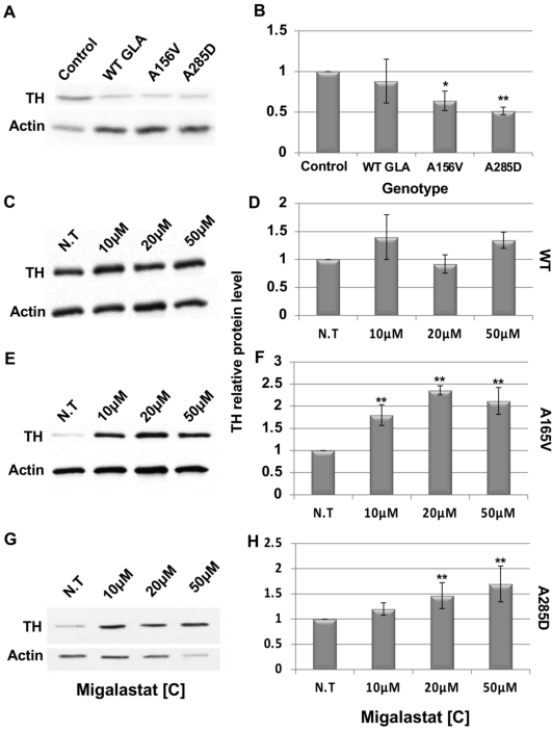

Figure 6. Western blot analysis of tyrosine hydroxylase in brains of *GLA* transgenic flies. (**A**) Protein lysates, prepared from heads of 10 control flies or flies expressing the different α-Gal A variants at day 22 post-eclosion, were subjected to Western blotting. The corresponding blots were interacted with anti-TH antibodies. As a loading control, the blots were interacted with anti-actin antibodies. (**B**) To quantify the results, TH intensity in each lane was divided by that of actin in the same lane, and the number obtained for Control was considered 1. Results represent the mean ± SEM of four independent experiments. Statistical analysis included one-way ANOVA with post-hoc Dunnett test. (**C**,**D**) Protein lysates prepared from flies expressing the WT α-Gal A, treated with the shown migalastat concentrations, were manipulated as in (**A**). To quantify the results, TH intensity in each lane was divided by that of actin in the same lane, and the number obtained for N.T. was considered to be 1. Results represent the mean ± SEM of four independent experiments. (**E**,**F**) Protein lysates prepared from flies expressing the A156V α-Gal A, treated with the shown migalastat concentrations, were manipulated as in (**A**). Quantification was as in (**D**). (**G**,**H**) Protein lysates prepared from flies expressing the A285D α-Gal A, treated with the shown migalastat concentrations, were manipulated as in (**A**), and quantification of results was as in (**D**). In (**D**,**F**,**H**), statistical analysis included two-way ANOVA (to determine significant differences between genotypes' reaction to concentrations) followed by one-way ANOVA with post-hoc Dunnett t-test. Significance: * $p < 0.05$; ** $p < 0.01$. N.T: Non-Treated. The expression of the α-Gal A mutant variants was under the dopa decarboxylase GAL4 driver (DdcGAL4).

2.5. Survival of Transgenic α-Gal a Expressing Flies

Life span of flies expressing the different α-Gal A variants was followed, with and without migalastat treatment. The results showed premature death of transgenic flies expressing mutant α-Gal A variants, in comparison to flies expressing the WT human α-Gal A (Figure 7A). Furthermore, the flies expressing the A285D α-Gal A mutation presented earlier death in comparison to flies expressing the A156V α-Gal A mutation (Figure 7A). In order to examine the effect of chaperone treatment on life span, α-Gal A-expressing flies were treated with different concentrations of migalastat from eclosion to death. The use of migalastat at different concentrations did not alter life span of flies expressing the human WT α-Gal A protein (Figure 7B) but significantly prolonged the life span of flies expressing the A156V α-Gal A mutant (Figure 7C). There was a small change in the survival of flies expressing the A285D α-Gal A mutation treated with 50 μM migalastat, which should not be ignored (Figure 6D). Interestingly 50% survival was also significantly increased for both A156V and A285D mutations (Figure 6E).

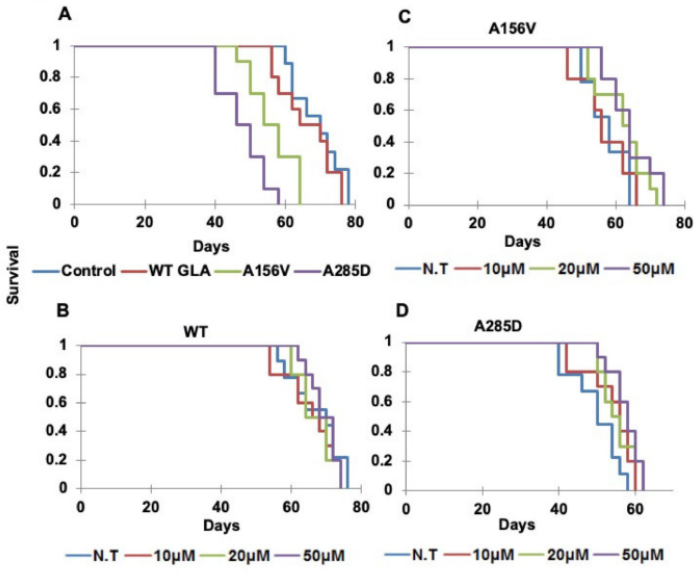

E

Genotype	Control	WT *GLA*	A156V *GLA*	A285D *GLA*
Longest survival (Days)	78	76	64	58
p-value	-	0.015	0.0003	<0.0001
50% survival (Days)	66	64	54	50
WT *GLA*	**N.T**	**10μM**	**20μM**	**50μM**
Longest survival (Days)	76	76	76	74
p-value	-	0.387	0.332	0.214
50% survival (Days)	64	66	64	68
A156V *GLA*	**N.T**	**10μM**	**20μM**	**50μM**
Longest survival (Days)	64	66	72	74
p-value	-	0.01	0.003	0.0025
50% survival (Days)	54	56	62	64
A285D *GLA*	**N.T**	**10μM**	**20μM**	**50μM**
Longest survival (Days)	58	60	60	62
p-value	-	0.018	0.007	0.004
50% survival (Days)	50	56	54	58

Figure 7. Survival of flies. (**A**) Kaplan–Meier curve showing the overall survival rates of flies expressing different *GLA* transgenes compared to normal control (Oregon-R) flies. (**B**–**D**) Kaplan–Meier curve showing the overall survival rates of flies expressing the different α-Gal A variants, treated with different migalastat concentrations. The expression of the α-Gal A mutant variants was under the dopa decarboxylase GAL4 driver (DdcGAL4). N.T.: non-treated. (**E**) A table showing the day reached by

50% of the flies (50% survival) and the longest survival time (days) reached by the different lines as well as statistical significance measured by Kaplan–Meier's multiple comparisons. In this test statistical significance is $p < 0.01$ as compared to the wild type (**A**) or N.T. (**B–D**).

3. Discussion

Mutations in the *GLA* gene cause Fabry disease, an X-linked lysosomal disease characterized by progressive accumulation of GL-3 in cells. The accumulation leads to tissue damage and eventual organ failure. There are more than 1000 known mutations in the *GLA* gene [36,50]. Most of the mutations disrupt the hydrophobic core of the protein, presumably leading to protein misfolding and degradation in the ER [31,51–53]. Thus, Fabry disease is primarily a protein misfolding lysosomal disease.

In the present study we used *Drosophila melanogaster* to model misfolding of Fabry disease-associated mutant α-Gal A variants. We did so by creating transgenic flies expressing WT and mutant α-Gal A variants and assessing development of ER stress and activation of the ER stress response, and their relief with a known α-Gal A chaperone, migalastat. We tested two classical human mutant *GLA* variants, A156V, known to have 4.3% in vitro enzyme activity of WT, and the A285D α-Gal A mutation, with no residual enzymatic activity [21,52,54]. Our results clearly showed that the A156V and the A285D mutant proteins were misfolded and ER-retained. Their ER retention led to UPR activation, which could be reduced by migalastat treatment. Migalastat, also known as AT1001, is an active site-specific chaperone. It was first found as a potent competitive inhibitor of α-Gal A. However, it effectively enhances α-Gal A activity in Fabry-derived cells, when given at concentrations lower than that usually required for intracellular inhibition of the enzyme [31]. Migalastat is the first pharmacological chaperone approved for treating Fabry disease patients with known responsive mutations [17].

We also documented ERAD of the tested mutant α-Gal A variants. Thus, the level of two mutant proteins, A156V and the A285D, were elevated in transfected HEK293T cells, in the presence of the proteasome inhibitor MG132. By decreasing UPR parameters, we could achieve an increase in the number of TH containing dopaminergic cells in the brain, an improvement in motor abilities and expanded life span of the mutant flies, which were more significant in the A156V containing flies.

Our results corroborated published studies on the responsiveness of the different Fabry mutations to migalastat, arguing that they are misfolded. In an early report, Ishii et al. showed that in COS-1 cells transfected with plasmids expressing the R301Q or Q279E, there was a fraction of α-Gal A that was aggregated at the top of the gel and had no enzyme activity. The authors argued that the aggregate originated from the ER [55]. Using confocal microscopy, Yam et al. showed that following chaperone treatment, ER retained mutant α-Gal A successfully trafficked to the lysosomes and degraded GL-3 in fibroblasts that derived from Fabry disease patients. The authors suggested that migalastat reduced BiP binding to α-Gal A in the ER and allowed its trafficking [56,57]. Ishii et al. documented protein stabilization by Western blot analysis of several α-Gal A mutations, including the A156V variant, following either treatment with the ER mannosidase I inhibitor, kifunensine [58] or with the proteasomal inhibitor, lactacystin [59], in COS-7 cells transfected with plasmids expressing the tested mutations. The results indicated protein misfolding and ERAD of mutant α-Gal A variants. In addition, increase in activity following migalastat treatment was shown [60].

A large number of publications documented the effect of migalastat on stabilization and increase in activity of α-Gal A [32,61,62]. Improvement in enzyme activity of different mutant α-Gal A was shown in HEK293-transfected cells treated with either migalastat [21,63,64] or migalastat and ambroxol [65], the known pharmacological chaperone of glucocerebrosidase, deficient in Gaucher disease [66]. There was a synergistic effect when treating cells with both chaperones [65]. The described results strongly indicated ERAD of mutant α-Gal A variants.

Currently, there is a mouse model in which the endogenous gene was knocked out, and it expresses a human mutant R301Q α-Gal A cDNA under the human α-Gal A promoter [67]. While ERAD and UPR were not specifically shown in this model, decreased accumulation of GL-3 was documented

following its treatment with migalastat [67,68]. These results strongly indicated misfolding of the R301Q mutant α-Gal A variant in the ER and its folding and trafficking to the lysosomes in the presence of the chaperone.

It is of note that De Francesco et al. ruled out apoptotic death associated with ER stress and UPR by evaluating caspase 4 and UPR genes in peripheral blood mononuclear cells derived from Fabry patients [69].

To summarize, in the present work we were able to document, using a fly model expressing α-Gal A variants, that the A156V and the A285D mutant variants are misfolded, are retained in the ER, undergo ERAD and activate the UPR. UPR activation by the A156V amenable mutation can be relieved by the pharmacological chaperone migalastat. On the other hand, treatment of the A285D-expressing flies with migalastat does not alleviate UPR parameters.

4. Materials and Methods

4.1. Antibodies

The antibodies used in the present project are as follows. Primary antibodies: rabbit polyclonal anti-tyrosine hydroxylase antibodies AB152 (Millipore, MA, USA); mouse monoclonal anti-Myc antibody (Cell Signaling Technology, Beverly, MA, USA); mouse monoclonal anti-actin antibody (Sigma-Aldrich, Rehovot, Israel); rabbit polyclonal anti-ERK antibodies (Santa Cruz Biotechnology, CA, USA). Secondary antibodies: horseradish peroxidase-conjugated goat anti-mouse antibodies; horseradish peroxidase-conjugated goat anti-rabbit antibodies, all from Jackson ImmunoResearch Laboratories, West Grove, PA, USA).

4.2. Fly Strains

Control strain in all experiments was Oregon-R obtained from the Bloomington *Drosophila* Stock Center, Indiana University, Bloomington, IN, USA). Transgenic flies, harboring pUAST- MycHis-WT *GLA* on the second chromosome, pUAST-MycHis-A156V *GLA* and pUAST-MycHis- A285D *GLA* on the third chromosome, were established by BestGene Inc. (Chino Hills, CA, USA). Da-GAL4 and Ddc-GAL4 were from Bloomington Stock Center (Indiana University, Bloomington, IN, USA). Strains were maintained on standard cornmeal-molasses medium at 25 °C.

4.3. Cell Lines and Transfections

HEK293T cells (ATCC® CRL-11268™) were grown in Dulbecco's modified Eagle's medium (DMEM DMEM; Gibco, purchased from Biological industries, Beit-Haemek, Israel), supplemented with 10% FCS (Beit-Haemek, Israel) at 37 °C in the presence of 5% CO2. Cells were transfected using calcium phosphate solutions. A mixture of DNA in 250 µL of 250 mM CaCl2 was dropped into a tube containing HBSX2 solution (50 mM Hepes, 280 mM NaCl, 1.5 mM Na2HPO4, pH 7.09) and incubated for 20 min at RT. The mixture was then added dropwise to sub-confluent cells. Forty-eight hours later, cell lysates were prepared for SDS–PAGE and Western blot analysis.

4.4. MG132 (Carbobenzoxy-L-leucyl-L-leucyl-L-leucinal) Treatment

HEK293T-transfected cells were treated with 25 µM of MG132 24 h post transfection (Calbiochem, San Diego, CA, USA) for 20 h.

4.5. Plasmid Preparation

Gibson assembly (New England Biolabs, Beverly, MA, USA) was employed to create the pUAST-MycHis or the pcDNA4-MycHis-B plasmids, containing the different *GLA* cDNAs. The inserts were amplified from pcDNA3.1/V5-His-*GLA* (WT/A156V/A285D) plasmids (described in [21]), with primers shown in Table 1. PCR was executed in 20 µL containing 30 ng of plasmid DNA, 4 µl of 5× ISO buffer, 0.4 mM dNTPS, 3% DMSO, 20 units/mL of fusion polymerase (New England,

Bio Labs, Beverly, MA, USA) and 10 pM each of forward and reverse primers. Thermal cycling conditions were 30 s at 98 °C, then thirty-five cycles of 98 °C (10 s), 68 °C (1 min) and 72 °C (1 min), following by 10 min at 72 °C for final extension. PCR reactions were carried out in Eorff Mastercycler EP Gradient S (Eorf, Hamburg, Germany). PCR products were separated on 1% agarose gels, and inserts were purified using "RBC Bioscience" kits, according to the manufacturer's instructions. The PCR products contained XhoI sequences on both sides (See Table 1 for primer sequences). The vector plasmids pUAST-MycHis or pcDNA4-MycHis-B were linearized with the restriction enzyme XhoI. Assembly and transformation were performed using a Gibson Assembly Cloning Kit (New England, Bio Labs, Beverly, MA, USA), following the manufacturer's instructions.

Table 1. Primers used for Gibson assembly.

Primer Name	Primer Sequence
FP-*GLA*(ATG) + pUAST/mycHis-left arm	5′-CAGATCTGCGGCCGCGGCTCGAGGATGCAGCTGAGGAACCCAGAACTAC-3′
RP-*GLA*(TAA) + pUAST/mycHis-right arm	5′-GCCCTCTAGAGGTACCCTCGAGCCAAGTAAGTCTTTTAATGACATCTG-3′
FP-*GLA*(ATG) + pcDNA4/myc-His-B-left arm	5′-CAGCACAGTGGCGGCCGGTCGAGTATGCAGCTGAGGAACCCAGAA-3
RP-*GLA*(TAA) +pcDNA4/myc-His-B-right arm	5′-CCGCGGGCCCTCTAGACTCGAGCGAAGTAAGTCTTTTAATGACATC-3′

4.6. RNA Preparation

For RNA extraction from flies, adult flies were frozen in liquid nitrogen and then homogenized in TRIzol® Reagent (Life Technologies, Carlsbad, CA, USA), according to the manufacturer's instructions.

4.7. cDNA Preparation and qRT-PCR

Two micrograms of RNA were reverse transcribed with M-MLV reverse transcriptase (Promega Corporation, CA, USA), using oligo dT primer in a total volume of 20 µL at 42 °C for 60 min. Reactions were stopped by incubation at 70 °C for 15 min. Three microliters of cDNA were used for qRT-PCR. qRT-PCR was performed using power SYBR green QPCR mix reagent kit (Applied Biosystems, Foster City, CA, USA) Rotor-Gene 6000. The reaction mixture contained 50% QPCR mix, 300 nM of forward primer and 300 nM of reverse primer, in a final volume of 10 µL. Thermal cycling conditions were 10 min at 95 °C, 40 cycles of: 95 °C (10 s) 60 °C (20 s) and 72 °C (20 s). Relative gene expression was determined by Ct value. The list of primers used for qRT-PCR is shown in Table 2.

Table 2. Primers used for qRT-PCR.

Primer Name	Primer Sequence
ATF4 F	5′-AGACGCTGCTTCGCTTCCTTC-3′
ATF4 R	5′-GCCCGTAAGTGCGAGTACGCT-3′
Hsc 70-3 F	5′-GCTGGTGTTATTGCCGGTCTGC-3′
Hsc 70-3 R	5′-GATGCCTCGGGATGGTTCCTTGC-3′
Xbp1 F	5′-CCGAACTGAAGCAGCAACAGC-3′
Xbp1 R	5′-GTATACCCTGCGGCAGATCC-3′
RP49 F	5′-TAAGAAGCGCACAAAGCACT-3′
RP49 R	5′-GGGCATCAGATATTGTCCCT-3′

4.8. Endonuclease-H Sensitivity

Endonuclease-H (endo-H) sensitivity was tested essentially as described elsewhere [7]. Briefly, cell lysates, containing 80 µg of total protein, were subjected to an overnight incubation with endo-H (New England Biolabs, Beverly, MA, USA), according to the manufacturer's instructions.

4.9. SDS–PAGE and Western Blotting

For each preparation, either confluent cells or 10 or more flies were homogenized in NP-40 lysis buffer (20 mM Tris HCL pH 7.5, 100 mM NaCl, 1 mM $MgCl_2$, 5 Mm EDTA and 0.5% NP-40) containing

protease inhibitors (10 µg/mL leupeptin, 10 µg/mL aprotinin and 0.1 mM PMSF, all from Sigma-Aldrich, St. Louis, MO, USA). Samples containing the same amount of protein were electrophoresed through 10% SDS–PAGE and electroblotted onto a nitrocellulose membrane (Schleicher and Schuell BioScience, Keene, NH, USA), which was interacted with the appropriate antibodies. The blots were developed and analyzed by ChemiDoc™ XRS (Bio-Rad laboratories, GmbH, Munich, Germany).

4.10. Immunofluorescence and Confocal Microscopy

Brains of adult flies were fixed with 4% paraformaldehyde for 60 min. Following rinsing with PBT (1× PBS supplemented with 0.3% Triton X-100), primary antibody, diluted in BBT (1× PBS supplemented with 0.1% BSA, 0.1% Tween-20 and 250 mM NaCl) was added for overnight incubation at 4 °C with shaking. Following three washes with PBT, secondary antibodies were added and were incubated under shaking for 2 h at room temperature. After three washes with PBT, the brain samples were mounted with Galvanol mounting reagent (Mowiol 4-88, Calbiochem, CA, USA). Slides were visualized using an LSM510 Meta (ZEISS) confocal microscope. For quantitative studies, Z-projections of confocal sections (exposed and processed identically) were analyzed. Images of a given experiment were exposed and processed identically, unless otherwise detailed. Captured images were analyzed using ImageJ software. The ImageJ software ((NIH, Bethesda, MD, USA) automatically subtracts background staining. Pixel intensity (in arbitrary units) was used to quantify fluorescence in the indicated experiments. Data was statistically evaluated using one-way ANOVA with post-hoc Dunnett test.

4.11. Chaperone Treatment

Eighty microliters of 1-deoxygalactonojirimycin hydrochloride (DGJ/AT1001/migalastat) purchased from Sigma-Aldrich, Israel, at concentrations of 10 µM, 20 µM or 50 µM were poured on top of 10 mL food-containing vials, which were kept at room temperature for at least 1 day before use. Chaperone was diluted in DDW from a 10 mM stock solution.

4.12. Climbing Assay

Climbing behavior of adult flies was measured using a countercurrent apparatus essentially as described elsewhere [70]. Briefly, groups of 30 flies (both males and females) were given 10 min to adapt in the starting tube, which could slide along the apparatus, and then 20 s to move upwards against gravity to the upper frame's tube. The top frame of tubes was then shifted to the right so that the start tube came into register with a second bottom tube, and flies, which successfully climbed up, were tapped down again, falling into tube 2. The upper frame was then returned to the left, and the flies were once again allowed to climb into the upper tube. After five runs, the number of the flies in each tube was counted. For each time point, at least four cohorts from each genotype were scored. The Climbing index (CI) was calculated using the following formula: CI (the weighted mean) = $\Sigma(mn_m)/N$; m–number of test vial, nm–number of flies in the m^{th} vial, N–total number of flies. CI ranged from 1 (min) to 6 (max).

4.13. Survival Assay

For each fly strain, 10 vials, each containing 5 males and 5 females (total of 100 flies), was maintained on food from day one post-eclosion. Flies were flipped into tubes containing fresh food every second day, and deaths were recorded. Kaplan–Meier was used to plot survival using the XLSTAT software. Results are presented relative to the initial number of flies in each vial.

4.14. Statistical analysis

Parametric statistical tests were used for all comparisons. Data, obtained from 3–6 independent experiments (in each experiment, 10–30 flies were used), were expressed as mean ± standard error of the mean (SEM). Comparisons between the groups were performed using one-way, two-way or

three-way ANOVA according to the number of variants, followed by either post-hoc Dunnett test or t-test. The tests used for the different experiments are detailed in each figure legend. All statistical analyses were preformed using the SPSS software (IBM Corp., Armonk, NY, USA). Kaplan–Meier analysis was performed using the XLSTAT software (Addinsoft Inc., New York, NY, USA).

Supplementary Materials: The following is available online at http://www.mdpi.com/1422-0067/21/19/7397/s1, Figure S1: Mutant α-Gal A undergoes ERAD.

Author Contributions: Conceptualization, M.H.; methodology, H.B., M.P., G.M., J.L.; wring—original draft preparation, M.H., H.B.; writing—review and editing, M.H., H.B., M.P., G.M., J.L., A.R.; supervision, M.H.; funding acquisition, M.H.; All authors have read and agreed to the published version of the manuscript.

Funding: This study was supported by an Unrestricted Research Grant from Pfizer Pharmaceuticals Israel Ltd., (Ramot no. 4691).

Conflicts of Interest: The authors declare no conflict of interest. The funder had no role in the design of the study; in the collection, analyses or interpretation of data; in the writing of the manuscript; or in the decision to publish the results.

Abbreviations

DW	Double distilled water
ER	Endoplasmic reticulum
ERAD	Endoplasmic reticulum associated degradation
M-MLV	Murine Molony leukemia virus
PCR	Polymerase chain reaction
SDS-PAGE	Sodium dodecyl sulphate polyacrylamise gel electrophoresis
SEM	Standard error of mean
TH	Tyrosine hydroxylase
qRT-PCR	Quantitative real time PCR
UPR	Unfolded protein response
WT	Wild type

References

1. Walter, P.; Ron, D. The unfolded protein response: From stress pathway to homeostatic regulation. *Science* **2011**, *334*, 1081–1086. [CrossRef] [PubMed]
2. Wang, S.; Kaufman, R.J. The impact of the unfolded protein response on human disease. *J. Cell Biol.* **2012**, *197*, 857–867. [CrossRef] [PubMed]
3. Bendikov-Bar, I.; Maor, G.; Filocamo, M.; Horowitz, M. Ambroxol as a pharmacological chaperone for mutant glucocerebrosidase. *Blood Cells Mol. Dis.* **2013**, *50*, 141–145. [CrossRef] [PubMed]
4. Bendikov-Bar, I.; Ron, I.; Filocamo, M.; Horowitz, M. Characterization of the ERAD process of the L444P mutant glucocerebrosidase variant. *Blood Cells Mol. Dis.* **2011**, *46*, 4–10. [CrossRef]
5. Braunstein, H.; Maor, G.; Chicco, G.; Filocamo, M.; Zimran, A.; Horowitz, M. UPR activation and CHOP mediated induction of GBA1 transcription in Gaucher disease. *Blood Cells Mol. Dis.* **2018**, *68*, 21–29. [CrossRef]
6. Maor, G.; Rencus-Lazar, S.; Filocamo, M.; Steller, H.; Segal, D.; Horowitz, M. Unfolded protein response in Gaucher disease: From human to Drosophila. *Orphanet J. Rare Dis.* **2013**, *8*, 140. [CrossRef]
7. Ron, I.; Horowitz, M. ER retention and degradation as the molecular basis underlying Gaucher disease heterogeneity. *Hum. Mol. Genet.* **2005**, *14*, 2387–2398. [CrossRef]
8. Maor, G.; Cabasso, O.; Krivoruk, O.; Rodriguez, J.; Steller, H.; Segal, D.; Horowitz, M. The contribution of mutant GBA to the development of Parkinson disease in Drosophila. *Hum. Mol. Genet.* **2016**, *25*, 2712–2727. [CrossRef]
9. Aerts, J.M.F.G.; Groener, J.E.; Kuiper, S.; Donker-Koopman, W.E.; Strijland, A.; Ottenhoff, R.; Van Roomen, C.; Mirzaian, M.; Wijburg, F.A.; Linthorst, G.E.; et al. Elevated globotriaosylsphingosine is a hallmark of Fabry disease. *Proc. Natl. Acad. Sci. USA* **2008**, *105*, 2812–2817. [CrossRef]
10. Brady, R.O.; Gal, A.E.; Bradley, R.M.; Martensson, E.; Warshaw, A.L.; Laster, L. Enzymatic defect in Fabry's disease. *N. Engl. J. Med.* **1967**, *276*, 1163–1167. [CrossRef]

11. Desnick, R.J.; Wasserstein, M.P. Fabry disease: Clinical features and recent advances in enzyme replacement therapy. *Adv. Nephrol. Necker Hosp.* **2001**, *31*, 317–339. [PubMed]
12. Kint, J.A. The enzyme defect in Fabry's disease. *Nat. Cell Biol.* **1970**, *227*, 1173. [CrossRef] [PubMed]
13. Okada, S.; O'Brien, J.S.; Chase, L.R.; Aurbach, G.D. Generalized gangliosidosis: Beta-galactosidase deficiency. *Science* **1968**, *160*, 1002–1004. [CrossRef] [PubMed]
14. Brady, R.O. Enzymatic abnormalities in diseases of sphingolipid metabolism. *Clin. Chem.* **1967**, *13*, 565–577. [CrossRef]
15. Saifudeen, Z.; Desnick, R.J.; Ehrlich, M. A mutation in the 5′ untranslated region of the human α-galactosidase A gene in high-activity variants inhibits specific protein binding. *FEBS Lett.* **1995**, *371*, 181–184. [CrossRef]
16. Germain, D.P. Fabry disease. *Orphanet J. Rare Dis.* **2010**, *5*, 30. [CrossRef]
17. McCafferty, E.H.; Scott, L.J. Migalastat: A review in Fabry disease. *Drugs* **2019**, *79*, 543–554. [CrossRef]
18. Doheny, D.; Srinivasan, R.; Pagant, S.; Chen, B.; Yasuda, M.; Desnick, R.J. Fabry disease: Prevalence of affected males and heterozygotes with pathogenic GLA mutations identified by screening renal, cardiac and stroke clinics, 1995–2017. *J. Med Genet.* **2018**, *55*, 261–268. [CrossRef]
19. Whybra, C.; Wendrich, K.; Ries, M.; Gal, A.; Beck, M. Clinical manifestation in female Fabry disease patients. *Contrib. Nephrol.* **2001**, 245–250. [CrossRef]
20. Wilcox, W.R.; Oliveira, J.P.; Hopkin, R.J.; Ortiz, A.; Banikazemi, M.; Feldt-Rasmussen, U.; Sims, K.; Waldek, S.; Pastores, G.M.; Lee, P.; et al. Females with Fabry disease frequently have major organ involvement: Lessons from the Fabry registry. *Mol. Genet. Metab.* **2008**, *93*, 112–128. [CrossRef]
21. Lukas, J.; Giese, A.-K.; Markoff, A.; Grittner, U.; Kolodny, E.; Mascher, H.; Lackner, K.J.; Meyer, W.; Wree, P.; Saviouk, V.; et al. Functional characterisation of alpha-galactosidase a mutations as a basis for a new classification system in Fabry disease. *PLoS Genet.* **2013**, *9*, e1003632. [CrossRef] [PubMed]
22. Benjamin, E.R.; Della Valle, M.C.; Wu, X.; Katz, E.; Pruthi, F.; Bond, S.; Bronfin, B.; Williams, H.; Yu, J.; Bichet, D.-G.; et al. The validation of pharmacogenetics for the identification of Fabry patients to be treated with migalastat. *Genet. Med.* **2016**, *19*, 430–438. [CrossRef] [PubMed]
23. Brady, R.O. Enzyme replacement for lysosomal diseases. *Annu. Rev. Med.* **2006**, *57*, 283–296. [CrossRef] [PubMed]
24. Lidove, O.; West, M.L.; Pintos-Morell, G.; Reisin, R.; Nicholls, K.; Figuera, L.E.; Parini, R.; Carvalho, L.R.; Kampmann, C.; Pastores, G.M.; et al. Effects of enzyme replacement therapy in Fabry disease-A comprehensive review of the medical literature. *Genet. Med.* **2010**, *12*, 668–679. [CrossRef] [PubMed]
25. Schiffmann, R.; Brady, R.O. Development of enzyme replacement therapy for Fabry disease. In *Fabry Disease: Perspectives from 5 Years of FOS*; Oxford PharmaGenesis: Oxford, UK, 2006.
26. Barbey, F.; Lidove, O.; Schwarting, A. Fabry nephropathy: 5 years of enzyme replacement therapy-A short review. *Clin. Kidney J.* **2007**, *1*, 11–19. [CrossRef]
27. Schiffmann, R.; Hughes, D.; Linthorst, G.E.; Ortiz, A.; Svarstad, E.; Warnock, D.G.; West, M.L.; Wanner, C.; Bichet, D.-G.; Christensen, E.I.; et al. Screening, diagnosis, and management of patients with Fabry disease: Conclusions from a "Kidney Disease: Improving Global Outcomes" (KDIGO) Controversies Conference. *Kidney Int.* **2017**, *91*, 284–293. [CrossRef]
28. Araki, K.; Nagata, K. Protein folding and quality control in the ER. *Cold Spring Harb. Perspect. Biol.* **2011**, *3*, a007526. [CrossRef]
29. Cortez, L.; Sim, V. The therapeutic potential of chemical chaperones in protein folding diseases. *Prion* **2014**, *8*, 197–202. [CrossRef]
30. Fan, J.-Q. A contradictory treatment for lysosomal storage disorders: Inhibitors enhance mutant enzyme activity. *Trends Pharmacol. Sci.* **2003**, *24*, 355–360. [CrossRef]
31. Fan, J.-Q.; Ishii, S.; Asano, N.; Suzuki, Y. Accelerated transport and maturation of lysosomal α-galactosidase A in Fabry lymphoblasts by an enzyme inhibitor. *Nat. Med.* **1999**, *5*, 112–115. [CrossRef]
32. Asano, N.; Ishii, S.; Ikeda, K.; Kato, A.; Fan, J.-Q.; Kizu, H.; Yasuda, K.; Martin, O.R. In vitro inhibition and intracellular enhancement of lysosomal α-galactosidase A activity in Fabry lymphoblasts by 1-deoxygalactonojirimycin and its derivatives. *JBIC J. Biol. Inorg. Chem.* **2000**, *267*, 4179–4186. [CrossRef] [PubMed]
33. Benjamin, E.R.; Flanagan, J.J.; Schilling, A.; Chang, H.H.; Agarwal, L.; Katz, E.; Wu, X.; Pine, C.; Wustman, B.; Desnick, R.J.; et al. The pharmacological chaperone 1-deoxygalactonojirimycin increases α-galactosidase A levels in Fabry patient cell lines. *J. Inherit. Metab. Dis.* **2009**, *32*, 424–440. [CrossRef] [PubMed]

34. Germain, D.P.; Fan, J.-Q. Pharmacological chaperone therapy by active-site-specific chaperones in Fabry disease: In vitro and preclinical studies. *Int. J. Clin. Pharmacol. Ther.* **2009**, *47*, S111–S117. [PubMed]
35. Hamanaka, R.; Shinohara, T.; Yano, S.; Nakamura, M.; Yasuda, A.; Yokoyama, S.; Fan, J.-Q.; Kawasaki, K.; Watanabe, M.; Ishii, S. Rescue of mutant α-galactosidase A in the endoplasmic reticulum by 1-deoxygalactonojirimycin leads to trafficking to lysosomes. *Biochim. et Biophys. Acta (BBA)-Mol. Basis Dis.* **2008**, *1782*, 408–413. [CrossRef] [PubMed]
36. Lukas, J.; Cimmaruta, C.; Liguori, L.; Pantoom, S.; Iwanov, K.; Petters, J.; Hund, C.; Bunschkowski, M.; Hermann, A.; Cubellis, M.V.; et al. Assessment of gene variant amenability for pharmacological chaperone therapy with 1-deoxygalactonojirimycin in Fabry disease. *Int. J. Mol. Sci.* **2020**, *21*, 956. [CrossRef] [PubMed]
37. Seemann, S.; Ernst, M.; Cimmaruta, C.; Struckmann, S.; Cozma, C.; Koczan, D.; Knospe, A.-M.; Haake, L.R.; Citro, V.; Bräuer, A.U.; et al. Proteostasis regulators modulate proteasomal activity and gene expression to attenuate multiple phenotypes in Fabry disease. *Biochem. J.* **2020**, *477*, 359–380. [CrossRef] [PubMed]
38. Duffy, J.B. GAL4 system indrosophila: A fly geneticist's swiss army knife. *Genesis* **2002**, *34*, 1–15. [CrossRef]
39. Brand, A.H.; Perrimon, N. Targeted gene expression as a means of altering cell fates and generating dominant phenotypes. *Development* **1993**, *118*, 401–415.
40. Smith, J.E.; Cronmiller, C. Faculty of 1000 evaluation for The Drosophila daughterless gene autoregulates and is controlled by both positive and negative cis regulation. *Development* **2001**, *128*, 4705–4714. [CrossRef]
41. Maley, F.; Trimble, R.B.; Tarentino, A.L.; Plummer, T.H. Characterization of glycoproteins and their associated oligosaccharides through the use of endoglycosidases. *Anal. Biochem.* **1989**, *180*, 195–204. [CrossRef]
42. Trimble, R.B.; Tarentino, A.L. Identification of distinct endoglycosidase (endo) activities in *Flavobacterium meningosepticum*: Endo F1, endo F2, and endo F3. Endo F1 and endo H hydrolyze only high mannose and hybrid glycans. *J. Boil. Chem.* **1991**, *266*, 1646–1651.
43. Narasimhan, S.; Stanley, P.; Schachter, H. Control of glycoprotein synthesis. Lectin-resistant mutant containing only one of two distinct N-acetylglucosaminyltransferase activities present in wild type Chinese hamster ovary cells. *J. Biol. Chem.* **1977**, *252*, 3926–3933. [PubMed]
44. Tai, T.; Yamashita, K.; Ito, S.; Kobata, A. Structures of the carbohydrate moiety of ovalbumin glycopeptide III and the difference in specificity of endo-beta-N-acetylglucosaminidases CII and H. *J. Boil. Chem.* **1977**, *252*, 6687–6694.
45. Goldberg, A.L. Selective inhibitors of the proteasome-dependent and vacuolar pathways of protein degradation in *Saccharomyces cerevisiae*. *J. Biol. Chem.* **1996**, *271*, 27280–27284. [CrossRef]
46. Lee, D.H.; Goldberg, A.L. Proteasome inhibitors: Valuable new tools for cell biologists. *Trends Cell Boil.* **1998**, *8*, 397–403. [CrossRef]
47. Rock, K.L.; Gramm, C.; Rothstein, L.; Clark, K.; Stein, R.; Dick, L.; Hwang, D.; Goldberg, A.L. Inhibitors of the proteasome block the degradation of most cell proteins and the generation of peptides presented on MHC class I molecules. *Cell* **1994**, *78*, 761–771. [CrossRef]
48. Feany, M.B.; Bender, W.W. A Drosophila model of Parkinson's disease. *Nat. Cell Biol.* **2000**, *404*, 394–398. [CrossRef]
49. Mao, Z.; Davis, R.L. Eight different types of dopaminergic neurons innervate the Drosophila mushroom body neuropil: Anatomical and physiological heterogeneity. *Front. Neural Circuits* **2009**, *3*, 5. [CrossRef]
50. Tuttolomondo, A.; Simonetta, I.; Duro, G.; Pecoraro, R.; Miceli, S.; Colomba, P.; Zizzo, C.; Nucera, A.; Daidone, M.; Di Chiara, T.; et al. Inter-familial and intra-familial phenotypic variability in three Sicilian families with Anderson-Fabry disease. *Oncotarget* **2017**, *8*, 61415–61424. [CrossRef]
51. Eng, C.M.; Desnick, R.J. Molecular basis of fabry disease: Mutations and polymorphisms in the human α-galactosidase A gene. *Hum. Mutat.* **1994**, *3*, 103–111. [CrossRef]
52. Okumiya, T.; Ishii, S.; Kase, R.; Kamei, S.; Sakuraba, H.; Suzuki, Y. α-Galactosidase gene mutations in Fabry disease: Heterogeneous expressions of mutant enzyme proteins. *Qual. Life Res.* **1995**, *95*, 557–561. [CrossRef] [PubMed]
53. Romeo, G.; D'Urso, M.; Pisacane, A.; Blum, E.; De Falco, A.; Ruffilli, A. Residual activity of α-galactosidase A in Fabry's disease. *Biochem. Genet.* **1975**, *13*, 615–628. [CrossRef] [PubMed]
54. Shabbeer, J.; Yasuda, M.; Benson, S.D.; Desnick, R.J. Fabry disease: Identification of 50 novel α-galactosidase A mutations causing the classic phenotype and three-dimensional structural analysis of 29 missense mutations. *Hum. Genom.* **2006**, *2*, 1–13. [CrossRef] [PubMed]

55. Ishii, S.; Kase, R.; Okumiya, T.; Sakuraba, H.; Suzuki, Y. Aggregation of the inactive form of human α -galactosidase in the endoplasmic reticulum. *Biochem. Biophys. Res. Commun.* **1996**, *220*, 812–815. [CrossRef]
56. Yam, G.H.-F.; Bosshard, N.; Zuber, C.; Steinmann, B.; Roth, J. Pharmacological chaperone corrects lysosomal storage in Fabry disease caused by trafficking-incompetent variants. *Am. J. Physiol. Physiol.* **2006**, *290*, C1076–C1082. [CrossRef]
57. Yam, G.H.-F.; Zuber, C.; Roth, J. A synthetic chaperone corrects the trafficking defect and disease phenotype in a protein misfolding disorder. *FASEB J.* **2005**, *19*, 12–18. [CrossRef]
58. Movsichoff, F.; Castro, O.A.; Parodi, A.J. Characterization of *Schizosaccharomyces pombe* ER α-Mannosidase: A reevaluation of the role of the enzyme on ER-associated degradation. *Mol. Biol. Cell* **2005**, *16*, 4714–4724. [CrossRef]
59. Fenteany, G.; Standaert, R.; Lane, W.; Choi, S.; Corey, E.; Schreiber, S. Inhibition of proteasome activities and subunit-specific amino-terminal threonine modification by lactacystin. *Science* **1995**, *268*, 726–731. [CrossRef]
60. Ishii, S.; Chang, H.-H.; Kawasaki, K.; Yasuda, K.; Wu, H.-L.; Garman, S.C.; Fan, J.-Q. Mutant α-galactosidase A enzymes identified in Fabry disease patients with residual enzyme activity: Biochemical characterization and restoration of normal intracellular processing by 1-deoxygalactonojirimycin. *Biochem. J.* **2007**, *406*, 285–295. [CrossRef]
61. Andreotti, G.; Citro, V.; De Crescenzo, A.; Orlando, P.; Cammisa, M.; Correra, A.; Cubellis, M.V. Therapy of Fabry disease with pharmacological chaperones: From in silico predictions to in vitro tests. *Orphanet J. Rare Dis.* **2011**, *6*, 66. [CrossRef]
62. Shin, S.-H.; Murray, G.J.; Kluepfel-Stahl, S.; Cooney, A.M.; Quirk, J.M.; Schiffmann, R.; Brady, R.O.; Kaneski, C.R. Screening for pharmacological chaperones in Fabry disease. *Biochem. Biophys. Res. Commun.* **2007**, *359*, 168–173. [CrossRef] [PubMed]
63. Lukas, J.; Scalia, S.; Eichler, S.; Pockrandt, A.-M.; Dehn, N.; Cozma, C.; Giese, A.-K.; Rolfs, A. Functional and clinical consequences of novel α-galactosidase a mutations in Fabry disease. *Hum. Mutat.* **2015**, *37*, 43–51. [CrossRef] [PubMed]
64. Wu, X.; Katz, E.; Della Valle, M.C.; Mascioli, K.; Flanagan, J.J.; Castelli, J.P.; Schiffmann, R.; Boudes, P.; Lockhart, D.J.; Valenzano, K.J.; et al. A pharmacogenetic approach to identify mutant forms of α-galactosidase a that respond to a pharmacological chaperone for Fabry disease. *Hum. Mutat.* **2011**, *32*, 965–977. [CrossRef] [PubMed]
65. Lukas, J.; Pockrandt, A.-M.; Seemann, S.; Sharif, M.; Runge, F.; Pohlers, S.; Zheng, C.; Glaser, A.; Beller, M.; Rolfs, A.; et al. Enzyme enhancers for the treatment of Fabry and Pompe disease. *Mol. Ther.* **2015**, *23*, 456–464. [CrossRef]
66. Maegawa, G.; Tropak, M.B.; Buttner, J.D.; Rigat, B.A.; Fuller, M.; Pandit, D.; Tang, L.; Kornhaber, G.J.; Hamuro, Y.; Clarke, J.T.R.; et al. Identification and characterization of ambroxol as an enzyme enhancement agent for Gaucher disease. *J. Biol. Chem.* **2009**, *284*, 23502–23516. [CrossRef]
67. Khanna, R.; Soska, R.; Lun, Y.; Feng, J.; Frascella, M.; Young, B.; Brignol, N.; Pellegrino, L.; Sitaraman, S.A.; Desnick, R.J.; et al. The pharmacological chaperone 1-deoxygalactonojirimycin reduces tissue globotriaosylceramide levels in a mouse model of Fabry disease. *Mol. Ther.* **2010**, *18*, 23–33. [CrossRef]
68. Young-Gqamana, B.; Brignol, N.; Chang, H.-H.; Khanna, R.; Soska, R.; Fuller, M.; Sitaraman, S.A.; Germain, D.P.; Giugliani, R.; Hughes, D.A.; et al. Migalastat HCl reduces globotriaosylsphingosine (Lyso-Gb3) in Fabry transgenic mice and in the plasma of Fabry patients. *PLoS ONE* **2013**, *8*, e57631. [CrossRef]
69. De Francesco, P.N.; Mucci, J.M.; Ceci, R.; Fossati, C.A.; Rozenfeld, P.A. Higher apoptotic state in Fabry disease peripheral blood mononuclear cells. *Mol. Genet. Metab.* **2011**, *104*, 319–324. [CrossRef]
70. Inagaki, H.K.; Kamikouchi, A.; Ito, K. Methods for quantifying simple gravity sensing in Drosophila melanogaster. *Nat. Protoc.* **2009**, *5*, 20–25. [CrossRef]

International Journal of
Molecular Sciences

MDPI

Article

Mechanistic Insight into the Mode of Action of Acid β-Glucosidase Enhancer Ambroxol

Supansa Pantoom [1], Larissa Hules [1], Christopher Schöll [2], Andranik Petrosyan [2], Maria Monticelli [3], Jola Pospech [2], Maria Vittoria Cubellis [3,4], Andreas Hermann [1,5,6] and Jan Lukas [1,5,*]

[1] Translational Neurodegeneration Section "Albrecht-Kossel", Department of Neurology, University Medical Center Rostock, 18147 Rostock, Germany; supansapantoom@yahoo.com (S.P.); larissa.hules@uni-rostock.de (L.H.); andreas.hermann@med.uni-rostock.de (A.H.)
[2] Leibniz Institute for Catalysis, University of Rostock, 18059 Rostock, Germany; christopher.schoell@ur.de (C.S.); andpharm@gmail.com (A.P.); jola.pospech@catalysis.de (J.P.)
[3] Department of Biology, University Federico II, 80126 Napoli, Italy; maria.monticelli@yahoo.com (M.M.); cubellis@unina.it (M.V.C.)
[4] Istituto di Chimica Biomolecolare—CNR, 80078 Pozzuoli, Italy
[5] Center for Transdisciplinary Neurosciences Rostock (CTNR), University Medical Center Rostock, University of Rostock, 18147 Rostock, Germany
[6] German Center for Neurodegenerative Diseases (DZNE) Rostock/Greifswald, 18147 Rostock, Germany
* Correspondence: jan.lukas@med.uni-rostock.de; Tel.: +49-381-494-4894

Abstract: Ambroxol (ABX) is a mucolytic agent used for the treatment of respiratory diseases. Bioactivity has been demonstrated as an enhancement effect on lysosomal acid β-glucosidase (β-Glu) activity in Gaucher disease (GD). The positive effects observed have been attributed to a mechanism of action similar to pharmacological chaperones (PCs), but an exact mechanistic description is still pending. The current study uses cell culture and in vitro assays to study the effects of ABX on β-Glu activity, processing, and stability upon ligand binding. Structural analogues bromohexine, 4-hydroxybromohexine, and norbromohexine were screened for chaperone efficacy, and in silico docking was performed. The sugar mimetic isofagomine (IFG) strongly inhibits β-Glu, while ABX exerts its inhibitory effect in the micromolar range. In GD patient fibroblasts, IFG and ABX increase mutant β-Glu activity to identical levels. However, the characteristics of the banding patterns of Endoglycosidase-H (Endo-H)-digested enzyme and a substantially lower half-life of ABX-treated β-Glu suggest different intracellular processing. In line with this observation, IFG efficiently stabilizes recombinant β-Glu against thermal denaturation in vitro, whereas ABX exerts no significant effect. Additional β-Glu enzyme activity testing using Bromohexine (BHX) and two related structures unexpectedly revealed that ABX alone can refunctionalize β-Glu in cellula. Taken together, our data indicate that ABX has little in vitro ability to act as PC, so the mode of action requires further clarification.

Keywords: Gaucher disease; small molecule therapy; pharmacological chaperone; drug repositioning; lysosomal storage disease; rare disease; thermal shift assay

check for updates

Citation: Pantoom, S.; Hules, L.; Schöll, C.; Petrosyan, A.; Monticelli, M.; Pospech, J.; Cubellis, M.V.; Hermann, A.; Lukas, J. Mechanistic Insight into the Mode of Action of Acid β-Glucosidase Enhancer Ambroxol. *Int. J. Mol. Sci.* **2022**, *23*, 3536. https://doi.org/10.3390/ijms23073536

Academic Editor: Shoshana Revel-Vilk

Received: 24 February 2022
Accepted: 23 March 2022
Published: 24 March 2022

Publisher's Note: MDPI stays neutral with regard to jurisdictional claims in published maps and institutional affiliations.

1. Introduction

The pharmacological chaperones (PCs) represent a novel form of therapy for diseases involving protein misfolding, such as lysosomal storage disorders (LSDs). PCs specifically bind to folded or partially folded proteins to provide enhanced stabilization and enable trafficking of mutant but intrinsically functional protein to the target organelle [1,2]. Most PCs are reversible competitive inhibitors of their target protein, even though the inhibitory activity is not desired [3]. The development of efficient PCs is an unmet need for all LSDs as the efficacy of existing therapies (e.g., enzyme replacement therapy and substrate reduction therapy) is limited by their inability to cross the blood-brain barrier or by undesirable side effects.

Gaucher disease (GD; MIM# 230800, 230900, 231000) is a rare autosomal LSD caused by mutations in the *GBA1* gene (MIM# 606463) encoding for the lysosomal enzyme acid β-glucosidase (β-Glu, EC 3.2.1.45). GD has an estimated incidence of 1/40,000 in the general population and an incidence of 1/1000 in the Ashkenazi Jewish population [4]. The resulting decrease in enzymatic activity leads to a progressive accumulation of glucosylceramide and glucosylsphingosine in lysosomes, causing organ enlargement, anemia, and bone disease (Type I) and additional neurological impairment (Types II and III) [5]. A range of different *GBA1* gene variants, including the prevalent p.Asn370Ser allele associated with Type I GD, have been tested for their response to various PCs [6–8], so GD can be considered a reasonable target for PC development. One such PC, the iminosugar isofagomine (IFG), selectively inhibits β-Glu in cell lysates in a competitive manner, with IC_{50} values of 30 (5) nM (wildtype β-Glu) and 128 (18) nM (p.Asn370Ser variant) at pH 5.2 (7.2) using 3 mM of 4-methylumbelliferyl-β-D-glucopyranoside (4-MUG) [9]. A similar result was obtained for wildtype β-Glu in a later study using recombinant enzyme [1]. A six-month Phase 2 clinical trial was carried out in 19 adults with Type I GD, but the drug was not advanced to Phase 3 development due to a lack of meaningful reduction in disease symptoms in the majority of the patients [10]. It can be assumed that potent competitive inhibitors harbor the risk of interfering with the natural reaction conditions in the cells in an adverse manner. Thus, it may seem that the development of either allosteric, non-inhibitory, or less-potent isosteric PCs is imperative to comply with safety demands in the drug approval process.

Around the same time as IFG failed in clinical trials, the substituted benzylamin ambroxol (trans-4-(2-amino-3,5-dibromobenzylamino)-cyclohexanol ($C_{13}H_{18}Br_2N_2O$, ABX) was identified by thermal denaturation assay [11]. In this study, recombinant β-Glu was subjected to heat treatment at 51 °C for 12 min, and it was found that ABX-treated β-Glu exhibited higher enzyme activity compared to untreated enzyme. The evident advantage of this assay was that ABX was detected by means of its β-Glu enzyme stabilizing effect rather than β-Glu inhibition. Maegawa and colleagues further investigated the inhibition mode and binding site and characterized ABX as a mixed-type inhibitor that exerts its inhibitory effect in the micromolar range [11]. It is of note that ABX is a derivative of BHX; however, BHX did not prove to be a PC but exhibited inhibitory function towards β-Glu [1,11,12]. Numerous studies followed in which patient fibroblasts with different mutations, e.g., p.Arg120Trp, p.Phe213Ile, and in some cases p.Leu444Pro, responded significantly positively to ABX exposure [13–15]. The positive effects could be reproduced in other cell and animal models, such as mouse and fruit fly [16–19]. ABX treatment achieved a positive outcome on blood parameters and organ volume in a pilot study of six previously untreated Type I GD patients and was well-tolerated [20]. Later studies concluded with a similarly promising result in Type III GD patients using ABX as either mono- or combination treatment with enzyme replacement therapy [21,22].

Successive studies suggested that ABX does not act solely as a PC but also at the cell biological level as a transcriptional regulator, for example by increasing *GBA1* and transcription factor *TFEB* mRNA [23,24] and the transcription of the ER stress-related transcription factor CHOP [19,25], which are thought to play a role in the expression process of β-Glu [26,27]. However, no conclusive link has been established between chaperoning and the influence on cellular physiology. Similarly, in studies on Fabry disease, a beneficial effect of ABX on mutant α-Galactosidase A (α-Gal) was observed, but the mechanism of action remained obscure [28,29]. Nevertheless, ABX was not efficient in single application, whereas combinatory treatment indicated a PC-supportive effect. Furthermore, the study by Seemann et al. [29] demonstrated that the efficient α-Gal enhancer compounds each showed both an inhibitory effect on the proteasome and a positive gene regulatory effect on the α-Gal target gene itself. Neither effect could be shown for ABX. Since both the α-Gal and β-Glu data do not currently allow the enzyme-enhancing effect of ABX to be mechanistically termed "chaperoning", in the present work we have studied the effects of ABX and IFG on β-Glu in various biochemical and cell biological experiments. There are remarkable differences in the processing and stability of the enzyme under IFG and

ABX influence in cells, and the investigation in a quantifiable in vitro β-Glu thermostability assay indicated a much weaker ABX-mediated stabilization effect.

2. Results and Discussion

2.1. β-Glu Enzyme Is Weakly Inhibited by Ambroxol

Most of the identified PCs for lysosomal hydrolases are isosteric inhibitors. They are biosimilar sugar compounds of the natural substrate. The benzylamin compounds ABX and BHX are an exception among the inhibitor structures for β-Glu. All these structures have in common the aim to increase the stability of both normal and mutant enzyme forms. In this way, the activity of functionally compromised enzyme variants can be recovered. Unlike IFG, which was confirmed as a competitive inhibitor, the mode of action for ABX and BHX was characterized as mixed inhibition [1]. In this study, we reproduced the inhibitory activity of the substances. The half-maximal inhibitory concentration (IC_{50}) of the active site-inhibitor IFG was 0.32 ± 0.0015 nM at pH 4.7 when 0.026 µM recombinant β-Glu was used and at a substrate concentration of 1.5 mM 4-MUG (Figure 1a,d). The considerable dependence on pH, enzyme-substrate ratio, and other parameters such as buffer substance were not considered in our experiment. The same applies to the other experiment series. For ABX, an inhibition effect was measured that was almost three orders of magnitude lower under the applied conditions, with an IC_{50} of 254.0 ± 0.12 µM (Figure 1b,d). The half-maximal inhibitory concentration represents the concentration of an inhibitor that is required to reduce enzyme activity by 50%. For ABX, we defined it as the concentration at which the half-maximal inhibitory effect was achieved, since the inhibition by ABX was incomplete (as known from previous studies) [12,30]. In the current experiment, the residual enzyme activity was about 70%. Remarkably, BHX had no significant inhibitory effect in the tested concentration range (Figure 1c,d). While it has been suggested that the strength of the inhibitory effect has a positive predictive value for the efficiency of the chaperone effect [31], robust data for this hypothesis are not available. At this point, the statement can once again be supported that IFG is a strong inhibitor while ABX is a weak inhibitor. It should be noted that IFG shows a proven altered kinetics with mutated enzyme [9], which can also be assumed for ABX as different binding affinities have been calculated using molecular dynamics simulation for different drugs to the abnormal enzyme variants [32].

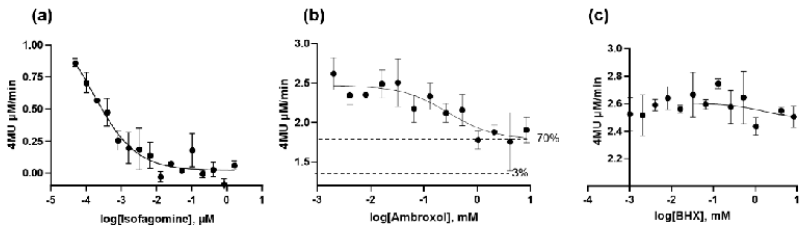

(d)

Cmpd	IC_{50}, µM
IFG	0.32 ± 0.0015
ABX	254.0 ± 0.12
BHX	>1500 µM (No inhibition effect)

Figure 1. Inhibition of recombinant acid β-glucosidase (β-Glu). Endpoint enzyme activity measurement was recorded in the presence of different concentrations of isofagomine (IFG) (**a**), ambroxol (ABX) (**b**), and bromohexine (BHX) (**c**) after a 20 min incubation phase using 1.5 mM 4-methylumbelliferyl-β-D-glucopyranoside (4-MUG) synthetic substrate at pH 4.7. (**d**) IC_{50} was calculated from the dose–response curves using the function "log(inhibitor) vs. response" (GraphPad Prism 5 for Windows, GraphPad Software, La Jolla, CA, USA).

2.2. Enzyme Activity Is Enhanced in Cell Culture

The p.Asn370Ser mutation is the most common GD associated mutation. It is present in over 70% of Ashkenazi Jewish Type I GD patients (who are either homoallelic or heteroallelic with another GD mutation) [33]. We analyzed the PC response in two p.Asn370Ser/84GG compound heterozygous cell lines: GM00852 and GM00372. The two cell lines exhibited β-Glu enzyme activity of 8.3 (±1.4) nmol 4-MUG × mg protein^{-1} × h^{-1} and 5.0 (±0.5) nmol 4-MUG × mg protein^{-1} × h^{-1}, respectively. The wildtype cell line used for comparison, GM01653, exhibited β-Glu activity of 83.6 (±10.3) nmol 4-MUG × mg protein^{-1} × h^{-1} (Figure 2a–c). The reported activity of the p.Asn370Ser mutant ranges from 14% to 30% [6,33]. The somewhat lower percentage activity of the two GD lines under investigation here might be explained by the fact that the second allele is a NULL allele carrying the nonsense mutation 84GG [34]. ABX and IFG treatment of the cells for 5 days plus a short washout step of 6 h showed significant responsiveness of β-Glu in both GD lines (Figure 2a,b) and maintenance of activity in the WT cells (Figure 2c).

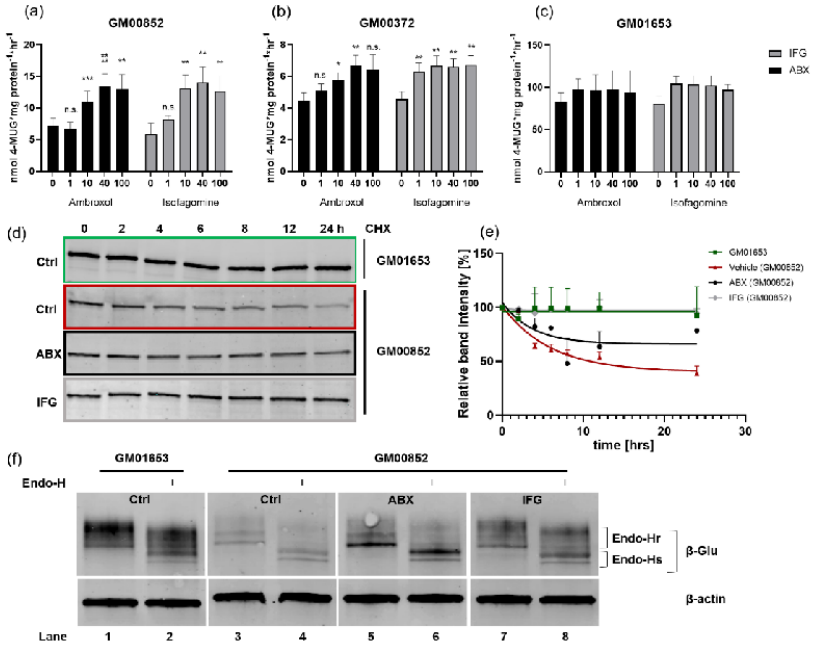

Figure 2. Acid β-glucosidase (β-Glu) enzyme activity, stability, and glycosylation in compound-treated patient fibroblasts. (**a–c**) β-Glu activity in ambroxol/isofagomine (ABX/IFG)-treated cells. Three cell lines of unrelated patients harboring either compound heterozygous p.Asn370Ser/84GG (GM00852, GM00372) mutations or wildtype *GBA1* (GM01653) were cultured for 5 days in absence and presence of ABX (black columns) or IFG (grey columns). The cells were harvested following a 6 h washout period, lysed, and subjected to enzyme measurement using 3 mM 4-methylumbelliferyl-β-D-glucopyranoside (4-MUG). Data are provided as mean ± SEM from 6–12 (**a**,**b**) and 3 (**c**) independent experiments. Differences between the groups were analyzed using one-way ANOVA. Post-hoc Dunnett test was used to analyze each column with the respective value of the untreated cells (significance level is represented by *, **, *** as *p*-values of 0.05, 0.01 and 0.001); n.s., not significant. (**d**) Cycloheximide (CHX) chase experiment. Patient fibroblasts of line GM00852 and control cells (GM01653) were cultured for 5 days in the presence or absence of treatment. Then, in addition to treatment, CHX was added for at 0, 2, 4, 6, 8, 12, and 24 h to study intracellular stability of β-Glu. Cell lysates containing 20–30 µg were digested with PNGase F to obtain a singular protein band in

immunoblot using anti-β-Glu (2E2) antibody. (**e**) Decay curves of β-Glu in fibroblast cells. Each β-Glu band was normalized to its corresponding β-Actin band (not shown). All normalized values obtained were referenced to the 0 h time point of each treatment series before CHX chase start (100%). The values are provided as mean ± SD from 2–3 independent experiments. For each treatment regimen, a nonlinear fit analysis of the resulting values was performed. (**f**) Glycosylation analysis of cellular β-Glu. Cell lysates of ABX, IFG or control-treated fibroblasts were subjected to Endo-H digestion and Western blot. Qualitative band analysis was repeated in two independent experiments: Endo-Hr, Endoglycosidase H-resistant; Endo-Hs, Endoglycosidase H-sensitive.

GM00852 cells showed increases of up to 14.1 (±2.5) nmol 4-MUG × mg protein^{-1} × h^{-1} and 13.5 (±1.9) nmol 4-MUG × mg protein^{-1} × h^{-1} after treatment with IFG and ABX, respectively, at the most effective concentrations of 40 μM each (Figure 2a). GM00372 had elevated β-Glu activity up to 6.7 nmol 4-MUG × mg protein^{-1} × h^{-1} for IFG and ABX at 100 μM and 40 μM, respectively. In a previous study on a series of deoxynojirimycin derivatives as PC candidates, the two GD lines showed maximum responsiveness of 1.7-fold (GM00372) and up to 2.4-fold (GM00852) after 4 days of treatment [35]. In other studies with cells carrying the p.Asn370Ser mutation, similar relative increases were also observed after application of different molecular drugs [7,35–39]. The values are generally in the same range as the fold changes from the analyses carried out here (Table 1). IFG showed a weak, insignificant β-Glu chaperoning activity of 1.3-fold (1–100 μM) on the wildtype enzyme in GM01653 cells. ABX also barely affected the activity (1.1-fold increase at 5–40 μM). However, it is an important indication of the safety that normal activity is not hampered by either of the PC treatments. Specifically, PCs for β-Glu might be a potential drug in combating Parkinson's disease [13,40] due to the association between mutations in the *GBA1* gene and an increased risk of early Parkinsonism [41,42]. These patients carry the WT allele in addition to a mutant *GBA1* allele. It has previously been demonstrated that cells carrying the p.Leu444Pro mutation are amenable to ABX [11,14]. We did not intend to reproduce these results in this study because we concluded that the positive effects of ABX and IFG on mutant β-Glu activity in cell culture has been sufficiently verified. Another indication of the safety of the treatment is the result of the MTT viability assay (Supplementary Materials Figure S1a). Only high ABX concentrations (>40 μM) showed slightly toxic effects in all three cell lines in vitro. Since it is known that even long-term treatment with a high dose of ABX of up to 21 mg/kg/day is well-tolerated by the organism [43], it cannot be excluded that the ABX toxicity here is a cell-culture-specific outcome.

Table 1. Maximum acid β-glucosidase (β-Glu) activity increases in cells.

Cmpd	β-Glu Activity [FC] (GM00852)	β-Glu Activity [FC] (GM00372)	β-Glu Activity [FC] (GM01653)
ABX	2.0 ± 0.15 † (40 μM), ****	1.6 ± 0.12 (40 μM), **	1.3 ± 0.12 (20 μM), n.s.
IFG	2.4 ± 0.17 (40 μM), **	1.6 ± 0.16 (100 μM), **	1.3 ± 0.17 (100 μM), n.s.
BHX	1.1 ± 0.09 (40 μM), n.s.	n/a	n/a
D1	1.3 ± 0.16 (40 μM), n.s.	n/a	n/a
D2	1.2 ± 0.05 (40 μM), n.s.	n/a	n/a

Experiments were repeated ($n = 6$; except † $n = 12$). Statistical analysis was carried out as specified in the legend for Figure 2a–c. Asterisks indicate significance level compared to the untreated state: **, $p < 0.01$; ****, $p < 0.0001$; n.s., not significant; n/a, not analyzed.

2.3. Differential β-Glu Stability and Processing Level Following ABX and IFG Treatment

Treatment with active-site-occupying compounds leads to a prolongation of the half-life of the mutant enzyme [44]. To determine whether stabilization of β-Glu in GM00852 is equally efficient, we cultured the cells for 5 days with or without addition of ABX or IFG. Thereafter, the cells were treated with the protein translation inhibitor cycloheximide (CHX) for an additional 2, 4, 6, 8, 12, and 24 h to prevent de novo protein synthesis. PC treatment was continued in each case. We found that ABX was able to slow intracellular β-Glu degradation compared to the native state (Figure 2d,e). After 24 h, 61.5% of native β-Glu

(Figure 2e, red curve) was degraded. ABX-treated intracellular β-Glu showed degradation by 21.5%, less than half of the untreated enzyme (black curve). IFG was so efficient that after 24 h hardly any protein degradation was detectable (gray curve). The wildtype enzyme in GM01653 cells (Figure 2e, inlayed picture, green curve) also showed stable enzyme levels and insignificant β-Glu degradation.

Lysosomal enzymes are synthesized in the ER. N-glycan conjugation allows further transport to the Golgi apparatus, where sugar-chain modification leads to the formation of high-order complex carbohydrates. Endoglycosidase H (Endo-H) cleaves high-mannose but not complex oligosaccharides. The Endo-H reaction therefore identifies post-Golgi processed protein by causing Endo-H sensitive (Endo-Hs) protein to undergo a size shift, whereas Endo-H resistant (Endo-Hr) protein does not change size. Thus, indirect statements about the cellular localization of proteins can be made. After 5 days of culturing GD fibroblasts with the appropriate treatment and harvesting without a washout period, cell lysates were obtained. The results of this experiment are shown in Figure 2f. The first finding is that mutant p.Asn370Ser β-Glu in GM00852 had approximately 36% residual protein level (Figure 2f, lane 3) compared with wildtype enzyme in GM01653 cells (Figure 2f, lane 1). Endo-H handled samples showed Endo-Hr and Endo-Hs protein fractions at around 67 kDa and 54 kDa, respectively. The overall increase of β-Glu total enzyme by the treatments with ABX and IFG compared to the untreated condition is evident. The p.Asn370Ser β-Glu of IFG-treated cells showed a wildtype-like band pattern before and after Endo-H digestion. ABX-treated enzyme shows a characteristic, particularly pronounced Endo-Hs β-Glu band in the blot, while less Endo-Hr form was expressed.

2.4. ABX-Related Structures Do Not Increase Intracellular p.Asn370Ser β-Glu Activity

As mentioned above, BHX had no effect in the former chaperone study [11]. We synthesized two related BHX/ABX derivatives: 4-hydroxybromohexine (D1) contains an additional hydroxyl substituent on the cyclohexyl ring of bromohexine, yielding (1s,4s)-4-((2-amino-3,5-dibromobenzyl)(methyl)amino)cyclohexan-1-ol; in addition, the nor-derivative of bromohexine 2,4-dibromo-6-((cyclohexylamino)methyl)aniline (norbromohexine, D2) was synthesized. The latter structure lacks both the hydroxycyclohexyl and the aminomethyl group. Neither compound had a significant effect on β-Glu activity (Table 1). In silico docking revealed that the binding of ABX to β-Glu is dependent on hydrogen bonding between the 4-hydroxyl group of ABX with Asp127 and Trp381 providing the acceptor and donor sidechains, respectively [45]. We propose that additional H-bond formation between the amino group and Glu235 of the β-Glu enzyme assists in the orientation of the cyclohexane group to point inside the binding pocket (Supplementary Materials Figure S2a). The presence of a methyl group at the amine, as for BHX (and D1), prevents the interaction with Glu235, therefore switching compound orientation so that the dibromophenyl ring is pointing inside the binding pocket instead. In this case, the π-π and salt bridge interactions between the dibromophenyl ring and its positively charged NH2+ with Tyr313 and Ser345, respectively, may compensate for the lack of the hydrogen bonding interaction and, thus, explain the rather similar binding scores of the different compounds (Supplementary Materials Figure S2c). Moreover, this binding model would provide an obvious explanation for the observation that both the presence of the 4-hydroxyl group and the absence of the aminomethyl group are crucial for the intracellular chaperone effect of ABX.

2.5. Stabilizing Capacity of ABX and IFG on β-Glu Enzyme Defined

Heat-induced melting profiles of recombinant β-Glu were recorded by thermal shift at a pH value of 5.5 in the presence of 2 mM compound or respective vehicle as a control. The enzyme was heated from 20 to 90 °C in the presence of Sypro Orange, similar to the recent report for recombinant α-Gal enzyme [46]. ABX had a lesser stabilizing effect than IFG (Figure 3). This reflects the fact that ABX has lower affinity than IFG for β-Glu

(K_i 10 µM and 0.02 µM, respectively) [1]. The denaturing temperature of ABX-treated β-Glu was 53.6 °C, which corresponded to a ΔT_M of merely +2.3 °C (Figure 3a,c) at a concentration in the millimolar range, whereas ABX plasma peak concentration can be considered well below 1 mM even in high-dose treatments [43]. IFG effectively stabilized the β-Glu enzyme with a ΔT_M of +22 °C up to 64.0 °C (Figure 3b,c). It should be noted that a pronounced solvent effect was observed with ethanol (Figure 3b). BHX showed a similar low stabilizing effect to ABX with a ΔT_M of +1.2 °C (Figure 3c). Hence, we show here that ABX only mildly stabilizes β-Glu in vitro, whereas the active site-specific competitive inhibitor IFG produced a significant increase in thermodynamic heat resistance of β-Glu. It is unlikely that technical aspects hamper the elucidation of stable enzyme:ABX interaction in vitro since previous reports on the inhibitory effect of ABX cover a broad range of conditions [1,7,39] with robust outcomes, indicating that the stabilizing effect cannot be enhanced dramatically by changing assay conditions. Effective PCs typically have binding affinities in the nanomolar to low micromolar range. Usually this is reflected not only in the inhibitory effect but also in a stabilization of the target enzyme in vitro while the enzyme: PC complex is formed [46,47]. Thus, the β-Glu stabilizing effect of ABX observed intracellularly is most likely not due to direct interaction between the molecules alone. Although it is conceivable that intracellular binding of the enzyme to ABX lowers the energy needed for folding so the complex can be shuttled to the lysosome, the observed incomplete processing of the enzyme in fibroblasts argues against it. Moreover, in direct binding studies, unphysiological amounts of ABX were used that exceeded obtainable ABX plasma concentration [11]. In agreement with previous results, we find that ABX is a weak in vitro stabilizer of β-Glu [24], but we cannot observe any significant gene regulatory effect of ABX on gene expression in our cells [29,45]. The formerly described beneficial effects of ABX in GD, as well as the prevention of α-synuclein protein aggregation in Parkinson's disease [24,40], based on putative direct β-Glu stabilizing effects require reevaluation in this light. It is possible that our data may indicate an overestimation of the PC activity of ABX and thus indicate limited applicability of ABX.

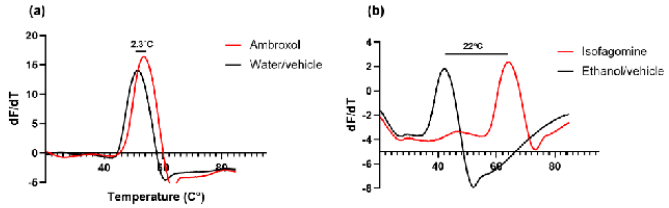

(c)

Compounds	Thermal shift (°C)
IFG	22.0
ABX	2.3
BHX	1.2

Figure 3. Heat-induced melting profiles of recombinant acid β-glucosidase (β-Glu) with and without ambroxol (ABX) and isofagomine (IFG). Recombinant β-Glu was mixed with different concentrations of ABX (**a**), IFG (**b**), or respective vehicle. Sypro Orange was added to a final concentration of 12.5 µM. Incrementally increased temperature over a range of 20–90 °C using the Lightcycler qRT PCR system resulted in increasing denaturation of the enzyme. (**c**) Thermal shift values were obtained by using first derivatives of raw data and were depicted for IFG, ABX, and bromohexine (BHX).

In Pompe and Fabry diseases, the outcome of a combination therapy consisting of ERT and PCT utilizing the two iminosugar PCs DNJ and DGJ is expected to provide additional benefit over ERT monotherapy [48,49]. The recently published study of a combination therapy of ERT + ABX in Type III GD attended to increased β-Glu activity and encourage normalization of the lyso-Gb1 biomarker [43]. PCT can achieve effects via two different modes of action: firstly, by functionalizing and increasing the level of endogenous mutant

β-Glu and secondly by stabilizing and thus increasing the half-life of the recombinant replacent enzyme of ERT. It can be assumed from our in vitro data that ABX did not act via the second mechanism because the low stabilizing effect of ABX suggests that it is not suitable as an adjuvant for ERT, whereas strong PCs such as the DGJ, DNJ, or IFG iminosugars may be an option.

We hypothesized that a combination therapy consisting of two distinct PCTs using ABX and IFG may be an option because of the apparent partial difference in mechanism of action. A cell culture experiment showed that ABX/IFG combination-treated GM00852 and GM00372 cells displayed additive drug effects on β-Glu enzyme activity elevation compared to monotherapy with either treatment (Supplementary Materials Figure S3). Even though the exact mechanism of action of ABX remains unclear, our data suggest that additional intracellular factors are required to achieve the ABX effect, e.g., by utilizing gene regulatory function and exploiting endogenous molecular chaperones that exert a positive effect on β-Glu [19,23–27,50]. This peculiarity of ABX also makes it a potential drug candidate for other LSDs. Conversely, this aspect should be appreciated in future studies on the utility of ABX as PD therapy, as its putative direct effect on the correct folding of β-Glu may be overestimated.

3. Materials and Methods

3.1. IC_{50} Measurements

Imiglucerase (Cerezyme®, Genzyme Corporation, Cambridge, MA, USA) was a left-over from a patient who did not attend therapy in our outpatient clinic. Imiglucerase is also referred to as (recombinant) β-Glu in the text hereinafter. The powder was reconstituted in Sörensen buffer, pH 4.7, containing 0.125% sodium taurocholate on the day of the experiment. IFG, ABX, or BHX was mixed with Imiglucerase (final concentration: 0.026 μM) in a 384-well black plate (Thermo Scientific, Waltham, MA, USA) and briefly pre-incubated. An equivalent volume of 1.5 mM 4-methylumbelliferyl β-D-glucopyranoside (4-MUG, Sigma–Aldrich, Steinheim, Germany) was added and incubated for 20 min at room temperature. The reaction was stopped with glycine–NaOH buffer pH 10.5. Liberated 4-methylumbelliferone was measured (excitation 365 nm; emission 440 nm) with a Tecan Spark multimode microplate reader (Tecan, Männedorf, Switzerland).

3.2. Cell Culture

Cell lines GM00372 and GM00852 (both p.Asn370Ser/84GG) and wildtype control cell line GM01653 (all obtained from Coriell Institute Cell Repository, Camden, NJ, USA) were cultured under standard conditions at 37 °C under a 5% CO_2 atmosphere. Typically, cells were seeded in T125 flasks in DMEM and 15% FBS with the addition of penicillin/streptomycin and sub-cultured while confluence was reached. Medium was changed every 4 days.

3.3. Enzyme Activity Assay

The GM00372, GM00852, and GM01653 cells were seeded in 6-well assay plates and incubated overnight. The next day, the medium was replaced with fresh medium containing the respective compound dissolved in either dimethyl sulfoxide or water (ABX) or a mixture of ethanol and water at a ratio of 1:1 (v/v) (IFG). The fibroblasts were incubated for 5 days. After half the incubation period, the medium was replaced with fresh treatment medium. The incubation was followed by a 6 h washout period in medium without the drug. The cells were harvested by trypsination (0.25% trypsin/EDTA) and spun at 3000× g in a benchtop centrifuge to pellet the cells. Cell pellets were washed twice with phosphate-buffered saline and lysed by the freeze-and-thaw method in ultrapure water supplemented with 0.15% Triton X-100. The protein amount of each sample was determined by the BCA method (Thermo Scientific, Waltham, MA, USA). Lysosomal β-Glu activity was evaluated by mixing 5 μg of total protein with 3 mM of 4-MUG (Sigma–Aldrich, Steinheim, Germany) dissolved in Sorenson's phosphate buffer (pH 5.3) containing 0.15% Triton X-100 and

0.125% taurocholate in a total volume of 30 µL in 96-well reaction plates. The reaction was incubated at 37 °C and terminated after 1 h by the addition of 0.2 mL of glycine buffer (pH 10.5). The fluorescence was measured (excitation 360 nm; emission 465 nm) in a Tecan Spark plate reader (Tecan AG, Männedorf, Switzerland).

3.4. Cycloheximide Assay

Cells were plated into 6-well assay plates and treated with ABX, IFG, or the vehicle control for 5 days. Fresh treatment medium was then added with additional CHX (100 µg/mL) for the indicated period. Then, the cells were harvested in order to obtain β-Glu degradation kinetics via Western blot.

3.5. Western Blot

Cells were lysed on ice using RIPA buffer containing Roche complete protease inhibitor cocktail, and the protein amount of each sample was determined as above. If applicable, Endoglycosidase H (Endo-H) and peptide:N-glycosidase F (PNGase) treatment of cell lysates was carried out prior to SDS-PAGE, containing 20–30 µg of total protein, according to the company specifications (New England Biolabs, Ipswich, MA, USA). Aliquots of cell lysates were separated using Criterion precast 4–15% Tris-HCl gels (Bio-Rad, Munich, Germany) as described earlier [51]. Western blot analysis was conducted using monoclonal anti-β-Glu 2E2 antibody (Sigma–Aldrich, Steinheim, Germany) at 3 µg/mL and mouse monoclonal β-actin antibody at a 1:10,000 dilution (cat-no. A5441, Sigma–Aldrich, Steinheim, Germany) each diluted in Tris-buffered saline supplemented with 0.1% Tween-20 and 3% skim milk powder. For fluorescence detection, appropriate secondary antibodies were used (Thermo Fisher Scientific, Dreieich, Germany) for digital visualization via Odyssey Infrared Imaging system (Li-Cor Biosciences, Lincoln, NE, USA). β-Glu protein level was quantified and normalized to the internal loading control, β-actin, using the Odyssey software version 2.1.

3.6. Thermal Shift Assay

Imiglucerase (final concentration: 1 mg/mL) was mixed with 10X Sypro orange dye (final concentration: 12.5 µM) in MES buffer, pH 5.5 (50 mM MES, 50 mM NaCl, and 2 mM DTE) in LightCycler® 96-well white plates (Roche Applied Science, Penzberg, Germany). The compounds were added to a final concentration of 2 mM and thoroughly mixed. The plate was measured using Lightcycler 480 instrument II (Roche Applied Science, Penzberg, Germany) at an excitation wavelength of 533 nm and emission wavelength of 610 nm. The program melt curve was used to detect protein melting curves with a temperature range between 20–95 °C at 1 °C/min. T_m value was determined from the peak of the first derivatives of the melting curve using GraphPad Prism 5.0 (GraphPad Software, La Jolla, CA, USA).

3.7. Chemical Synthesis of D1 and D2

Synthesis of (1s,4s)-4-((2-amino-3,5-dibromobenzyl)(methyl)amino)cyclohexan-1-ol (D1).

3.7.1. Synthesis of *tert*-Butyl-hydroxycarbamate

Following the literature procedure [52], a suspension of $NH_2OH{\cdot}HCl$ (4.8 g, 68.7 mmol, 1.5 eq) and K_2CO_3 (9.5 g, 68.7 mmol, 1.5 eq) in Et_2O (100 mL) and H_2O (12 mL) was stirred for 1 h at ambient temperature (evolution of CO_2). Subsequently, a solution of di-*tert*-butyldicarbonate (10.0 g, 45.8 mmol, 1.0 eq) in Et_2O (100 mL) was added dropwise to the stirring suspension at 0 °C, and the resulting suspension was stirred at ambient temperature for 2 h. H_2O (20 mL) was added to the reaction mixture till a clear two-phase system was obtained and the layers were separated. The aqueous phase was extracted with Et_2O (3 × 60 mL), the combined organic layers were dried over Na_2SO_4 and concentrated under reduced pressure. The crude product was purified by column chromatography (SiO_2, *n*-pentane:EtOAc = 5:1) to afford *tert*-butyl-hydroxycarbamate (6.1 g, 45.8 mmol, quant.) as a colorless solid. R_f = 0.23 (*n*-pentane:EtOAc = 2:1, $KMnO_4$). m.p. 51 °C. ^{1}H NMR

(300 MHz, $CDCl_3$) δ 7.15 (s, 1H), 1.46 (s, 9H). ^{13}C NMR (75 MHz, $CDCl_3$) δ 159.0, 82.3, 28.3. GCMS (EI, *m*/*z*, relative intensity): 133 (0.1) $[M]^+$, 59 (56), 57 (100), 43 (15), 41 (45), 39 (12). HRMS (ESI-TOF, *m*/*z*): calcd. for $C_5H_{11}NO_3$ [M] 133.0733; found 133.0739. IR (ATR, neat, cm^{-1}): 3356(m), 3282(w), 2979(w), 2940(w), 1679(s), 1514(m), 1459(m), 1393(m), 1367(s), 1282(s), 1252(s), 1161(s), 1119(s), 1048(m), 1014(m), 861(m), 774(m), 752(m), 517(s), 479(s).

3.7.2. Synthesis of *tert*-Butyl-2-oxa-3-azabicyclo[2.2.2]oct-5-ene-3-carboxylate

tert-Butyl-2-oxa-3-azabicyclo[2.2.2]oct-5-ene-3-carboxylate was synthesized following a modified literature procedure [53]. CuCl (146.0 mg, 1.5 mmol, 0.2 eq) and pyridine (58.9 µL, 57.6 mg, 0.7 mmol, 0.1 eq) were added to *tert*-butyl-hydroxycarbamate (982.0 mg, 7.4 mmol, 1.0 eq) and 1,3-cyclohexadiene (843.3 µL, 709.2 mg, 8.9 mmol, 1.2 eq) in THF (30 mL). The resulting mixture was stirred vigorously for 4 h at RT and open to air. The reaction was quenched with aqueous NH_3 (25%, 30 mL), THF was removed under reduced pressure, the aqueous phase was extracted with EtOAc (3 × 40 mL), and the combined organic layers were dried over Na_2SO_4 and concentrated under reduced pressure. The crude product was purified by column chromatography (SiO_2, *n*-pentane:EtOAc = 5:1) to afford the title compound (1.4 g, 6.7 mmol, 90%) as a colorless solid. R_f = 0.60 (*n*-pentane:EtOAc = 2:1, $KMnO_4$). m.p. 34.5–36.5 °C. ^1H NMR (300 MHz, $CDCl_3$) δ 6.58-6.43 (m, 2H), 4.75-4.63 (m, 2H), 2.21-2.01 (m, 2H), 1.43 (s, 9H), 1.53-1.25 (m, 2H). ^{13}C NMR (75 MHz, $CDCl_3$) δ 157.8, 131.8, 131.6, 81.6, 70.7, 50.2, 28.3, 23.7, 20.6. GCMS (EI, *m*/*z*, relative intensity): 211 (2) $[M]^+$, 111 (13), 80 (39), 79 (66), 78 (12), 77 (12), 57 (100), 41 (30), 39 (12). HRMS (ESI-TOF, *m*/*z*): calcd. for $C_{11}H_{17}NO_3$ [M] 211.1203; found 211.1208. IR (ATR, neat, cm^{-1}): 2979(m), 2937(w), 1673(s), 1615(w), 1455(m), 1395(s), 1360(s), 1293(m), 1253(s), 1162(s), 1125(m), 1110(s), 1076(s), 1049(s), 993(m), 957(m), 918(m), 879(s), 849(m), 818(m), 797(m), 745(s), 713(s), 680(m), 666(m), 614(m), 492(m), 429(m).

3.7.3. Synthesis of 3-*N*-Methyl-2-oxa-3-azabicyclo[2.2.2]oct-5-ene

3-*N*-methyl-2-oxa-3-azabicyclo[2.2.2]oct-5-ene was synthesized following a modified literature procedure [54]. A solution of *tert*-butyl-2-oxa-3-azabicyclo[2.2.2]oct-5-ene-3-carboxylate (6.3 g, 30.0 mmol, 1.0 eq) in tetrahydrofuran (50 mL) was added dropwise to a stirring suspension of $LiAlH_4$ (2.3 g, 60.0 mmol, 2.0 eq) in tetrahydrofuran (50 mL) at 0 °C. The ice-bath was removed, and the reaction mixture was stirred at ambient temperature for 1 h. Afterwards, the reaction mixture was cooled to 0 °C and quenched carefully with methanol and aqueous K_2CO_3 (pH = 10). The insoluble material was filtered off, and volatiles were removed under reduced pressure. The crude product was dissolved in dichloromethane and the aqueous phase was extracted with dichloromethane (5 × 50 mL). The combined organic layers were dried over Na_2SO_4, and the crude product was purified by column chromatography (SiO_2, CH_2Cl_2:EtOAc = 20:1 + 2% NEt_3→CH_2Cl_2:EtOAc = 5:1 + 2% NEt_3), affording 3-*N*-methyl-2-oxa-3-azabicyclo[2.2.2]oct-5-ene (2.6 g, 20.7 mmol, 69%) as a brown oil. R_f = 0.60 (CH_2Cl_2:MeOH = 10:1, $KMnO_4$). ^1H NMR (300 MHz, $CDCl_3$) δ 6.66-6.56 (m, 1H), 6.33-6.22 (m, 1H), 4.39-4.28 (m, 1H), 3.57-3.46 (m, 1H), 2.37 (s, 3H), 2.11-1.93 (m, 2H), 1.48-1.18 (m, 2H). ^{13}C NMR (75 MHz, $CDCl_3$) δ 132.8, 129.4, 68.0, 56.0, 44.8, 23.2, 22.4. GCMS (EI, *m*/*z*, relative intensity): 125 (10) $[M]^+$, 124 (92), 111 (10), 97 (17), 96 (17), 95 (20), 83 (10), 81 (13), 80 (91), 79 (100), 78 (24), 77 (49), 69 (12), 68 (16), 67 (37), 57 (13), 55 (15), 54 (13), 46 (70), 43 (11), 41 (23), 39 (17). HRMS (ESI-TOF, *m*/*z*): calcd. for $C_7H_{11}NO$ [M] 125.0841; found 125.0849. IR (ATR, neat, cm^{-1}): 3051(w), 2953(m), 2877(m), 1452(m), 1431(m), 1368(m), 1310(w), 1220(w), 1179(m), 1164(m), 1087(w), 1058(m), 998(m), 986(m), 955(s), 931(s), 853(m), 816(m), 801(m), 718(s), 704(s), 654(s), 569(m), 478(m), 438(s).

3.7.4. Synthesis of (*Syn*)-4-(methylamino)cyclohexan-1-ol

Following a modified literature procedure [55], a solution of (1*R*,4*S*)-3-methyl-2-oxa-3-azabicyclo[2.2.2]oct-5-ene 22 (1.0 g, 8.0 mmol, 1.0 eq) in dry methanol (40 mL) was hydrogenated in the presence of 5% Pd/C (1.7 g, 0.8 mmol, 0.1 eq) at RT under atmospheric pressure of H_2 (balloon) for 24 h. The catalyst was removed by filtration through celite, and the crude

product was purified by column chromatography (SiO_2, EtOAc:MeOH = 5:1 + 2% NEt_3) and sublimation (0.02 mbar, 50 °C) to afford (*syn*)-4-(methylamino)cyclohexan-1-ol (227.3 mg, 1.8 mmol, 22%) as a colorless solid. R_f = 0.06 (EtOAc:MeOH = 5:1 + 2%NEt_3, $KMnO_4$). m.p. 84–85 °C. ^{1}H NMR (300 MHz, CD_2Cl_2) δ 3.87-3.73 (m, 1H), 2.59 (s, 1H), 2.49-2.35 (m, 1H), 2.37 (s, 3H), 1.78-1.43 (m, 8H). ^{13}C NMR (75 MHz, CD_2Cl_2) δ 67.3, 57.1, 33.7, 31.6, 27.5. GCMS (EI, *m*/*z*, relative Intensity): 129 (12) $[M]^+$, 71 (17), 70 (100), 57 (38), 42 (7), 30 (4). HRMS (ESI-TOF, *m*/*z*): calcd. for $C_7H_{15}NO$ [M] 129.1154; found 129.1162. IR (ATR, neat, cm^{-1}): 3261(m), 3087(m), 2974(w), 2936(s), 2849(s), 2785(s), 2676(w), 1563(w), 1499(w), 1430(m), 1368(s), 1353(m), 1330(m), 1309(w), 1284(m), 1261(s), 1218(m), 1137(m), 1119(s), 1090(m), 1060(m), 1031(m), 974(s), 902(s), 824(m), 763(m), 686(m), 651(m), 507(m), 494(m), 464(w), 416(m).

3.7.5. General Procedure for the Syntheses of 2,4-Dibromo-6-((cyclohexylamino)methyl) aniline-derivatives (GP1)

2-amino-3,5-dibromobenzaldehyde (1.0 eq) and cyclohexylamine-derivative (1.5 eq) were dissolved in dry iPrOH (0.1 M) in a preheated flask under Ar and at 40 °C. Then, $Ti(OiPr)_4$ (2.0 eq) was added dropwise to the stirring reaction mixture. After the reaction was continued at 40 °C for 24 h, $NaBH_4$ (2.5 eq) was added to the reaction solution in portions and stirred at 40 °C for an additional 24 h. After completion, H_2O was added to the solution to quench the reaction and precipitate a large amount of solid, which was removed by suction filtration. The solvent was evaporated, the aqueous phase adjusted to pH = 10, extracted with EtOAc (3 × 20 mL), dried, and purified by column chromatography.

3.7.6. Synthesis of (1s,4s)-4-((2-Amino-3,5-dibromobenzyl)(methyl)amino)cyclohexan-1-ol (D1)

Following the general procedure GP1, 2-amino-3,5-dibromobenzaldehyde (215.9 mg, 0.8 mmol, 1.0 eq) and *cis*-4-(methylamino)cyclohexan-1-ol (150.0 mg, 1.2 mmol, 1.5 eq) were first treated with $Ti(OiPr)_4$ (469.5 µL, 439.9 mg, 1.6 mmol, 2.0 eq) and then with $NaBH_4$ (73.2 mg, 1.9 mmol, 2.5 eq). Purification by column chromatography (SiO_2, *n*-pentane:EtOAc = 5:1) yielded the title compound D1 (190.8 mg, 0.5 mmol, 63%) as a yellow viscous oil. R_f = 0.25 (*n*-pentane:EtOAc = 1:1, $KMnO_4$). ^{1}H NMR (300 MHz, $CDCl_3$) δ 7.46 (d, *J* = 2.2 Hz, 1H), 7.04 (d, *J* = 2.2 Hz, 1H), 5.45 (s, 2H), 3.99 (p, *J* = 3.2 Hz, 1H), 3.60 (s, 2H), 2.50-2.34 (m, 1H), 2.14 (s, 3H), 1.93-1.69 (m, 4H), 1.66-1.41 (m, 4H). ^{13}C NMR (75 MHz, $CDCl_3$) δ 144.1, 133.2, 131.8, 110.2, 108.2, 65.8, 61.2, 58.0, 36.6, 32.2, 22.1. GCMS (EI, *m*/*z*, relative Intensity): 394 (7) $[M]^+$, 392 (13) $[M]^+$, 390 (7) $[M]^+$, 335 (10), 333 (20), 331 (10), 307 (10), 305 (21), 303 (11), 295 (32), 291 (34), 266 (28), 335 (10), 264 (57), 262 (30), 142 (15), 128 (29), 104 (16), 77 (10), 70 (100), 57 (10), 44 (14), 42 (15). HRMS (ESI-TOF, *m*/*z*): calcd. for $C_{14}H_{20}ON_2{}^{79}Br_2$ [M] 389.9937; found 389.9928; calcd. for $C_{14}H_{20}ON_2{}^{79}Br^{81}Br$ [M] 391.9916; found 391.9925. IR (ATR, neat, cm^{-1}): 3429(w), 3258(w), 2926(m), 2850(m), 2792(w), 1604(m), 1575(w), 1550(m), 1459(s), 1379(m), 1356(m), 1291(m), 1256(m), 1232(m), 1196(m), 1123(m), 1100(m), 1072(m), 1031(s), 987(m), 958(s), 929(m), 905(m), 885(m), 856(s), 816(m), 736(m), 679(s), 646(s), 551(s), 444(s).

3.7.7. Synthesis of 2,4-Dibromo-6-((cyclohexylamino)methyl)aniline (D2)

Following the general procedure GP1, 2-amino-3,5-dibromobenzaldehyde 18 (253.1 mg, 0.9 mmol, 1.0 eq) and cyclohexylamine (156.9 µL, 135.0 mg, 1.4 mmol, 1.5 eq) were first treated with $Ti(OiPr)_4$ (550.5 µL, 515.8 mg, 1.8 mmol, 2.0 eq) and then with $NaBH_4$ (85.8 mg, 2.3 mmol, 2.5 eq). Purification by column chromatography (SiO_2, *n*-pentane:EtOAc = 10:1) yielded the title compound D2 (292.7 mg, 0.8 mmol, 89%) as a light yellow oil. R_f = 0.13 (*n*-pentane:EtOAc = 10:1, UV). ^{1}H NMR (300 MHz, $CDCl_3$) δ 7.46 (d, *J* = 2.3 Hz, 1H), 7.09 (dt, *J* = 2.3, 0.7 Hz, 1H), 5.41 (s, 2H), 3.79 (t, *J* = 0.5 Hz, 2H), 2.54-2.34 (m, 1H), 1.98-1.83 (m, 2H), 1.79-1.66 (m, 2H), 1.65-1.55 (m, 1H), 1.39-0.97 (m, 5H). ^{13}C NMR (75 MHz, $CDCl_3$) δ 144.1, 133.2, 131.4, 127.1, 110.5, 108.3, 56.2, 50.3, 33.6, 26.2, 25.0. GCMS (EI, *m*/*z*, relative Intensity): 364 (8) $[M]^+$, 362 (15) $[M]^+$, 360 (8) $[M]^+$, 293 (13), 291 (27), 289 (15), 281 (49), 280 (10), 279 (100), 277 (52), 266 (42), 264 (87), 262 (45), 183 (10), 112 (12), 104 (16), 293 (13), 98 (67), 56 (18), 55 (12), 41 (11). HRMS (ESI-TOF, *m*/*z*): calcd. for

$C_{13}H_{18}N_2{}^{79}Br^{81}Br$ [M] 361.9811; found 361.9806; calcd. for $C_{13}H_{18}N_2{}^{81}Br_2$ [M] 363.9790; found 375.9799. IR (ATR, neat, cm^{-1}): 3435(w), 3265(w), 2922(s), 2849(m), 1606(m), 1577(w), 1552(m), 1459(s), 1408(m), 1371(m), 1346(m), 1284(w), 1242(m), 1195(m), 1144(w), 1111(m), 1077(s), 988(w), 956(m), 889(m), 858(s), 818(m), 799(m), 758(m), 682(s), 621(s), 551(s), 509(m), 448(s).

3.8. Statistical Evaluation

All statistical analyses were calculated using GraphPad Prism, versions 5.0 and 9.1.0 (for Windows).

4. Conclusions

Pharmacological chaperones merit attention as candidate drugs for the treatment of Gaucher disease, specifically because they promise hope for the treatment of Type III GD. The present report juxtaposes the specific properties of the effects of ambroxol with those of the known PC isofagomine using molecular and biochemical examinations. ABX increases β-Glu activity measured in lysates of GD patient fibroblasts, quantitatively indistinguishable from IFG. Nevertheless, the ability of ABX to stabilize recombinant β-Glu in vitro is limited compared with IFG, and cellular stabilization of mutant β-Glu is also less effective, as verified by evidence of incomplete cellular processing.

Closely related structural ABX analogues show no chaperone effect on β-Glu, and in silico docking reveals a possible position reversal in the binding pocket of compounds with an aminomethyl group, suggesting that ABX and derivatives might enter the active site in reverse position, with similar binding enthalpies but different stabilizing efficiency. Thus, the efficacy of ABX as a GCase binder and stabilizer in GD (and likely as a protein aggregation inhibitor for Parkinson's disease) must be questioned. Our data emphasize the possibility that ABX function may be due to an as-yet-unexplained mode of action in the cellular context.

Supplementary Materials: The following supporting information can be downloaded at: https://www.mdpi.com/article/10.3390/ijms23073536/s1.

Author Contributions: Conceptualization, S.P. and J.L.; methodology, S.P., L.H., C.S. and A.P.; validation, M.M. and M.V.C.; formal analysis, J.P. and M.V.C.; investigation, S.P., L.H. and J.L.; resources, J.P. and A.H.; data curation, A.H.; writing—original draft preparation, S.P. and J.L.; writing—review and editing, M.V.C. and A.H.; visualization, S.P. and J.L.; supervision, A.H.; project administration, J.L.; funding acquisition, J.L. All authors have read and agreed to the published version of the manuscript.

Funding: This work was supported by the European Union (grant number ESF/14-BM-A55-0046/16).

Institutional Review Board Statement: Not applicable.

Informed Consent Statement: Not applicable.

Data Availability Statement: Data is contained within the article and supplementary material.

Acknowledgments: The authors would like to thank Mia Horowitz of the Shmunis School of Biomedicine and Cancer Research for critical discussion on the manuscript. We also thank Franziska Alfen for technical assistance and data management.

Conflicts of Interest: The authors declare no conflict of interest.

References

1. Shanmuganathan, M.; Britz-McKibbin, P. Inhibitor screening of pharmacological chaperones for lysosomal β-glucocerebrosidase by capillary electrophoresis. *Anal. Bioanal. Chem.* **2011**, *399*, 2843–2853. [CrossRef] [PubMed]
2. Monticelli, M.; Liguori, L.; Allocca, M.; Andreotti, G.; Cubellis, M.V. β-Glucose-1,6-Bisphosphate Stabilizes Pathological Phophomannomutase2 Mutants In Vitro and Represents a Lead Compound to Develop Pharmacological Chaperones for the Most Common Disorder of Glycosylation, PMM2-CDG. *Int. J. Mol. Sci.* **2019**, *20*, 4164. [CrossRef]

3. Liguori, L.; Monticelli, M.; Allocca, M.; Hay Mele, B.; Lukas, J.; Cubellis, M.V.; Andreotti, G. Pharmacological Chaperones: A Therapeutic Approach for Diseases Caused by Destabilizing Missense Mutations. *Int. J. Mol. Sci.* **2020**, *21*, 489. [CrossRef]
4. Mehta, A. Epidemiology and natural history of Gaucher's disease. *Eur. J. Intern. Med.* **2006**, *17*, S2–S5. [CrossRef] [PubMed]
5. Lukas, J.; Cozma, C.; Yang, F.; Kramp, G.; Meyer, A.; Neßlauer, A.-M.; Eichler, S.; Böttcher, T.; Witt, M.; Bräuer, A.U.; et al. Glucosylsphingosine Causes Hematological and Visceral Changes in Mice-Evidence for a Pathophysiological Role in Gaucher Disease. *Int. J. Mol. Sci.* **2017**, *18*, 2192. [CrossRef]
6. Yu, Z.; Sawkar, A.R.; Whalen, L.J.; Wong, C.-H.; Kelly, J.W. Isofagomine- and 2,5-anhydro-2,5-imino-D-glucitol-based glucocerebrosidase pharmacological chaperones for Gaucher disease intervention. *J. Med. Chem.* **2007**, *50*, 94–100. [CrossRef] [PubMed]
7. Castilla, J.; Rísquez, R.; Cruz, D.; Higaki, K.; Nanba, E.; Ohno, K.; Suzuki, Y.; Díaz, Y.; Ortiz Mellet, C.; García Fernández, J.M.; et al. Conformationally-locked N-glycosides with selective β-glucosidase inhibitory activity: Identification of a new non-iminosugar-type pharmacological chaperone for Gaucher disease. *J. Med. Chem.* **2012**, *55*, 6857–6865. [CrossRef] [PubMed]
8. Navo, C.D.; Corzana, F.; Sánchez-Fernández, E.M.; Busto, J.H.; Avenoza, A.; Zurbano, M.M.; Nanba, E.; Higaki, K.; Ortiz Mellet, C.; García Fernández, J.M.; et al. Conformationally-locked C-glycosides: Tuning aglycone interactions for optimal chaperone behaviour in Gaucher fibroblasts. *Org. Biomol. Chem.* **2016**, *14*, 1473–1484. [CrossRef]
9. Steet, R.A.; Chung, S.; Wustman, B.; Powe, A.; Do, H.; Kornfeld, S.A. The iminosugar isofagomine increases the activity of N370S mutant acid beta-glucosidase in Gaucher fibroblasts by several mechanisms. *Proc. Natl. Acad. Sci. USA* **2006**, *103*, 13813–13818. [CrossRef]
10. Khanna, R.; Benjamin, E.R.; Pellegrino, L.; Schilling, A.; Rigat, B.A.; Soska, R.; Nafar, H.; Ranes, B.E.; Feng, J.; Lun, Y.; et al. The pharmacological chaperone isofagomine increases the activity of the Gaucher disease L444P mutant form of beta-glucosidase. *FEBS J.* **2010**, *277*, 1618–1638. [CrossRef] [PubMed]
11. Maegawa, G.H.B.; Tropak, M.B.; Buttner, J.D.; Rigat, B.A.; Fuller, M.; Pandit, D.; Tang, L.; Kornhaber, G.J.; Hamuro, Y.; Clarke, J.T.R.; et al. Identification and characterization of ambroxol as an enzyme enhancement agent for Gaucher disease. *J. Biol. Chem.* **2009**, *284*, 23502–23516. [CrossRef] [PubMed]
12. Sharif, M.; Pews-Davtyan, A.; Lukas, J.; Schranck, J.; Langer, P.; Rolfs, A.; Beller, M. Palladium-Catalyzed Carbonylative Transformations of Bromhexine into Bioactive Compounds as Glucocerebrosidase Inhibitors. *Eur. J. Org. Chem.* **2014**, *2014*, 222–230. [CrossRef]
13. Bendikov-Bar, I.; Maor, G.; Filocamo, M.; Horowitz, M. Ambroxol as a pharmacological chaperone for mutant glucocerebrosidase. *Blood Cells Mol. Dis.* **2013**, *50*, 141–145. [CrossRef]
14. Bendikov-Bar, I.; Ron, I.; Filocamo, M.; Horowitz, M. Characterization of the ERAD process of the L444P mutant glucocerebrosidase variant. *Blood Cells Mol. Dis.* **2011**, *46*, 4–10. [CrossRef]
15. Luan, Z.; Li, L.; Higaki, K.; Nanba, E.; Suzuki, Y.; Ohno, K. The chaperone activity and toxicity of ambroxol on Gaucher cells and normal mice. *Brain Dev.* **2013**, *35*, 317–322. [CrossRef]
16. Panicker, L.M.; Miller, D.; Awad, O.; Bose, V.; Lun, Y.; Park, T.S.; Zambidis, E.T.; Sgambato, J.A.; Feldman, R.A. Gaucher iPSC-derived macrophages produce elevated levels of inflammatory mediators and serve as a new platform for therapeutic development. *Stem Cells* **2014**, *32*, 2338–2349. [CrossRef]
17. Sanchez-Martinez, A.; Beavan, M.; Gegg, M.E.; Chau, K.-Y.; Whitworth, A.J.; Schapira, A.H.V. Parkinson disease-linked GBA mutation effects reversed by molecular chaperones in human cell and fly models. *Sci. Rep.* **2016**, *6*, 31380. [CrossRef]
18. Migdalska-Richards, A.; Daly, L.; Bezard, E.; Schapira, A.H.V. Ambroxol effects in glucocerebrosidase and α-synuclein transgenic mice. *Ann. Neurol.* **2016**, *80*, 766–775. [CrossRef]
19. Maor, G.; Cabasso, O.; Krivoruk, O.; Rodriguez, J.; Steller, H.; Segal, D.; Horowitz, M. The contribution of mutant GBA to the development of Parkinson disease in Drosophila. *Hum. Mol. Genet.* **2016**, *25*, 2712–2727. [CrossRef]
20. Zimran, A.; Altarescu, G.; Elstein, D. Pilot study using ambroxol as a pharmacological chaperone in type 1 Gaucher disease. *Blood Cells Mol. Dis.* **2013**, *50*, 134–137. [CrossRef]
21. Narita, A.; Shirai, K.; Itamura, S.; Matsuda, A.; Ishihara, A.; Matsushita, K.; Fukuda, C.; Kubota, N.; Takayama, R.; Shigematsu, H.; et al. Ambroxol chaperone therapy for neuronopathic Gaucher disease: A pilot study. *Ann. Clin. Transl. Neurol.* **2016**, *3*, 200–215. [CrossRef] [PubMed]
22. Ciana, G.; Dardis, A.; Pavan, E.; Da Riol, R.M.; Biasizzo, J.; Ferino, D.; Zanatta, M.; Boni, A.; Antonini, L.; Crichiutti, G.; et al. In vitro and in vivo effects of Ambroxol chaperone therapy in two Italian patients affected by neuronopathic Gaucher disease and epilepsy. *Mol. Genet. Metab. Rep.* **2020**, *25*, 100678. [CrossRef] [PubMed]
23. Magalhaes, J.; Gegg, M.E.; Migdalska-Richards, A.; Schapira, A.H. Effects of ambroxol on the autophagy-lysosome pathway and mitochondria in primary cortical neurons. *Sci. Rep.* **2018**, *8*, 1385. [CrossRef] [PubMed]
24. McNeill, A.; Magalhaes, J.; Shen, C.; Chau, K.-Y.; Hughes, D.; Mehta, A.; Foltynie, T.; Cooper, J.M.; Abramov, A.Y.; Gegg, M.; et al. Ambroxol improves lysosomal biochemistry in glucocerebrosidase mutation-linked Parkinson disease cells. *Brain* **2014**, *137*, 1481–1495. [CrossRef] [PubMed]
25. Maor, G.; Rencus-Lazar, S.; Filocamo, M.; Steller, H.; Segal, D.; Horowitz, M. Unfolded protein response in Gaucher disease: From human to Drosophila. *Orphanet J. Rare Dis.* **2013**, *8*, 140. [CrossRef] [PubMed]

26. Lu, J.; Yang, C.; Chen, M.; Ye, D.Y.; Lonser, R.R.; Brady, R.O.; Zhuang, Z. Histone deacetylase inhibitors prevent the degradation and restore the activity of glucocerebrosidase in Gaucher disease. *Proc. Natl. Acad. Sci. USA* **2011**, *108*, 21200–21205. [CrossRef] [PubMed]
27. Braunstein, H.; Maor, G.; Chicco, G.; Filocamo, M.; Zimran, A.; Horowitz, M. UPR activation and CHOP mediated induction of GBA1 transcription in Gaucher disease. *Blood Cells Mol. Dis.* **2018**, *68*, 21–29. [CrossRef] [PubMed]
28. Lukas, J.; Pockrandt, A.-M.; Seemann, S.; Sharif, M.; Runge, F.; Pohlers, S.; Zheng, C.; Gläser, A.; Beller, M.; Rolfs, A.; et al. Enzyme enhancers for the treatment of Fabry and Pompe disease. *Mol. Ther.* **2015**, *23*, 456–464. [CrossRef] [PubMed]
29. Seemann, S.; Ernst, M.; Cimmaruta, C.; Struckmann, S.; Cozma, C.; Koczan, D.; Knospe, A.-M.; Haake, L.R.; Citro, V.; Bräuer, A.U.; et al. Proteostasis regulators modulate proteasomal activity and gene expression to attenuate multiple phenotypes in Fabry disease. *Biochem. J.* **2020**, *477*, 359–380. [CrossRef] [PubMed]
30. Sharif, M.; Pews-Davtyan, A.; Lukas, J.; Pohlers, S.; Rolfs, A.; Langer, P.; Beller, M. Palladium-catalysed Suzuki–Miyaura coupling reactions of Bromhexine and Ambroxol. *Tetrahedron* **2014**, *70*, 5128–5135. [CrossRef]
31. Asano, N.; Ishii, S.; Kizu, H.; Ikeda, K.; Yasuda, K.; Kato, A.; Martin, O.R.; Fan, J.Q. In vitro inhibition and intracellular enhancement of lysosomal alpha-galactosidase A activity in Fabry lymphoblasts by 1-deoxygalactonojirimycin and its derivatives. *Eur. J. Biochem.* **2000**, *267*, 4179–4186. [CrossRef] [PubMed]
32. Thirumal Kumar, D.; Iyer, S.; Christy, J.P.; Siva, R.; Tayubi, I.A.; George Priya Doss, C.; Zayed, H. A comparative computational approach toward pharmacological chaperones (NN-DNJ and ambroxol) on N370S and L444P mutations causing Gaucher's disease. *Adv. Protein Chem. Struct. Biol.* **2019**, *114*, 315–339. [CrossRef] [PubMed]
33. Balwani, M.; Fuerstman, L.; Kornreich, R.; Edelmann, L.; Desnick, R.J. Type 1 Gaucher disease: Significant disease manifestations in "asymptomatic" homozygotes. *Arch. Intern. Med.* **2010**, *170*, 1463–1469. [CrossRef] [PubMed]
34. Diaz, G.A.; Gelb, B.D.; Risch, N.; Nygaard, T.G.; Frisch, A.; Cohen, I.J.; Miranda, C.S.; Amaral, O.; Maire, I.; Poenaru, L.; et al. Gaucher disease: The origins of the Ashkenazi Jewish N370S and 84GG acid beta-glucosidase mutations. *Am. J. Hum. Genet.* **2000**, *66*, 1821–1832. [CrossRef]
35. Yu, L.; Ikeda, K.; Kato, A.; Adachi, I.; Godin, G.; Compain, P.; Martin, O.; Asano, N. Alpha-1-C-octyl-1-deoxynojirimycin as a pharmacological chaperone for Gaucher disease. *Bioorg. Med. Chem.* **2006**, *14*, 7736–7744. [CrossRef] [PubMed]
36. Mu, T.-W.; Fowler, D.M.; Kelly, J.W. Partial restoration of mutant enzyme homeostasis in three distinct lysosomal storage disease cell lines by altering calcium homeostasis. *PLoS Biol.* **2008**, *6*, e26. [CrossRef]
37. Mu, T.-W.; Ong, D.S.T.; Wang, Y.-J.; Balch, W.E.; Yates, J.R.; Segatori, L.; Kelly, J.W. Chemical and biological approaches synergize to ameliorate protein-folding diseases. *Cell* **2008**, *134*, 769–781. [CrossRef] [PubMed]
38. Ong, D.S.T.; Mu, T.-W.; Palmer, A.E.; Kelly, J.W. Endoplasmic reticulum Ca2+ increases enhance mutant glucocerebrosidase proteostasis. *Nat. Chem. Biol.* **2010**, *6*, 424–432. [CrossRef] [PubMed]
39. Kato, A.; Nakagome, I.; Sato, K.; Yamamoto, A.; Adachi, I.; Nash, R.J.; Fleet, G.W.J.; Natori, Y.; Watanabe, Y.; Imahori, T.; et al. Docking study and biological evaluation of pyrrolidine-based iminosugars as pharmacological chaperones for Gaucher disease. *Org. Biomol. Chem.* **2016**, *14*, 1039–1048. [CrossRef] [PubMed]
40. Mullin, S.; Smith, L.; Lee, K.; D'Souza, G.; Woodgate, P.; Elflein, J.; Hällqvist, J.; Toffoli, M.; Streeter, A.; Hosking, J.; et al. Ambroxol for the Treatment of Patients With Parkinson Disease With and Without Glucocerebrosidase Gene Mutations: A Nonrandomized, Noncontrolled Trial. *JAMA Neurol.* **2020**, *77*, 427–434. [CrossRef] [PubMed]
41. Clark, L.N.; Ross, B.M.; Wang, Y.; Mejia-Santana, H.; Harris, J.; Louis, E.D.; Cote, L.J.; Andrews, H.; Fahn, S.; Waters, C.; et al. Mutations in the glucocerebrosidase gene are associated with early-onset Parkinson disease. *Neurology* **2007**, *69*, 1270–1277. [CrossRef] [PubMed]
42. Nichols, W.C.; Pankratz, N.; Marek, D.K.; Pauciulo, M.W.; Elsaesser, V.E.; Halter, C.A.; Rudolph, A.; Wojcieszek, J.; Pfeiffer, R.F.; Foroud, T. Mutations in GBA are associated with familial Parkinson disease susceptibility and age at onset. *Neurology* **2009**, *72*, 310–316. [CrossRef] [PubMed]
43. Kim, Y.-M.; Yum, M.-S.; Heo, S.H.; Kim, T.; Jin, H.K.; Bae, J.-S.; Seo, G.H.; Oh, A.; Yoon, H.M.; Lim, H.T.; et al. Pharmacologic properties of high-dose ambroxol in four patients with Gaucher disease and myoclonic epilepsy. *J. Med. Genet.* **2020**, *57*, 124–131. [CrossRef] [PubMed]
44. Ben Bdira, F.; Kallemeijn, W.W.; Oussoren, S.V.; Scheij, S.; Bleijlevens, B.; Florea, B.I.; van Roomen, C.P.A.A.; Ottenhoff, R.; van Kooten, M.J.F.M.; Walvoort, M.T.C.; et al. Stabilization of Glucocerebrosidase by Active Site Occupancy. *ACS Chem. Biol.* **2017**, *12*, 1830–1841. [CrossRef]
45. Lukas, J.; Seemann, S.; Sharif, M.; Zheng, C.; Cimmaruta, C.; Braunstein, H.; Pews-Davtyan, A.; Mieske, E.; Andreotti, G.; Cubellis, M.V.; et al. Ambroxol and bromhexine derivatives as pharmacological chaperones for mutant glucocerebrosidase. *Mol. Genet. Metab.* **2017**, *120*, S87. [CrossRef]
46. Andreotti, G.; Monticelli, M.; Cubellis, M.V. Looking for protein stabilizing drugs with thermal shift assay. *Drug Test. Anal.* **2015**, *7*, 831–834. [CrossRef]
47. Yoshimizu, M.; Tajima, Y.; Matsuzawa, F.; Aikawa, S.-I.; Iwamoto, K.; Kobayashi, T.; Edmunds, T.; Fujishima, K.; Tsuji, D.; Itoh, K.; et al. Binding parameters and thermodynamics of the interaction of imino sugars with a recombinant human acid alpha-glucosidase (alglucosidase alfa): Insight into the complex formation mechanism. *Clin. Chim. Acta* **2008**, *391*, 68–73. [CrossRef] [PubMed]

48. Khanna, R.; Flanagan, J.J.; Feng, J.; Soska, R.; Frascella, M.; Pellegrino, L.J.; Lun, Y.; Guillen, D.; Lockhart, D.J.; Valenzano, K.J. The pharmacological chaperone AT2220 increases recombinant human acid α-glucosidase uptake and glycogen reduction in a mouse model of Pompe disease. *PLoS ONE* **2012**, *7*, e40776. [CrossRef]
49. Xu, S.; Lun, Y.; Brignol, N.; Hamler, R.; Schilling, A.; Frascella, M.; Sullivan, S.; Boyd, R.E.; Chang, K.; Soska, R.; et al. Coformulation of a Novel Human α-Galactosidase A With the Pharmacological Chaperone AT1001 Leads to Improved Substrate Reduction in Fabry Mice. *Mol. Ther.* **2015**, *23*, 1169–1181. [CrossRef] [PubMed]
50. Yang, C.; Swallows, C.L.; Zhang, C.; Lu, J.; Xiao, H.; Brady, R.O.; Zhuang, Z. Celastrol increases glucocerebrosidase activity in Gaucher disease by modulating molecular chaperones. *Proc. Natl. Acad. Sci. USA* **2014**, *111*, 249–254. [CrossRef]
51. Lukas, J.; Giese, A.-K.; Markoff, A.; Grittner, U.; Kolodny, E.; Mascher, H.; Lackner, K.J.; Meyer, W.; Wree, P.; Saviouk, V.; et al. Functional characterisation of alpha-galactosidase a mutations as a basis for a new classification system in fabry disease. *PLoS Genet.* **2013**, *9*, e1003632. [CrossRef]
52. Frazier, C.P.; Engelking, J.R.; Read de Alaniz, J. Copper-catalyzed aerobic oxidation of hydroxamic acids leads to a mild and versatile acylnitroso ene reaction. *J. Am. Chem. Soc.* **2011**, *133*, 10430–10433. [CrossRef]
53. Frazier, C.P.; Bugarin, A.; Engelking, J.R.; Read de Alaniz, J. Copper-catalyzed aerobic oxidation of N-substituted hydroxylamines: Efficient and practical access to nitroso compounds. *Org. Lett.* **2012**, *14*, 3620–3623. [CrossRef]
54. Yamashita, M.; Yamashita, T.; Aoyagi, S. Toward the racemic total synthesis of hederacines A and B: Construction of an advanced tricyclic intermediate. *Org. Lett.* **2011**, *13*, 2204–2207. [CrossRef] [PubMed]
55. Moutel, S.; Shipman, M.; Martin, O.R.; Ikeda, K.; Asano, N. Synthesis of a trihydroxylated azepane from d-arabinose by way of an intramolecular alkene nitrone cycloaddition. *Tetrahedron Asymmetry* **2005**, *16*, 487–491. [CrossRef]

PLOS ONE

RESEARCH ARTICLE

Identification of an Allosteric Binding Site on Human Lysosomal Alpha-Galactosidase Opens the Way to New Pharmacological Chaperones for Fabry Disease

Valentina Citro[1☯], Jorge Peña-García[2☯], Helena den-Haan[2], Horacio Pérez-Sánchez[2*], Rosita Del Prete[1], Ludovica Liguori[1,3], Chiara Cimmaruta[1,3], Jan Lukas[4], Maria Vittoria Cubellis[1*], Giuseppina Andreotti[3]

1 Dipartimento di Biologia, Università Federico II, Napoli, 80126, Italy, **2** Bioinformatics and High Performance Computing Research Group (BIO-HPC), Computer Engineering Department, Universidad Católica San Antonio de Murcia (UCAM), Spain, **3** Istituto di Chimica Biomolecolare–CNR, Pozzuoli, 80078, Italy, **4** Albrecht-Kossel-Institute for Neuroregeneration, Medical University Rostock, Rostock, Germany

☯ These authors contributed equally to this work.
* cubellis@unina.it (MVC); hperez@ucam.edu (HPS)

OPEN ACCESS

Citation: Citro V, Peña-García J, den-Haan H, Pérez-Sánchez H, Del Prete R, Liguori L, et al. (2016) Identification of an Allosteric Binding Site on Human Lysosomal Alpha-Galactosidase Opens the Way to New Pharmacological Chaperones for Fabry Disease. PLoS ONE 11(10): e0165463. doi:10.1371/journal.pone.0165463

Editor: Stephan N. Witt, Louisiana State University Health Sciences Center, UNITED STATES

Received: May 10, 2016

Accepted: October 12, 2016

Published: October 27, 2016

Data Availability Statement: All data are included in the paper and in its Supporting Information files.

Funding: Funding was provided by Telethon - Italy (Grant no. GGP12108). This work was partially supported by the Fundación Séneca del Centro de Coordinación de la Investigación de la Región de Murcia under Project 18946/JLI/13. Powered@NLHPC: This research was partially supported by the supercomputing infrastructure of the NLHPC (ECM-02). The funders had no role in

Abstract

Personalized therapies are required for Fabry disease due to its large phenotypic spectrum and numerous different genotypes. In principle, missense mutations that do not affect the active site could be rescued with pharmacological chaperones. At present pharmacological chaperones for Fabry disease bind the active site and couple a stabilizing effect, which is required, to an inhibitory effect, which is deleterious. By *in silico* docking we identified an allosteric hot-spot for ligand binding where a drug-like compound, 2,6-dithiopurine, binds preferentially. 2,6-dithiopurine stabilizes lysosomal alpha-galactosidase *in vitro* and rescues a mutant that is not responsive to a mono-therapy with previously described pharmacological chaperones, 1-deoxygalactonojirimycin and galactose in a cell based assay.

Introduction

Fabry disease (FD) is a rare pathology, but accounts for 8.8% of the patients affected by inherited disorders of metabolism [1]. It is caused by mutations in the gene *GLA*, which is located on the X chromosome and encodes lysosomal alpha-galactosidase (AGAL) [2]. Enzyme replacement (ERT) is the only approved specific therapy for FD; it is well tolerated and safe [3]. The large phenotypic and genotypic spectrum of the disease poses several problems and the cost-effectiveness of ERT is still debated, in particular for patients who have residual enzyme activity [4]. In FD, about 40% of all missense mutations are associated with a biochemically mildly damaged enzyme [5]. A therapy with sub-inhibitory concentrations of 1-deoxygalactonojirimycin (DGJ) was first proposed by Suzuki and co-workers [6] and then tested in cells [7–13], in mouse models of FD [14] [15] and in clinical trials [16] [17]. Such therapy is suitable

study design, data collection and analysis, decision to publish, or preparation of the manuscript.

Competing Interests: The authors have declared that no competing interests exist.

Abbreviations: FD, Fabry disease; AGAL, lysosomal alpha-galactosidase; ERT, Enzyme replacement therapy; DGJ, 1-deoxygalactonojirimycin; DTP, 2,6-dithiopurine; GLA, alpha-D-galactose; GAL, beta-D-galactose.

only for patients carrying specific mutations (40%-60% of missense mutants tested in cell based assays [11, 12]) and requires fine-tuning of the dosage regimen because DGJ is an inhibitor of AGAL. The approach with small molecules for FD is promising, but DGJ is not yet the ideal drug. Molecules that either substitute DGJ or act in synergy with it to enable reduced dosage of DGJ should be sought, in particular for mutants that do not respond to a monotherapy with DGJ. Analogues of DGJ have been developed [18] [19]. A new family of arylthioureas showed a better balance between the stabilizing effect, which is required, and the inhibitory effect, which is detrimental [20]. However, these molecules bind the active site, as demonstrated by x-ray crystallography, and enhance enzymatic activity only at micromolar concentration, not dissimilarly from DGJ, when administered to eukaryotic cells expressing AGAL mutants [20].

Ambroxol, a mucolytic agent used in the treatment of respiratory diseases, proved to be useful in association with DGJ to rescue some AGAL mutants [21]. Its mechanism of action is not clear since ambroxol is not specific for AGAL, but it is effective also on lysosomal beta-glucocerebrosidase [22] and alpha-glucosidase mutants [21].

Discovery of chaperones directed against the active site is facilitated by focusing on molecules with structural similarity to galactose, a natural product of AGAL. Conversely, the discovery allosteric ligands, i.e. ligands that bind AGAL at sites outside the active site, is complicated by the fact that they may not chemically resemble any known substrates or products. We performed *in silico* molecular docking (virtual screening) of over ten thousand low molecular weight structurally diverse compounds previously filtered from ZINC database [23], by looking for molecules that bind preferentially at a site different from the active site. Among the top ranking hits we found one molecule, 2,6-dithiopurine (DTP). This molecule was chosen for further studies since it has already passed some safety tests, is a known chemiopreventive agent [24] [25] and it is safe when administered to mice [26]. DTP is able to stabilize AGAL against thermal and urea-induced denaturation and is able to rescue a mutant that is not sensitive to DGJ. It acts *in vivo* in synergy with galactose and with very low concentrations of DGJ.

Methods and Materials

Virtual screening

We selected a random subset of 9 million molecules (including FDA-approved drugs) from the ZINC database [23] for performing the virtual screening calculations in this study. Molecular docking calculations were carried out on the structure deposited in the PDB with the code 3S5Z [27] with the Leadfinder [28] docking program using default parameters. Protein structure 3S5Z contains 2 ligands: alpha-D-galactose (GLA) bound at the active site through D92, D93, K168, E203, R227, D231 (GLA site) and beta-D-galactose (GAL) bound at a different site through D255 and K374 (GAL site). Thus, two boxes (x, y, z dimensions 40 Å), centered on the position occupied by either GLA or GAL, were set for docking. Using the global shape similarity tool WEGA [29] alpha-D-galactose (the natural substrate of AGAL) was processed against the selected compound library and those molecules with the highest values for similarity score, ranging from 0.8 to 0.95, were selected for posterior docking studies. In total ten thousand purchasable molecules obtained after filtering with WEGA were selected for docking.

Thermal unfolding

Thermal shift assay [30, 31] was adapted as described [32] using commercially available wt-AGAL, Fabrazyme® (Genzyme, Cambridge, MA). Melting profiles were recorded under different conditions by thermal shift assay with the StepOne Real-Time PCR System (Applied Biosystems). The protein (0.5–1 mg/mL final concentration) was equilibrated in Na-Hepes 20

mM, NaCl 150 mM, pH 7.4 with Sypro Orange 2.5X (Invitrogen Molecular Probes, lifetechnologies.com), either without ligands or in the presence of ligands (6 mM DTP, 0.040 mM DGJ (SIGMA, Milan, Italy). The samples were distributed in 48-well PCR plates (0.025 mL in each well), sealed and heated from 20 to 90° at 1°C/min with increments of 0.6°C. The excitation wavelength of 490 nm and the emission wavelength of 575 nm, which are optimal for fluorescein, were adapted to detect Sypro Orange. Melting profiles of recombinant human phosphomannomutase2 were recorded similarly, the only exception was the presence of 1mM MgCl2 in the buffer. Phosphomannomutase 2 had been expressed and purified as described [33].

In order to verify the reversibility of the effect of DTP on Fabrazyme®, the enzyme equilibrated in Na-Hepes 20 mM, NaCl 150 mM, pH 7.4 was incubated for 1 hour at 4°C in the presence of 6 mM DTP dissolved in DMSO, then the sample was dialysed by ultrafiltration (by using Centrifugal ultrafiltration unit 15-mL MWCO 10 kDa, Merck-Millipore). A control experiment was also conducted incubating the enzyme with DMSO and dialysing it. Each dialysed sample was analysed by enzymatic assay (at pH 7.5) and by TSA (the experiment was conducted either in the presence of 6 mM DTP or with only DMSO) as described above.

Urea-induced unfolding

The experiment was carried out with a method firstly described by Kim et al [34] and adapted as described [35]. In brief, Fabrazyme® (0.32 mg/mL) was induced to unfold by urea in Hepes buffer at pH 7.4, with or without DTP 6 mM, in a final volume of 0.028 mL. The enzyme was incubated in the presence of urea concentrations ranging from 0 to 5 M. The samples were incubated at 10°C overnight, then each sample was treated with the appropriate amount of thermolysin necessary to obtain a 1:5 protease to protein ratio in the presence of $CaCl_2$ (10 mM final concentration). After 1 min incubation at 37°C the reaction was stopped by the addition of EDTA (40 mM final concentration). The samples were separated by SDS-PAGE and coloured by Coomassie Blue Staining, then undigested proteins (Fabrazyme® and thermolysin) were quantified with a ChemiDoc XRS (Bio-Rad Laboratories, Hercules, CA-USA). Two rectangular boxes were used to define specific protein bands, one for Fabrazyme® and one for thermolysin as shown in S1 File. The intensity of bands was corrected subtracting the appropriate background (adjusted volumes), the ratio between the corrected values was calculated for Fabrazyme® and thermolysin in each lane and was plotted against urea concentration.

Transfection into COS-7 cells

COS-7cells were cultured in DMEM containing 10% FBS at 37°C and 5% CO2. The cells were transfected with individual plasmids containing mutant AGAL-encoding ORF using the LipofectAMINE2000 cationic lipid reagent in suspension [36].

67.5 micrograms of plasmid DNA in 13.5 mL Opti-MEM (Invitrogen) were mixed with 0.135 mL LipofectAMINE2000 reagent (Invitrogen) and incubated for 30 min at room temperature. COS-7 cells were harvested by trypsin treatment and resuspended in DMEM containing 10% FBS.

COS-7 in suspension (40.5 mL) were added to the transfection mix solution, distributed into 27 wells of six-well plates at 60% confluency and allowed to adhere for 5h.

The medium was substituted by fresh DMEM, 10% FBS, 1% DMSO (used to solubilize DTP and ambroxol) (1 mL), and drugs were added either in monotherapy or in binary combination as indicated in the specific figure legends. After 48 h incubation, the cells were washed in PBS (5 times), scraped and harvested by centrifugation. Dry pellets were resuspended in 0.030 mL of water and lysed by freeze-thawing. Three independent transfections were carried out for A230T, C56Y, C63Y, two for the other mutants, E341D, A37T, P40S, M42T, M42V, S126C,

C172G, R118C, Q280K, L300F, L310F and G360C. Water-soluble extracts were used for enzyme assays or western blot. The Bradford colorimetric assay was used for protein quantification [37] using the Bio-Rad Protein Assay with bovine serum albumin as standard.

Alpha-galactosidase assay

Tests on transfected mutants were carried out as described in [36]. Briefly: cell lysates (1–2 microliters) were added to 38 microliters of AGAL assay buffer (sodium citrate 27 mM-sodium phosphate dibasic 46 mM, 4-methylumbelliferyl-alpha-D-galactopyranoside 5 mM and N-acetyl-D-galactosamine 100 mM, pH 4.5) and incubated for 0.5–1 h at 37°C. All chemicals were obtained from Sigma. The reaction was stopped by adding 0.360 mL of 1 M sodium carbonate buffer [10]. Fluorescence was detected using a fluorescence spectrophotometer (Cary Eclypse-Varian) at 355 nm excitation and 460 nm emission.

A 4-methylumbelliferone standard curve ranging from 5 nM to 0.025 mM was run in parallel for conversion of fluorescence data to AGAL activity expressed as nmol/mg protein per min.

In order to measure the enzymatic activity in the presence of DTP 6 mM a spectrophotometric assay was run. Fabrazyme (1–2 microliters 0.25 mg/ml) were added to 0.038 mL of AGAL assay buffer (4-Nitrophenyl α-D-galactopyranoside 17 mM in Hepes 40 mM pH 7.4) and incubated for 3–15 min at 37°C. The reaction was stopped by adding 0.360 mL of 1 M sodium carbonate and the absorbance at 405nm was measured. The assay was conducted in the presence of DTP 6 mM (previously dissolved in DMSO) or DMSO.

Western blot analysis

Western blot analysis for the detection of AGAL was performed using rabbit polyclonal antibodies (Abcam 70520) and HRP-coniugated anti-rabbit IgG antibody produced in goat (Bio-Rad 1706515). After SDS-PAGE (15% acrylamide), proteins were transferred to a PVDF membrane. The membrane was blocked with 5% (w/v) non-fat dried skimmed milk in blot solution at 4°C overnight, then treated with the primary antibody diluted in a blot solution 1:500 for 1 hour at room temperature. After washing, the detection was performed by using the Precision Plus Protein™ (Bio-Rad). GAPDH was revealed with mouse monoclonal anti lapine GAPDH (AbD seroTec (cat:4699–9555) 1:2000. All other chemicals were from Bio-Rad. Uncropped images of the gels are provided as S1 File.

Deglycosylation

Deglycosylation of A230T expressed in COS7 cells (treated or untreated with DTP 6 mM) (10 μg f each) was performed according to the producer's instructions. wt-AGAL was processed at the same way as a control. Briefly, EDTA and SDS were added to the proteins (final concentrations were 20 mM and 0.1% respectively). The samples were then boiled for 5 min, immediately cooled before the addition of NP-40 to a final condition of 0.7% and N-Glycosidase F (0.5 unit) and incubated overnight at 37°C. A parallel experiment was conducted avoiding the denaturation step (SDS and heating) before adding NP-40. The samples was analysed by western blotting as described elsewhere.

Bioinformatic and Statistical analysis

Standard deviations and p values (paired two-tailed Student's t-test) were obtained using Microsoft Excel (Microsoft Office professional 2010).

The effect of mutation on protein stability was predicted either running SDM on-line [38] or running MUPRO1.1[39] locally. Secondary structure was assigned with SEGNO [40]. Accessibility to solvent was calculated by SDM. Active site residues were identified with DroseP [41]. Molecular dynamics was run with Yasara program under default conditions for 50 nsec [42] and flexibility assessed as described [43]. Protein damaging scores based on sequence conservation were derived using PolyPhen-2 software [44] or Fabry_CEP [45].

Results

Molecular docking calculations were carried out on the AGAL structure deposited in the pdb with the code 3S5Z [27]. In this model AGAL binds two ligands per chain: alpha-D-galactose at the active site through D92, D93, K168, E203, R227 and D231 (GLA site) and beta-D-galactose at a different site through D255 and K374 (GAL site). This structure offers a good target to identify molecules that have little inhibitory activity and/or act in synergy with drugs directed against the active site. In proximity to the GAL site, we identified a hot-spot for binding that will be referred to as the allosteric site. It comprises residues A37, R38, T39, P40, T41, M42, E87, Y88 and does not overlap with the active site that is lined by W47, D92, D93, Y134, C142, K168, D170, E203, L206, Y207, R227, D231, S297 (Fig 1). The allosteric site is different from the GAL binding site.

We looked for molecules that bind the allosteric site with a high score, but bind the active site with a very low score. Drug repositioning, which should always be considered as the first choice when developing new therapies for rare diseases [46], could not be used because none of the approved drugs tested (FDA database) bound specifically the allosteric site (results not shown).

As a second choice we selected DTP, which is not an approved drug, but is a good candidate because it is safe when tested on human skin cells [25] and on mice [24] [26]. Even if the docking simulations started at GAL site DTP contacted the allosteric site. As a control we carried out a simulation limiting the search to a box centred on the active site as described in the methods. We show the interactions of DTP with the allosteric site in Fig 1B, and the corresponding energetic contributions in Fig 2A, the potential interactions of DTP with the active site (GLA site) in Fig 1C and the corresponding energetic contributions in Fig 2B. Docking simulations calculated a binding affinity at GLA's binding site 52% lower (absolute value) than at the allosteric site (Fig 2). Scores calculated with Leadfinder [28] are reported as kcal/mol in Fig 2, but are meant only for rank-ordering different docking poses of DTP and cannot provide accurate binding energy predictions.

DTP does not inhibit AGAL (Fabrazyme®, Genzyme) when tested at 6 mM concentration using 4-Nitrophenyl α-D-galactopyranoside 17 mM in Hepes 40 mM pH 7.4, whereas DGJ blocks completely the enzyme (1% residual activity) at concentration as low as 0.001 mM.Thermal shift assay was used to evaluate the ability of DTP (6mM) to stabilize wt-AGAL, (Fabrazyme®, Genzyme) in the presence or in the absence of DGJ. DTP is able to stabilize the enzyme against thermal denaturation alone or in synergy with the iminosugar (Fig 3A). without forming covalent bonds. To prove the reversibility of this stabilising effect, DTP (6 mM) was incubated with enzyme and subsequently removed by dialysis before thermal shift assay. Results are indicated in Fig 3B (filled squares DTP/DTP; open squares DMSO/DTP; filled circles; DTP/DMSO; open circles DMSO/DMSO) where the first word of the label corresponds to the pretreatment and the second part corresponds to the presence of the compound during the thermal scan. The specificity of effect of DTP was tested running thermal shift assay on phosphomannomutase2, an enzyme structurally and functionally unrelated to AGAL in the presence of DTP 6 mM or a positive control, glucose 1–6 bisphosphate 0.5 mM (S1 Fig).

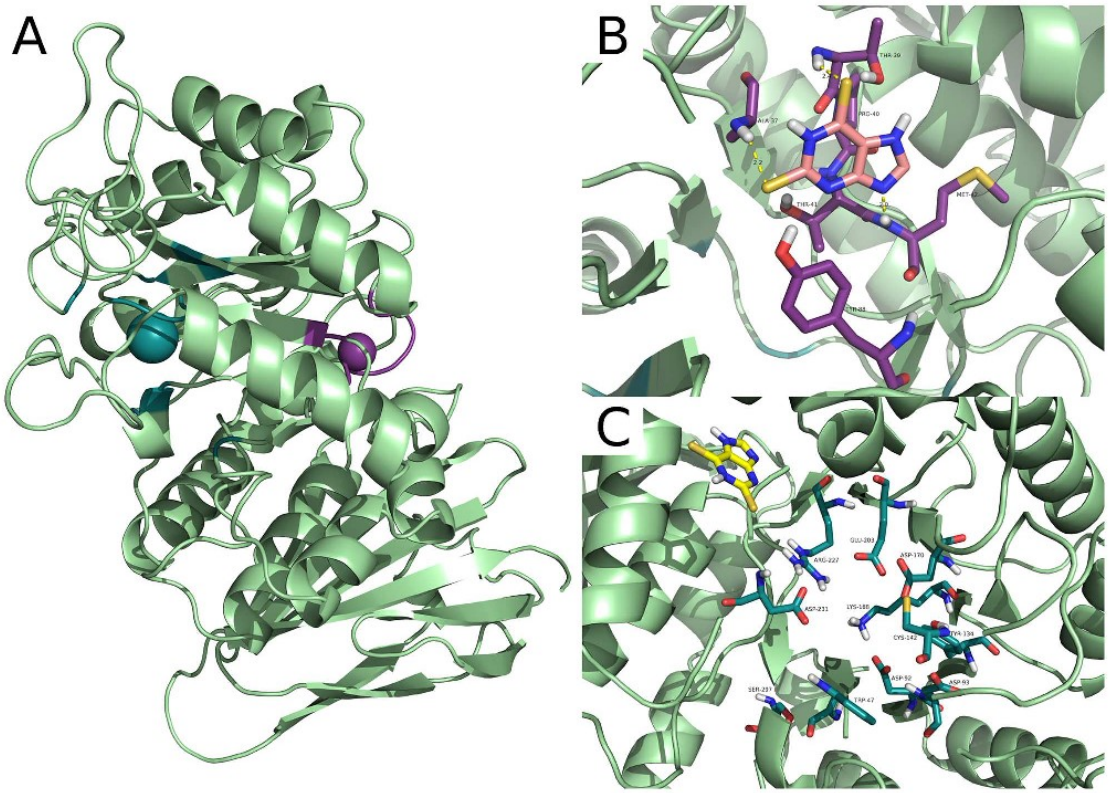

Fig 1. The active site and the allosteric binding site in human lysosomal alpha-galactosidase. The structure of lysosomal alpha-galactosidase is shown as a cartoon. In Panel A the active site (GLA site) is pinpointed by a blue sphere while the allosteric binding site is pinpointed by a violet sphere. Residues involved in the 2,6-dithiopurine allosteric and alpha-galactose binding site respectively are shown as sticks in Panel B or C respectively along with docked DTP. Predicted hydrogen bonds between DTP and AGAL within the allosteric binding site are shown as yellow dashed lines in Panel B. Best ranked pose of DTP in the alpha-galactose binding site area is shown in Panel C.

doi:10.1371/journal.pone.0165463.g001

The stability of AGAL in the presence or in the absence of DTP was tested by unfolding induced by a range of urea concentrations, followed by limited proteolysis. The enzyme unfolds at 2.7 M urea in the absence of DTP, and at 3 M urea in the presence of DTP (Fig 4). A minor band, which might represent a differently glycosylated form of AGAL, is observed in Fig 4. Its intensity correlates with that of the major band (data not shown).

AGAL mutants were expressed transiently in COS-7 cells. We tested the effect of DTP on the mutant A230T [47], which is non-responsive to DGJ [36], but eligible for PC therapy [48].

After transfection of A230T into COS-7 cells, specific bands were revealed by Western blot (WB) and the total alpha-galactosidase activity was measured in cell extracts. In order to interpret results it is worth remembering that AGAL is synthesized as a precursor of 50 kDa, but it is converted into a mature form of 46 kDa. A detailed analysis of Ishii and co-workers [49] demonstrated that when AGAL mutants are correctly processed into a 46 kDa form, they are also transferred into lysosomes. In Fig 5A we show the migration of transfected wt-AGAL (90 ±9 U/mg activity in the lysates) as a reference. A230T shows a faint band corresponding to the precursor form of AGAL. This is not induced by the treatment with acknowledged PCs, DGJ,

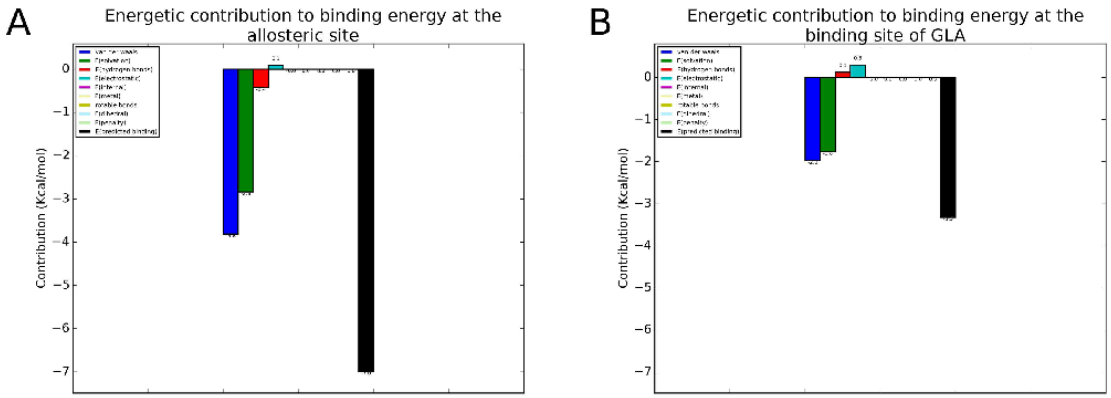

Fig 2. Energetic contributions to the binding of 2–6 dithiopurine to the allosteric site and the active site of human lysosomal alpha-galctosidase. Depicted energetic contributions are: van der Waals interactions (dark blue), volume-based free energy of solvation (green), hydrogen bonds (red), electrostatic energy (cyan), internal energy (pink), metal interactions (light yellow), energy of entropic losses associated with ligand's rotatable bonds (dark yellow), dihedral energy (light blue), internal energy penalty (light green) and total predicted binding affinity (black). A) Decomposition for the allosteric site, and B), decomposition for the active site.

doi:10.1371/journal.pone.0165463.g002

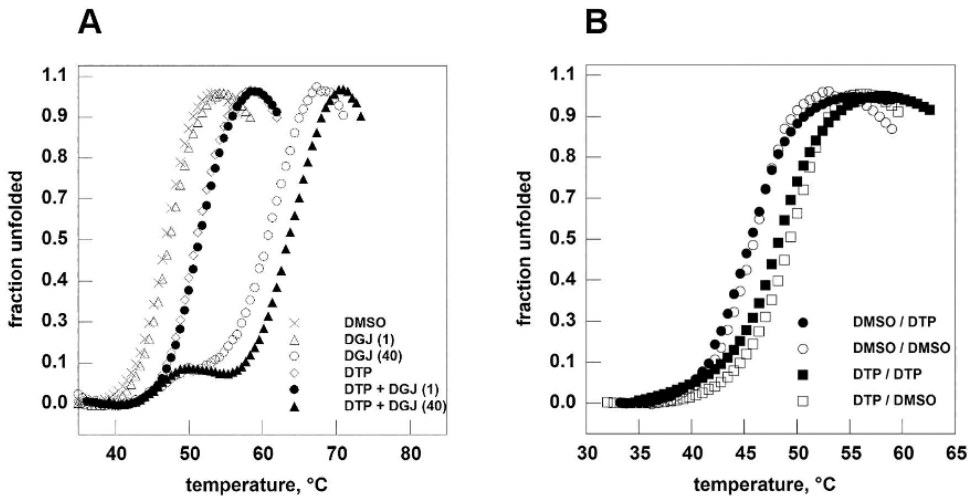

Fig 3. 2–6 dithiopurine stabilizes human lysosomal alpha-galactosidase in thermal shift assay. Panel A. Fabrazyme® (in Na-Hepes 20 mM, NaCl 150 mM, pH 7.4) was equilibrated in the presence of ligands dissolved in DMSO 20%: DGJ 1 microM (empty triangle) or 40 microM (empty circle); DTP 6 mM (empty diamond); DTP 6 mM plus DGJ 1 microM (filled circle); DTP 6 mM plus DGJ 40 microM (filled triangle). A control (with only DMSO) was also shown (x). Panel B. Fabrazyme® (in Na-Hepes 20 mM, NaCl 150 mM, pH 7.4) was incubated in the presence of DTP 6 mM for 1 hour at 4˚C then DTP was eliminated by dialysis. A control experiment was conducted by incubating the enzyme only with DMSO. Both the aliquots of Fabrazyme® were analysed by thermal shift assay in the presence of DTP 6 mM or in the presence of DMSO. Filled squares: DTP/DTP; open squares: DMSO/DTP; filled circles: DTP/DMSO; open circles: DMSO/DMSO where the first word of the label corresponds to the pretreatment and the second part corresponds to the presence of the compound during the thermal scan. The protein samples were heated from 20 to 90˚ at 1˚C/min in the presence of Sypro Orange 2.5x. Data were shown as normalized curves.

doi:10.1371/journal.pone.0165463.g003

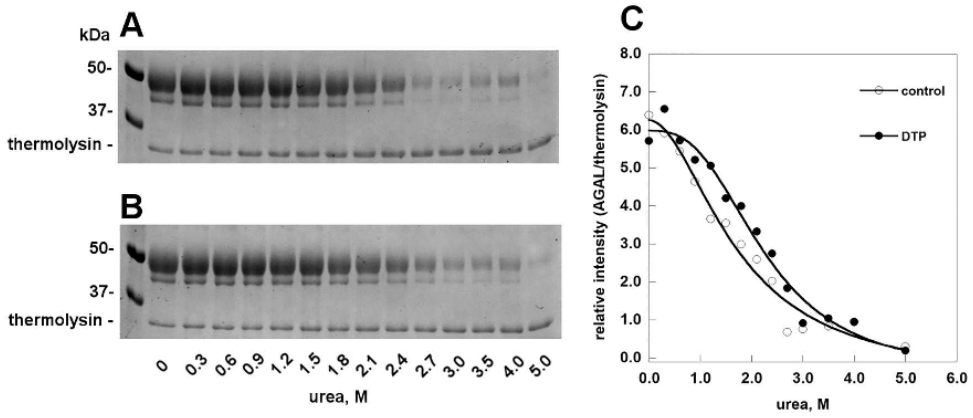

Fig 4. 2–6 dithiopurine protects human alpha-galactosidase against urea-induced unfolding. Fabrazyme® was incubated in the presence of urea (from 0 to 5 M), with (B) or without (A) DTP 6 mM, at 10˚C over night, then each sample was treated for 1 min at 37˚C with thermolysin (1:5 protease to protein ratio). Folded undigested proteins were visualized by SDS-PAGE. The intensity of the bands was quantified and the relative intensity of major band of Fabrazyme® and thermolysin in each lane was plotted against urea concentration (C).

doi:10.1371/journal.pone.0165463.g004

galactose [50] or ambroxol [21], at the dosages commonly used to measure their chaperoning effect on transfected mutants, 0.020 mM, 100 mM or 0.040 mM respectively. However, DTP 6 mM promotes the maturation of A230T. Moreover, its effect is potentiated by galactose and DGJ, even at very low concentration (0.001mM), but not by ambroxol (Fig 5A, 5B and 5C).

The lowest concentration at which DTP promotes A230T maturation is 2 mM (Fig 5D and 5E). The different bands visualised on WB represent different glycosylated forms, as demonstrated by treatment of A230T or wt-AGAL with N-Glycosidase F Fig 5F.

We tested the effect of DTP 6 mM on further mutants expressed in COS-7 cells: C56Y (Fig 6A), C63Y (Fig 6B) and E341D (Fig 6C). In these cases, enzymatic activity was not recovered (Fig 6D), possibly because the proteins are not catalytically active, but increased protein processing was detectable. C63Y and E341D are not responsive do DGJ [12, 13]. C56Y activity increases in the presence of DGJ although it does not meet the criteria chosen Lukas *et al* [13] to define responsiveness.

We tested four mutations affecting residues in the allosteric site, A37T, P40S, M42T, M42V. None of these mutants responds to DTP (Fig 7). A37T [12], M42T [13] and M42V [8, 9, 12] are responsive to 0.020 mM DGJ, whereas P40S is not [10, 11, 13]. This finding supports the idea that DTP binds the allosteric site found *in silico*, although it does not prove it, because the same molecule has no effect on mutations that do *not* affect the allosteric site. An example is provided by S126C, C172G, and R118C which are not responsive to DGJ, [10–12, 51] (S2 Fig) and by Q280K, L300F, L310F and G360C (S3 Fig), which are responsive to DGJ [12] [36].

Discussion

The catalytic domain of AGAL is formed by a TIM-barrel and the active site is located at the carboxyterminal end of beta-strands, as expected [52].

We identified a different druggable pocket located at the opposite side of the TIM-barrel of AGAL. Some molecules resulting from our virtual screening bind better to the allosteric site than to the active site. One of these molecules, a chemopreventive 2,6-dithiopurine DTP, appeared particularly promising because it is actively transported into mammalian cells where it accumulates at millimolar concentration [25] and it is safe [24] [26].

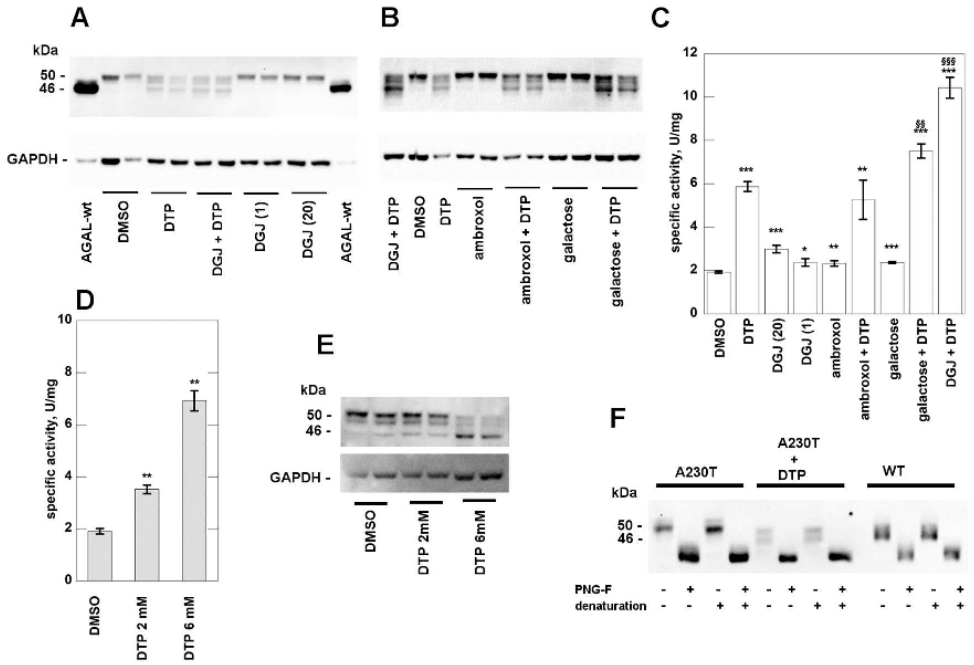

Fig 5. 2–6 dithiopurine rescues mutant human alpha-galactosidase in monotherapy or in synergy. COS-7 cells were cultured in conventional medium and transfected with plasmid containing A230T mutant. Cells were treated with: DTP 6 mM, DGJ 1 microM, DGJ 20 microM, ambroxol 40 microM, ambroxol 40 microM plus DTP 6 mM, galactose 100 mM, galactose 100 mM plus DTP 6 mM, DGJ 1microM plus DTP 6 mM. All the molecules were dissolved in DMSO and an appropriate control was realized. After 48 h incubation, the cells were scraped and lysed then water-soluble extracts were analysed by western blotting (A and B) and enzyme assay (C). The effect of DTP 2 mM is shown in D and E. Cell extracts were treated with N-Glycosidase F and then analysed by WB (F). Standard deviations is indicated by bars and differences that are statistically significant are flagged by * when compared to the control with DMSO ($p < 0.05$:*; $p < 0.01$: **; $p < 0.001$:***), are flagged by § when compared to DTP ($p < 0.01$:§§; $p < 0.001$:§§§).

doi:10.1371/journal.pone.0165463.g005

DTP promotes the processing of some mutants of AGAL that are not responsive to DGJ and in one case, A230T, enhances its activity in monotherapy as well as in synergy with DGJ or galactose.

Not all missense mutations associated with FD are responsive to PC and we have not yet found molecular features that are necessary and sufficient to determine responsiveness. Mutations occurring at non conserved sites are generally less severe and responsive to PC, but there are exceptions to this rule. The best example we encountered is A230T, a mutation occurring at a non conserved site. A230 is exposed to solvent and exhibits moderate flexibility (Root mean square fluctuation, RMSF, of alpha carbon 0.74 ±0.02 Å). A230 is not directly implicated in catalysis, but it flanks D231, a proton donor that is essential for the hydrolysis of the substrate and belongs to a short stretch in polyproline II conformation. Its mutation to Threonine is classified as mildly destabilizing by MUPRO [39] or SDM [38]. The position specific substitution score, which measures the tolerability of the mutation in orthologous sequences and correlates with responsiveness to DGJ, is benign [48]. A230T is classified as possibly damaging or benign by HumDiv- and HumVar-trained PolyPhen-2 models respectively [44]. To summarize, A230T is eligible for PC therapy and does respond to DTP, although it does not respond to DGJ. Although DTP might be active only on a minority of AGAL missense mutations, we

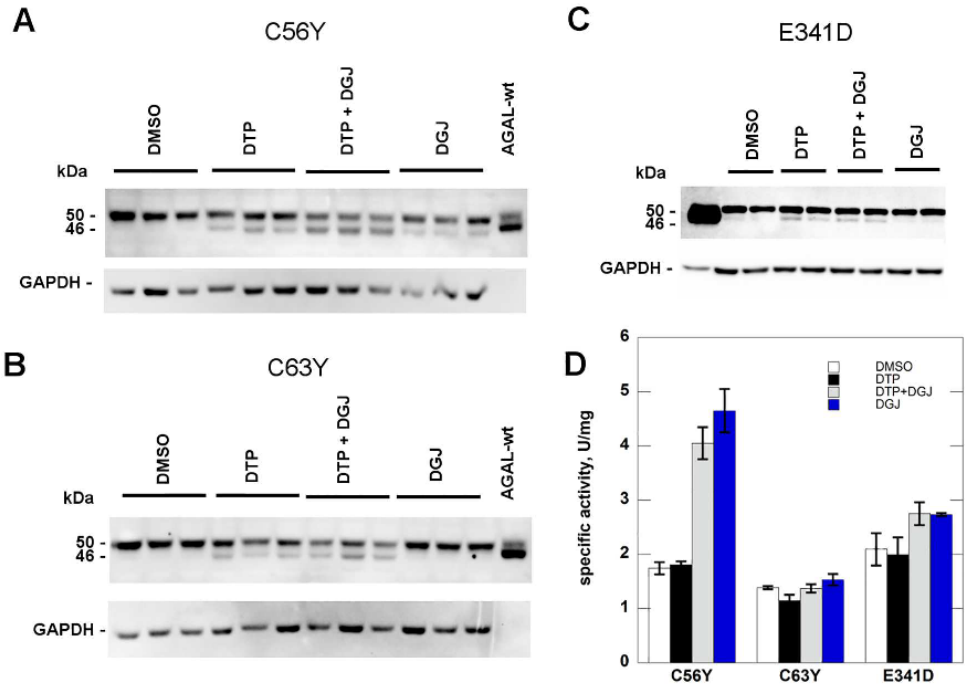

Fig 6. 2–6 dithiopurine promotes processing of some mutant human alpha-galactosidase. COS-7 cells were cultured in conventional medium and transfected with plasmid containing C56Y, C63Y and E341D mutants. Cells were treated with: DTP 6 mM, DGJ 1 microM, DGJ 1 microM plus DTP 6 mM. All the molecules were dissolved in DMSO and an appropriate control was realized. After 48 h incubation, the cells were scraped and lysed then water-soluble extracts were analysed by western blotting (A, B and C) and enzyme assay (D). Standard deviations are indicated by bars.

doi:10.1371/journal.pone.0165463.g006

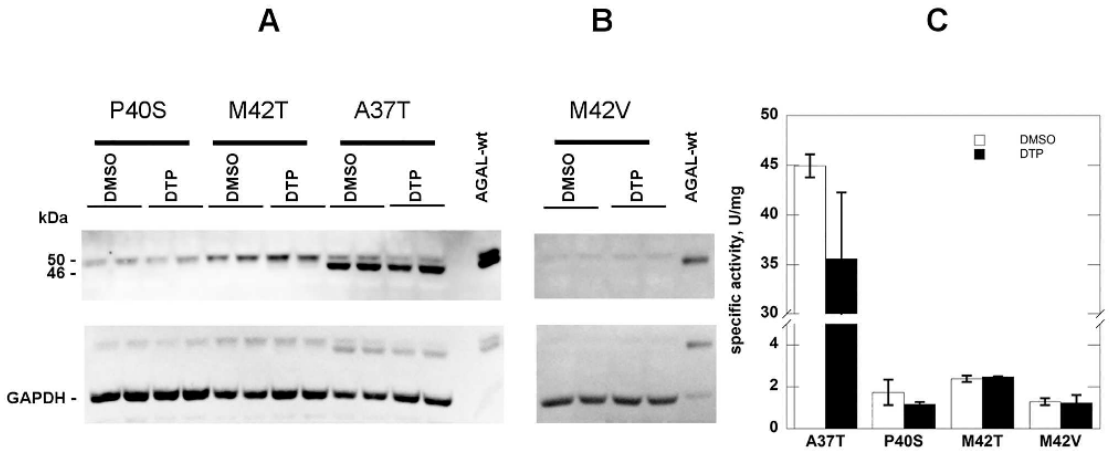

Fig 7. 2–6 dithiopurine has no effect on mutations affecting the allosteric site. COS-7 cells were cultured in conventional medium and transfected with plasmid containing A37T, P40S, M42T, M42V mutants. Cells were treated with DTP 6 mM dissolved in DMSO and an appropriate control was realized. After 48 h incubation, the cells were scraped and lysed then water-soluble extracts were analysed by western blotting (A and B) and enzyme assay (C). Standard deviations are indicated by bars.

doi:10.1371/journal.pone.0165463.g007

suggest that it should be tested in the cases that receive a positive score with Fabry_CEP [45], but fail to respond to DGJ. We are aware that the interaction of DTP with AGAL, which occurs in vitro only at high concentration, cannot exclude non specific off-target effects of the drug on protein homeostasis. Derivatives of DTP obtained by techniques of lead optimization and medicinal chemistry might prove to be effective at lower doses and more specific.

Supporting Information

S1 Fig. 2–6 dithiopurine does not stabilizes human lysosomal phosphomannomutase2 in thermal shift assay. Human Phosphomannomutase2 (in Na-Hepes 20 mM, NaCl 150 mM, $MgCl_2$ 1mM pH 7.4) was equilibrated in the presence of ligands dissolved in DMSO 20%: DTP 6 mM (empty circle) and glucose 1, 6 bisphosphate (G16) 0.5 mM (filled squares) as a positive control. A control (with only DMSO) was also shown (filled circles).
(TIF)

S2 Fig. 2–6 dithiopurine has no effect on some mutations that are not responsive to DGJ. COS-7 cells were cultured in conventional medium and transfected with plasmid containing R118C, S126C and C172G mutants. Cells were treated with: DTP 6 mM, DGJ 1 microM, DGJ 1 microM plus DTP 6 mM. All the molecules were dissolved in DMSO and an appropriate control was realized. After 48 h incubation, the cells were scraped and lysed then water-soluble extracts were analysed by western blotting (A, B and C) and enzyme assay (D). Standard deviations are indicated by bars.
(TIF)

S3 Fig. 2–6 dithiopurine has no effect on some mutations that are responsive to DGJ. COS-7 cells were cultured in conventional medium and transfected with plasmid containing L310F, L300F, Q280K and G360C mutants. Cells were treated with DTP 6 mM. All the molecules were dissolved in DMSO and an appropriate control was realized. After 48 h incubation, the cells were scraped and lysed then water-soluble extracts were analysed by western blotting (A, B) and enzyme assay (C). Standard deviations are indicated by bars.
(TIF)

S1 File. Uncropped gels. Images are relative to gels shown in Figs 4, 5, 6 and 7.
(PDF)

Acknowledgments

The authors gratefully acknowledge the computer resources and the technical support provided by the Plataforma Andaluza de Bioinformática of the University of Málaga. We thank E. Castelluccio, V.Mirra, A.Paone and A.Siciliano for technical assistance. We thank D.J.G. Mackay for copyediting the manuscript. This work is dedicated to our friend and colleague Dr Maria Malanga.

Author Contributions

Conceptualization: VC HP-S GA.

Data curation: HP-S MVC.

Formal analysis: VC GA.

Funding acquisition: HP-S MVC GA.

Investigation: JP-G Hd-H RDP LL CC.

Methodology: JP-G Hd-H RDP LL CC.

Project administration: GA.

Resources: HP-S JL MVC GA.

Software: JP-G Hd-H HP-S.

Supervision: HP-S MVC GA.

Validation: VC RDP LL CC.

Visualization: VC HP-S.

Writing – original draft: MVC GA.

Writing – review & editing: JL MVC GA.

References

1. Sirrs S, Hollak C, Merkel M, Sechi A, Glamuzina E, Janssen MC, et al. The Frequencies of Different Inborn Errors of Metabolism in Adult Metabolic Centres: Report from the SSIEM Adult Metabolic Physicians Group. JIMD Rep. 2015. Epub 2015/10/10. doi: 10.1007/8904_2015_435 PMID: 26450566.
2. Germain DP. Fabry disease. Orphanet J Rare Dis. 2010; 5:30. PMID: 21092187. doi: 10.1186/1750-1172-5-30
3. Beck M, Hughes D, Kampmann C, Larroque S, Mehta A, Pintos-Morell G, et al. Long-term effectiveness of agalsidase alfa enzyme replacement in Fabry disease: A Fabry Outcome Survey analysis. Mol Genet Metab Rep. 2015; 3:21–7. Epub 2016/03/05. [pii]. PMID: 26937390; PubMed Central PMCID: PMC4750577.
4. Rombach SM, Hollak CE, Linthorst GE, Dijkgraaf MG. Cost-effectiveness of enzyme replacement therapy for Fabry disease. Orphanet J Rare Dis. 2013; 8:29. Epub 2013/02/21. [pii]. PMID: 23421808; PubMed Central PMCID: PMC3598841.
5. Lukas J, Scalia S, Eichler S, Pockrandt AM, Dehn N, Cozma C, et al. Functional and Clinical Consequences of Novel alpha-Galactosidase A Mutations in Fabry Disease. Hum Mutat. 2016; 37(1):43–51. Epub 2015/09/30. doi: 10.1002/humu.22910 PMID: 26415523.
6. Fan JQ, Ishii S, Asano N, Suzuki Y. Accelerated transport and maturation of lysosomal alpha-galactosidase A in Fabry lymphoblasts by an enzyme inhibitor. Nat Med. 1999; 5(1):112–5. PMID: 9883849. doi: 10.1038/4801
7. Shin SH, Kluepfel-Stahl S, Cooney AM, Kaneski CR, Quirk JM, Schiffmann R, et al. Prediction of response of mutated alpha-galactosidase A to a pharmacological chaperone. Pharmacogenet Genomics. 2008; 18(9):773–80. PMID: 18698230. doi: 10.1097/FPC.0b013e32830500f4
8. Shimotori M, Maruyama H, Nakamura G, Suyama T, Sakamoto F, Itoh M, et al. Novel mutations of the GLA gene in Japanese patients with Fabry disease and their functional characterization by active site specific chaperone. Hum Mutat. 2008; 29(2):331. PMID: 18205205. doi: 10.1002/humu.9520
9. Park JY, Kim GH, Kim SS, Ko JM, Lee JJ, Yoo HW. Effects of a chemical chaperone on genetic mutations in alpha-galactosidase A in Korean patients with Fabry disease. Exp Mol Med. 2009; 41(1):1–7. PMID: 19287194. doi: 10.3858/emm.2009.41.1.001
10. Benjamin ER, Flanagan JJ, Schilling A, Chang HH, Agarwal L, Katz E, et al. The pharmacological chaperone 1-deoxygalactonojirimycin increases alpha-galactosidase A levels in Fabry patient cell lines. J Inherit Metab Dis. 2009; 32(3):424–40. PMID: 19387866. doi: 10.1007/s10545-009-1077-0
11. Wu X, Katz E, Della Valle MC, Mascioli K, Flanagan JJ, Castelli JP, et al. A pharmacogenetic approach to identify mutant forms of alpha-galactosidase A that respond to a pharmacological chaperone for Fabry disease. Hum Mutat. 2011; 32(8):965–77. PMID: 21598360. doi: 10.1002/humu.21530
12. Lukas J, Giese AK, Markoff A, Grittner U, Kolodny E, Mascher H, et al. Functional characterisation of alpha-galactosidase a mutations as a basis for a new classification system in fabry disease. PLoS Genet. 2013; 9(8):e1003632. Epub 2013/08/13. [pii]. PMID: 23935525; PubMed Central PMCID: PMC3731228.
13. Lukas J, Scalia S, Eichler S, Pockrandt AM, Dehn N, Cozma C, et al. Functional and Clinical Consequences of Novel alpha-Galactosidase A Mutations in Fabry Disease. Hum Mutat. 2015. Epub 2015/09/30. doi: 10.1002/humu.22910 PMID: 26415523.

14. Ishii S, Chang HH, Yoshioka H, Shimada T, Mannen K, Higuchi Y, et al. Preclinical efficacy and safety of 1-deoxygalactonojirimycin in mice for Fabry disease. J Pharmacol Exp Ther. 2009; 328(3):723–31. PMID: 19106170. doi: 10.1124/jpet.108.149054

15. Khanna R, Benjamin ER, Pellegrino L, Schilling A, Rigat BA, Soska R, et al. The pharmacological chaperone isofagomine increases the activity of the Gaucher disease L444P mutant form of beta-glucosidase. Febs J. 2010; 277(7):1618–38. PMID: 20148966. doi: 10.1111/j.1742-4658.2010.07588.x

16. Germain DP, Giugliani R, Hughes DA, Mehta A, Nicholls K, Barisoni L, et al. Safety and pharmacodynamic effects of a pharmacological chaperone on alpha-galactosidase A activity and globotriaosylceramide clearance in Fabry disease: report from two phase 2 clinical studies. Orphanet J Rare Dis. 2012; 7:91. PMID: 23176611. doi: 10.1186/1750-1172-7-91

17. Giugliani R, Waldek S, Germain DP, Nicholls K, Bichet DG, Simosky JK, et al. A Phase 2 study of migalastat hydrochloride in females with Fabry disease: Selection of population, safety and pharmacodynamic effects. Mol Genet Metab. 2013; 109(1):86–92. PMID: 23474038. doi: 10.1016/j.ymgme.2013.01.009

18. Tsukimura T, Chiba Y, Ohno K, Saito S, Tajima Y, Sakuraba H. Molecular mechanism for stabilization of a mutant alpha-galactosidase A involving M51I amino acid substitution by imino sugars. Mol Genet Metab. 2011; 103(1):26–32. PMID: 21353612. doi: 10.1016/j.ymgme.2011.01.013

19. Jenkinson SF, Fleet GW, Nash RJ, Koike Y, Adachi I, Yoshihara A, et al. Looking-glass synergistic pharmacological chaperones: DGJ and L-DGJ from the enantiomers of tagatose. Org Lett. 2011; 13 (15):4064–7. Epub 2011/07/13. doi: 10.1021/ol201552q PMID: 21744786.

20. Yu Y, Mena-Barragan T, Higaki K, Johnson JL, Drury JE, Lieberman RL, et al. Molecular basis of 1-deoxygalactonojirimycin arylthiourea binding to human alpha-galactosidase a: pharmacological chaperoning efficacy on Fabry disease mutants. ACS Chem Biol. 2014; 9(7):1460–9. Epub 2014/05/03. doi: 10.1021/cb500143h PMID: 24783948.

21. Lukas J, Pockrandt AM, Seemann S, Sharif M, Runge F, Pohlers S, et al. Enzyme enhancers for the treatment of fabry and pompe disease. Mol Ther. 2015; 23(3):456–64. Epub 2014/11/21. doi: 10.1038/mt.2014.224 [pii]. PMID: 25409744.

22. Bendikov-Bar I, Maor G, Filocamo M, Horowitz M. Ambroxol as a pharmacological chaperone for mutant glucocerebrosidase. Blood Cells Mol Dis. 2013; 50(2):141–5. Epub 2012/11/20. doi: 10.1016/j.bcmd.2012.10.007 [pii]. PMID: 23158495; PubMed Central PMCID: PMC3547170.

23. Irwin JJ, Shoichet BK. ZINC—a free database of commercially available compounds for virtual screening. J Chem Inf Model. 2005; 45(1):177–82. Epub 2005/01/26. doi: 10.1021/ci049714+ PMID: 15667143; PubMed Central PMCID: PMC1360656.

24. Boulware S, Fields T, McIvor E, Powell KL, Abel EL, Vasquez KM, et al. 2,6-Dithiopurine, a nucleophilic scavenger, protects against mutagenesis in mouse skin treated in vivo with 2-(chloroethyl) ethyl sulfide, a mustard gas analog. Toxicol Appl Pharmacol. 2012; 263(2):203–9. Epub 2012/06/27. doi: 10.1016/j.taap.2012.06.010S0041-008X(12)00269-4 [pii]. PMID: 22732900; PubMed Central PMCID: PMC3422404.

25. Powell KL, Boulware S, Thames H, Vasquez KM, MacLeod MC. 2,6-Dithiopurine blocks toxicity and mutagenesis in human skin cells exposed to sulfur mustard analogues, 2-chloroethyl ethyl sulfide and 2-chloroethyl methyl sulfide. Chem Res Toxicol. 2010; 23(3):497–503. Epub 2010/01/07. doi: 10.1021/tx9001918 PMID: 20050631; PubMed Central PMCID: PMC2838951.

26. Qing WG, Powell KL, Stoica G, Szumlanski CL, Weinshilboum RM, Macleod MC. Toxicity and metabolism in mice of 2,6-dithiopurine, a potential chemopreventive agent. Drug Metab Dispos. 1995; 23 (8):854–60. Epub 1995/08/01. PMID: 7493553.

27. Guce AI, Clark NE, Rogich JJ, Garman SC. The molecular basis of pharmacological chaperoning in human alpha-galactosidase. Chem Biol. 2011; 18(12):1521–6. PMID: 22195554. doi: 10.1016/j.chembiol.2011.10.012

28. Stroganov OV, Novikov FN, Stroylov VS, Kulkov V, Chilov GG. Lead finder: an approach to improve accuracy of protein-ligand docking, binding energy estimation, and virtual screening. J Chem Inf Model. 2008; 48(12):2371–85. Epub 2008/11/15. doi: 10.1021/ci800166p PMID: 19007114.

29. Yan X, Li J, Liu Z, Zheng M, Ge H, Xu J. Enhancing molecular shape comparison by weighted Gaussian functions. J Chem Inf Model. 2013; 53(8):1967–78. Epub 2013/07/13. doi: 10.1021/ci300601q PMID: 23845061.

30. Pantoliano MW, Petrella EC, Kwasnoski JD, Lobanov VS, Myslik J, Graf E, et al. High-density miniaturized thermal shift assays as a general strategy for drug discovery. J Biomol Screen. 2001; 6(6):429–40. Epub 2002/01/15. doi: 10.1089/108705701753364922 PMID: 11788061.

31. Lo MC, Aulabaugh A, Jin G, Cowling R, Bard J, Malamas M, et al. Evaluation of fluorescence-based thermal shift assays for hit identification in drug discovery. Anal Biochem. 2004; 332(1):153–9. Epub 2004/08/11. doi: 10.1016/j.ab.2004.04.031 [pii]. PMID: 15301960.

32. Andreotti G, Monticelli M, Cubellis MV. Looking for protein stabilizing drugs with thermal shift assay. Drug Test Anal. 2015. Epub 2015/04/08. doi: 10.1002/dta.1798 PMID: 25845367.

33. Andreotti G, Pedone E, Giordano A, Cubellis MV. Biochemical phenotype of a common disease-causing mutation and a possible therapeutic approach for the phosphomannomutase 2-associated disorder of glycosylation. Mol Genet Genomic Med. 2013; 1(1):32–44. doi: 10.1002/mgg3.3 PMID: 24498599

34. Kim MS, Song J, Park C. Determining protein stability in cell lysates by pulse proteolysis and Western blotting. Protein Sci. 2009; 18(5):1051–9. PMID: 19388050. doi: 10.1002/pro.115

35. Andreotti G, Citro V, Correra A, Cubellis MV. A thermodynamic assay to test pharmacological chaperones for Fabry disease. Biochim Biophys Acta. 2014; 1840(3):1214–24. Epub 2013/12/24. doi: 10.1016/j.bbagen.2013.12.018 [pii]. PMID: 24361605; PubMed Central PMCID: PMC3909460.

36. Andreotti G, Citro V, De Crescenzo A, Orlando P, Cammisa M, Correra A, et al. Therapy of Fabry disease with pharmacological chaperones: from in silico predictions to in vitro tests. Orphanet J Rare Dis. 2011; 6:66. Epub 2011/10/19. doi: 10.1186/1750-1172-6-66 [pii]. PMID: 22004918; PubMed Central PMCID: PMC3216245.

37. Bradford MM. A rapid and sensitive method for the quantitation of microgram quantities of protein utilizing the principle of protein-dye binding. Anal Biochem. 1976; 72:248–54. Epub 1976/05/07. S0003269776699996 [pii]. PMID: 942051.

38. Worth CL, Preissner R, Blundell TL. SDM—a server for predicting effects of mutations on protein stability and malfunction. Nucleic Acids Res. 2011; 39(Web Server issue):W215–22. PMID: 21593128. doi: 10.1093/nar/gkr363

39. Cheng J, Randall A, Baldi P. Prediction of protein stability changes for single-site mutations using support vector machines. Proteins. 2006; 62(4):1125–32. PMID: 16372356. doi: 10.1002/prot.20810

40. Cubellis MV, Cailliez F, Lovell SC. Secondary structure assignment that accurately reflects physical and evolutionary characteristics. BMC Bioinformatics. 2005; 6 Suppl 4:S8. PMID: 16351757. doi: 10.1186/1471-2105-6-S4-S8

41. Cammisa M, Correra A, Andreotti G, Cubellis MV. Identification and analysis of conserved pockets on protein surfaces. BMC Bioinformatics. 2013; 14 Suppl 7:S9. Epub 2013/07/17. doi: 10.1186/1471-2105-14-S7-S9 [pii]. PMID: 23815589; PubMed Central PMCID: PMC3633052.

42. Krieger E, Darden T, Nabuurs SB, Finkelstein A, Vriend G. Making optimal use of empirical energy functions: force-field parameterization in crystal space. Proteins. 2004; 57(4):678–83. PMID: 15390263. doi: 10.1002/prot.20251

43. Cubellis MV, Baaden M, Andreotti G. Taming molecular flexibility to tackle rare diseases. Biochimie. 2015; 113:54–8. Epub 2015/04/07. doi: 10.1016/j.biochi.2015.03.018 [pii]. PMID: 25841341; PubMed Central PMCID: PMC4441037.

44. Adzhubei IA, Schmidt S, Peshkin L, Ramensky VE, Gerasimova A, Bork P, et al. A method and server for predicting damaging missense mutations. Nat Methods. 2010; 7(4):248–9. Epub 2010/04/01. doi: 10.1038/nmeth0410-248 [pii]. PMID: 20354512; PubMed Central PMCID: PMC2855889.

45. Cammisa M, Correra A, Andreotti G, Cubellis MV. Fabry_CEP: a tool to identify Fabry mutations responsive to pharmacological chaperones. Orphanet J Rare Dis. 2013; 8:111. Epub 2013/07/26. doi: 10.1186/1750-1172-8-111 [pii]. PMID: 23883437; PubMed Central PMCID: PMC3729670.

46. Hay Mele B, Citro V, Andreotti G, Cubellis MV. Drug repositioning can accelerate discovery of pharmacological chaperones. Orphanet J Rare Dis. 2015; 10:55. Epub 2015/05/08. [pii]. PMID: 25947946; PubMed Central PMCID: PMC4429356.

47. Ashton-Prolla P, Tong B, Shabbeer J, Astrin KH, Eng CM, Desnick RJ. Fabry disease: twenty-two novel mutations in the alpha-galactosidase A gene and genotype/phenotype correlations in severely and mildly affected hemizygotes and heterozygotes. J Investig Med. 2000; 48(4):227–35. PMID: 10916280.

48. Andreotti G, Guarracino MR, Cammisa M, Correra A, Cubellis MV. Prediction of the responsiveness to pharmacological chaperones: lysosomal human alpha-galactosidase, a case of study. Orphanet J Rare Dis. 2010; 5:36. PMID: 21138548. doi: 10.1186/1750-1172-5-36

49. Ishii S, Chang HH, Kawasaki K, Yasuda K, Wu HL, Garman SC, et al. Mutant alpha-galactosidase A enzymes identified in Fabry disease patients with residual enzyme activity: biochemical characterization and restoration of normal intracellular processing by 1-deoxygalactonojirimycin. Biochem J. 2007; 406(2):285–95. PMID: 17555407. doi: 10.1042/BJ20070479

50. Okumiya T, Ishii S, Takenaka T, Kase R, Kamei S, Sakuraba H, et al. Galactose stabilizes various missense mutants of alpha-galactosidase in Fabry disease. Biochem Biophys Res Commun. 1995; 214(3):1219–24. Epub 1995/09/25. S0006-291X(85)72416-3 [pii] doi: 10.1006/bbrc.1995.2416 PMID: 7575533.

51. Spada M, Pagliardini S, Yasuda M, Tukel T, Thiagarajan G, Sakuraba H, et al. High incidence of later-onset fabry disease revealed by newborn screening. Am J Hum Genet. 2006; 79(1):31–40. PMID: 16773563. doi: 10.1086/504601

52. Vega MC, Lorentzen E, Linden A, Wilmanns M. Evolutionary markers in the (beta/alpha)8-barrel fold. Curr Opin Chem Biol. 2003; 7(6):694–701. Epub 2003/12/04. S136759310300139X [pii]. PMID: 14644177.

original article

Enzyme Enhancers for the Treatment of Fabry and Pompe Disease

Jan Lukas[1], Anne-Marie Pockrandt[1], Susanne Seemann[1], Muhammad Sharif[2,3], Franziska Runge[1], Susann Pohlers[1], Chaonan Zheng[1,2], Anne Gläser[1], Matthias Beller[2], Arndt Rolfs[1] and Anne-Katrin Giese[1]

[1]*Albrecht Kossel Institute, Medical University Rostock, Rostock, Germany;* [2]*Leibniz Institute for Catalysis, University of Rostock, Rostock, Germany;* [3]*Department of Chemistry, COMSATS Institute of Information Technology, Abbottabad, Pakistan*

Lysosomal storage disorders (LSD) are a group of heterogeneous diseases caused by compromised enzyme function leading to multiple organ failure. Therapeutic approaches involve enzyme replacement (ERT), which is effective for a substantial fraction of patients. However, there are still concerns about a number of issues including tissue penetrance, generation of host antibodies against the therapeutic enzyme, and financial aspects, which render this therapy suboptimal for many cases. Treatment with pharmacological chaperones (PC) was recognized as a possible alternative to ERT, because a great number of mutations do not completely abolish enzyme function, but rather trigger degradation in the endoplasmic reticulum. The theory behind PC is that they can stabilize enzymes with remaining function, avoid degradation and thereby ameliorate disease symptoms. We tested several compounds in order to identify novel small molecules that prevent premature degradation of the mutant lysosomal enzymes α-galactosidase A (for Fabry disease (FD)) and acid α-glucosidase (GAA) (for Pompe disease (PD)). We discovered that the expectorant Ambroxol when used in conjunction with known PC resulted in a significant enhancement of mutant α-galactosidase A and GAA activities. Rosiglitazone was effective on α-galactosidase A either as a monotherapy or when administered in combination with the PC 1-deoxygalactonojirimycin. We therefore propose both drugs as potential enhancers of pharmacological chaperones in FD and PD to improve current treatment strategies.

Received 21 April 2014; accepted 7 November 2014; advance online publication 20 January 2015. doi:10.1038/mt.2014.224

INTRODUCTION

Lysosomes contain acid hydrolase enzymes, which are involved in the degradation and recycling of macromolecules. For example, the enzymes α-galactosidase A (*GLA*, α-Gal A, NM_000169.2, EC 3.2.1.22) and acid α-glucosidase (GAA, acid maltase, NM_000152.3, EC 3.2.1.3) belong to the family of exoglycosidases that catalyze the cleavage of terminal α-D-galactoside and α-D-glycoside residues respectively.[1,2] Mutations within the genes encoding lysosomal acid hydrolases lead to accumulation of the corresponding substrates[3] with subsequent development of phenotypically distinct diseases described by the umbrella term "lysosomal storage disorders" (LSDs).

Fabry disease (FD, OMIM #301500), an X-linked lysosomal storage disorder causing the accumulation of glycosphingolipids (mainly globotriaosylceramides), classically presents with angiokeratoma, chronic pain, major pain crisis, anhidrosis, and gastrointestinal problems in childhood or adolescence with a progressive course.[4] Pompe disease (PD, OMIM #232300) is an autosomal recessive neuromuscular disorder typically fatal during the first 12 months of life due to respiratory insufficiency.[5,6] Despite different clinical presentations, both diseases share some important analogies. The two lysosomal enzymes involved belong to the same GH-D clan of the O-Glycosyl hydrolase group of the glycosyl hydrolases superfamily possessing an α/β_8 barrel fold in the domain containing the active site and a comparable catalytic mechanism (retaining aspartate acts as catalytic nucleophile) (www.cazy.org). Certain mutations in FD and PD are associated with a milder disease course, characterized by later onset and slower progression of symptoms.[7–9] These "mild" genotypes are missense mutations that disrupt the structure and stability of the lysosomal enzyme, resulting in misfolding, premature degradation, and failure to reach the target organelle.[10–12] This leads to loss of specific lysosomal hydrolytic activity. To date, the number of reported missense mutations associated with both diseases is high, ranging from >200 in Pompe to >400 in FD (HGMD Professional 2013.2, fabry-database).

Enzyme replacement therapy (ERT) based on the intravenous administration of human enzyme (Replagal, Shire Human Genetic Therapies; Fabrazyme, Lumizyme, Genzyme) is available for each disease. The effectiveness of ERT relies on mannose 6-phosphate residues being recognized by their widely distributed receptors in the plasma membranes of cells.[13] One main shortcoming of ERT is limited tissue penetrance.[14] Central nervous system manifestations such as cerebrovascular complications and neuropathic pain in FD cannot be addressed due to the blood–brain barrier, which is not penetrated by ERT. Another shortcoming is the risk of an immune response with potentially neutralizing antibodies generated against the therapeutic enzymes.[15–17] This might partly explain differences in ERT efficacy between individuals observed in long-term safety studies. A positive correlation has been noted between the deleterious effect of a mutation and the titer of cross-reactive immunological material;[18] so, patients with damaging

Correspondence: Arndt Rolfs, Albrecht Kossel Institute, Medical University Rostock, Gehlsheimer Str. 20, 18147 Rostock, Germany.
E-mail: arndt.rolfs@med.uni-rostock.de.

missense mutations are also at risk of developing antibodies, which can compromise the efficacy of ERT.[19]

A new strategy in the treatment of LSDs is the use of small molecules known as pharmacological chaperones (PC) to enhance lysosomal activity by binding to and stabilizing the mutant enzyme.[9,11,12,20–24] The prerequisite for this treatment approach, therefore, is the presence of a misfolded enzyme, which is still capable of functioning. The PC binds to the mutant enzyme, corrects protein folding, and recovers its lysosomal activity. A large number of mutations are potential candidates for PC therapy, although this is not yet clinically approved. For example, about half of all mutations described in FD are missense mutations and among those, about 50% respond *in vitro* to the PC galactose analog 1-deoxygalactonojirimycine (DGJ, Migalastat hydrochloride).[9,25,26] A recently published study revealed that 26 PD mutations responded to the PC glucose analogue 1-deoxynojirimycine (DNJ).[27] In Gaucher disease, the potent PC Ambroxol (ABX), exists to treat mutant enzymes resulting from the common missense mutations *p.N370S* and *p.L444P*, which together account for about two thirds of cases worldwide.[28,29] ABX was investigated in the current study as a potential PC for both FD and PD. The reason behind this approach is that lysosomal hydrolases share common structural and functional features. PC display little selectivity for their target due to promiscuity within the glycosidase enzyme family and therefore in theory may bind to various different lysosomal hydrolases. For instance, the imino sugar N-butyldeoxynojirimycin (NB-DNJ) was shown to be a PC for both PD and Gaucher disease.[23,24,30] In another example, DGJ potently inhibits α-Gal A and α-N-acetylgalactosaminidase.[31]

It has already been established that PC correct misfolding, stabilize protein structure, and prevent rejection in the quality control system of the endoplasmic reticulum (ER), thereby avoiding premature proteasomal degradation and facilitating transport to the lysosome. Another treatment approach used in Gaucher and Niemann-Pick type C disease, both aim to bypass early enzyme degradation in the ER by either upregulating molecular chaperones or inhibiting the ubiquitin-proteasome-system.[32–34] We therefore systematically investigated a broad range of small molecules for their ability to avoid premature enzyme degradation by either of these two mechanisms, *e.g.*, Tunicamycin, MG-132, Rosiglitazone (RSG), etc.

The most effective small molecules in enhancing mutant lysosomal enzyme function in our cell culture-based system were found to be Ambroxol, RSG/Pioglitazone, and Bezafibrate. The fact that Ambroxol has been shown to be effective in increasing activity of mutant enzymes in both FD (the current study) and GD (previous study) suggests that one single compound could potentially be used in the treatment of different LSDs.

RESULTS

A screening system for mutant glycosylase enhancement

The purpose of this study was to produce different mutant forms of the lysosomal hydrolase α-galactosidase A (α-Gal A) to investigate their response to small molecules with a view to (i) elucidating cellular pathways that can potentially be modulated in order to increase mutant enzyme activity and (ii) to identify potential compounds for the treatment of LSD. Substances with distinct biological and biochemical functions were investigated in an *in vitro* model for FD. HEK-293H cells were cultured and transfected with various mutant *GLA* cDNAs to produce α-Gal A with defects in folding but residual enzyme activity. These α-Gal A mutants were previously shown to be responsive to the pharmacological chaperone DGJ, which was used as an indicator of the capacity of the enzymes to gain functional recovery (**Supplementary Figure S1**). From the 32 mutations depicted in **Supplementary Figure S1**, a set of nine mutations was selected for further testing based on (i) residual activity (>1 % of wild type) and (ii) DGJ responsiveness (>1.5-fold increase, overall >5% of wild type), as established in an earlier article.[9]

The first candidate substance: ambroxol, a pharmacological chaperone effective in Gaucher disease

For FD, mutant misfolded α-Gal A enzymes were tested with Ambroxol (ABX), a recently identified PC for Gaucher disease. Several of the mutant α-Gal A enzymes appeared to show slightly elevated function after administration of 40 µmol/l ABX to the cell-culture medium, but a significant effect was only seen for wild-type α-Gal A and two specific mutants *p.A156V* and *p.R301Q* (**Figure 1a**). The concentration–response relationship was recorded for the wild-type enzyme (**Figure 1b**). ABX was effective at a concentration range of 10–60 µmol/l while displaying a decline to about 40% of the maximal effect at 120 µmol/l ABX; we used sigmoidal curve fit and calculated an EC_{50} of 17.4 µmol/l. The drop in activity detected at concentrations >80 µmol/l could actually be caused by a harmful effect on the cultured cells that has formerly been reported for ABX[28] rather than a specific inhibitory effect of the compound on the enzyme. A concentration–response curve was recorded for one mutant (*p.A156V*), resulting in a similar EC_{50} to that of the wild-type, of 13.0 µmol/l (**Supplementary Figure S2**). In the following experiments, ABX was also used at 40 µmol/l, which represents approximately twice EC_{50}. The mutations from **Figure 1a** were tested using a combination of 20 µmol/l DGJ and 40 µmol/l ABX, which resulted in increased enzyme activity for all nine mutations tested (*p.E59K*, *p.A73V*, *p.A143T*, *p.A156V*, *p.I232T*, *p.R301G*, *p.R301Q*, *p.R356W*, and *p.R363H*) when compared to treatment with DGJ alone (**Figure 1c**). The mutants *p.A73V*, *p.I232T*, and *p.R363H* attained close to normal enzyme activity, while the mutants *p.A143T* and *p.R301Q* exceeded 50% activity thereby crossing the estimated threshold for the normal range.[35] This increase in activity was associated with a parallel increase in the level of α-Gal A protein in the cells (**Figure 1d**). The stronger α-Gal A signals suggest a potential stabilizing effect of the double treatment and/or enhanced transport into the lysosome. In summary, double treatment with DGJ and ABX resulted in increased enzyme activity for all mutations tested. This in turn prompted a similar double-treatment study using galactose and ABX (galactose, like DGJ, is also a PC in FD). A subset of six mutations responded with an elevated α-Gal A activity using this particular double treatment (**Supplementary Figure S3**).

Ambroxol stabilizes α-Gal A in combination with DGJ *in vitro*

We wanted to test the previous suggestion that the DGJ/ABX double treatment stabilized the enzyme. We therefore carried out a

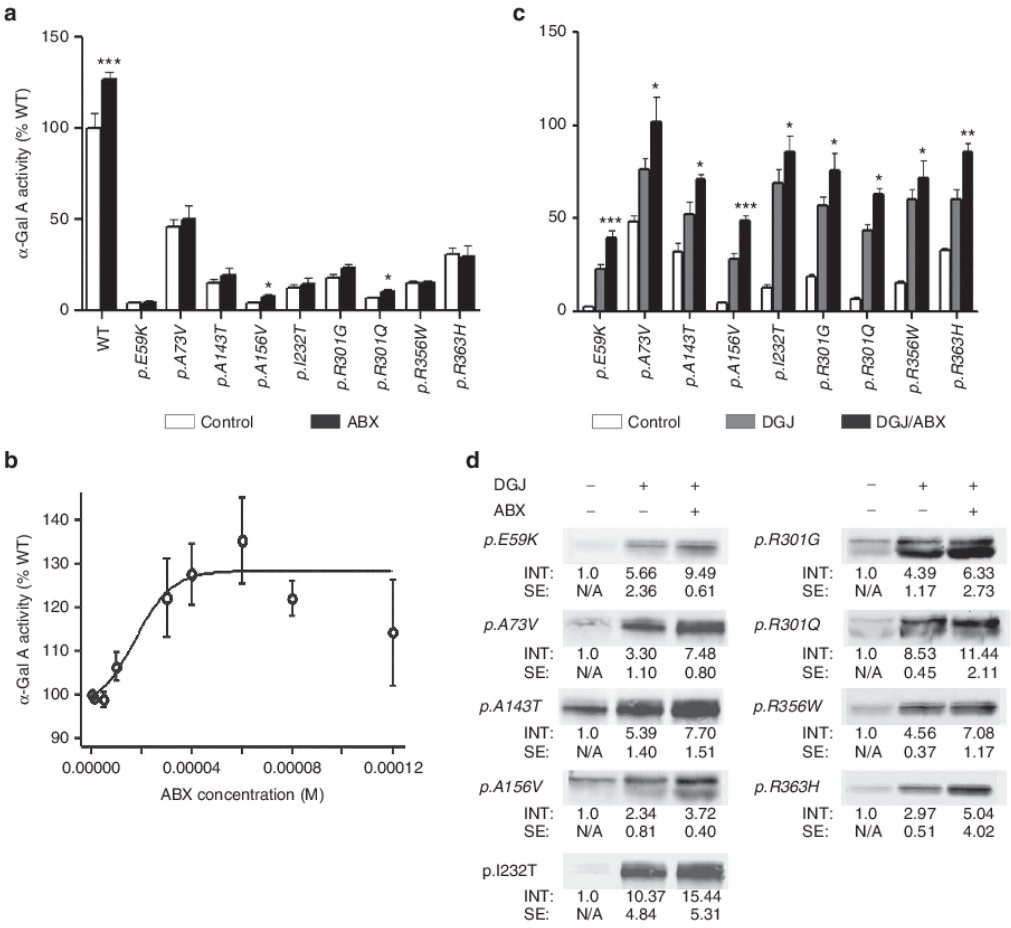

Figure 1 Effect of ABX on overexpressed mutant forms of α-Gal A in HEK-293H cells. ABX was administered 6 hours after transfection of the *GLA* cDNA-containing plasmids and then cultured for 60 hours changing the media any other day adding fresh treatment as described in the Materials and Methods section (**a**) Bona fide analysis with 40 µmol/l ABX revealed a tendency to mildly increase intracellular activities of several mutant α-Gal A forms that was significant for *p.A156V* and *p.R301Q*. Wild-type enzyme increased markedly upon the addition of the compound as well. (**b**) Concentration–response relation analysis showed increasing wild-type α-Gal A activity. An EC_{50} of 17.4 µmol/l was calculated by a nonlinear regression analysis A maximum stimulatory effect was obtained at 60 µmol/l. At concentrations ≥80 µmol/l, the α-Gal A activity dropped back to normal. (**c**) In the same culture system as under (**a**), the *GLA* expressing HEK-293H cells were DGJ or DGJ/ABX combination-treated. The DGJ-responsive α-Gal A forms (see also **Supplementary Figure S1**) displayed considerable gains from the additional administration of ABX. (**d**) Western blot of the mutant α-Gal A forms indicated higher levels of intracellular enzyme after treatment with DGJ in combination with 40 µmol/l ABX compared to the monotherapy. Western blots were repeated at least three times. In each lane 30 µg of total protein was loaded and separated by SDS-PAGE. Semiquantitative analysis was carried out using the Odyssey software v1.2. Calculated intensities were normalized for GAPDH internal loading control (not shown). The average intensities ("INT") are given as fold change ± standard error. Enzyme activity values are shown as mean ± SEM ($n \geq 5$). Results were considered significant if $^*P < 0.05$, $^{**}P < 0.01$, $^{***}P < 0.005$. Control treatment denotes the respective carrier solvent used for the compounds (DGJ was diluted in hypure H_2O as a 10 mmol/l stock solution, ABX was typically diluted in DMSO (100 mmol/l).

thermal denaturation test in a cell-free environment using human α-galactosidase A produced in a human fibroblast cell line (agalsidase alfa, Shire Human Genetic Therapies, Berlin, Germany), to examine the hypothesis that ABX could act *via* pharmacological chaperoning (*i.e.*, bind to the enzyme and in turn lead to stabilization). Briefly, the method involves incubation of agalsidase alfa at 51 °C for 60 minutes in a 96-well plate with or without the respective additive (DGJ, ABX or a combination of both) as previously described.[26] A control plate with the same sample set up was kept on ice. Enzyme activity was measured with the artificial substrate 4-methylumbelliferyl-α-D-galactopyranoside (4-MUG). The thermal incubation of mock-treated (DMSO) α-Gal A at 51 °C led to a decreased active enzyme fraction of about 29.9% compared to control incubation on ice (Figure 2). Increasing DGJ concentrations attenuated α-Gal A thermal denaturation (restoring up to 63.4% of normal activity at 2.5 µmol/l) whereas increasing concentrations of ABX led to an accelerated loss of enzyme activity (reducing to 18.8% of normal activity at 2.5 mmol/l). Coadministration of DGJ and 2.5 mmol/l ABX led to a further stabilization compared to DGJ alone. The conclusion

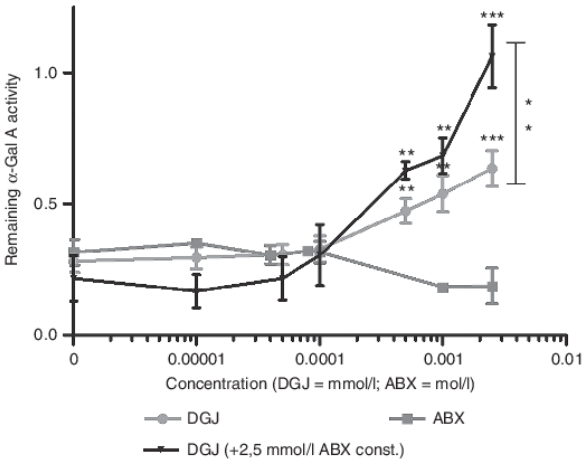

Figure 2 Thermal denaturation of α-Gal A. Replagal was mixed with increasing amount of compound. The mixture was incubated at 51 °C for 60 minutes and the enzymatic reaction was started upon the addition of substrate directly thereafter. The decrease of activity was compared to a reference sample kept on ice for 60 minutes before the enzymatic assay. The curve obtained for DGJ showed attenuated denaturation heat-treated enzyme in a concentration-dependent manner (light-grey graph) and significant stabilization at 500 nmol/l onwards. ABX showed no change compared to the untreated state at concentrations up to 200 µmol/l (dark–grey graph). In millimolar concentrations ABX accelerated the denaturation resulting in lowered enzyme activity compared to the untreated enzyme. In combination with a constant addition of 2.5 mmol/l ABX, the DGJ treatment led to enhanced stabilization of the enzyme at higher DGJ concentrations. At 2.5 µmol/l DGJ, the enzyme was more effectively stabilized under combination compared to monotherapy. Data was obtained from at least five independent experiments, each experiment included duplicate measurements. Values are shown as mean ± SEM ($n \geq 5$). Results were considered significant if $^{*}P < 0.05$, $^{**}P < 0.01$, $^{***}P < 0.005$.

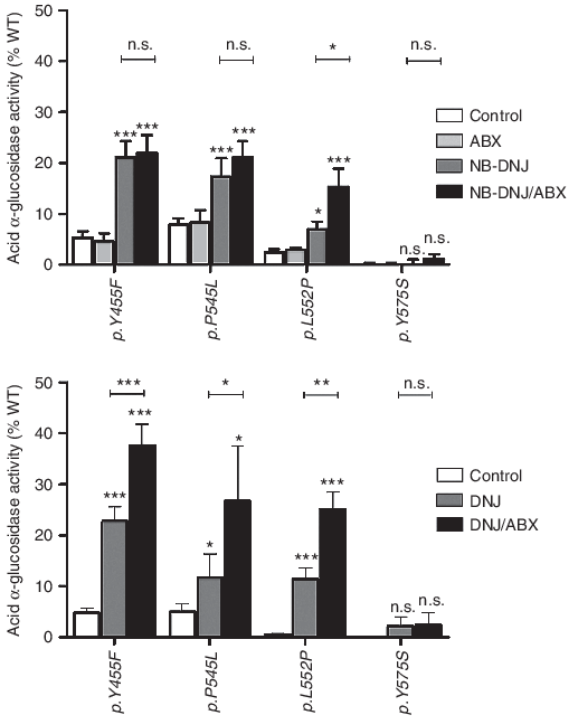

Figure 3 Acid α-glucosidase (GAA) activity in HEK-293H cells expressing mutant forms of the enzyme treated with a pharmacological chaperone (NB-DNJ or DNJ) and a combination consisting of NB-DNJ/ABX and DNJ/ABX. Upper: PC-responsive mutations of GAA were treated with 40 µmol/l ABX, 20 µmol/l NB-DNJ and a combination of 20 µmol/l NB-DNJ and 40 µmol/l ABX. The monotreatment with ABX did not beneficially influence mutant GAA activity. The NB-DNJ was effective on *p.Y455F*, *p.P545L*, and *p.L552P*, but not *p.Y575S*. The mutant *p.L552P* was amenable to the double treatment whereas *p.Y455F* and *p.P545L* did not display synergistic effects from the combination of the PC with ABX. Lower: In the same set of mutations, DNJ provoked a similar response compared to NB-DNJ. In combination with ABX, the mutations (except for *p.Y575S*) showed a siginificant synergistic effect with the imino sugar compared to the monotherapy. Values are shown as mean ± SEM ($n \geq 3$). Results were considered significant if $^{*}P < 0.05$, $^{**}P < 0.01$, $^{***}P < 0.005$.

drawn is that following heat denaturation, ABX alone does not preserve enzyme activity but when used with DGJ has a synergistic positive effect.

Can the effect of ABX be applied mutatis mutandis to other LSD cell culture models?

In a similar heterologous expression system as described for *GLA* mutations in FD, ABX was combined with a PC to analyze the effect on mutant GAA in PD. Mutations with a known ability to respond to PC treatment were investigated in this study.[23,24] For example, *p.Y455F*, *p.P545L*, and *p.L552P* showed a significant benefit from the 60-hour N-butyl-deoxynojirimycine (NB-DNJ) treatment, whereas no effect was achieved with the ABX (**Figure 3**, upper part). Surprisingly, mutant *p.L552P* showed a significant benefit from the combination of NB-DNJ and ABX indicated by an increase of activity from 6.9 to 15.3% of wild type, compared to monotherapy with NB-DNJ. The same did not hold true for *p.Y455F* and *p.P545L*. The effect of another pharmacological chaperone DNJ, was also triggered by the addition of ABX, increasing activity of the mutant *p.L552P* from 11.4 to 25.1% (**Figure 3**, lower part), which corresponds to the ratio observed with NB-DNJ (2.2-fold increase). A significant improvement in enzyme activity using a combination of DNJ and ABX was also seen for mutants *p.Y455F* (1.6-fold) and *p.P545L* (2.3-fold). Apparently, in the case of the GAA enzyme, the success of combined administration with ABX strongly depended on the chaperone used and the type of mutation. The combination DNJ/ABX was efficient on all tested mutations except *p.Y575S*.

RSG, a known inhibitor of the ubiquitin-proteasome-system, acts as enhancer of intracellular mutant α-Gal A activity

ER stress inducers and ubiquitin-proteasome-system inhibitors have both been proposed as potential drugs in several LSDs.[32–34] Both strategies aim to modulate cellular proteostasis in order to beneficially influence enzyme folding and subsequently deliver mutant enzymes to the lysosome. We treated mutant α-Gal A (*p.R301Q*), overexpressed in HEK-293H cells, in the presence or absence of DGJ, with different ER stress inducing agents: Kifunensine (an α-mannosidase inhibitor), Thapsigargin (an

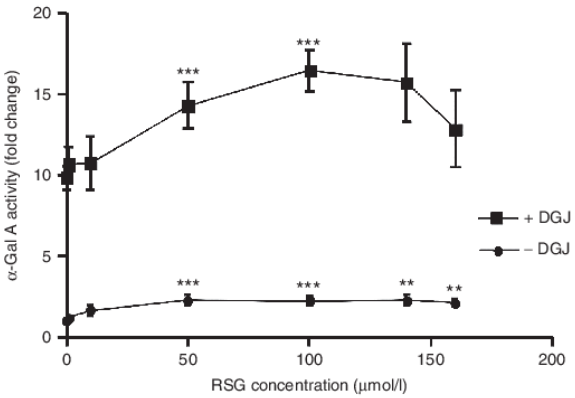

Figure 4 Mutant *p.R301Q* α-Gal A activity under treatment with Rosiglitazone. The *GLA* mutation *p.R301Q* was overexpressed in HEK-293H cells and treated with the known ubiquitination modifying agent RSG in the presence or absence of 20 μmol/l DGJ. Significant enzyme activity enhancement was gained at concentrations ≥50 μmol/l. In a therapeutic margin of 50–140 μmol/l RSG proved to be an effective enhancer of mutant α-Gal A activity.

ER Calcium releaser and reuptake inhibitor), and Tunicamycin (an inhibitor of N-glycosidic linkage formation). None of these three agents produced a positive effect on cellular enzyme activity (**Supplementary Figure S4**). Thapsigargin even had a negative effect on α-Gal A activity in a concentration-dependent manner and at concentrations >50 nmol/l, it appeared to be toxic to the cells. MG-132, an inhibitor of proteasomal activity, showed a modest, but not statistically significant increase on *p.R301Q* enzyme activity at 50 nmol/l (1.2-fold) (**Supplementary Figure S4**). The effect was also detected when MG-132 was administered in combination with 20 μmol/l DGJ leading to a 1.1-fold increase over DGJ monotherapy (from 8.6- to 9.5-fold of the untreated control). Other inhibitors of proteasomal activity, Lactacystin, Bortezomib, and Ritonavir, were also tested, but did not show an effect on mutant α-Gal A function (data not shown). **Supplementary Table S1** shows the effect on the distinct proteasomal activities (Chymotrypsin-, Trypsin-, and Caspase-like activity) in the cell system used at different concentrations. Remarkably, MG-132 had no inhibitory effect on the proteasome when applied at a concentration of 100 nmol/l. Only at a concentration of 1 μmol/l, an inhibitory effect on all three proteasomal activities was noticeable. However, due to the cytotoxic effect of MG-132, it was not feasible to apply concentrations above 100 nmol/l over long periods (such as 60 hours) in the present cell system. A short-term treatment with 1 μmol/l MG-132 for 12 hours preceding cell harvest did not significantly change α-Gal A activity either (data not shown).

Contrary to the findings for MG-132, a major response to RSG, a Peroxisome proliferator–activated receptor-γ (PPAR-γ) agonist reported to inhibit global cellular ubiquitination,[36] was observed for *p.R301Q*. The administration of 50–140 μmol/l RSG led to approximately threefold increase of *p.R301Q* activity. RSG in combination with DGJ was even more effective in enhancing activity of the mutant *p.R301Q* enzyme (**Figure 4**). Therefore, other mutant α-Gal A forms, which had previously been classified as DGJ nonresponders were also tested for responsiveness (compare **Supplementary Figure S1**). Mutant α-Gal A forms *p.R118C*, *p.A156V*, *p.R301Q*, and *p.T385A* were exposed to 20 μmol/l DGJ, 100 μmol/l RSG, and a combination of 20 μmol/l DGJ and 100 μmol/l RSG (**Figure 5a**). The DGJ nonresponding mutants *p.R118C* and *p.T385A* showed a 1.2- and 1.1-fold increase in activity when DGJ was administered, which increased to a 1.4- and 1.3-fold increase when RSG was added, respectively. According to the established responder criteria, both drugs failed to increase the enzyme activity >1.5-fold. However, taking into account the fact that *p.R118C* and *p.T385A* retain intrinsic activities of 22.9% and 47.0% of wild type respectively, both mutations can be considered as RSG responders, because activity was increased by over 5% up to 30.7 and 62.5%, respectively. The efficiency of the combinational treatment exceeded the monotherapy. *p.A156V* and *p.R301Q* are strong DGJ responders and the addition of RSG boosted the monotherapy by 1.8-fold (*p.R301Q*) and 1.3-fold (*p.A156V*). Pioglitazone is a structural and functional analogue of RSG. The combination of DGJ/Pioglitazone was equally effective as DGJ/RSG on *p.R301Q* activity.

The corresponding effect on the protein level is shown in **Figure 5b**. As shown before, the mutant enzyme forms responded to the administration of 20 μmol/l DGJ, 100 μmol/l RSG, and the combination of both. In the case of *p.R118C* and *p.T385A*, the band signal of 100 μmol/l RSG-treated mutants was stronger than for DGJ-treated mutants, but the combination revealed the strongest effect. For mutants *p.A156V* and *p.R301Q*, RSG alone increased the amount of the 50 kDa immature form of the enzyme, whereas DGJ apparently enhanced maturation resulting in higher levels of the 46 kDa mature form. With the combination therapy, an enhancement of the effect of DGJ on the 46 kDa mature form was observed. In order to clarify whether the inhibitory effect on global cellular ubiquitination or the PPAR-γ agonism was key for the α-Gal A activity elevation, Ubiquitin-activating enzyme (E1) inhibitor Pyr-41 and PPAR-α/γ agonizing agent Bezafibrate were tested. Pyr-41 did not enhance α-Gal A activity, whereas Bezafibrate increased *p.R301Q* activity significantly in 100, 200, and 500 μmol/l with or without the simultaneous administration of DGJ (**Figure 5c**). This evidence shows that PPAR function may play a role in mutant α-Gal A activity elevation rather than ubiquitination inhibition alone.

DISCUSSION

To date, large scale screenings to identify compounds, which enhance enzyme activity in LSD have been based on direct interaction with the lysosomal enzyme *in vitro*.[28,37,38] Our approach was to instead use HEK-293H cells and screen for compounds that enhanced activity of mutant lysosomal enzymes within a cellular environment. The advantage of a cell-based system over a cell-free *in vitro* system is that any beneficial compounds identified may be (i) more relevant for clinical applications and (ii) generally applicable to different diseases sharing the same biochemical basis. A particular problem however, is the relatively low throughput of this system due to the time and labor demands of cell culture with a high number of repetitions required for each compound.

In order to discover substances counteracting the loss of enzyme activity in lysosomal storage disorders, Ambroxol (ABX) was tested in the HEK-293H cellular model of Fabry and PD. ABX

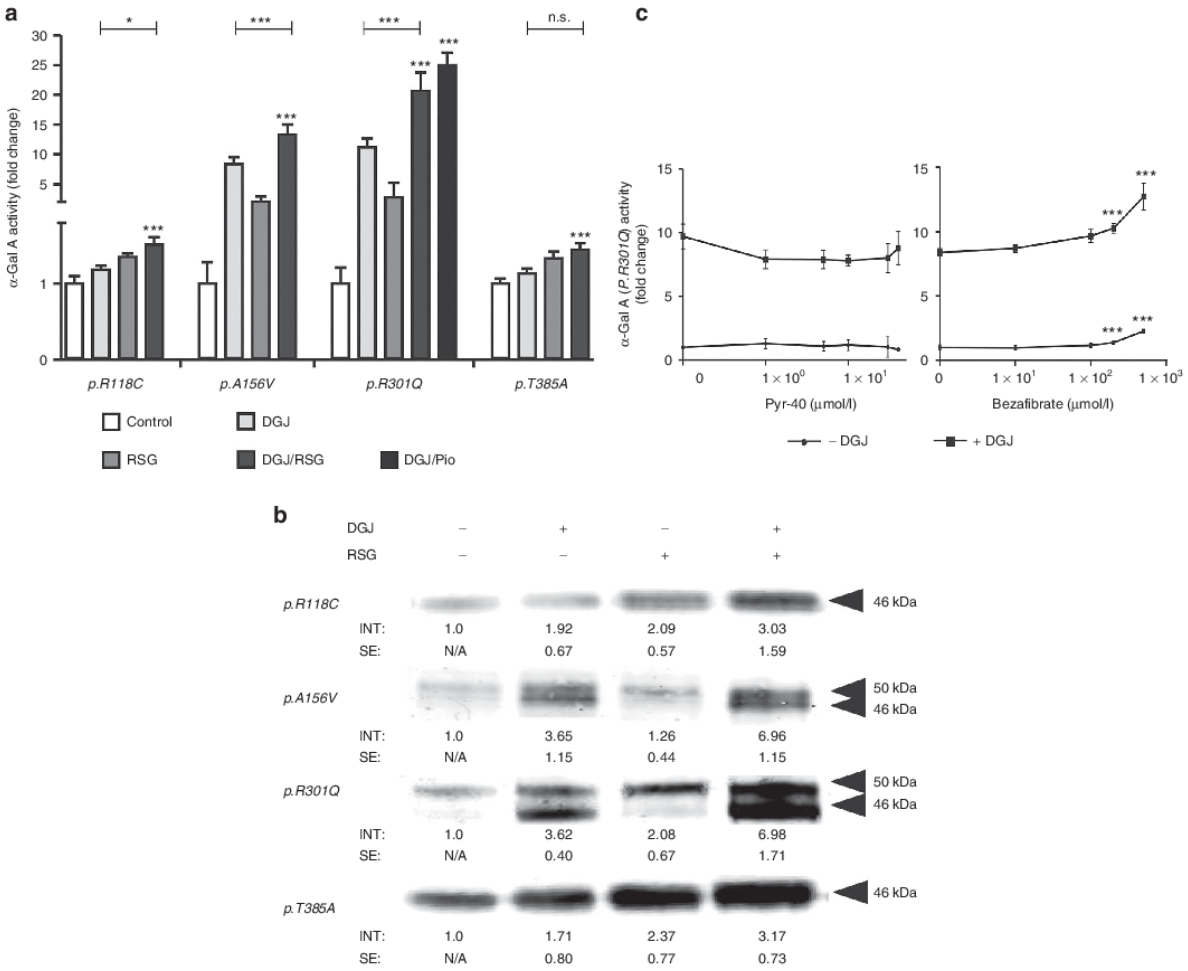

Figure 5 Mutant α-Gal A forms respond to PPAR-γ agonist drugs. HEK-293H cells were transfected and treated as described in Materials and Methods ("Transient *GLA/GAA* expression in HEK-293H cells"). (**a**) The administration of 100 μmol/l RSG increased the enzyme activity of mutant forms of α-Gal A. In the case of *p.A156V* and *p.R301Q* the DGJ treatment is an efficacious single treatment, but the combination with RSG leads to a further increase of activity. A structural and functional analogue of RSG, Pioglitazone (Pio), administered at 100 μmol/l is similarly effective on *p.R301Q* in combination with DGJ. RSG had a distinct effect on mutants *p.R118C* and *p.T385A* that did not respond to DGJ (see **Supplementary Figure S1**). The combination of both drugs was most effective. Values are shown as mean ± SEM ($n \geq 3$). Students *T*-test was used to investigate significance of the combined treatment compared to control and to DGJ monotherapy. Results were considered significant if $^{*}P < 0.05$, $^{**}P < 0.01$, $^{***}P < 0.005$. (**b**) Western blot analysis of different mutant α-Gal A forms under DGJ, RSG and DGJ/RSG combination treatment. In accordance with (**a**) the mutant enzyme forms displayed best responsiveness towards the combination of pharmacological chaperone DGJ and RSG. Experiments were repeated at least 3 times for reliability. Western blot analysis was taken out essentially as described under **Fig. 1d**. (**c**) E1 ubiquitin activating enzyme inhibitor Pyr-41 and PPAR-α/γ agonist Bezafibrate were tested on overexpressed *p.R301Q* mutant in HEK-293H cells. No change of α-Gal A activity was observed for Pyr-41 over a concentration range of 0.1–40 μmol/l. By contrast, treatment with Bezafibrate led to an increase from 8.4- to 12.7-fold and from 1.0 to 2.3 with or without additional administration of DGJ, respectively.

is a compound formerly tested in Gaucher disease that was shown to interact with GCase, causing diminished enzyme activity *in vitro* but increased activity of mutant enzymes in fibroblasts,[28] (*p.N370S* in non-neuronopathic type I GD and *p.L444P*[29] in subacute neuronopathic type III GD). In the current study, ABX alone was applied to HEK-293H cells expressing either normal (wild type) or mutant α-Gal A (Figure 1a,b). Combined treatment with ABX and synthetic α-Gal A PC DGJ was also tested (Figure 1c). Wild-type α-Gal A showed a 1.4-fold increase in activity after the addition of 60 μmol/l ABX, but its effectiveness was less pronounced at concentrations ≥100 μmol/l. Mutants of α-Gal A, which were DGJ-responsive, showed an additional benefit from combined treatment with ABX (Figure 1c) leading to higher enzyme levels after 60 hours of treatment (Figure 1d). This was due to a stabilizing effect of DGJ/ABX on the enzyme as demonstrated by an *in vitro* heat-treatment experiment using the pharmaceutical form of α-Gal A (agalsidase alfa). DGJ monotherapy was not as effective in stabilizing the enzyme as when used in combination with ABX (Figure 2). In contrast, ABX monotherapy i*n vitro* led to accelerated loss of enzyme activity.

Hypothetically, binding of ABX to the enzyme and stabilization could be enhanced by structural changes induced by DGJ binding. However, ligand binding to the protein has been reported to barely affect the conformation of the enzyme.[39] Moreover, ABX monotherapy provoked a significant, though modest, activity elevation of α-Gal A wild-type, *p.A156V* and *p.R301Q* enzyme forms in HEK-293H cells, which could argue for an alternative work mechanism of ABX *via* a general cellular process, affecting protein maturation and transport. For example, it has been reported that ABX regulates the efflux of extracellular Ca^{2+} in dorsal root ganglion cells[40] possibly mediated by inhibition of voltage-gated sodium and calcium channels.[41] Calcium is a critical agent for protein folding. Manipulating the release of Ca^{2+} from the ER, the largest intracellular Ca^{2+} store, was shown to have an influence on mutant GCase enzyme in Gaucher disease.[33] Since α-Gal A mutants show an increased propensity to aggregate within the cell,[42] we can speculate that ABX perhaps enhances the effect of the pharmacological chaperone *via* modulation of the protein folding conditions in the ER. Besides the chaperoning effect, ABX was recently speculated to impact on GBA expression and function in Gaucher disease fibroblasts.[43] Therefore, the utilized cell culture system cannot elucidate the specific mode of action of substances that have a diverse functional spectrum.

Anyhow, ABX did not act as an *in vitro* inhibitor of α-Gal A activity (**Supplementary Figure S5**), so evidently does not bind the active site in a substrate competitive manner. Allosteric binders of mutant lysosomal enzymes are regarded as promising treatment options, because the risk of undesired side-effects and overdosage is minimized.[44]

Mutant GAA activity was also beneficially influenced by the combination of a PC and ABX (**Figure 3**). ABX alone had no effect on mutant GAA; a differential effect was shown for both PCs, NB-DNJ and DNJ, when used in combination with ABX. While DNJ and NB-DNJ as a monotherapy had a similar outcome, it is not yet clear why DNJ/ABX had a synergistic effect on mutants *p.Y455F* and *p.P545L* and NB-DNJ/ABX did not.

PPAR-γ agonist RSG increased mutant α-Gal A activity (*p.R301Q*, *p.A156V*, *p.R118C*, *p.T385A*). It was assumed that RSG mediates its effect *via* inhibition of cellular ubiquitination, thereby avoiding α-Gal A degradation. However, the ubiquitination inhibitor Pyr-41 did not increase α-Gal A activity. Interruption of the ubiquitin–proteasome system by the use of proteasomal inhibitors (*e.g.*, MG-132) was also ineffective. An earlier report suggested that treatment with the proteasomal inhibitor Lactacystin led to increased amounts of α-Gal A in COS7 cells expressing several mutant forms of the enzyme, but without a concurrent enhancement of enzyme activity.[45] Western blot analysis performed in our laboratory did indeed show that Lactacystin and MG-132 increased the amount of *p.R301Q, but not p.A156V* (**Supplementary Figure S6**), which is in accordance with the results from Ishii *et al*. Since only the immature 50 kDa band of *p.R301Q* is markedly increased, we conclude that this α-Gal A form does not significantly contribute to enzyme activity under the applied assay conditions.

On the other hand PPAR-γ agonist Bezafibrate did enhance activity of *p.R301Q* which suggests that increased PPAR-γ activity may instead play a role. However, it cannot be excluded that both increased PPAR-γactivity and inhibition of ubiquitination enhance enzyme activity since there is crosstalk between PPAR-γ-mediated transcriptional regulation and the ubiquitination machinery.[46] For example, PPAR-γ itself is an E3 ubiquitin ligase that facilitates the degradation of NF-κb.[47] Certain players in the ubiquitin machinery have been shown to interact with mutant GCase[48,49] indicating a role in its premature degradation. Elucidation of why RSG was operative demands further investigation. The use of more specific drugs could reveal the pivotal mechanism of action. Interestingly, RSG did not display an effect on GAA (data not shown).

Prospectively, these compounds need to be tested in patient-derived cell systems (*i.e.*, lymphoblastoid or fibroblast cell lines) in order to verify the suspected effects. Such cell systems do not require previous transfection of plasmid vectors harboring cDNA of the mutations and allow for more flexible and optimized treatment regimes.[50] This is an advantage over more "synthetic" cell systems such as the HEK-293H system used here, in which transient expression (*de novo* enzyme synthesis) confounds the beneficial effect of small molecules. Patient cell lines are therefore a convenient solution for temporal-oriented studies and should be applied as a second step. Testing findings in a humanized mouse model is also practical.[51] Regrettably, to our knowledge, a mouse model does not yet exist for PD.

This work delivers a novel step forward in drug development for LSD. Our use of FDA-approved compounds renders this study an attractive target for further research to elucidate the role of proposed pathways in the enhancement of mutant enzyme stability and activity as a prelude to preclinical and clinical testing.

In particular, ABX and RSG could potentially be suitable compounds as additional treatments in Fabry (or Pompe) patients where monotherapy with a pharmacological chaperone is not sufficiently effective. As described above, the combination of DGJ and ABX was successful in restoring either near normal α-Gal A activity (*e.g.*, *p.A73V*) or boosting activity to >50% to cross the threshold into the normal range (*e.g.*, *p.R301Q*). Both outcomes are potentially associated with an amelioration of the disease (Fabry) not obtained using PC monotherapy. Moreover, for mutants with residual activity but not responsive to DGJ, like *p.R118C* and *p.T385A*, the usage of RSG could be an alternative treatment strategy because it exceeds the effect of DGJ (**Figure 5**).

In PD, a genotype/phenotype correlation model is not available, but it can be assumed that an elevation of GAA activity from 11.4% (DNJ) to 25.1% (DNJ/ABX) of normal, as observed for the mutant *p.L552P*, is likely to be clinically relevant.

Lately, it was demonstrated that small molecules can also have synergistic effects in ERT.[52] Evidently, we must endeavor to find the most effective course of treatment for patients with FD and PD, not limited to just one active agent. It is important to note that combination treatments have possible implications for other LSDs as well.[40,53]

MATERIALS AND METHODS

Materials. HEK-293H cell line was purchased from Invitrogen (Carlsbad, CA). Ambroxol hydrochloride, Bezafibrate, 1-deoxygalactonojirimycine hydrochloride, 1-Deoxynojirimycin, α-Lobelin, RSG, Thapsigargin, Tunicamycin, and the synthetic fluorogenic substrates for α-Gal A and GAA were purchased from Sigma Aldrich (Steinheim, Germany). Kifunensine,

MG-132 were obtained from Merck (Darmstadt, Germany). Lactacystin and bortezomib were purchased from Biomol (Hamburg, Germany). A rabbit polyclonal antibody targeted against human α-galactosidase A was custom-made (Eurogentec, Liège, Belgium)[9] and mouse anti-GAPDH (ab8245) was purchased from abcam (Cambridge, UK). Secondary antibody Alexa Fluor 680 Goat Anti-Rabbit IgG (H+L) was purchased from Molecular Probes (Eugene, OR) and Anti-Mouse IgG (H&L) IRDye800 was purchased from Rockland (Gilbertsville, PA).

All primers were obtained from MWG Operon (Ebersberg, GER). A register of used primers is shown in **Supplementary Table S2**.

Cultivation of HEK-293H cells. HEK-293H were maintained in Dulbecco's modified Eagle medium containing 4,500 mg glucose/l supplemented with 10% fetal bovine serum (both from Gibco, Carlsbad, CA) and 1% Penicillin/Streptomycin.

Cloning. Human cDNA clones of α-Gal A (IRAUp969H0320D, *GLA*, NM_000169.2) and GAA (IRATp970C0971D, *GAA*, NM_000152.3) were obtained from Source BioScience (Berlin, GER). cDNAs were amplified by PCR (for primer sequences refer to **Supplementary Table S2**). After subcloning into pGEM-T (Promega, Mannheim, GER) or pCRII TOPO (Invitrogen), respectively, the fragments were obtained via restriction digestion using the respective restriction endonucleases indicated in **Supplementary Table S2** and ligated into a mammalian expression vector (pcDNA3.1/V5-His TOPO, Invitrogen). Gene sequence integrity was confirmed by standard sequencing and alignment analysis as described earlier.[9]

Mutagenesis. Site-directed mutagenesis of *GLA* and *GAA* plasmids were carried out as described before.[9] **Supplementary Table S2** reports the list of applied primers for all *GLA* and *GAA* mutations.

Transient* GLA/GAA *expression in HEK-293H cells. Commonly, HEK-293H cells were seeded at a density of 1.5×10^5 cells/well of a 24-well plate (Greiner Bio-One, Frickenhausen, GER) the day before transfection. On the day of transfection, mutant *GLA* or *GAA* plasmid was transfected using Lipofectamine 2000 (Invitrogen) according to the manufacturer's guidelines. The compounds were added 6 hours after transfection and left for a 60-hour cultivation unless indicated otherwise. Fresh medium and treatment was added every other day. Transfection control was carried out by parallel transfections of the wild-type and mutant *GLA*/*GAA*, which differ by just one base pair.[25] Additionally, enzyme activity of every mutant was checked for coherence and stability, indicating maintained plasmid quality.

For the compound serial tests, HEK-293H cells were plated on 10 cm cell culture dishes and transfected with pcDNA3.1 *p.A156V* and *p.R301Q* mutated *GLA* inserts. Six hours after transfection, the cells were trypsinized, collected in a 50 ml tube, and spun down at 1,000 × g. The cells were then aliquoted in medium containing the respective compound or compound combination and plated at a density of 2×10^5/well on 24-well plates in order to obtain identical transfection efficiencies for all samples.

In vitro ***enzyme activity measurements in HEK-293H cell lysates.*** α-Gal A and GAA activities were measured in cell lysates of transiently expressing HEK-293H cells. On the day of cell harvest, 66 hours after transfection, medium was aspirated with a vacuum pump (KNF Neuberger, Freiburg i. Breisgau, GER) and washed in phosphate buffered saline. The cells were then collected in 150 µl sterile distilled water and transferred to fresh 1.5 ml centrifugation tubes. The proteins were yielded using five cycles freeze and thaw in liquid nitrogen. For normalization purposes, the protein was quantified using BCA protein assay kit (Thermo Scientific, Braunschweig, GER). The crude protein extract was subsequently used for enzyme activity measurement (0.5 µg for α-Gal A and 5 µg for GAA) employing synthetic fluorogenic substrates 4-methylumbelliferyl-α-D-galactopyranoside (for α-Gal A) and 4-methylumbelliferyl-α-D-glucopyranoside (for GAA), respectively.

α-Gal A enzyme thermal denaturation test. *In vitro* thermal denaturation was carried out using 200 ng of human α-Gal A (agalsidase alfa, Replagal, Shire Human Genetic Therapies, Berlin, Germany) in a whole volume of 25 µl (in 0.06 mol/l phosphate-citrate buffer, pH 6.7). The enzyme was pipetted in 96-well plates (Greiner bio-one GmbH, Frickenhausen, GER) and incubated at 51 °C for 60 minutes with the respective additive DGJ, ABX or a combination of both basically as reported elsewhere.[26] A reference plate was kept on ice during that period. Thereafter, 4 volumes of 0.06 mol/l phosphate-citrate buffer (pH 4.7) were added to the wells and mixed. Twenty-five microliters of the mixture were transferred into a fresh 96-well plate. The enzyme activity measurement was started by addition of 20 µl of the substrate 4-methylumbelliferyl-α-D-galactopyranoside solution (stock concentration: 2.0 mol/l. Samples were kept under slight agitation in a 37 °C water bath for 20 minutes. To stop the reaction, 200 µl of glycine-NaOH buffer (pH 10.5) was added and substrate turnover was immediately surveyed as described above. Comparison of heat-treated versus reference sample was used to measure the reduction in enzyme activity.

Western blot analysis. Western blot analysis was carried out basically as described before.[9]

PPAR-γ transcriptional regulation reporter assay. The HEK-293H cells were seeded at a density of 4×10^4 in a 96-well plate in antibiotic free medium 24 hours before transfection. On the day of transfection, the medium was changed prior to adding the transfection solution (Lipofectamine 2000, Invitrogen) containing the reporter plasmid constructs (Cignal PPAR Reporter (luc) Kit, Qiagen, Hilden, GER). Six hours post-transfection, the compounds were added. The treatment was carried out for 18 hours before the cells were lysed in passive lysis buffer (Dual-Luciferase Reporter Assay System, Promega GmbH). The detected firefly luciferase activity was normalized against intrinsic renilla luciferase contained in the transfection solution at a plasmid ratio of 1:40. Samples were diluted to ensure that the signal was in the linear assay range, transferred to polypropylene round bottom tubes and measured in a luminometer (Lumat LB9507, Berthold Technologies, Bad Wildbad, GER) with the respective substrates.

SUPPLEMENTARY MATERIAL

Figure S1. Excerpt of pharmacological chaperone- (DGJ-) treated GLA mutations.
Figure S2. ABX concentration-dependent increase of PC-treated *p.A156V* α-Gal A activity.
Figure S3. Synergistic effect of a galactose/ABX combination on galactose-responsive GLA mutations.
Figure S4. ER protein homeostasis re-modeling agents did not have a significant effect on *p.R301Q* α-Gal A activity.
Figure S5. Agalsidase alfa inhibition assay with DGJ and ABX.
Figure S6. Proteasomal inhibitors MG-132 and Lactacystin increased cellular α-Gal A mutants.
Table S1. Proteasomal activities in compound-treated HEK-293H cells.
Table S2. Primer registry.

ACKNOWLEDGMENTS

This work was conducted with excellent technical support by Tina Czajka, Mandy Loebert, and Sebastian Rost (Albrecht-Kossel-Institute, Medical University Rostock). We greatly thank Ulrike Grittner (Charité Berlin) for her appreciated advice and statistical support and Jenny Creed Geraghty (Centogene AG, Rostock) for critical manuscript revision. This work was supported by the Medical University Rostock by an internal funding program. Replagal was a kind gift of Werner Foeller (Shire Human Genetic Therapies Inc., Berlin, GER). The International patent "Combination of a Compound having the Ability to Rearrange a Lysosomal Enzyme and Ambroxol and/or a derivative of Ambroxol" (International application no: PCT/EP2012/005363) was filed according to the findings presented in this manuscript.

REFERENCES

1. Golubev, AM, Nagem, RA, Brandão Neto, JR, Neustroev, KN, Eneyskaya, EV, Kulminskaya, AA *et al.* (2004). Crystal structure of alpha-galactosidase from Trichoderma reesei and its complex with galactose: implications for catalytic mechanism. *J Mol Biol* **339**: 413–422.
2. Moreland, RJ, Jin, X, Zhang, XK, Decker, RW, Albee, KL, Lee, KL *et al.* (2005). Lysosomal acid alpha-glucosidase consists of four different peptides processed from a single chain precursor. *J Biol Chem* **280**: 6780–6791.
3. Meikle, PJ, Fuller, M and Hopwood, JJ (2003). Mass spectrometry in the study of lysosomal storage disorders. *Cell Mol Biol (Noisy-le-grand)* **49**: 769–777.
4. Mehta, A, Beck, M, Eyskens, F, Feliciani, C, Kantola, I, Ramaswami, U *et al.* (2010). Fabry disease: a review of current management strategies. *QJM* **103**: 641–659.
5. Kishnani, PS, Beckemeyer, AA and Mendelsohn, NJ (2012). The new era of Pompe disease: advances in the detection, understanding of the phenotypic spectrum, pathophysiology, and management. *Am J Med Genet C Semin Med Genet* **160C**: 1–7.
6. Güngör, D, de Vries, JM, Hop, WC, Reuser, AJ, van Doorn, PA, van der Ploeg, AT *et al.* (2011). Survival and associated factors in 268 adults with Pompe disease prior to treatment with enzyme replacement therapy. *Orphanet J Rare Dis* **6**: 34.
7. Spada, M, Pagliardini, S, Yasuda, M, Tukel, T, Thiagarajan, G, Sakuraba, H *et al.* (2006). High incidence of later-onset fabry disease revealed by newborn screening. *Am J Hum Genet* **79**: 31–40.
8. Herzog, A, Hartung, R, Reuser, AJ, Hermanns, P, Runz, H, Karabul, N *et al.* (2012). A cross-sectional single-centre study on the spectrum of Pompe disease, German patients: molecular analysis of the GAA gene, manifestation and genotype-phenotype correlations. *Orphanet J Rare Dis* **7**: 35.
9. Lukas, J, Giese, AK, Markoff, A, Grittner, U, Kolodny, E, Mascher, H *et al.* (2013). Functional characterisation of alpha-galactosidase a mutations as a basis for a new classification system in fabry disease. *PLoS Genet* **9**: e1003632.
10. Schmitz, M, Alfalah, M, Aerts, JM, Naim, HY and Zimmer, KP (2005). Impaired trafficking of mutants of lysosomal glucocerebrosidase in Gaucher's disease. *Int J Biochem Cell Biol* **37**: 2310–2320.
11. Yam, GH, Zuber, C and Roth, J (2005). A synthetic chaperone corrects the trafficking defect and disease phenotype in a protein misfolding disorder. *FASEB J* **19**: 12–18.
12. Flanagan, JJ, Rossi, B, Tang, K, Wu, X, Mascioli, K, Donaudy, F *et al.* (2009). The pharmacological chaperone 1-deoxynojirimycin increases the activity and lysosomal trafficking of multiple mutant forms of acid alpha-glucosidase. *Hum Mutat* **30**: 1683–1692.
13. Coutinho, MF, Prata, MJ and Alves, S (2012). Mannose-6-phosphate pathway: a review on its role in lysosomal function and dysfunction. *Mol Genet Metab* **105**: 542–550.
14. Dietz, HC (2010). New therapeutic approaches to mendelian disorders. *N Engl J Med* **363**: 852–863.
15. Kemper, AR, Hwu, WL, Lloyd-Puryear, M and Kishnani, PS (2007). Newborn screening for Pompe disease: synthesis of the evidence and development of screening recommendations. *Pediatrics* **120**: e1327–e1334.
16. El Dib, RP, Pastores, GM (2010). Enzyme replacement therapy for Anderson-Fabry disease. *Cochrane Database Syst Rev* **5**: CD006663.
17. Wilcox, WR, Linthorst, GE, Germain, DP, Feldt-Rasmussen, U, Waldek, S, Richards, SM *et al.* (2012). Anti-α-galactosidase A antibody response to agalsidase beta treatment: data from the Fabry Registry. *Mol Genet Metab* **105**: 443–449.
18. Wang, J, Lozier, J, Johnson, G, Kirshner, S, Verthelyi, D, Pariser, A *et al.* (2008). Neutralizing antibodies to therapeutic enzymes: considerations for testing, prevention and treatment. *Nat Biotechnol* **26**: 901–908.
19. Patel, TT, Banugaria, SG, Case, LE, Wenninger, S, Schoser, B and Kishnani, PS (2012). The impact of antibodies in late-onset Pompe disease: a case series and literature review. *Mol Genet Metab* **106**: 301–309.
20. Fan, JQ, Ishii, S, Asano, N and Suzuki, Y (1999). Accelerated transport and maturation of lysosomal alpha-galactosidase A in Fabry lymphoblasts by an enzyme inhibitor. *Nat Med* **5**: 112–115.
21. Asano, N, Ishii, S, Kizu, H, Ikeda, K, Yasuda, K, Kato, A *et al.* (2000). *In vitro* inhibition and intracellular enhancement of lysosomal alpha-galactosidase A activity in Fabry lymphoblasts by 1-deoxygalactonojirimycin and its derivatives. *Eur J Biochem* **267**: 4179–4186.
22. Sawkar, AR, Cheng, WC, Beutler, E, Wong, CH, Balch, WE and Kelly, JW (2002). Chemical chaperones increase the cellular activity of N370S beta -glucosidase: a therapeutic strategy for Gaucher disease. *Proc Natl Acad Sci USA* **99**: 15428–15433.
23. Okumiya, T, Kroos, MA, Vliet, LV, Takeuchi, H, Van der Ploeg, AT and Reuser, AJ (2007). Chemical chaperones improve transport and enhance stability of mutant alpha-glucosidases in glycogen storage disease type II. *Mol Genet Metab* **90**: 49–57.
24. Parenti, G, Zuppaldi, A, Gabriela Pittis, M, Rosaria Tuzzi, M, Annunziata, I, Meroni, G *et al.* (2007). Pharmacological enhancement of mutated alpha-glucosidase activity in fibroblasts from patients with Pompe disease. *Mol Ther* **15**: 508–514.
25. Andreotti, G, Citro, V, De Crescenzo, A, Orlando, P, Cammisa, M, Correra, A *et al.* (2011). Therapy of Fabry disease with pharmacological chaperones: from in silico predictions to *in vitro* tests. *Orphanet J Rare Dis* **6**: 66.
26. Wu, X, Katz, E, Della Valle, MC, Mascioli, K, Flanagan, JJ, Castelli, JP *et al.* (2011). A pharmacogenetic approach to identify mutant forms of α-galactosidase A that respond to a pharmacological chaperone for Fabry disease. *Hum Mutat* **32**: 965–977.
27. Benjamin, E, Do, HV, Wu, X, Flanagan, J, Wustman, B (2014). Method to predict response to pharmacological chaperone treatment of diseases. Amicus Therapeutics: USA. US Patent No 14/054,369.
28. Maegawa, GH, Tropak, MB, Buttner, JD, Rigat, BA, Fuller, M, Pandit, D *et al.* (2009). Identification and characterization of ambroxol as an enzyme enhancement agent for Gaucher disease. *J Biol Chem* **284**: 23502–23516.
29. Bendikov-Bar, I, Ron, I, Filocamo, M and Horowitz, M (2011). Characterization of the ERAD process of the L444P mutant glucocerebrosidase variant. *Blood Cells Mol Dis* **46**: 4–10.
30. Sánchez-Ollé, G, Duque, J, Egido-Gabás, M, Casas, J, Lluch, M, Chabás, A *et al.* (2009). Promising results of the chaperone effect caused by imino sugars and aminocyclitol derivatives on mutant glucocerebrosidases causing Gaucher disease. *Blood Cells Mol Dis* **42**: 159–166.
31. Clark, NE, Metcalf, MC, Best, D, Fleet, GW and Garman, SC (2012). Pharmacological chaperones for human α-N-acetylgalactosaminidase. *Proc Natl Acad Sci USA* **109**: 17400–17405.
32. Mu, TW, Ong, DS, Wang, YJ, Balch, WE, Yates, JR 3rd, Segatori, L *et al.* (2008). Chemical and biological approaches synergize to ameliorate protein-folding diseases. *Cell* **134**: 769–781.
33. Wang, F, Agnello, G, Sotolongo, N and Segatori, L (2011). Ca2+ homeostasis modulation enhances the amenability of L444P glucosylcerebrosidase to proteostasis regulation in patient-derived fibroblasts. *ACS Chem Biol* **6**: 158–168.
34. Zampieri, S, Bembi, B, Rosso, N, Filocamo, M and Dardis, A (2012). Treatment of Human Fibroblasts Carrying NPC1 Missense Mutations with MG132 Leads to an Improvement of Intracellular Cholesterol Trafficking. *JIMD Rep* **2**: 59–69.
35. Andreotti, G, Guarracino, MR, Cammisa, M, Correra, A and Cubellis, MV (2010). Prediction of the responsiveness to pharmacological chaperones: lysosomal human alpha-galactosidase, a case of study. *Orphanet J Rare Dis* **5**: 36.
36. Marfella, R, D'Amico, M, Esposito, K, Baldi, A, Di Filippo, C, Siniscalchi, M *et al.* (2006). The ubiquitin-proteasome system and inflammatory activity in diabetic atherosclerotic plaques: effects of rosiglitazone treatment. *Diabetes* **55**: 622–632.
37. Zheng, W, Padia, J, Urban, DJ, Jadhav, A, Goker-Alpan, O, Simeonov, A *et al.* (2007). Three classes of glucocerebrosidase inhibitors identified by quantitative high-throughput screening are chaperone leads for Gaucher disease. *Proc Natl Acad Sci USA* **104**: 13192–13197.
38. Tropak, MB, Blanchard, JE, Withers, SG, Brown, ED and Mahuran, D (2007). High-throughput screening for human lysosomal beta-N-Acetyl hexosaminidase inhibitors acting as pharmacological chaperones. *Chem Biol* **14**: 153–164.
39. Lieberman, RL, D'aquino, JA, Ringe, D and Petsko, GA (2009). Effects of pH and iminosugar pharmacological chaperones on lysosomal glycosidase structure and stability. *Biochemistry* **48**: 4816–4827.
40. Gasperini, RJ, Hou, X, Parkington, H, Coleman, H, Klaver, DW, Vincent, AJ *et al.* (2011). TRPM8 and Nav1.8 sodium channels are required for transthyretin-induced calcium influx in growth cones of small-diameter TrkA-positive sensory neurons. *Mol Neurodegener* **6**: 19.
41. Weiser, T (2008). Ambroxol: a CNS drug? *CNS Neurosci Ther* **14**: 17–24.
42. Siekierska, A, De Baets, G, Reumers, J, Gallardo, R, Rudyak, S, Broersen, K *et al.* (2012). α-Galactosidase aggregation is a determinant of pharmacological chaperone efficacy on Fabry disease mutants. *J Biol Chem* **287**: 28386–28397.
43. McNeill, A, Magalhaes, J, Shen, C, Chau, KY, Hughes, D, Mehta, A *et al.* (2014). Ambroxol improves lysosomal biochemistry in glucocerebrosidase mutation-linked Parkinson disease cells. *Brain* **137**(Pt 5): 1481–1495.
44. Porto, C, Ferrara, MC, Meli, M, Acampora, E, Avolio, V, Rosa, M *et al.* (2012). Pharmacological enhancement of α-glucosidase by the allosteric chaperone N-acetylcysteine. *Mol Ther* **20**: 2201–2211.
45. Ishii, S, Chang, HH, Kawasaki, K, Yasuda, K, Wu, HL, Garman, SC *et al.* (2007). Mutant alpha-galactosidase A enzymes identified in Fabry disease patients with residual enzyme activity: biochemical characterization and restoration of normal intracellular processing by 1-deoxygalactonojirimycin. *Biochem J* **406**: 285–295.
46. Kilroy, GE, Zhang, X and Floyd, ZE (2009). PPAR-gamma AF-2 domain functions as a component of a ubiquitin-dependent degradation signal. *Obesity (Silver Spring)* **17**: 665–673.
47. Hou, Y, Moreau, F and Chadee, K (2012). PPARγ is an E3 ligase that induces the degradation of NFκB/p65. *Nat Commun* **3**: 1300.
48. Ron, I, Rapaport, D and Horowitz, M (2010). Interaction between parkin and mutant glucocerebrosidase variants: a possible link between Parkinson disease and Gaucher disease. *Hum Mol Genet* **19**: 3771–3781.
49. Maor, G, Filocamo, M and Horowitz, M (2013). ITCH regulates degradation of mutant glucocerebrosidase: implications to Gaucher disease. *Hum Mol Genet* **22**: 1316–1327.
50. Steet, RA, Chung, S, Wustman, B, Powe, A, Do, H and Kornfeld, SA (2006). The iminosugar isofagomine increases the activity of N370S mutant acid beta-glucosidase in Gaucher fibroblasts by several mechanisms. *Proc Natl Acad Sci USA* **103**: 13813–13818.
51. Khanna, R, Soska, R, Lun, Y, Feng, J, Frascella, M, Young, B *et al.* (2010). The pharmacological chaperone 1-deoxygalactonojirimycin reduces tissue globotriaosylceramide levels in a mouse model of Fabry disease. *Mol Ther* **18**: 23–33.
52. Khanna, R, Flanagan, JJ, Feng, J, Soska, R, Frascella, M, Pellegrino, LJ *et al.* (2012). The pharmacological chaperone AT2220 increases recombinant human acid α-glucosidase uptake and glycogen reduction in a mouse model of Pompe disease. *PLoS One* **7**: e40776.
53. Porto, C, Pisani, A, Rosa, M, Acampora, E, Avolio, V, Tuzzi, MR *et al.* (2012). Synergy between the pharmacological chaperone 1-deoxygalactonojirimycin and the human recombinant alpha-galactosidase A in cultured fibroblasts from patients with Fabry disease. *J Inherit Metab Dis* **35**: 513–520.

Biochemical Journal (2020) **477** 359–380
https://doi.org/10.1042/BCJ20190513

Research Article

Proteostasis regulators modulate proteasomal activity and gene expression to attenuate multiple phenotypes in Fabry disease

Susanne Seemann[1], Mathias Ernst[2], Chiara Cimmaruta[1,3,4], Stephan Struckmann[2], Claudia Cozma[5], Dirk Koczan[6], Anne-Marie Knospe[1], Linda Rebecca Haake[1], Valentina Citro[4], Anja U. Bräuer[7,8,9], Giuseppina Andreotti[3], Maria Vittoria Cubellis[3,4], Georg Fuellen[2], Andreas Hermann[1,10,11], Anne-Katrin Giese[12,13], Arndt Rolfs[5,14] and Jan Lukas[1,10]

[1]Translational Neurodegeneration Section "Albrecht-Kossel", Department of Neurology, University Medical Center Rostock, University of Rostock, 18147 Rostock, Germany; [2]Institute for Biostatistics and Informatics in Medicine and Ageing Research, University Medical Center Rostock, 18057 Rostock, Germany; [3]Institute of Biomolecular Chemistry, CNR, 80078 Pozzuoli, Italy; [4]Department of Biology, University Federico II, 80126 Naples, Italy; [5]Centogene AG, Rostock, Germany; [6]Institute of Immunology, University Medical Center Rostock, 18057 Rostock, Germany; [7]Institute of Anatomy, University Medical Center Rostock, 18057 Rostock, Germany; [8]Research Group Anatomy, School of Medicine and Health Sciences, Carl von Ossietzky University Oldenburg, 26129 Oldenburg, Germany; [9]Research Center for Neurosensory Science, Carl von Ossietzky University Oldenburg, Oldenburg, Germany; [10]Center for Transdisciplinary Neurosciences Rostock (CTNR), University Medical Center Rostock, University of Rostock, 18147 Rostock, Germany; [11]German Center for Neurodegenerative Diseases (DZNE) Rostock/Greifswald, 18147 Rostock, Germany; [12]Department of Neurology, Massachusetts General Hospital, Harvard Medical School, Boston, MA, U.S.A.; [13]Program in Medical and Population Genetics, Broad Institute of MIT and Harvard, Cambridge, MA, U.S.A.; [14]University Medical Center Rostock, University of Rostock, 18057 Rostock, Germany

Correspondence: Jan Lukas (jan.lukas@med.uni-rostock.de)

The lysosomal storage disorder Fabry disease is characterized by a deficiency of the lysosomal enzyme α-Galactosidase A. The observation that missense variants in the encoding *GLA* gene often lead to structural destabilization, endoplasmic reticulum retention and proteasomal degradation of the misfolded, but otherwise catalytically functional enzyme has resulted in the exploration of alternative therapeutic approaches. In this context, we have investigated proteostasis regulators (PRs) for their potential to increase cellular enzyme activity, and to reduce the disease-specific accumulation of the biomarker globotriaosylsphingosine in patient-derived cell culture. The PRs also acted synergistically with the clinically approved 1-deoxygalactonojirimycine, demonstrating the potential of combination treatment in a therapeutic application. Extensive characterization of the effective PRs revealed inhibition of the proteasome and elevation of *GLA* gene expression as paramount effects. Further analysis of transcriptional patterns of the PRs exposed a variety of genes involved in proteostasis as potential modulators. We propose that addressing proteostasis is an effective approach to discover new therapeutic targets for diseases involving folding and trafficking-deficient protein mutants.

Received: 17 July 2019
Revised: 17 December 2019
Accepted: 2 January 2020

Accepted Manuscript online: 3 January 2020
Version of Record published: 29 January 2020

Introduction

Fabry disease (FD, OMIM 301500) is one of more than 40 lysosomal storage diseases (LSD) [1]. According to recent data, FD is possibly the most common LSD with an incidence found to be 1 : 1 250 to 1 : 37 800 [2] depending on the severity of symptoms. FD is caused by mutations in the X-linked gene encoding the lysosomal enzyme α-Galactosidase A (gene symbol: *GLA*, protein: α-Gal A) leading to absent or diminished activity of the enzyme [3]. Many missense variants of the *GLA* gene lead to impaired protein processing within the endoplasmic reticulum (ER) and an altered conformation that results in ER retention and premature ER-associated degradation (ERAD) [4]. Deficient activity of α-Gal A, in turn, causes progressive accumulation of Globotriaosylceramide (Gb3)

PORTLAND PRESS

Biochemical Journal (2020) **477** 359–380
https://doi.org/10.1042/BCJ20190513

or its metabolite Globotriaosylsphingosine (lyso-Gb3) [3]. The measurement of lyso-Gb3 in plasma and whole blood is considered of diagnostic as well as of prognostic value for the assessment of the clinical outcome of *GLA* mutations [5–7].

The current therapeutic strategy involves enzyme replacement therapy (ERT) with intravenous infusions of α-Gal A. Different formulations are available from different sources and manufacturers. The benefit of ERT may be impaired by many limitations including an insufficient penetration in key tissues [8], an immune response leading to the formation of IgG antibodies that may hamper the effectiveness of the treatment [9], the patient burden of a life-long inconvenient intravenous therapy and high cost. The clinical approval of the orally available pharmacological chaperone (PC) therapy using the active-site specific sugar mimetic 1-deoxygalactonojirimycine (DGJ) represents a recent therapeutic advance for a fraction of FD patients [10]. These patients harbor missense variants, which are associated with a destabilized though catalytically active α-Gal A enzyme. The effectiveness of DGJ is based on its direct binding to the immature α-Gal A within the ER. The variant enzyme then attains a thermodynamically favored folding state, which leads to a reduced elimination by ERAD and, consequently, to a shift to a greater enzyme fraction being further transported along the secretory route to the lysosomes raising the level of available, active α-Gal A [11].

New therapeutic approaches include the use of small molecules, which have the capacity to modify proteostasis, including protein synthesis, folding and degradation. They either increase the folding capacity of the ER or enhance the degradation of misfolded proteins in order to resolve the protein overload [12]. Therefore, they are referred to as proteostasis regulators (PRs). Many of these have been proposed as potential candidate drugs in protein misfolding and aggregation diseases (e.g. Cystic Fibrosis, Alzheimer's disease, retinitis pigmentosa) [12–15] and particularly LSD [16–20]. Either the protein variants that have resulted in the diseases are to be removed from the system, since toxic gain-of-function variants have developed, or the functionality of the protein must be restored by preventing degradation, i.e. a rescue of loss-of-function. Depending on the goal to be pursued, the properties of an effective drug are determined. Proteostasis is maintained by a highly conserved cellular machinery that regulates protein folding in general, and specifically, the protein misfolding-induced unfolded protein response (UPR) which activates the ERAD [21–23]. Signal integration within the proteostasis network is associated with extensive gene regulation [24,25] and leads to cell type-specific transcriptional patterns in response to stress in order to restore homeostasis [26]. The relation between protein folding diseases and the expression of proteostasis genes is being examined by a growing research community [16,17,21,23,27–33]. Additionally, the role of gene expression regulation, particularly of genes involved in proteostasis processes, has been proposed to be part of the work mechanism of PRs besides their primary biochemical function [16,17,21,27–30,33]. This gene regulator function of PRs might have an impact on the rescue of misfolded proteins. First indications for a meaningful use of PRs in FD can be found in earlier studies [34,35].

The aim of this study was to screen for candidates able to increase variant α-Gal A activity in patient-derived fibroblasts harboring the PC amenable variants c.902G>A (p.R301Q) and c.901C>G (p.R301G), respectively, and to provide a profound characterization of the effects on the proteostasis network.

Materials and methods

Chemicals

Chemicals were purchased from Sigma–Aldrich (Steinheim, Germany) except for 17-AAG (Abcam, Cambridge, U.K.); Rosiglitazon, Clasto-Lactacystin β-lactone (CLC), Eeyarestatin I (EerI) and Ritonavir (Cayman Chemicals, Ann Arbor, MI, U.S.A.); Pifithrin-μ (Enzo Life Sciences, Lörrach, Germany); Lacidipine (Key Organics, Cornwall, U.K.); MG132 (Merck (Darmstadt, Germany); 15d-PGJ2 (Santa Cruz Biotechnology, Dallas, TX, U.S.A.); Kifunensine and 1-deoxygalactonojirimycine hydrochloride (Toronto Research Chemicals, Toronto, Canada) and Bortezomib (USBiological, Salem, MA, U.S.A.).

Cell culture

Wild-type (WT) fibroblast cell lines GM01653 (wild-type 1, WT1), GM23249 (WT2), GM23250 (WT3), GM23968 (WT4) from healthy male donors and Fabry fibroblasts hemizygous for the c.901C>G (p.R301G) variant (GM00882, $GLA^{p.R301G/o}$) were purchased from Coriell Institute cell repository (Camden, U.S.A.). Male Fabry fibroblasts hemizygous for the c.902G>A (p.R301Q) variant ($GLA^{p.R301Q/o}$) were a kind gift of Amicus Therapeutics (Cranbury, NJ, U.S.A.). Both variants were reported to be amenable to PC treatment [5,35]. All lines were sequenced prior to use to verify the genotypes. Fabry disease was excluded for all healthy donors.

Biochemical Journal (2020) **477** 359–380
https://doi.org/10.1042/BCJ20190513

PORTLAND PRESS

However, GM23249 carried the intronic haplotype found to be associated with reduced mRNA expression [36]. Fibroblasts were cultured in Dulbecco's modified Eagle medium containing 4.5 g glucose/l (Gibco, Carlsbad, CA, U.S.A.) supplemented with 15% heat-inactivated fetal bovine serum (Gibco) and 1% Penicillin/Streptomycin (Invitrogen, Carlsbad, CA, U.S.A.) at 37°C in 5% CO_2. Monolayers were passaged with 0.25% Trypsin-EDTA (Fisher Scientific, Schwerte, Germany) when reaching full confluency.

Drug treatment

The patients' fibroblasts were seeded one day prior to the treatment to give the cells time to adhere to the surface of the culture vessel. At the beginning of the treatment, the cells typically had ∼80% confluency. The cells were treated with PR, DGJ, and a combination of both. The exact duration of the treatment and the drug concentrations used can be seen in the figures. Typically, the treatment was followed by a 6-h off-treatment period ('washout') for enzyme activity measurement, because α-Gal A required this recovery phase for stable assessment after DGJ treatment (Supplementary Figure S1) and a 4 days washout for biomarker measurements as reported before [37]. The PR treatment was also discontinued for the washout period. After the treatment, the cells were processed according to the downstream application as described in the following paragraphs.

α-Galactosidase A activity assay

After the treatment for the indicated time, the activity assay was run. The cells were harvested with 0.25% Trypsin-EDTA, washed with phosphate-buffered saline (PBS), resuspended in deionized water and lysed during five freezing and thawing cycles. The protein amount in the cell lysates was determined using the BCA protein assay kit (Thermo Scientific, Waltham, MA, U.S.A.). Five micrograms of total protein was used for enzyme activity measurement with the substrate analog 4-methylumbelliferyl-α-D-galactopyranoside. The reaction product 4-methylumbelliferone was recorded at 360 nm excitation and 460 nm emission in a fluorescence plate reader as described earlier [38].

Lyso-Gb3 determination in patient-derived fibroblasts

We seeded 2×10^5 fibroblast cells and treated them with PRs for the specified period of time. On the day of harvest, the cells were trypsinized then pelleted, washed with PBS, resuspended in 70 µl deionized water and vortexed for 3 min. The cell suspension was lysed during six cycles of freezing in liquid nitrogen and sonication for 5 min. Samples were centrifuged and the supernatant with the protein extract was transferred to a new tube. The protein amount in the cell lysates was determined using the BCA protein assay kit (Thermo Scientific). Sample preparation for lyso-Gb3 determination and the mass spectrometric analysis was performed as described [39]. For each batch of analyses, a calibration curve was added with a concentration range from 0 to 1 000 ng/ml in water. The concentration of the lyso-Gb3 was recorded in ng/mg protein extract.

Lipid extraction

Lipids were extracted according to Bligh and Dyer [40] with slight modifications. 1×10^6 human fibroblasts were seeded and cultured for the indicated time points with and without treatment. On the day of cell harvest, the cells were pelleted in non-adhesive wall glass tubes (Schott AG, Mainz, Germany) allowing for lipid extraction. A mixture of chloroform, methanol and hydrochloric acid (2 : 4 : 0.1) was added to the samples together with 1% butylated hydroxytoluol, to prevent lipid oxidation. In addition, a fluorescent internal standard, TopFluor® Lyso PA was added at a concentration of 1 mg/ml to ensure the reproducibility of the lipid extraction. The compound is a synthetic lipid, and therefore absent from the real samples. The fluorescence was later measured by CAMAG visionCATS at 366 nm. Chloroform was added to the homogenized samples and vortexed three times with a 10 min break in between. Next, water was added to the samples and vortexed three times with a 10 min break in between, followed by 30 min incubation and centrifugation at 1260 ×***g*** for 10 min. A biphasic separation was visible, and the bottom phase containing a mix of chloroform and lipids was transferred into a new non-adhesive wall glass vessel. Finally, the chloroform was evaporated in an N_2 chamber, fresh chloroform was added, and the bottles were stored at −20°C until use.

PORTLAND PRESS

Biochemical Journal (2020) **477** 359–380
https://doi.org/10.1042/BCJ20190513

Separation and analysis of Gb3 by high-performance thin-layer chromatography (HPTLC) and Far-Eastern blot

Samples were transferred to the HPTLC with an automatic TLC Sampler 4 (ATS 4) from CAMAG. The stationary phase was 10 × 10 cm silica gel (60 F254 Merck, KGaA, Darmstadt, Germany). For the mobile phase a chloroform (SupraSolv Merck KGaA, Darmstadt, Germany), methanol (LiChroSolv Merck KGaA, Darmstadt, Germany), ammonia 32% (HiPerSolv VWR Chemicals, Radnor, PA, U.S.A.), water (Rotisolv Carl Roth GmbH, Karlsruhe, Germany) solution at a ratio of 161 : 75 :5 : 10 was used. Lipids then developed on the HPTLC plate were sprayed with primuline reagent (Derivatizer, CAMAG) and visualized under ultraviolet light (366 nm, TLC Visualizer, CAMAG).

Far-Eastern blotting was made according to Taki et al. [41], with slight modifications (TLC blot (far-eastern blot)) and its applications. The plate was immersed in a mixture of isopropanol 0.2% $CaCl_2$: methanol (40 : 20 : 7, v/v/v) for 2 s, then covered with an activated polyvinylidene difluoride (PVDF) membrane (0.45 μm GE Healthcare Amersham Hybond, Fisher Scientific, Pittsburgh, PA, U.S.A.) and a glass microfiber filter (APFF, Merck, KGaA, Darmstadt, Germany). The transfer cassette was pressed for 30 s with an iron heated at 180°C, after which the PVDF membrane was separated from the plate and dried.

PVDF membrane was blocked over night at 4°C with 0.1% BSA diluted in PBS followed by antibody incubation with anti-Gb3 (1 : 1000, TCI, amsbio, Mainz, Germany) in 3% BSA/PBS for 2 h at RT. The secondary antibody used was Mouse Ig, HRP-Linked Whole Ab, Sheep (1 : 5000, ECL) conjugated to horseradish peroxidase. After incubation for 1 h at RT, Gb3 was detected using clarity western ECL Substrate (Bio-Rad 1705061 1 : 1) and analyzed by using ImageLab 6.0 software (Bio-Rad Laboratories, Hercules, CA, U.S.A.).

Synergy analysis

All calculations were performed using R 3.3.0. The synergyfinder [42] tool was used in version 1.3.0 (with minor patches, see https://github.com/struckma/synergyfinder). For calculating the three-dimensional interaction surface over the dose matrix, the package synergyfinder was used as well. For synergy analysis, the enzyme activity after the treatment of $GLA^{p.R301Q/o}$ was calculated as the percentage of the maximal determined activity. The enzyme activity of the untreated control cells was subtracted from the non-control samples. Synergy values (*excess over bliss*, *eob*) were determined by calculating the difference between the actual enzyme activity after the combined treatment and the expected additive drug effect given by the BLISS independence model [43] and calculated with the following equation: $E_D + E_B - E_D * E_B$. Here, E_D represents the enzyme activity after single treatment with DGJ and E_B describes the effect of the respective Bortezomib (BTZ) concentration. Synergy was called if the achieved enzyme activity after the combined treatment was higher than the expected additive effect. The BLISS synergy scores for each treatment were plotted as a function of the two drug concentrations.

Western blot analysis

Cultured WT and $GLA^{p.R301Q/o}$ fibroblasts were pelleted, washed with PBS and resuspended in 45 μl RIPA buffer containing complete protease inhibitor cocktail (Roche Diagnostics, Mannheim, Germany) followed by a 20 min incubation on ice to complete the lysis. After centrifugation of the samples, the supernatants were used for protein measurement using the BCA protein assay kit (Thermo Scientific) according to the specifications by the manufacturer. The PNGase digestion was carried out using the PNGase F kit from New England Biolabs (Ipswich, MA, U.S.A.) according to the manufacturer's specifications. Hundred micrograms of protein per sample were mixed with Laemmli buffer and incubated for 5 min at 95°C. For the separation of the proteins, SDS–PAGE was performed using the precast 4–15% Criterion™ TGX Stain-Free™ Protein Gels (Bio-Rad Laboratories). Proteins were transferred to a nitrocellulose membrane (GE Healthcare, Braunschweig, Germany), using the Trans-Blot® Turbo™ Midi Nitrocellulose Transfer Packs and the Trans-Blot® Turbo™ Transfer System (Bio-Rad Laboratories). The membrane was blocked in 5% non-fat dried skim milk solution for 1 h at room temperature and incubated with primary rabbit polyclonal GAPDH antibody (Abcam, Cambridge, U.K.) at a 1 : 10 000 dilution in TBS-Tween 20 supplemented with 3% non-fat dried skim milk at 4°C overnight. Afterwards, the membrane was washed five times with TBS-Tween 20, incubated with mouse monoclonal α-Gal A antibody at a 1 : 500 dilution in TBS-Tween 20 supplemented with 3% non-fat dried skim milk (Abcam, Cambridge, U.K.) for 2 h at room temperature and washed again with TBS-Tween 20. Then, the membrane was treated with 1 : 20 000 diluted secondary goat anti-rabbit antibody (LI-COR Biosciences,

Biochemical Journal (2020) **477** 359–380
https://doi.org/10.1042/BCJ20190513

Lincoln, NE, U.S.A.) and 1 : 10 000 diluted goat anti-mouse antibody (Rockland Immunochemicals, Limerick, PA, U.S.A.), both diluted in TBS-Tween 20 including 3% non-fat dried skim milk, for 2 h at room temperature protected from light. After a final washing step, the blots were visualized using an Odyssey® Infrared Imager (LI-COR Biosciences). The determination of the protein size and the quantification of the bands were done using the Odyssey Application Software version 1.2.

Proteasomal activity assay

Specific proteasome inhibition was examined using the Cell-Based Proteasome-Glo™ Assays (Promega, Madison, WI, U.S.A.) according to the manufacturer's protocol. One day before the assay *GLA*$^{p.R301Q/o}$ fibroblasts were seeded in 24-well plates (Sarstedt, Nümbrecht, Germany) and cultured overnight. The experiment was initiated by the addition of the compound. The cells were incubated for 2 h. For the luminometric measurement, the cells were harvested by scraping and 20 000 cells were dissolved in 100 µl PBS + compound. An equal volume of Proteasome Proteasome™-Glo Reagent (Promega) specific for chymotrypsin-like activity determination was added [44] and the suspension was incubated for 10 min followed by a measurement with a Lumat 9507 instrument (Berthold Technologies, Bad Wildbad, Germany) with a measurement time of 2 s.

Quantitative real-time PCR

GLA$^{p.R301Q/o}$ fibroblasts were treated for 24 h. The cells were harvested and 2 µl of the crude RNA extract was reverse transcribed using the FastLane Cell cDNA kit (Qiagen, Hilden, Germany) according to the manufacturer's specification. PCR samples were prepared with the FastStart Essential DNA Green Master kit (Roche, Mannheim, Germany) according to the manufacturer's specification. Primer sequences were 5′-TTCAAAAGCCCAATTATACAGAAA-3′ (forward) and 5′-CTGGTCCAGCAACATCAACA-3′ (reverse) for *GLA* and 5′-TGCCCCCGACCGTCTAC-3′ (forward) and 5′-ATGCGGTTCCAGCCTATCTG-3′ (reverse) for *G6PD*, respectively. PCR was carried out with the LightCycler® Nano (Roche, Mannheim, Germany) in combination with the LightCycler® Nano SW 1.1 software. Changes of mRNA amounts were calculated using the efficiency corrected relative quantification model [45].

Microarray analysis

1.2×10^6 *GLA*$^{p.R301Q/o}$ fibroblasts were seeded in 10 cm dishes and treated with the indicated compound for 24 h (see Supplementary Table S1). Each condition was performed in quadruplicate. The cells were homogenized in Buffer RLT Plus of the RNeasy Plus Mini Kit (Qiagen, Hilden, Germany). Total RNA was purified utilizing the RNeasy Plus Mini Kit according to the manufacturer's specification. Microarray-based gene expression analysis was performed with GeneChip® Human Transcriptome Arrays 2.0 (Affymetrix, St. Clara, CA, U.S.A.). The RNA samples were amplified and labeled using the GeneChip® WT PLUS Reagent Kit (Thermo Fisher Scientific) according to the manufacturer's instructions. For the overnight hybridization, the GeneChip® Hybridization Oven (Affymetrix) was utilized and the visualization was done using the GeneChip Scanner 3000/7G (Affymetrix). The original data were subjected to quality control using the Expression Console Software (Version 1.4.1.46, Affymetrix). Background correction and normalization were performed using the Robust Multichip Average procedure [46]. Differentially expressed genes were identified by moderated *t*-test with Benjamini–Hochberg *P*-value adjustment. An absolute fold change ≥ 1.5 coupled with an adjusted *P*-value ≤ 0.05 were considered significant.

Wikipathways analysis

Transcriptional signatures of MG132, BTZ, CLC and EerI were analyzed for pathway annotation. WikiPathways analysis was performed using the R software version 3.2.3 utilizing the Bioconductor package org.Hs.eg.db [47].

Extended proteostasis gene signature

We compiled an extended ERAD/proteasome gene signature. We obtained a list of known ERAD/proteostasis genes [23]. We then constructed a gene-centric interaction network based on the STRING 10.0 interactome database. Querying this network with the candidate genes yielded multiple network subcomponents. We identified genes that could parsimoniously bridge these subcomponents, yielding a set of additional ERAD/proteostasis candidate genes. We subjected these candidate genes to a manual review to positively establish their involvement in ERAD/proteostasis, assessing whether they were annotated with GO terms related to ER

PORTLAND PRESS

Biochemical Journal (2020) **477** 359–380
https://doi.org/10.1042/BCJ20190513

protein folding, UPR or ERAD. Finally, the candidate gene list was augmented by adding ubiquitin associated E1/E2 and proteasome-associated genes utilizing the respective HGNC gene lists. Three hundred and fifty-seven genes were identified that are in the described context with proteostasis.

Statistical analysis

Statistical data analysis was carried out using GraphPad Prism 5 (GraphPad Software Inc., U.S.A.), Excel software (Microsoft, U.S.A.) and R software (R Foundation). Experimental data are given as mean ± SD. Differences between treatment groups were analyzed using One-way ANOVA with post-hoc Dunnett test as indicated (*, **, ***, ****P-values of 0.05, 0.01, 0.001 and <0.0001). The number of independent experiments is indicated in the figure legends.

Results

Abnormal changes in Fabry patient-derived fibroblasts

Enzymatic α-Gal A activity in patient-derived fibroblasts from adult male hemizygous Fabry patients harboring the variants p.R301Q ($GLA^{p.R301Q/o}$) and p.R301G ($GLA^{p.R301G/o}$) was initially compared with four fibroblast cell lines from healthy age and sex-matched donors (WT 1–4) (Figure 1A). The values for the enzyme activity in $GLA^{p.R301Q/o}$ (16.70 ± 3.70 nmol 4-MU/mg protein/h) and $GLA^{p.R301G/o}$ (12.28 (±4.93) nmol 4-MU/mg protein/h) fibroblasts, respectively, were reduced compared with the WT cells (58.5 (±31.1) nmol 4-MU/mg protein/h). Both common FD storage products lyso-Gb3 and Gb3 were also analyzed. Lyso-Gb3 showed a significant increase in both patient cell lines compared with WT1 cells (Figure 1B). The Gb3 level of $GLA^{p.R301Q/o}$ fibroblasts was also found to be elevated (Supplementary Figure S2).

Proteostasis regulators as effective α-Gal A enhancers

In this study, we first screened 23 PRs as potential variant α-Gal A activity enhancers (Table 1). To this end, $GLA^{p.R301Q/o}$ fibroblasts were treated with proteostasis regulating substances of varying concentrations for 5 days. For the treatment with DGJ and all DGJ combinations, a 6-h non-treatment phase was applied before cells were harvested (see Materials and methods). A substance was considered effective if the mean value of enzyme activity increased by more than 1.2 times compared with untreated $GLA^{p.R301Q/o}$ fibroblasts and statistical significance was obtained from at least three independent measurements. The proteasome inhibitors MG132, BTZ and CLC were classified as effective activity enhancers of variant p.R301Q. Enzyme activity in $GLA^{p.R301Q/o}$ cells was elevated up to 2.1-fold by MG132 and BTZ, which is comparable to the 1.9-fold increase observed with 50 μM DGJ (Figure 2A). CLC increased the activity of α-Gal A up to 1.7-fold. The concentration-dependent effect of the active PRs is shown in Supplementary Figure S3. When testing the substances with $GLA^{p.R301G/o}$ fibroblasts, the concentrations most effective in the $GLA^{p.R301Q/o}$ cells showed a high efficacy, enhancing the variant p.R301G enzyme up to 6.5-fold (MG132), 8.5-fold (BTZ) and 4.1-fold (CLC), respectively (Figure 2B).

Proteostasis regulators with synergistic effects in combination with DGJ

Both the $GLA^{p.R301Q/o}$ and the $GLA^{p.R301G/o}$ cell lines were treated with a combination of the PRs and 50 μM DGJ. After 5 days of treatment, α-Gal A activity was significantly increased when compared with the single treatment with DGJ (Figure 3A,B). Evidently, MG132 and BTZ increased the DGJ effect from 2-fold up to 6.5-fold and 6.8-fold, respectively, in $GLA^{p.R301Q/o}$ cells, and up to 13.2-fold and 17.8-fold, respectively, in $GLA^{p.R301G/o}$ cells. The combination of DGJ and CLC resulted in a 4-fold and 7-fold increase in enzyme activity in $GLA^{p.R301Q/o}$ and $GLA^{p.R301G/o}$ fibroblasts, respectively. EerI, which inhibits the Sec61-mediated protein translocation from the ER into the cytosol, had no significant effect in $GLA^{p.R301Q/o}$ fibroblasts when used as a single substance (Figure 2A), but in combination with DGJ, a significant effect beyond that of DGJ single treatment was observed up to 3.3-fold of the untreated and 1.9-fold of the DGJ single treated state, respectively (Figure 3A). In $GLA^{p.R301G/o}$ cells a 4.3-fold increase above untreated and 2.2-fold above DGJ single treatment was achieved (Figure 3B). Hence, EerI was evaluated as an effective substance. The secretolytic and mucoactive agent Ambroxol (ABX) was formerly described as a potential PC for FD [35]. ABX at a concentration of 10 μM slightly elevated the effect obtained with DGJ single treatment by 1.1-fold in $GLA^{p.R301Q/o}$ (Figure 3A) and by 1.3-fold in $GLA^{p.R301G/o}$ fibroblasts (Figure 3B), respectively. Even though this was a bit less than the effect observed on these two variants in HEK293H cells in the previous study, ABX was included in the further

Biochemical Journal (2020) **477** 359–380
https://doi.org/10.1042/BCJ20190513

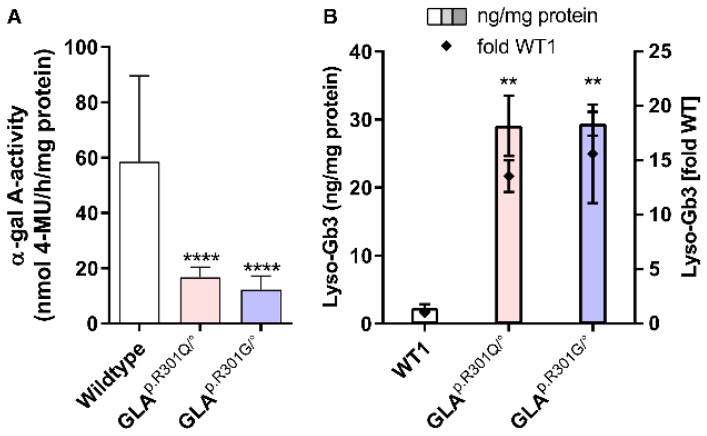

Figure 1. Determination of the pathophysiology of Fabry patient-derived fibroblasts.

(**A**) WT and FD fibroblasts were cultured for 5 days. Cell homogenates were used to determine enzyme activity with 4-methylumbelliferyl-α-D-galactopyranoside as a substrate. Shown is the substrate turnover per hour per mg protein as the mean. The wild-type control bar represents the activity obtained from four different fibroblast cell lines. The data are reported as mean ± SD. Each individual wild-type cell line was tested at least four times. The FD cell activity was obtained from 16 independent experiments. (**B**) WT1, *GLA*$^{p.R301Q/o}$ and *GLA*$^{p.R301G/o}$ fibroblasts were cultured for 7 days followed by lyso-Gb3 determination, which was normalized to the protein amount in each sample (left *y*-axis). The data are reported as mean ± SD ng lyso-Gb3/mg protein (left *y*-axis) and fold change (right *y*-axis) from three independent experiments. Statistics: Differences between the groups were analyzed using One-way ANOVA with post-hoc Dunnett test (*, **, ***, ****P-values of 0.05, 0.01, 0.001 and <0.0001). For (**B**), the statistical evaluation refers to the left *y*-axis.

analyses. The remaining PRs listed in Table 1 were inactive in both single and combination treatment with DGJ (data not shown).

Based on the BLISS independence model, the synergistic mechanism of action was determined for the combinations of DGJ plus BTZ. The BLISS model provides a formula for the investigation of the interaction of two simultaneously applied compounds to determine the efficacy of combination treatments. To examine the dynamics of the most effective combination treatment, different concentration ranges of DGJ (1–200 μM) and BTZ (1–10 nM) were combined for the treatment of *GLA*$^{p.R301Q/o}$ fibroblasts (Figure 3C). Exceeding the clinically achievable plasma concentration by 20 times, DGJ at a concentration of 200 μM triggered an increase in α-Gal A activity up to 60% of the mean normal activity obtained from four WT fibroblast lines (35.3 (±5.4) nmol 4-MU/mg protein/h). However, only 5 nM BTZ were sufficient to increase the activity of variant α-Gal A in combination with the clinically effective 10 μM DGJ up to the normal level (84.6 (±6.8) nmol 4-MU/mg protein/h). The maximum effect was achieved with the combination of 200 μM DGJ + 5 nM BTZ. To get a better overview of the synergy of DGJ and BTZ, an analysis based on the BLISS independence model was performed. Drug interaction of BTZ and DGJ in the *GLA*$^{p.R301Q/o}$ fibroblasts featured synergy as demonstrated by the BLISS synergy scores of the combined treatment (Figure 3D).

Bortezomib corrects the Fabry-related cellular phenotype

The α-Gal A protein undergoes a complicated process involving folding and transport in the cell en route to the lysosome. Higher enzyme activity should correlate with an improved processing of variant α-Gal A. For a quantitative assessment of α-Gal A, *GLA*$^{p.R301Q/o}$ fibroblasts were treated with DGJ and BTZ for 5 days with subsequent washout for 6 h. The occurrence of several N-glycosylated α-Gal A forms renders its quantification difficult (Figure 4A). *In vitro* deglycosylation of the enzyme prior to western blot analysis using PNGase F was applied to collect all cellular α-Gal A forms in a distinct band for a more comprehensive measurement (Figure 4B). Quantification of the indicated 39 kDa band revealed a reduced α-Gal A protein level by half in the *GLA*$^{p.R301Q/o}$ cell line in relation to WT1 fibroblasts (Figure 4C). α-Gal A level tended to be slightly elevated after the single treatment with 50 μM DGJ or 5 nM BTZ to 1.3-fold and 1.5-fold, respectively (Figure 4C). In

PORTLAND PRESS

Biochemical Journal (2020) **477** 359–380
https://doi.org/10.1042/BCJ20190513

Table 1 Panel of proteostasis regulators used in this study

Molecular function	Small molecule	Disease examined	Proteostasis regulator reference
Ca^{2+} channel blocker	Lacidipine	Gaucher disease	Wang et al. *Chem Biol.* (2011)
	Dantrolene	Gaucher disease	Wang et al. *ACS Chem. Biol.* (2011) Ong et al. *Nat. Chem. Biol.* (2010)
	Diltiazem	Gaucher disease	Ong et al. *Nat. Chem, Biol.* (2010)
Coinducer of heat shock proteins (HSPs)	Arimoclomol	NPC1	Kirkegaard et al. *Sci. Transl. Med.* (2016)
Inhibitor of cyclooxygenase	Ibuprofen	Cystic fibrosis	Carlile et al. *J. Cyst Fibros.* (2015)
ERAD inhibitor	17-AAG (HSP90)	Glioblastoma multiforme	Sauvageot et al. *Neuro Oncol.* (2009)
	Bortezomib (proteasome)	Pompe disease	Shimada et al. *JIMD Rep.* (2015)
	Celastrol (proteasome)	Gaucher disease, Tay-Sachs disease	Mu et al. *Cell* (2008)
	Clasto-Lactacystin β-lactone (proteasome)	Fabry disease	Ishii et al. *Biochem. J.* (2007)
	Eeyarestatin I (VCP)	Gaucher disease	Wang et al. *J. Biol. Chem.* (2011)
	Kifunensine (MAN1B1)	Gaucher disease	Wang et al. *J. Biol. Chem.* (2011)
	MG132 (proteasome)	Gaucher disease, Tay-Sachs disease	Mu et al. *Cell* (2008)
	Pifithrin-μ (HSP70)	Cancer	Leu et al. *Mol. Cell* (2009)
	Pyr41 (ubiquitination)	Fabry disease	Lukas et al. *Mol. Ther.* (2015)
	Ritonavir (proteasome)	Solid malignancies	Kraus et al. *Mol. Cancer Ther.* (2008)
	SAHA (histone deacetylase)	NPC1, Gaucher disease	Pipalia et al. *Proc. Natl Acad. Sci. U.S.A.* (2011), Lu et al. *Proc. Natl Acad. Sci. U.S.A.* (2011)
	TSA (histone deacetylase)	NPC1	Pipalia et al. *Proc. Natl Acad. Sci. U.S.A.* (2011)
Na^{+} channel blocker/PC	Ambroxol	Fabry disease/Pompe disease, Gaucher disease	Lukas et al. *Mol. Ther.* (2015), McNeill et al. *Brain* (2014)
PC	DGJ	Fabry disease	Fan et al. *Nat. Med.* (1999)
Peroxisome Proliferator-Act-ivated Receptor agonist	Rosiglitazone (PPARγ)	Fabry disease	Lukas et al. *Mol. Ther.* (2015)
	Pioglitazone (PPARγ)	Alzheimer's disease	Papadopoulos et al. *PLoS One* (2013)
	15d-PGJ_2 (PPARγ)	Multiple myeloma	Sperandio et al. *Exp. Mol. Pathol.* (2017)
	Bezafibrate (PPARα/δ/γ)	Fabry disease	Lukas et al. *Mol Ther.* (2015)

accordance with the enzyme activity measurement (Figure 3A), the combined treatment with DGJ/BTZ increased the α-Gal A to supraphysiological levels.

It is not possible to prove with certainty how high a potential gain in protein stability or enzyme activity must be in order to restore normal cell physiology and, hence, provide a clinical benefit. Therefore, an important result of the treatment is a functional reduction in pathophysiological lyso-Gb3 levels. $GLA^{p.R301Q/o}$

Biochemical Journal (2020) **477** 359–380
https://doi.org/10.1042/BCJ20190513

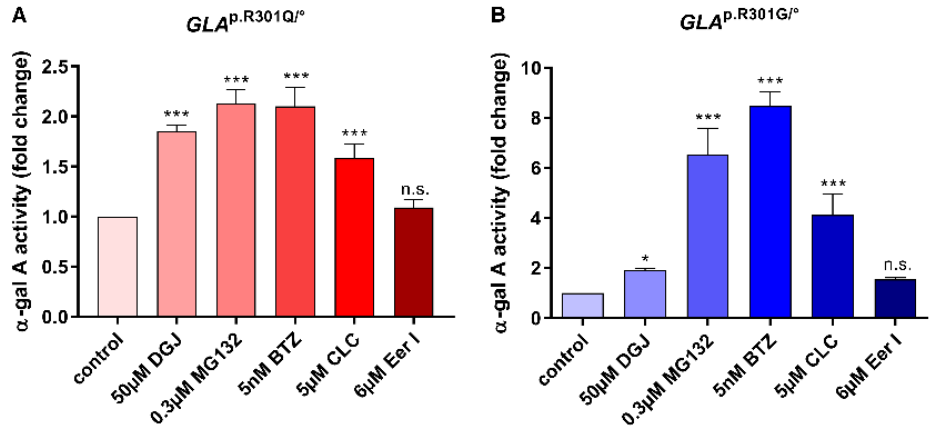

Figure 2. Enhancement of mutant α-Gal A activity by proteostasis regulators.

GLA$^{p.R301Q/°}$ (**A**) and *GLA*$^{p.R301G/°}$ (**B**) fibroblasts were treated for 5 days with the pharmacological chaperone DGJ and different proteostasis regulating drugs (MG132, BTZ, CLC and Eerl). Reported enzyme activity was normalized to the activity of untreated mutant control cells. Data are reported as mean ± SD of at least three independent experiments. One-way ANOVA with post-hoc Dunnett test was carried out to test statistical significance (*, ***P*-values of 0.05 and 0.001); n.s., not significant.

fibroblasts were treated with 50 μM DGJ and 5 nM BTZ for 7 and 14 days with a subsequent washout for 4 days. After 7 (+4) days, DGJ (10%) and BTZ (32%) single treatment caused an insignificant reduction in lyso-Gb3 in the cells (Figure 5A). In contrast, the combination of DGJ and BTZ lowered the cellular lyso-Gb3 significantly by 49%. Increasing treatment time to 14 days did not improve the effect of DGJ but enhanced the BTZ effect after single treatment (60%) as well as in combination with DGJ (70%) (Figure 5B). However, the differences between the 7-day and 14-day treatment have not been significant being $P = 0.2140$ for the single and $P = 0.4081$ for the combination treatment (unpaired two-sample *t*-test). The lyso-Gb3 clearance after the single and combined treatment with DGJ and BTZ followed relatively slow kinetics. It behaves in an almost linear way within the monitored time of the experiment. Moreover, the lyso-Gb3 level is far from normal, being 3.8 times higher than in the control fibroblast cell line after the 14-day treatment. Enzyme activity, however, approached (in case of DGJ, BTZ single treatment) or even exceeded (in case of combined treatment) the normal level after 5 days (compare Figures 2A and 3A). Therefore, we wanted to determine how enzyme activity changes during prolonged exposure to treatment and whether the effect can become exhausted, or potentially, increase over time. At first, only the duration of treatment was adjusted to 14 days, but the washout time was left at 6 h specified for DGJ (Figure 5C). As expected, enzyme activity increase after DGJ and BTZ single treatments remained relatively stable compared with 5 days. A slight trend was observed indicating a stronger increase using longer incubation periods (DGJ: 1.9-fold (5 days) vs. 2.3-fold (14 days), $P = 0.0173$; BTZ: 2.1-fold (5 days) vs. 3.0-fold (14 days), $P = 0.0921$, unpaired two-sample *t*-test). The combined treatment was significantly more effective and achieved a 24-fold increase in the initial activity (DGJ/BTZ: 6.8-fold (5 days) vs. 24.0-fold (14 days), $P < 0.0001$, unpaired two-sample *t*-test). We then adjusted the washout period likewise to 4 days in accordance with the lyso-Gb3 experiments (Figure 5D). The DGJ effect resembled the level observed for the 5-day treatment and 6-h washout regimen while the beneficial effect of BTZ single treatment on the α-Gal A activity could not be observed after 4 days of washout. The combined treatment of DGJ and BTZ yielded an elevation identical with the level observed for 5-day treatment and 6-h washout (6.8-fold). Although the combination treatment after 4 days of washout still resulted in a significant increase in activity compared with the DGJ single treatment, the reduced activity compared with the 14-day treatment and 6-h washout (6.8-fold vs. 24.0-fold, $P < 0.0001$, unpaired two-sample *t*-test) indicates that a part of the BTZ effect was eliminated by the discontinuation of treatment.

Altogether, these data suggest that the DGJ effect on α-Gal A will persist for prolonged periods of time when treatment is discontinued. Although the effect produced by BTZ is temporary and decreased rapidly when cells

PORTLAND PRESS

Biochemical Journal (2020) **477** 359–380
https://doi.org/10.1042/BCJ20190513

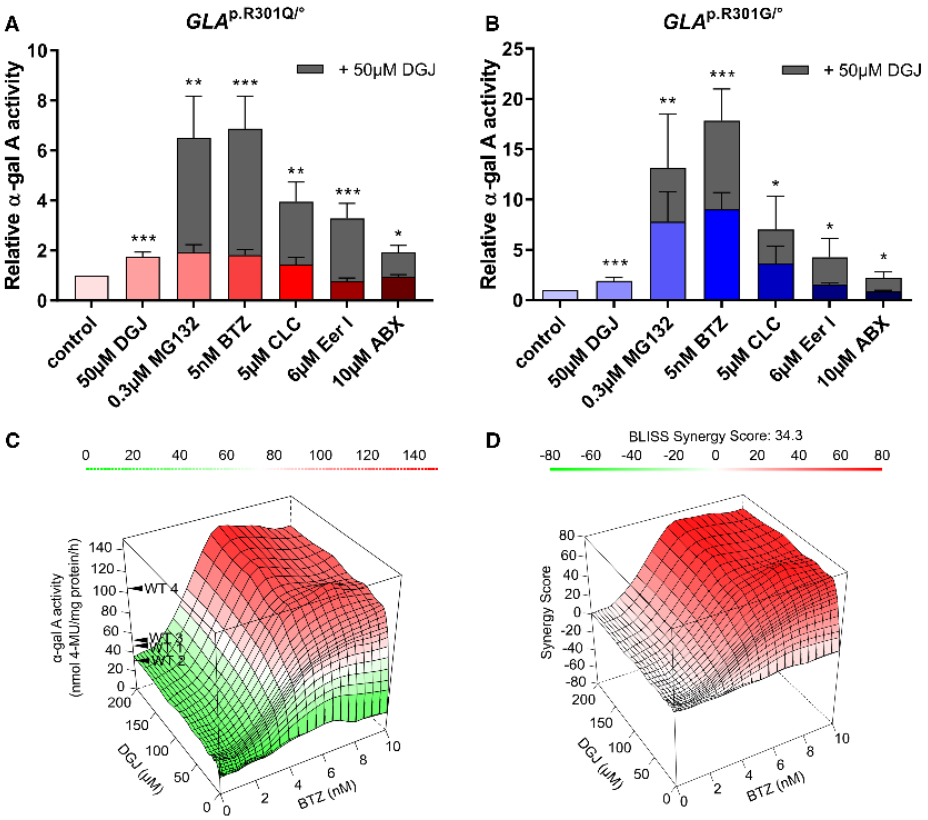

Figure 3. Drug synergy of PRs and the pharmacological chaperone DGJ on Fabry disease mutants.
GLA$^{p.R301Q/o}$ (**A**) and *GLA*$^{p.R301G/o}$ (**B**) fibroblasts, respectively, were treated with combinations of DGJ and various PRs. Reported enzyme activity was normalized to the activity of untreated mutant control cells. For the statistical evaluation, DGJ treatment was compared with the untreated condition, the combinations were compared with DGJ single treatment. (**C**) Drug interaction landscape for enzyme activity in *GLA*$^{p.R301Q/o}$ fibroblasts was established for DGJ and BTZ. **(D)** Drug interaction landscape for enzyme activity in *GLA*$^{p.R301Q/o}$ fibroblasts based on the BLISS model revealed BLISS Synergy Score of 34.3 as the representative mean of all calculated single Synergy Scores. Data in (**A**) and (**B**) are representative of mean ± SD of at least three independent experiments. Data in (**C**) and (**D**) are reported as mean of 3 independent experiments. Statistics (**A**,**B**): One-way ANOVA with post-hoc Dunnett test (*, **, ***P-values of 0.05, 0.01 and 0.001).

were no longer exposed to treatment, the BTZ effect could reach very high levels through prolonged treatment time (Figure 5C). Moreover, the lyso-Gb3 reducing effect of BTZ also appears to be sustainable in the interrupted treatment regime (Figure 5A,B). The *GLA*$^{p.R301G/o}$ fibroblasts showed a significant reduction in lyso-Gb3 with all applied substances using the 7 (+4)-day washout treatment regimen (Figure 5E) and confirmed the principle trend in the *GLA*$^{p.R301Q/o}$ cells.

Proteostasis regulators display different effects on the proteasome

The proteasome is a major effector of the PRs by definition, and MG132, BTZ and CLC are known inhibitors of the proteasomal activity. The decrease in proteasomal function in *GLA*$^{p.R301Q/o}$ fibroblasts was observed after the application of the effective concentrations of MG132, BTZ and CLC, but the level of reduction was obviously very different being 19.8%, 56.5% and 1.5% of the normal activity, respectively (Figure 6A). A concentration of 50 nM BTZ could further lower the proteasomal activity but had no additional effect on variant α-Gal

Biochemical Journal (2020) **477** 359–380
https://doi.org/10.1042/BCJ20190513

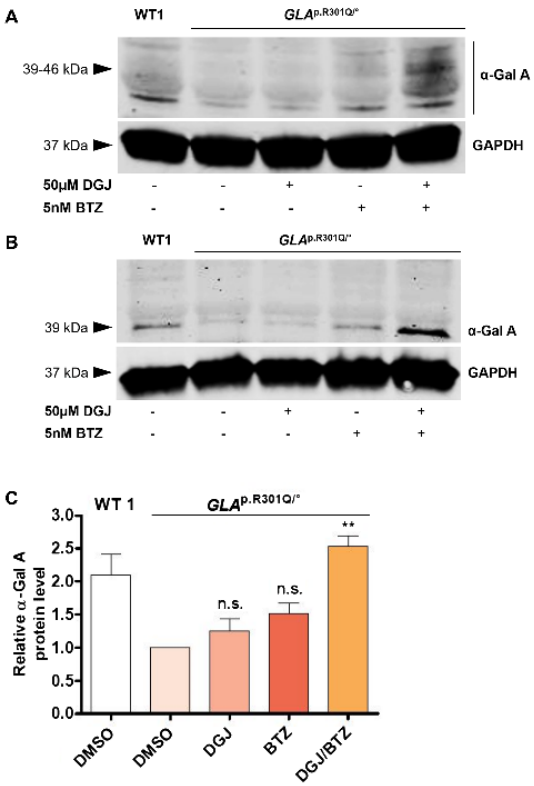

Figure 4. Protein level of α-Gal A in *GLA*$^{p.R301Q/o}$ fibroblasts after treatment with DGJ and BTZ.
WT1 cells and *GLA*$^{p.R301Q/o}$ fibroblasts were treated for 5 days with 50 μM DGJ and 5 nM BTZ with subsequent washout for 6 h. (**A**) Protein level of α-Gal A was reduced in *GLA*$^{p.R301Q/o}$ fibroblasts in comparison with WT1 cells. Treatment with DGJ and BTZ increased the protein level of α-Gal A in *GLA*$^{p.R301Q/o}$ fibroblasts above the WT level. (**B**) Deglycosylation with PNGase F prior to western blot resulted in a condensation of all antibody-reactive material in a distinct band at ~39 kDa. (**C**) Quantification of (**B**). Fluorescence intensity of the α-Gal A bands was normalized to the corresponding GAPDH band and to untreated *GLA*$^{p.R301Q/o}$ cells. Data represent three independent experiments and are plotted as mean ± SD. Statistics: Differences between the groups of treated *GLA*$^{p.R301Q/o}$ fibroblasts were analyzed using One-way ANOVA with post-hoc Dunnett test (**P*-value of 0.01); n.s., not significant.

A activity (Supplementary Figure S3C). Thus, BTZ was most effective in increasing the activity of α-Gal A at sub-IC50 concentrations related to proteasomal inhibition [48]. Application of DGJ, EerI and ABX had no effect on the proteasome. Celastrol (CTR) was included in this analysis as a proteasomal inhibitor that was unable to increase α-Gal A activity in the *GLA*$^{p.R301Q/o}$ cells in order to obtain a mechanistic explanation for this finding. Treatment with CTR resulted in an inhibition of the proteasomal activity down to 75.0%. It is crucial to investigate whether there is a critical threshold of proteasomal activity necessary for the rescue of variant α-Gal A or, more generally, whether regulation of the degradation of α-Gal A via the proteasome is a relevant factor at all.

GLA gene expression elevation in *GLA*$^{p.R301Q/o}$ cells by proteostasis regulators

PRs have an impact on the transcriptome. An obvious suspicion is that the PRs investigated here up-regulate the mutated *GLA* gene itself. Thus, we tested whether the effective PRs could trigger *GLA* gene expression in

PORTLAND PRESS

Biochemical Journal (2020) **477** 359–380
https://doi.org/10.1042/BCJ20190513

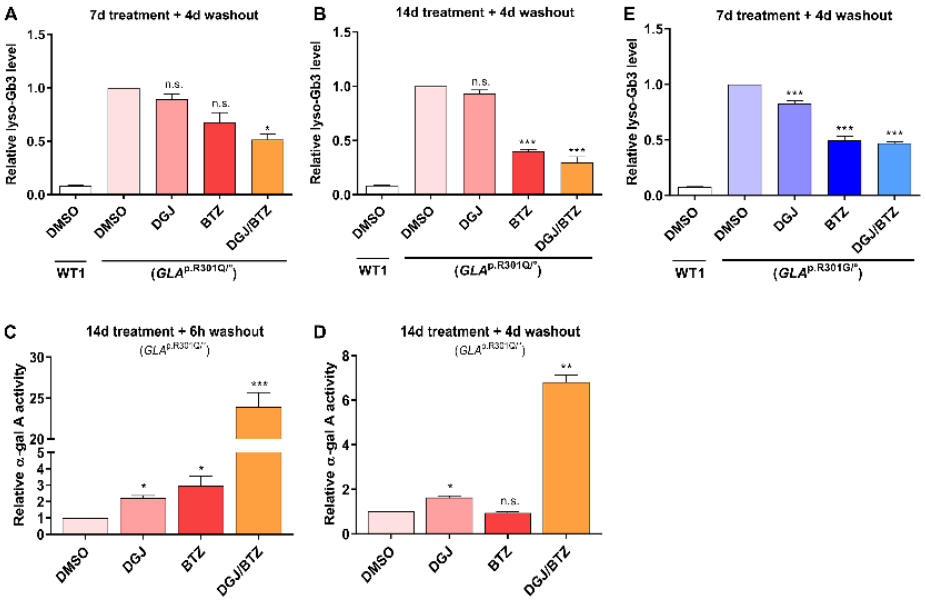

Figure 5. Lyso-Gb3 level and α-Gal A activity in *GLA*$^{p.R301Q/o}$ cells in response to prolonged treatment with DGJ and BTZ.

GLA$^{p.R301Q/o}$ fibroblasts were treated for 7 days (**A**) or 14 days (**B**) with 50 μM DGJ, 5 nM BTZ and the DGJ/BTZ combination with subsequent washout for 4 days. Lyso-Gb3 values were normalized to DMSO-treated *GLA*$^{p.R301Q/o}$ cells. The white barshows the lyso-Gb3 level in DMSO-treated WT1 fibroblasts. (**C**) α-Gal A activity after the prolonged 14-day treatment and 6-h washout analogous to the described treatment scheme (Figure 2) and (**D**) an additional 4-day washout. Reported enzyme activity was normalized to the activity of untreated mutant control cells. For the statistical evaluation, DGJ and BTZ single treatments were compared with the untreated condition, the combination was compared with DGJ single treatment. (**E**) *GLA*$^{p.R301G/o}$ fibroblasts were treated for 7 days as in **(A)** and lyso-Gb3 was normalized to the DMSO-treated cells. All results are normalized to the untreated *GLA*$^{p.R301Q/o}$ cells. Data are plotted as mean ± SD from 4 (**A**) or 3 (**B–E**) independent experiments. Statistics: Differences between the groups were analyzed using One-way ANOVA with post-hoc Dunnett test (*, **, ****P*-values of 0.05, 0.01 and 0.001); n.s., not significant.

the *GLA*$^{p.R301Q/o}$ fibroblasts. MG132, BTZ, CLC and EerI induced increases in expression levels of up to 7.9-fold, 8.4-fold, 9.2-fold and 5.4-fold (Figure 6B). The application of DGJ and ABX had no effect on *GLA* expression. CTR increased the expression level of *GLA* up to 2.6-fold which indicates that the ability to elevate *GLA* gene expression is an important, but not an exclusive attribute of a PR that acts as an enhancer of α-Gal A activity, and it appears that a critical limit must be exceeded to trigger a functional enzyme activity boost.

Potential role of transcriptional regulation in α-Gal A activity restoration

Given the global impact of PRs on the transcriptome and the proteostasis interactome, in particular, it is of great relevance to identify genes whose expression level in the cell is significantly altered by the effective PRs. Unbiased transcriptional profiling could unveil deeper mechanistic insights into PR function and lead to the identification of new therapeutic targets. Whole transcriptome microarray analysis was therefore performed on *GLA*$^{p.R301Q/o}$ fibroblasts after treatment with DGJ and the effective PRs.

We performed principal component analysis (PCA) on the global gene expression profiles (29 799 probesets) (Supplementary Figure S4). Broadly, the samples can be grouped into three clusters, which are distinguished by their PC1 scores, having high inter- and low intra-cluster variance. One of the clusters comprises the untreated DMSO controls, single treatments of ABX and DGJ and the combination treatment thereof. This indicates that the global impact of those treatments on the transcriptome is rather limited. On the other hand, a cluster

Biochemical Journal (2020) **477** 359–380
https://doi.org/10.1042/BCJ20190513

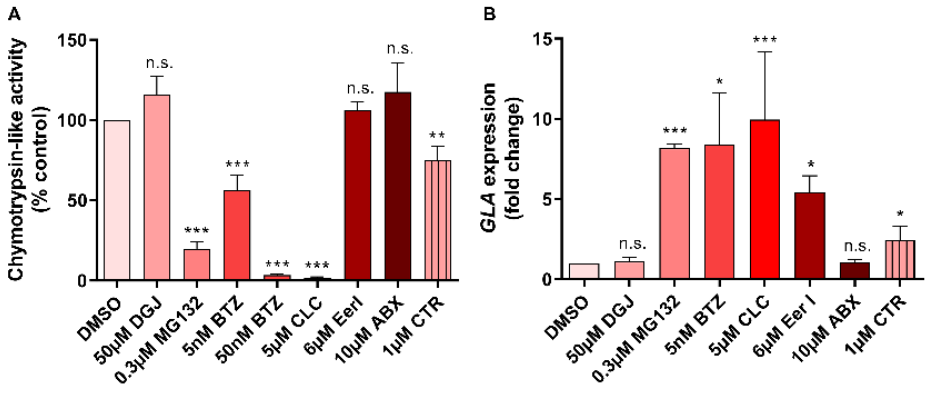

Figure 6. PRs show distinct effects on proteasomal activity and *GLA* gene expression in *GLA*$^{p.R301Q/o}$ fibroblasts.
(**A**) Proteasomal activity under the influence of proteostasis regulators. *GLA*$^{p.R301Q/o}$ fibroblasts were PR-treated for 2 h and immediately harvested in PBS. The obtained cell suspensions were then used for the luminometric measurement of chymotrypsin-like proteasomal activity. Results were normalized to the DMSO-treated *GLA*$^{p.R301Q/o}$ cells. The data are reported as mean ± SD of five independent experiments. Statistics: One-way ANOVA with post-hoc Dunnett test (*, **, ***P-values of 0.05, 0.01 and 0.001); n.s., not significant. (**B**) PRs with different effects on *GLA* expression. Relative *GLA* mRNA expression was analyzed by quantitative RT-PCR. Ahead of RT-PCR, *GLA*$^{p.R301Q/o}$ fibroblasts were treated for 24 h with indicated concentrations of PRs. The data represent 3–5 independent experiments and are plotted as mean ± SD relative to DMSO treatment. Statistics: Differences between the groups were analyzed using One-way ANOVA with post-hoc Dunnett test (*, **, ***P-values of 0.05, 0.01 and 0.001); n.s., not significant.

containing single treatments of BTZ and MG132 and the combination treatment of the latter with DGJ is located at a considerable distance from the cluster containing the controls, indicating a major impact on transcription. This is in line with our findings on the phenotypic effects of these proteostasis modifiers as shown above. Finally, a cluster containing CLC and EerI features PC1 scores close to zero; this suggests that the transcriptomic effect of those drugs is smaller than that of MG132 and BTZ. Furthermore, the underlying gene expression changes are likely to affect distinct sets of genes, implying different modes of action of the drugs.

The treatment with MG132 and BTZ regulated the expression of 1332 and 1060 genes, respectively (Supplementary Tables S2 and S3). CLC and EerI changed the expression of 471 and 512 genes, respectively. The intersection of those four sets of differentially expressed genes contained 235 genes. Treatment with DGJ and ABX caused no substantial change in gene expression, with zero and two differentially expressed genes, respectively. We identified 86 biological pathways by enrichment analysis using the WikiPathways collection [49] that show gene content overlap with the 235 consensus genes, and calculated the statistical significance thereof; Table 2 gives the most significant pathways ($P \leq 0.001$, hypergeometric test) of which Hs_Proteasome_Degradation (WP183), Hs_Parkin-Ubiquitin_Proteasomal_System_pathway (WP2359) and Hs_NRF2_pathway (WP2884) stand out, as these are directly proteostasis-related pathways. Other pathways such as Hs_Histone_Modifications (WP2369), Hs_Cell_Cycle (WP179) and Hs_Nucleotide_Metabolism (WP404) may be indicative of involved gene regulatory mechanisms. An effect on various proteostasis-associated pathways can also be demonstrated using the differentially expressed genes of each individual treatment (Supplementary Tables S4–S7).

To obtain a more proteostasis/ERAD focused view, we intersected the list of differentially expressed genes with our proteostasis genes identified (see Materials and methods). Indeed, of the 357 proteostasis-related genes, 6 were not annotated on the microarray and, hence, excluded from the analysis, and 64 (18.2%), were differentially expressed in at least one of the treatments (Figure 7A, Tables 3, Supplementary Tables S8 and S9), significantly more than expected by chance ($P \leq 4.13 \times 10^{-20}$, hypergeometric test). It is of note that of those 64 differentially expressed genes, 60 were up-regulated, while only 4 were down-regulated, in at least one treatment (Figure 7A). Altogether, 29 signature genes were common to all four treatments (BTZ, MG132, CLC and

PORTLAND PRESS

Biochemical Journal (2020) **477** 359–380
https://doi.org/10.1042/BCJ20190513

Table 2 Overrepresented signaling pathways within the intersection of global transcriptional signatures obtained from MG132, BTZ, CLC and EerI

No.	WIKI pathway
1	**Hs_Proteasome_Degradation_WP183**
2	Hs_Histone_Modifications_WP2369
3	Hs_Retinoblastoma_(RB)_in_Cancer_WP2446
4	**Hs_Parkin-Ubiquitin_Proteasomal_System_pathway_WP2359**
5	Hs_Gastric_Cancer_Network_1_WP2361
6	Hs_Pentose_Phosphate_Pathway_WP134
7	**Hs_NRF2_pathway_WP2884**
8	Hs_Benzo(a)pyrene_metabolism_WP696
9	Hs_Cell_Cycle_WP179
10	Hs_Polyol_Pathway_WP690
11	Hs_Nucleotide_Metabolism_WP404
12	Hs_Oxytocin_signaling_WP2889

Shown are the significantly overrepresented pathways with the 12 lowest corresponding *P*-values. bold: proteostasis-associated pathways.

EerI). Fifty-seven genes underwent differential expression upon BTZ treatment (Figure 7B). Mapping these genes on the functional chart of proteostasis suggests their involvement in subcategories like 'misfolded protein recognition' and 'proteasomal degradation' (Figure 7C). To investigate whether there were already differences in baseline gene expression in the $GLA^{p.R301Q/o}$ cells, we compared the gene expression profiles of the FD cells with the 4 WT cell lines. PCA was applied to all 29 799 (Supplementary Figure S5A) and the 351 proteostasis related (Supplementary Figure S5B) probesets. The high inter-cluster variance was observed for all five cell lines indicating that the FD cells were no less different than the WT lines among themselves. A more detailed view at the proteostasis genes showed no signs of differential regulation or ER stress. Only 19 genes were different between the $GLA^{p.R301Q/o}$ cells and at least one WT line, but not a single proteostasis gene showed rectified regulation to all 4 WT lines (Supplementary Figure S5C).

Discussion

The aim of the present study was to identify candidate small molecules able to increase mutant α-Gal A activity in patient-derived fibroblasts, and to provide a deeper understanding of the mechanisms initiated by the PRs that may be responsible for the effect on α-Gal A. We have demonstrated the efficacy of the PRs MG132, BTZ, CLC and EerI as potential drugs for FD by increasing enzyme activity of variant forms of the α-Gal A. We have further shown synergistic increase in mutant α-Gal A activity by combination of PRs with the clinically approved drug DGJ (trade name: Galafold [50]). The results of the current study can, therefore, be a valuable indication for a future clinical combination application of PRs with one of the approved treatments, e.g. the PC.

Due to a large number of variants leading to marginally stable α-Gal A protein, FD can be referred to as a protein misfolding disease for this portion of the variants. Misfolding of α-Gal A results in premature proteasomal degradation of the often still catalytically active enzyme [34]. Thus, an insufficient number of enzyme molecules are transported to the lysosomes, resulting in a diminished degradation of substrates and their accumulation within the cells and the extracellular space [6,51,52]. A first step towards the elimination of cellular dysfunction in protein misfolding diseases associated with loss-of-function mutations seems to be to increase the reduced protein amount of the damaged protein or enzyme in the cells. Proteostasis regulating drugs are interesting options to correct these particular phenotypes. In an approach to identify novel highly effective PRs and unravel their mode of action, we identified BTZ amongst others as being (i) highly effective and (ii) superior to the FDA-approved PC DGJ in attenuating hallmark pathology (increase in α-Gal A activity and decrease

Biochemical Journal (2020) **477** 359–380
https://doi.org/10.1042/BCJ20190513

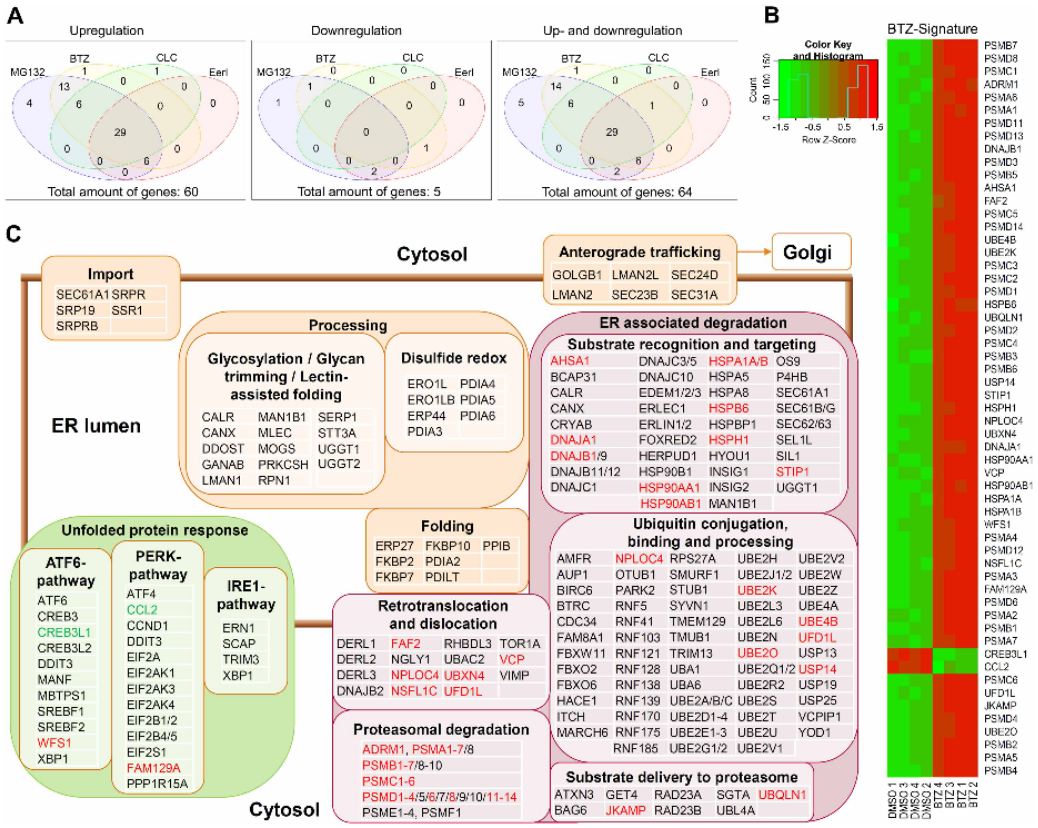

Figure 7. Proteostasis-associated transcriptional signature of PR-treated *GLA*$^{p.R301Q/o}$ fibroblasts.
(**A**) VENN diagram of differentially expressed proteostasis genes after the treatment of *GLA*$^{p.R301Q/o}$ fibroblasts with PRs. An intersection of 29 proteostasis genes was differentially expressed in all four treatments. The majority of the proteostasis genes was up-regulated and only a few were down-regulated. For detail, please refer to Supplementary Tables S8 and S9 (**B**) Heatmap of the 57 BTZ-regulated genes. (**C**) Visualization of the proteostasis gene signature of BTZ on a functional chart of ERAD/proteostasis. The chart includes 254 of the 357 manually reviewed proteostasis components based on their biological function in the network. Differentially expressed genes are indicated in red (up-regulation) and green (down-regulation). Differential gene expression was defined by >1.5-fold difference with a *P*-value threshold of 0.05.

Table 3 Number of differentially expressed proteostasis genes after the treatment with DGJ and PRs

	Treatment								
Genes	**DGJ**	**MG132**	**BTZ**	**CLC**	**Eerl**	**ABX**	**DGJ + MG132**	**DGJ + Eerl**	**DGJ + ABX**
Up-regulated genes	0	58	55	36	35	0	64	41	0
Down-regulated genes	0	4	2	0	3	0	3	2	0
Sum of regulated genes	0	62	57	36	38	0	67	43	0

PORTLAND PRESS

Biochemical Journal (2020) **477** 359–380
https://doi.org/10.1042/BCJ20190513

in biomarker lyso-Gb3 levels in patient fibroblast) by acting on several involved pathways (increasing gene expression, decreasing proteasomal activity). Of note, BTZ is an FDA-approved proteasome inhibitor for the treatment of plasmocytome (trade name: Velcade ® [53]) and is thus available for re-positioning approaches.

In the $GLA^{p.R301Q/o}$ fibroblasts DGJ was able to increase enzyme activity in a concentration-dependent manner. A 2-fold increase in enzyme activity restored ∼60% of wild-type activity in the $GLA^{p.R301Q/o}$ fibroblasts cells at a concentration of 200 μM (Supplementary Figure S3A). Nevertheless, a washout phase of 6 h after treatment had to elapse to unfold the full DGJ effect. The screening of different PRs revealed that MG132, BTZ and CLC showed the ability to increase the activity of α-Gal A as well, with concentrations of 0.3 μM (for a 2.1-fold increase), 0.005 μM (2.1-fold increase) and 5 μM (1.7-fold increase) for MG132, BTZ and CLC, respectively (Figure 2A). EerI was able to increase α-Gal A activity in combination with DGJ above the level of the single DGJ treatment and was, therefore, also regarded as an effective PR. The optimal concentration of BTZ to increase α-Gal A activity was 5 nM and, therefore, lower than BTZ concentrations used in other studies on NPC1 and Pompe disease [20,54].

The results for a second cell line, $GLA^{p.R301G/o}$ fibroblasts, could reproduce the efficacy of the individual PRs, using the most effective concentration established in the first cell line. It is noteworthy that the treatment with the PRs MG132, BTZ and CLC as a mono-therapy as well as in combination with DGJ showed a trend towards a stronger responsiveness of the p.R301G variant than observed in the $GLA^{p.R301Q/o}$ cells. EerI also tended to be effective as a mono-therapy in the $GLA^{p.R301G/o}$ fibroblasts (FC: 1.54 ± 0.14, not significant, Figure 2B) at a concentration of 6 μM, while no activity change was observed in $GLA^{p.R301Q/o}$ fibroblasts (FC: 1.09 ± 0.25, not significant, Figure 2A). DGJ, on the other hand, demonstrated a comparable efficacy in both fibroblast lines. It is still too early to conclude about the different responsiveness of the two *GLA* variants since only one cell line per genotype was tested. Although there is not much work on genetic and epigenetic factors as FD phenotype modifiers, it can be assumed that there are factors independent of the primary *GLA* gene mutation that have a direct influence on α-Gal A activity in cell culture and may thus also have an influence on the PR effect. Yet, it is not unlikely that the p.R301G variant may have a higher effect potential for the PRs used. Since p.R301Q and p.R301G are known DGJ amenable *GLA* gene variants [5,55], we can only speculate whether non-amenable variants also respond positively to the PRs. Due to the observed promising effects on variant enzyme activity and the biomarker lyso-Gb3, an extension of the mutation spectrum should be considered in future studies. Even though we only assessed cells from male hemizygous FD patients, PR treatment is a mutation-specific therapy such as the PC therapy. Therefore, the tested drugs have the potential for usage in both male and female patients likewise as is the case with PC therapy, provided the therapy is approved for the respective variant [56].

The approach to administer combinations of a chaperone and a compound with the capability to remodel cellular proteostasis is relatively new, but it has already been shown to be a promising approach to render future therapies more efficient [57]. In the present study, it was demonstrated for the first time that the use of DGJ in combination with the PR BTZ leads to a synergistic increase in variant α-Gal A activity. The combination of the clinically approved DGJ and BTZ even normalized α-Gal A activity in the patient cells. The combination of therapeutically used 10 μM DGJ [58] with 5 nM BTZ increased the enzyme activity in $GLA^{p.R301Q/o}$ fibroblasts up to the normal level (compare Figure 3C). It is worth mentioning that the maximum plasma concentration of BTZ during standard therapy of patients with multiple myeloma is ∼290 nM [53,59]. The most effective concentration of BTZ for increasing α-Gal A activity in this study was 5 nM. This high potency of BTZ with regard to enzyme activity increase is a good prerequisite for initiating long-term studies with BTZ. Since FD is a progressive genetic disorder and the therapy has to last a lifetime, the use of a low concentration formulation will likely reduce adverse effects.

It has already been described that lyso-Gb3 contributes to the pathophysiology of FD [3,60]. A recent study suggests plasma lyso-Gb3 as an appropriate clinical marker to measure the biochemical response to DGJ since the levels were found to reflect the disease course in the patients examined [61]. Lyso-Gb3 induces the proliferation of smooth muscle cells *in vitro* [3], inhibits cell growth and differentiation of fibroblasts [62] and contributes to the sensitization of peripheral nociceptive neurons [60]. Thus, therapeutic intervention is expected to reduce lyso-Gb3 in order to improve FD pathology. After a period of 7 days the BTZ treatment lowered lyso-Gb3 by 32% in $GLA^{p.R301Q/o}$ fibroblasts (Figure 5A), after 14 days, the cells demonstrated a 60% reduction (Figure 5B). Even though enzyme activity was close to normal (or even completely normalized in the DGJ/BTZ combination), lyso-Gb3 clearance progressed slowly. After 14 days the level was still markedly above the level within the wild-type cells. Of note, lyso-Gb3 was only marginally reduced by DGJ even though mono-therapy was as effective as the BTZ mono-therapy when considering enzyme activity. Since DGJ is a reversible

Biochemical Journal (2020) **477** 359–380
https://doi.org/10.1042/BCJ20190513

competitive inhibitor of α-Gal A and acts as active-site-specific chaperone [63], its efficacy seems to depend very much on the washout period and not on the on-treatment period, as after 7 (+4)-day and 14 (+4)-day washout phases no significant difference was found. Another study has demonstrated that Gb3 degradation was inhibited by the structurally similar lyso-Gb3 *in vitro* and *in vivo*, likely due to direct inhibition of α-Gal A [3], which may jeopardize the usefulness of ERT or another inhibitor of the enzyme such as DGJ for certain advanced FD patients with very high lyso-Gb3 levels.

In contrast, the obtained reduction using BTZ seems to be linear to the 'on-treatment' period, as the doubled treatment duration led to a further ∼50% reduction in the lyso-Gb3 level. BTZ function could be influenced by its ability to increase autophagy [64,65] and lysosomal exocytosis [66], which could contribute to the better clearance effect in an α-Gal A independent manner. This argues for an extension of the range of applications to patients who carry variants that do not respond sufficiently to DGJ or who do not express any functional enzyme at all, for example in combination with ERT [67]. Despite therapeutic success in FD patients harboring the amenable p.N215S α-Gal A variant, in which it was also noted that lyso-Gb3 was reduced under treatment, chaperone treatment may not be sufficiently effective for all gene variants whose *in vitro* amenability is proven [61]. Combination therapy using DGJ/BTZ is highly likely to be a more effective option here.

Mechanistically, we were able to highlight that an important aspect of effective PRs in FD is the ability to induce *GLA* gene expression. It has already been shown in a previous study that *GLA* expression is particularly highly responsive to MG132 treatment compared with other lysosomal genes in Gaucher patient fibroblasts [28]. This conclusion can be extended to the effect that all tested proteasomal inhibitors as well as EerI cause a significant increase in *GLA* gene expression. However, the ineffective CTR also increased *GLA* gene expression significantly. In addition, we addressed the aspect of inhibition of proteasomal activity. It has already been shown that proteasome inhibitors reduce the degradation of misfolded lysosomal proteins, thus increasing their transport to the lysosomes [15,16,53]. Our data show that the most effective concentrations of MG132, BTZ and CLC were able to inhibit the proteasome. There are indications that proteasome inhibition plays a central role in the observed effects on the α-Gal A, but since there appears to be no correlation between the intensity of proteasome inhibition and the increase in α-Gal A activity, the need for a concomitant proteasome inhibition on the quality of the α-Gal A enhancing effect needs further investigation.

Several studies describe that the mechanism of action of PRs is, amongst others, based on the regulation of gene expression of proteostasis genes [15,16,27]. Furthermore, it is known that the proteasomal system crucially influences gene expression [68]. We took a detailed look at gene expression in $GLA^{p.R301Q/o}$ fibroblasts and demonstrated that the effective PRs have a strong impact on global and proteostasis-associated gene expression. The transcriptional signatures of MG132, BTZ, CLC and EerI exhibited regulation of numerous ERAD genes, most of which were up-regulated. MG132 and BTZ showed similar, only slightly different, patterns regarding the globally regulated genes. Of the 1332 (MG132) and 1060 (BTZ) regulated genes, 990 were found in both signatures. Both treatments were statistically indistinguishable ($P < 2 \times 10^{-16}$, hypergeometric test), indicating the mechanistic identity and equiefficacy at the applied concentrations that were most effective on variant α-Gal A (0.3 μM MG132; 5 nM BTZ). However, proteasomal inhibition was significantly different at the concentrations we used (Figure 6A), which suggests a subordinate role for the strength of the inhibitory effect. This is also supported by the fact that the application of 50 nM BTZ increased the inhibition of the proteasome but did not lead to an increased α-Gal A activity (Supplementary Figure S3C). Furthermore, many proteasomal genes were induced. One reason for this might be based on the transcription factors Nrf1 and Nrf2, whose degradation is reduced under treatment with proteasomal inhibitors [69]. Downstream genes of Nrf2 are related to oxidative stress [70] and this pathway was identified by our analysis of the signature genes (Table 2). However, even though EerI slightly elevated proteasomal activity, proteasomal genes were likewise elevated. EerI inhibits the retrograde transport of proteins from the ER into the cytosol, which are intended for degradation. We speculate that a feedback pathway between proteasome and nucleus leads to an increase in the expression of proteasomal subunits, as the proteasomes cannot perceive or degrade substrate material due to this blockade.

Transcriptional signatures also demonstrated the regulation of *PERK* and *ATF6* signaling pathways while the *IRE1* pathway was not affected (Figure 7C). The latter is mainly associated with ERAD while *PERK* and *ATF6* are associated with increased folding capacities in the ER [71]. Various ER-associated chaperones were up-regulated as well, indicating an increased cellular protein folding capacity. Therefore, the effect on transcriptional regulation may be beneficial to enhance variant α-Gal A. We assume that among the differentially regulated proteostasis components, some could potentially be suitable for more specific pharmacological targeting. Although the potential to identify new treatment targets these pronounced gene expression signatures, such

PORTLAND PRESS

Biochemical Journal (2020) **477** 359–380
https://doi.org/10.1042/BCJ20190513

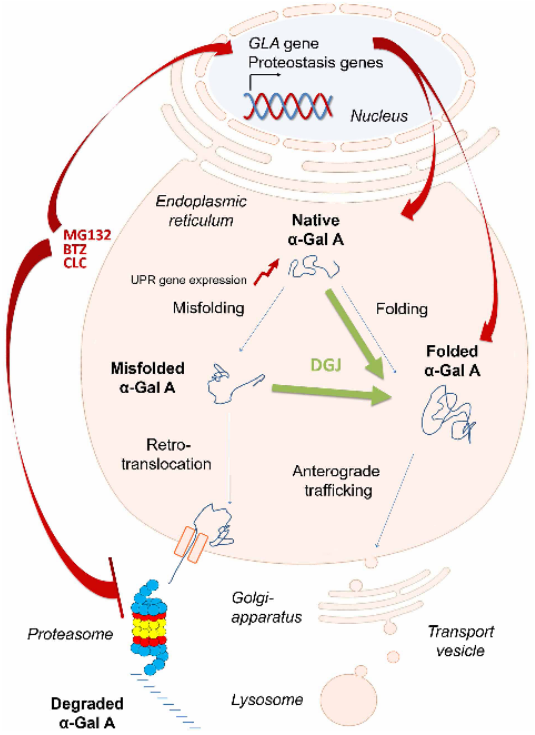

Figure 8. Model of the DGJ and BTZ mechanism leading to synergy in the recovery of α-Gal A function.
α-Gal A level is determined by mRNA transcription and efficiency of synthesis and protein folding. In the state of falsely incorporated amino acids due to point mutations, there is a shift in the balance between folding and misfolding of the protein. The pharmacological chaperone DGJ binds to the active site of the enzyme causing the enzyme to fold into a thermodynamically more stable state and α-Gal A is then less efficiently retained by the ER quality control. BTZ inhibits proteasomal activity and may, therefore, make a higher amount of α-Gal A available for DGJ. An equally important aspect of the BTZ effect seems to be its influence on the induction of the *GLA* gene expression and, speculatively, also the influence on the expression of many other genes putatively involved in proteostasis. As a result, more α-Gal A leaves the ER and is transported to the lysosomes.

phenotypes may raise the question of therapeutic versus adverse effects. This aspect should not be ignored when using proteasomal inhibitors as drug candidates. DGJ, on the other hand, appears to be in this aspect an extraordinarily neutral drug.

Low molecular mass compounds such as PC and PRs have proven to be promising approaches to overcoming protein folding diseases in recent years. In our study, the mechanisms of action complement each other in such a way that the synergy of the active substances can be accomplished. While DGJ increases the processing and transport of variant α-Gal A and therefore reduces its degradation [63], the studied PRs apparently mediate their effect via effective proteasomal degradation inhibition and a pronounced effect on cellular gene regulation (Figure 8). The positive-inducing effect on the *GLA* gene itself, which provides an increased amount of α-Gal A in the ER for folding and processing indicates the strong association between proteasomal and lysosomal systems. Indeed, 33 (7.6%, $P \leq 0.006$, hypergeometric test) of the 432 annotated signature genes [72] were differentially expressed in any of the PRs treatments including genes deficient in other LSD (Supplementary Figure S6, Supplementary Table S10). In sum, the PRs had a vast effect on the cellular gene expression regulation of degradational pathways, more specifically on the proteostasis network, which is likely to support the action of the drugs.

Biochemical Journal (2020) **477** 359–380
https://doi.org/10.1042/BCJ20190513

It can be assumed that a positive effect can only be achieved if the properties of the PRs are combined in a proportion that does justice to the respective misfolded protein variant. In FD, the proteasomal inhibitors studied here seem to best fulfill this need and are therefore candidates for clinical application.

In conclusion, we identified PRs that effectively elevate mutant α-Gal A activity and reduce lyso-Gb3 in the cells. The mechanism of action of the effective PRs included marked inhibition of the proteasome and a pronounced elevation of *GLA* gene expression as two main effectors on α-Gal A enzyme activity. Additionally, we analyzed the transcriptional effects of the PRs and identified a panel of commonly regulated proteostasis genes. We suggest that these transcriptional effects describe important aspects that influence the efficacy of PRs.

Availability of data, software and research materials

All materials used to conduct the research in this study will be made available to any researcher for purposes of reproducing the results or replicating the procedure. Affymetrix GeneChip® Human Transcriptome Arrays 2.0 CEL files are made available via Gene Expression Omnibus (GEO) database repository.

Abbreviations

ABX, Ambroxol; BTZ, Bortezomib; CLC, Clasto-Lactacystin β-lactone; CTR, Celastrol; DGJ, 1-deoxygalactonojirimycin; EerI, Eeyarestatin I; ER, endoplasmic reticulum; ERAD, ER-associated degradation; ERT, enzyme replacement therapy; FC, fold change; FD, Fabry disease; Gb3, globotriaosylceramide; *GLA*, gene symbol of human α-Galactosidase A; HPTLC, high-performance thin-layer chromatography; LSD, lysosomal storage diseases; lyso-Gb3, globotriaosylsphingosine; n.s., not significant; OMIM, Online Mendelian Inheritance in Man; PBS, phosphate-buffered saline; PC, pharmacological chaperone; PCA, principal component analysis; PRs, proteostasis regulators; PVDF, polyvinylidene difluoride; RT-PCR, Reverse transcription-polymerase chain reaction; UPR, unfolded protein response; WT, wild-type; α-Gal A, *GLA* gene product.

Acknowledgements

We thank Amicus Therapeutics for providing the Fabry patient-derived $GLA^{p.R301Q/o}$ cells. We also thank Sebastian Rost, Sebastian Oppermann, Laura Demuth, Robin Piecha and Saskia Ohse for excellent technical assistance. We would like to thank Dr. Gene Frickey for constructive criticism of the manuscript.

Author Contribution

S.S., C.C., A.-M.K. and L.R.H. carried out the cell culture experiments. S.S., M.E., S.S., D.K. and G.F. performed the transcriptomics analyses. C.C. and A.U.B. performed the lipid biomarker measurements. V.C., G.A., M.V.C., A.H., A.-K.G. and A.R. compiled and visualized data and provided method and material resources and critical review. J.L. and A.R. were responsible for study design, project administration and funding acquisition. All authors participated to the writing of the manuscript.

Funding

This work was supported by the European Union [grant number ESF/14-BM-A55-0046/16].

Competing Interests

The authors declare that there are no competing interests associated with the manuscript.

References

1 Futerman, A.H. and Van Meer, G. (2004) The cell biology of lysosomal storage disorders. *Nat. Rev. Mol. Cell Biol.* **5**, 554–565 https://doi.org/10.1038/nrm1423
2 Hwu, W.-L., Chien, Y.H., Lee, N.C., Chiang, S.C., Dobrovolny, R., Huang, A.C. et al. (2009) Newborn screening for Fabry disease in Taiwan reveals a high incidence of the later-onset GLA mutation c.936 + 919G > A (IVS4 + 919G > A). *Hum. Mutat.* **30**, 1397–1405 https://doi.org/10.1002/humu.21074
3 Aerts, J.M., Groener, J.E., Kuiper, S., Donker-Koopman, W.E., Strijland, A., Ottenhoff, R. et al. (2008) Elevated globotriaosylsphingosine is a hallmark of Fabry disease. *Proc. Natl. Acad. Sci.U.S.A.* **105**, 2812–2817 https://doi.org/10.1073/pnas.0712309105
4 Germain, D.P. (2010) Fabry disease. *Orphanet J. Rare Dis.* **5**, 30 https://doi.org/10.1186/1750-1172-5-30
5 Lukas, J., Giese, A.K., Markoff, A., Grittner, U., Kolodny, E., Mascher, H. et al. (2013) Functional characterisation of alpha-galactosidase a mutations as a basis for a new classification system in Fabry disease. *PLoS Genet.* **9**, e1003632 https://doi.org/10.1371/journal.pgen.1003632
6 Nowak, A., Mechtler, T., Kasper, D.C. and Desnick, R.J. (2017) Correlation of Lyso-Gb3 levels in dried blood spots and sera from patients with classic and later-onset Fabry disease. *Mol. Genet. Metab.* **121**, 320–324 https://doi.org/10.1016/j.ymgme.2017.06.006

PORTLAND PRESS

Biochemical Journal (2020) **477** 359–380
https://doi.org/10.1042/BCJ20190513

7 Niemann, M., Rolfs, A., Störk, S., Bijnens, B., Breunig, F., Beer, M. et al. (2014) Gene mutations versus clinically relevant phenotypes lyso-gb3 defines fabry disease. *Circ. Cardiovasc. Genet.* **7**, 8–16 https://doi.org/10.1161/CIRCGENETICS.113.000249
8 Parenti, G. (2009) Treating lysosomal storage diseases with pharmacological chaperones: from concept to clinics. *EMBO Mol. Med.* **1**, 268–279 https://doi.org/10.1002/emmm.200900036
9 van der Veen, S.J., van Kuilenburg, A.B.P., Hollak, C.E.M., Kaijen, P.H.P., Voorberg, J. and Langeveld, M. (2019) Antibodies against recombinant alpha-galactosidase A in Fabry disease: subclass analysis and impact on response to treatment. *Mol. Genet. Metab.* **126**, 162–168 https://doi.org/10.1016/j.ymgme.2018.11.008
10 Cammisa, M., Correra, A., Andreotti, G. and Cubellis, M.V. (2013) Fabry_CEP: a tool to identify Fabry mutations responsive to pharmacological chaperones. *Orphanet J. Rare Dis.* **8**, 111 https://doi.org/10.1186/1750-1172-8-111
11 Hamanaka, R., Shinohara, T., Yano, S., Nakamura, M., Yasuda, A., Yokoyama, S. et al. (2008) Rescue of mutant α-galactosidase A in the endoplasmic reticulum by 1-deoxygalactonojirimycin leads to trafficking to lysosomes. *Biochim. Biophys. Acta* **1782**, 408–413 https://doi.org/10.1016/j.bbadis.2008.03.001
12 Calamini, B., Silva, M.C., Madoux, F., Hutt, D.M., Khanna, S., Chalfant, M.A. et al. (2012) Small-molecule proteostasis regulators for protein conformational diseases. *Nat. Chem. Biol.* **8**, 185–196 https://doi.org/10.1038/nchembio.763
13 Carlile, G.W., Robert, R., Goepp, J., Matthes, E., Liao, J., Kus, B. et al. (2015) Ibuprofen rescues mutant cystic fibrosis transmembrane conductance regulator trafficking. *J. Cyst. Fibros.* **14**, 16–25 https://doi.org/10.1016/j.jcf.2014.06.001
14 Papadopoulos, P., Rosa-Neto, P., Rochford, J. and Hamel, E. (2013) Pioglitazone improves reversal learning and exerts mixed cerebrovascular effects in a mouse model of Alzheimer's disease with combined amyloid-β and cerebrovascular pathology. *PLoS One* **8**, e68612 https://doi.org/10.1371/journal.pone.0068612
15 Chiang, W.-C., Messah, C. and Lin, J.H. (2012) IRE1 directs proteasomal and lysosomal degradation of misfolded rhodopsin. *Mol. Biol. Cell* **23**, 758–770 https://doi.org/10.1091/mbc.e11-08-0663
16 Mu, T.W., Ong, D.S., Wang, Y.J., Balch, W.E., Yates, III, J.R., Segatori, L. et al. (2008) Chemical and biological approaches synergize to ameliorate protein-folding diseases. *Cell* **134**, 769–781 https://doi.org/10.1016/j.cell.2008.06.037
17 Wang, F., Song, W., Brancati, G. and Segatori, L. (2011) Inhibition of endoplasmic reticulum-associated degradation rescues native folding in loss of function protein misfolding diseases. *J. Biol. Chem.* **286**, 43454–43464 https://doi.org/10.1074/jbc.M111.274332
18 Pipalia, N.H., Cosner, C.C., Huang, A., Chatterjee, A., Bourbon, P., Farley, N. et al. (2011) Histone deacetylase inhibitor treatment dramatically reduces cholesterol accumulation in Niemann-Pick type C1 mutant human fibroblasts. *Proc. Natl. Acad. Sci.U.S.A.* **108**, 5620–5625 https://doi.org/10.1073/pnas.1014890108
19 Nakasone, N., Nakamura, Y.S., Higaki, K., Oumi, N., Ohno, K. and Ninomiya, H. (2014) Endoplasmic reticulum-associated degradation of Niemann-Pick C1: evidence for the role of heat shock proteins and identification of lysine residues that accept ubiquitin. *J. Biol. Chem.* **289**, 19714–19725 https://doi.org/10.1074/jbc.M114.549915
20 Shimada, Y., Nishimura, E., Hoshina, H., Kobayashi, H., Higuchi, T., Eto, Y. et al. (2015) Proteasome inhibitor Bortezomib enhances the activity of multiple mutant forms of lysosomal α-glucosidase in Pompe disease. *JIMD Rep.* **18**, 33–39 https://doi.org/10.1007/8904_2014_345
21 Ryno, L.M., Wiseman, R.L. and Kelly, J.W. (2013) Targeting unfolded protein response signaling pathways to ameliorate protein misfolding diseases. *Curr. Opin. Chem. Biol.* **17**, 346–352 https://doi.org/10.1016/j.cbpa.2013.04.009
22 Minamino, T., Komuro, I. and Kitakaze, M. (2010) Endoplasmic reticulum stress as a therapeutic target in cardiovascular disease. *Circ. Res.* **107**, 1071–1082 https://doi.org/10.1161/CIRCRESAHA.110.227819
23 Christianson, J.C., Olzmann, J.A., Shaler, T.A., Sowa, M.E., Bennett, E.J., Richter, C.M. et al. (2012) Defining human ERAD networks through an integrative mapping strategy. *Nat. Cell Biol.* **14**, 93–105 https://doi.org/10.1038/ncb2383
24 Lindquist, S.L. and Kelly, J.W. (2011) Chemical and biological approaches for adapting proteostasis to ameliorate protein misfolding and aggregation diseases-progress and prognosis. *Cold Spring Harb. Perspect. Biol.* **3**, a004507 https://doi.org/10.1101/cshperspect.a004507
25 Hegde, R.N., Parashuraman, S., Iorio, F., Ciciriello, F., Capuani, F., Carissimo, A. et al. (2015) Unravelling druggable signalling networks that control F508del-CFTR proteostasis. *eLife* **4**, e10365 https://doi.org/10.7554/eLife.10365
26 Shoulders, M.D., Ryno, L.M., Genereux, J.C., Moresco, J.J., Tu, P.G., Wu, C. et al. (2013) Stress-independent activation of XBP1s and/or atf6 reveals three functionally diverse ER proteostasis environments. *Cell Rep.* **3**, 1279–1292 https://doi.org/10.1016/j.celrep.2013.03.024
27 Plate, L. and Wiseman, R.L. (2017) Regulating secretory proteostasis through the unfolded protein response: from function to therapy. *Trends Cell Biol.* **27**, 722–737 https://doi.org/10.1016/j.tcb.2017.05.006
28 Wang, F., Agnello, G., Sotolongo, N. and Segatori, L. (2011) Ca^{2+} homeostasis modulation enhances the amenability of L444P glucosylcerebrosidase to proteostasis regulation in patient-derived fibroblasts. *ACS Chem. Biol.* **6**, 158–168 https://doi.org/10.1021/cb100321m
29 Mu, T.W., Fowler, D.M. and Kelly, J.W. (2008) Partial restoration of mutant enzyme homeostasis in three distinct lysosomal storage disease cell lines by altering calcium homeostasis. *PLoS Biol.* **6**, e26 https://doi.org/10.1371/journal.pbio.0060026
30 Kirkegaard, T., Gray, J., Priestman, D.A., Wallom, K.L., Atkins, J., Olsen, O.D. et al. (2016) Heat shock protein-based therapy as a potential candidate for treating the sphingolipidoses. *Sci. Transl. Med.* **8**, 355ra118 https://doi.org/10.1126/scitranslmed.aad9823
31 Wei, H., Kim, S.J., Zhang, Z., Tsai, P.C., Wisniewski, K.E. and Mukherjee, A.B. (2008) ER and oxidative stresses are common mediators of apoptosis in both neurodegenerative and non-neurodegenerative lysosomal storage disorders and are alleviated by chemical chaperones. *Hum. Mol. Genet.* **17**, 469–477 https://doi.org/10.1093/hmg/ddm324
32 Concilli, M., Iacobacci, S., Chesi, G., Carissimo, A. and Polishchuk, R. (2016) A systems biology approach reveals new endoplasmic reticulum-associated targets for the correction of the ATP7B mutant causing Wilson disease. *Metallomics* **8**, 920–930 https://doi.org/10.1039/C6MT00148C
33 Plate, L., Cooley, C.B., Chen, J.J., Paxman, R.J., Gallagher, C.M., Madoux, F. et al. (2016) Small molecule proteostasis regulators that reprogram the ER to reduce extracellular protein aggregation. *eLife* **5**, e15550 https://doi.org/10.7554/eLife.15550
34 Ishii, S., Chang, H.H., Kawasaki, K., Yasuda, K., Wu, H.L., Garman, S.C. et al. (2007) Mutant alpha-galactosidase A enzymes identified in Fabry disease patients with residual enzyme activity: biochemical characterization and restoration of normal intracellular processing by 1-deoxygalactonojirimycin. *Biochem. J.* **406**, 285–295 https://doi.org/10.1042/BJ20070479
35 Lukas, J., Pockrandt, A.M., Seemann, S., Sharif, M., Runge, F., Pohlers, S. et al. (2015) Enzyme enhancers for the treatment of Fabry and Pompe disease. *Mol. Ther.* **23**, 456–464 https://doi.org/10.1038/mt.2014.224

Biochemical Journal (2020) **477** 359–380
https://doi.org/10.1042/BCJ20190513

36 Zeevi, D.A., Hakam-Spector, E., Herskovitz, Y., Beeri, R., Elstein, D. and Altarescu, G. (2014) An intronic haplotype in α galactosidase A is associated with reduced mRNA expression in males with cryptogenic stroke. *Gene* **549**, 275–279 https://doi.org/10.1016/j.gene.2014.08.004
37 Benjamin, E.R., Flanagan, J.J., Schilling, A., Chang, H.H., Agarwal, L., Katz, E. et al. (2009) The pharmacological chaperone 1-deoxygalactonojirimycin increases alpha-galactosidase A levels in Fabry patient cell lines. *J. Inherit. Metab. Dis.* **32**, 424–440 https://doi.org/10.1007/s10545-009-1077-0
38 Citro, V., Cammisa, M., Liguori, L., Cimmaruta, C., Lukas, J., Cubellis, M.V. et al. (2016) The large phenotypic spectrum of fabry disease requires graduated diagnosis and personalized therapy: a meta-analysis can help to differentiate missense mutations. *Int. J. Mol. Sci.* **17**, E2010 https://doi.org/10.3390/ijms17122010
39 Lukas, J., Scalia, S., Eichler, S., Pockrandt, A.M., Dehn, N., Cozma, C. et al. (2016) Functional and clinical consequences of novel α-galactosidase a mutations in Fabry disease. *Hum. Mutat.* **37**, 43–51 https://doi.org/10.1002/humu.22910
40 Bligh, E.G. and Dyer, W.J. (1959) A rapid method of total lipid extraction and purification. *Can. J. Biochem. Physiol.* **37**, 911–917 https://doi.org/10.1139/y59-099
41 Taki, T., Gonzalez, T.V., Goto-Inoue, N., Hayasaka, T. and Setou, M. (2009) TLC blot (far-eastern blot) and its applications. *Methods Mol. Biol.* **536**, 545–556 https://doi.org/10.1007/978-1-59745-542-8_55
42 He, L., Kulesskiy, E., Saarela, J., Turunen, L., Wennerberg, K., Aittokallio, T. et al. (2018) Methods for high-throughput drug combination screening and synergy scoring. *Methods Mol. Biol.* **1711**, 351–398 https://doi.org/10.1007/978-1-4939-7493-1_17
43 Bliss, C.I. (1939) The toxicity of poisons applied jointly. *Ann. Appl. Biol.* **26**, 585–615 https://doi.org/10.1111/j.1744-7348.1939.tb06990.x
44 Goldberg, A.L. (2012) Development of proteasome inhibitors as research tools and cancer drugs. *J. Cell Biol.* **199**, 583–588 https://doi.org/10.1083/jcb.201210077
45 Pfaffl, M.W. (2001) A new mathematical model for relative quantification in real-time RT–PCR. *Nucleic Acids Res.* **29**, e45 https://doi.org/10.1093/nar/29.9.e45
46 Irizarry, R.A., Hobbs, B., Collin, F., Beazer-Barclay, Y.D., Antonellis, K.J., Scherf, U. et al. (2003) Exploration, normalization, and summaries of high density oligonucleotide array probe level data. *Biostatistics* **4**, 249–264 https://doi.org/10.1093/biostatistics/4.2.249
47 Carlson, M. (2015) org.Hs.eg.db: Genome wide annotation for Human. R package version 3.2.3
48 Codony-Servat, J., Tapia, M.A., Bosch, M., Oliva, C., Domingo-Domenech, J., Mellado, B. et al. (2006) Differential cellular and molecular effects of bortezomib, a proteasome inhibitor, in human breast cancer cells. *Mol Cancer Ther.* **5**, 665–675 https://doi.org/10.1158/1535-7163.MCT-05-0147
49 Kutmon, M., Riutta, A., Nunes, N., Hanspers, K., Willighagen, E.L., Bohler, A. et al. (2016) Wikipathways: capturing the full diversity of pathway knowledge. *Nucleic Acids Res.* **44**, D488–D494 https://doi.org/10.1093/nar/gkv1024
50 Markham, A. (2016) Migalastat: first global approval. *Drugs* **76**, 1147–1152 https://doi.org/10.1007/s40265-016-0607-y
51 Gervas-Arruga, J., Cebolla, J.J., Irun, P., Perez-Lopez, J., Plaza, L., Roche, J.C. et al. (2015) Increased glycolipid storage produced by the inheritance of a complex intronic haplotype in the α-galactosidase A (GLA) gene. *BMC Genet.* **16**, 109 https://doi.org/10.1186/s12863-015-0267-z
52 Sanchez-Niño, M.D., Sanz, A.B., Carrasco, S., Saleem, M.A., Mathieson, P.W., Valdivielso, J.M. et al. (2011) Globotriaosylsphingosine actions on human glomerular podocytes: implications for Fabry nephropathy. *Nephrol. Dial. Transplant.* **26**, 1797–1802 https://doi.org/10.1093/ndt/gfq306
53 Reece, D.E., Sullivan, D., Lonial, S., Mohrbacher, A.F., Chatta, G., Shustik, C. et al. (2011) Pharmacokinetic and pharmacodynamic study of two doses of bortezomib in patients with relapsed multiple myeloma. *Cancer Chemother. Pharmacol.* **67**, 57–67 https://doi.org/10.1007/s00280-010-1283-3
54 Macías-Vidal, J., Girós, M., Guerrero, M., Gascón, P., Serratosa, J., Bachs, O. et al. (2014) The proteasome inhibitor bortezomib reduced cholesterol accumulation in fibroblasts from Niemann-Pick type C patients carrying missense mutations. *FEBS J.* **281**, 4450–4466 https://doi.org/10.1111/febs.12954
55 Benjamin, E.R., Della Valle, M.C., Wu, X., Katz, E., Pruthi, F., Bond, S. et al. (2017) The validation of pharmacogenetics for the identification of Fabry patients to be treated with migalastat. *Genet Med.* **19**, 430–438 https://doi.org/10.1038/gim.2016.122
56 Amicus Therapeutics U.S., Inc. GALAFOLD™ Prescribing Information; Revised: 08/2018; https://www.galafold.com/app/uploads/2018/08/galafold.pdf
57 Mohamed, F.E., Al-Gazali, L., Al-Jasmi, F. and Ali, B.R. (2017) Pharmaceutical chaperones and proteostasis regulators in the therapy of lysosomal storage disorders: current perspective and future promises. *Front. Pharmacol.* **8**, 448 https://doi.org/10.3389/fphar.2017.00448
58 Hughes, D.A., Nicholls, K., Shankar, S.P., Sunder-Plassmann, G., Koeller, D., Nedd, K. et al. (2017) Oral pharmacological chaperone migalastat compared with enzyme replacement therapy in Fabry disease: 18-month results from the randomised phase III ATTRACT study. *J. Med. Genet.* **54**, 288–296 https://doi.org/10.1136/jmedgenet-2016-104178
59 Hanley, M.J., Mould, D.R., Taylorm, T.J., Gupta, N., Suryanarayan, K., Neuwirth, R. et al. (2017) Population pharmacokinetic analysis of Bortezomib in pediatric leukemia patients: model-based support for body surface area-based dosing over the 2- to 16-year age range. *J. Clin. Pharmacol.* **57**, 1183–1193 https://doi.org/10.1002/jcph.906
60 Ferraz, M.J., Marques, A.R., Appelman, M.D., Verhoek, M., Strijland, A., Mirzaian, M. et al. (2016) Lysosomal glycosphingolipid catabolism by acid ceramidase: formation of glycosphingoid bases during deficiency of glycosidases. *FEBS Lett.* **590**, 716–725 https://doi.org/10.1002/1873-3468.12104
61 Lenders, M., Stappers, F., Niemietz, C., Schmitz, B., Boutin, M., Ballmaier, P.J. et al. (2019) Mutation-specific Fabry disease patient-derived cell model to evaluate the amenability to chaperone therapy. *J. Med. Genet.* **56**, 548–556 https://doi.org/10.1136/jmedgenet-2019-106005
62 Choi, J.Y., Shin, M.Y., Suh, S.H. and Park, S. (2015) Lyso-globotriaosylceramide downregulates KCa3.1 channel expression to inhibit collagen synthesis in fibroblasts. *Biochem. Biophys. Res. Commun.* **468**, 883–888 https://doi.org/10.1016/j.bbrc.2015.11.050
63 Fan, J.Q., Ishii, S., Asano, N. and Suzuki, Y. (1999) Accelerated transport and maturation of lysosomal α-galactosidase A in Fabry lymphoblasts by an enzyme inhibitor. *Nat. Med.* **5**, 112–115 https://doi.org/10.1038/4801
64 Ji, C.H. and Kwon, Y.T. (2017) Crosstalk and interplay between the ubiquitin-proteasome system and autophagy. *Mol. Cells* **40**, 441–449 https://doi.org/10.14348/molcells.2017.0115
65 Cha-Molstad, H., Sung, K.S., Hwang, J., Kim, K.A., Yu, J.E., Yoo, Y.D. et al. (2015) Amino-terminal arginylation targets endoplasmic reticulum chaperone BiP for autophagy through p62 binding. *Nat. Cell Biol.* **17**, 917–929 https://doi.org/10.1038/ncb3177
66 Samie, M.A. and Xu, H. (2014) Lysosomal exocytosis and lipid storage disorders. *J. Lipid Res.* **55**, 995–1009 https://doi.org/10.1194/jlr.R046896
67 Song, H.Y., Chiang, H.C., Tseng, W.L., Wu, P., Chien, C.S., Leu, H.B. et al. (2016) Using CRISPR/Cas9-mediated GLA gene knockout as an in vitro drug screening model for Fabry disease. *Int. J. Mol. Sci.* **17**, E2089 https://doi.org/10.3390/ijms17122089

PORTLAND PRESS

Biochemical Journal (2020) **477** 359–380
https://doi.org/10.1042/BCJ20190513

68 Kwak, J., Workman, J.L. and Lee, D. (2011) The proteasome and its regulatory roles in gene expression. *Biochim. Biophys. Acta* **1809**, 88–96 https://doi.org/10.1016/j.bbagrm.2010.08.001
69 Xie, Y. (2010) Feedback regulation of proteasome gene expression and its implications in cancer therapy. *Cancer Metastasis Rev.* **29**, 687–693 https://doi.org/10.1007/s10555-010-9255-y
70 Ma, Q. (2013) Role of nrf2 in oxidative stress and toxicity. *Annu. Rev. Pharmacol. Toxicol.* **53**, 401–426 https://doi.org/10.1146/annurev-pharmtox-011112-140320
71 Hampton, R.Y. (2003) IRE1: a role in UPREgulation of ER degradation. *Dev. Cell* **4**, 144–146 https://doi.org/10.1016/S1534-5807(03)00032-7
72 Brozzi, A., Urbanelli, L., Germain, P.L., Magini, A. and Emiliani, C. (2013) hLGDB: a database of human lysosomal genes and their regulation. *Database (Oxford)* **2013**, bat024 https://doi.org/10.1093/database/bat024